SSC-395

SHIP MAINTENANCE PROJECT

Phases II and III- Volume 2

Study of Fatigue of Proposed Critical Structural Details in Double Hull Tankers

SHIP STRUCTURE COMMITTEE

1997

c.1

SHIP STRUCTURE COMMITTEE

The SHIP STRUCTURE COMMITTEE is constituted to prosecute a research program to improve the hull structures of ships and other marine structures by an extension of knowledge pertaining to design, materials, and methods of construction.

RADM J. C. Card, USCG (Chairman)
Chief, Office of Marine Safety, Security
and Environmental Protection
U. S. Coast Guard

Mr. John Grinstead
Director, Policy and Legislation
Marine Regulatory Directorate
Transport Canada

Mr. Edwin B. Schimler
Associate Administrator for Ship-
building and Technology Development
Maritime Administration

Dr. Donald Liu
Senior Vice President
American Bureau of Shipping

Mr. Robert McCarthy
Director, Survivability and Structural
Integrity Group (SEA 03P)
Naval Sea Systems Command

Mr. Thomas Connors
Acting Director of Engineering (N7)
Military Sealift Command

Dr. Ross Grahm
Head, Hydronautics Section
Defence Research Establishment-Atlantic

EXECUTIVE DIRECTOR

CDR Stephen E. Sharpe, USCG
U. S. Coast Guard

CONTRACTING OFFICER TECHNICAL REPRESENTATIVE

Mr. William J. Siekierka
Naval Sea Systems Command

SHIP STRUCTURE SUBCOMMITTEE

The SHIP STRUCTURE SUBCOMMITTEE acts for the Ship Structure Committee on technical matters by providing technical coordination for determinating the goals and objectives of the program and by evaluating and interpreting the results in terms of structural design, construction, and operation.

MILITARY SEALIFT COMMAND

Mr. Robert E. Van Jones (Chairman)
Mr. Rickard A. Anderson
Mr. Michael W. Touma
Mr. Jeffrey E. Beach

MARITIME ADMINISTRATION

Mr. Frederick Seibold
Mr. Richard P. Voelker
Mr. Chao H. Lin
Dr. Walter M. Maclean

U. S. COAST GUARD

CAPT George Wright
Mr. Walter Lincoln
Mr. Rubin Sheinberg

AMERICAN BUREAU OF SHIPPING

Mr. Glenn Ashe
Mr. John F. Conlon
Mr. Phillip G. Rynn
Mr. William Hanzalek

NAVAL SEA SYSTEMS COMMAND

Mr. W. Thomas Packard
Mr. Charles L. Null
Mr. Edward Kadala
Mr. Allen H. Engle

TRANSPORT CANADA

Mr. Peter Timonin
Mr. Felix Connolly
Mr. Francois Lamanque

DEFENCE RESEARCH ESTABLISHMENT ATLANTIC

Dr. Neil Pegg
LCDR Stephen Gibson
Dr. Roger Hollingshead
Mr. John Porter

SHIP STRUCTURE SUBCOMMITTEE LIAISON MEMBERS

SOCIETY OF NAVAL ARCHITECTS AND
MARINE ENGINEERS
Dr. William Sandberg

CANADA CENTRE FOR MINERALS AND
ENERGY TECHNOLOGIES
Dr. William R. Tyson

U. S. NAVAL ACADEMY
Dr. Ramswar Bhattacharyya

U. S. MERCHANT MARINE ACADEMY
Dr. C. B. Kim

U. S. COAST GUARD ACADEMY
CDR Bruce R. Mustain

U. S. TECHNICAL ADIVSORY GROUP TO THE
INTERNATIONAL STANDARDS ORGANIZATION
CAPT Charles Piersall

AMERICAN WELDING SOCIETY
Mr. Richard French

NATIONAL ACADEMY OF SCIENCES -
MARINE BOARD
Dr. Robert Sielski

NATIONAL ACADEMY OF SCIENCES -
COMMITTEE ON MARINE STRUCTURES
Dr. John Landes

WELDING RESEARCH COUNCIL
Dr. Martin Prager

AMERICAN IRON AND STEEL INSTITUTE
Mr. Alexander D. Wilson

OFFICE OF NAVAL RESEARCH
Dr. Yapa D. S. Rajapaske

MASSACHUSETTS INSTITUTE OF TECHNOLOGY
CAPT Alan J. Brown

STUDENT MEMBER
Mr. Jason Miller
Massachusetts Institute of Technology

C.3

c.2.

**Ship
Structure
Committee**

An Interagency Advisory Committee

SSC-395
SR-1360
SR-1371

February 27, 1997

SHIP MAINTENANCE PROJECT
Phases II and III

This report presents the results of the second and third phases of the subject project of which phase one was first presented in our four volume set -- SSC-386. These studies investigated the development of engineering technology that could lead improvements in structural maintenance for new and existing tankers. These projects built further upon the work started in phase I specifically focusing on critical structural details and corrosion limits.

The report has been divided into five volumes, each of which may stand alone. Volume one opens with a summary of all three phases by Professor Robert G. Bea, the coordinating investigator for the program and follows with a report on corrosion limits for tankers. The second and fifth volumes look into evaluation of cracked critical structural details in tankers. The third volume presents theory and user instructions for software to manage repair of critical structural details. The fourth volume applies to fatigue classification of critical structural details. The software developed in the project will be available on the next Ship Structure Committee CD Rom release, which is anticipated to be released in the next year. The industry is encouraged to contact Professor Bea at the University of California, Berkeley to discuss further possibilities in application of the work undertaken here in the industry.

C. CARD
Rear Admiral, U.S. Coast Guard
Chairman, Ship Structure Committee

1. Report No. SSC-395-2	2. Government Accession No. PB97-142830	3. Recipient's Catalog No.
4. Title and Subtitle Ship Maintenance Project Phases II and III Volume 2 Study of Fatigue of Proposed Critical Structural Details in Double Hull Tankers		5. Report Date 1997
		6. Performing Organization Code
		8. Performing Organization Report No.
7. Author(s) Robert Bea, Tao Xu		
9. Performing Agency Name and Address University of California at Berkeley Department of Naval Architecture and Ocean Engineering Berkeley, CA 94720		10. Work Unit No. (TRAIS)
		11. Contract or Grant No.
		13. Type of Report and Period Covered Final
12. Sponsoring Agency Name and Address Ship Structure Committee U. S. Coast Guard (G-MSE/SSC) 2100 Second St. S.W. Washington, DC 21\0593-0001		
		14. Sponsoring Agency Code G-M

15. Supplementary Notes
Sponsored by the Ship Structure Committee. Jointly funded by other organizations as a joint industry project. See inside the report for futher details on sponsors.

16. Abstract

This report presents the results of the second and third phases of the subject project of which phase one was first presented in our four volume set - SSC-386. These studies investigated the development of engineering technology that could lead to improvements in structural maintenance for new and existing tankers. These projects built further upon the work started in phase I specifically focusing on critical structural details and corrosion limits.

The report has been divided into five volumes, each of which may stand alone. Volume one opens with a summary of all three phases by Professor Robert G. Bea, the coordinating investigator for the program, and follows with a report on corrosion limits for tankers. The second and fifth volumes look into evaluation of cracked critical structural details in tankers. The third volume presents theory and user instructions for software to manage repair of critical structural details. The fourth volume applies to fatigue classification of critical structural details. The software developed in the project will be available on the next Ship Structure Committee CD Rom release which is anticipated to be released in the next year. The industry is encouraged to contact Professor Bea at the University of California, Berkeley to discuss further possibilities in application of the work undertaken here in the industry.

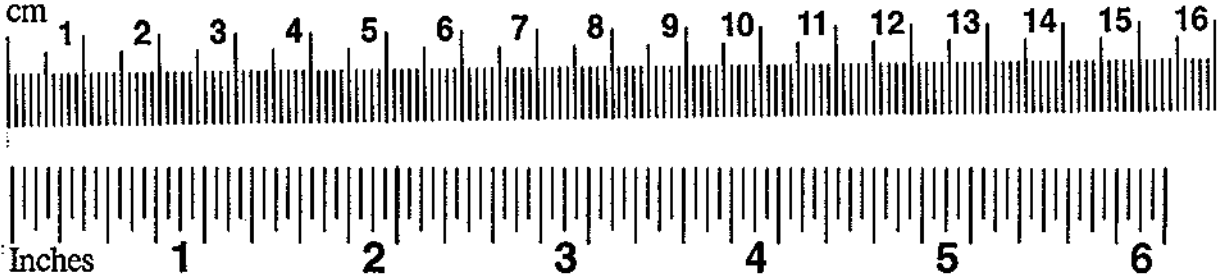| 17. Key Words fatigue, critical structural details, tanker structures, fatigue classification	18. Distribution Statement Distribution unlimited, available from: National Technical Information Service U.S. Department of Commerce Springfield, VA 22151 (703)487-4690		
19. Security Classif. (of this report) Unclassified	20. SECURITY CLASSIF. (of this page) Unclassified	21. No. of Pages 514	22. Price $67.00 Paper

Form DOT F 1700.7 (8/72)   Reproduction of form and completed page is authorized.

3

NIST

METRIC CONVERSION CARD

Approximate Conversions to Metric Measures

Symbol	When You Know	Multiply by	To Find	Symbol
LENGTH				
in	inches	2.5	centimeters	cm
ft	feet	30	centimeters	cm
yd	yards	0.9	meters	m
mi	miles	1.6	kilometers	km
AREA				
in²	square inches	6.5	square centimeters	cm²
ft²	square feet	0.09	square meters	m²
yd²	square yards	0.8	square meters	m²
mi²	square miles	2.6	square kilometers	km²
	acres	0.4	hectares	ha
MASS (weight)				
oz	ounces	28	grams	g
lb	pounds	0.45	kilograms	kg
	short tons (2000 lb)	0.9	metric ton	t
VOLUME				
tsp	teaspoons	5	milliliters	mL
Tbsp	tablespoons	15	milliliters	mL
in³	cubic inches	16	milliliters	mL
fl oz	fluid ounces	30	milliliters	mL
c	cups	0.24	liters	L
pt	pints	0.47	liters	L
qt	quarts	0.95	liters	L
gal	gallons	3.8	liters	L
ft³	cubic feet	0.03	cubic meters	m³
yd³	cubic yards	0.76	cubic meters	m³
TEMPERATURE (exact)				
°F	degrees Fahrenheit	subtract 32, multiply by 5/9	degrees Celsius	°C

Approximate Conversions from Metric Measures

Symbol	When You Know	Multiply by	To Find	Symbol
LENGTH				
mm	millimeters	0.04	inches	in
cm	centimeters	0.4	inches	in
m	meters	3.3	feet	ft
m	meters	1.1	yards	yd
km	kilometers	0.6	miles	mi
AREA				
cm²	square centimeters	0.16	square inches	in²
m²	square meters	1.2	square yards	yd²
km²	square kilometers	0.4	square miles	mi²
ha	hectares (10,000 m²)	2.5	acres	
MASS (weight)				
g	grams	0.035	ounces	oz
kg	kilograms	2.2	pounds	lb
t	metric ton (1,000 kg)	1.1	short tons	
VOLUME				
mL	milliliters	0.03	fluid ounces	fl oz
mL	milliliters	0.06	cubic inches	in³
L	liters	2.1	pints	pt
L	liters	1.06	quarts	qt
L	liters	0.26	gallons	gal
m³	cubic meters	35	cubic feet	ft³
m³	cubic meters	1.3	cubic yards	yd³
TEMPERATURE (exact)				
°C	degrees Celsius	multiply by 9/5, add 32	degrees Fahrenheit	°F

Temperature scale:

°C	-40	-20	0	20	37	60	80	100
°F	-40	0	32	80	98.6	160	212

water freezes — body temperature — water boils

cm / Inches ruler (1–16 cm, 1–6 inches)

4
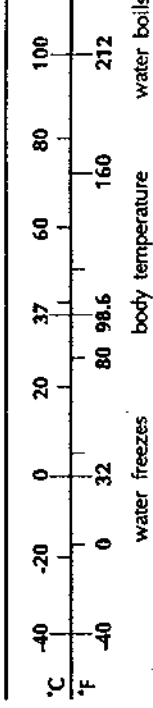
Ship Structural Maintenance Projects II and III
Cross Reference Listing

SSC Vol	SMP #	Title	Authors	Date	NTIS Number
	II				
2	-1	Fatigue Analysis of CSD in a 150K DWT Double-Hull Tanker	Xu, Bea	10/93	PB97-142830
2	-2	Fatigue Analysis of CSD in a 190K DWT Double-Hull Tanker	Xu, Bea	10/93	PB97-142830
2	-3	CSD Library and Finite Element Stress Contours	Xu, Bea	10/93	PB97-142830
1	-4	Development of a Rational Basis for Defining Corrosion Limits in Tankers	Mayoss, Bea	12/93	PB97-142822
3	-4a	RMS for CSD in Ships – User Manual	Ma, Bea	9/93	PB97-142848
3	-4b	RMS for CSD in Ships – Theory	Ma, Bea	9/93	PB97-142848
4		Fatigue Classification of CSD in Tankers	Schulte-Strathaus, Bea	1/94	PB97-142855
	III				
3	-1-1	RMS for Fatigue Cracks in Ship CSDs	Ma, Bea	10/94	PB97-142848
5	-2-1	Fitness for Purpose Analysis Procedure of Cracked CSDs in Tankers	Xu, Bea	1/95	PB97-142863
5	-2-2	A Load Shedding Model of Fracture Mechanics Analysis of Cracked SCDs in Tankers	Xu, Bea	1/95	PB97-142863
5	-2-3	FRACTURE- A Computer Code for Fracture Mechanics Analysis of Crack Growth of Cracked CSD in Tankers	Xu, Bea	1/95	PB97-142863
5	-5	Pro-IMR: A Computer Code for Probability-Based Inspection Planning	Xu, Bea	10/94	PB97-142863

5, 6y

Study of Fatigue of Proposed Critical Structural Details in Double Hull Tankers

Fatigue Analysis of Critical Structural Details in a 150,000 DWT Double Hull Tanker

Tao Xu
and
Professor Robert G. Bea

Department of Naval Architecture and Offshore Engineering
University of California, Berkeley

7,8ל

Table of Contents

Chapter 6 Fatigue Uncertainty

Chapter 7 Summary and Conclusions

List of Figures

11, 12x

Chapter 1

Introduction

1.1 Background

Tankers operate in an enviroment characterized by cyclic load which can cause fatigue cracking in welded critical structural details. If the critical structural detail (CSD) are not designed to resist fatigue cracking, the tanker's economic profitability from repair costs can be affected and the economic life shortened. it is desirable to develop techniques that enable ship structural designers to minimize the extent of fatigue damage and to ensure structural integrity throughout the tanker's service life.

A Joint Industry Project **Structural Maintenance for New and Existing Ships (SMP)** conducted by The Department of Naval Architecture and Offshore Engineering University of California at Berkeley from 1990 to 1992 addressed a long-term fatigue analysis procedure. This Joint Industry Project **Study of Fatigue of Proposed Critical Structural Details (CSD) in Double-Hull Tankers** is the direct extension of SMP project. The objective of this project is to conduct analytical studies of proposed CSD for new double-hull tankers to assure that they have desirable durability and robustness charcteristics. In this study, we proposed to perform analysis of several important CSD from two structural systems that are intended for the next-generation of VLCC's and ULCC's. The first study of a proposed 150,000 DWT double-hull tanker was conducted to determine if the CSD and framing system possess desirable degrees of durability. This report summarizes the fatigue analysis of this proposed 150,000 DWT double-hull tanker.

1.2 Ship Characteristics and Design Conditions

The overall dimensions of the 150,000 DWT proposed VLCC are described in Table (1). The general arrangement is shown in Fig.1.1. The midship section is shown in Fig.1.2.

Principal Dimensions

The principal dimensions of the 150,000 DWT double-hull tanker are:
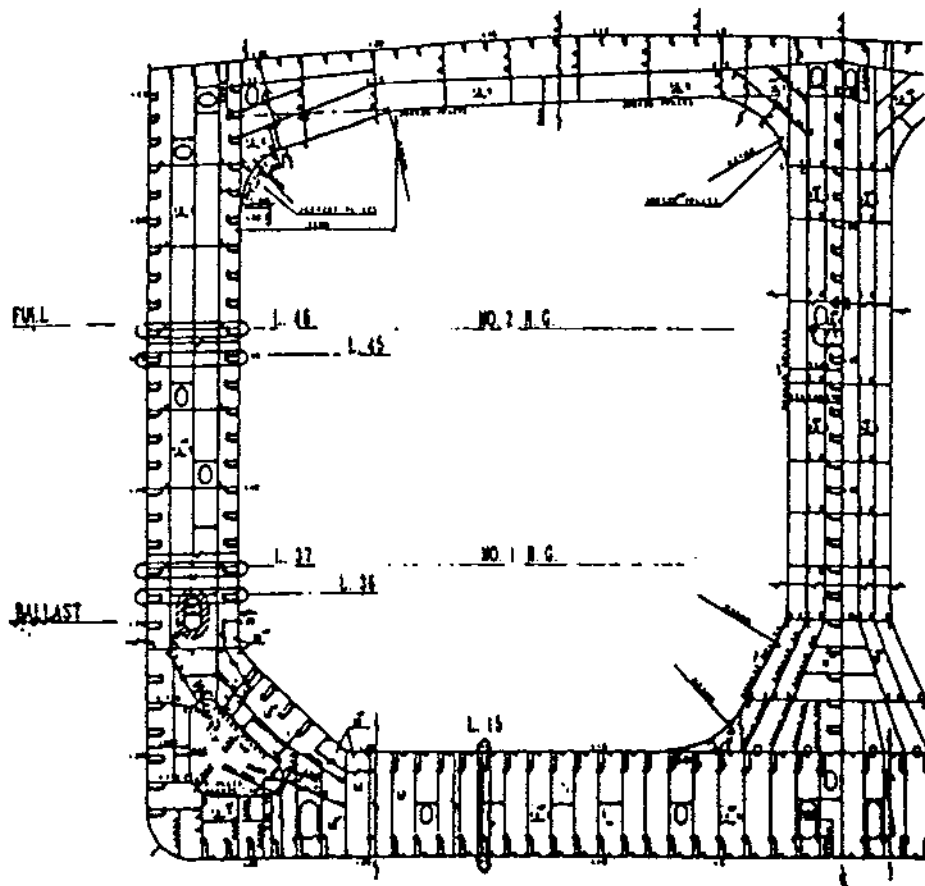
Figure 1.2 Midship Section

5

Chapter 2

Long-Term Extreme Loading

2.1 Introduction

The quantification of the response of tanker structures to wave action is crucial for fatigue evaluation. The alternating excitation induced in the marine structures by wave action produces different types of responses such as motions and stresses.

2.2 Ship Motion Analysis

A ship motion analysis was performed to generate Response Amplitude Operators (RAO) for ship bending moments and hydrodynamic (outer) pressures in various headings. In addition, the accelerations generated by the ship motion were used to determine inner pressures.

Strip Method

Station	21
Form	Lewis Form (Fig.2.2)

Calculation Condition

Ship Condition	Full Condition
	Ballast Condition
Heading Angle	0 to 180 (15)
Wave Length (Wl/Lpp)	0.277 to 6.25 (20 cases)
Ship Speed	11.175 knots (75% of design speed) : Full
	12.22 knots (75% of design speed) : Ballast

Rolling Motion

Rolling Period

$$T = 2 \times Kxx / (GoM)^{1/2}$$

Full Load	Ballast
17.1 sec	9.2 sec

$$Kxx = 0.39 \times B$$

Rolling Angle (10^{-8})

$$\theta = 20 \times (30/B)^{1/4} \text{ (deg)}$$
$$= 17.6 \text{ deg}$$

Roll Damping Factor

The roll damping factor is determined so that the rolling angle for 20 years obtained by the strip method is the same value as the above value (θ)

RAO - Results

The Response Amplitude Operator (RAO) for ship bending moments and hydrodynamic (outer) pressures in various headings and the accelerations used for inner pressure determination was generated by ship motion analysis.(Ref 3)

2.3 Long-Term Prediction

Long-Term Wave Environment

The purpose of defining the long-term wave enviroment was to select a scatter wave diagram, showing the annual average probability of occurence for various seastates for the anticipated ship trading route.

A North Atlantic All Season wave scatter diagram (according to Walden's wave data given in Fig.2.1) was selected for proposed 150,000 DWT double-hull tanker.

Walden's wave table was developed based on wave data collected from many wave measurement stations over many years. Each block in the table is the annual averaged probability of occurrence with respect to the seastate, represented by the modified Pierson Moskowitz (I.S.S.C) wave spectrum, having the significant wave height and average period indicated for that block.

Short-Term Response Statistics

A short-term statistics analysis was performed to predict the variance of the bending moment and outer pressure response spectra for each sea state in Walden's wave table. The variance was represented by the square of the root mean squared (RMS) value of the response spectrum. The bending and pressure response spectra were determined by multiplying respective RAO for each heading by the I.S.S.C. wave spectrum representing each wave condition in Walden's wave table.

LEWIS 2
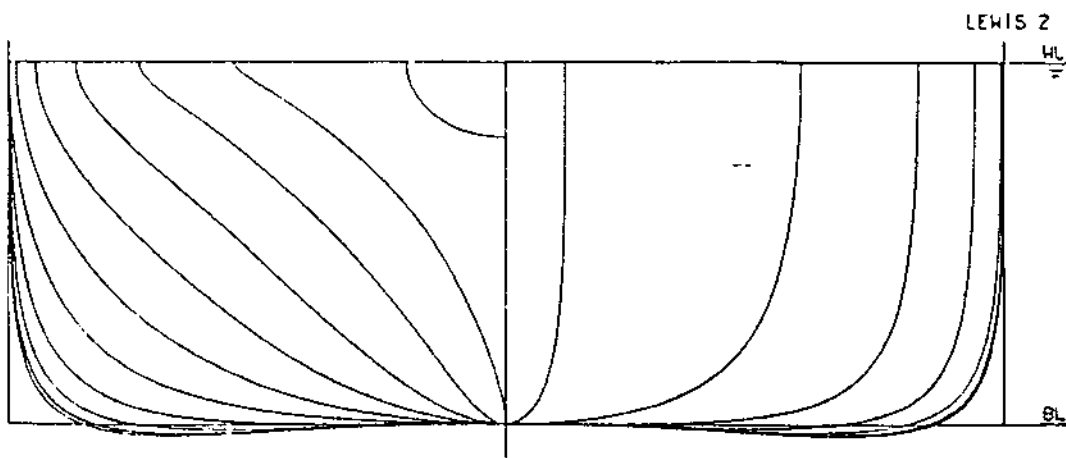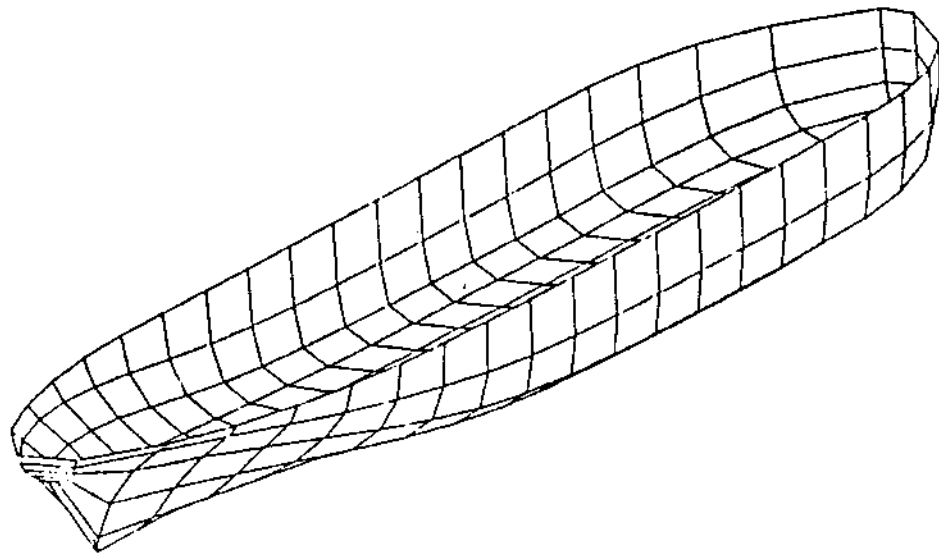
Figure 2.2

22

WAVE BENDING MOMENT

Fig 2.3

Wave Table
Walden - North Atlantic
All Seasons

Full.   ○ ――――
BALLAST   ― · ― · ○ ― · ―

Reference :
W.M.Mt. of Rule
542506 T-M

MAX 668000 T-M
(FULL.)

MAX 771800 T-M
(BALLAST)

MOMENT
(T-M)

11
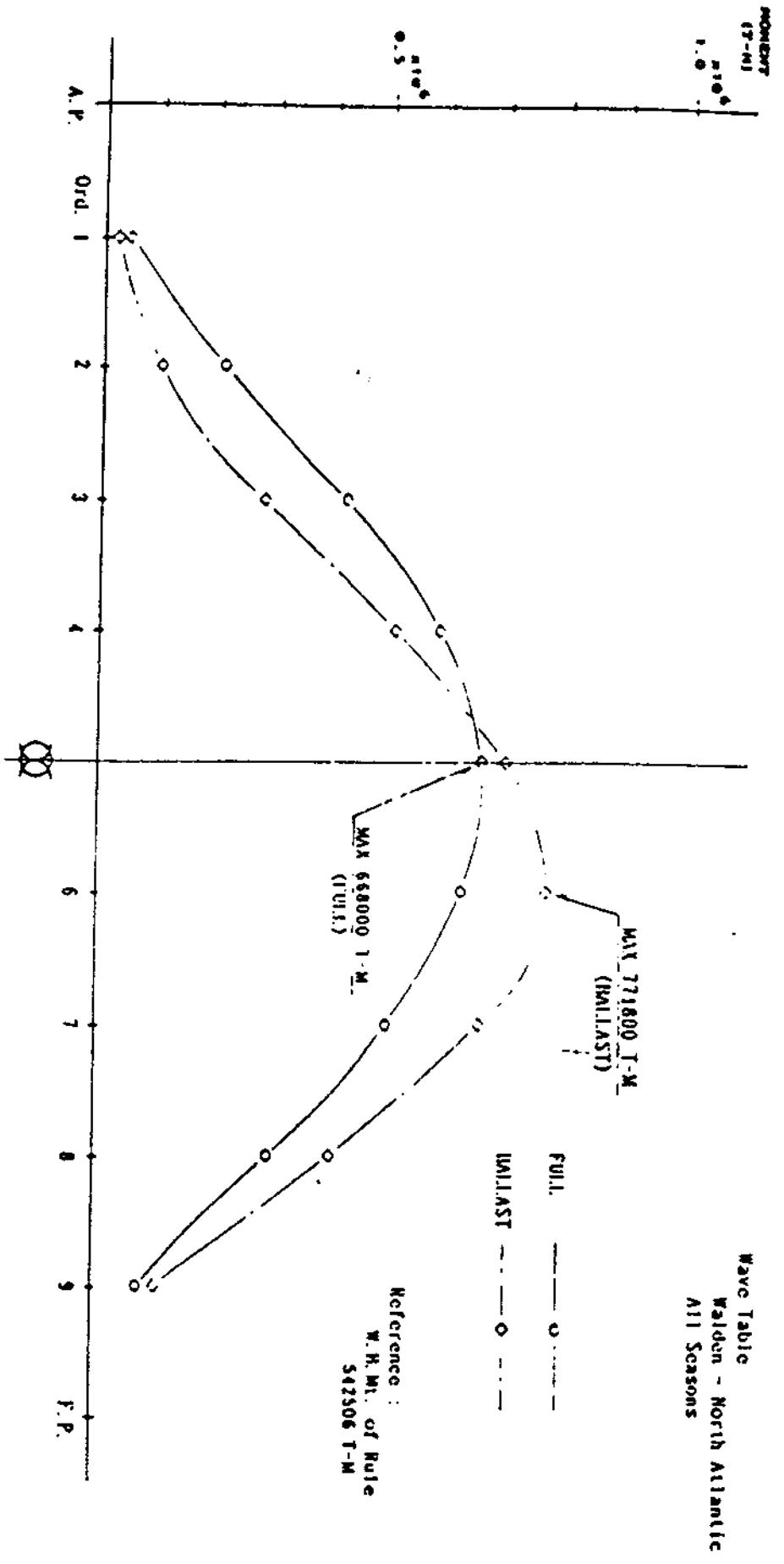
Length (L), m	261
Length (scantling), m	258.311
Length (l. w. l)	266.3
Breadth mld. (B), m	50.0
Depth mld (D), m	25.1
Draft mld. (d) (designed), m	16.76
Cb mld. (at scantling draft)	0.7916

Cb   Block Cofficient

Design Parameters

The response and fatigue calculation were performed in full load and ballast conditions. The design parameters used in these two conditions are summarized as follows:

Design Parameter	Full Load	Ballast
L x B x D	261.0 x 50.0 x 25.1	261.0 x 50 x 25.1
d	17.14	7.56
Cb	0.7834	0.7194
Co	0.9987	0.9970
OG (+ ; aft, - : fore)	-10.37	-10.39
KG	14.71	10.19
GoM	5.19	17.87
Displacement	180,701 MT	71,216 MT
Speed	11.175 knot	12.22 knot
Head Angle	0 to 360 deg	0 to 360 deg
Wave Length (Wl/L)	0.277 to 6.25	0.277 to 6.25

where   Cb = Block Coefficient
Co = Mid-ship section coefficient
OG = Center of gravity
KG = Distance of OG from the kneel
GoM = The metacentric height
Wl = Wave Length

The speed used in the motion analyses was 75% of design speed.

1.3 Steel Properties

The majority of the steel used in the proposed double-hull tanker was HTS Grade "AH32" steel. The mechanical properties of this type of steel are :

Tensile Strength .... min. 48kg/mm^2
Yield Strength .... min. 32kg/mm^2

'4

Critical Structural Details selected for the fatigue analysis are all constructed with grade "AH32" steel.

15

ROUGH ARRANGEMENT

PRINCIPAL DIMENSIONS

Length	b.p.	261.00	m
Breadth	mld.	50.00	m
Depth	mld.	25.10	m
Designed draught mld.		16.76	m
Scantling draught mld.		17.18	m

U-TYPE

COT

3,340

3,340

COT

COT

S-TY

J-TY

SLOP T.(S)
SLOP T.(P)
NO. 6 COT(S)
NO. 6 COT(P)
NO. 5 COT(S)
NO. 5 COT(P)
NO. 4 COT(S)
NO. 4 COT(P)
NO. 3 COT(S)
NO. 3 COT(P)
NO. 2 COT(S)
NO. 2 COT(P)
NO. 1 COT(S)
NO. 1 COT(P)

S-J (P/S)
S-J (P/S)
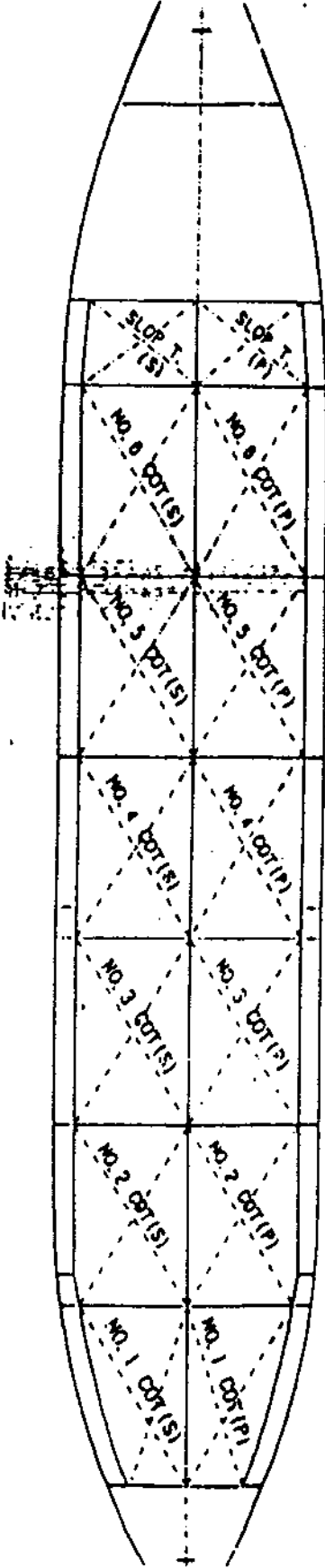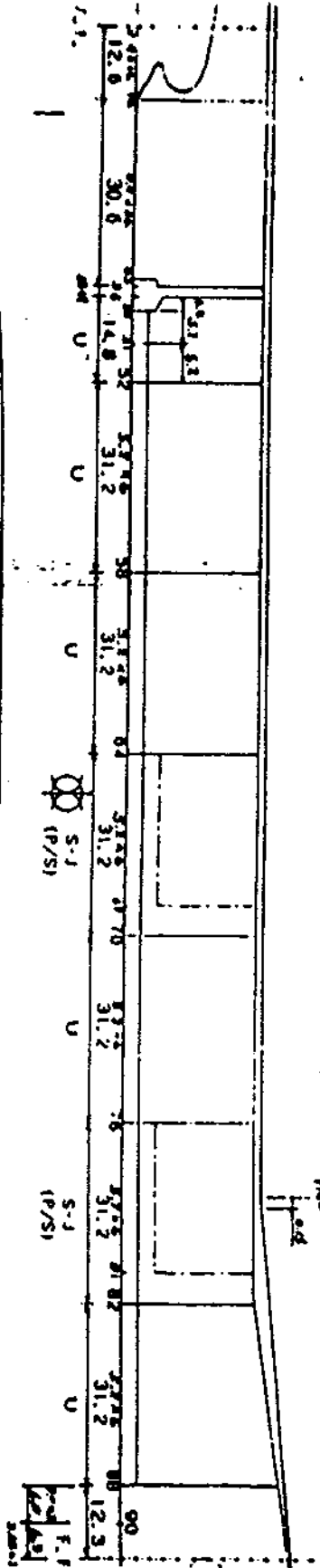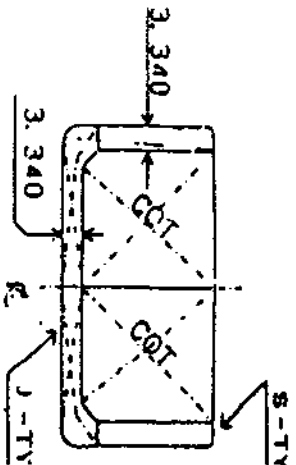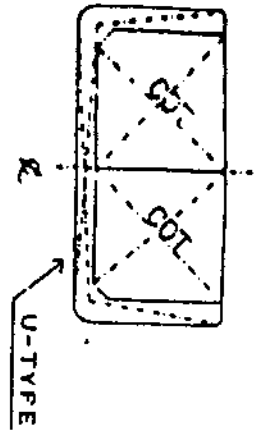
1.1 General Arrangement

16

Chapter 3

Finite Element Analysis

3.1 Introduction

The purpose of the Finite Element Analysis (FEA) was to determine the maximum stress range for the CSD hotspot. For the fatigue analysis, the following three stress components are considered.

1) Wave-induced pressure on ship body (for transverse memebers)
2) Wave-induced longitudinal bending moment (for longitudinal memebers)
3) Loading-unloading of cargo.

The long-term probable maximum pressure distribution were input to a finite element analysis to derive the maximum stress range for transverse members.

The longitudinal wave -induced bending moment was used to compute the longitudinal stress by beam theory.

3.2 Global Finite Element Analysis

A global FEA was performed to obtain the overall response of the vessel for the particular loading and seaway condition. The response in the form of deflections was the basis of boundary conditions for the local FEA.

FE Global Model

The calculated zone and support condition of the proposed double hull are shown in Fig.3.1. The FE global model is shown in Fig.3.2.

Loading Conditions.

Eight loading conditions were considered for the finite element analysis. They are:

Full Load Condition

F-1: Outer - Wave Crest + Still (Full)   Inner - Still
F-2: Outer - Wave Hollow + Still (Full)   Inner - Still

12

ユ ↳

F-3: Outer - Still (Full)   Inner - Max. Cargo Pressure
F-4: Outer - Still (Full)   Inner - Min. Cargo Pressure

Ballast Condition

B-1: Outer - Wave Crest + Still (Ballast)   Inner - Still
B-2: Outer - Wave Hollow + Still (Ballast)   Inner - Still
B-3: Outer - Still (Ballast)   Inner - Max. Ballast Pressure
B-4: Outer - Still (Ballast)   Inner - Min. Ballast Pressure

The details of these eight loading condition are shown in Fig.3.3

3.3 Local FE Analysis

Once the global stress distribution was determined, a zooming model for each structural detail was then used for determining the hotspot stress. Fig.3.4 shows the locations of the CSD selected for the fatigue analysis. Fig.3.5 shows the geometry of CSD and Fig.3.6 shows the FE mesh of the CSD.

3.4 Extreme Stress Range

In order to perform the probabilistic fatigue analysis, stress range of wave-induced pressure on the ship body (transverse members), longitudinal bending moments (longitudinal members) and loading-unloading conditions are considered as follows.

Stress Due to Wave-Induced Pressure : Transverse Member

$$\sigma_{R\ Full} = [(\sigma_{F1} - \sigma_{F2})^2 + (\sigma_{F3} - \sigma_{F4})^2]^{1/2}$$

$$\sigma_{R\ Ball} = [(\sigma_{B1} - \sigma_{B2})^2 + (\sigma_{B3} - \sigma_{B4})^2]^{1/2}$$

Varable Stress	Outer Pressure	Inner Pressure
σ_{F1}	wave crest	still
σ_{F2}	wave hollow	still
σ_{F3}	still	max.
σ_{F4}	still	min.
σ_{B1}	wave crest	still
σ_{B2}	wave hollow	still
σ_{B3}	still	max.
σ_{B4}	still	min.

25

Stress Due to Longitudinal Bending Moment : Longitudinal Memeber

σ_R Full = Moment Amp. at Full Load x 2

σ_R Ball = Moment Amp. at Ballast x 2

Stress Due to Loading - Unloading

σ_R: Full (Still Water) - Ballast (Still Water)

Discussion

The extreme stress ranges for three different components for the proposed Double-Hull's CSD were derived based on the above procedure The finite element results are applied in the fatigue analysis. It should be pointed out that the stress due to pressure which is derived from finite element analysis is the hotspot stress while the stress due to longitudinal wave bending which is derived from beam theory is the nominal stress. In order to cover this problem, fatigue analysis was performed based on two S-N curves in snext chapter. One is S-N curve for nominal stress while the other is S-N curve for hotspot stress which is one level higher than the nominal stress S-N curve.

26

CALCULATION ZONE

EXAMINED HOLD

UPP. DK.

INN. BOTT.

BOTT.

FR. 58   FR. 64   FR. 70   FR. 78

SEC. ⓐ   SEC. ⓑ

Figure 3.1

15

Fig 3.2

28

Full load

Outer

Inner

Ballast

Outer

Inner

f — 1

f — 2

f — 3

still

still(full)

still(full)

still(full)

still(full)

MIN. cargo pressure

MAX. cargo pressure

wave crest
+still(full)

wave hollow
+still(full)

B — 1

B — 2

B — 3

B — 4

still

still

still(ballast)

still(ballast)

wave crest
+still(ballast)

wave hollow
+still(ballast)

MAX. ballast pressure

MIN. ballast pressure

Fig 3.3

17

S.SHELL & L.BHD.

600   600

50   20'   450R   400

LONG. BKT. (T.BHD.)

T.BHD.

S.SHELL & L.BHD.

DET.

FC. PL. TAPER 10'

LONG. BKT.

Figure 3.4

30

LONG. TYPE (L2)

S. SHELL

39.5

110

L. BHD.

LONG. BKT. (Ond. T.Ring)

S. SHELL & L. BHD.

480R

6.??R

450

400   220   450

Figure 3.5

19

31

V. STIFF. (T. BHD.)

Figure 3.6

Chapter 4

Fatigue Damage Evaluation

4.1 Introduction

The objective of this chapter is to summarize the methodogy used to perform the fatigue analyses in tankers and to conduct a comprehensive fatigue analysis in the proposed double-hull tanker. The proposed double-hull tanker is built based on relatively new double-hull VLCC structural design in which the details adopted an apple-shaped slot opening at the connections between longitudinals and web plates without stiffeners, A deterministic fatigue analyses was conducted to identify the critical location for the fatigue damage in this new design and evaluate whether or not these details meet the design criteria.

The calculation of the fatigue damage for the CSD is based on several random variables. In order to account for this randomness, implicit and explicit factors of safety are widely used. The safety factors are to some extent subjective measures that are calibrated based on past experience. Thus the information about the degree of uncertainty of different variables can not be used effectively. Probabilistic fatigue analysis offers a way to include uncertainty of different variables in the fatigue damage calculation. A probabilistic fatigue analysis of the proposed double-hull tanker was conducted to give more insight into fatigue damage.

4.2 Fatigue Damage Evaluation Model

In this study the S-N curve approach combined with the use of Miner's summation rule was used to calculate fatigue damage. The Weibull approximation for the randomness in loading was applied in a probablilistic fatigue analysis.

4.2.1 S-N Classification

The accuracy of the estimated fatigue life of a structural detail depends strongly on the accuracy of the evaluated loadings and fatigue capacity. The capacity to resist

metal fatigue can be expressed by the S-N curve used for the hotspot location that is of interest. The S-N curve recommended by the Department of Energy (DnE) was used to describe the fatigue strength at the hotspots of the CSD. Fig.4.1 shows these S-N curves and a summary of the curve parameters. The S-N curve classsification for different hotspots of CSD is described in Ref.2. It should be pointed out that the deterministic fatigue analytsis is based on mean S-N curves while the probabilistic fatigue analysis is based on the S-N curves with mean value =1 and standard deviation =0.3.

4.2.2 Fatigue Damage Assessment

It is assumed that the curve characterizing fatigue behavior under constant cyclic loading is of the form

$$NS^m = K$$

where
    N = Number of cycles to failure
    S = Stress range
    m = Empirical constant
    K = Empirical constant

When the Miner's rule is applied, Fatigue damage is given by

$$D = N_T DE(S^m) / K$$

where

    N_T = Total number of cycles in time T
    T = Time
    D = Damage
    $E(S^m)$ = Expected, mean, or average value of S^m
    S = Stress range (random variable)

To account for the uncertainties in the stress calculation the following relation between the actual stress range Sa, and the estimated stress range S is introduced

$$Sa = BS$$

where

    B the bias that quantifies the modelling error. (random variable)

If we define the average frequency of stress cycles as

$$fo = N_T/T$$

Then the fatigue damage can be rewritten as

$$D = T\, B^m \Omega / K$$

where

$$\Omega = foE(S^m) = \text{stress parameter}$$

4.2.3 Weibull Model

The Weibull distribution was used to calculate Ω and thus the fatigue damage. It is assumed that the long-term distribution of the stress range could be fitted by the Weibull distribution. The three important Weibull parameters in this distribution are S_m, ξ and N_T. Then the stress parameter can be calculated as

$$\Omega = \lambda(m)foS_m{}^m[lnN_T]^{-m/\xi}\, \Gamma(\frac{M}{\xi} + 1)$$

where

S_m = Extreme stress range during the life time
ξ = Stress range parameter (Weibull shape parameter)
N_T = Total number of stress ranges in design life
λ = 1, unless Rayleigh assumption was made in analysis

4.3 Determinstic Analysis : Miner's Cumulative Damage Model

Based on the stress transfer function, Walden wave data for the North Atlantic Ocean and selected S-N curve, fatigue life is predicted for the locations of structural details of interest using the Miner's cumulative damage hypothesis. Evaluation of fatigue life was carried out on the following criteria:

Estimated Life:
$$Lt = (\frac{0.5}{Lf} + \frac{0.5}{Lb})^{-1} > 20 \text{ years}$$

where,
Lt : total fatigue life
Lf: fatigue life for full load condition
Lb: fatigue life for ballast condition

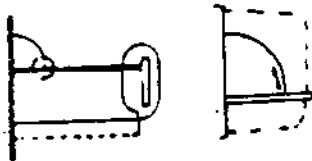### 4.3.1 Numerical Results

L36 - Slot on Sideshell Longitudinal

Design Fatigue Life = 20 year
Weibull Parameter = 0.942
Number of Cycles N= 1 x 10^8
N$_{Full}$= 0.5 x 10^8 N$_{Ballast}$= 0.5x 10^8
Load and unload N =500

Table 1.1.1

Typical CSD and Hotspot

S. SHELL LONG

Load Component	S-N	Stress Range (N/mm**2)	Fatigue Life (Year)
Pressure Full	F	152.586	121.085
	E	152.586	230.609
Pressure Ballast	F	111.132	313.412
	E	111.132	597.056
Wave Bending Full	–	–	–
Wave Bending Ballst	–	–	–
Load Unload	F	46.256	.
	E	46.256	.

Note : F Curve   Standard Weld
       E Curve   Improved Weld

Fatigue Life is for F Curve : 136.61Years
Fatigue Life for E Curve : 260.078 Years

Table 1.1.2

Typical CSD and Hotspot

S SHELL LONG

Load Component	S-N	Stress Range (N/mm**2)	Fatigue Life (Year)
Pressure Full	F	31.85	13313.9
	E	31.85	25363.2
Pressure Ballast	F	96.824	473.897
	E	96.824	962.784
Wave Bending Full	–	–	–
Wave Bending Ballst	–	–	–
Load Unload	F	144.55	.
	E	144.55	.

Note : F Curve   Standard Weld
       E Curve   Improved Weld

Fatigue Life for F Curve : 699.3 years
Fatigue Life for E Curve : 1855.287 years

36

Since Δ, K, B are random variables, T is also a random variable. The probability of fatigue failure is defined as

$$Pf = P\,(T < Ts\,)$$

where

Ts = Service life of the structure.

The use of the lognormal format has the advantage that a simple closed form expression for Pf can be found.

$$Pf = \Phi(-\beta)$$

where

Φ = standard normal distribution function and β= safety index

$$\beta = \frac{\ln(\overline{T}/T)}{\sigma_{\ln T}}$$

where $\overline{T}$ is the median value of T and is equal to

$$T = \frac{\Delta K}{B^m \Omega}$$

The standard deviation of ln T is given by

$$\sigma_{\ln T} = (\ln(1 + C_\Delta^2)(1+C_K^2)(1+C_B^2)^{m^2})^{1/2}$$

where the C's denote the coefficients of variation, COV, of each variable.

4.4.1 Bias for the Probabilistic Model

For a reliability analysis it is necessary to specify the median and the coefficient of variation of K,B and Δ, which are assumed to be lognormally distributed. The median value for K is obtained from least square analysis of the S-N data. The COV of K, Ck is obtained by approximating an equal probability curve with a straight line.

The variables B and Δ are used to quantify the modeling bias associated with assumptions made in the stress analysis and the description of fatigue strength. Several sources can contribute to the bias B. That is

B_M = Fabrication and assembly operations

B_S = Sea state description

B_F = Wave load prediction

B_N = Nominal member loads

B_H = Estimation of hotspot stress concentration factors.

Table 4.2 summarizes frequently used values for the medians and COV's of the B's .

Using these 5 bias factors, the following represntation of B is obtained

$$B = B_M B_S B_F B_N B_H$$

Assuming that each random variable is lognormally distributed the median and the COV of B are, respectively

$$B = B_M B_S B_F B_N B_H$$

$$C_B = \sqrt{(1+C_M^2)(1+C_S^2)(1+C_F^2)(1+C_N^2)(1+C_H^2) - 1}$$

For the random variable Δ, describing the model error associated with Miner's rule, the following values for Δ and C_Δ are widely used. $\Delta = 1.0$ and $C_\Delta = 0.3$.

4.4.2 Probability of Failure of CSD's 20 Year Service Life

Uncertainties play an important role in probabilistic fatigue analysis. Following is the general overview of the uncertainties which are involved in probabilistic fatigue analysis. More detailed analysis will be conducted in Chapter 6.

4.4.3 Uncertainties in Proposed Claculation

Uncertainties are involved in the estimation of the long-term stress distribution. These uncertainties account for the total modeling error involved in the fatigue damage evaluation procedure. It's the reasonable assumption that the uncertainties follow the lognormal distribution so that the uncertainty information can be represented through the two parameters mean value and coefficient of variation.

A lot of different contributors to the modeling error are involved in the fatigue damage evaluation. A good comprehensive summary of the uncertainties in the cumulative fatigue damage is given in (Ref.5).

The combination of the different contributing factors for the modeling errors defines the total modeling error or bias. The total coefficient of variation of the modeling error or bias is obtained through a combination of the individual coefficients of variation.

For the evaluation of the fatigue damage for the CSDs in this Chapter, only the total modeling bias (its mean and coefficient of variation) are varied. These values essential represent the systematic error and the confidence in the estimation of the long-term stress range distribution. The more details about the uncertainty effects due to different factors were studied in Chapter 6 to quantity different effects due to different factors.

Table 1.1.2

Typical CSD and Hotspot

S. SHELL LONG

Load Component	S-N	Stress Range (N/mm**2)	Probability
Pressure Full	F	31.85	0.0
	E	31.85	0.0
Pressure Ballast	F	96.824	0.0
	E	96.824	0.0
Wave Bending Full	–	–	–
Wave Bending Ballst	–	–	–
Load Unload	F	144.55	0.0
	E	144.55	0.0

Note : F Curve   Hotspot Stress
       E Curve   Nominal Stress

Total Probability of Failure Pf = 0.0% for F Curve
Total Probability of Failure Pf = 0.0% for E Curve

Table 1.1.3

Typical CSD and Hotspot

S SHELL LONG

Load Component	S-N	Stress Range (N/mm**2)	Probability
Pressure Full	F2	258.034	60.36%
	F	258.034	27.27%
Pressure Ballast	F2	192.668	1.807%
	F	192.668	0.1525%
Wave Bending Full	F2	–	–
	F		
Wave Bending Ballst	F2	–	–
	F		
Load Unload	F2	197.862	0.0
	F	197.862	0.0

Note:F2 Curve   Hotspot Stress
      F Curve   Nominal Stress

Total Probability of Failure Pf = 62.16% for F2 Curve
Total Probability of Failure Pf =27.4225% for F Curve

41

4.5 Discussion and Conclusion

From the comprehensive fatigue analysis, the following conclusions are derived:

The new design adopted an apple-shaped slot opening at the connections between longitudinals and web plates making the stiffeners unncessary.

The conventional practice is to attach stiffeners to the face plate of longitudinals, However, the attaching of stiffeners tends to cause stress concentration at the connections, and therefore generate fatigue cracks unless careful and detailed design is made for stiffener end. But the current design without stiffeners for the CSDs increased the fatigue life dramatically according to the present analysis.

Fatigue damage on side longitudinals around the load water line is severe, for example : L45, L46. These are the critical areas in tanker structure.

Outline of Damage

It is found that the fatigue damage is severe around the water line. It's fatigue life is usually less than 20 years.

It is found that the fatigue damage is severe at the intersection of the above longitudinals with the transverse bulkhead. (See Apprendix A, Table 3.3.1)

Cause of Damage

Based on results from this study, following are the reason for the fatigue damage.

a) The wave loads are maximum around the load waterline and the stress range in the vicinty of this area is found to be higher than others.

b) The HT-steel results in an increase in the stress range without an increase in the fatigue strength

c) The relative deflection of transverse webs against the transverse bulkheads is large. Therefore, the secondary higher bending stress may be incurred at the intersection of the longitudinals with the transverse bulkheads.

The selection of bias values and the coefficients of variation for these values are discussed extensively in (Ref. 5). Based on the previous study, the following ranges for the bias and the coefficient of variation of the bias have been selected for the proposed CSD. The reason for the CovBias = 0.0 is to compare with the previous analysis results. (Ref 1)

	Bias	Median Vaule	CovBias
1	Fabrication and Assembly	1.20	0.00
2	Seastate Characteristics	1.10	0.00
3	Wave Load Prediction	0.80	0.00
4	Determination of Member Load	0.90	0.00
5	Estimation of SCF	1.00	0.00
	Median Bias	Cov Bias	
	1.0	0.0	

	Median	Cov
S-N Curve	1.0	0.3

4.4.4 Numerical Results

L36 - Slot on Sideshell Longitudinal

Design Fatigue Life = 20 year
Weibull Parameter = 0.942
Number of Cycles N= 1 x 10^8
NFull= 0.5 x 10^8 NBallast= 0.5x 10^8
Load and unload N =500

Typical CSD and Hotspot

SHELL LONG

Table 1.1.1

Load Component	S-N	Stress Range (N/mm**2)	Probability
Pressure Full	F	152.586	4.4E-7
	E	152.586	2.0E-11
Pressure Ballast	F	111.132	0.0
	E	111.132	0.0
Wave Bending Full	–	–	–
Wave Bending Ballst	–	–	–
Load Unload	F	46.256	0.0
	E	46.256	0.0

Total Probability of Failure Pf = 0.00004448% for F Curve
Total Probability of Failure Pf = 0.0% for E Curve

40

Typical CSD and Hotspot

SHELL LONG

Table 1.1.3

Load Component	S-N	Stress Range (N/mm**2)	Fatigue Life (Year)
Pressure Full	F2	258.034	18.13
	F	258.034	25.04
Pressure Ballast	F2	192.668	43.57
	F	192.668	60.14
Wave Bending Full	F2	–	–
	F		
Wave Bending Ballst	F2	–	–
	F		
Load Unload	F2	197.862	-
	F	197.862	-

Note:F2 Curve   Standard Weld
F Curve   Improved Weld

Fatigue Life for F2 Curve : 25.6 year
Fatigue Life for F Curve : 35.357 year

The results of additional analyses of CSD in the proposed double-hull tanker are given in Apprendix A.

4.4 Probabilistic Analysis : Lognormal Format

It is assumed that the lognormal format for the probability distributions of all factors of the fatigue damage expressions. This format has been demonstrated to be valid for the variables involved in the fatigue damage analysis, specially for the variables Δ and K. Miner's rule, which states the failure occurs when the fatigue damage $D > 1$ is modified to

$$D > \Delta$$

where Δ is a random variable denoting damage at failure. This quantifies the modeling errors associated with Miner's rule.

To account for the uncertainties in fatigue strength, the S-N curve pamaeter K is defined as a random variable.
The time to failue T is then given as

$$T = \frac{\Delta K}{B^m \Omega}$$

25

37

Chapter 5

Residual Life of Cracked CSD

5.1 Introduction

From the previous analysis, it is found that the fatigue damage is severe in some CSDs in proposed 150,000 DWT double hull tanker and may cause fatigue crack during 20 years design life. Thus, inspection, maintenance and repair (IMR) is important and necessary in the tanker's service life. That is to say that the fatigue crack may occur during its service life. So the next problem is how to calculate the residual life of these cracked CSDs. This chapter will deal with the residual life of the cracked CSD in proposed Double-Hull tanker by linear fracture mechanics.

Linear fracture mechanics is an appropriate tool to deal with the fatigue crack and residual life of cracked CSD. The basis of LEFM is an analysis of the elastic stress field at the tip of a crack. In general there are three different opening modes for cracks. Their superposition describes the general case of cracking. For the purpose of the residual life of cracked CSD, only mode I is considered.

In this chapter, we adopted Hybrid Methods (Ref 7), a general fracture mechanics approach to derived the equivalent S-N curves for the cracked details based on its initial crack length. Later, we used these equivalent S-N curves to predict the residual life for the cracked CSDs.

mode I Opening Mode   mode II Sliding mode   mode III tearing mode
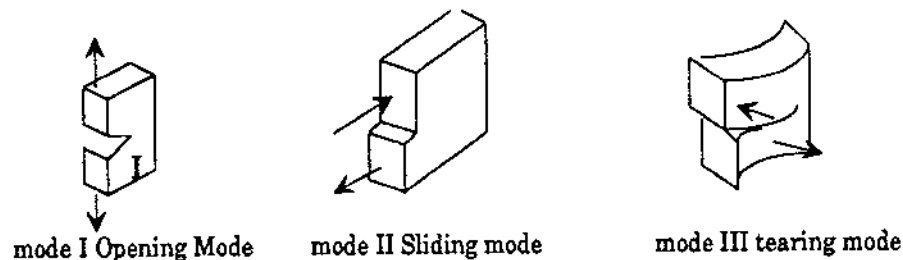
Fig 5.1 Fatigue Cracking Modes

The following documents the analysis procedure and numerical results.

5.2 Residual Life of Cracked CSD

For residual life assessment of welded details with flaws, no rules are issued by Claasification Societies or Regulatory bodies. Instead some organizations have specified recommended practices for residual life assessment. The general approach is based on fracture mechanics.

For the assessment of residual life of a cracked CSD a fracture mechanics approach has to be used. For engineering practice, it is usually conservative and sufficient to use the Paris equation to calculate the crack growth da/dN.

$$\frac{da}{dN} = C(\Delta K)^m$$

Here C and m are constants, which depend on the material and the applied conditions, and ΔK is the range of the stress intensity factor.

For $\Delta K < \Delta Ko$, da/dN is assumed to be zero.

The stress intensity factor range, ΔK, is a function of structuiral geometry, stress range and crack length:

$$\Delta K = Y(\Delta \sigma)$$

By integrating, the overall life can be predicted :

$$Nres = \int_a^{af} \frac{da}{da/dN} = \frac{1}{Const.(\Delta \sigma)} \int_a^{af} \frac{da}{(\Delta K/\Delta \sigma)^m}$$

with:

$$\frac{\Delta K}{\Delta \sigma} = Y(a)$$

Then the equivalent S-N curve is

$$Nres(\Delta \sigma)^m = Const$$

where the above constant depends on the initial crack length a. It is therefore possible to obtain a set of S-N curves, where each curve represents a specific initial crack length.

45

In order to obtain S-N curves for cracked CSDs by using the above approach to predict the residual life, the stress intensity factors for the cracked CSDs has to be found. What follows is an explanation of the two general methods used to calculate the stress intensity factor.

5.2.1 Simplified Approach - Analytical Solution for ΔK

This approach is based on the assumption that the stress intensity factor is dependent on the cracklength and fracture toughness parameter C. From the above assumption, the following closed form expression for the number of cycles can be derived [9]:

$$N = \frac{1}{C\Delta\sigma\pi^{m/2}F^m} \frac{a_f^{1-m/2} - a_i^{1-m/2}}{1-m/2}$$

where:

ai:	initial cracklength
af:	final cracklength
C:	crack growth parameter
m:	crack growth parameter
F:	influence function
Δσ:	stress range

Comparing this equation with the standard equation for the S-N curve

$$N = K(\Delta\sigma)^{-m}$$

It can be seen that the S-N curve parameter K can be derived using the above closed form fracture mechanics equation.

$$N = \frac{1}{C\pi^{m/2}F^m} \frac{a_f^{1-m/2} - a_i^{1-m/2}}{1-m/2}$$

The crack growth parameter m is in general assumed to be 3.0. Based on crack propagation results an empirical formula has been established for crack growth parameter C

$$C = \frac{1.315 10^7}{28.31^m} \frac{da}{dN} \Delta K$$

It should be noticed that this simplified approach does not take into account the complex stress distribution of CSD in tankers.

46

5.2.2 Complex Approach - Hybrid Method for ΔK

The hybrid method is actually an influence function and a superposition method. As described previously, the stress intensity factor K contains all information regarding the geometry and stress distribution of the said details. For general details, K is of the general form as:

$$K = \sigma\sqrt{\pi a}F$$

With F being a correction factor in the above equation taking into account, for instance, the effects of

a free surface close to the crack tip
a finite sheet thickness
finite sheet width
crack shape
curvature of a cylindrical shell
non-uniform stresses
crack tip plasticity

Consequently the equation for F has the following form:

$$F = F_S\ F_T\ F_W\ F_E\ F_C\ F_G\ F_P$$

with
F_S = free surface correction factor
F_T = finite thickness correction factor
F_W = finite width correction factor
F_E = crack shape correction factor
F_C = curvature correction factor
F_G = non-uniform stress correction factor
F_P = plasticity correction factor

The factor F_C can be set to be 1. Also the factor F_P, which accounts for the plasticity at the crack tip is set to 1 since the majority of fatigue situation, the extension of a plastic zone tends to be small compared with the crack length.

Part-through Crack Case

Newman and Raju derived a procedure to calculate crack growth by means of an empirical stress intensity factor equation that considers both tension and bending stresses through the thickness of the plate.

47

$$K = (\sigma_t + H\sigma_b) \sqrt{\frac{\pi a}{Q}} F(a/t, a/c, c/b, \varphi)$$

with

σ_t = remote uniform-tension stress

σ_b = remote uniform-bending stress

H = function, depend on φ, a/t, a/c

a = depth of surface crack

Q = shape factor for elliptical crack

F = stress intensity boundary-correction factor

t = plate thickness

c = half-length of surface crack

b = half-width of cracked plate

φ = parametric angle of the ellipse

see Fig.(5.2)

The factor Q takes into account the effect of crack front curvature, i.e. crack shape. A useful approximation for Q has been developed by Rawe:

$$Q = 1 + 1.464(a/c)^{1.65} \qquad\qquad a/c < 1$$

The functions F and H are defined so that the boundary correction factor for tension is equal to F and the correction factor for bending is equal to the product of F and H.

The function F was obtained from a systematic curve-fitting procedure by using double-series polynomials in terms of a/c,a/t, and angular functions of φ. The function F was taken to be

$$F = [M_1 + M_2(a/t)^2 + M_3(a/t)^4]f_\varphi g f_w$$

where

$$M_1 = 1.13 - 0.09(a/t)$$

$$M_2 = -0.54 + \frac{0.89}{0.2 + (a/c)}$$

$$M_3 = 0.5 - \frac{1.0}{0.65 + (a/c)} + 1.4(1.0 - \frac{a}{c})$$

$$g = 1 + [0.1 + 0.35(\frac{a}{t})^2](1 - \sin\varphi)^2 \qquad (=1 \text{ for } \varphi = \pi/2)$$

The function f_φ an angular function from the embedded elliptical-crack solution is

$$f_\varphi = [(\frac{a}{t})^2\cos^2\varphi + \sin^2\varphi]^{1/4} \qquad (=1 \text{ for } \varphi = \pi/2)$$

The function f_w, a finite width correction factor is

$$f_w = [\sec(\frac{\pi c \alpha}{2b\,t})]^{1/2}$$

36

The function H is of the form

$$H = H_1 + (H_2 - H_1) \sin^2\varphi \qquad (= H_2 \text{ for } \varphi = \pi/2)$$

where

$$p = 0.2 + \frac{a}{c} + 0.6\frac{a}{t}$$

$$H_1 = 1 - 0.34\frac{a}{t} - 0.11\frac{a}{c}(\frac{a}{t})$$

$$H_2 = 1 + G_1(\frac{a}{t}) + G_2(\frac{a}{t})^2$$

In this equation for H_2

$$G_1 = -1.22 - 0.12\frac{a}{c}$$

$$G_2 = 0.55 - 1.05(\frac{a}{c})^{0.75} + 0.47(\frac{a}{c})^{1.5}$$

The remote bending stress σ_b and tension stress σ_t in the equation for the stress intensity factor refer to the pure bending or tension stress. Therefore a correction of Newman-Raju's equation with regard to the actual stress gradients has to be made.

The stress gradient correction factor F_G (also called " geometry correction factor ") can be derived from known solutions for K. This solution of a crack stress field problem can be visualized as a two step process.

1. The stress distribution problem is solved in a manner satisfying the boundary conditions (displacements, stresses) but with the crack considered absent.

2. To this stress field is superposed another stress field which cancels any stresses acting directly across the crack along the line of the crack.

Step 1 is a non-singular elasticity problem and can be solved by a FEM analysis. As the addition of a non-singular stress field ($\sigma(x)$, Step 1) does not affect the value of K (caused by $-\sigma(x)$, Step 2) the resulting K will be identical with that obtained from Step 2.

To evaluate K from Step 2, an influence (Green's) function method is employed. An influence function can be defined as

$$G_1(b,a) = \frac{1}{P}K_{IP}(b,a)$$

where K_{IP} = due to a load P at x = b

44

P = load per unit sheet thickness / width

Hence, $G_I(b,a)$ is the K_I value arising from a unit force (per unit thickness/width) applied at abscissa $x = b$. $G_I(b,a)$ is independent of loading and depends merely on all the geometry parameters of the cracked body. If a solution for the stress intensity factor is known for any particular load system, then this information is sufficient to determine the stress intensity factor for any other load system.

A pressure $p(x)$ applied on an infinitesimal surface t(or W) dx results in an infinitesimal stress factor.

$$dK_I(x,a) = G_I(x,a)p(x)dx$$

Thus, the K_I resulting from the total crack surface loading is

$$K_I = \int_0^a G_I(x,a)p(x)dx$$

In a part- through crack case the computation of the stress gradient corrector F_G maight be based on the following solution of the problem shown in fig.5.1

$$K_I = \frac{2P}{\sqrt{\pi a}} \frac{1}{\sqrt{1-(b/a)^2}} F(b/a)$$

Therefore the influence function in this case is

$$G_I = \frac{2}{\sqrt{\pi a}} \frac{1}{\sqrt{1-(b/a)^2}} F(b/a)$$

With the condition of $p(x) = \sigma(x)$, yields

$$K_I = \frac{2}{\pi} \sqrt{\pi a} \int_0^a \sigma(x) F(x/a)dx$$

where $\sigma(x)$ can be obtained from a FEM analysis.

The stress distribution could be represented by a polynomial expression and could be intergrated analytically. However it is more convenient to use a discretized stress distribution and the above equation then may be reformulated as

38

50

$$K = \frac{2}{\pi}\sqrt{\pi a} \sum_{1}^{ni} \sigma_{bi} \, F(b/a) \int_{bi}^{bi+1} \frac{dx}{\sqrt{a^2 - b^2}}$$

where σ_{bi} = stress in block no. "i"

$bi = 1/2(bi + bi_{+1})$

The integration is carried out over the block width, and the summation over the number of blocks. After factoring out the nominal stress σ, applied remotely from the crack, integration leads to

$$K = \sigma\sqrt{\pi a} \left\{ \frac{2}{\pi} \sum_{1}^{ni} \sigma_{bi}/\sigma \, F(bi/a) \, [\arcsin\frac{x}{a}]_{bi+1}^{bi} \right\}$$

$$= \sqrt{\pi a} \left\{ \frac{2}{\pi} \sum_{1}^{ni} \sigma_{bi}/\sigma \, w_{bi} \right\}$$

$$= \sigma\sqrt{\pi a}F$$

where $\quad$ w_{bi} = weight of block no. "i".

For the case of an edge crack described here the effect of the stress gradient on the stress surface correction factor Fs can be included in FG in the following way.

$$F_G = \frac{F}{1.122}$$

The resulting expression used in computing FG in the case of an edge crack might then be written as

$$F_G = \frac{2}{1.122\pi}$$

In order to apply Newman - Raju's empirical stress intensity factor equation in the case of an arbitrary stress field the following transformations have to be made.

For tension stresses $\quad$ F is replaced by F*FG,at
For bending stresses $\quad$ F is replaced by F*FG,ab
$\qquad\qquad\qquad\quad$ H is replaced by H/FG,nb

FG,at and FG,ab are correction factors, which account for the difference between a uniform and a non-uniform tension or bending stress distribution in the crack growth plane. These factors are calculated using the above equation with the actual through

39

thickness stress distributions (tension for Fσ,at and bending for Fσ,ab). A calculation for pure bending provided the extraction on the effect of this distribution and gave Fσ,nb.

Through Crack Case

The problem of estimating the stress intensity factor K for the case of a through thickness crack can be solved by using the hybrid method only. Here it is only necessary to take the finite width correction factor Fw and the stress gradient correction factor Fσ into account. It is therefore not necessary to apply the Newman / Raju method.

$$K = \sigma\sqrt{\pi a}F$$

Here F is a function of the stress gradient correction factor Fσ and the finite width correction factor Fw only.

$$K = \sigma\sqrt{\pi a}\, F_\sigma F_w$$

The computation of Fσ in the case of a through crack might be based on a solution of the problem shown in Fig. 5.3

As described for the part-through crack the stress gradient correction factor can be determined by using a superposition method combined with an influence (Green's) function method.

The following exact solution for the stress intensity factor for a crack in an infinite sheet subjected to a pair of splitting forces, which do not have to be at the center of the crack is used.

This yields the following expression of Fσ :

$$F_G = \frac{2}{1.122 \cdot \pi} \cdot \sum_{i=1}^{n} \left\{ \frac{\sigma_{b_i}}{\sigma} \cdot F(\bar{b}_i/a) \cdot \left[\arcsin \frac{b_{i+1}}{a} - \arcsin \frac{b_i}{a} \right] \right\}$$

where b in (-a, +a)

The finite width correction factor Fw can be calculated using the general methods in (Ref 8)

Since part through- thickness cracks are hardly ever detected in ship inspections, they are not considered in this analysis. So only the methods to calculate the stress intensity factors for through-thickness cracks are applied in numerical calculation.

52

5.3 Corrosion Fatigue

A corrosive enviroment might, in addition to influence the fatigue material parameters in the fatigue model, lead to a general increase in the stress level with time due to a reduction in the steel thickness.

In this analysis, the increase in the stress level is expressed as,

$$S_{cor}(t) = \frac{z}{z - k_{cor}t} = \frac{z}{z - k_{cor}N_t/(r\upsilon_0)} \qquad t < z/k_{cor}$$

where z is the steel thickness, k_{cor} is the corrosion rate and N_t is the number of load cycles at time t. r is the frcation of the lifetime the ship is expected to be at sea and υ_0 is the average rate of stress cycles over the lifetime. The rate of corrosion will depend on the type of corrosive environment and on the use of cathodic protection in the area where the investigated detail is located. The influence of the thickness reduction on the long-term stress level is then,

$$\sum_{i=0}^{N_T}(\Delta\sigma S_{cor}(t_i))^m = \sum_{i=0}^{N_T}(\Delta\sigma \frac{z}{z - k_{cor}(i-1)/r\upsilon_0})^m$$

$$= E[\Delta\sigma^m]\sum_{i=0}^{N_T}(\frac{z}{z - k_{cor}(i-1)/r\upsilon_0})^m$$

$$= E[\Delta\sigma^m]\int_0^{rt\upsilon_0}(\frac{z}{z - k_{cor}(i-1)/r\upsilon_0})^m)dx$$

$$= E[\Delta\sigma^m]\frac{zr\upsilon_0}{k_{cor}(m-1)}((\frac{z}{z - k_{cor}(i-1)/r\upsilon_0})^{m-1} - 1)$$

The expression is rewritten as,

$$\sum_{i=0}^{N_T}(\Delta\sigma S_{cor}(t_i))^m = rt\upsilon_0 E[\Delta\sigma^m]B_{cor}(t)$$

where,

$$B_{cor}(t) = \frac{zr\upsilon_0}{k_{cor}(m-1)}((\frac{z}{z - k_{cor}(i-1)/r\upsilon_0})^{m-1} - 1)$$

accounts for the effect of increased stress level over time due to corrosion. The derivation is based on the assumption of a stationary stress range process over the lifetime.

41

5.4 Numerical Illustrations - Residual Life for Cracked CSD

The previous comprehensive probabilistic fatigue analysis has identified that the probability of failure of some CSDs in proposed double-hull tanker will be larger than 1. That means that the fatigue cracks or fatigue failure may occur during its service life. For these details, the deterministic fatigue analysis is performed first to determine its fatigue life. Then the analysis for the cracked CSD will be performed later to determine its residual life. The residual life calculation is based on the above two approaches, fracture mechanics approach for uncorroded details and corrosion fatigue approach.for corrode details. Following are some results.

Case I : *L37 - Slot on Sideshell Longitudinal*

$$Weibull\ Parameter = 0.942$$
$$Number\ of\ Cycles\ N = 1 \times 10^{8}$$
$$N_{Full} = 0.5 \times 10^{8}\ N_{Ballast} = 0.5 \times 10^{8}$$
$$Load\ and\ unload\ N = 500$$

Typical CSD and Hotspot

S. SHELL LONG.
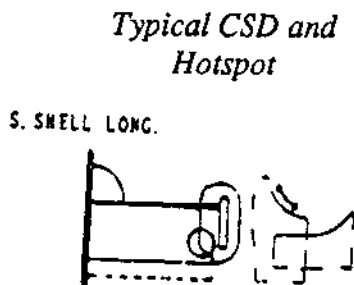
Table 1.2.5

Load Component	S-N	Stress Range	Probability
Pressure Full	F2	497.448	> 1
	F	497.448	> 1
Pressure Ballast	F2	406.112	> 1
	F	406.112	> 1
Wave Bending Full	F2	--	-
	F	-.-	
Wave Bending Ballst	F2	-	--
	F		
Load Unload	F2	36.352	0.0
	F	36.352	0.0

Note:F2 Curve   Hotspot Stress
       F Curve   Nominal Stress

Total Probability of Failure Pf > 1 for F2 Curve
Total Probability of Failure Pf > 1 for F Curve

Step 1 : Fatigue life Calculation

Fatigue Life Calculation

Typical CSD and Hotspot

S. SHELL LONG.
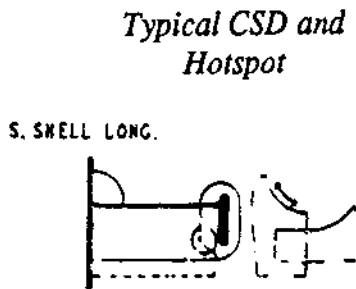
Load Component	S-N	Stress Range	Fatigue Life
Pressure Full	F2	497.448	4 year
	F	497.448	7.5 year
Pressure Ballast	F2	406.112	7.26 year
	F	406.112	13.82 year
Wave Bending Full	F2	–	–
	F		
Wave Bending Ballst	F2	–	–
	F		
Load Unload	F2	36.352	–
	F	36.352	

Note:F2 Curve   Hotspot Stress
F Curve   Nominal Stress

Based on the above results, an suumption has been made that the initial crack length is 2mm at the service life of 5.63 years for F2 curve and 10.66 years for F curve. From this assumption, the residual life of that cracked is in next table.

Step 2 : Residual Life Calculation Fracture Mechanics Approach

Residual Life Calculation
(Crack Growth Rate 0.9)

Load Component	Stress Range	Residual Life
Pressure Full	497.448	2.7
Pressure ballast	406.112	4
Wave Bending Full	--	
WaveBendingBallast	--	
Load Unload	36.352	--

55

Case 2 : L46 - Slot on LongBHD Longitudinal

Weibull Parameter = 0.942
Number of Cycles N= 1 x 10^8
NFull= 0.5 x 10^8 NBallast= 0.5x 10^8
Load and unload N =500

Table 2.4.5

Typical CSD and Hotspot

L. BHD LONG.

Load Component	S-N	Stress Range (N/mm**2)	Probability
Pressure Full	F2	369.264	71.67%
	F	369.264	63.58%
Pressure Ballast	F2	233.044	41.98%
	F	233.044	36.47%
Wave Bending Full	F2	–	–
	F		
Wave Bending Ballst	F2	–	–
	F		
Load Unload	F2	132.594	0.0
	F	132.594	0.0

Note:F2 Curve   Hotspot Stress
    F Curve   Nominal Stress

Total Probability of Failure Pf > 1 for F2 Curve
Total Probability of Failure Pf > 1 for F Curve

56

Step 1 : Fatigue life Calculation

Fatigue Life Calculation

Typical CSD and Hotspot	*Load Component*	*S-N*	*Stress Range (N/mm**2)*	*Fatigue Life (Year)*
	Pressure Full	*F2*	*369.264*	*7 year*
		F	*369.264*	*9.65 year*
	Pressure Ballast	*F2*	*233.044*	*27.8 year*
		F	*233.044*	*38.4 year*
	Wave Bending Full	*F2*	*–*	*–*
		F		
	Wave Bending Ballst	*F2*	*–*	*–*
		F		
	Load Unload	*F2*	*132.594*	*–*
		F	*132.594*	

Note:F2 Curve   Standard Weld
F Curve   Improved Weld

L. BHD LONG.

Based on the above results, a suumption has been made that the initial crack length is 3mm at the service life of 10 year. From this assumption, the residual life of that cracked CSD is

Step 2 : Residual Life Calculation Fracture Mechanics Approach

Residual Life Calculation
(Crack Growth Rate 0.9)

Load Component	Stress Range	Residual Life
Pressure Full	369.264	6.6
Pressure ballast	233.044	26.31
Wave Bending Full	--	
WaveBendingBallast	--	
Load Unload	132.594	--

57

5.5 Numerical Illustrations - Corrosion Fatigue for CSD

Case I : *L36 - Slot on Sideshell Longitudinal*

Weibull Parameter = 0.942
Number of Cycles N= 1 x 10^8
NFull= 0.5 x 10^8 NBallast= 0.5x 10^8
Load and unload N =500

Fatigue Life Calculation

Typical CSD and Hotspot

S SHELL LONG
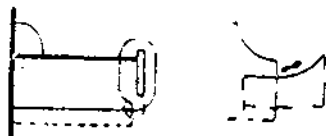
Load Component	S-N	Stress Range (N/mm**2)	Fatigue Life (Year)
Pressure Full	F2	258.034	18.13
	F	258.034	25.04
Pressure Ballast	F2	233.044	43.57
	F	233.044	60.14
Wave Bending Full	F2	–	–
	F		
Wave Bending Ballst	F2	–	–
	F		
Load Unload	F2	197.862	–
	F	197.862	

Note:F2 Curve   Hotspot Stress
F Curve   Nominal Stress

Corrosion-Fatigue Life Calculation

Typical CSD and Hotspot

S SHELL LONG
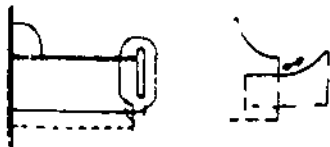
Load Component	S-N	Stress Range (N/mm**2)	Fatigue Life (Year)
Pressure Full	F2	258.034	18.32
	F	258.034	25.3
Pressure Ballast	F2	233.044	44.023
	F	233.044	60.27
Wave Bending Full	F2	–	–
	F		
Wave Bending Ballst	F2	–	–
	F		
Load Unload	F2	197.862	–
	F	197.862	

58

Case II : L37 - Slot on Sideshell Longitudinal

Weibull Parameter = 0.942
Number of Cycles N= 1 x 10^8
NFull= 0.5 x 10^8 NBallast= 0.5x 10^8
Load and unload N =500

Fatigue Life Calculation

Typical CSD and Hotspot

S. SHELL LONG.

Load Component	S-N	Stress Range (N/mm**2)	Fatigue Life (Year)
Pressure Full	F2	269.5	21.97
	F	269.5	41.87
Pressure Ballast	F2	261.09	24.17
	F	261.09	46.04
Wave Bending Full	F2	–	–
	F		
Wave Bending Ballst	F2	–	–
	F		
Load Unload	F2	94.766	–
	F	94.766	

Note:F2 Curve   Standard Weld
     F Curve   Improved Weld

Corrosion-Fatigue Life Calculation

Typical CSD and Hotspot

S. SHELL LONG.
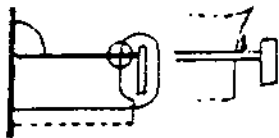
Load Component	S-N	Stress Range (N/mm**2)	Fatigue Life (Year)
Pressure Full	F2	269.5	22.2
	F	269.5	42.3
Pressure Ballast	F2	261.09	24.42
	F	261.09	46.52
Wave Bending Full	F2	–	–
	F		
Wave Bending Ballst	F2	–	–
	F		
Load Unload	F2	94.766	–
	F	94.766	

Note:F2 Curve   Standard Weld
     F Curve   Improved Weld

5.6 Conclusion

Residual life for cracked CSDs were calculated by an equivalent S-N approach which was developed from linear fracture mechanics. A series of equivelent S-N curves are constructed by repeating the computation of different initial crack lengths and implemented in SMP fatigue damage evaluation software. These equivalent S-N curves are combined into a single conventional S-N equation by representing the intercept of the S-N curve as a function of the crack length. Users who have little knowledge of fracture mechanics can easily use the software to predict the residual life of cracked CSds based on some knowledge of conventional S-N fatigue analysis procedure.

The calculation of corrosion fatigue was conducted to evaluate the effects of corrosion on fatigue. Although the results show that the corrosion does not have any great effects on fatigue due to the small corrosion rate. It does have a great effect on tanker details' duribility. The most important point is that corrosion fatigue is a synergistic effect in which corrosion and fatigue occur simultaneously. It's not only the increase of the stress level due to corrosion. Actually, the synergistic effect, in which corrosion and fatigue ocur simultaneously produces a reduction in strength which is greater than the sum of the individual effects due to corrosion and fatigue acting separately. The model developed here is only the first step for corrosion fatigue. It is recommended that further study on corrosion fatigue should be conducted.

60

Chapter 6

Fatigue Uncertainty Analysis

6.1 Introduction

As we know, fatigue is an important consideration in critical structural detail design. For tankers, fatigue is one of the two main damage modes, and thus safety requirements associated with fatigue reliability dictate design decisions.

A S-N approach for fatigue analysis consists of the following steps:

a) modeling the loading environment,
b) modeling loads exerted by the environment on the ships,
c) evaluation of nominal loads,
d) evaluation of stresses at hotshot
e) evaluation of cumulative fatigue damage over the tanker's service time.
f) evaluation of the probability of failure in tanker's service life.

In this chapter,the fatigue uncertainty analysis is based on the fatigue analysis approach which is developed in SMP project in Department of Naval Architecture & Offshore Engineering University of California at Berkeley (Ref 1). Errors in calculating stress vector in unit load approach were quantitied. Errors involved in all the steps of fatigue analysis are combined together and uncertainties are quantitied in fatigue damage, for the case that the SMP approach is used. the importance of the different uncertainties are investigated through the study of proposed CSD.

6.2 Uncertainties in cumulative fatigue damage

Studies of fatigue reliability of marine structures assume that the effect of random uncertainties on the cumulative damage is negligible. Thus, the previous studies account for modeling uncertainties in stress evaluation processes (Ref 9). Although the effect of random uncertainties reduces with the number of load cycles increasing, no study has proven that this effect is negligible.

61

The objective of this chapter presented here is to address the above issue, estimate uncertainties in the cumulative fatigue damage over the lifetime of CSDs in double-hull tankers, and study the relative importance of each uncertainty.

The following are the basic assumption in uncertainty analysis.

a) Fatigue life can be estimated by using the S-N curves. The integrated Paris law gives the same form, assuming no threshold level and no sequence effects. The slope of these curves is constant for any number of cycles, N.

b) Miner's rule can be used to estimate fatigue damage.

c) The stress amplitude distribution is known as the Weibull distribution for long-term fatigue analysis.

d) The mean and standard deviation of the cumulative damage, D, can be estimated by linearizing the expression relating D with all random variables around the mean values of these variables. This is a crude approximation since the derivatives of the damage with respect to the values of the random variables are not constant. But the objective of this study is to identify the most important uncertainties and obtain estimates of the COV of D. It can be applied in fatigue uncertainty analysis.

e) The bias for the S-N curves. Design S-N curves are based on median S-N curves with standard deviation 2σ.

Under the above assumptions, fatigue damage can be calculated by the following equation (Ref 9) :

$$D = \frac{B_{II}{}^m \Sigma S_i{}^m}{A}$$

where,

B_{II} represents the modeling error in the stress at the hot spot

m, is the exponent in the S-N curves,

S_i, is the predicted stress amplitude at the ith load application, and

A, is the constant at the right hand side of the S-N equations.

The summation is for all load applications.

The above equation is based on the assumption that the stress is narrow band process. The stress might be wide band which effects the fatigue damage and the life of the structure. It can be accounted by using the rainflow correction factor (Ref 10) or binomial correction factor (Ref 11)

The modeling bias B_{II} is given by the following equation:

$$B_{II} = B_M B_S B_F B_N B_H$$

where,

B_M represents uncertainties in the geometry due to manufacturing imperfections,

B_S represents uncertainties in seastate description,

B_F represents uncertainties in wave load predictions,

B_N is the bias for errors in static and dynamic structural analysis, and

B_H is the bias for uncertainties in stress vectors

By using a first order Taylor series expansion of the expression for D about the mean values of all random variables, we obtain the mean value of D,

$$E(D) = \frac{\cdot E^m(B_{II}) \Sigma E^m(S_i)}{E(A)}$$

Assuming that the statistics of the predicted stress are the same for all load cycles, we have,

$$E(D) = \frac{E^m(B_{II}) N E^m(S_i)}{E(A)}$$

where N is the number of cycles over the lifetime of the ship.

The coefficient of variation of fatigue damage D is

$$COV_D = (m^2 COV_{B_{II}}^2 + COV_A^2 + COV^2_{\Sigma S^m})^{1/2}, \text{ where}$$

$COV_{B_{II}}$ is the COV of modeling bias,

where

$$C_{\mathbf{s}} \cdot \sqrt{(1+C_{\mathbf{M}}^2)(1+C_{\mathbf{S}}^2)(1+C_{\mathbf{F}}^2)(1+C_{\mathbf{N}}^2)(1+C_{\mathbf{H}}^2)} \cdot 1$$

COV_A is the COV of A, and

$COV_{\Sigma S^m}$ is the COV of the sum ΣS^m

Note that subscript i has been dropped.

The first term in the expression with the square root, represents the effect of modeling uncertainties. The second term is associated with uncertainties in S-N curves and the third represents the effect of random uncertainties.

6.3 Relative importance for random uncertainties

Based on E.Nikolaidis' study (ref 12), it has been found that the effect of random uncertainties is small. E. Nikolaidis considered two cases. In the first case the maxima of

63

the stress, Si follows the Rayleigh distribution, while in the second they follow the Weibull distribution. He assumes that the distribution coefficient between the ith and the kth stress maxima, σi and σk, is, $r\sigma i\sigma k = \rho_{\sigma i,\sigma i+1}^{|i-k|}$, where $\rho_{Si,Si+1}$ is the correlation coefficient between two subsequent peaks. In his study, he considered different values $\rho_{Si,Si+1}$ for in the range from 0. to 0.99. After some derivation, the following equation was derived for the COV of random uncertainties:

$$COV_{\Sigma S^m} = \frac{COV_{S^m}(\frac{1+\rho}{1-\rho} - \frac{2\rho}{N(1-\rho)^2})^{1/2}}{N^{1/2}}$$

where COVs is the COV of a local maximum.

It is observed that the COV increases with the correlation coefficient between subsequent maxima increasing. Moreover, the COV for random uncertainties decreases, with the number of load cycles, N, increasing. The $COV_{\Sigma S^m}$ is almost zero for large values of N, for any values of ρ less than one.

The COV for random uncertainties is presented in Table 6.1 for three cases, the stress amplitude follows the rayleigh distribution, while in the latter two cases, it follows the Weibull distribution (Ref. 12) with Weibull exponent c equal to 0.7 and 1.0, respectively.

Distribution of Stress Amplitude		COV of Cumulative Damage				
		Correlation Coefficient of Subsequent Peaks				
		0.0	0.5	0.8	0.9	0.99
Rayleigh		0.0	0.0	0.01	0.01	0.03
Weibull	1.0	0.01	0.01	0.01	0.02	0.06
Weibull	0.7	0.01	0.01	0.02	0.03	0.10

It is observed that the effect of random uncertainties is small. Moreover, a similar calculation for $N=10^8$, which is a typical number of load application over the lifetime of a marine structure, showed that the COV due to random uncertainties is practically zero.

6.4 Relative Contribution of Various Types of uncertainty on Fatigue Damage

The equation of the previous section allow to quantify the uncertainties in the cumulative fatigue damage. The average bias and COV of fatigue damage for CSDs in tankers was calculated by the above equations.

The data on various uncertainties , which are involved in fatigue analysis, are presented in Table 6.2 and Table 6.3.

64

Table 6.2 Summary of Bias and COV of B_{II} Uncertainties

Uncertainties in fatigue analysis	Bias	COV
B_M	0.9 - 1.0	0.1 - 0.3
B_S	0.6 - 1.2	0.4 - 0.6
B_F	0.6 - 1.0	0.1 -0.3
B_N	0.8 - 1.0	0.2 -0.4
B_H	0.8 - 1.2	0.1 - 0.5

Table 6.3 Summary of Bias and COV of Fatigue Uncertainties

Uncertainties in fatigue analysis	Bias	COV
A	1.0	0.3 -0.6
ΣS^m	1.0	0.0

The influence of fatigue uncertainties in fatigue analysis is shown in fig.6.1 - fig.6.6. The following conclusions can be extracted from the tables and figures.

a) Uncertainty in cumulative damage is very large for tankers. The reason is that fatigue damage is extremely sensitive to the amplitude of the applied loads, In other words, a small change in the amplitude results to a large change in the fatigue damage and the expected fatigue life.

b) For the case of tankers, the uncertainties in stress analysis is the most important. The next important uncertainty is that in S-N curve selection.

c) The effect of random uncertainties is small because these uncertainties are averaged out in the procedure for evaluating fatigue damage. Moreover, the statistical correlation between consecutive stress peaks is unimportant in fatigue. This is the theoretical foundation for the long-term Weibull distribution of stress range.

6.5 Recommendation and Conclusion

The following are the main conclusions from the uncertainty analysis.

65

1. It is believed that the effect way to reduce uncertainty is to distinguish between ships with different characteristics and operational schedules, and quantify uncertainties separately in uncertain analysis.

2. In order to predict long-term loading for fatigue damage accurately, linear seakeeping methods can not estimate hydrodynamic pressures on the ship hull with acceptable accuracy although it is effective in calculating global loads and wave bending moments. Nonlinear effects should be considered for the CSDs in tankers since local pressure plays more important role in CSDs especially for transverse members. For the bow and stern of ship hull, wave slamming is another important factor. The combination of the slamming and wave bending moments should be treated in more proper way since the previous Turkstra's rule, or the peak coincidence approximation may involve large uncertainty.

3. The following are the most important uncertainties in fatigue analysis in tankers.

     - Local pressure for the CSDs in tankers.
     - Stress Vector in fatigue analysis which means the selection of the appropriate stress vector and corresponding S-N curves.
     - combination of wave and slamming bending moments for stern and bow of the ship hull.
     - still loads effects.

Based on the above studies, it is recommended that we should modeling uncertainties closer and in more detail in ships although various studies have been conducted previously in offshore structures. (Ref 12). It is suggested that the study should consider the following factors.

     1) What is the best way to account for modeling uncertainties in ships ?
     2) How do the errors in various steps of fatigue analysis procedure propagate when estimating fatigue damage in tankers ?
     3) Are the existing databases on measured response of ships sufficient to quantify modeling uncertainties ?

Critical Structural Detail in Chevron Double-Hull Tanker
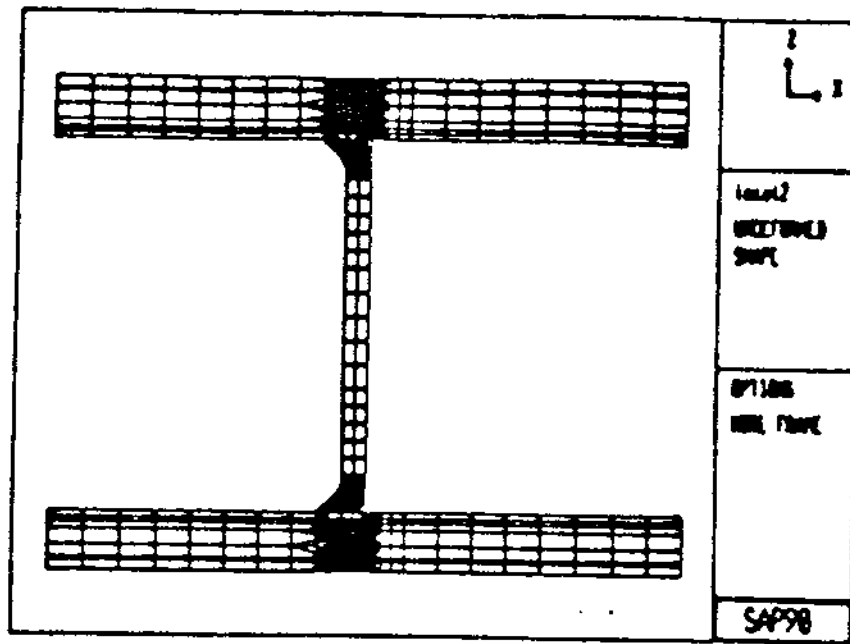
Computation Results of Long-Term Loading

Weibull Scale Parameter	Weibull Shape Parameter
4.21	0.821

Fig 6.1 Finite Element for fatigue Uncertainty Analysis
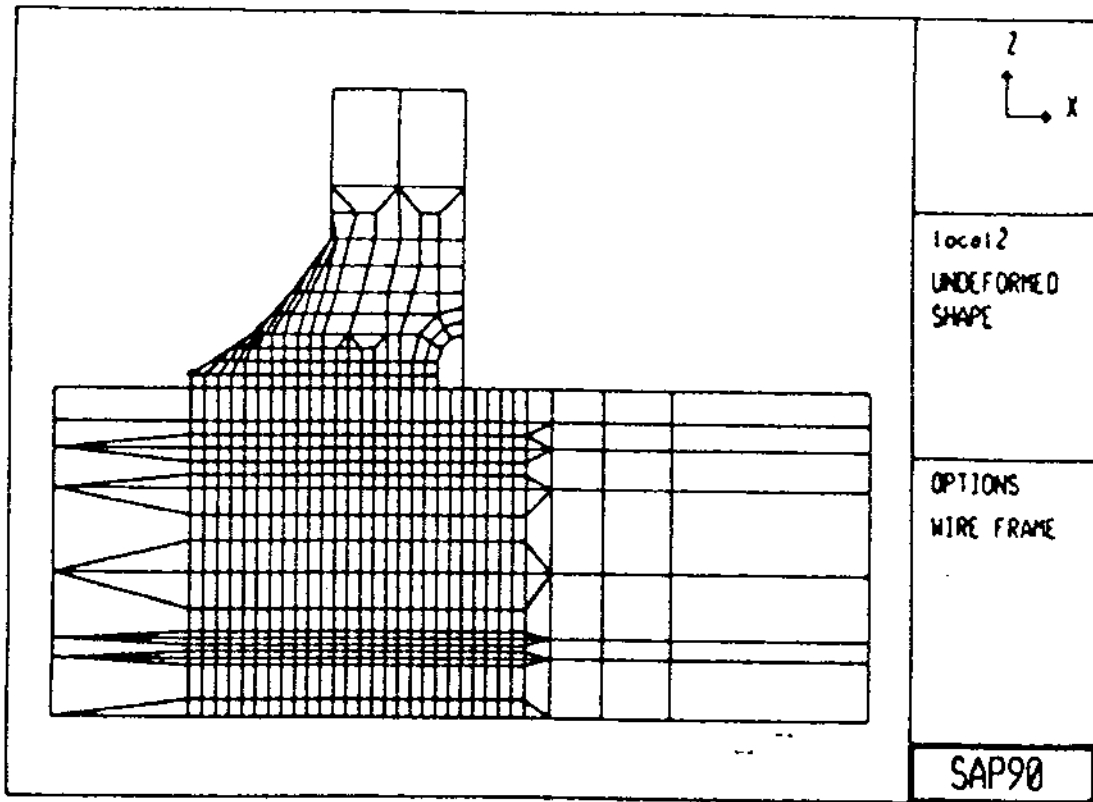
Fig 6.2 Finite Element Model for the Hotspot Area (Zooming)

68

Fig 6.2 Finite Element Model for the Hotspot Area (Zooming)

68

Probability of Failure vs Bias (COV=0.9)
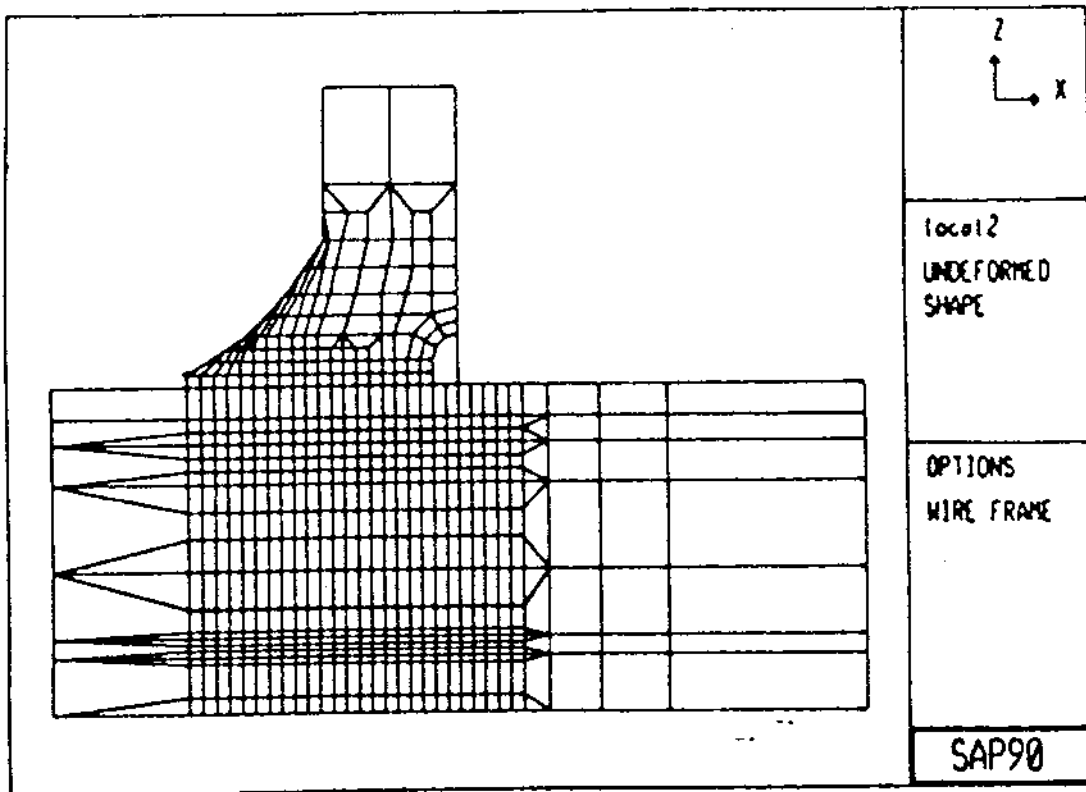
Probability of Failure vs COV of Bias (Mean=1)
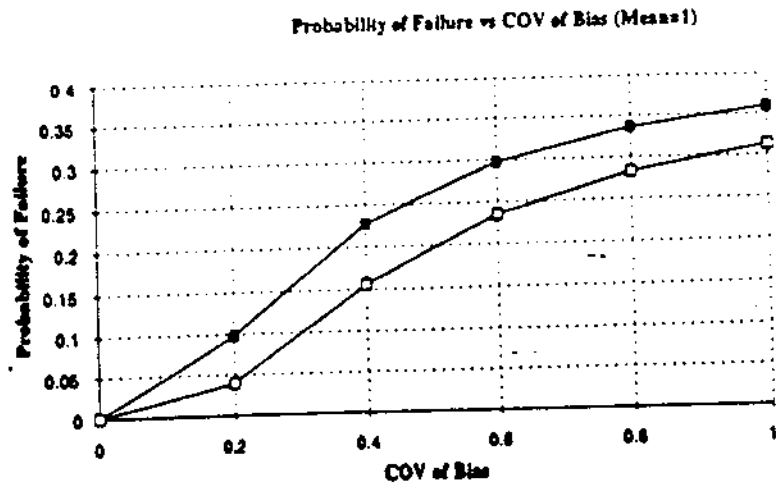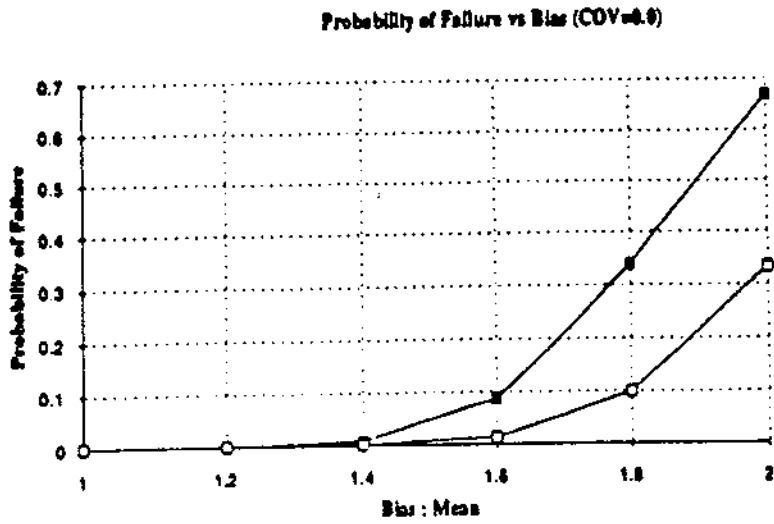
$$\text{Bias} = \frac{\text{True Value of Tf}}{\text{Predicted Value of Tf}}$$

Fig 6.3 Probability of Failure vs Total Uncertainty
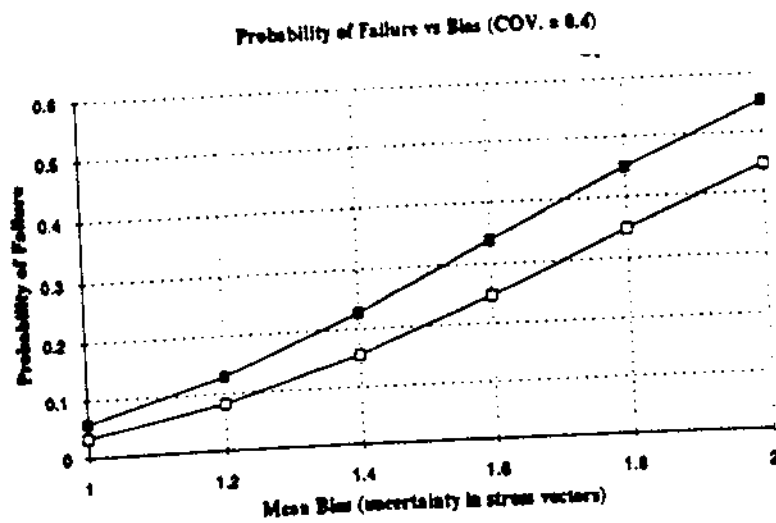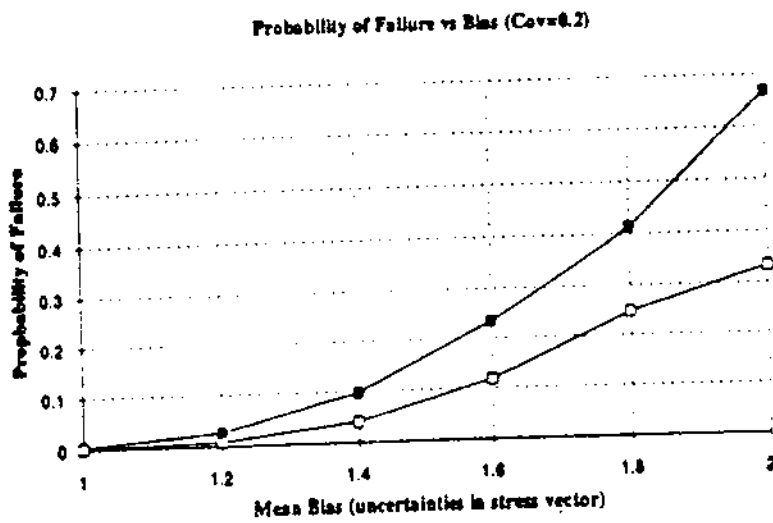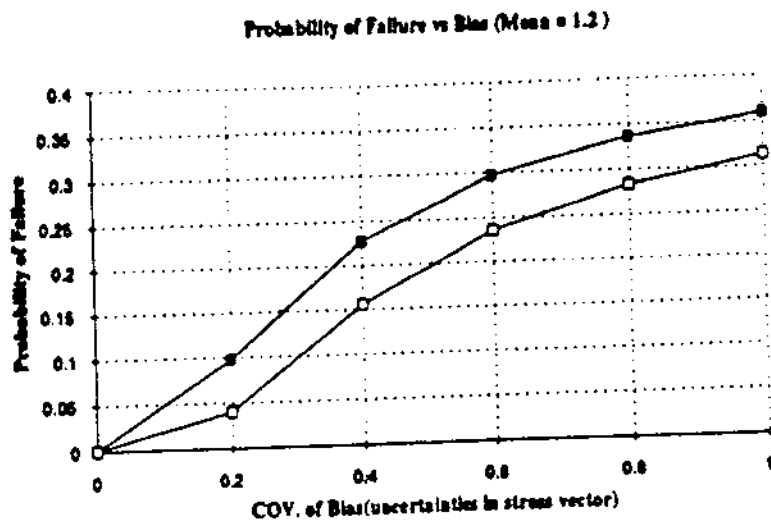
Fig 6.4 Datigue Uncertainty due to Detail Stress Analysis

Probability of Failure vs Bias (Cov=0.2)
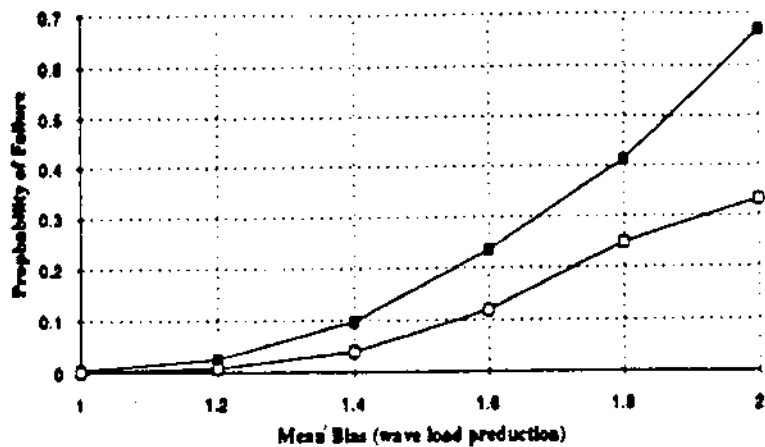
Probability of Failure vs Bias (COV. = 0.4)
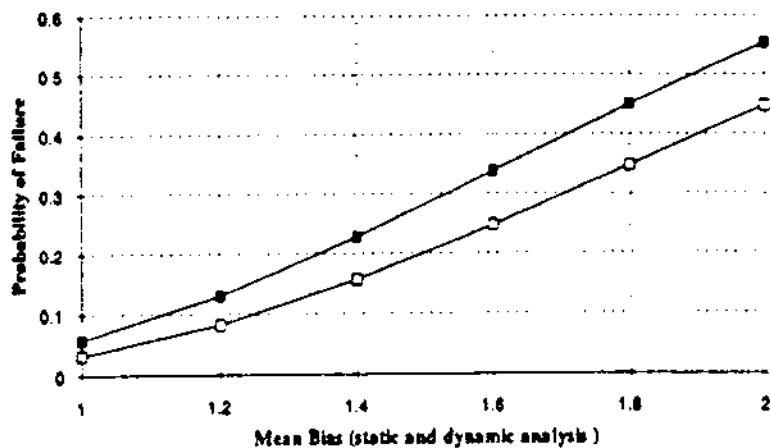
Probability of Failure vs Bias (COV. = 0.6)
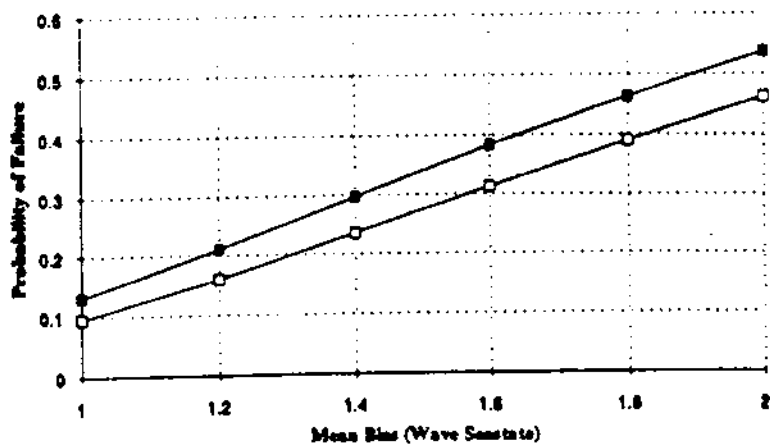
Fig 6.5 Fatigue Uncertainty due to Other factors

Chapter 7

Conclusions and Recommendations

7.1 Summary

In the high seas, the continuous cyclic stress induced by the wave sagging and hogging causes fatigue problems in ships. These problems were addressed in detail in the joint industry project **Structural Maintenance for New and Existing Ships**. Since fatigue problems are impossible to address by the empirical equations embedded in the conventional design methods. two identical oil tankers may not have the same level of fatigue performance. Depending on the trade routes, one may have fatigue cracks just after one year service, and the other may last for years without fatigue cracks. This inconsistent level of performance is attributed primarily to inadequate analytical methods existed in current ship design and analysis of the fatigue problems.

The reasons for the increased number fatigue related cracks in oil tankers are as follows:

1) The trend of reducing ship scantlings based on detailed stress analyses and the increased use of high tensile steel have resulted in an increase of the general stress level. The increase has in general not been offset by improved detail design to cause a reduction of the SCF value for CSD in order to achieve a comparable fatigue endurance.

2) Tankers operating on the TAPS trade route (California - Alaska) experience the most severe cyclic loadings.

3) The presence of corrosion in ballast tanks results in a reduction of the fatigue life of CSD.

This report documents in detail computation analysis of the fatigue of the proposed CSD in the proposed double-hull tankers. Both the probabilistic and deterministic fatigue analysis was conducted to determine the probability of failure during the tanker's service life and fatigue life of the proposed CSD in the proposed double-hull tankers. The residual life for the cracked CSD was carried out by linear fracture mechanics. Corrosion fatigue was studied based on the increase in the stress level for the hotspot of CSD. Fatigue uncertainties were investigate to quantify errors in all the steps of fatigue analysis and quantify the uncertainties in fatigue damage evaluation.

7.2 Conclusions

Fatigue Design

Much concern has recently arisen over fatigue as probable or dominant failure mode of some critical structural details. This is especially true of the side-longitudinal CSD in its draft range when the structural details are made of higher strength steels.

Previous studies addressed that the fatigue cracks were severe at the sideshell longitudinal stiffener connection. (Ref.2). In order to avoid the fatigue cracks in longitudinal stiffener connection, a new design was proposed in the proposed double-hull tankers which adopts an apple-shaped slot opening at the connections between longitudinals and web plates to make the stiffeners unnecessary. But it caused a severe fatigue problem around the apply-shaped cutout under current construction for this relative new design. More, it should be pointed out that the secondary stresses may be raised by the deflection of the primary members due to the reduction of the stiffness of the hull structures without stiffeners.

Original Design   fatigue life 11.17 for hotspot

Proposed Improved Design   fatigue life for hotspot 85.74 years
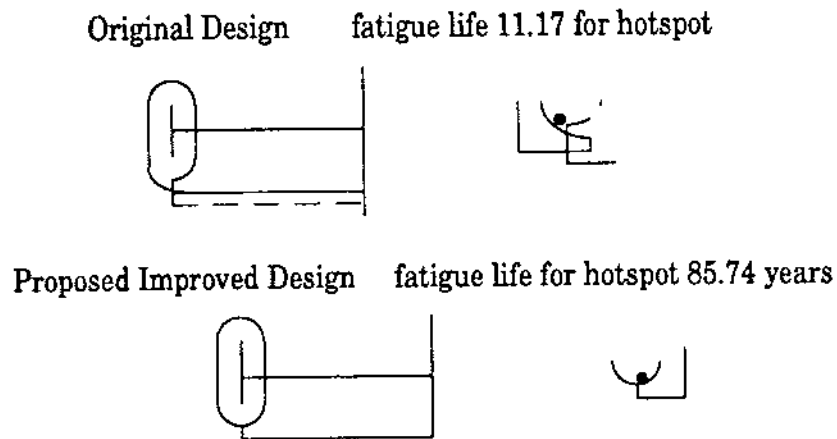
Fig 7.1 Original Design and Improved Design

It is necessary to develop a high quality construction technique for the proposed fatigue design.

Several design modification have been proposed for the CSD based on the study. Following is the general summary

(a) Add bracket to relieve the stress concentration hot spot or improve force transmission for the sideshell longitudinal bracket connection.

(b) Add lug, collar plate or closing plate to the cutout to improve the shear force carrying capacity and fatigue strength around the cutout.

61

(c) Configuration changes - soft toe, new place plate, radius change to improve the local strength and fatigue strength.

Corrosion Fatigue

Corrosion fatigue is defined as a synergistic effect in which corrosion and fatigue occur simultaneously. The combined effect of an aggressive environment with a cyclic stress or strain is usually more severe than the sum of the two effects of corrosion and fatigue acting separately.

No single mechanism completely governs the entire corrosion fatigue process and it seems that there is no general theoretical model for the corrosion fatigue. Of course, the influence of corrosion on fatigue can be clearly represented by comparing the S-N curves for fatigue tests carried out in both air and a more aggressive environment. It seems that the general effect of corrosion is to be a reduction in fatigue strength, but it is significant that the synergistic effect, in which corrosion and fatigue occur simultaneously, produces a reduction in strength which is greater than the sum of the individual effects due to corrosion and fatigue acting separately. Unfortunately, few works have been conducted in this area which is very important in ship structural integrity. The model presented in this report only considered the reduction in fatigue strength. It is based on the effect of increased stress level over time due to corrosion. Although it can not present the whole mechanism of corrosion, it's still useful to point out the influence of the fatigue material parameters in the fatigue model due to corrosion. Following is one numerical example:

fatigue life is 23.57 years for hotspot

corrosion fatigue life is 19.34 for the corrosion rate 1mm
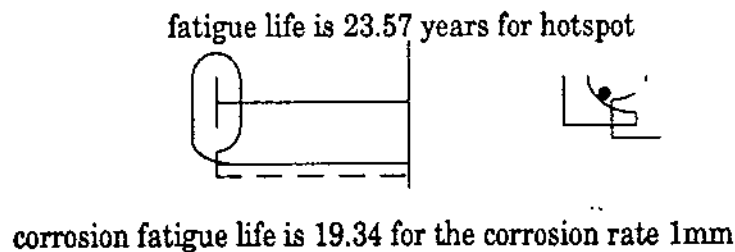
Fig 7.2 CSD Corrosion Fatigue

It should be pointed out that the corrosion rate is generally based on the corrosion database in SMP project. It is highly recommended that further study and experiment on corrosion fatigue should be conducted since the question to be answered concerning the structural strength is " At what point in the life of the structure should one be assessing the corrosion and fatigue?". This is a new question. Obviously, the estimation of fatigue life based on uncorroded scantling is overly optimistic. But even the fatigue analysis which accounted the increase of local stresses for a structural detail may not be enough in some cases since the corrosion fatigue is the synergistic effect.

74

Residual Life for Cracked CSD

From the comprehensive fatigue analysis, it was found that the fatigue damage is severe in some CSDs in proposed double hull tanker and cause fatigue cracks during 20 years service life. Based on the fatigue analysis, residual life calculation was conducted for cracked CSDs by linear fracture mechanics.

For residual life assessment of welded details with flaws, no rules has been issued by Classification Societies or Regulatory bodies. Instead some organizations have specified recommended practices for residual life assessment. The general approach is based on fracture mechanics.

This study conducted the residual life assessment based on an equivalent S-N approach. Linear fracture mechanics was used to derive a series of equivalent S-N curves which can be combined into a single conventional S-N equation by representing the intercept of the S-N curve as a function of the crack length. With this relationship, the method can be easily used by engineers to predict the remaining fatigue life with any initial crack length.

It has been found that the residual life for the cracked details is shorter. Thus inspection, maintenance and repair (IMR) is important and necessary in the tanker's service life. It is highly recommended that the further study about the calibration of cracked details should be studied based on fracture mechanics and existing fracture data base.

Fatigue Uncertainty

For the fatigue uncertainty analysis, following assumptions have been made.

(a) Fatigue life can be estimated by using the S-N curves. The integrated Paris law gave the same form as S-N model assuming no threshold level and sequence effects. The slope of these S-N curves is constant for any number of cycles, N.

(b) Miner's rule can be used to estimate fatigue damage

(c) The stress amplitude distribution is known as Weibull distribution for long-term fatigue analysis.

(d) The mean and standard deviation of the cumulative damage, D can be estimated by linearizing the expression relating D with all random variables around the mean values of these variables. This is a crude approximation since the derivatives of the damage with respect to the values of the random variables are not constant. But the objective of the fatigue uncertainty analysis in this report is to identify the most important uncertainties and obtain the COV of D. It can be applied here for the fatigue uncertainty analysis.

Based on the above assumptions, a detailed uncertainty analysis was conducted to quantify the uncertainties in the cumulative damage model. The following is the summary of the conclusions.

(a) Uncertainty in cumulative damage is very larger for tankers. The reason is that fatigue damage is extremely sensitive to the amplitude of the applied loads. In other words, a small change in the amplitude results to a large change in the fatigue damage and expected fatigue life.

(b) For the case of tankers, the uncertainties in stress analysis is the most important factor in fatigue analysis. Corresponding to the stress analysis, the selection of S-N curves play a key role in the fatigue estimation.

(c) The effect of random uncertainty is small because these uncertainties are averaged out in the procedure for evaluating fatigue damage. Moreover, the statistical correlation between consecutive stress peaks is unimportant in fatigue. These are the theoretical foundation for the long-term Weibull distribution of the stress range.

(d) In order to predict long-term loading for fatigue damage accurately, linear seakeeping methods can not estimate hydrodynamic pressures on the ship hull with acceptable accuracy although it is effective in calculating global loads and wave bending moments. Nonlinear effects should be considered for the CSD in tankers since local pressure plays more important role in CSD especially for transverse members.

Inspection, Maintenance and Repair

Regardless of fatigue considerations taken in design, inspection, maintenance and repair plays a more and more important role in the tanker industry. But the repair work may be costly and inconvenient. In most cases carefully planned inspection and repair procedures can improve cost effectiveness. Such procedures can be established if the crack growth can be predicted and the maximum crack size to which the crack may be allowed to grow can be estimated for realistic details with a reasonable accuracy. Unfortunately, it's still hard to do it now.

As for repairs, once the crack is detected, it is common practice to repair as soon as possible. This practice is applied irrespective of crack propagation rate, or possible unloading resulting in the crack stopping to grow.

For early cracks the remedy is improved detail design, and better workmanship. For fatigue cracks the common practice is to weld the crack often combined with improved detail design. Occasionally, also renewal of material is considered necessary.

Reference

1. *148,800 LTDW Diesel Oil Tanker Strcutural Analysis* Advanced Analysis Technology Dept. Ishikawajima-Harima Heavy Industries Co. Ltd

2. *Structural Maintenance for New and Existing Ships*, Reports SMP 1-1 through 5-2, Department of Naval Architecture and Offshore Engineering, University of California at Berkeley, September 1992.

3 *Guide for the Fatigue Strength Assessment of Tanker*, American Bureau of Shipping, New York, NY 1992.

4 *Definition and Validation of a Practical Rationally-Based Method for the Fatigue Analysis and Design of Ship Hulls*. Society of Naval Architects and Marine Engineers T&R Report No. R-41

5. *Uncertainties in Stress Analysis on Marine Structures* Ship Structure Committee Report SSC-363

6 *Fatigue handbook, Offshore Steel Structures*. A. Almar-Naess Tapir, 1985

7 *Life - A Computer Program for Fracture Mechanics Analysis of Crack Growth in Welded Structural Components*. Technical Report No. 5.8, SINTEF - Norwegian Institute of Technology, 1984

8 *Fatigue Reliability* (a series of papers) ASCE Committee on Fatigue and Fracture Reliability Journal of Structural Division 1982.

9 *Marine Structural Integrity Programs*. Ship Structure Committee Report SSC-365

10 *Long-term Corrosion Fatigue of Welded Marine Steels* Ship Structure Committee Report SSC-326

11. Olufsen, A., and Bea, R.G *"Uncertainties in Extreme Wave Loadings on Fixed Offshore Platforms"* O.M.A.E. 90 Proceedings.

12 Wirsching, P.H. and Chen, Y.N., *"Consideration of Probability-Based Fatigue Design for Marine Structures,"* Proceeding of the Marine Structural Reliability Symposium, 1987, pp31-43, also in Marine Structures, Vol. 1, No. 1 1988, pp. 23-45

Apprendix A Results for Fatigue Life Calculation

79

Fatigue life calculation for CSDs in Proposed Double-Hull

L36 - Slot on Sideshell Longitudinal

Design Fatigue Life = 20 year
Weibull Parameter = 0.942
Number of Cycles N= 1 x 10^8
NFull= 0.5 x 10^8 NBallast= 0.5x 10^8
Load and unload N =500

Typical CSD and Hotspot

SHELL LONG

Table 1.1.1

Load Component	S-N	Stress Range	Fatigue Life
Pressure Full	F	152.586	121.085
	E	152.586	230.609
Pressure Ballast	F	111.132	313.412
	E	111.132	597.056
Wave Bending Full	–	–	–
Wave Bending Ballst	–	–	–
Load Unload	F	46.256	-
	E	46.256	-

Note : F Curve   Standard Weld
E Curve   Improved Weld

Fatigue Life is for F Curve : 136.61Years
**Fatigue Life for E Curve : 260.078 Years**

Typical CSD and Hotspot

S. SHELL LONG
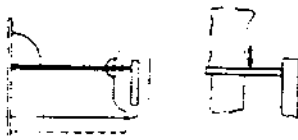
Table 1.1.2

Load Component	S-N	Stress Range	Fatigue Life
Pressure Full	F	31.85	13313.9
	E	31.85	25363.2
Pressure Ballast	F	96.824	473.897
	E	96.824	962.784
Wave Bending Full	–	–	–
Wave Bending Ballst	–	–	–

81

| Load Unload | F | 144.55 | - |
| | E | 144.55 | - |

Note : F Curve   Standard Weld
E Curve   Improved Weld

Fatigue Life for F Curve : 699.3 years
Fatigue Life for E Curve : 1855.287 years

Typical CSD and Hotspot

S SHELL LONG

Table 1.1.3

Load Component	S-N	Stress Range	Fatigue Life
Pressure Full	F2	258.034	18.13
	F	258.034	25.04
Pressure Ballast	F2	192.668	43.57
	F	192.668	60.14
Wave Bending Full	F2	–	–
	F		
Wave Bending Ballst	F2	–	–
	F		
Load Unload	F2	197.862	-
	F	197.862	-

Note:F2 Curve   Standard Weld
F Curve   Improved Weld

Fatigue Life for F2 Curve : 25.6 year
Fatigue Life for F Curve : 35.357 year

L37 - Slot on Sideshell Longitudinal

Design Fatigue Life = 20 year
Weibull Parameter = 0.942
Number of Cycles N= 1 x 10 ^{8}
NFull= 0.5 x 10 ^{8} NBallast= 0.5x 10 ^{8}
Load and unload N =500

Table 1.2.1

Typical CSD and Hotspot

Load Component	S-N	Stress Range	Fatigue Life
Pressure Full	F	178.164	76.06
	E	178.164	144.9
Pressure Ballast	F	132.3	186
	E	132.3	359
Wave Bending Full	F	–	–
	E		
Wave Bending Ballst	F	–	–
	E		

A-4
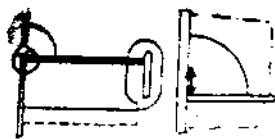
Load Unload	F	35.574	-
	E	35.574	-

Note : F Curve   Standard Weld
        E Curve   Improved Weld

Fatigue Life for F Curve : 107.97 years
Fatigue Life for E Curve : 206.47 years

Typical CSD and Hotspot

S. SHELL LONG.

Table 1.2.2
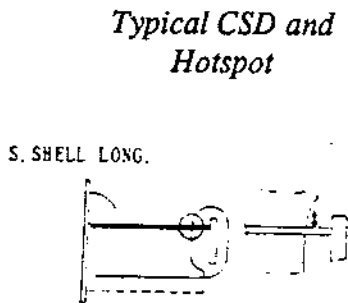
Load Component	S-N	Stress Range	Fatigue Life
Pressure Full	F	269.5	21.97
	E	269.5	41.866
Pressure Ballast	F	261.09	24.17
	E	261.09	46.04
Wave Bending Full	F	–	–
	E		
Wave Bending Ballst	F	–	–
	E		
Load Unload	F	94.766	-
	E	94.766	-

Note : F Curve   Standard Weld
        E Curve   Improved Weld

Fatigue Life for F Curve : 23.02 year
Fatigue Life for E Curve : 43.854 years

Typical CSD and Hotspot

S. SHELL LONG.

Table 1.2.3
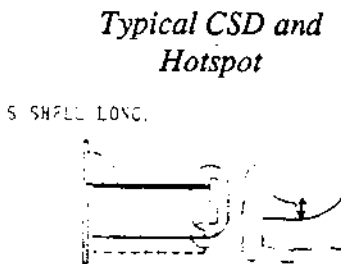
Load Component	S-N	Stress Range	Fatigue Life
Pressure Full	F2	104.86	270.27
	F	104.86	373.08
Pressure Ballast	F2	85.946	490.86
	F	85.946	677.57
Wave Bending Full	F2	–	–
	F		
Wave Bending Ballst	F2	–	–
	F		
Load Unload	F2	70.56	-
	F	70.56	-

Note:F2 Curve   Standard Weld
        F Curve   Improved Weld

Fatigue Life for F2 Curve : 348.6 years
Fatigue Life for F Curve : 481.23 years

83

Typical CSD and Hotspot

S. SHELL LONG.
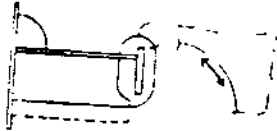
Table 1.2.4

Load Component	S-N	Stress Range	Fatigue Life
Pressure Full	C	490.686	22.84
Pressure Ballast	C	373.87	59.15
Wave Bending Full	C	–	–
Wave Bending Ballst	C	–	–
Load Unload	C	101.332	–

Note: C Curve   Standard Weld
                       Improved Weld

Fatigue Life for C Curve : 32.946 years

Typical CSD and Hotspot

S. SHELL LONG.
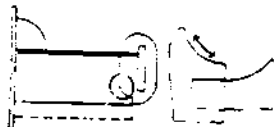
Table 1.2.5

Load Component	S-N	Stress Range	Fatigue Life
Pressure Full	F2	497.448	2.5
	F	497.448	3.5
Pressure Ballast	F2	406.112	4.65
	F	406.112	6.42
Wave Bending Full	F2	–	–
	F		
Wave Bending Ballst	F2	–	–
	F		
Load Unload	F2	36.352	–
	F	36.352	

Note: F2 Curve   Standard Weld
       F Curve   Improved Weld

Fatigue Life for F2 Curve : 3.25 years
Fatigue Life for F Curve : 4.53 years

L45 - Slot on Sideshell Longitudinal

Design Fatigue Life = 20 year
Weibull Parameter = 0.942
Number of Cycles $N = 1 \times 10^8$
$N_{Full} = 0.5 \times 10^8$ $N_{Ballast} = 0.5 \times 10^8$
Load and unload $N = 500$

84

Table 1.3.1

Typical CSD and Hotspot

S. SHELL LONG.
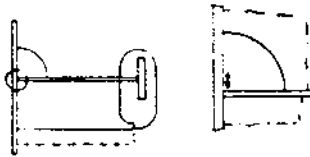
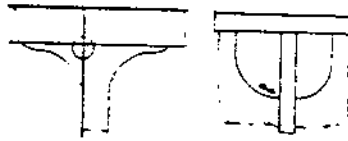| Load Component	S-N	Stress Range	Fatigue Life
Pressure Full	F	236.376	32.57
	E	236.376	62.05
Pressure Ballast	F	166.698	92.86
	E	166.698	176.9
Wave Bending Full	F	–	–
	E		
Wave Bending Ballst	F	–	–
	E		
Load Unload	F	29.792	–
	E	29.792	

Note : F Curve   Standard Weld
E Curve   Improved Weld

Fatigue Life for F Curve : 48.24 years
Fatigue Life for E Curve : 91.87 years

Table 1.3.2

Typical CSD and Hotspot

S. SHELL LONG.
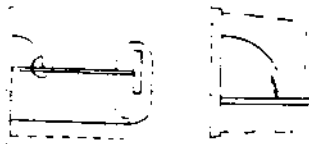
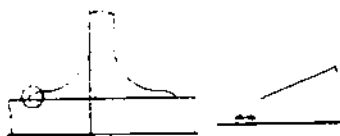| Load Component	S-N	Stress Range	Fatigue Life
Pressure Full	F	334.278	13.01
	E	334.278	24.79
Pressure Ballast	F	260.974	27.34
	E	260.974	52.09
Wave Bending Full	F	–	–
	E		
Wave Bending Ballst	F	–	–
	E		
Load Unload	F	43.022	–
	E	43.022	

Note : F Curve   Standard Weld
E Curve   Improved Weld

Fatigue Life for F Curve : 17.63 years
Fatigue Life for E Curve : 33.6 years

Table 1.3.3

Typical CSD and Hotspot

Load Component	S-N	Stress Range	Fatigue Life
Pressure Full	F	113.876	329
	E	113.876	627

A-7
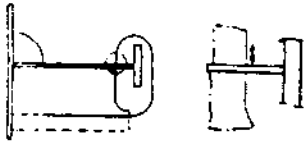
Pressure Ballast	F	110.446	360.77
	E	110.446	687.28
Wave Bending Full	F	–	–
	E		
Wave Bending Ballst	F	–	–
	E		
Load Unload	F	43.022	–
	E	43.022	

Note:F Curve   Standard Weld
     E Curve   Improved Weld

Fatigue Life for F Curve : 344.116 years
Fatigue Life for E Curve : 655.74 years

Typical CSD and
Hotspot
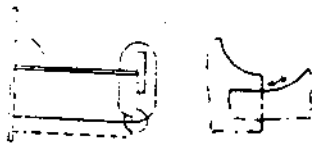
S. SHELL LONG.

Table 1.3.4

Load Component	S-N	Stress Range	Fatigue Life
Pressure Full	F2	235.592	26.93
	F	235.592	37.17
Pressure Ballast	F2	161.504	83.586
	F	161.504	115.38
Wave Bending Full	F2	–	–
	F		
Wave Bending Ballst	F2	–	–
	F		
Load Unload	F2	294.196	–
	F	294.194	

Note:F2 Curve   Standard Weld
     F Curve   Improved Weld

Fatigue Life for F2 Curve : 40.736 years
Fatigue Life for F Curve : 56.23 years

Typical CSD and
Hotspot

S. SHELL LONG.

Table 1.3.5

Load Component	S-N	Stress Range	Fatigue Life
Pressure Full	C	385.434	61.31
Pressure Ballast	C	189.826	731.364
Wave Bending Full	C	–	–
Wave Bending Ballst	C	–	–

Load Unload	C	279.496	–

Note:C Curve Standard Weld
Improved Weld

Fatigue Life for C Curve : 113.14 years

L46 - Slot on Sideshell Longitudinal

Design Fatigue Life = 20 year
Weibull Parameter = 0.942
Number of Cycles $N = 1 \times 10^{8}$
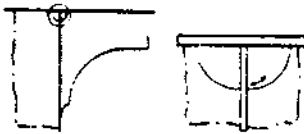$N_{Full} = 0.5 \times 10^{8}$ $N_{Ballast} = 0.5 \times 10$
Load and unload N = 500

Table 1.4.1

Typical CSD and Hotspot

S. SHELL LONG.

Load Component	S-N	Stress Range	Fatigue Life
Pressure Full	F	93.492	594.78
	E	93.492	1133.07
Pressure Ballast	F	62.818	1960.78
	E	62.818	3735.33
Wave Bending Full	F	–	–
	E		
Wave Bending Ballst	F	–	–
	E		
Load Unload	F	29.498	–
	E	29.498	

Note : F Curve Standard Weld
E Curve Improved Weld

Fatigue Life for F Curve : 912.74 years
Fatigue Life for E Curve : 1739.13 years

Table 1.4.2

Typical CSD and Hotspot
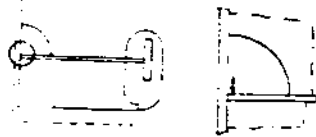
S. SHELL LONG.

Load Component	S-N	Stress Range	Fatigue Life
Pressure Full	F	117.992	295.886
	E	117.992	563.669
Pressure Ballast	F	78.89	989.956
	E	78.89	1885.89
Wave Bending Full	F	–	–
	E		
Wave Bending Ballst	F	–	–
	E		
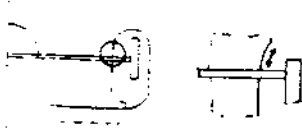
Typical CSD and Hotspot

L. BHD LONG.
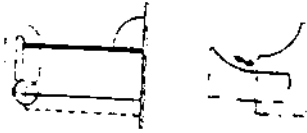
Table 2.1.2

Load Component	S-N	Stress Range	Fatigue Life
Pressure Full	F	0.0	–
	E	0.0	
Pressure Ballast	F	0.0	–
	E	0.0	
Wave Bending Full	–	–	–
Wave Bending Ballst	–	–	–
Load Unload	F	125.44	–
	E	125.44	

Note : F Curve   Standard Weld
       E Curve   Improved Weld

Fatigue Life for F Curve : - years
Fatigue Life for E Curve : - years

Typical CSD and Hotspot

L. BHD LONG.
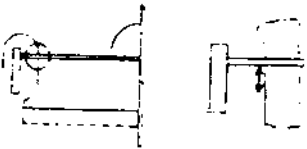
Table 2.1.3

Load Component	S-N	Stress Range	Fatigue Life
Pressure Full	F2	109.172	270.6
	F	109.172	373.55
Pressure Ballast	F2	125.93	176.32
	F	125.93	243.38
Wave Bending Full	F2	–	–
	F		
Wave Bending Ballst	F2	–	–
	F		
Load Unload	F2	294.294	–
	F	294.294	

Note:F2 Curve   Standard Weld
       F Curve   Improved Weld

Fatigue Life for F2 Curve : 213.52 years
Fatigue Life for F Curve : 294.724 years

L37 - Slot on LongBHD Longitudinal

Design Fatigue Life = 20 year
Weibull Parameter = 0.942
Number of Cycles N= 1 x 10^8
*NFull= 0.5 x 10^8 NBallast= 0.5x 10^8*

A-12

90

Table 2.2.1

Typical CSD and Hotspot

L. BHD LONG.
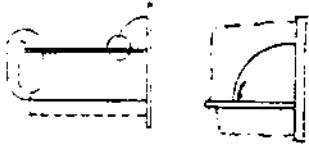
Load Component	S-N	Stress Range	Probability
Pressure Full	F	214.718	49.1
	E	214.718	93.5
Pressure Ballast	F	201.488	59.42
	E	201.488	113.2
Wave Bending Full	F	–	–
	E		
Wave Bending Ballst	F	–	–
	E		
Load Unload	F	42.532	–
	E	42.532	

Note : F Curve   Standard Weld
         E Curve   Improved Weld

Fatigue Life for F Curve : 53.76 years
Fatigue Life for E Curve : 102.41 years

Table 2.2.2

Typical CSD and Hotspot

L. FHD LONG.

Load Component	S-N	Stress Range	Fatigue Life
Pressure Full	F	259.7	27.75
	E	259.7	52.86
Pressure Ballast	F	201.586	59.33
	E	201.586	113.03
Wave Bending Full	F	–	–
	E		
Wave Bending Ballst	F	–	–
	E		
Load Unload	F	154.938	–
	E	154.938	

Note : F Curve   Standard Weld
         E Curve   Improved Weld

Fatigue Life for F Curve : 37.81 years
Fatigue Life for E Curve : 72.046 years

Table 2.2.3

Typical CSD and Hotspot

Load Component	S-N	Stress Range	Fatigue Life
Pressure Full	F2	50.372	2754.95
	F	50.372	3802.89

A-13

91

L BHD LONG.
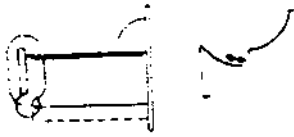
Pressure Ballast	F2 F	35.476 35.476	7886.38 10885.2
Wave Bending Full	F2 F	–	–
Wave Bending Ballst	F2 F	–	–
Load Unload	F2 F	82.124 82.124	–

Note: F2 Curve — Standard Weld
F Curve — Improved Weld

Fatigue Life for F2 Curve : 4084.96 years
Fatigue Life for F Curve : 5640.16 years

Typical CSD and Hotspot

BHD LONG.

Table 2.2.4
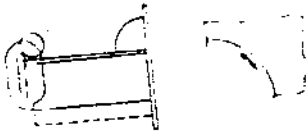
Load Component	S-N	Stress Range	Fatigue Life
Pressure Full	C	480.592	28.32
Pressure Ballast	C	363.972	74.93
Wave Bending Full	C	–	–
Wave Bending Ballst	C	–	–
Load Unload	C	139.552	–

Note: C Curve — Standard Weld
Improved Weld

Fatigue Life for C Curve : 41.1 years

Typical CSD and Hotspot
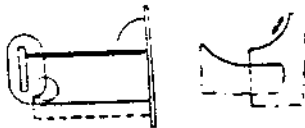
L. BHD LONG.

Table 2.2.5

Load Component	S-N	Stress Range	Fatigue Life
Pressure Full	F2 F	246.862 246.862	23.4 32.3
Pressure Ballast	F2 F	171.794 171.794	69.44 95.86
Wave Bending Full	F2 F	–	–
Wave Bending Ballst	F2 F	–	–

92

| Load Unload | F2 | 245.588 | – |
| | F | 245.588 | |

Note:F2 Curve   Standard Weld
F Curve   Improved Weld

Fatigue Life for F2 Curve : 35 years
Fatigue Life for F Curve : 48.31 years

L45 - Slot on LongBHD Longitudinal

Design Fatigue Life = 20 year
Weibull Parameter = 0.942
Number of Cycles $N = 1 \times 10^{8}$
$N_{Full} = 0.5 \times 10^{8}$ $N_{Ballast} = 0.5 \times 10^{8}$
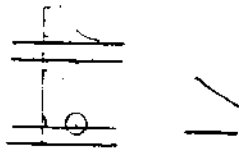Load and unload N = 500

Table 2.3.1

Typical CSD and Hotspot

L. BHD LONG.

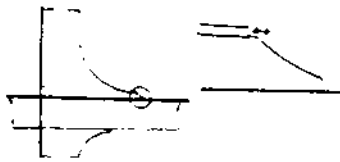| Load Component	S-N	Stress Range	Fatigue Life
Pressure Full	F	204.624	56.73
	E	204.624	108.07
Pressure Ballast	F	147.098	152.7
	E	147.098	290.9
Wave Bending Full	F	–	–
	E		
Wave Bending Ballst	F	–	–
	E		
Load Unload	F	185.122	–
	E	185.122	

Note : F Curve   Standard Weld
E Curve   Improved Weld

Fatigue Life for F Curve : 82.7 years
Fatigue Life for E Curve : 157.6 years

Table 2.3.2

Typical CSD and Hotspot
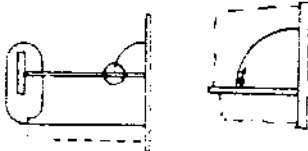
L. BHD LONG.

Load Component	S-N	Stress Range	Fatigue Life
Pressure Full	F	150.332	143.06
	E	150.332	272.54
Pressure Ballast	F	95.486	558.75
	E	95.486	1064.43
Wave Bending Full	F	–	–
	E		

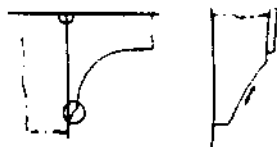| Wave Bending Ballst | F
E | – | – |
| Load Unload | F
E | 252.742
252.742 | – |

Note : F Curve   Standard Weld
        E Curve   Improved Weld

Fatigue Life for F Curve : 227.8 years
Fatigue Life for E Curve : 434.03 years

Table 2.3.3

Typical CSD and Hotspot

! BHL LONG.
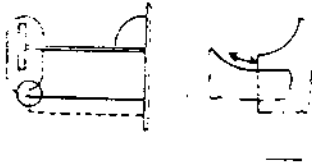
Load Component	S-N	Stress Range	Fatigue Life
Pressure Full	F2 F	187.964 187.964	53.02 73.2
Pressure Ballast	F2 F	157.094 157.094	90.82 125.37
Wave Bending Full	F2 F	–	–
Wave Bending Ballst	F2 F	–	–
Load Unload	F2 F	343.392 343.392	–

Note:F2 Curve   Standard Weld
      F Curve   Improved Weld

Fatigue Life for F2 Curve : 66.955 years
Fatigue Life for F Curve : 92.43 years

Table 2.3.4

Typical CSD and Hotspot

! BHD LONG.

Load Component	S-N	Stress Range	Fatigue Life
Pressure Full	C	189.238	739.35
Pressure Ballast	C	148.078	1744.46
Wave Bending Full	C	–	–
Wave Bending Ballst	C	–	–
Load Unload	C	366.814	–

Note:C Curve   Standard Weld
                  Improved Weld

L46 - Slot on LongBHD Longitudinal

Design Fatigue Life = 20 year
Weibull Parameter = 0.942
Number of Cycles N= 1 x 10^8
NFull= 0.5 x 10^8 NBallast= 0.5x 10^8
Load and unload N =500

Typical CSD and Hotspot

L. BHD LONG.
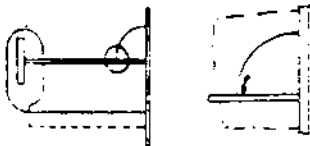
Table 2.4.1

Load Component	S-N	Stress Range	Fatigue Life
Pressure Full	F	78.694	997.37
	E	78.694	1900.0
Pressure Ballast	F	50.176	3847.63
	E	50.176	7329.82
Wave Bending Full	F	–	–
	E		
Wave Bending Ballst	F	–	–
	E		
Load Unload	F	22.05	–
	E	22.05	

Note : F Curve   Standard Weld
E Curve   Improved Weld

Fatigue Life for F Curve : 1584.28 years
Fatigue Life for E Curve : 3018.4 years

Typical CSD and Hotspot

L. BHD LONG.

Table 2.4.2

Load Component	S-N	Stress Range	Fatigue Life
Pressure Full	F	14.994	–
	E	14.994	
Pressure Ballast	F	31.752	–
	E	31.752	
Wave Bending Full	F	–	–
	E		
Wave Bending Ballst	F	–	–
	E		
Load Unload	F	7.056	–
	E	7.056	

Note : F Curve   Standard Weld
E Curve   Improved Weld

Table 2.4.3

Typical CSD and Hotspot

L. BHD LONG.
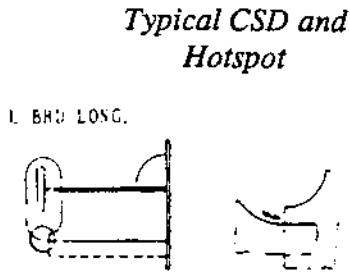
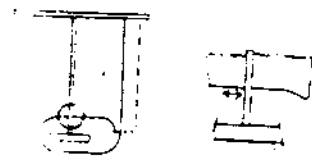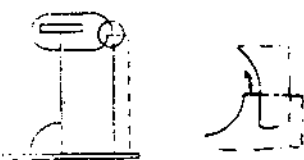| Load Component	S-N	Stress Range	Fatigue Life
Pressure Full	F2	186.592	54.2
	F	186.592	74.8
Pressure Ballast	F2	112.896	244.7
	F	112.896	337.8
Wave Bending Full	F2	–	–
	F		
Wave Bending Ballst	F2	–	–
	F		
Load Unload	F2	77.48	–
	F	77.48	

Note:F2 Curve   Standard Weld
      F Curve   Improved Weld

Fatigue Life foe F2 Curve : 88.74 years
Fatigue Life for F Curve : 122.48 years

Table 2.4.4

Typical CSD and Hotspot

L. BHD LONG.
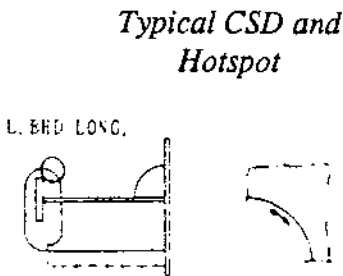
Load Component	S-N	Stress Range	Fatigue Life
Pressure Full	C	389.158	59.3
Pressure Ballast	C	232.946	357.26
Wave Bending Full	C	–	–
Wave Bending Ballst	C	–	–
Load Unload	C	89.278	–

Note:C Curve   Standard Weld
               Improved Weld

Fatigue Life for C Curve : 101.73 years

Table 2.4.5

Typical CSD and Hotspot
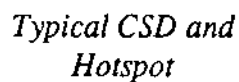
Load Component	S-N	Stress Range	Fatigue Life
Pressure Full	F2	369.264	6.99
	F	369.264	9.65

L. BHD LONG.
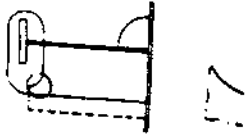
Pressure Ballast	F2 F	233.044 233.044	27.82 38.4
Wave Bending Full	F2 F	–	–
Wave Bending Ballst	F2 F	–	–
Load Unload	F2 F	132.594 132.594	–

Note:F2 Curve   Standard Weld
      F Curve   Improved Weld

Fatigue Life for F2 Curve : 11.17 years
Fatigue Life for F Curve : 15.42 years

L37 -Long.BKT. (Ord.T.Ring)

Design Fatigue Life = 20 year
Weibull Parameter = 0.942
Number of Cycles $N = 1 \times 10^8$
$N_{Full} = 0.5 \times 10^8$ $N_{Ballast} = 0.5 \times 10^8$
Load and unload $N = 500$

Table 3.1.1

Typical CSD and Hotspot

S. SHELL

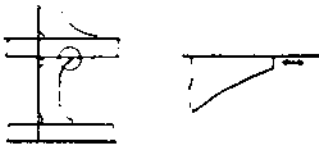| Load Component	S-N	Stress Range	Fatigue Life
Pressure Full	F2 F	161.112 161.112	84.2 116.2
Pressure Ballast	F2 F	145.04 145.04	115.4 159.3
Wave Bending Full	F2 F	–	–
Wave Bending Ballst	F2 F	–	–
Load Unload	F2 F	125.538 125.538	–

Note:F2 Curve   Standard Weld
      F Curve   Improved Weld

Fatigue Life for F2 Curve : 97.34 years
Fatigue Life for F Curve : 134.37 years

Table 3.1.2

Typical CSD and Hotspot

Load Component	S-N	Stress Range	Fatigue Life

S. SHELL
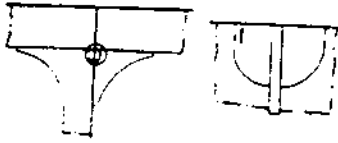
Load Component	S-N	Stress Range	Fatigue Life
Pressure Full	F2	157.584	89.88
	F	157.584	124.2
Pressure Ballast	F2	122.99	189.27
	F	122.99	261.26
Wave Bending Full	F2	–	–
	F		
Wave Bending Ballst	F2	–	–
	F		
Load Unload	F2	123.872	–
	F	123.872	

Note: F2 Curve   Standard Weld
     F Curve   Improved Weld

Fatigue Life for F2 Curve : 121.88 years
Fatigue Life for F Curve : 168.35 years

Typical CSD and Hotspot

S. SHELL

Table 3.1.3
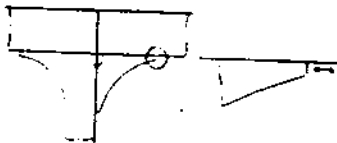
Load Component	S-N	Stress Range	Fatigue Life
Pressure Full	F2	154.448	95.57
	F	154.448	131.93
Pressure Ballast	F2	172.774	68.27
	F	172.774	94.24
Wave Bending Full	F2	–	–
	F		
Wave Bending Ballst	F2	–	–
	F		
Load Unload	F2	177.086	–
	F	177.086	

Note: F2 Curve   Standard Weld
     F Curve   Improved Weld

Fatigue Life for F2 Curve : 80.32 years
Fatigue Life for F Curve : 109.94 years

Typical CSD and Hotspot

L. BHD

Table 3.1.4

Load Component	S-N	Stress Range	Fatigue Life
Pressure Full	F	67.228	1599.67
	E	67.228	3047.41
Pressure Ballast	F	90.944	646.12
	E	90.944	1231.0
Wave Bending Full	F	–	–
	E		

98

Wave Bending Ballst	F	–	–
	E		
Load Unload	F	188.16	–
	E	188.16	

Note: F Curve   Standard Weld
E Curve   Improved Weld

Fatigue Life for F Curve : 920.8 years
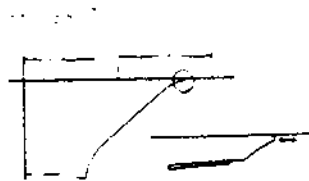**Fatigue Life for E Curve : 1754.38 years**

Typical CSD and Hotspot
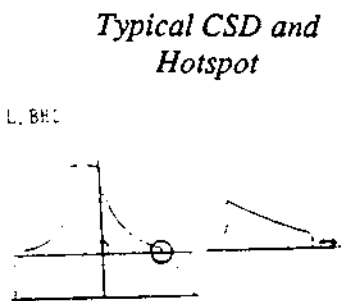
L. BHⅭ

Table 3.1.5

Load Component	S-N	Stress Range	Fatigue Life
Pressure Full	F2	72.912	908.416
	F	72.912	1253.96
Pressure Ballast	F2	84.574	582.0
	F	84.574	803.5
Wave Bending Full	F2	–	–
	F		
Wave Bending Ballst	F2	–	–
	F		
Load Unload	F2	214.032	–
	F	214.032	

Note: F2 Curve   Standard Weld
F Curve   Improved Weld

Fatigue Life for F2 Curve : 709.22 years
Fatigue Life for F Curve : 979.43 years

L46 -Long.BKT. (Ord.T.Ring)

Design Fatigue Life = 20 year
Weibull Parameter = 0.942
Number of Cycles $N = 1 \times 10^8$
$N_{Full} = 0.5 \times 10^8$ $N_{Ballast} = 0.5 \times 10^8$
Load and unload $N = 500$

Table 3.2.1

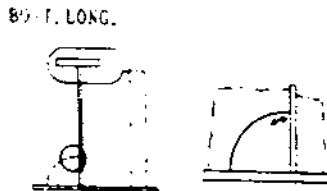*Typical CSD and Hotspot*

Load Component	S-N	Stress Range	Probability
Pressure Full	F2	66.052	1221.87
	F	66.052	1686.65
Pressure Ballast	F2	28.91	–
	F	28.91	

A-21

99
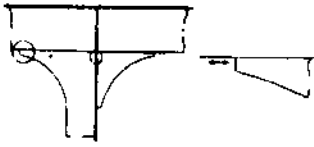
Wave Bending Full	F2 F	–	–
Wave Bending Ballst	F2 F	–	–
Load Unload	F2 F	50.764 50.764	–

Note: F2 Curve   Standard Weld
       F Curve   Improved Weld

Fatigue Life for F2 Curve : 2443.74 years
Fatigue Life for F Curve : 3373.3 years

Table 3.2.2

Typical CSD and Hotspot

S. SHELL
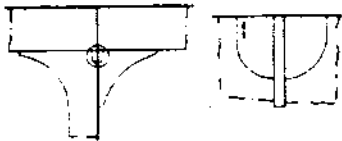
Load Component	S-N	Stress Range	Fatigue Life
Pressure Full	F2 F	144.256 144.256	117.3 161.9
Pressure Ballast	F2 F	92.12 92.12	450.422 621.756
Wave Bending Full	F2 F	–	–
Wave Bending Ballst	F2 F	–	–
Load Unload	F2 F	84.28 84.28	–

Note: F2 Curve   Standard Weld
       F Curve   Improved Weld

Fatigue Life for F2 Curve : 186.05 years
Fatigue Life for F Curve : 257.07 years

Table 3.2.3

Typical CSD and Hotspot
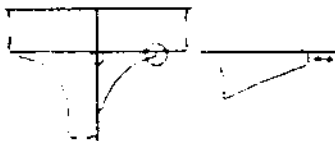
S. SHELL

Load Component	S-N	Stress Range	Fatigue Life
Pressure Full	F2 F	54.096 54.096	–
Pressure Ballast	F2 F	32.144 32.144	–
Wave Bending Full	F2 F	–	–
Wave Bending Ballst	F2 F	–	–
Load Unload	F2 F	73.5 73.5	–

100

Typical CSD and Hotspot

S. SHELL LONG.
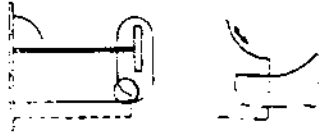
Table 1.4.5

Load Component	S-N	Stress Range	Fatigue Life
Pressure Full	F2	514.304	2.58
	F	514.304	4.32
Pressure Ballast	F2	323.89	3.57
	F	323.89	5.89
Wave Bending Full	F2	--	--
	F		
Wave Bending Ballst	F2	--	--
	F		
Load Unload	F2	19.502	--
	F	19.502	

Note: F2 Curve   Standard Weld
        F Curve   Improved Weld

Fatigue Life for F2 Curve : 3 years
**Fatigue Life for F Curve : 5 years**

L36 - Slot on LongBHD Longitudinal

Design Fatigue Life = 20 year
Weibull Parameter = 0.942
Number of Cycles $N = 1 \times 10^8$
$N_{Full} = 0.5 \times 10^8$ $N_{Ballast} = 0.5 \times 10^8$
Load and unload N =500

Typical CSD and Hotspot

L. BHD LONG.
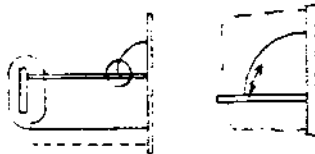
Table 2.1.1

Load Component	S-N	Stress Range	Fatigue Life
Pressure Full	F	90.062	665.36
	E	90.062	1267.53
Pressure Ballast	F	65.562	1724.75
	E	65.562	3285.68
Wave Bending Full	--	--	--
Wave Bending Ballst	--	--	--
Load Unload	F	116.62	--
	E	116.62	

Note : F Curve   Standard Weld
       E Curve   Improved Weld

Fatigue Life for F Curve : 960.43 years
Fatigue Life for E Curve : 1829.8 years

89

Load Unload	F	49.196	–
	E	49.196	

Note : F Curve   Standard Weld
        E Curve   Improved Weld

Fatigue Life for F Curve : 455.58 years
Fatigue Life for E Curve : 867.98 years

Table 1.4.3

Typical CSD and Hotspot

S. SHELL LONG.
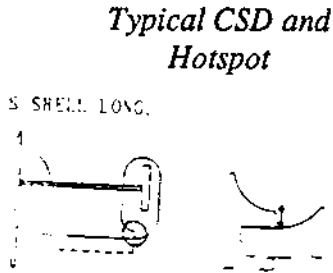
Load Component	S-N	Stress Range	Fatigue Life
Pressure Full	F2	87.122	532.47
	F	87.122	735.02
Pressure Ballast	F2	54.684	2153.28
	F	54.684	2979.32
Wave Bending Full	F2	–	–
	F		
Wave Bending Ballst	F2	–	–
	F		
Load Unload	F2	4.01	–
	F	4.01	

Note:F2 Curve   Standard Weld
        F Curve   Improved Weld

Fatigue Life for F2 Curve : 853.82 years
Fatigue Life for F Curve : 1179.2 years

Table 1.4.4

Typical CSD and Hotspot

S. SHELL LONG.
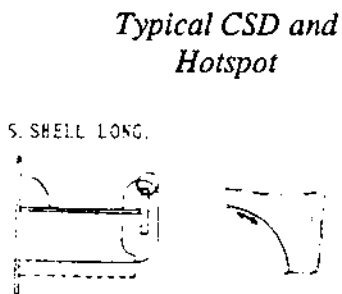
Load Component	S-N	Stress Range	Fatigue Life
Pressure Full	C	392.392	57.6
Pressure Ballast	C	253.428	266.
Wave Bending Full	C	–	–
Wave Bending Ballst	C	–	–
Load Unload	C	17.052	–

Note:C Curve   Standard Weld
                 Improved Weld

Fatigue Life for C Curve : 94.7 years

88

Table 3.2.4

Typical CSD and Hotspot

L. BHC
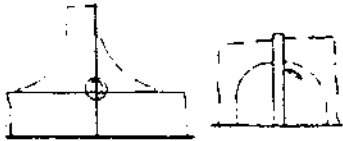
Load Component	S-N	Stress Range	Fatigue Life
Pressure Full	F	64.68	–
	E	64.68	
Pressure Ballast	F	49.392	–
	E	49.392	
Wave Bending Full	F	–	–
	E		
Wave Bending Ballst	F	–	–
	E		
Load Unload	F	51.058	–
	E	51.058	

Note:C Curve   Standard Weld
             Improved Weld

Fatigue Life for F Curve : - years
Fatigue Life for E Curve : - years

Table 3.2.5

Typical CSD and Hotspot

L. BHC
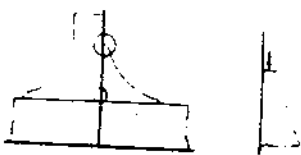
Load Component	S-N	Stress Range	Fatigue Life
Pressure Full	F2	68.208	–
	F	62.208	
Pressure Ballast	F2	46.942	–
	F	46.942	
Wave Bending Full	F2	–	–
	F		
Wave Bending Ballst	F2	–	–
	F		
Load Unload	F2	71.344	–
	F	71.344	

Note:F2 Curve   Standard Weld
       F Curve   Improved Weld

Fatigue Life for F2 Curve - years
Fatigue Life for F Curve - years

Design Fatigue Life = 20 year
Weibull Parameter = 0.979
Number of Cycles N= 1 x 10 ^{8}
NPull= 0.5 x 10 ^{8} NBallast= 0.5x 10 ^{8}
Load and unload N =500

Table 3.3.1

Typical CSD and Hotspot

S. SHELL
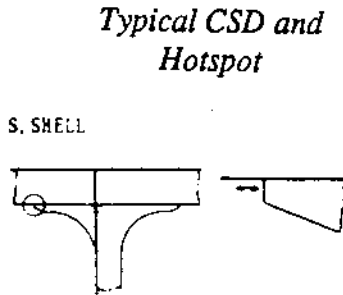
Load Component	S-N	Stress Range	Fatigue Life
Pressure Full	F2	319.774	8.86
	F	319.114	12.23
Pressure Ballast	F2	227.85	24.5
	F	227.85	33.8
Wave Bending Full	F2	–	–
	F		
Wave Bending Ballst	F2	–	–
	F		
Load Unload	F2	87.906	–
	F	87.906	

Note:F2 Curve   Standard Weld
     F Curve   Improved Weld

Fatigue Life for F2 Curve : 13.01 years
Fatigue Life for F Curve : 17.96 years

Table 3.3.2

Typical CSD and Hotspot

S. SHELL
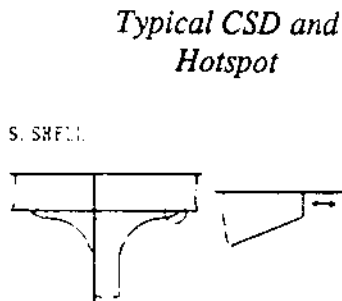
Load Component	S-N	Stress Range	Fatigue Life
Pressure Full	F2	279.986	13.2
	F	279.986	18.2
Pressure Ballast	F2	184.828	45.87
	F	184.828	63.32
Wave Bending Full	F2	–	–
	F		
Wave Bending Ballst	F2	–	–
	F		
Load Unload	F2	80.458	–
	F	80.458	

Note:F2 Curve   Standard Weld
     F Curve   Improved Weld

Fatigue Life for F2 Curve : 20.5 years
Fatigue Life for F Curve : 28.27 years

102

Table 3.3.3

Typical CSD and Hotspot

S. SHELL
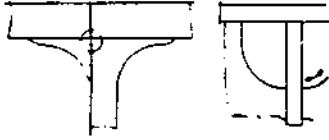
Load Component	S-N	Stress Range	Fatigue Life
Pressure Full	F	324.674	11.68
	E	324.674	22.25
Pressure Ballast	F	223.93	35.6
	E	223.93	67.8
Wave Bending Full	F	–	–
	E		
Wave Bending Ballst	F	–	–
	E		
Load Unload	F	109.956	–
	E	109.956	

Note: F Curve   Standard Weld
       E Curve   Improved Weld

Fatigue Life for F Curve : 17.59 years
Fatigue Life for E Curve : 33.5 years

Table 3.3.4

Typical CSD and Hotspot

L. BH
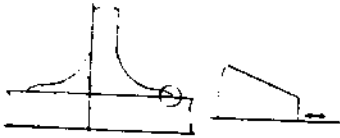
Load Component	S-N	Stress Range	Fatigue Life
Pressure Full	F2	193.844	39.76
	F	193.844	54.89
Pressure Ballast	F2	127.694	47.46
	F	127.694	192.02
Wave Bending Full	F2	–	–
	F		
Wave Bending Ballst	F2	–	–
	F		
Load Unload	F2	182.182	–
	F	182.182	

Note: F2 Curve   Standard Weld
       F Curve   Improved Weld

Fatigue Life for F2 Curve : 43.27 years
Fatigue Life for F Curve : 85.368 years

Table 3.3.5

Typical CSD and Hotspot

Load Component	S-N	Stress Range	Fatigue Life
Pressure Full	F	231.574	32.2
	E	231.574	61.33
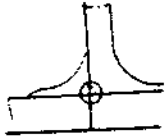
Load Component	S-N	Stress Range	Fatigue Life
Pressure Ballast	F	165.228	88.63
	E	165.228	168.85
Wave Bending Full	F	–	–
	E		
Wave Bending Ballst	F	–	–
	E		
Load Unload	F	284.2	⸱
	E	284.2	

Note: F Curve   Standard Weld
      E Curve   Improved Weld

Fatigue Life for F Curve : 47.24 years
Fatigue Life for E Curve : 89.98 years

L.45 -Long.BKT. (T.BHD)

Design Fatigue Life = 20 year
Weibull Parameter = 0.979
Number of Cycles $N = 1 \times 10^{8}$
$N_{Full} = 0.5 \times 10^{8}$ $N_{Ballast} = 0.5 \times 10^{8}$
Load and unload N = 500

Table 3.4.1

Typical CSD and Hotspot

S. SHELL
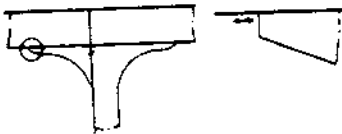
Load Component	S-N	Stress Range	Fatigue Life
Pressure Full	F2	253.82	17.7
	F	253.82	24.45
Pressure Ballast	F2	146.6	91.9
	F	146.6	126.9
Wave Bending Full	F2	–	–
	F		
Wave Bending Ballst	F2	–	–
	F		
Load Unload	F2	24.402	–
	F	24.402	

Note: F2 Curve   Standard Weld
      F Curve   Improved Weld

Fatigue Life for F2 Curve : 29.68 years
Fatigue Life for F Curve : 41 years

Table 3.4.2

Typical CSD and Hotspot

Load Component	S-N	Stress Range	Fatigue Life

S. SHELL
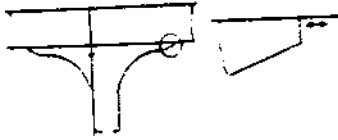
Load Component	S-N	Stress Range	Fatigue Life
Pressure Full	F2	202.664	34.8
	F	202.664	48.03
Pressure Ballast	F2	113.778	196.646
	F	113.778	271.448
Wave Bending Full	F2	–	–
	F		
Wave Bending Ballst	F2	–	–
	F		
Load Unload	F2	27.342	–
	F	27.342	

Note: F2 Curve   Standard Weld
F Curve   Improved Weld

Fatigue Life for F2 Curve : 59.13 years
Fatigue Life for F Curve : 81.62 years

Table 3.4.3

Typical CSD and Hotspot

S. SHELL

Load Component	S-N	Stress Range	Fatigue Life
Pressure Full	F	307.8	6.6
	E	307.8	9.1
Pressure Ballast	F	186.102	44.93
	E	186.102	62.03
Wave Bending Full	F	–	–
	E		
Wave Bending Ballst	F	–	–
	E		
Load Unload	F	67.228	–
	E	67.228	

Note: F Curve   Standard Weld
E Curve   Improved Weld

Fatigue Life for F2 Curve : 11.51 years
Fatigue Life for F Curve : 15.87 years

Table 3.4.4

Typical CSD and Hotspot

L. BHD

Load Component	S-N	Stress Range	Fatigue Life
Pressure Full	F2	221.578	26.02
	F	221.578	36.75
Pressure Ballast	F2	142.982	99.08
	F	142.982	136.78
Wave Bending Full	F2	–	–
	F		

105

Wave Bending Ballst	F2 F	–	–
Load Unload	F2 F	151.41 151.41	–

Note: F2 Curve — Standard Weld
F Curve — Improved Weld

Fatigue Life for F2 Curve : 41.216 years
Fatigue Life for F Curve : 57.93 years

Typical CSD and Hotspot

L. BHD

Table 3.4.5

Load Component	S-N	Stress Range	Fatigue Life
Pressure Full	F E	220.598 220.598	26.98 37.24
Pressure Ballast	F E	146.118 146.118	92.84 128.16
Wave Bending Full	F E	–	–
Wave Bending Ballst	F E	–	–
Load Unload	F E	205.72 205.72	–

Note: F Curve — Standard Weld
E Curve — Improved Weld

Fatigue Life for F Curve : 41.81 years
Fatigue Life for E Curve : 57.71 years

L36 -Long.BKT. (N0.1 H.G)

Design Fatigue Life = 20 year
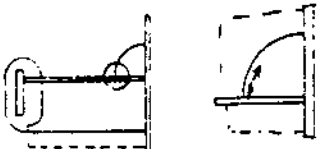Weibull Parameter = 0.942
Number of Cycles $N = 1 \times 10^8$
$N_{Full} = 0.5 \times 10^8$ $N_{Ballast} = 0.5 \times 10^8$
Load and unload N = 500
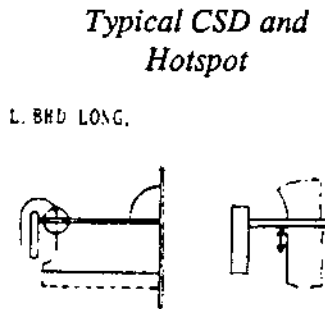
Table 4.1.1

Typical CSD and Hotspot

Load Component	S-N	Stress Range	Fatigue Life
Pressure Full	F E	32.83 32.83	–
Pressure Ballast	F E	65.072 65.072	–

S. SHELL

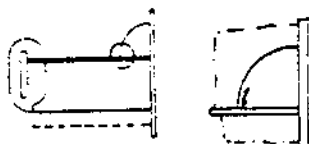| Wave Bending Full	F		
	E	–	–
Wave Bending Ballst	F	–	–
	E		
Load Unload	F	57.232	
	E	57.232	–

Note:F Curve   Standard Weld
    E Curve   Improved Weld

Fatigue Life for F Curve : - years
Fatigue Life for E Curve : - years

Table 4.1.2

Typical CSD and Hotspot

S. SHELL
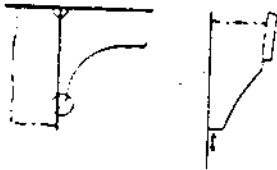
Load Component	S-N	Stress Range	Fatigue Life
Pressure Full	F	46.354	
	E	46.354	–
Pressure Ballast	F	19.796	
	E	19.796	–
Wave Bending Full	F	–	–
	E		
Wave Bending Ballst	F	–	–
	E		
Load Unload	F	98.882	
	E	98.882	–

Note:F Curve   Standard Weld
    E Curve   Improved Weld

Fatigue Life for F2 Curve : - years
Fatigue Life for F Curve : - years

Table 4.1.3

Typical CSD and Hotspot

L. SHL.
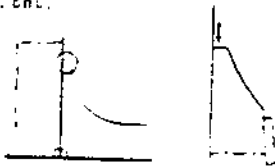
Load Component	S-N	Stress Range	Fatigue Life
Pressure Full	F	50.176	3164.99
	E	50.176	6029.38
Pressure Ballast	F	70.07	1162.16
	E	70.07	2213.93
Wave Bending Full	F	–	–
	E		
Wave Bending Ballst	F	–	–
	E		
Load Unload	F	50.764	
	E	50.764	–

101

Fatigue Life for F Curve :1695.2 years
Fatigue Life for E Curve : 3239.4 years

Table 4.1.4

Typical CSD and Hotspot

.. BHD.
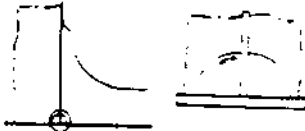
Load Component	S-N	Stress Range	Fatigue Life
Pressure Full	F	31.556	–
	E	31.556	
Pressure Ballast	F	19.796	–
	E	19.796	
Wave Bending Full	F	–	–
	E		
Wave Bending Ballst	F	–	–
	E		
Load Unload	F	98.882	–
	E	98.882	

Note:F Curve   Standard Weld
      E Curve   Improved Weld

Fatigue Life for F Curve : - years
Fatigue Life for E Curve : - years

Table 4.1.5

Typical CSD and Hotspot

S. SHELL

Load Component	S-N	Stress Range	Fatigue Life
Pressure Full	F	95.256	462.57
	E	95.256	881.22
Pressure Ballast	F	80.948	753.77
	E	80.948	1435.96
Wave Bending Full	F	–	–
	E		
Wave Bending Ballst	F	–	–
	E		
Load Unload	F	106.33	–
	E	106.33	

Note:F Curve   Standard Weld
      E Curve   Improved Weld

Fatigue Life for F Curve : 573.33 years
Fatigue Life for E Curve : 1092.42 years

Design Fatigue Life = 20 year
Weibull Parameter = 0.942
Number of Cycles N= 1 x 10^8
NFull= 0.5 x 10^8 NBallast= 0.5x 10^8
Load and unload N =500

Table 4.2.1

Typical CSD and
Hotspot

S. SHELL
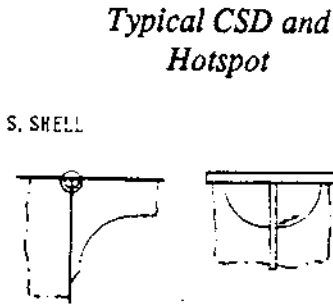
Load Component	S-N	Stress Range	Fatigue Life
Pressure Full	F	90.944	531.54
	E	90.944	1012.6
Pressure Ballast	F	110.152	299.15
	E	110.152	569.88
Wave Bending Full	F	–	–
	E		
Wave Bending Ballst	F	–	–
	E		
Load Unload	F	23.128	–
	E	23.128	

Note:F Curve   Standard Weld
E Curve   Improved Weld

Fatigue Life for F Curve : 382.85 years
Fatigue Life for E Curve : 729.4 years

Table 4.2.2

Typical CSD and
Hotspot

S. SHELL
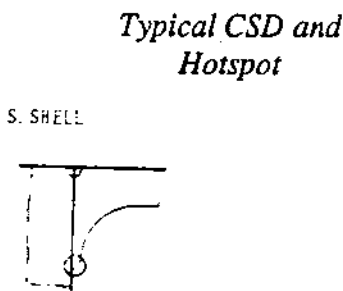
Load Component	S-N	Stress Range	Fatigue Life
Pressure Full	F	64.288	1504.77
	E	64.288	2866.63
Pressure Ballast	F	45.864	4144.24
	E	45.864	7894.87
Wave Bending Full	F	–	–
	E		
Wave Bending Ballst	F	–	–
	E		
Load Unload	F	54.88	–
	E	54.88	

109

Fatigue Life for F Curve : 2208 years
Fatigue Life for E Curve : 4207 years

Typical CSD and Hotspot

L. BHD
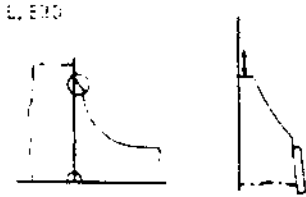
Table 4.2.3

Load Component	S-N	Stress Range	Fatigue Life
Pressure Full	F	39.004	–
	E	39.004	
Pressure Ballast	F	34.006	–
	E	34.006	
Wave Bending Full	F	–	–
	E		
Wave Bending Ballst	F	–	–
	E		
Load Unload	F	61.25	–
	E	61.25	

Note:F Curve   Standard Weld
E Curve   Improved Weld

Fatigue Life for F Curve : - years
Fatigue Life for E Curve : - years

Typical CSD and Hotspot

L. BHD

Table 4.2.4

Load Component	S-N	Stress Range	Fatigue Life
Pressure Full	F	110.25	289.35
	E	110.25	568.36
Pressure Ballast	F	132.398	172.27
	E	132.398	328.18
Wave Bending Full	F	–	–
	E		
Wave Bending Ballst	F	–	–
	E		
Load Unload	F	38.122	–
	E	38.122	

Note:F Curve   Standard Weld
E Curve   Improved Weld

Fatigue Life for F Curve : 215.96 years
Fatigue Life for E Curve : 416.11 years

110

Typical CSD and Hotspot

BOTT. LONG.
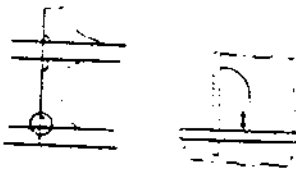
Table 4.2.5

Load Component	S-N	Stress Range	Fatigue Life
Pressure Full	F	139.35	147.75
	E	139.35	281.47
Pressure Ballast	F	95.746	455.5
	E	95.746	867.76
Wave Bending Full	F	–	–
	E		
Wave Bending Ballst	F	–	–
	E		
Load Unload	F	79.576	–
	E	79.576	

Note: F Curve   Standard Weld
        E Curve   Improved Weld

Fatigue Life for F Curve : 223.13 years
Fatigue Life for E Curve : 425.1 years

L.15 -Long.BKT.

Design Fatigue Life = 20 year
Weibull Parameter = 0.849
Number of Cycles N= 1 x 10 ^{8}
N_{Full}= 0.5 x 10 ^{8} $N_{Ballast}$= 0.5x 10 ^{8}
Load and unload N =500

Typical CSD and Hotspot

DK. LONG.

Table 5.1.1
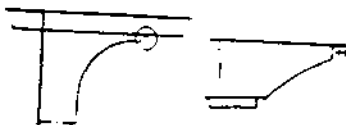
Load Component	S-N	Stress Range	Fatigue Life
Pressure Full	F2	171.892	119.5
	F	171.892	164.95
Pressure Ballast	F2	131.124	269.2
	F	131.124	371.6
Wave Bending Full	F2	243.628	42
	F	243.628	58
Wave Bending Ballst	F2	326.732	17.4
	F	326.732	24.02
Load Unload	F2	15.19	–
	F	15.19	

Note: F2 Curve   Standard Weld
        F Curve   Improved Weld

Fatigue Life for F2 Curve : - years
Fatigue Life for F Curve : - years

111

Table 5.1.2

Typical CSD and Hotspot

DK. LONG.
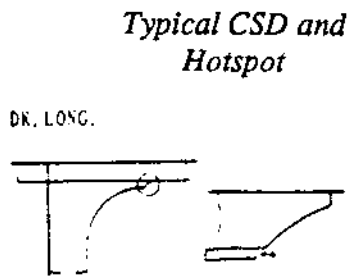
Load Component	S-N	Stress Range	Fatigue Life
Pressure Full	F	100.94	2345.46
	E	100.94	4468.15
Pressure Ballast	F	70.952	814.6
	E	70.952	1551.8
Wave Bending Full	F	98.392	879.5
	E	98.392	1675.5
Wave Bending Ballst	F	113.68	576.256
	E	113.68	1086.35
Load Unload	F	12.838	—
	E	12.838	

Note:F Curve   Standard Weld
       E Curve   Improved Weld

Fatigue Life for F Curve : 883.94 years
Fatigue Life for E Curve : 1677 years

L.15 -Long.BKT.

Design Fatigue Life = 20 year
Weibull Parameter = 0.899
Number of Cycles $N = 1 \times 10^8$
$N_{Full} = 0.5 \times 10^8$ $N_{Ballast} = 0.5 \times 10^8$
Load and unload N = 500

Table 5.2.1

Typical CSD and Hotspot

INN. BUTT. LONG.
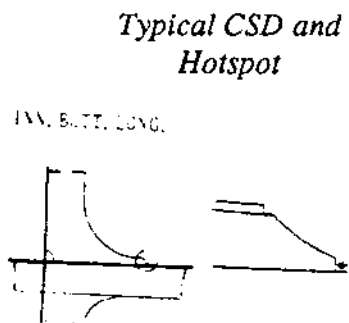
Load Component	S-N	Stress Range	Fatigue Life
Pressure Full	F2	63.896	1718.6
	F	63.896	2372.4
Pressure Ballast	F2	86.828	684.9
	F	86.828	945.4
Wave Bending Full	F2	164.836	100.1
	F	164.836	138.2
Wave Bending Ballst	F2	190.512	64.84
	F	190.512	89.5
Load Unload	F2	17.836	—
	F	17.836	

Note:F2 Curve   Standard Weld
      F Curve   Improved Weld

A-34

BOTT. LONG.

Pressure	F	81.83	1129.44
Full	E	81.83	2151.62
Pressure	F	91.14	817.47
Ballast	E	91.14	1557.31
Wave Bending	F	104.076	548.97
Full	E	104.076	1045.8
Wave Bending	F	235.2	47.56
Ballst	E	235.2	90.61
Load Unload	F	124.068	–
	E	124.068	

Note: F Curve   Standard Weld
        E Curve   Improved Weld

Fatigue Life for F2 Curve : 160.28 years
Fatigue Life for F Curve : 305.4 years

Table 5.2.5

Typical CSD and Hotspot

INN. BOTT. LONG.

Load Component	S-N	Stress Range	Fatigue Life
Pressure	F	198.744	78.85
Full	E	198.774	156.2
Pressure	F	292.922	24.6
Ballast	E	292.922	46.9
Wave Bending	F	118.776	369.33
Full	E	118.776	703.58
Wave Bending	F	137.04	240.45
Ballst	E	137.04	458.1
Load Unload	F	70.168	–
	E	70.168	

Note: F Curve   Standard Weld
        E Curve   Improved Weld

Fatigue Life for F2 Curve : 66.445 years
Fatigue Life for F Curve : 127.68 years

Table 5.2.6

Typical CSD and Hotspot

S. SHELL

Load Component	S-N	Stress Range	Fatigue Life
Pressure	F	85.652	984.9
Full	E	85.652	1876.25
Pressure	F	315.07	19.78
Ballast	E	315.07	37.69
Wave Bending	F	114.856	408.45
Full	E	114.856	778.11

Wave Bending	F	132.692	264.9
Ballst	E	132.692	504.6
Load Unload	F	372.106	
	E	372.106	–

Note: F Curve   Standard Weld
E Curve   Improved Weld

Fatigue Life for F2 Curve : 69.21 years
Fatigue Life for F Curve : 131.88 years

L.15 -V.STIFF. (Ord.T.Ring)

Design Fatigue Life = 20 year
Weibull Parameter = 0.899
Number of Cycles $N = 1 \times 10^8$
$N_{Full} = 0.5 \times 10^8$ $N_{Ballast} = 0.5 \times 10^8$
Load and unload N = 500

Typical CSD and
Hotspot

INN. BOTT. LONG.

Table 6.1.1
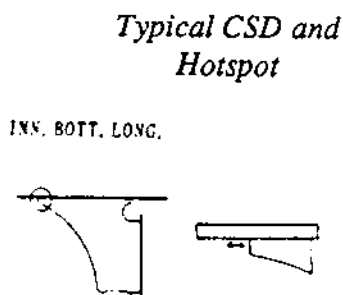
| Load Component	S-N	Stress Range	Fatigue Life
Pressure Full	F	28.91	–
	E	28.91	
Pressure Ballast	F	79.772	1219.13
	E	79.772	2322.47
Wave Bending Full	F	153.664	170.56
	E	153.664	324.93
Wave Bending Ballst	F	177.772	110.16
	E	177.772	209.85
Load Unload	F	133.28	–
	E	133.28	

Note: F Curve   Standard Weld
E Curve   Improved Weld

Fatigue Life for F2 Curve : - years
Fatigue Life for F Curve : - years

Table 6.1.2

Typical CSD and
Hotspot

Load Component	S-N	Stress Range	Fatigue Life
Pressure Full	F	85.946	974.822
	E	85.946	1857.06
Pressure Ballast	F	92.61	779.16
	E	92.61	1484.3

		Stress Range	Fatigue Life
Wave Bending Full	F	177.772	110.16
	E	177.772	209.85
Wave Bending Ballst	F	205.604	71.2
	E	205.604	135.65
Load Unload	F	416.794	–
	E	416.794	

Note: F Curve   Standard Weld
E Curve   Improved Weld

Fatigue Life for F2 Curve : 163.21 years
Fatigue Life for F Curve : 299.65 years

Table 6.1.3

Typical CSD and Hotspot
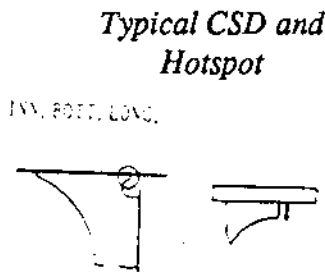
Load Component	S-N	Stress Range	Fatigue Life
Pressure Full	F	67.424	2019.1
	E	67.424	3846.4
Pressure Ballast	F	92.61	779.16
	E	92.61	1484.3
Wave Bending Full	F	166.404	134.311
	E	166.404	255.865
Wave Bending Ballst	F	192.472	86.8
	E	192.472	165.35
Load Unload	F	84.28	–
	E	84.28	

Note: F Curve   Standard Weld
E Curve   Improved Weld

Fatigue Life for F2 Curve : 192.83 years
Fatigue Life for F Curve : 367.3 years

Table 6.1.4
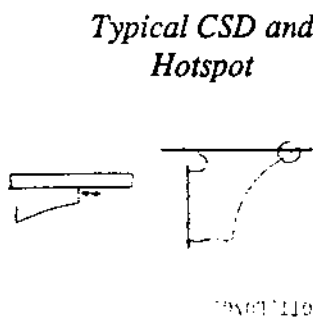
Typical CSD and Hotspot

Load Component	S-N	Stress Range	Fatigue Life
Pressure Full	F	164.052	140.17
	E	164.052	267.03
Pressure Ballast	F	283.024	27.3
	E	283.024	52.0
Wave Bending Full	F	214.424	62.77
	E	214.424	119.6
Wave Bending Ballst	F	247.94	40.6
	E	247.94	77.35
Load Unload	F	350.938	–
	E	350.938	

Load Unload	F	253.232	–
	E	253.232	

Note:F Curve   Standard Weld
     E Curve   Improved Weld

Fatigue Life for F2 Curve : 770.4 years
Fatigue Life for F Curve : 1686.34 years

Table 6.2.3

Typical CSD and Hotspot

INN BOTT. LONG.

Load Component	S-N	Stress Range	Fatigue Life
Pressure Full	F2	106.134	517.65
	F	106.134	986.14
Pressure Ballast	F2	137.2	239.63
	F	137.2	456.5
Wave Bending Full	F2	–	–
	F		
Wave Bending Ballst	F2	–	–
	F		
Load Unload	F2	545.37	–
	F	545.37	

Note:F2 Curve   Standard Weld
     F Curve   Improved Weld

Fatigue Life for F2 Curve : 327.6 years
Fatigue Life for F Curve : 624.14 years

Table 6.2.4

Typical CSD and Hotspot

BOTT LONG.

Load Component	S-N	Stress Range	Fatigue Life
Pressure Full	F	113.68	421.26
	E	113.68	802.51
Pressure Ballast	F	207.858	68.91
	E	207.858	131.28
Wave Bending Full	F	–	–
	E		
Wave Bending Ballst	F	–	–
	E		
Load Unload	F	235.572	–
	E	236.572	

Note:F2 Curve   Standard Weld
     F Curve   Improved Weld

Fatigue Life for F2 Curve : 118.4 years
Fatigue Life for F Curve : 225.65 years

Fatigue Life for F2 Curve : 145.7 years
Fatigue Life for F Curve : 201.13 years

Typical CSD and Hotspot

INN. BOTT. LONG.

Table 5.2.2
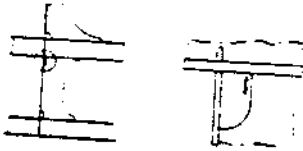
Load Component	S-N	Stress Range	Fatigue Life
Pressure Full	F	42.238	-
	E	42.238	
Pressure Ballast	F	61.25	-
	E	61.25	
Wave Bending Full	F	84.476	1026.6
	E	84.476	1955.7
Wave Bending Ballst	F	97.608	665.5
	E	97.608	1267.8
Load Unload	F	28.42	-
	E	28.42	

Note: F Curve   Standard Weld
E Curve   Improved Weld

Fatigue Life for F2 Curve : 807.56 years
Fatigue Life for F Curve : 1538.7 years

Typical CSD and Hotspot

INN. BOTT. LONG.

Table 5.2.3

Load Component	S-N	Stress Range	Fatigue Life
Pressure Full	F	83.79	1052.02
	E	83.79	2004.13
Pressure Ballast	F	126.91	302.77
	E	126.91	576.78
Wave Bending Full	F	203.448	73.5
	E	203.448	140.00
Wave Bending Ballst	F	235.2	47.56
	E	235.2	90.61
Load Unload	F	124.068	-
	E	124.068	

Note: F Curve   Standard Weld
E Curve   Improved Weld

Fatigue Life for F2 Curve : 102.87 years
Fatigue Life for F Curve : 195.96 years

Typical CSD and Hotspot

Table 5.2.4

Load Component	S-N	Stress Range	Fatigue Life

Typical CSD and Hotspot

FORE (FR.70)
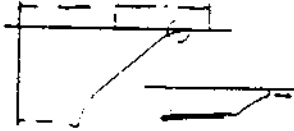
Table 7.1.4

Load Component	S-N	Stress Range	Fatigue Life
Pressure Full	F	3.234	–
	E	3.234	
Pressure Ballast	F	7.546	–
	E	7.546	
Wave Bending Full	F	–	–
	E		
Wave Bending Ballst	F	–	–
	E		
Load Unload	F	0.98	–
	E	0.98	

Note: F Curve   Standard Weld
E Curve   Improved Weld

Fatigue Life for F Curve : - years
Fatigue Life for E Curve : - years

No.2 H.Gir.

Design Fatigue Life = 20 year
Weibull Parameter = 0979
Number of Cycles $N = 1 \times 10^{8}$
$N_{Full} = 0.5 \times 10^{8}$ $N_{Ballast} = 0.5 \times 10^{8}$
Load and unload $N = 500$

Typical CSD and Hotspot

FORE (FR.70)
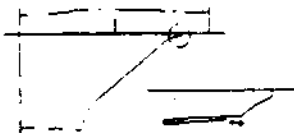
Table 7.1.1

Load Component	S-N	Stress Range	Fatigue Life
Pressure Full	F	58.604	–
	E	58.604	
Pressure Ballast	F	69.09	–
	E	69.09	
Wave Bending Full	F	–	–
	E		
Wave Bending Ballst	F	–	–
	E		
Load Unload	F	2.94	–
	E	2.94	

Note: F Curve   Standard Weld
E Curve   Improved Weld

Fatigue Life for F Curve : - years
Fatigue Life for E Curve : - years

A-41

119

Table 7.2.2

Typical CSD and Hotspot

AFT (FR.64)

Load Component	S-N	Stress Range	Fatigue Life
Pressure Full	F	29.89	—
	E	29.89	
Pressure Ballast	F	40.376	—
	E	40.376	
Wave Bending Full	F	—	—
	E		
Wave Bending Ballst	F	—	—
	E		
Load Unload	F	1.96	—
	E	1.96	

Note: F Curve   Standard Weld
       E Curve   Improved Weld

Fatigue Life for F Curve : - years
Fatigue Life for E Curve : - years

Table 7.2.3

Typical CSD and Hotspot

Load Component	S-N	Stress Range	Fatigue Life
Pressure Full	F	0.0	—
	E	0.0	
Pressure Ballast	F	0.0	—
	E		
Wave Bending Full	F	—	—
	E		
Wave Bending Ballst	F	—	—
	E		
Load Unload	F	0.0	—
	E	0.0	

Note: F Curve   Standard Weld
       E Curve   Improved Weld

Fatigue Life for F Curve : - years
Fatigue Life for E Curve : - years

Table 7.2.4

Typical CSD and Hotspot

Load Component	S-N	Stress Range	Fatigue Life
Pressure Full	F	11.172	—
	E	11.172	

FORE (FR. 70)

Pressure Ballast	F	14.7	–
	E	14.7	
Wave Bending Full	F	–	–
	E		
Wave Bending Ballst	F	–	–
	E		
Load Unload	F	0.0	' –
	E	0.0	

Note: F Curve   Standard Weld
       E Curve   Improved Weld

Fatigue Life for F Curve : - years
Fatigue Life for E Curve : - years

A-43

121

Table 6.2.5

Typical CSD and Hotspot

BOTT. LONG.

Load Component	S-N	Stress Range	Fatigue Life
Pressure Full	F	17.934	–
	E	17.934	
Pressure Ballast	F	39.004	–
	E	39.004	
Wave Bending Full	F	–	–
	E		
Wave Bending Ballst	F	–	–
	E		
Load Unload	F	142.68	–
	E	142.68	

Note: F Curve   Standard Weld
        E Curve   Improved Weld

Fatigue Life for F Curve : - years
*Fatigue Life for E Curve : - years*

No.1 H.Gir.

Design Fatigue Life = 20 year
Weibull Parameter = 0979
Number of Cycles $N = 1 \times 10^{8}$
$N_{Full} = 0.5 \times 10^{8}$ $N_{Ballast} = 0.5 \times 10^{8}$
Load and unload $N = 500$

Table 7.1.1

Typical CSD and Hotspot

B9 F. LONG.

Load Component	S-N	Stress Range	Fatigue Life
Pressure Full	F	7.448	–
	E	7.448	
Pressure Ballast	F	4.998	–
	E	4.998	
Wave Bending Full	F	–	–
	E		
Wave Bending Ballst	F	–	–
	E		
Load Unload	F	10.78	–
	E	10.78	

A-44

Table 7.1.2

Typical CSD and Hotspot

AFT (FR.64)

Load Component	S-N	Stress Range	Fatigue Life
Pressure Full	F	10.78	–
	E	10.78	
Pressure Ballast	F	5.648	–
	E	5.648	
Wave Bending Full	F	–	–
	E		
Wave Bending Ballst	F	–	–
	E		
Load Unload	F	0.98	–
	E	0.98	

Note:F Curve   Standard Weld
      E Curve   Improved Weld

Fatigue Life for F Curve : - years
Fatigue Life for E Curve : - years

Table 7.1.3

Typical CSD and Hotspot

AFT (FR.64)

Load Component	S-N	Stress Range	Fatigue Life
Pressure Full	F	12.544	–
	E	12.544	
Pressure Ballast	F	15.386	–
	E	15.386	
Wave Bending Full	F	–	–
	E		
Wave Bending Ballst	F	–	–
	E		
Load Unload	F	4.9	–
	E	4.9	

Note:F Curve   Standard Weld
      E Curve   Improved Weld

Fatigue Life for F Curve : - years
Fatigue Life for E Curve : - years

Fatigue Life for F2 Curve : 47.43 years
Fatigue Life for F Curve : 90.37 years

L.15 -Slot (Bott.Long)

Design Fatigue Life = 20 year
Weibull Parameter = 0.899
Number of Cycles $N= 1 \times 10^8$
$N_{Full}= 0.5 \times 10^8$ $N_{Ballast}= 0.5 \times 10^8$
Load and unload N =500

Typical CSD and
Hotspot

BOTT. LONG.

Table 6.2.1
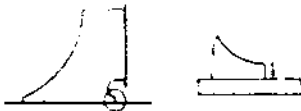
Load Component	S-N	Stress Range	Fatigue Life
Pressure Full	F2	150.136	132.5
	F	150.136	182.87
Pressure Ballast	F2	314.09	14.47
	F	314.09	19.97
Wave Bending Full	F2	–	–
	F		
Wave Bending Ballst	F2	–	–
	F		
Load Unload	F2	332.2	–
	F	332.2	

Note:F2 Curve   Standard Weld
    F Curve   Improved Weld

Fatigue Life for F2 Curve : 26.1 years
Fatigue Life for F Curve : 36 years

Table 6.2.2

Typical CSD and
Hotspot
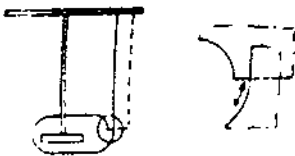
INN. BOTT. LONG.

Load Component	S-N	Stress Range	Fatigue Life
Pressure Full	F	58.114	3153.26
	E	58.114	6007.03
Pressure Ballast	F	106.232	514.77
	E	106.232	980.64
Wave Bending Full	F	–	–
	E		
Wave Bending Ballst	F	–	–
	E		

Apprendix B Results for Probabilistic Fatigue Analysis

125

Probabilistic fatigue analysis for CSDs in Proposed Double-Hull
(Service Life = 20 years)

L36 - Slot on Sideshell Longitudinal

Design Fatigue Life = 20 year
Weibull Parameter = 0.942
Number of Cycles N= 1 x 10 ^{8}
N_{Full}= 0.5 x 10 ^{8} $N_{Ballast}$= 0.5x 10 ^{8}
Load and unload N =500

Table 1.1.1

Typical CSD and Hotspot

SHELL LONG
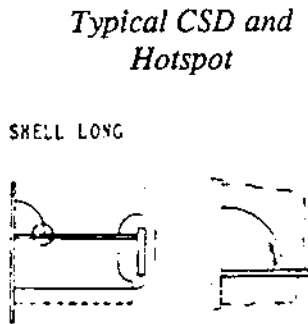
Load Component	S-N	Stress Range	Probability
Pressure Full	F	152.586	0.00004448%
	E	152.586	0.000000002%
Pressure Ballast	F	111.132	0.0
	E	111.132	0.0
Wave Bending Full	–	–	–
Wave Bending Ballst	–	–	–
Load Unload	F	46.256	0.0
	E	46.256	0.0

Note : F Curve   Standard Weld
E Curve   Improved Weld

Total Probability of Failure Pf = 0.00004448% for F Curve
**Total Probability of Failure Pf = 0.0% for E Curve**

Table 1.1.2

Typical CSD and Hotspot

S. SHELL LONG

Load Component	S-N	Stress Range	Probability
Pressure Full	F	31.85	0.0
	E	31.85	0.0
Pressure Ballast	F	96.824	0.0
	E	96.824	0.0
Wave Bending Full	–	–	–

Wave Bending Ballst	–	–	–
Load Unload	F	144.55	0.0
	E	144.55	0.0

Note : F Curve   Standard Weld
E Curve   Improved Weld

Total Probability of Failure Pf = 0.0% for F Curve
Total Probability of Failure Pf = 0.0% for E Curve

Table 1.1.3

Typical CSD and Hotspot

S SHELL LONG

Load Component	S-N	Stress Range	Probability
Pressure Full	F2	258.034	60.36%
	F	258.034	27.27%
Pressure Ballast	F2	192.668	1.807%
	F	192.668	0.1525%
Wave Bending Full	F2	–	–
	F		
Wave Bending Ballst	F2	–	–
	F		
Load Unload	F2	197.862	0.0
	F	197.862	0.0

Note:F2 Curve   Standard Weld
F Curve   Improved Weld

Total Probability of Failure Pf = 62.16% for F2 Curve
Total Probability of Failure Pf =27.4225% for F Curve

L37 - Slot on Sideshell Longitudinal

Design Fatigue Life = 20 year
Weibull Parameter = 0.942
Number of Cycles N= 1 x 10 ^{8}
NFull= 0.5 x 10 ^{8} NBallast= 0.5x 10 ^{1}
Load and unload N =500

Table 1.2.1

Typical CSD and Hotspot

Load Component	S-N	Stress Range	Probability
Pressure Full	F	178.164	0.013%
	E	178.164	0.000003411%
Pressure Ballast	F	132.3	0.000000073%
	E	132.3	0.0
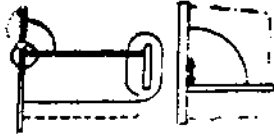
Load Component	S-N	Stress Range	Probability
Wave Bending Full	F	–	–
	E		
Wave Bending Ballst	F	–	–
	E		
Load Unload	F	35.574	0.0
	E	35.574	0.0

Note : F Curve   Standard Weld
     E Curve   Improved Weld

Total Probability of Failure Pf = 0.013% for F Curve
Total Probability of Failure Pf = 0.000003411% for E Curve

Table 1.2.2

Typical CSD and Hotspot

S. SHELL LONG.
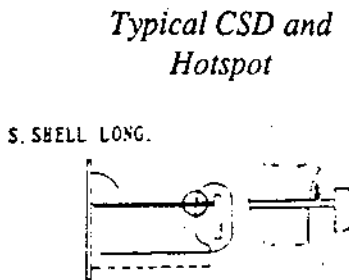
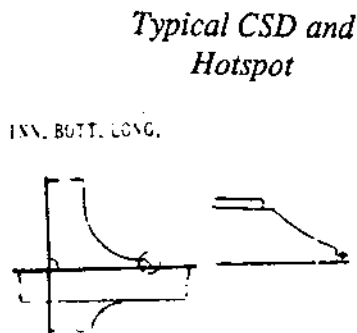| Load Component	S-N	Stress Range	Probability
Pressure Full	F	269.5	39.8%
	E	269.5	2.17%
Pressure Ballast	F	261.09	30.23%
	E	261.09	1.13%
Wave Bending Full	F	–	–
	E		
Wave Bending Ballst	F	–	–
	E		
Load Unload	F	94.766	0.0
	E	94.766	0.0

Note : F Curve   Standard Weld
     E Curve   Improved Weld

Total Probability of Failure Pf = 70.03% for F Curve
Total Probability of Failure Pf = 3.30% for E Curve

Table 1.2.3

Typical CSD and Hotspot

S. SHELL LONG.
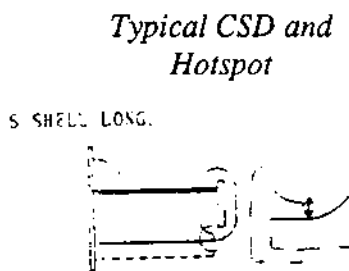
Load Component	S-N	Stress Range	Probability
Pressure Full	F2	104.86	0.0
	F	104.86	0.0
Pressure Ballast	F2	85.946	0.0
	F	85.946	0.0
Wave Bending Full	F2	–	–
	F		
Wave Bending Ballst	F2	–	–
	F		
Load Unload	F2	70.56	0.0
	F	70.56	0.0

128

Design Fatigue Life = 20 year
Weibull Parameter = 0.942
Number of Cycles N= 1 x 10^8
NFull= 0.5 x 10^8 NBallast= 0.5x 10^8
Load and unload N =500

Table 1.3.1

Typical CSD and Hotspot

S. SHELL LONG.
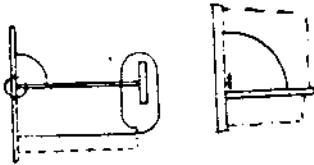
Load Component	S-N	Stress Range	Probability
Pressure Full	F	236.376	9.12%
	E	236.376	0.098%
Pressure Ballast	F	166.698	0.00136%
	E	166.698	0.0
Wave Bending Full	F	–	–
	E		
Wave Bending Ballst	F	–	–
	E		
Load Unload	F	29.792	0.0
	E	29.792	0.0

Note : F Curve   Standard Weld
       E Curve   Improved Weld

Total Probability of Failure Pf = 9.12136% for F Curve
Total Probability of Failure Pf = 0.098% for E Curve

Table 1.3.2

Typical CSD and Hotspot

S. SHELL LONG.
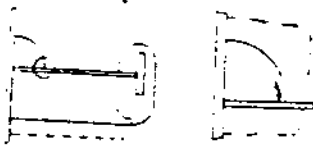
Load Component	S-N	Stress Range	Probability
Pressure Full	F	334.278	88%
	E	334.278	27.86%
Pressure Ballast	F	260.974	19.62%
	E	260.974	0.444%
Wave Bending Full	F	–	–
	E		
Wave Bending Ballst	F	–	–
	E		
Load Unload	F	43.022	0.0
	E	43.022	0.0

Note : F Curve   Standard Weld
       E Curve   Improved Weld

Total Probability of Failure Pf > 1 for F Curve
Total Probability of Failure Pf = 28.304% for E Curve

Table 1.3.3

130
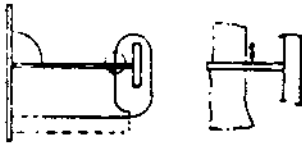
Typical CSD and Hotspot	Load Component	S-N	Stress Range	Probability
S. SHELL LONG.	Pressure Full	F	113.876	0.0
		E	113.876	0.0
	Pressure Ballast	F	110.446	0.0
		E	110.446	0.0
	Wave Bending Full	F	–	–
		E		
	Wave Bending Ballst	F	–	–
		E		
	Load Unload	F	43.022	0.0
		E	43.022	0.0

Note: F Curve   Standard Weld
E Curve   Improved Weld

Total Probability of Failure Pf = 0.0% for F Curve
Total Probability of Failure Pf = 0.0% for E Curve

### Table 1.3.4
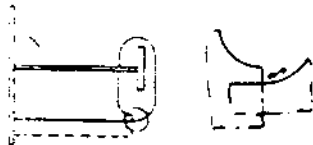
Typical CSD and Hotspot	Load Component	S-N	Stress Range	Probability
S. SHELL LONG.	Pressure Full	F2	235.592	21.17%
		F	235.592	4.77%
	Pressure Ballast	F2	161.504	0.00549%
		F	161.504	0.0001236%
	Wave Bending Full	F2	–	–
		F		
	Wave Bending Ballst	F2	–	–
		F		
	Load Unload	F2	294.196	0.0
		F	294.194	0.0

Note: F2 Curve   Standard Weld
F Curve   Improved Weld

Total Probability of Failure Pf = 21.1755% for F2 Curve
Total Probability of Failure Pf = 4.7701236% for F Curve

Table 1.3.5

Typical CSD and Hotspot	Load Component	S-N	Stress Range	Probability
	Pressure Full	C	385.434	0.086%
	Pressure Ballast	C	189.826	0.0

131
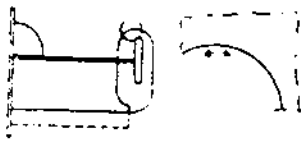
S. SHELL LONG.

Wave Bending Full	C	–	–
Wave Bending Ballst	C	–	–
Load Unload	C	279.496	0.0

Note:C Curve   Standard Weld
                  Improved Weld

Total Probability of Failure Pf = 0.086% for C Curve

L46 - Slot on Sideshell Longitudinal

Design Fatigue Life = 20 year
Weibull Parameter = 0.942
Number of Cycles $N= 1 \times 10^{8}$
$N_{Full}= 0.5 \times 10^{8}$ $N_{Ballast}= 0.5 \times 10^{8}$
Load and unload $N = 500$

Table 1.4.1

Typical CSD and Hotspot

S. SHELL LONG.
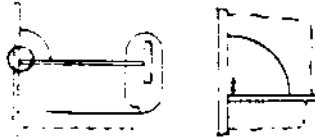
Load Component	S-N	Stress Range	Probability
Pressure Full	F	93.492	0.0
	E	93.492	0.0
Pressure Ballast	F	62.818	0.0
	E	62.818	0.0
Wave Bending Full	F	–	–
	E		
Wave Bending Ballst	F	–	–
	E		
Load Unload	F	29.498	0.0
	E	29.498	0.0

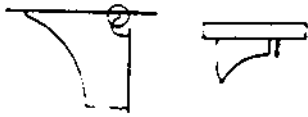Note : F Curve   Standard Weld
       E Curve   Improved Weld

Total Probability of Failure Pf = 0.0% for F Curve
Total Probability of Failure Pf = 0.0% for E Curve

Table 1.4.2

Typical CSD and Hotspot

Load Component	S-N	Stress Range	Probability
Pressure Full	F	117.992	0.0
	E	117.992	0.0
Pressure Ballast	F	78.89	0.0
	E	78.89	0.0

132

S. SHELL LONG.
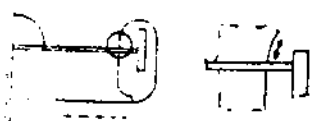
Wave Bending Full	F	–	–
	E		
Wave Bending Ballst	F	–	–
	E		
Load Unload	F	49.196	0.0
	E	49.196	0.0

Note : F Curve   Standard Weld
E Curve   Improved Weld

Total Probability of Failure Pf = 0.0% for F Curve
Total Probability of Failure Pf = 0.0% for E Curve

Table 1.4.3

Typical CSD and Hotspot

S. SHELL LONG.
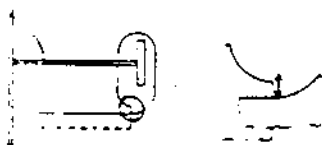
Load Component	S-N	Stress Range	Probability
Pressure Full	F2	87.122	0.0
	F	87.122	0.0
Pressure Ballast	F2	54.684	0.0
	F	54.684	0.0
Wave Bending Full	F2	–	–
	F		
Wave Bending Ballst	F2	–	–
	F		
Load Unload	F2	4.01	0.0
	F	4.01	0.0

Note:F2 Curve   Standard Weld
F Curve   Improved Weld

Total Probability of Failure Pf = 0.0% for F2 Curve
Total Probability of Failure Pf = 0.0% for F Curve
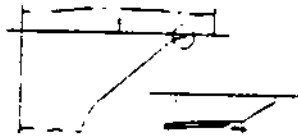
Table 1.4.4

Typical CSD and Hotspot

S. SHELL LONG.
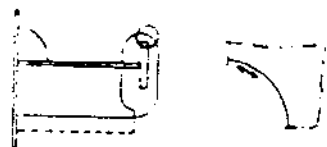
Load Component	S-N	Stress Range	Probability
Pressure Full	C	392.392	0.15%
Pressure Ballast	C	253.428	0.0
Wave Bending Full	C	–	–
Wave Bending Ballst	C	–	–
Load Unload	C	17.052	0.0

133
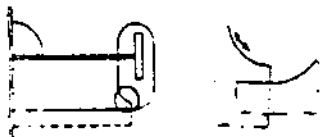
Total Probability of Failure Pf = 0.15% for C Curve

Typical CSD and Hotspot

S. SHELL LONG.

Table 1.4.5

Load Component	S-N	Stress Range	Probability
Pressure Full	F2	514.304	> 1
	F	514.304	63.76%
Pressure Ballast	F2	323.89	> 1
	F	323.89	56.79%
Wave Bending Full	F2	–	–
	F		
Wave Bending Ballst	F2	–	–
	F		
Load Unload	F2	19.502	0.0
	F	19.502	0.0

Note:F2 Curve   Standard Weld

F Curve   Improved Weld

Total Probability of Failure Pf > 1 for F2 Curve
Total Probability of Failure Pf > 1 for F Curve

L36 - Slot on LongBHD Longitudinal

Design Fatigue Life = 20 year
Weibull Parameter = 0.942
Number of Cycles $N= 1 \times 10^8$
$N_{Full}= 0.5 \times 10^8$ $N_{Ballast}= 0.5 \times 10^8$
Load and unload N =500

Typical CSD and Hotspot

L. BHD LONG.

Table 2.1.1

Load Component	S-N	Stress Range	Probability
Pressure Full	F	90.062	0.0
	E	90.062	0.0
Pressure Ballast	F	65.562	0.0
	E	65.562	0.0
Wave Bending Full	–	–	–
Wave Bending Ballst	–	–	–
Load Unload	F	116.62	0.0
	E	116.62	0.0

134

Table 2.1.2

Typical CSD and Hotspot

L. BHD LONG.

Load Component	S-N	Stress Range	Probability
Pressure Full	F	0.0	0.0
	E	0.0	0.0
Pressure Ballast	F	0.0	0.0
	E	0.0	0.0
Wave Bending Full	–	–	–
Wave Bending Ballst	–	–	–
Load Unload	F	125.44	0.0
	E	125.44	0.0

Note : F Curve   *Standard Weld*

E Curve   *Improved Weld*

Total Probability of Failure Pf = 0.0% for F Curve
Total Probability of Failure Pf = 0.0% for E Curve

Table 2.1.3

Typical CSD and Hotspot

L. BHD LONG.

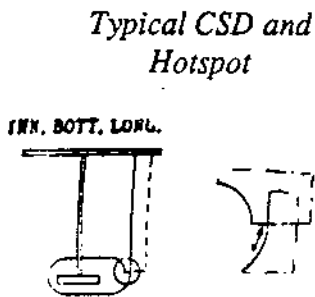| Load Component	S-N	Stress Range	Probability
Pressure Full	F2	109.172	0.0
	F	109.172	0.0
Pressure Ballast	F2	125.93	0.0
	F	125.93	0.0
Wave Bending Full	F2	–	–
	F		
Wave Bending Ballst	F2	–	–
	F		
Load Unload	F2	294.294	0.0
	F	294.294	0.0

Note:F2 Curve   *Standard Weld*

F Curve   *Improved Weld*

Total Probability of Failure Pf = 0.0% for F2 Curve
Total Probability of Failure Pf =0.0% for F Curve

L37 - Slot on LongBHD Longitudinal

135

Design Fatigue Life = 20 year
Weibull Parameter = 0.942
Number of Cycles N= 1 x 10 ^{8}
NFull= 0.5 x 10 ^{8} NBallast= 0.5x 10 ^{8}
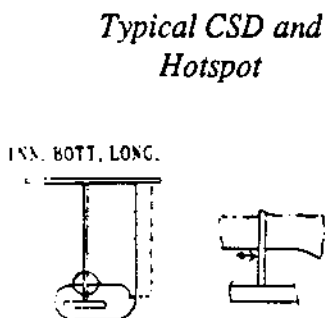*Load and unload N =500*

Table 2.2.1

Load Component	S-N	Stress Range	Probability
Pressure Full	F	214.718	0.704%
	E	214.718	0.001248%
Pressure Ballast	F	201.488	0.146%
	E	201.488	0.00011%
Wave Bending Full	F	–	–
	E		
Wave Bending Ballst	F	–	–
	E		
Load Unload	F	42.532	0.0
	E	42.532	0.0

Note : F Curve   Standard Weld
        E Curve   Improved Weld

Total Probability of Failure Pf = 0.85% for F Curve
**Total Probability of Failure Pf = 0.1358% for E Curve**

Table 2.2.2

Load Component	S-N	Stress Range	Probability
Pressure Full	F	259.7	18.5%
	E	259.7	0.39%
Pressure Ballast	F	201.586	14.06%
	E	201.586	0.226%
Wave Bending Full	F	–	–
	E		
Wave Bending Ballst	F	–	–
	E		
Load Unload	F	154.938	0.0
	E	154.938	0.0

Note : F Curve   Standard Weld
        E Curve   Improved Weld

Total Probability of Failure Pf = 32.56% for F Curve
Total Probability of Failure Pf = 0.616% for E Curve

Typical CSD and Hotspot

L. BHD LONG.

Table 2.2.3

Load Component	S-N	Stress Range	Probability
Pressure Full	F2	50.372	0.0
	F	50.372	0.0
Pressure Ballast	F2	35.476	0.0
	F	35.476	0.0
Wave Bending Full	F2	–	–
	F		
Wave Bending Ballst	F2	–	–
	F		
Load Unload	F2	82.124	0.0
	F	82.124	0.0

Note: F2 Curve   Standard Weld
       F Curve   Improved Weld

Total Probability of Failure Pf = 0.0% for F2 Curve
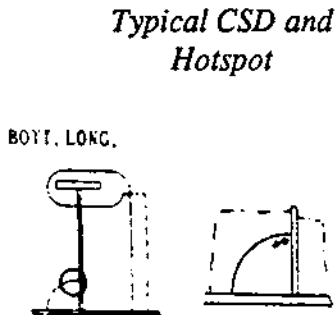*Total Probability of Failure Pf = 0.0% for F Curve*

Typical CSD and Hotspot

L. BHD LONG.

Table 2.2.4

Load Component	S-N	Stress Range	Probability
Pressure Full	C	480.592	16.52%
Pressure Ballast	C	363.972	0.011%
Wave Bending Full	C	–	–
Wave Bending Ballst	C	–	–
Load Unload	C	139.552	0.0

Note: C Curve   Standard Weld
                 Improved Weld

Total Probability of Failure Pf = 16.0531% for C Curve

Typical CSD and Hotspot

Table 2.2.5

Load Component	S-N	Stress Range	Probability
Pressure Full	F2	246.862	33.6%
	F	246.862	9.84%
Pressure Ballast	F2	171.794	0.04%
	F	171.794	0.012%
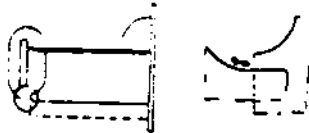
L BHD LONG.

|			
Wave Bending Full	F2 F	–	–
Wave Bending Ballst	F2 F	–	–
Load Unload	F2 F	245.588 245.588	0.0 0.0

Note: F2 Curve   Standard Weld
F Curve   Improved Weld

Total Probability of Failure Pf = 33.64% for F2 Curve
Total Probability of Failure Pf = 9.852% for F Curve

L45 - Slot on LongBHD Longitudinal

Design Fatigue Life = 20 year
Weibull Parameter = 0.942
Number of Cycles $N = 1 \times 10^8$
$N_{Full} = 0.5 \times 10^8$ $N_{Ballast} = 0.5 \times 10^8$
Load and unload N = 500

Table 2.3.1

Typical CSD and Hotspot

L BHD LONG.

Load Component	S-N	Stress Range	Probability
Pressure Full	F E	204.624 204.624	0.00000412% 0.0%
Pressure Ballast	F E	147.098 147.098	0.0% 0.0%
Wave Bending Full	F E	–	–
Wave Bending Ballst	F E	–	–
Load Unload	F E	185.122 185.122	0.0 0.0

Note : F Curve   Standard Weld
E Curve   Improved Weld

Total Probability of Failure Pf = 0.00000412% for F Curve
Total Probability of Failure Pf = 0.0% for E Curve

Table 2.3.2

Typical CSD and Hotspot

Load Component	S-N	Stress Range	Probability
Pressure Full	F E	150.332 150.332	0.435% 0.0241%

L. BHD LONG.
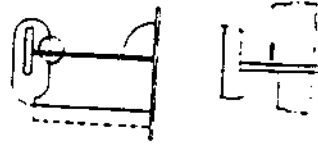
	S-N	Stress Range	Probability
Pressure	F	95.486	0.002345%
Ballast	E	95.486	0.000041%
Wave Bending	F		
Full	E	–	–
Wave Bending	F		
Ballst	E	–	–
Load Unload	F	252.742	0.0
	E	252.742	0.0

Note : F Curve   Standard Weld
        E Curve   Improved Weld

Total Probability of Failure Pf = 0.437345% for F Curve
Total Probability of Failure Pf = 0.00234541% for E Curve

Typical CSD and Hotspot

L. BHD LONG.

Table 2.3.3
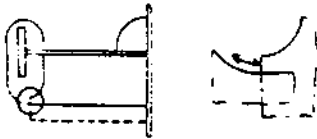
Load Component	S-N	Stress Range	Probability
Pressure	F2	187.964	0.0
Full	F	187.964	0.0
Pressure	F2	157.094	0.0
Ballast	F	157.094	0.0
Wave Bending	F2		
Full	F	–	–
Wave Bending	F2		
Ballst	F	–	–
Load Unload	F2	343.392	0.0
	F	343.392	0.0

Note:F2 Curve   Standard Weld
       F Curve   Improved Weld

Total Probability of Failure Pf = 0.0% for F2 Curve
Total Probability of Failure Pf = 0.0% for F Curve

Typical CSD and Hotspot

L. BHD LONG.

Table 2.3.4

Load Component	S-N	Stress Range	Probability
Pressure Full	C	189.238	0.0
Pressure Ballast	C	148.078	0.0
Wave Bending Full	C	–	–
Wave Bending Ballst	C	–	–

Load Unload	C	366.814	0.0

Note:C Curve   Standard Weld
                   Improved Weld

Total Probability of Failure Pf = 0.0% for C Curve

L46 - Slot on LongBHD Longitudinal

Design Fatigue Life = 20 year
Weibull Parameter = 0.942
Number of Cycles $N = 1 \times 10^8$
$N_{Full} = 0.5 \times 10^8$ $N_{Ballast} = 0.5 \times 10^8$
Load and unload $N = 500$

Table 2.4.1

Typical CSD and Hotspot

L. BHD LONG.

Load Component	S-N	Stress Range	Probability
Pressure Full	F	78.694	0.0
	E	78.694	0.0
Pressure Ballast	F	50.176	0.0
	E	50.176	0.0
Wave Bending Full	F	–	–
	E		
Wave Bending Ballst	F	–	–
	E		
Load Unload	F	22.05	0.0
	E	22.05	0.0

Note : F Curve   Standard Weld
        E Curve   Improved Weld

Total Probability of Failure Pf = 0.0% for F Curve
Total Probability of Failure Pf = 0.0% for E Curve

Table 2.4.2

Typical CSD and Hotspot

L. BHD LONG.

Load Component	S-N	Stress Range	Probability
Pressure Full	F	14.994	0.0
	E	14.994	0.0
Pressure Ballast	F	31.752	0.0
	E	31.752	0.0
Wave Bending Full	F	–	–
	E		
Wave Bending Ballst	F	–	–
	E		

140

| Load Unload | F | 7.056 | 0.0 |
| | E | 7.056 | 0.0 |

Note : F Curve   Standard Weld
     E Curve   Improved Weld

Total Probability of Failure Pf = 0.0% for F Curve
Total Probability of Failure Pf = 0.0% for E Curve

Typical CSD and Hotspot

L. BHD LONG.

Table 2.4.3

Load Component	S-N	Stress Range	Probability
Pressure Full	F2	186.592	0.365%
	F	186.592	0.019%
Pressure Ballast	F2	112.896	0.0
	F	112.896	0.0
Wave Bending Full	F2	–	–
	F		
Wave Bending Ballst	F2	–	–
	F		
Load Unload	F2	77.48	0.0
	F	77.48	0.0

Note:F2 Curve   Standard Weld
     F Curve   Improved Weld

Total Probability of Failure Pf = 0.365% for F2 Curve
Total Probability of Failure Pf = 0.019% for F Curve

Typical CSD and Hotspot

L. BHD LONG.
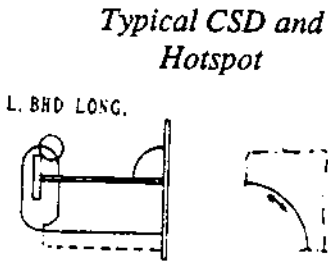
Table 2.4.4

Load Component	S-N	Stress Range	Probability
Pressure Full	C	389.158	0.11%
Pressure Ballast	C	232.946	0.0
Wave Bending Full	C	–	–
Wave Bending Ballst	C	–	–
Load Unload	C	89.278	0.0

Note:C Curve   Standard Weld
                Improved Weld

Total Probability of Failure Pf = 0.11% for C Curve

141

Table 2.4.5

Typical CSD and Hotspot

L. BHD LONG.

Load Component	S-N	Stress Range	Probability
Pressure Full	F2	369.264	100%
	F	369.264	100%
Pressure Ballast	F2	233.044	18.72%
	F	233.044	3.96%
Wave Bending Full	F2	–	–
	F		
Wave Bending Ballst	F2	–	–
	F		
Load Unload	F2	132.594	0.0
	F	132.594	0.0

Note: F2 Curve   Standard Weld
      F Curve   Improved Weld

Total Probability of Failure Pf > 1 for F2 Curve
Total Probability of Failure Pf > 1 for F Curve

L37 -Long.BKT. (Ord.T.Ring)

Design Fatigue Life = 20 year
Weibull Parameter = 0.942
Number of Cycles $N = 1 \times 10^8$
$N_{Full} = 0.5 \times 10^8$ $N_{Ballast} = 0.5 \times 10^8$
Load and unload N = 500

Table 3.1.1

Typical CSD and Hotspot

S. SHELL

Load Component	S-N	Stress Range	Probability
Pressure Full	F2	161.112	0.005504%
	F	161.112	0.0001124%
Pressure Ballast	F2	145.04	0.0001233%
	F	145.04	0.00000134%
Wave Bending Full	F2	–	–
	F		
Wave Bending Ballst	F2	–	–
	F		
Load Unload	F2	125.538	0.0
	F	125.538	0.0

Note: F2 Curve   Standard Weld
      F Curve   Improved Weld

Total Probability of Failure Pf = 0.005628% for F2 Curve
Total Probability of Failure Pf = 0.00011374% for F Curve
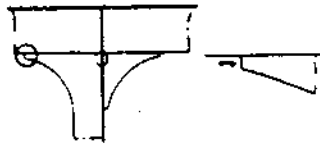
142

Table 3.1.2

Typical CSD and Hotspot

S. SHELL

Load Component	S-N	Stress Range	Probability
Pressure Full	F2	157.584	0.00261%
	F	157.584	0.0000464%
Pressure Ballast	F2	122.99	0.0
	F	122.99	0.0
Wave Bending Full	F2	–	–
	F		
Wave Bending Ballst	F2	–	–
	F		
Load Unload	F2	123.872	0.0
	F	123.872	0.0

Note: F2 Curve   Standard Weld
        F Curve   Improved Weld

Total Probability of Failure Pf = 0.00261% for F2 Curve
Total Probability of Failure Pf = 0.0000464% for F Curve

Table 3.1.3
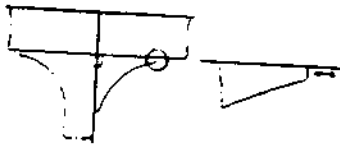
Typical CSD and Hotspot

S. SHELL

Load Component	S-N	Stress Range	Probability
Pressure Full	F2	154.448	0.001293%
	F	154.448	0.00002031%
Pressure Ballast	F2	172.774	0.0477168%
	F	172.774	0.0015255%
Wave Bending Full	F2	–	–
	F		
Wave Bending Ballst	F2	–	–
	F		
Load Unload	F2	177.086	0.0
	F	177.086	0.0

Note: F2 Curve   Standard Weld
        F Curve   Improved Weld

Total Probability of Failure Pf = 0.0490% for F2 Curve
Total Probability of Failure Pf = 0.00154% for F Curve

Table 3.1.4

Typical CSD and Hotspot

Load Component	S-N	Stress Range	Probability
Pressure Full	F	67.228	0.0
	E	67.228	0.0

L. BHD

Pressure	F	90.944	0.0
Ballast	E	90.944	0.0
Wave Bending	F	–	–
Full	E		
Wave Bending	F	–	–
Ballst	E		
Load Unload	F	188.16	0.0
	E	188.16	

Note: F Curve   Standard Weld
     E Curve   Improved Weld

Total Probability of Failure Pf = 0.0% for F Curve
Total Probability of Failure Pf = 0.0% for E Curve

Typical CSD and
Hotspot

L. BHD

Table 3.1.5
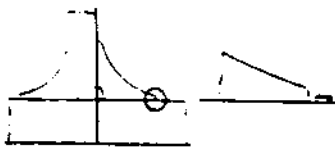
Load Component	S-N	Stress Range	Probability
Pressure	F2	72.912	0.0
Full	F	72.912	0.0
Pressure	F2	84.574	0.0
Ballast	F	84.574	0.0
Wave Bending	F2	–	–
Full	F		
Wave Bending	F2	–	–
Ballst	F		
Load Unload	F2	214.032	0.0
	F	214.032	0.0

Note: F2 Curve   Standard Weld
     F Curve   Improved Weld

Total Probability of Failure Pf = 0.0% for F2 Curve
Total Probability of Failure Pf = 0.0% for F Curve

L46 -Long.BKT. (Ord.T.Ring)

Design Fatigue Life = 20 year
Weibull Parameter = 0.942
Number of Cycles N= 1 x 10^8
NFull= 0.5 x 10^8 NBallast= 0.5x 10^8
Load and unload N =500

Table 3.2.1

Typical CSD and
Hotspot

Load Component	S-N	Stress Range	Probability

S. SHELL
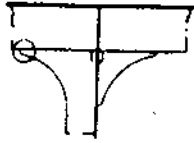
Pressure Full	F2	66.052	0.0
	F	66.052	0.0
Pressure Ballast	F2	28.91	0.0
	F	28.91	0.0
Wave Bending Full	F2	–	–
	F		
Wave Bending Ballst	F2	–	–
	F		
Load Unload	F2	50.764	0.0
	F	50.764	0.0

Note: F2 Curve   Standard Weld
       F Curve   Improved Weld

Total Probability of Failure Pf = 0.0% for F2 Curve
Total Probability of Failure Pf = 0.0% for F Curve

Typical CSD and Hotspot

S. SHELL

Table 3.2.2
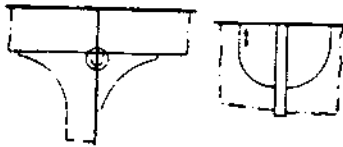
Load Component	S-N	Stress Range	Probability
Pressure Full	F2	144.256	0.0
	F	144.256	0.0
Pressure Ballast	F2	92.12	0.0
	F	92.12	0.0
Wave Bending Full	F2	–	–
	F		
Wave Bending Ballst	F2	–	–
	F		
Load Unload	F2	84.28	0.0
	F	84.28	0.0

Note: F2 Curve   Standard Weld
       F Curve   Improved Weld

Total Probability of Failure Pf = 0.0% for F2 Curve
Total Probability of Failure Pf = 0.0% for F Curve

Typical CSD and Hotspot

S. SHELL

Table 3.2.3
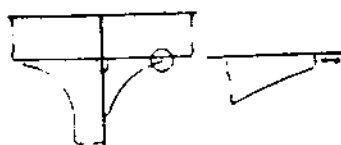
Load Component	S-N	Stress Range	Probability
Pressure Full	F2	54.096	0.0
	F	54.096	0.0
Pressure Ballast	F2	32.144	0.0
	F	32.144	0.0
Wave Bending Full	F2	–	–
	F		

145

Wave Bending Ballst	F2	–	–
	F		
Load Unload	F2	73.5	0.0
	F	73.5	0.0

Note: F2 Curve   Standard Weld
F Curve   Improved Weld

Total Probability of Failure Pf = 0.0% for F2 Curve
Total Probability of Failure Pf = 0.0% for F Curve

Typical CSD and Hotspot

L. BHD
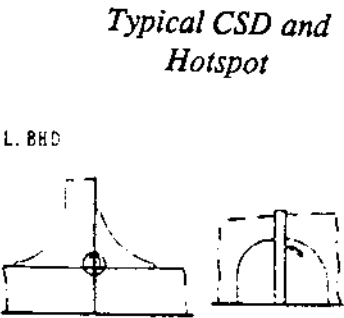
Table 3.2.4

Load Component	S-N	Stress Range	Probability
Pressure Full	F	64.68	0.0
	E	64.68	0.0
Pressure Ballast	F	49.392	0.0
	E	49.392	0.0
Wave Bending Full	F	–	–
	E		
Wave Bending Ballst	F	–	–
	E		
Load Unload	F	51.058	0.0
	E	51.058	0.0

Note: C Curve   Standard Weld
Improved Weld

Total Probability of Failure Pf = 0.0% for F Curve
Total Probability of Failure Pf = 0.0% for E Curve

Typical CSD and Hotspot

L. BHD
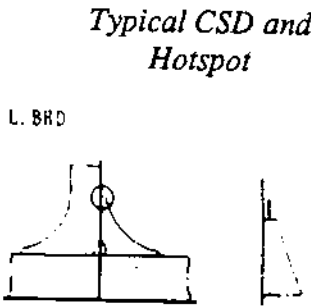
Table 3.2.5

Load Component	S-N	Stress Range	Probability
Pressure Full	F2	68.208	0.0
	F	62.208	0.0
Pressure Ballast	F2	46.942	0.0
	F	46.942	0.0
Wave Bending Full	F2	–	–
	F		
Wave Bending Ballst	F2	–	–
	F		
Load Unload	F2	71.344	0.0
	F	71.344	0.0

Total Probability of Failure Pf = 0.0% for F2 Curve
Total Probability of Failure Pf = 0.0% for F Curve

Typical CSD and
Hotspot

S. SHELL LONG.

Table 1.2.4
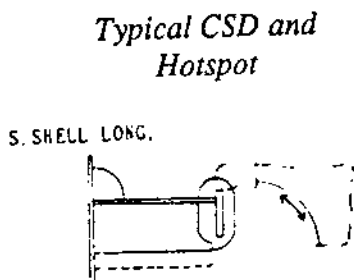
Load Component	S-N	Stress Range	Probability
Pressure Full	C	490.686	35.5%
Pressure Ballast	C	373.87	0.12%
Wave Bending Full	C	–	–
Wave Bending Ballst	C	–	–
Load Unload	C	101.332	0.0

Note:C Curve   Standard Weld
                      Improved Weld

Total Probability of Failure Pf = 35.62% for C Curve

Typical CSD and
Hotspot
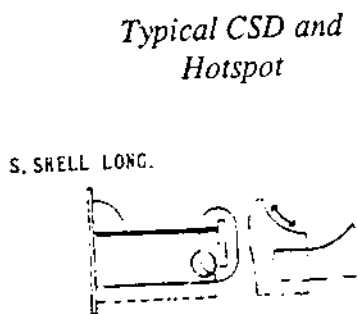
S. SHELL LONG.

Table 1.2.5

Load Component	S-N	Stress Range	Probability
Pressure Full	F2	497.448	100%
	F	497.448	100%
Pressure Ballast	F2	406.112	100%
	F	406.112	100%
Wave Bending Full	F2	–	–
	F		
Wave Bending Ballst	F2	–	–
	F		
Load Unload	F2	36.352	0.0
	F	36.352	0.0

Note:F2 Curve   Standard Weld
      F Curve   Improved Weld

Total Probability of Failure Pf > 1 for F2 Curve
Total Probability of Failure Pf > 1 for F Curve

L45 - Slot on Sideshell Longitudinal

Total Probability of Failure Pf = 0.0% for F2 Curve
Total Probability of Failure Pf = 0.0% for F Curve

L36 -Long.BKT. (T.BHD)

Design Fatigue Life = 20 year
Weibull Parameter = 0.979
Number of Cycles N= 1 x 10 ^{8}
NPull= 0.5 x 10 ^{8} NBallast= 0.5x 10 ^{8}
Load and unload N =500

Typical CSD and Hotspot

S. SHELL
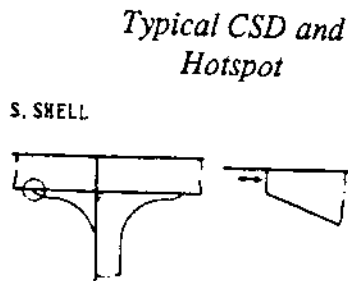
Table 3.3.1

Load Component	S-N	Stress Range	Probability
Pressure Full	F2	319.774	98%
	F	319.114	90%
Pressure Ballast	F2	227.85	29.3%
	F	227.85	7.9%
Wave Bending Full	F2	—	—
	F		
Wave Bending Ballst	F2	—	—
	F		
Load Unload	F2	87.906	0.0
	F	87.906	0.0

Note:F2 Curve   *Standard Weld*
F Curve   *Improved Weld*

Total Probability of Failure Pf > 1 for F2 Curve
Total Probability of Failure Pf = 97.9% for F Curve

Typical CSD and Hotspot

S. SHELL
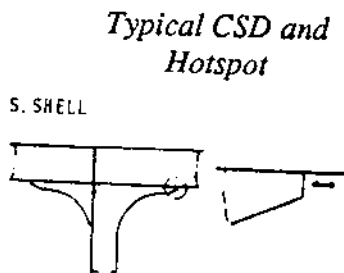
Table 3.3.2

Load Component	S-N	Stress Range	Probability
Pressure Full	F2	279.986	86.8%
	F	279.986	59.9%
Pressure Ballast	F2	184.828	1.27%
	F	184.828	0.0964%
Wave Bending Full	F2	—	—
	F		
Wave Bending Ballst	F2	—	—
	F		

147

| Load Unload | F2 | 80.458 | 0.0 |
| | F | 80.458 | 0.0 |

Note: F2 Curve   Standard Weld
       F Curve   Improved Weld

Total Probability of Failure Pf = 88.08% for F2 Curve
Total Probability of Failure Pf = 60% for F Curve

Table 3.3.3

Typical CSD and Hotspot

S. SHELL
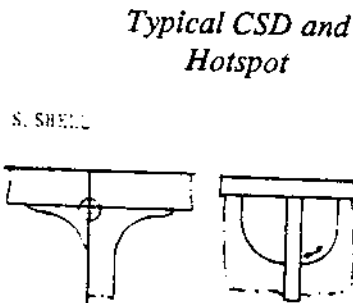
Load Component	S-N	Stress Range	Probability
Pressure Full	F	324.674	92.9%
	E	324.674	38.5%
Pressure Ballast	F	223.93	5.74%
	E	223.93	0.042%
Wave Bending Full	F	–	–
	E		
Wave Bending Ballst	F	–	–
	E		
Load Unload	F	109.956	0.0
	E	109.956	0.0

Note: F Curve   Standard Weld
     E Curve   Improved Weld

Total Probability of Failure Pf = 98.64% for F2 Curve
Total Probability of Failure Pf = 44.24% for F Curve

Table 3.3.4

Typical CSD and Hotspot
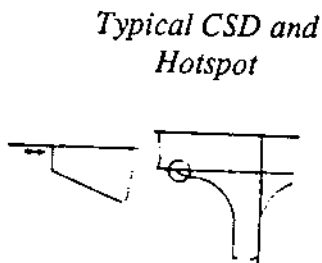
Load Component	S-N	Stress Range	Probability
Pressure Full	F2	193.844	3.22%
	F	193.844	0.332%
Pressure Ballast	F2	127.694	0.0
	F	127.694	0.0
Wave Bending Full	F2	–	–
	F		
Wave Bending Ballst	F2	–	–
	F		
Load Unload	F2	182.182	0.0
	F	182.182	0.0

Note: F2 Curve   Standard Weld
      F Curve   Improved Weld

Total Probability of Failure Pf = 3.22% for F2 Curve
Total Probability of Failure Pf = 0.332% for F Curve

Typical CSD and Hotspot

L. BHD

Table 3.3.5

Load Component	S-N	Stress Range	Probability
Pressure Full	F	231.574	9.66%
	E	231.574	0.11%
Pressure Ballast	F	165.228	0.00235%
	E	165.228	0.0
Wave Bending Full	F	–	–
	E		
Wave Bending Ballst	F	–	–
	E		
Load Unload	F	284.2	0.0
	E	284.2	0.0

Note:F Curve   Standard Weld
E Curve   Improved Weld

Total Probability of Failure Pf = 9.66235% for F Curve
Total Probability of Failure Pf = 0.11% for E Curve

L.45 -Long.BKT. (T.BHD)

Design Fatigue Life = 20 year
Weibull Parameter = 0.979
Number of Cycles N= 1 x 10 ^{8}
NFull= 0.5 x 10 ^{8} NBallast= 0.5x 10 ^{8}
Load and unload N =500

Typical CSD and Hotspot

S. SHELL
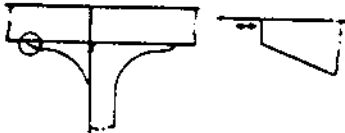
Table 3.4.1

Load Component	S-N	Stress Range	Probability
Pressure Full	F2	253.82	62.8%
	F	253.82	29.44%
Pressure Ballast	F2	146.6	0.00204%
	F	146.6	0.00003467%
Wave Bending Full	F2	–	–
	F		
Wave Bending Ballst	F2	–	–
	F		
Load Unload	F2	24.402	0.0
	F	24.402	0.0

Note:F2 Curve   Standard Weld
F Curve   Improved Weld

149

Total Probability of Failure Pf = 62.80204% for F2 Curve
Total Probability of Failure Pf = 29.4400347% for F Curve

Table 3.4.2

Typical CSD and Hotspot

S. SHELL
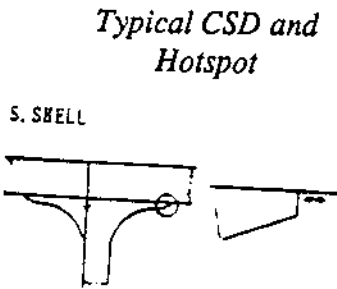
Load Component	S-N	Stress Range	Probability
Pressure Full	F2	202.664	6.81%
	F	202.664	0.92%
Pressure Ballast	F2	113.778	0.0
	F	113.778	0.0
Wave Bending Full	F2	–	–
	F		
Wave Bending Ballst	F2	–	–
	F		
Load Unload	F2	27.342	0.0
	F	27.342	0.0

Note: F2 Curve   Standard Weld
      F Curve   Improved Weld

Total Probability of Failure Pf = 6.81% for F2 Curve
Total Probability of Failure Pf = 0.92% for F Curve

Table 3.4.3

Typical CSD and Hotspot

S. SHELL
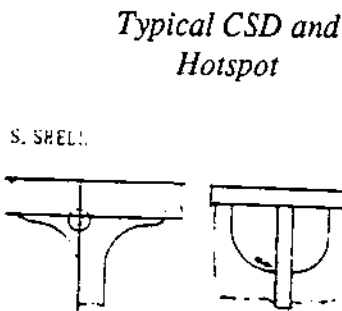
Load Component	S-N	Stress Range	Probability
Pressure Full	F	307.8	100%
	E	307.8	100%
Pressure Ballast	F	186.102	1.41%
	E	186.102	0.116%
Wave Bending Full	F	–	–
	E		
Wave Bending Ballst	F	–	–
	E		
Load Unload	F	67.228	0.0
	E	67.228	0.0

Note: F Curve   Standard Weld
      E Curve   Improved Weld

Total Probability of Failure Pf = 100% for F2 Curve
Total Probability of Failure Pf = 100% for F Curve

Table 3.4.4

Typical CSD and Hotspot

Load Component	S-N	Stress Range	Probability

150
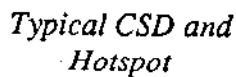
L. BHD
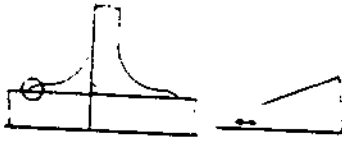
Pressure Full	F2	221.578	22.07%
	F	221.578	5.08%
Pressure Ballast	F2	142.982	0.000839%
	F	142.982	0.00001225%
Wave Bending Full	F2	–	–
	F		
Wave Bending Ballst	F2	–	–
	F		
Load Unload	F2	151.41	0.0
	F	151.41	0.0

Note: F2 Curve   Standard Weld
F Curve   Improved Weld

Total Probability of Failure Pf = 22.071% for F2 Curve
Total Probability of Failure Pf = 5.08% for F Curve

Typical CSD and Hotspot

L. BHD

Table 3.4.5

Load Component	S-N	Stress Range	Probability
Pressure Full	F	220.598	21.02%
	E	220.598	4.72%
Pressure Ballast	F	146.118	0.001817%
	E	146.118	0.0000303%
Wave Bending Full	F	–	–
	E		
Wave Bending Ballst	F	–	–
	E		
Load Unload	F	205.72	0.0
	E	205.72	0.0

Note: F Curve   Standard Weld
E Curve   Improved Weld

Total Probability of Failure Pf = 21.021817% for F Curve
Total Probability of Failure Pf = 4.72% for E Curve

L36 -Long.BKT. (N0.1 H.G)

Design Fatigue Life = 20 year
Weibull Parameter = 0.942
Number of Cycles $N = 1 \times 10^8$
$N_{Full} = 0.5 \times 10^8$ $N_{Ballast} = 0.5 \times 10^8$
Load and unload N = 500

Table 4.1.1

151

Typical CSD and
Hotspot

S. SBELL
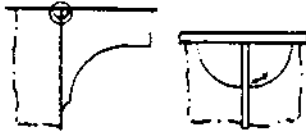
Load Component	S-N	Stress Range	Probability
Pressure Full	F	32.83	0.0
	E	32.83	0.0
Pressure Ballast	F	65.072	0.0
	E	65.072	0.0
Wave Bending Full	F	–	–
	E		
Wave Bending Ballst	F	–	–
	E		
Load Unload	F	57.232	0.0
	E	57.232	0.0

Note:F Curve   Standard Weld
      E Curve   Improved Weld

Total Probability of Failure Pf = 0.0% for F Curve
Total Probability of Failure Pf = 0.0% for E Curve

Table 4.1.2

Typical CSD and
Hotspot

S. SBELL
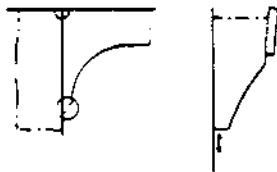
Load Component	S-N	Stress Range	Probability
Pressure Full	F	46.354	0.0
	E	46.354	0.0
Pressure Ballast	F	19.796	0.0
	E	19.796	0.0
Wave Bending Full	F	–	–
	E		
Wave Bending Ballst	F	–	–
	E		
Load Unload	F	98.882	0.0
	E	98.882	0.0

Note:F Curve   Standard Weld
      E Curve   Improved Weld

Total Probability of Failure Pf = 0.0% for F2 Curve
Total Probability of Failure Pf = 0.0% for F Curve

Table 4.1.3

Typical CSD and
Hotspot

Load Component	S-N	Stress Range	Probability
Pressure Full	F	50.176	0.0
	E	50.176	0.0
Pressure Ballast	F	70.07	0.0
	E	70.07	0.0

152

L. BHD.
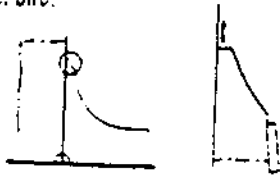
	S-N	Stress Range	Probability
Wave Bending Full	F	–	–
	E		
Wave Bending Ballst	F	–	–
	E		
Load Unload	F	50.764	0.0
	E	50.764	0.0

Note: F Curve   Standard Weld
       E Curve   Improved Weld

Total Probability of Failure Pf = 0.0% for F Curve
Total Probability of Failure Pf = 0.0% for E Curve

Table 4.1.4

Typical CSD and Hotspot

BHD.
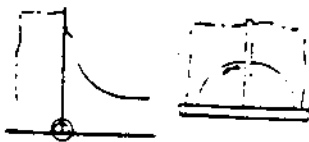
Load Component	S-N	Stress Range	Probability
Pressure Full	F	31.556	0.0
	E	31.556	0.0
Pressure Ballast	F	19.796	0.0
	E	19.796	0.0
Wave Bending Full	F	–	–
	E		
Wave Bending Ballst	F	–	–
	E		
Load Unload	F	98.882	0.0
	E	98.882	0.0

Note: F Curve   Standard Weld
       E Curve   Improved Weld

Total Probability of Failure Pf = 0.0% for F Curve
Total Probability of Failure Pf = 0.0% for E Curve

Table 4.1.5

Typical CSD and Hotspot

S. SHELL
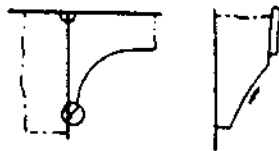
Load Component	S-N	Stress Range	Probability
Pressure Full	F	95.256	0.0
	E	95.256	0.0
Pressure Ballast	F	80.948	0.0
	E	80.948	0.0
Wave Bending Full	F	–	–
	E		
Wave Bending Ballst	F	–	–
	E		
Load Unload	F	106.33	0.0
	E	106.33	0.0

153

L.46 -Long.BKT. (N0.2 H.G)

Design Fatigue Life = 20 year
Weibull Parameter = 0.942
Number of Cycles N= 1 x 10^8
$N_{Full}= 0.5 x 10^8$ $N_{Ballast}= 0.5x 10^8$
Load and unload N =500

Table 4.2.1

Typical CSD and Hotspot

S. SHELL
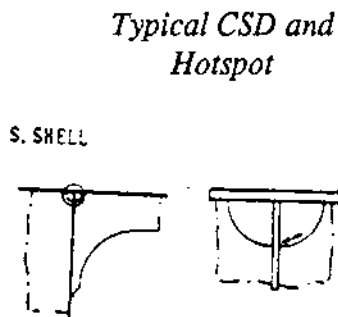
Load Component	S-N	Stress Range	Probability
Pressure Full	F	90.944	0.0
	E	90.944	0.0
Pressure Ballast	F	110.152	0.0
	E	110.152	0.0
Wave Bending Full	F	–	–
	E		
Wave Bending Ballst	F	–	–
	E		
Load Unload	F	23.128	0.0
	E	23.128	0.0

Note:F Curve   Standard Weld
     E Curve   Improved Weld

Total Probability of Failure Pf = 0.0% for F Curve
Total Probability of Failure Pf = 0.0% for E Curve

Table 4.2.2

Typical CSD and Hotspot

S. SHELL
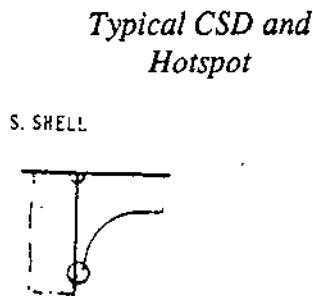
Load Component	S-N	Stress Range	Probability
Pressure Full	F	64.288	0.0
	E	64.288	0.0
Pressure Ballast	F	45.864	0.0
	E	45.864	0.0
Wave Bending Full	F	–	–
	E		
Wave Bending Ballst	F	–	–
	E		

| Load Unload | F | 54.88 | 0.0 |
| | E | 54.88 | 0.0 |

Note: F Curve   Standard Weld
        E Curve   Improved Weld

Total Probability of Failure Pf = 0.0% for F Curve
Total Probability of Failure Pf = 0.0% for E Curve

Table 4.2.3

Typical CSD and Hotspot

L. BHD
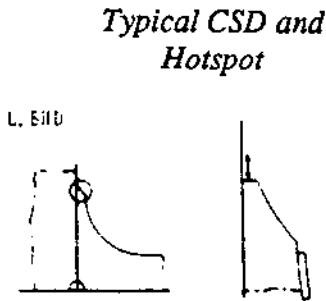
Load Component	S-N	Stress Range	Probability
Pressure Full	F	39.004	0.0
	E	39.004	0.0
Pressure Ballast	F	34.006	0.0
	E	34.006	0.0
Wave Bending Full	F	–	–
	E		
Wave Bending Ballst	F	–	–
	E		
Load Unload	F	61.25	0.0
	E	61.25	0.0

Note: F Curve   Standard Weld
        E Curve   Improved Weld

Total Probability of Failure Pf = 0.0% for F Curve
Total Probability of Failure Pf = 0.0% for E Curve

Table 4.2.4

Typical CSD and Hotspot

L. BHD
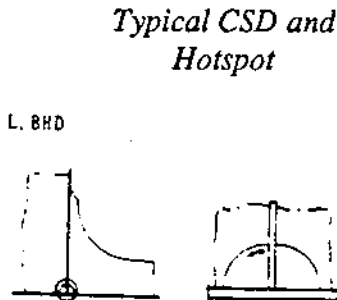
Load Component	S-N	Stress Range	Probability
Pressure Full	F	110.25	0.0
	E	110.25	0.0
Pressure Ballast	F	132.398	0.0
	E	132.398	0.0
Wave Bending Full	F	–	–
	E		
Wave Bending Ballst	F	–	–
	E		
Load Unload	F	38.122	0.0
	E	38.122	0.0

Note: F Curve   Standard Weld
        E Curve   Improved Weld

Total Probability of Failure Pf = 0.0% for F Curve
Total Probability of Failure Pf = 0.0% for E Curve

155

Table 4.2.5

Typical CSD and Hotspot

S. SHELL

Load Component	S-N	Stress Range	Probability
Pressure Full	F	139.35	0.0
	E	139.35	0.0
Pressure Ballast	F	95.746	0.0
	E	95.746	0.0
Wave Bending Full	F	–	–
	E		
Wave Bending Ballst	F	–	–
	E		
Load Unload	F	79.576	0.0
	E	79.576	0.0

Note:F Curve   Standard Weld
E Curve   Improved Weld

Total Probability of Failure Pf = 0.0% for F Curve
Total Probability of Failure Pf = 0.0% for E Curve

L.15 -Long.BKT.

Design Fatigue Life = 20 year
Weibull Parameter = 0.849
Number of Cycles $N = 1 \times 10^{8}$
$N_{Full} = 0.5 \times 10^{8}$ $N_{Ballast} = 0.5 \times 10^{8}$
Load and unload N =500

Table 5.1.1

Typical CSD and Hotspot

DK. LONG.

Load Component	S-N	Stress Range	Probability
Pressure Full	F2	171.892	0.0
	F	171.892	0.0
Pressure Ballast	F2	131.124	0.0
	F	131.124	0.0
Wave Bending Full	F2	243.628	2.3%
	F	243.628	0.21%
Wave Bending Ballst	F2	326.732	64.6%
	F	326.732	31.1%
Load Unload	F2	15.19	0.0
	F	15.19	0.0

Note:F2 Curve   Standard Weld
F Curve   Improved Weld

156

Total Probability of Failure Pf = 66.9% for F2 Curve
Total Probability of Failure Pf = 31.31% for F Curve

Table 5.1.2

Typical CSD and Hotspot

DK. LONG.

Load Component	S-N	Stress Range	Probability
Pressure Full	F	100.94	0.0
	E	100.94	0.0
Pressure Ballast	F	70.952	0.0
	E	70.952	0.0
Wave Bending Full	F	98.392	0.0
	E	98.392	0.0
Wave Bending Ballst	F	113.68	0.0
	E	113.68	0.0
Load Unload	F	12.838	0.0
	E	12.838	0.0

Note: F Curve   Standard Weld
      E Curve   Improved Weld

Total Probability of Failure Pf = 0.0% for F Curve
Total Probability of Failure Pf = 0.0% for E Curve

L.15 -Long.BKT.

Design Fatigue Life = 20 year
Weibull Parameter = 0.899
Number of Cycles N= 1 x 10 ^{8}
NFull= 0.5 x 10 ^{8} NBallast= 0.5x 10 ^{8}
Load and unload N =500

Table 5.2.1

Typical CSD and Hotspot

INN. BOTT. LONG.

Load Component	S-N	Stress Range	Probability
Pressure Full	F2	63.896	0.0
	F	63.896	0.0
Pressure Ballast	F2	86.828	0.0
	F	86.828	0.0
Wave Bending Full	F2	164.836	0.0
	F	164.836	0.0
Wave Bending Ballst	F2	190.512	0.0
	F	190.512	0.0
Load Unload	F2	17.836	0.0
	F	17.836	0.0

157

Total Probability of Failure Pf = 0.0% for F2 Curve
Total Probability of Failure Pf = 0.0% for F Curve

Typical CSD and Hotspot

INN. BOTT. LONG.

Table 5.2.2

Load Component	S-N	Stress Range	Probability
Pressure Full	F	42.238	0.0
	E	42.238	0.0
Pressure Ballast	F	61.25	0.0
	E	61.25	0.0
Wave Bending Full	F	84.476	0.0
	E	84.476	0.0
Wave Bending Ballst	F	97.608	0.0
	E	97.608	0.0
Load Unload	F	28.42	0.0
	E	28.42	0.0

Note:F Curve   Standard Weld
E Curve   Improved Weld

Total Probability of Failure Pf = 0.0% for F Curve
Total Probability of Failure Pf = 0.0% for E Curve

Typical CSD and Hotspot

INN. BOTT. LONG.

Table 5.2.3
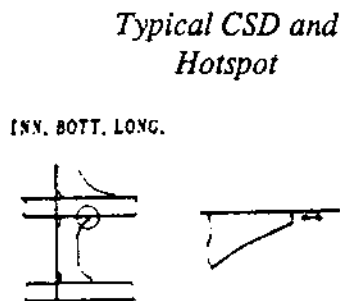
Load Component	S-N	Stress Range	Probability
Pressure Full	F	83.79	0.0
	E	83.79	0.0
Pressure Ballast	F	126.91	0.0
	E	126.91	0.0
Wave Bending Full	F	203.448	0.01873%
	E	203.448	0.0
Wave Bending Ballst	F	235.2	0.894%
	E	235.2	0.00182%
Load Unload	F	124.068	0.0
	E	124.068	0.0

Note:F Curve   Standard Weld
E Curve   Improved Weld

Total Probability of Failure Pf = 0.91273% for F Curve
Total Probability of Failure Pf = 0.00182% for E Curve

Table 5.2.4

151

Typical CSD and Hotspot

INN. BOTT. LONG.
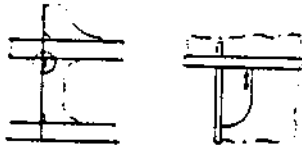
Load Component	S-N	Stress Range	Probability
Pressure Full	F	81.83	0.0
	E	81.83	0.0
Pressure Ballast	F	91.14	0.0
	E	91.14	0.0
Wave Bending Full	F	104.076	0.0
	E	104.076	0.0
Wave Bending Ballst	F	235.2	0.89%
	E	235.2	0.0018%
Load Unload	F	124.068	0.0
	E	124.068	0.0

Note:F Curve   Standard Weld
E Curve   Improved Weld

Total Probability of Failure Pf = 0.89% for F Curve
Total Probability of Failure Pf = 0.0018% for E Curve

Table 5.2.5

Typical CSD and Hotspot

BOTT. LONG.
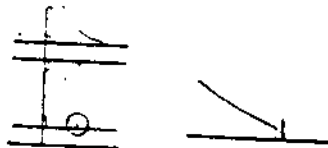
Load Component	S-N	Stress Range	Probability
Pressure Full	F	198.744	0.00888%
	E	198.774	0.0
Pressure Ballast	F	292.922	28.55%
	E	292.922	0.99%
Wave Bending Full	F	118.776	0.0
	E	118.776	0.0
Wave Bending Ballst	F	137.04	0.0
	E	137.04	0.0
Load Unload	F	70.168	0.0
	E	70.168	0.0

Note:F Curve   Standard Weld
E Curve   Improved Weld

Total Probability of Failure Pf = 25.55888% for F Curve
Total Probability of Failure Pf = 0.99% for E Curve

Table 5.2.6

Typical CSD and Hotspot

Load Component	S-N	Stress Range	Probability
Pressure Full	F	85.652	0.0
	E	85.652	0.0
Pressure Ballast	F	315.07	51.1%
	E	315.07	4.1%

159

BOTT. LONG.
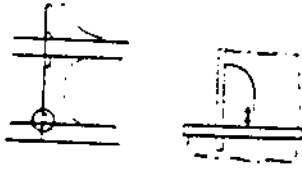
Wave Bending Full	F	114.856	0.0
	E	114.856	0.0
Wave Bending Ballst	F	132.692	0.0
	E	132.692	0.0
Load Unload	F	372.106	0.0
	E	372.106	0.0

Note: F Curve   Standard Weld
        E Curve   Improved Weld

Total Probability of Failure Pf = 51.1% for F Curve
Total Probability of Failure Pf = 4.1% for E Curve

L.15 -V.STIFF. (Ord.T.Ring)

Design Fatigue Life = 20 year
Weibull Parameter = 0.899
Number of Cycles $N= 1 \times 10^{8}$
$N_{Full}= 0.5 \times 10^{8}$ $N_{Ballast}= 0.5 \times 10^{8}$
Load and unload N =500

Typical CSD and Hotspot

INV. BOTT. LONG.
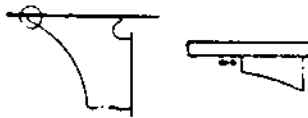
Table 6.1.1

Load Component	S-N	Stress Range	Probability
Pressure Full	F	28.91	0.0
	E	28.91	0.0
Pressure Ballast	F	79.772	0.0
	E	79.772	0.0
Wave Bending Full	F	153.664	0.0
	E	153.664	0.0
Wave Bending Ballst	F	177.772	0.00015876%
	E	177.772	0.0
Load Unload	F	133.28	0.0
	E	133.28	0.0

Note: F Curve   Standard Weld
        E Curve   Improved Weld

Total Probability of Failure Pf = 0.0001588% for F Curve
Total Probability of Failure Pf = 0.0% for E Curve

Typical CSD and Hotspot

Table 6.1.2

Load Component	S-N	Stress Range	Probability
Pressure Full	F	85.946	0.0
	E	85.946	0.0

INN. BOTT. LONG.

Pressure	F	92.61	0.0
Ballast	E	92.61	0.0
Wave Bending	F	177.772	0.0001588%
Full	E	177.772	0.0
Wave Bending	F	205.604	0.026%
Ballst	E	205.604	0.0
Load Unload	F	416.794	0.0
	E	416.794	0.0

Note:F Curve   Standard Weld
      E Curve   Improved Weld

Total Probability of Failure Pf = 0.0261588% for F Curve
Total Probability of Failure Pf = 0.0% for E Curve

Table 6.1.3

Typical CSD and Hotspot

BOTT. LONG.
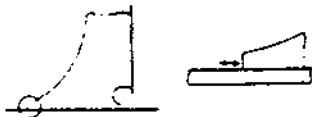
Load Component	S-N	Stress Range	Probability
Pressure	F	67.424	0.0
Full	E	67.424	0.0
Pressure	F	92.61	0.0
Ballast	E	92.61	0.0
Wave Bending	F	166.404	0.0000103%
Full	E	166.404	0.0
Wave Bending	F	192.472	0.003018%
Ballst	E	192.472	0.0
Load Unload	F	84.28	0.0
	E	84.28	0.0

Note:F Curve   Standard Weld
      E Curve   Improved Weld

Total Probability of Failure Pf = 0.00302803% for F Curve
Total Probability of Failure Pf = 0.0% for E Curve

Table 6.1.4

Typical CSD and Hotspot

Load Component	S-N	Stress Range	Probability
Pressure	F	164.052	0.0
Full	E	164.052	0.0
Pressure	F	283.024	19.7%
Ballast	E	283.024	2.45%
Wave Bending	F	214.424	0.088%
Full	E	214.424	0.0000527%
Wave Bending	F	247.94	2.6%
Ballst	E	247.94	0.011%

Total Probability of Failure Pf = 0.0% for F Curve
Total Probability of Failure Pf = 0.0% for E Curve

Typical CSD and Hotspot

AFT (FR.64)
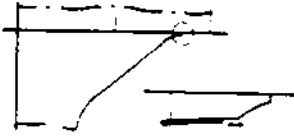
Table 7.1.2

Load Component	S-N	Stress Range	Probability
Pressure Full	F	10.78	0.0
	E	10.78	0.0
Pressure Ballast	F	5.648	0.0
	E	5.648	0.0
Wave Bending Full	F	–	–
	E		
Wave Bending Ballst	F	–	–
	E		
Load Unload	F	0.98	0.0
	E	0.98	0.0

Note:F Curve   *Standard Weld*
E Curve   *Improved Weld*

Total Probability of Failure Pf = 0.0% for F Curve
Total Probability of Failure Pf = 0.0% for E Curve

Typical CSD and Hotspot

FORE (FR.70)
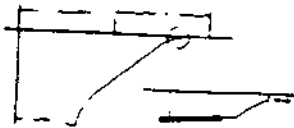
Table 7.1.3

Load Component	S-N	Stress Range	Probability
Pressure Full	F	12.544	0.0
	E	12.544	0.0
Pressure Ballast	F	15.386	0.0
	E	15.386	0.0
Wave Bending Full	F	–	–
	E		
Wave Bending Ballst	F	–	–
	E		
Load Unload	F	4.9	0.0
	E	4.9	0.0

Note:F Curve   *Standard Weld*
E Curve   *Improved Weld*

Total Probability of Failure Pf = 0.0% for F Curve
Total Probability of Failure Pf = 0.0% for E Curve

Table 7.1.4

Typical CSD and Hotspot

FORE (FR. 70)

Load Component	S-N	Stress Range	Probability
Pressure Full	F	3.234	0.0
	E	3.234	0.0
Pressure Ballast	F	7.546	0.0
	E	7.546	0.0
Wave Bending Full	F	–	–
	E		
Wave Bending Ballst	F	–	–
	E		
Load Unload	F	0.98	0.0
	E	0.98	0.0

Note: F Curve   Standard Weld
      E Curve   Improved Weld

Total Probability of Failure Pf =0.0% for F Curve
Total Probability of Failure Pf = 0.0% for E Curve

No.2 H.Gir.

Design Fatigue Life = 20 year
Weibull Parameter = 0979
Number of Cycles N= 1 x 10^8
NFull= 0.5 x 10^8 NBallast= 0.5x 10^8
Load and unload N =500

Table 7.1.1

Typical CSD and Hotspot

AFT (FR. 64)
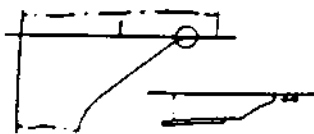
Load Component	S-N	Stress Range	Probability
Pressure Full	F	58.604	0.0
	E	58.604	0.0
Pressure Ballast	F	69.09	0.0
	E	69.09	0.0
Wave Bending Full	F	–	–
	E		
Wave Bending Ballst	F	–	–
	E		
Load Unload	F	2.94	0.0
	E	2.94	0.0

Note: F Curve   Standard Weld
      E Curve   Improved Weld

Total Probability of Failure Pf = 0.0% for F Curve
Total Probability of Failure Pf = 0.0% for E Curve

Table 7.2.2

Typical CSD and Hotspot

AFT (FR.64)

Load Component	S-N	Stress Range	Probability
Pressure Full	F	29.89	0.0
	E	29.89	0.0
Pressure Ballast	F	40.376	0.0
	E	40.376	0.0
Wave Bending Full	F	–	–
	E		
Wave Bending Ballst	F	–	–
	E		
Load Unload	F	1.96	0.0
	E	1.96	0.0

Note: F Curve   Standard Weld
E Curve   Improved Weld

Total Probability of Failure Pf = 0.0% for F Curve
Total Probability of Failure Pf = 0.0% for E Curve

Table 7.2.3

Typical CSD and Hotspot

Load Component	S-N	Stress Range	Probability
Pressure Full	F	0.0	0.0
	E	0.0	0.0
Pressure Ballast	F	0.0	0.0
	E		0.0
Wave Bending Full	F	–	–
	E		
Wave Bending Ballst	F	–	–
	E		
Load Unload	F	0.0	0.0
	E	0.0	0.0

Note: F Curve   Standard Weld
E Curve   Improved Weld

Total Probability of Failure Pf = 0.0% for F Curve
Total Probability of Failure Pf = 0.0% for E Curve

Table 7.2.4

Typical CSD and Hotspot

Load Component	S-N	Stress Range	Probability
Pressure Full	F	11.172	0.0
	E	11.172	0.0
Pressure Ballast	F	14.7	0.0
	E	14.7	0.0
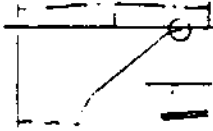
157

FORE (FR. 70)

Wave Bending Full	F	–	–
	E		
Wave Bending Ballst	F	–	–
	E		
Load Unload	F	0.0	0.0
	E	0.0	0.0

Note: F Curve   Standard Weld
       E Curve   Improved Weld

Total Probability of Failure Pf =0.0% for F Curve
Total Probability of Failure Pf = 0.0% for E Curve

Load Unload	F	350.938	0.0	
	E	350.938	0.0	

Note:F Curve   Standard Weld
E Curve   Improved Weld

Total Probability of Failure Pf =22.388 for F Curve
Total Probability of Failure Pf = 2.461% for E Curve

L.15 -Slot (Bott.Long)

Design Fatigue Life = 20 year
Weibull Parameter = 0.899
Number of Cycles $N = 1 \times 10^{8}$
$N_{Full} = 0.5 \times 10^{8}$ $N_{Ballast} = 0.5 \times 10^{8}$
Load and unload N =500

Table 6.2.1

Typical CSD and Hotspot

INN. BOTT. LONG.

Load Component	S-N	Stress Range	Probability
Pressure Full	F2	150.136	0.0
	F	150.136	0.0
Pressure Ballast	F2	314.09	80.8%
	F	314.09	50.1%
Wave Bending Full	F2	–	–
	F		
Wave Bending Ballst	F2	–	–
	F		
Load Unload	F2	332.2	0.0
	F	332.2	0.0

Note:F2 Curve   Standard Weld
F Curve   Improved Weld

Total Probability of Failure Pf = 80.8% for F2 Curve
Total Probability of Failure Pf = 50.1% for F Curve

Table 6.2.2

Typical CSD and Hotspot

INN. BOTT. LONG.

Load Component	S-N	Stress Range	Probability
Pressure Full	F	58.114	0.0
	E	58.114	0.0
Pressure Ballast	F	106.232	0.0
	E	106.232	0.0
Wave Bending Full	F	–	–
	E		

Wave Bending Ballst	F E	–	–
Load Unload	F	253.232	0.0
	E	253.232	0.0

Note:F Curve — Standard Weld
E Curve — Improved Weld

Total Probability of Failure Pf = 0.0% for F Curve
Total Probability of Failure Pf = 0.0% for E Curve

Table 6.2.3

Typical CSD and Hotspot

BOTT. LONG.
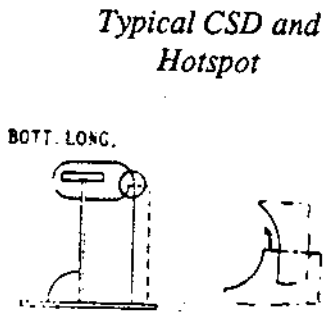
Load Component	S-N	Stress Range	Probability
Pressure Full	F2	106.134	0.0
	F	106.134	0.0
Pressure Ballast	F2	137.2	0.0
	F	137.2	0.0
Wave Bending Full	F2	–	–
	F		
Wave Bending Ballst	F2	–	–
	F		
Load Unload	F2	545.37	0.0
	F	545.37	0.0

Note:F2 Curve — Standard Weld
F Curve — Improved Weld

Total Probability of Failure Pf = 0.0% for F2 Curve
Total Probability of Failure Pf = 0.0% for F Curve

Table 6.2.4

Typical CSD and Hotspot

BOTT. LONG.
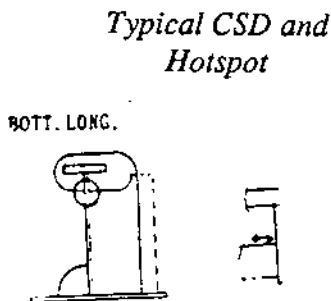
Load Component	S-N	Stress Range	Probability
Pressure Full	F	113.68	0.0
	E	113.68	0.0
Pressure Ballast	F	207.858	0.036%
	E	207.858	0.0000143%
Wave Bending Full	F	–	–
	E		
Wave Bending Ballst	F	–	–
	E		
Load Unload	F	235.572	0.0
	E	236.572	0.0

Note:F2 Curve — Standard Weld
F Curve — Improved Weld

163

Total Probability of Failure Pf = 0.036% for F Curve
Total Probability of Failure Pf = 0.0000143% for E Curve

Typical CSD and Hotspot

BOTT. LONG.

Table 6.2.5

Load Component	S-N	Stress Range	Probability
Pressure Full	F	17.934	0.0
	E	17.934	0.0
Pressure Ballast	F	39.004	0.0
	E	39.004	0.0
Wave Bending Full	F	–	–
	E		
Wave Bending Ballst	F	–	–
	E		
Load Unload	F	142.68	0.0
	E	142.68	0.0

Note: F Curve   Standard Weld
      E Curve   Improved Weld

Total Probability of Failure Pf = 0.0% for F Curve
Total Probability of Failure Pf = 0.0% for E Curve

No.1 H.Gir.

Design Fatigue Life = 20 year
Weibull Parameter = 0979
Number of Cycles N= 1 x 10^8
NFull= 0.5 x 10^8 NBallast= 0.5x 10^8
Load and unload N =500

Table 7.1.1

Typical CSD and Hotspot

AFT (FR.84)
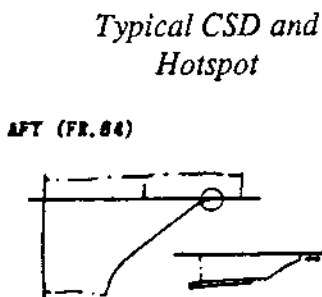
Load Component	S-N	Stress Range	Probability
Pressure Full	F	7.448	0.0
	E	7.448	0.0
Pressure Ballast	F	4.998	0.0
	E	4.998	0.0
Wave Bending Full	F	–	–
	E		
Wave Bending Ballst	F	–	–
	E		
Load Unload	F	10.78	0.0
	E	10.78	0.0

Study of Fatigue of Proposed Critical Structural Details in Double Hull Tankers

Fatigue Analysis of Critical Structural Details in a 190,000 DWT Double Bottom Tanker

Tao Xu
and
Professor Robert G. Bea

Department of Naval Architecture and Offshore Engineering
University of California, Berkeley

169, 170v

Table of Contents

Chapter 6 CSD Design Alternatives

7 Summary and Conclusions

List of Figures

List of Tables

175, 176 ∀

Chapter 1

Introduction

The steel structure of tankers is subject to various cyclic loads during its lifetime. Structural cracks that develop during the life of the ship result from the cyclic stresses. Cracks frequently occur at welded joints. Cracks also are found at cutouts and other discontinuities in the base material. Recently, experience with highly optimized design of relatively new (less than 5 years old) VLCC's and ULCC's has indicated the presence of significant cracking in CSD. Fundamentally, these problems appear to be the result of excessively high nominal stresses in the CSD that are derived from the use of higher strength steels, improperly configured details, incorrectly defined fatigue stresses and inappropriate S-N curves.

Recently, the classification rules such as those of DNV, ABS have included requirements for fatigue strength of critical structural details (CSD) [Ref.1.1,1.2]. They are based on nominal stresses. The nominal stress approach has two disadvantages. First, it is in many cases not possible to define a reasonable nominal stress, Second, suitable fatigue test results are often not available for the wide variety of CSD found in hull structures. The definition of the nominal stress may be rather difficult, if the overall stress analysis of the structure is performed with the aid of the finite element method. This is increasingly the case with modern ships having highly utilized structural members.

Approaches for the fatigue strength assessment on the basis of critical hot spot stresses (HSS) help overcome some of these difficulties. Such an approach defines the local stress such that the structural (or geometric) notch effect is considered while the notch effect caused by the weld toe is not considered. This idea has been applied especially in the offshore technology by the development of the HSS approach for the fatigue assessment of tubular joints. In the joint industry project **Fatigue Classification of Critical Structural Details in Tankers** conducted by Department of Naval Architecture & Offshore Engineering, University of California at Berkeley (1992-1993), the HSS approach was applied to develop a coherent and calibrated method for the selection and classification of cyclic stress range - number of cycles to failure (S-N) relationships for use in fatigue analyses of CSD in tankers.

The objective of joint industry project **Study of Fatigue of Proposed Critical Structural Details in Double-Hull Tankers** was to conduct an analyitical study of

proposed critical structural details (CSD) for new double-hull tankers to assure that they have desirable durability characteristics.

In this study, we proposed to perform analyses of 10 CSDs from two structural systems that are proposed to the next generation of double-hull tankers.

In this project, two level analyses were performed to determine the fatigue durability.
1) Finite element analysis for the CSD to provide an accurate model for the load-displacement behavior of the CSD and the stress distribution at the element level for the fatigue damage evaluation.
2) Fatigue analysis to assure that the CSD has desirable durability and robustness characteristics.

Fig. 1 and Fig. 2 show the general fatigue analysis procedure for proposed CSD in double-hull tankers.

In conjunction with the study of **Fatigue Classification of Critical Structural Details in Tankers**, the finite element analyses were performed to determine the hot spot stress concentration factors (SCF) by systematic calculation of typical CSD. The fatigue analysis of proposed CSD was conducted based on the S-N curve selection of hot spot stress. A sensitivity analysis was conducted to determine the geometry sensitivity of stress concentration factors.

Based on the two level analysis, several design alternatives were studied to determine effective means of increasing the durability and robustness characteristics.

178

```
┌─────────────────────────┐
│   Loading Condition     │
│   (cargo, Ballast)      │
└─────────────────────────┘
             │
             ▼
┌─────────────────────────┐              ┌─────────────────────────┐
│    Wave Condition       │              │                         │
│  (Wave Length, Height   │              │     Unit Loading        │
│      direction)         │              │                         │
└─────────────────────────┘              └─────────────────────────┘
             │                                        │
             ▼                                        ▼
┌─────────────────────────┐              ┌─────────────────────────┐
│    Ship Motion Wave     │              │     3-Dimensional       │
│                         │              │    Finite Element       │
│        Loads            │              │       Analysis          │
└─────────────────────────┘              └─────────────────────────┘
             │                                        │
             ▼                                        ▼
┌─────────────────────────┐              ┌─────────────────────────┐
│ Response Function of Wave│             │                         │
│     Induced Forces      │◄─────────────│    Stress Transfer      │
│  ( Pressure, Wave Loads,│              │      Functions          │
│      Acceleration)      │              │                         │
└─────────────────────────┘              └─────────────────────────┘
             │
             ▼
┌─────────────────────────┐
│   Stress Time Histories │
└─────────────────────────┘
             │
             ▼
┌─────────────────────────┐              ┌─────────────────────────┐
│ Stress Response Functions│────────────▶│░░░Long -Term░░░░░░░░░░░░│
│                         │              │░░░Stress Range░░░░░░░░░░│
└─────────────────────────┘              └─────────────────────────┘
```
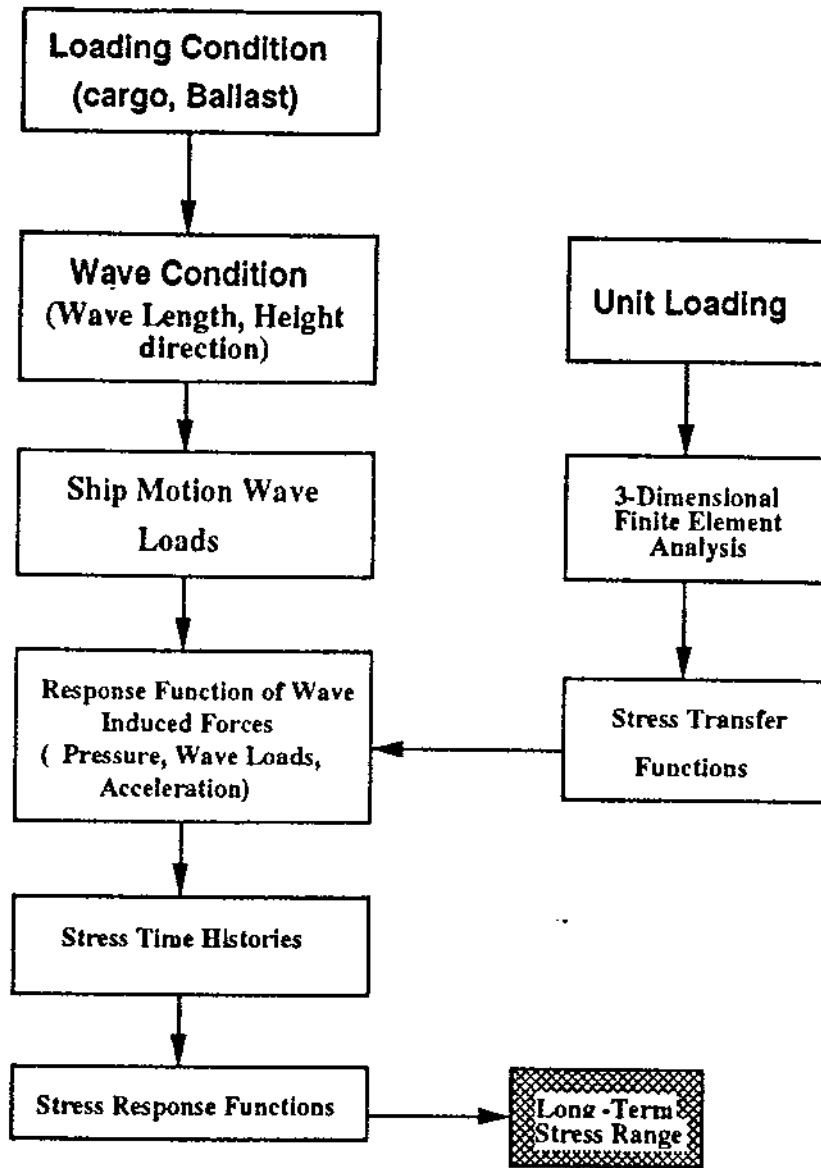
Fig 1.1 Long-term Loading Procedure for Proposed CSD in Tankers

3
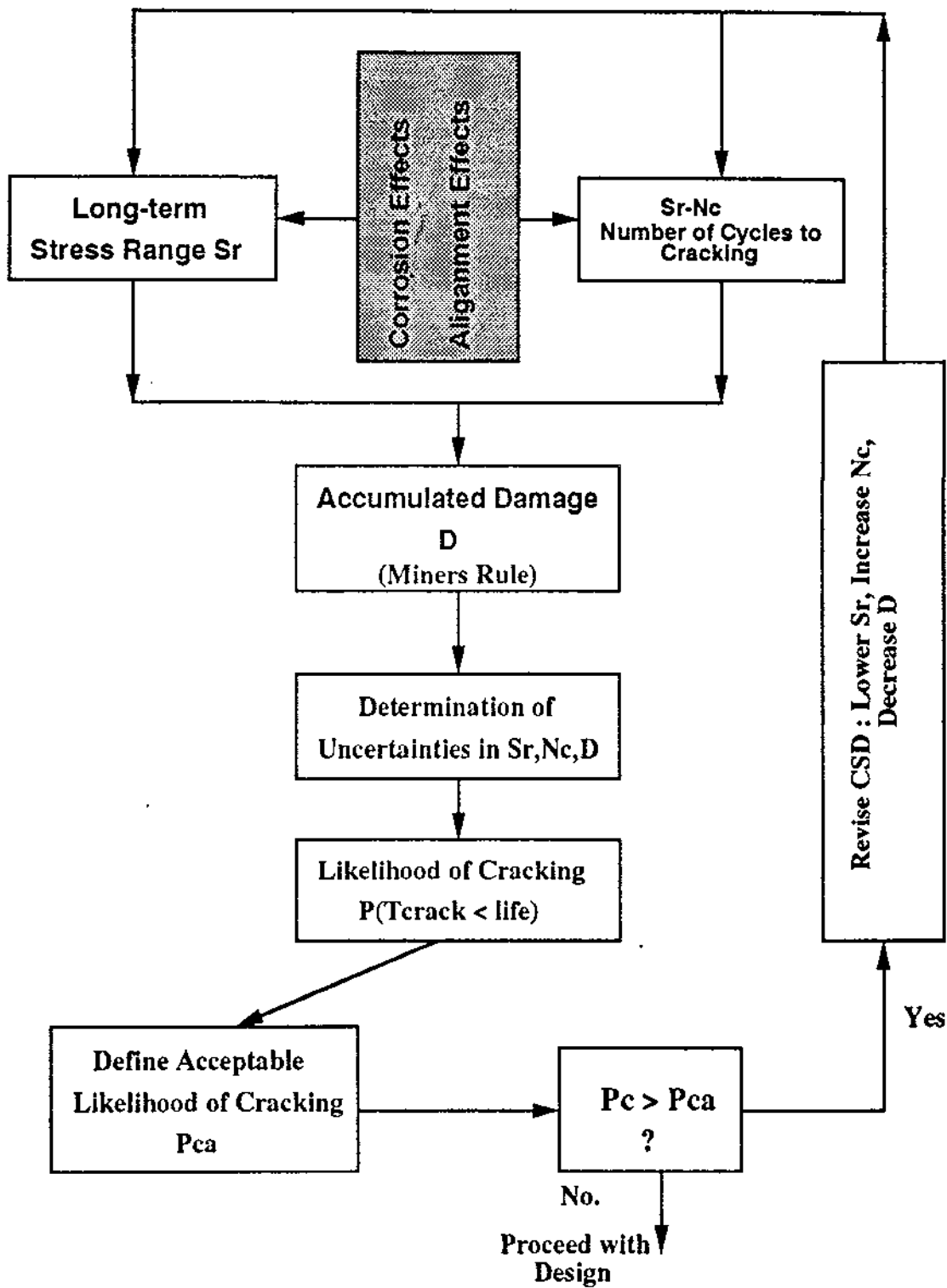
Fig 1.2 Fatigue Analysis Procedure for Proposed CSD in Tanker

4

180

Chapter 2

Ship Characteristics and Motion

2.1 General

A VLCC with 190,000 DWT was studied as the second proposed tanker. The overall dimensions are described in Table (2.1). The general arrangement is shown in Fig 2.1. The midship section is shown in Fig 2.2.

2.2 Voyage Profile for Service Life

The proposed tanker was assumed to travel exclusively on the TAPS trade route. The travel routes are defined by the time the vessel spends in the specified Marsden zones and the total harbor time. A description of the Marsden zones and a complete listing of the wave statistics for each zone can be found in Ref .1

The proposed tanker operates on the TAPS trade route between California and Alaska. This route passes through the Marsden zones 6,7,13,14,22. Fig 2.3 shows these Marsden zones and the courses and destinations.

The SMP project has summarized the voyage profile for the proposed tanker over 15 years (Ref.1). The tanker spends about 60% of the time at sea and 40% at port.

The calculation of the long-term distribution of the stress ranges is based on the time the tanker spend in different Marsden zones and the total harbor time. background on the procedure can be found in Ref. 2

For each of the above Marsden zones the estimated percentage is multiplied by the service life of the proposed tanker.

$$T_i = \lambda_i T_s$$

where

T_i = Time in Marsden zone i
λ_i = Relative Time in Marsden zone i [%]

5

181

T_s = Service life of Vessel
i = {6,7,13,14,22}

2.3 Maneuvering Philosophy

Information about the proposed tanker speed laden and under ballast is needed to calculate the transfer functions for the tanker using a ship motion program. Course changes and speed reductions due to bad weather will also strongly affect the long-term distribution of the ship responses. This information is therefore also required input for the estimation of the long-term distribution of the ship response.

The following information is required .

Fraction of time in Load case 1
Steer speed in Load case 1
Cruising speed in Load case 1
Fraction of time in Load case 2
Cruising speed in Load case 2
Course change for Hs in head, beam and following sea
Cruising speed change in head, beam and following sea
Steering speed change in head, beam and following sea

The data for the above information has been obtained from the operator of the vessel used for the proposed tanker. In general course changes due to bad weather are avoided. According to the owner/operator speed reduction to prevent damage to the ship in bad weather is only used in extreme condition since the increased resistance caused by high sea states will automatically result in a reduced speed.

Table 2.2 contains a summary of the information that is used to describe the maneuvering philosophy for the proposed tanker.

2.4 Steel Properties

The major of the steel used in the proposed tanker was the HTS Grade "AH32" steels. The mechanical properties of this type of steel are :
Tensile Strength...min. 48kg/mm^2
Yield Strength...min. 32kg/mm^2

6

182

2.5 Ship Motion Response

The quantification of the response of tanker structure to wave is crucial for fatigue evaluation. The alternating excition induced in tanker structures by wave action produces different types of response such as motions and stresses.

A ship motion analysis was performed to generate Response Amplitude Operators (RAO's) for tanker bending moments and hydrodynamic (outer) pressures in various headings, In addition, the accelerations generated by the ship motion were used to determine inner pressures.

Based on the RAO, the short-term and long-term statistics was performed to determine the long-term loading for the tanker during its service life.

The ship motion analysis were performed in previous SMP project. More details can be found in Ref. 2. In this project, the corresponding loading were applied in Global and Local Finite element analysis.

183

DWT	LOA	LBP	Breadth Molded	Depth Molded	Draft	Construction
190,000	290.4	279.5	50.6	23.8	18.1	Double-Bottom

Table 2.1 Overall Dimensions for Double-Bottom Tanker

Information	Input Data
Fraction of time *ballast*	45
Steering speed *ballast*	2.3 m/s
Cruising speed *ballast*	7.9 m/s
Fraction of time *laden*	55
Steering speed *laden*	2.05 m/s
Cruising speed *laden*	7.46 m/s
Course change for H_S in head, beam and following sea	12, 12, 12
Cruising speed change for H_S in head, beam and following sea	10, 9, 10
Steering speed change for H_S in head, beam and following sea	11, 10, 11

Table 2.2 Maneuvering Philosophy and Speed Characteristics
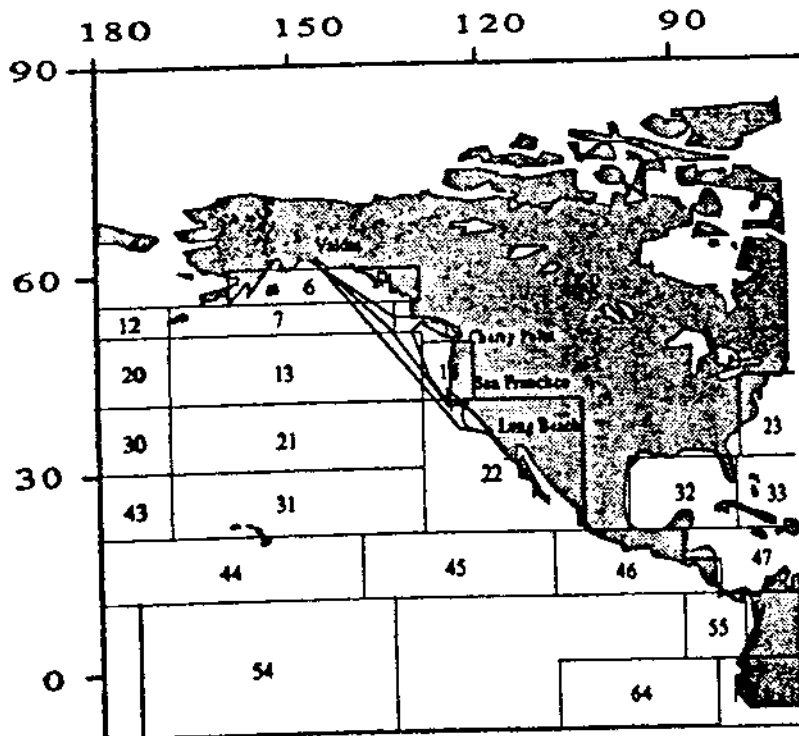
Fig 2.3 Marsden Zones for North Pacific

184

Tank 5 | Tank 4 | Tank 3 | Tank 2 | Tank 1

135 114   71   62   53 48   43   32   23   0

Profile

68   Upper Deck
                                    48
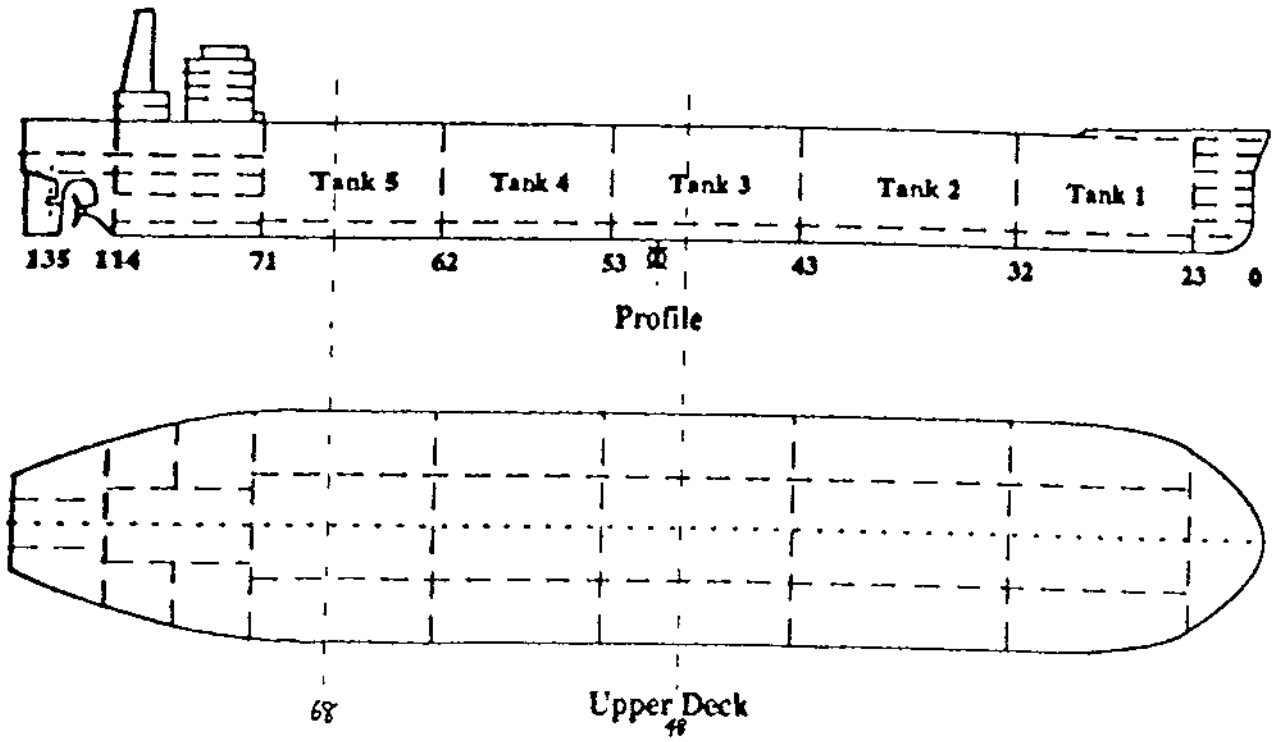
Fig 2.1 General Arrangement

9

185
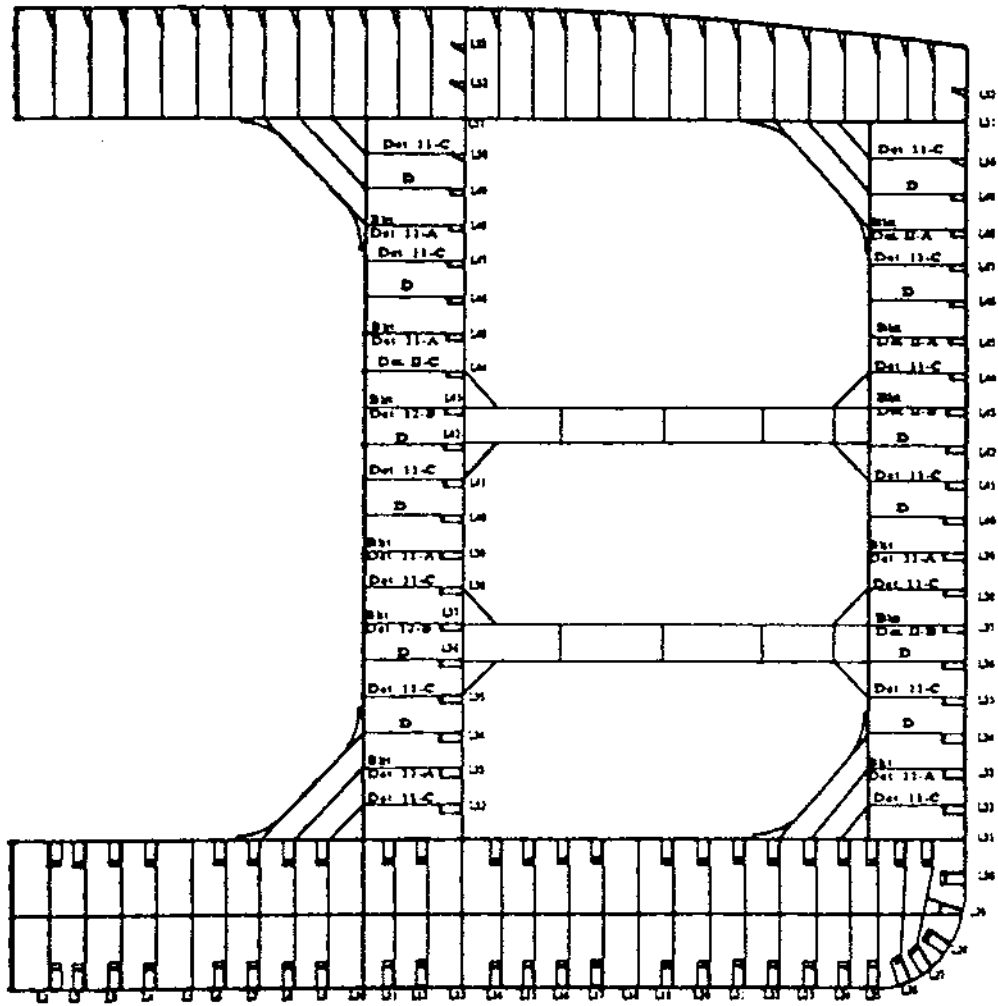
Shell and Longl. Bhd Longitudinals

Shell Longls	Bhd Longls	Size	Spacing 36"
50, 51, 52	50, 51, 52, 53	12" x 45.9 FB	
47, 48, 49	47, 48, 49	14" x 4" x.5",.75"	
46	45, 46	15" x 5" x.5",.75"	
43, 44, 45	43, 44	16" x 5" x.5",.75"	
40, 41, 42	39, 40, 41, 42	18" x 6" x.5",.75"	
36, 37, 38, 39	35, 36, 37, 38	21" x 6" x.5",.75"	
32, 33, 34, 35	32, 33, 34	21" x 8" x.5",.75"	

Fig 2.2 Midship Section

186

Chapter 3

Global Finite Element Analysis

3.1 General

A three dimensional finite element analysis was performed for the parallel mid-body cargo tanks between frame 66 and frame 48 which is shown in Fig 3.1. The objective of this analysis was to obtain boundary conditions and loads for the subsequent fine mesh analysis for local details.

3.2 Global Model

The extent of the global model is from vessel frame 48 to frame 66. It is assumed that the loads are symmetrical with respect to the longitudinal axis. Only the port half of the tanker is modeled. The vessel was modeled using various finite elements whose geometry configuration and stiffeness closely approximate the actual structures. The deck, longitudinal bulkhead, transverse bulkhead, sideshell, inner bottom and outer bottom were shell plate element. Frame element were used for longitudinal and sideshell stiffeners. Selection hidden line plot are shown in Fig 3.2 for global FE model and in Fig. 3.3 for web frame selection for corresponding model.

3.3 Global Loading

Since the objective of the FEM analysis is to determine the SCF of the hotspot in local details, the normal loading for the stillwater ballast condition was applied to the global model. For this case tanks 5P, 5S, 3P and 3S are filled with saltwater ballast. A schematic showing about the ballast distribution is shown in Fig. 3.4. To obtain realistic stresses, boundary moments derived from ship motion analysis were applied at the end of the model. The magnitude of these boundary moments were determined such that the total bending moment at the middle of the model, the line of symmetry, would satisfy the ABS rule requirements while the sideshell and bottom pressure were applied as the equivalent weight loads.In this case, load information was obtained from the previous SMP project (Ref .1 and Ref. 2). The shear and bending moment diagrams are presented in Fig. 3.5 and Fig 3.6.

187

3.4 Results and Discussion

The objective of the global finite element analysis is to derive the appropriate boundary conditions for nonsideshell longitudinal details to calculate the hotspot SCFs. The plot for stress contours are presented in Ref. 3. It was found that the double bottom connections are one of the high stress region. A more fine analysis was conducted and is summarized in Chapter 4. For the general sideshell longitudinal details, global finite element analysis is neglected in the SMP fatigue analysis procedure (Ref. 1 and Ref. 2) while the global finite element was used for local finite element analysis to calculate the stress concentration factors.

188

Profile

Tank 5 | Tank 4 | Tank 3 | Tank 2 | Tank 1

135 114   71   62   53 42   43   32   23 0

Upper Deck

68   42
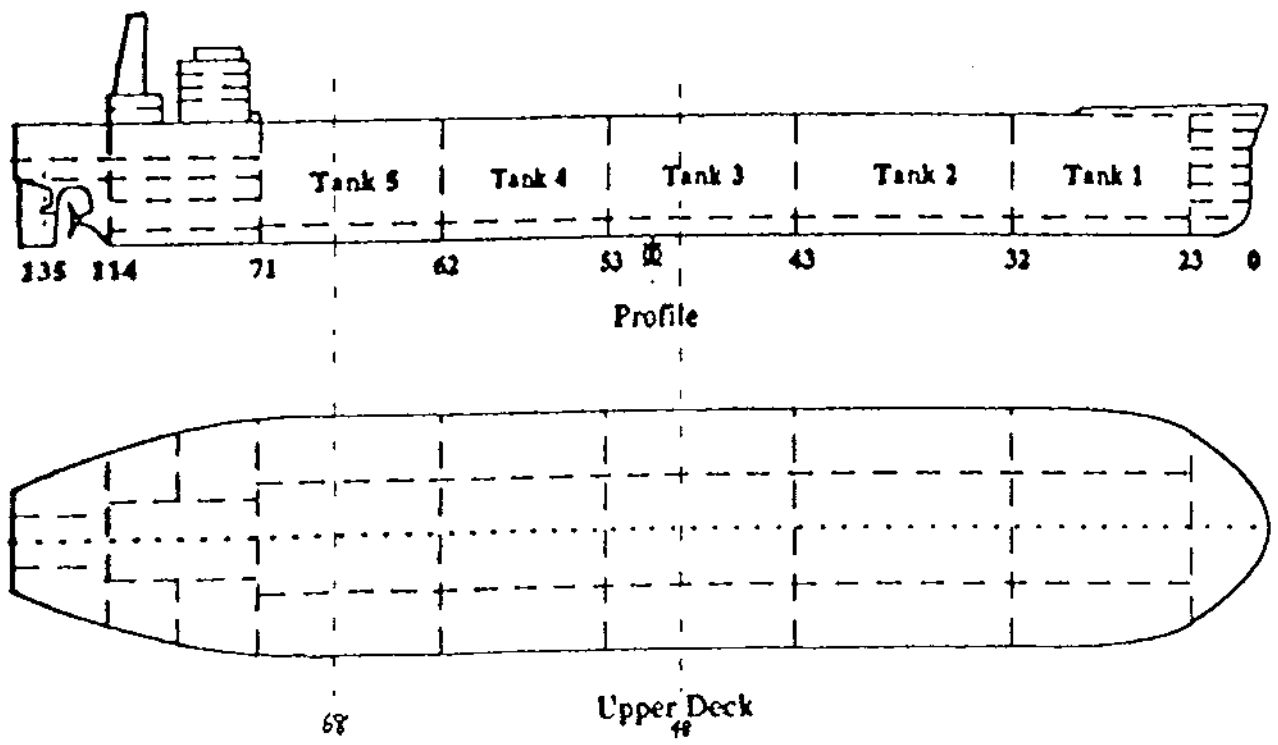
Fig 3.1 Parallel Mid-Body Tanker

13   189
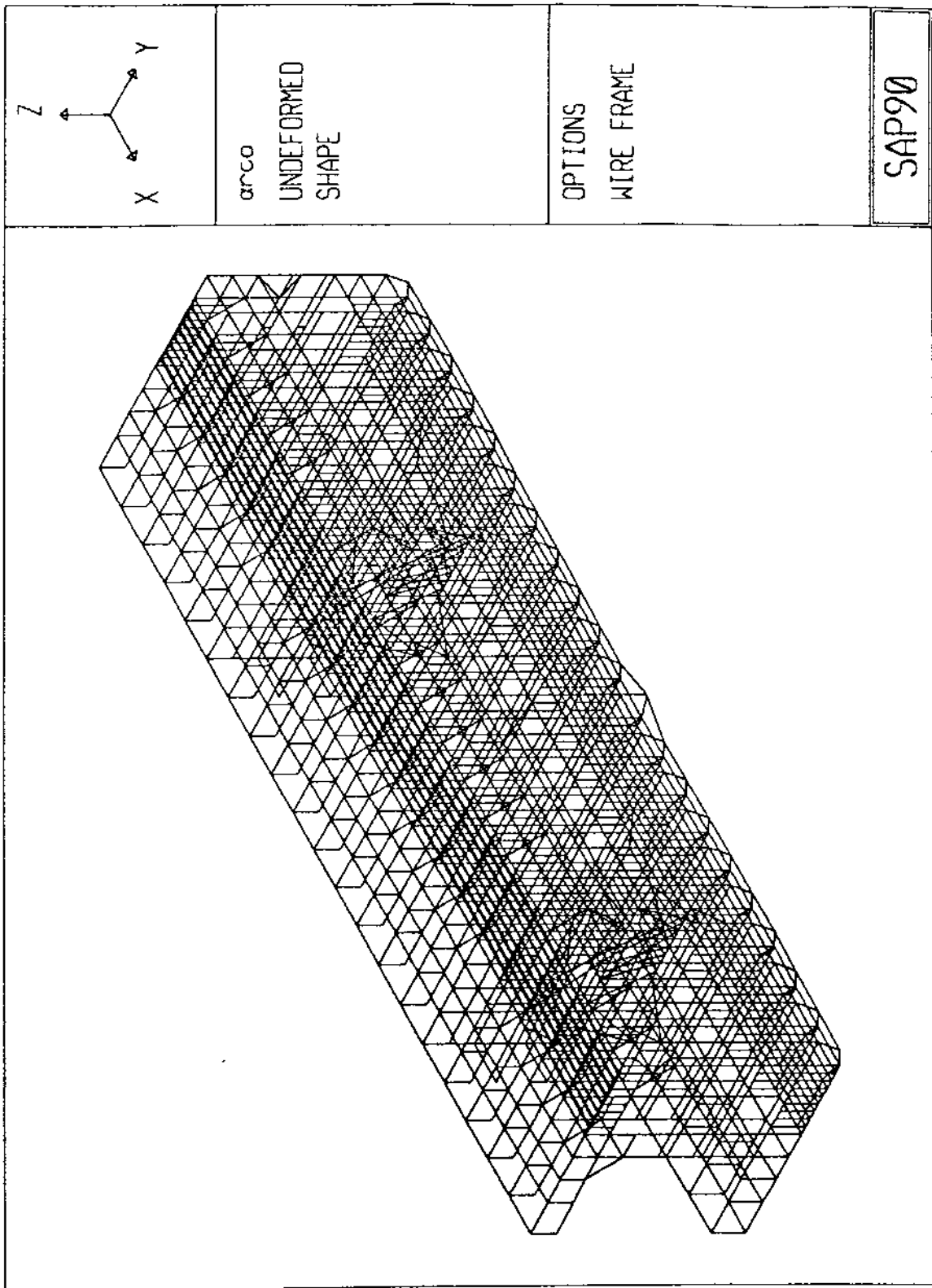
Fig 3.2 Global FEM Model

14
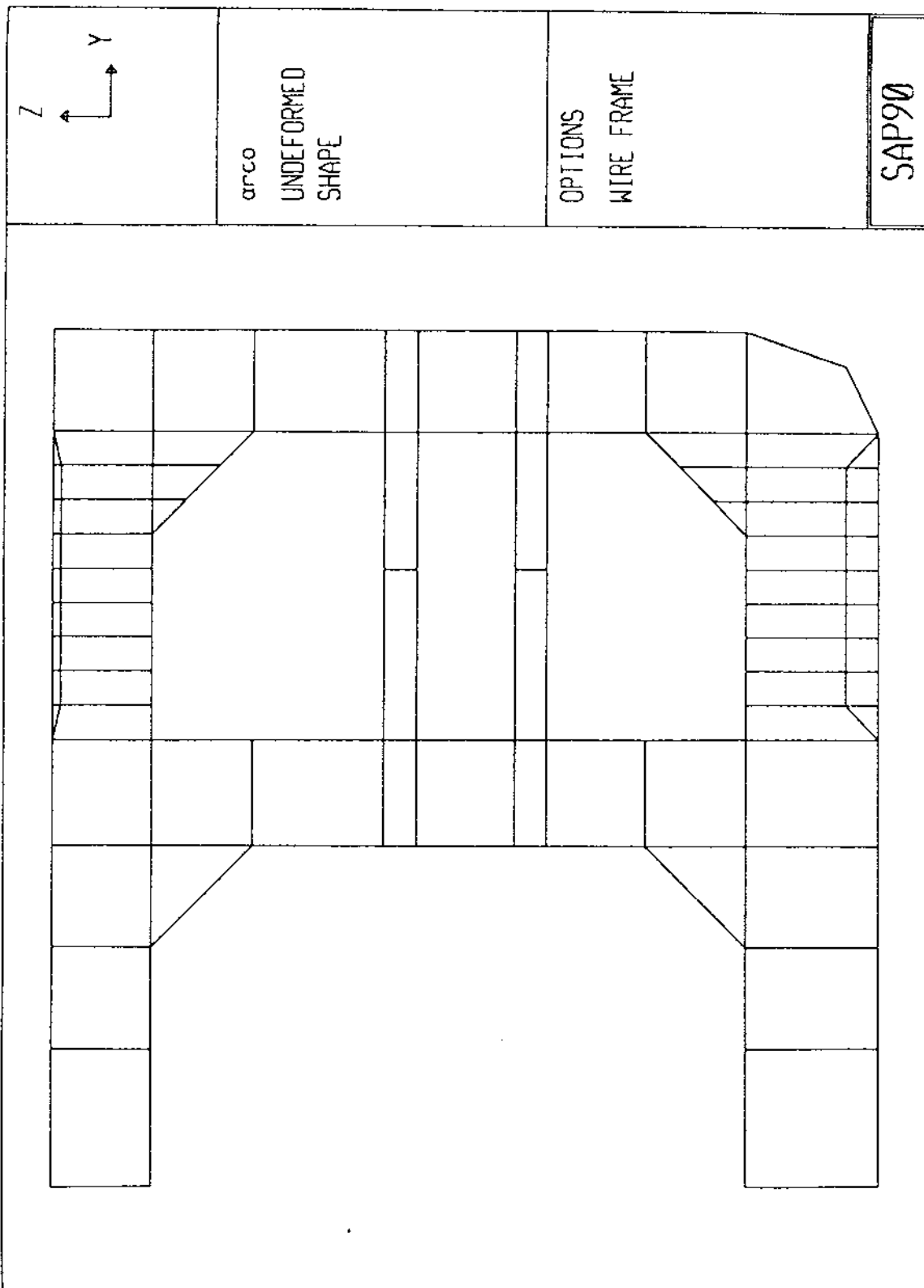
Fig 3.3 FEM Model for Midship Section

Profile

Upper Deck
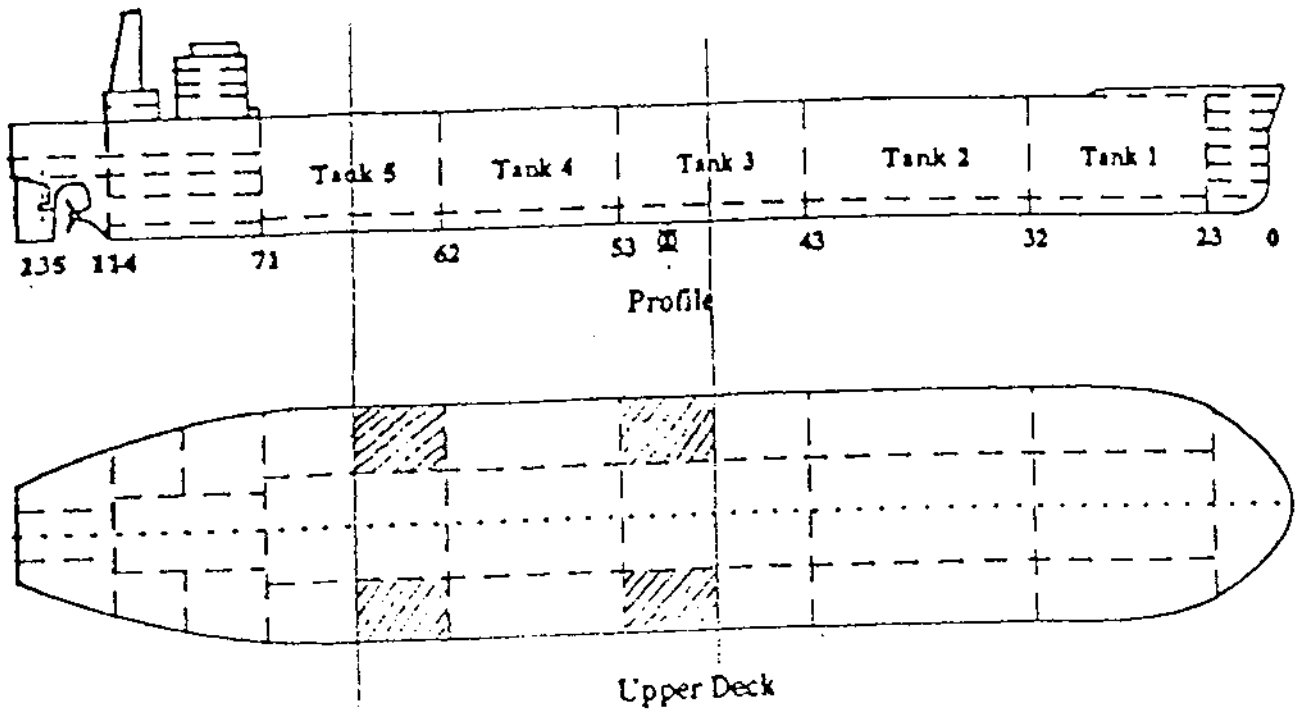
Fig 3.4 Ballast Layout
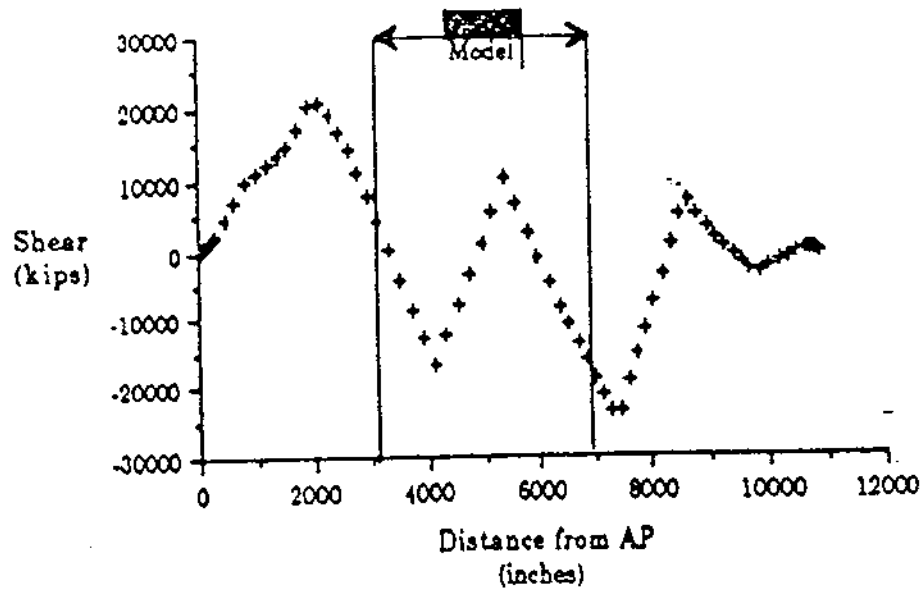
Fig 3.5 Global Shear Force

Chapter 4

Local Finite Element Analysis

4.1 General

The objective of this chapter is to conduct a systematic finite element analysis of CSD to determine the stress concentration factors. The use of stress concentration factors (SCFs) is preferable in practical design. If dependence of the main geometric parameters is taken into account, a relatively simple optimization of structural details becomes possible.

4.2 Finite Element Modeling

Preparation of a "standard" finite element model of a CSD is rather straightforward although it's time consuming. But we still have to consider some factors which, if ignored, may invalidate an otherwise apparently well constructed model.

In this chapter, a series 3-D finite element models were created to conduct the study of SCFs. The extent of the model was over 2 frame spacings, a frame spacing to either side of the trans web. The vertical extent was one longitudinal spacing above and below the bracket detail. All the plating was idealized by shell bending element while the longitudinal flange was modeled by frame elements. Fig. 4.1 and Fig 4.2 show the typical 3-D finite element models.

One of the difficult aspects of finite element analysis is the assignment of boundary conditions. Boundary conditions must be applied to the model to simulate the remaining part of the structure which are not included in the model itself. At these boundary locations, forces or displacements are usually applied. Improperly distributed or applied boundary forces may cause a high stress area around the boundary region or result in large (unrealistic) rigid body displacement. During the SMP project conducted by Department of Naval Architecture & Offshore Engineering, University of California at Berkeley from 1990 to 1992. A general procedure to determine the applied boundary conditions for the general sideshell longitudinal details was developed. (Ref. 1 and Ref. 2). The boundary conditions for the general sideshell longitudinal details can be applied directly in SMP software. But it can not handle the nonsideshell details which the boundary displacements derived from global finite element analysis are applied.

18

194

4.3 Systematic Calculation of Stress Concentration Factors

The stress concentration factors are important in CSD fatigue design. First, it can be used to be a relative evaluation about the CSD stress distribution. Second, it can be applied in preliminary CSD fatigue optimization design.

Systematic finite element analysis were performed for various CSD with the objective of establishing approximation formula for hot spot SCFs. The proposed CSD was the interaction of longitudinal L34 with Frame F53. The finite element analysis for various configurations about cut out and stiffeners were conducted to determine the hotspot stress around the cut out, bracket -toe and so on.

4.4 General Sideshell Longitudinal Details

Fig 4.3 is the typical web frame section and general sideshell detail location. Fig 4.4 is the typical geometry and dimensions for the proposed general sideshell detail. The applied loads are derived from the global finite element analysis.

4.4.1 Transverse Web frame Cutout

In general side shell CSD, cutouts in web frame or transverse bulkhead are usually the high stress area. Damage statistics for the tankers show that about 70% of cracks repaired, occurr at the connection between the longitudinal and transverse web of intricate nature, which in turn demands a detailed analysis procedure. Unfortunately, the Classification Society's Rules do not govern the design of these connections and cutouts in details. From the systematic analysis of the transverse web with different cutouts, results about the SCFs around the cutouts have been provided which may be useful in preliminary optimization structural design. Fig 4.6 and Fig 4.7 shows the typical CSD and corresponding FEM model.

From the systematic analysis of the transverse web with different cutouts, several results about the SCFs around the cutout has been provided which may be useful in preliminary structural design. Following is the summarize of the study performed by Finite Element Analysis. The stress contours are presented in Ref. 3

195

Y Z X	
arcob UNDEFORMED SHAPE	
OPTIONS WIRE FRAME	
SAP90	
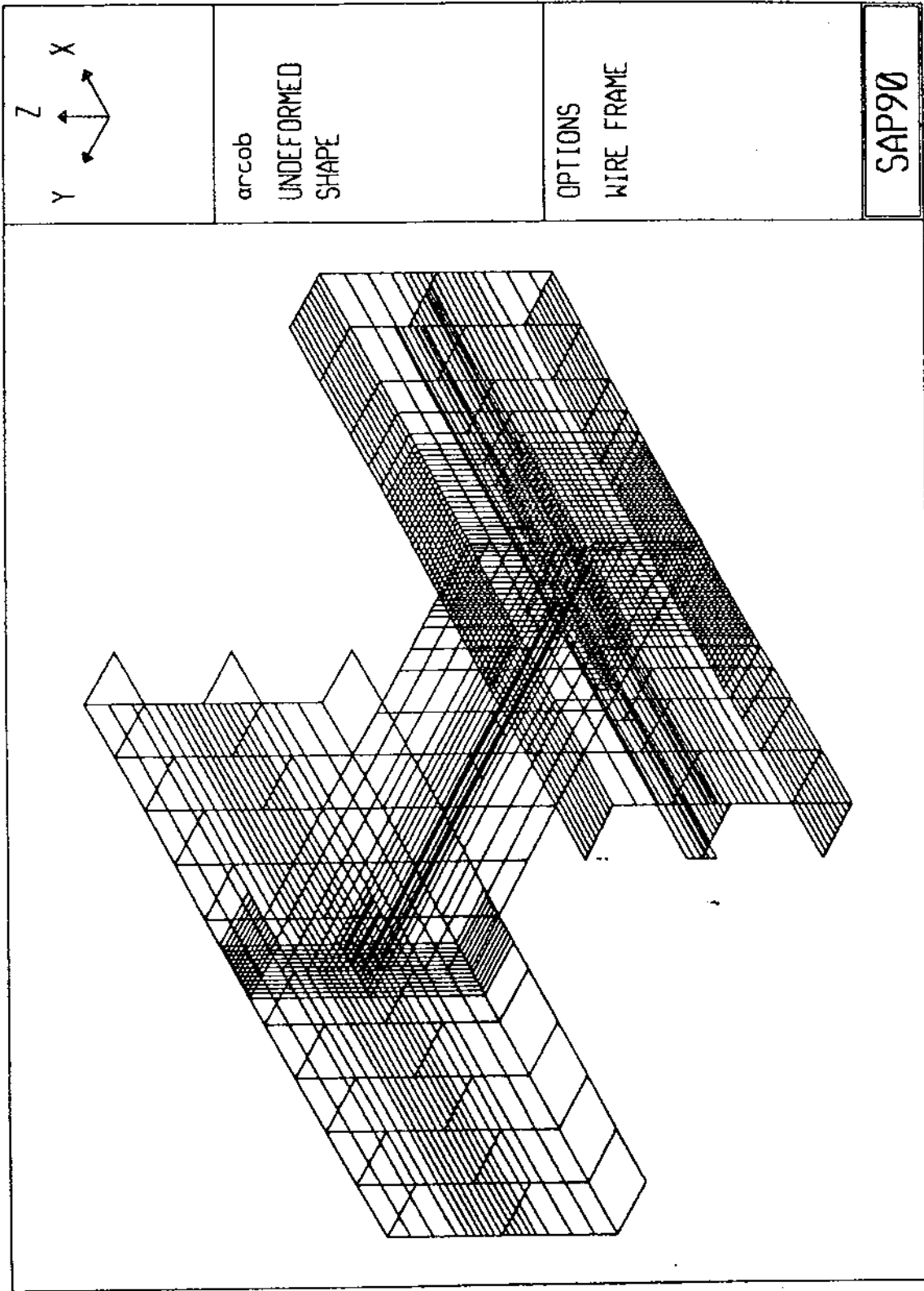
Fig 4.1 Typical CSD FE Model - Double-Bottom CSD

20

Z ↑ Y ←→ X	SL 1 UNDEFORMED SHAPE	OPTIONS WIRE FRAME

SAP90
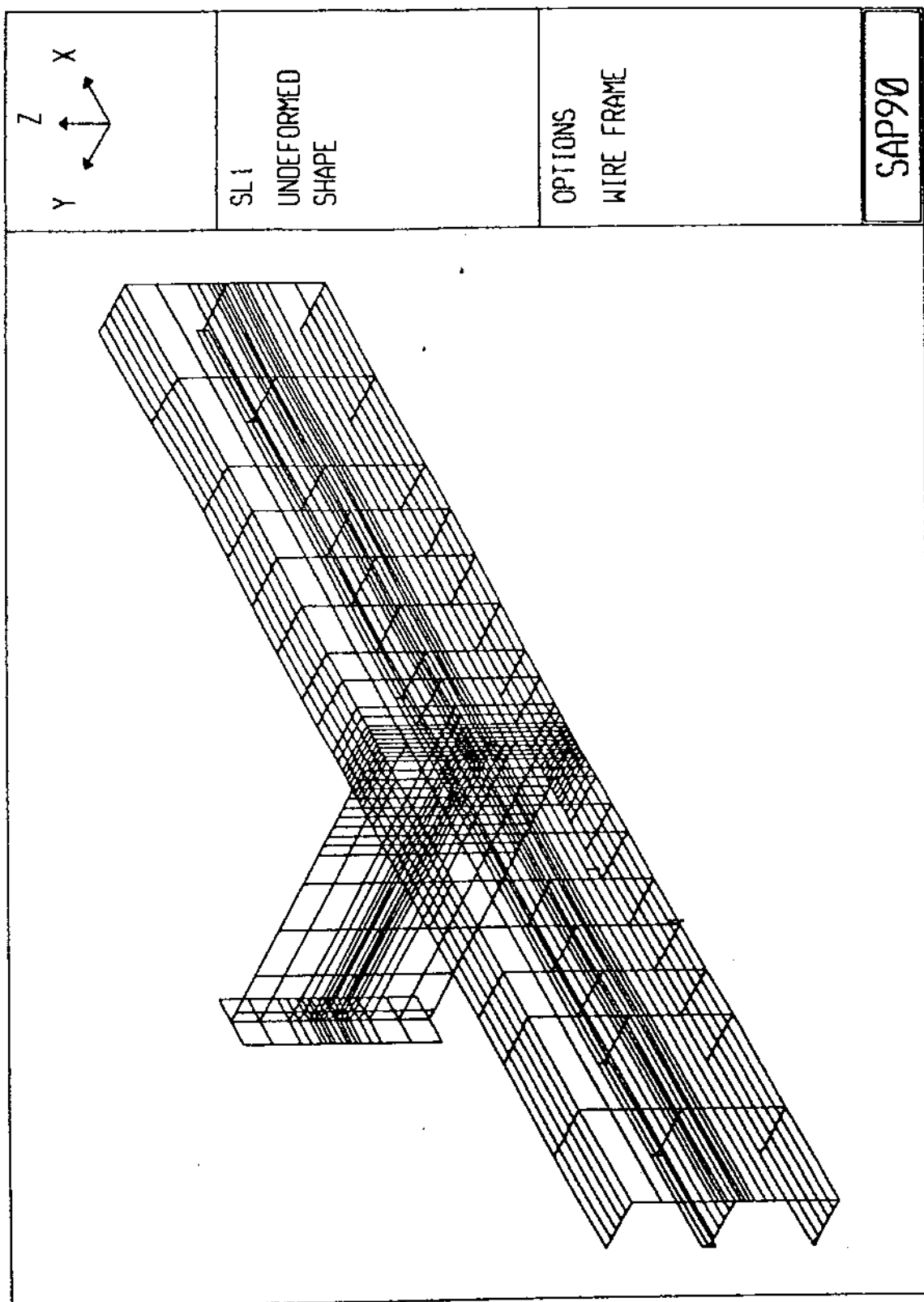
Fig 4.2 Typical CSD FEM Model - General Side shell CSD

21
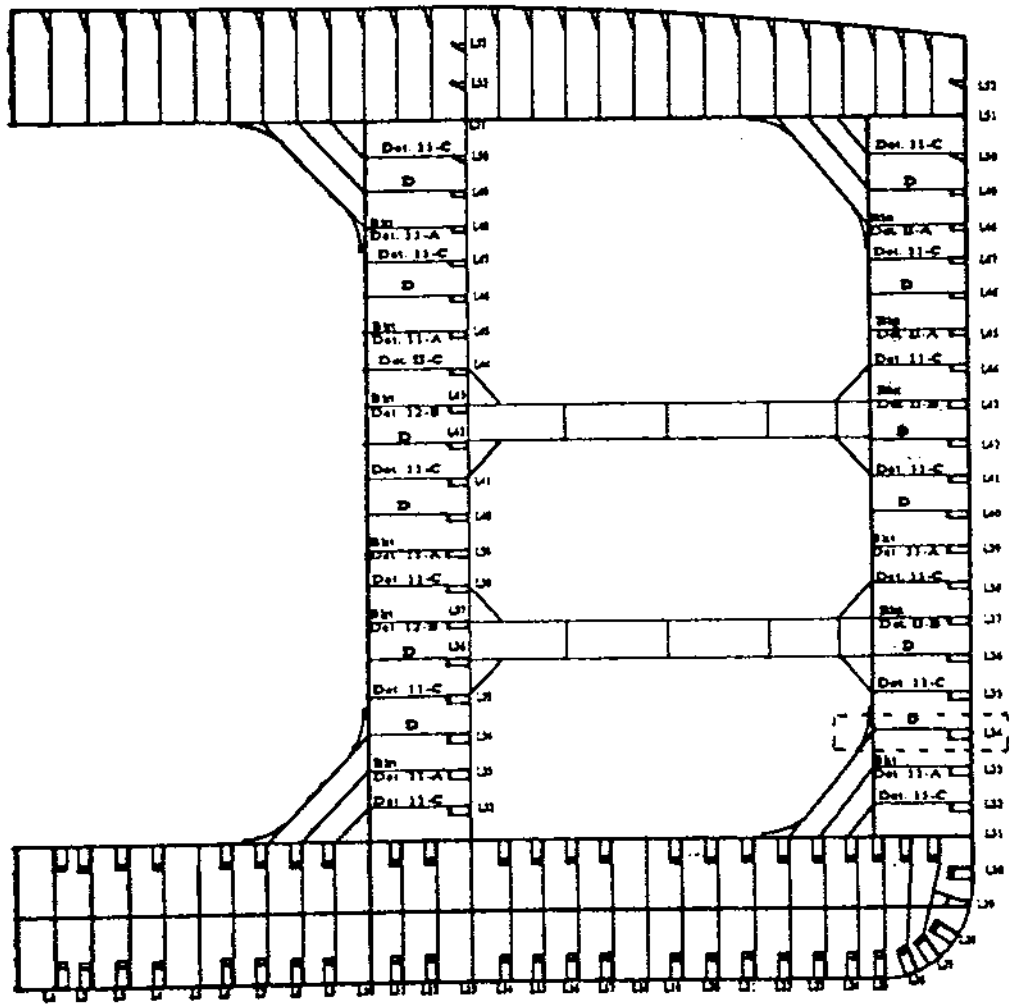
Fig 4.3 Web frame Section and General Sideshell Detail Location

198
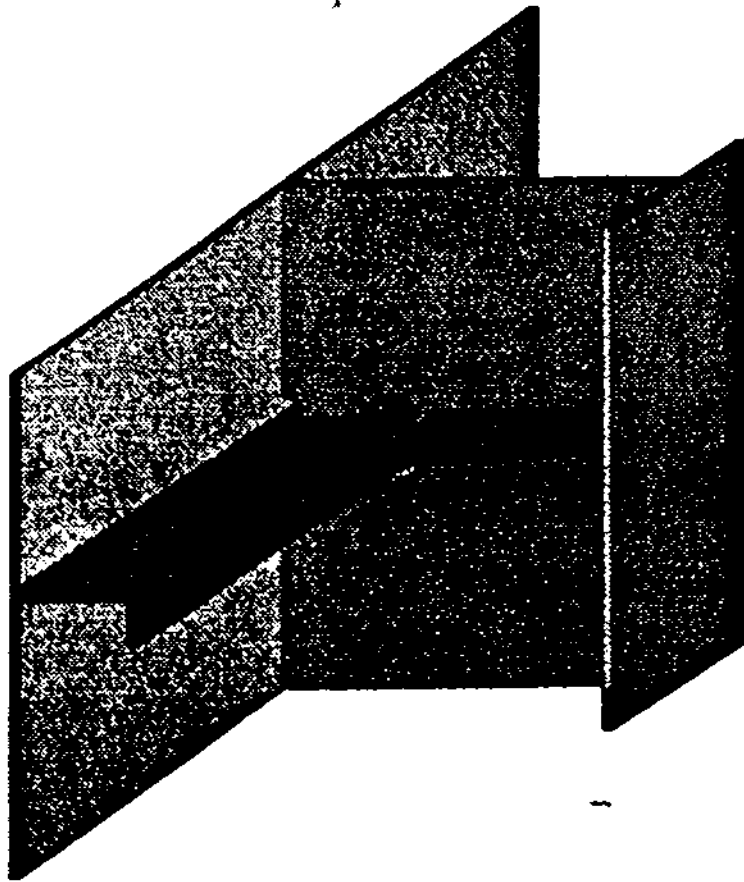
Fig 4.4 Typical Sideshell CSD - Configuration

199

```
Z
Y ↖  ↑  ↗ X

SL1
UNDEFORMED
SHAPE

OPTIONS
WIRE FRAME

SAP90
```
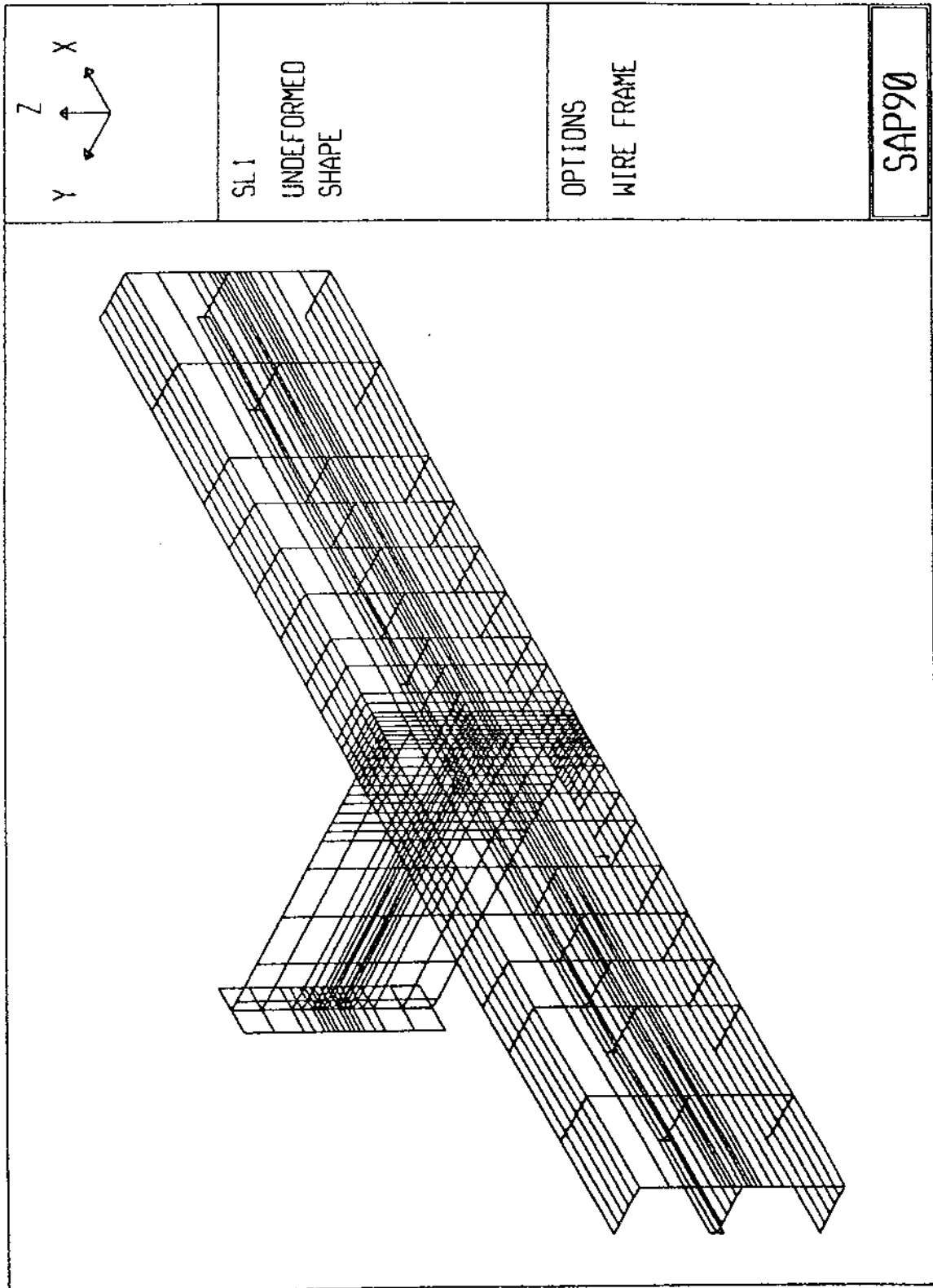
Fig 4.5 Typical Sideshell CSD - FE Model

200
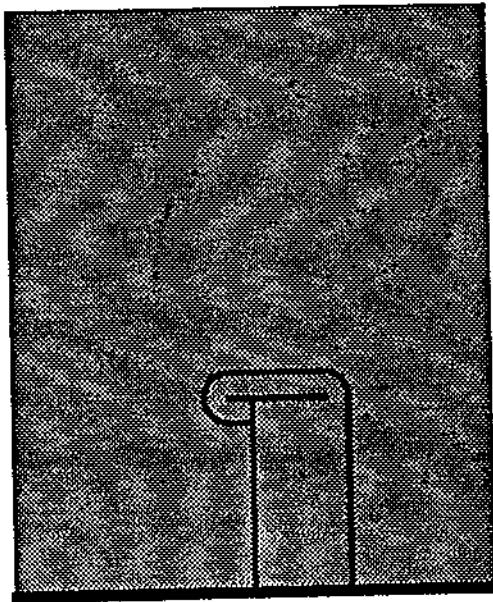
Fig. 4.6 Cut-out in General CSD
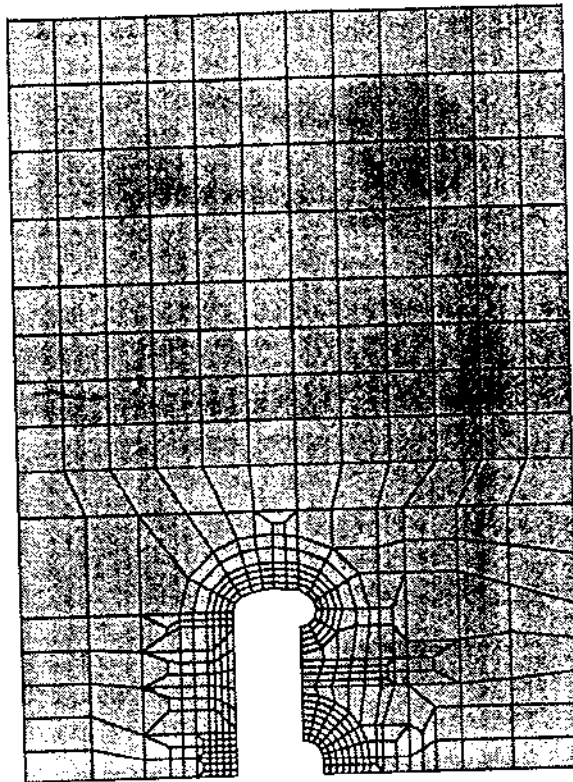
Fig 4.7 FEM Model for Corresponding Cut out

SCF=1.47   SCF=1.23

Cut-out Design 1

SCF=2.31   SCF=1.57

Cut-out Design 2

SCF = 2.12

SCF=1.47

Cut - out Design 3

SCF=2.33

SCF=1.51

Cut-out Design 4

SCF=1.34
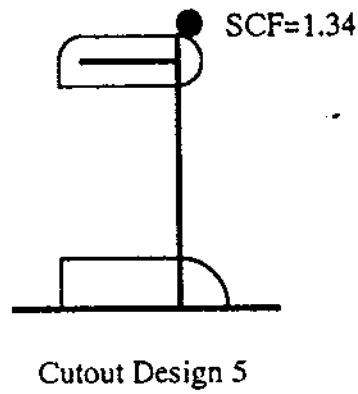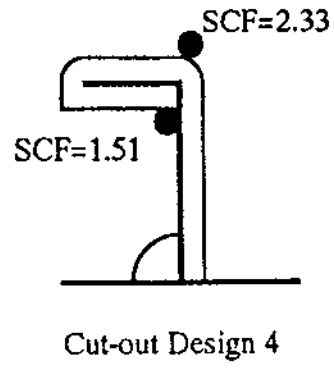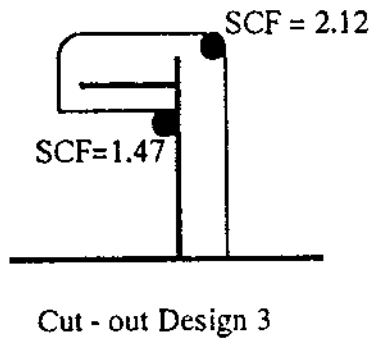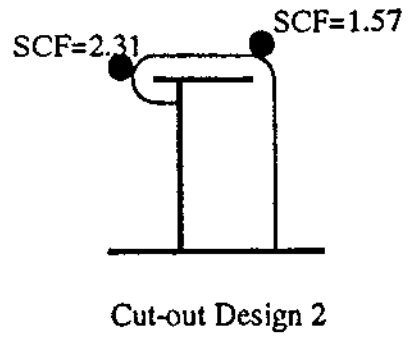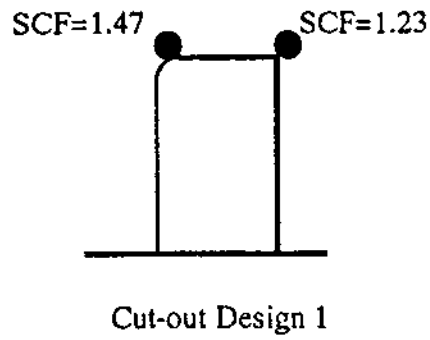
Cutout Design 5

Fig 4.8 Stress Concentration Factors for Transverse Cut-out for General Sideshell CSD

202

SCF=1.54

Cutout Design 7

SCF=1.33

Cutout Design 6

SCF=3.45

Cutout Design 8

SCF=3.97

Cutout Design 9

SCF=2.31
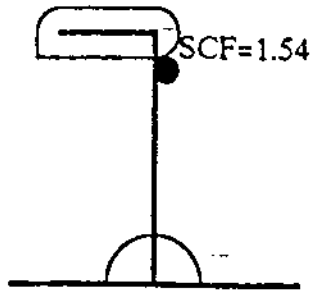
Cutout Design 10

Fig 4.9 Stress Concentration Factors for Cutout in Transverse Web
for General Sideshell CSD (Continued)

203

4.3.3 Stiffener and Bracket-toe

This detail is used in ship structural design in longitudinal as well as transverse members and has frequently shown fatigue damage. For brackets on continuous plates or flanges, different shape exist: without or with soft transition, and without or with additional buckling stiffener. Fig 4.10 and Fig 4.11 shows the typical geometry and fini'e element mesh. The stress concentration factors for the proposed CSDs are presented in Fig 4.12. The stress contours are presented in Ref 3.
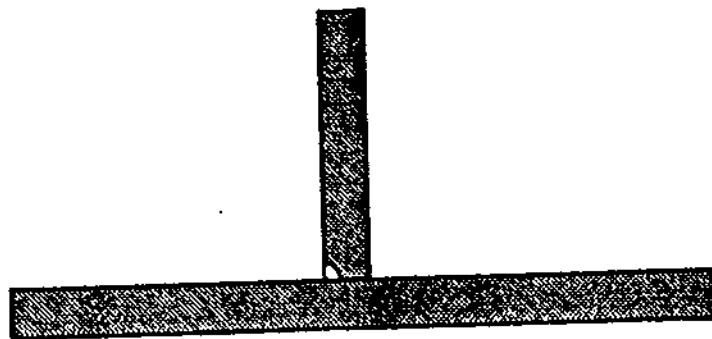
Fig 4.10 Configurations for Typical Stiffener or Bracket-toe
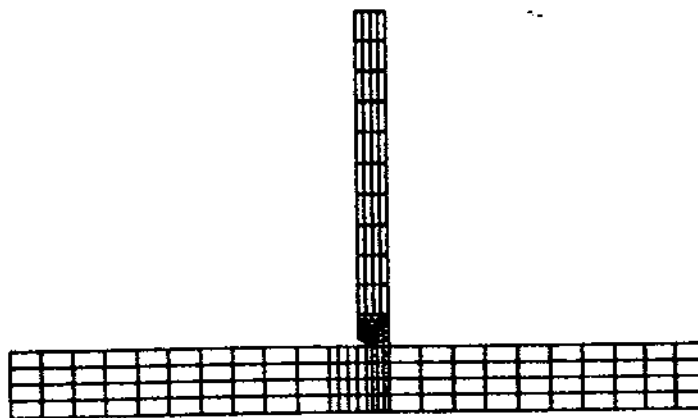
Fig 4.11 Finite Element Model for Typical Bracket-toe or Stiffener

204
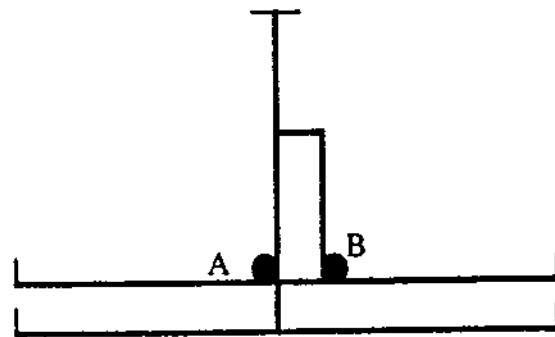
Stress Concentration Factor K$_A$ = 2.37
Stress Concentration Factor K$_B$= 1.78
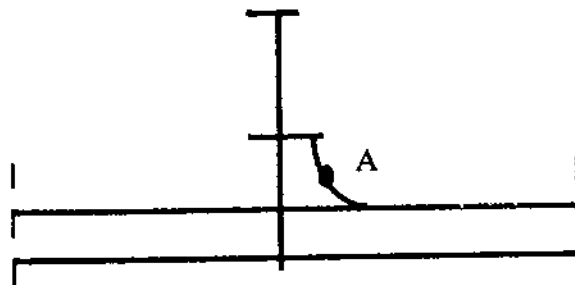
Stress Concentration Factor K$_A$=1.2
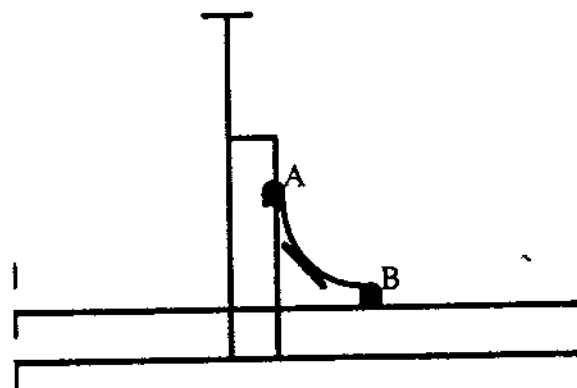
Stress Concentration Factor K$_A$=1.74
Stress Concentration Factor K$_B$= 1.89

Fig 4.12A Stress Concentration Factors for Bracket-toe or Stiffeners

205

Stress Concentration Factor KA=2.03

Stress Concentration Factor KA=1.34

Stress Concentration Factor KA=2.01
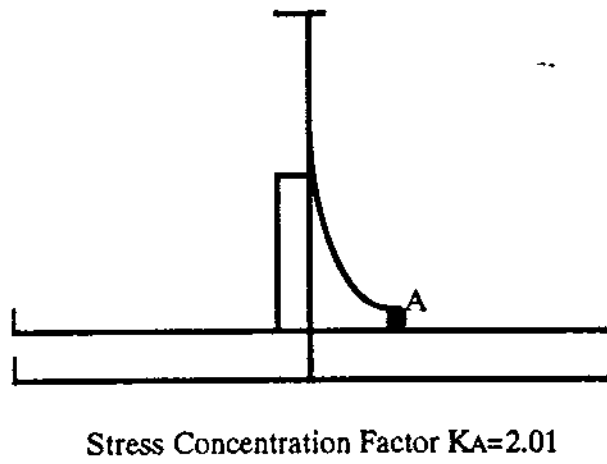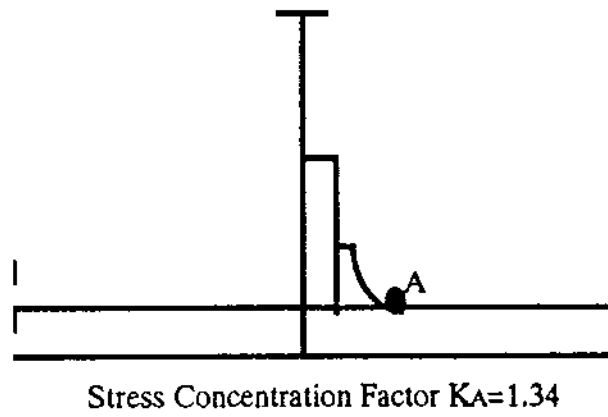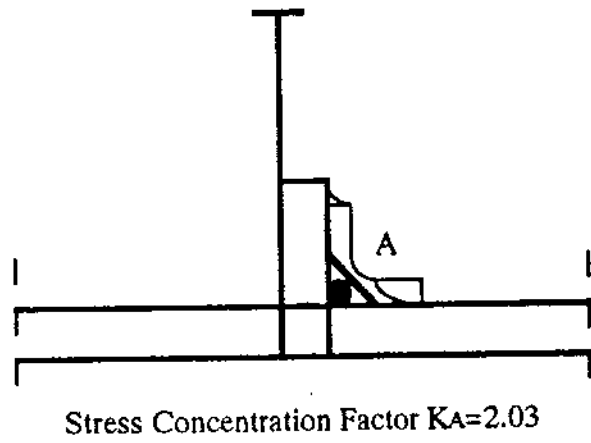
Fig 4.12B Stress Concentration Factors for Bracket-toe or Stiffeners (Continued)

206

4.5 General Nonsideshell Longitudinal Details

The proposed nonsideshell longitudinal details are longitudinal transverse bulkhead and web frame connections. The longitudinal transverse bulkhead is on the similar location as the general sideshell longitudinal details. It's L34 and Frame 53. The web frame connection is on from L32 to L21 on Frame 52 which is shown in Fig 4.13.

4.5.1 Web frame Connection

Web frame connections are usually the high stress area in tankers. Due to the specific interests from the sponsors, several design alternatives for the web frame connection were conducted in this project. Fig 4.14 and Fig 4.15 show the typical geometry and corresponding FEM mesh. The stress contours are presented in Ref 4.4.

Fig 4.13 Location for Double-Bottom Connection

31

207

Fig 4.14 Double-Bottom Connection - Configuration
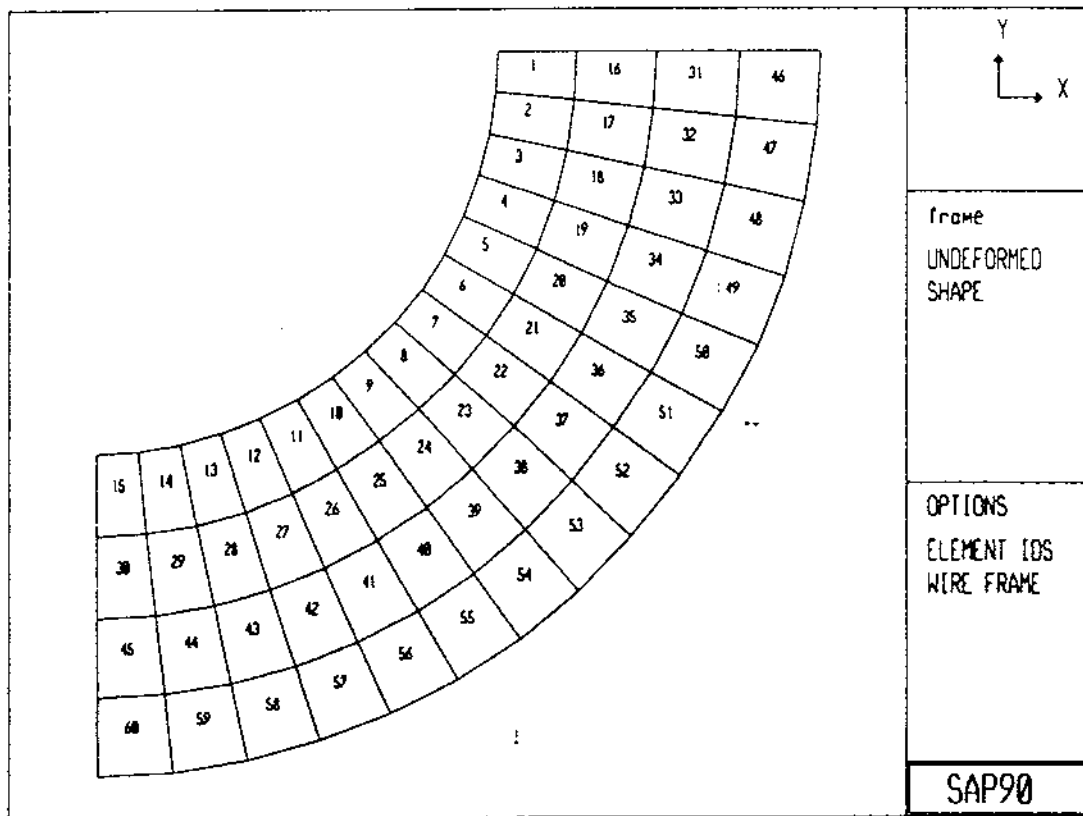
Fig 4.15 Finite Element Mesh for Double-Bottom Connection
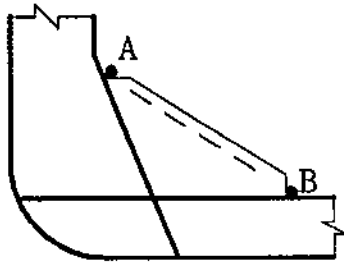
Stress Concentration Factor K $_A$ = 2.64 K $_B$=3.0
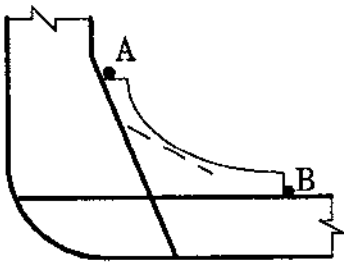
Stress Concentration Factors K $_A$ = 1.96 K $_B$ = 2.2
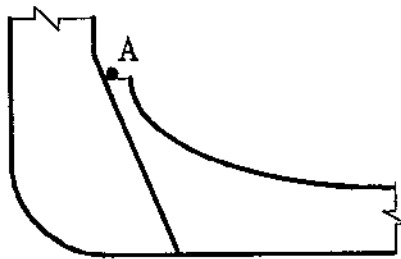
Stress Concentration Factor K $_A$=1.48
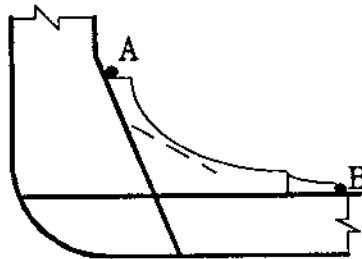
Stress Concentration Factor K $_A$=1.96 K $_B$=1.65

Fig 4.16 Stress Concentration Factors for Double-Bottom Connections

33

209
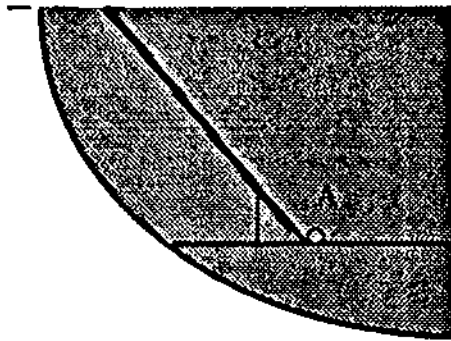
Stress Concentration Factor KA=2.79
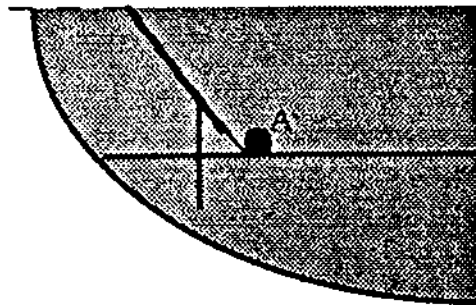
Stress Concentration Factor KA=3.87
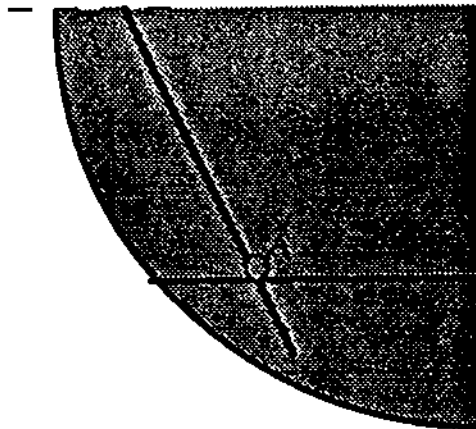
Stress Concentration Factor   KA=2.34

Fig 4.17 Stress Concentration Factors for Double-Bottom Connection (Continued)

210

4.5.2 Longitudinal Transverse Bulkhead Connection

From the SMP fatigue database (Ref. 1 and Ref. 2), it is found that fatigue cracks in transverse bulkhead are severe. A systematic finite element analysis was performed to determine the stress concentration factors (SCF). The applied boundary conditions are the displacements derived from global finite element analysis. Fig 4.18 is the geometry and dimensions. Fig 4.19 is the finite element model. Fig 4.20 is the stress concentration factors for various cutouts, stiffeners and bracket-toes. The stress contours are presented in Ref .3
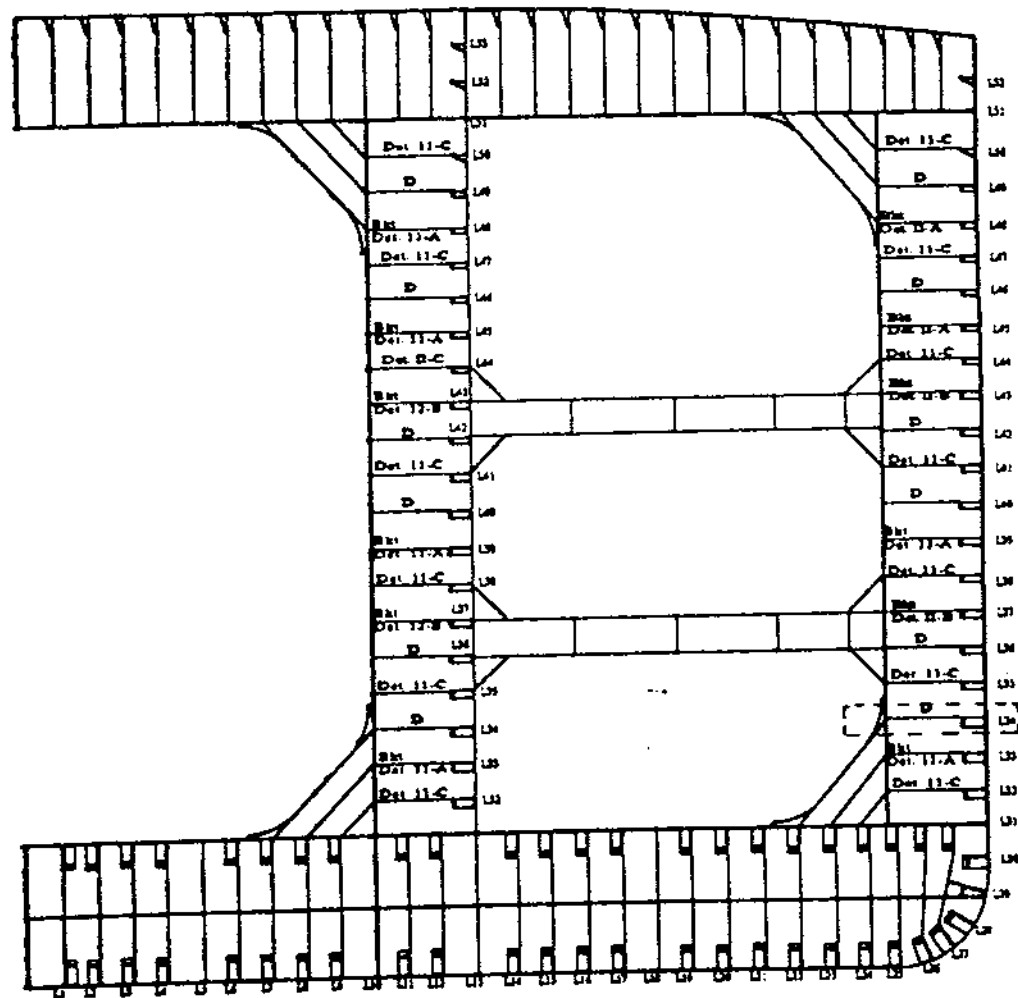
Fig 4.18 General Nonsideshell CSD - Longitudinal Transverse Bulkhead Connection
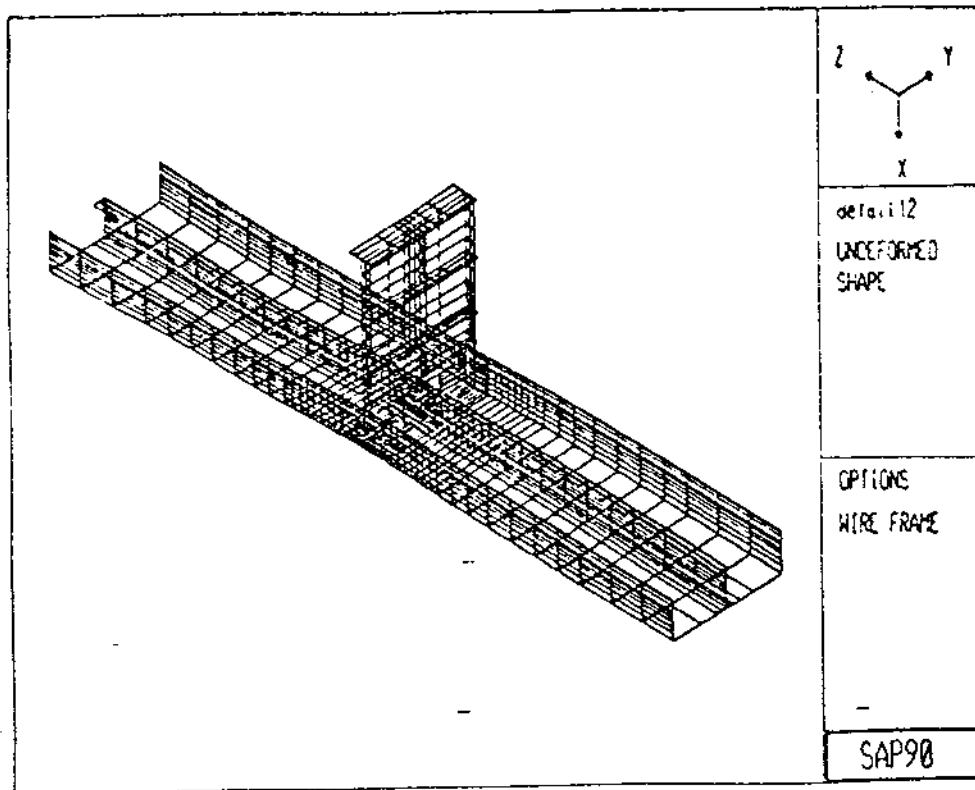
Fig 4.19 General Nonsideshell CSD FE Model - Longitudinal Bulkhead Connection

SCF=1.34   SCF=1.43

Cut-out Design 1

SCF=1.87   SCF=1.17

Cut-out Design 2

SCF=2.34

SCF=1.67

Cut - out Design 3

SCF=2.13

SCF=1.34

Cut-out Design 4
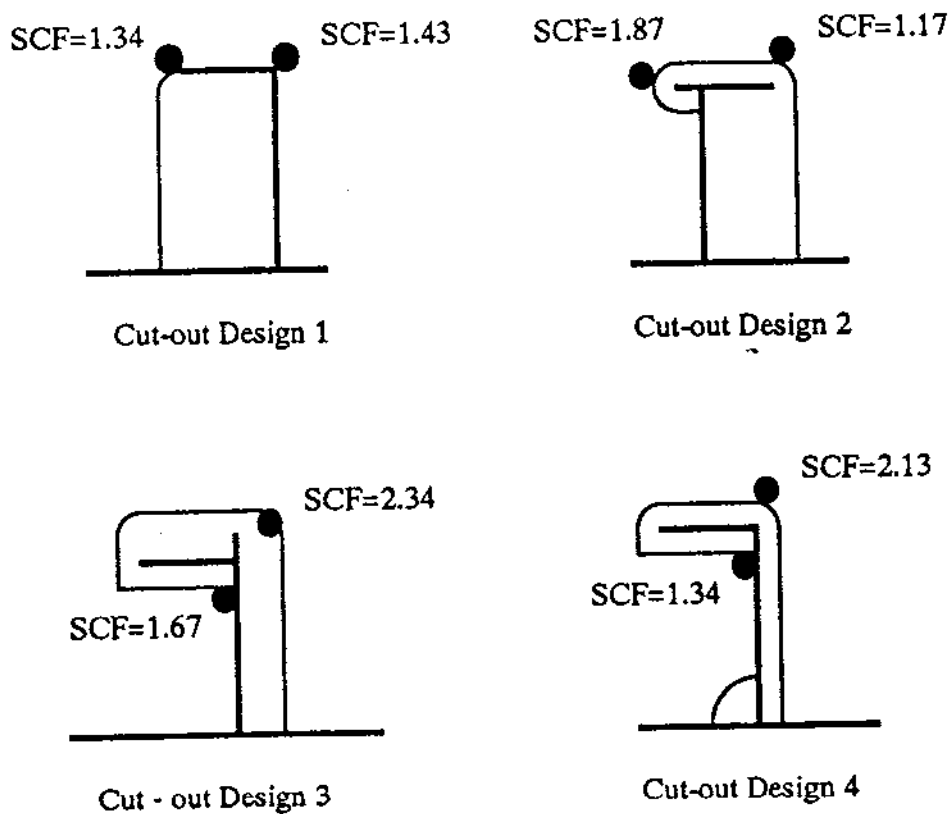
Fig 4.19 Stress Concentration Factors in Cutout for Transverse Bulkhead

212
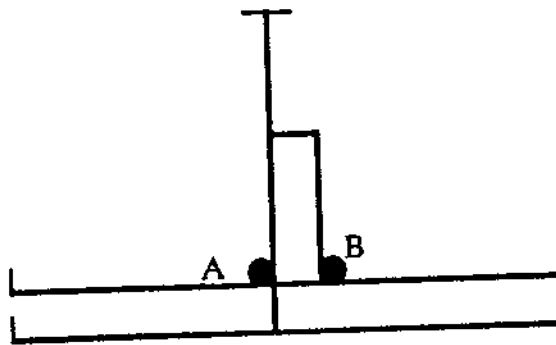
Stress Concentration Factor K_A = 1.79

Stress Concentration Factor K_B = 1.47
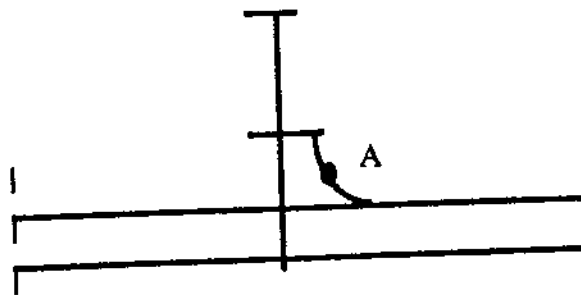
Stress Concentration Factor K_A = 1.3
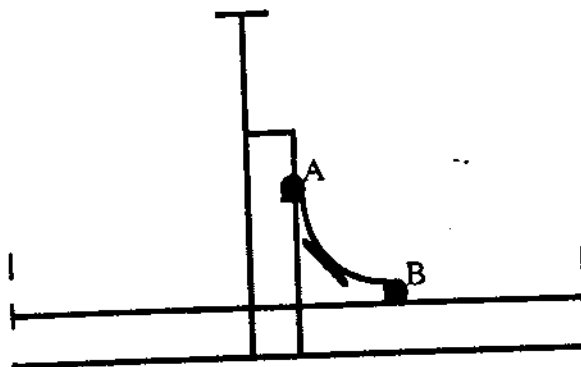
Stress Concentration Factor K_A = 1.44

Stress Concentration Factor K_B = 2.13

Fig 4.20A Stress Concentration Factors for Stiffener and Bracket-toes
for Transverse Bulkhead Connection

213

Stress Concentration Factor $K_A = 1.93$

Stress Concentration Factor $K_A = 1.41$

Stress Concentration Factor $K_A = 1.79$
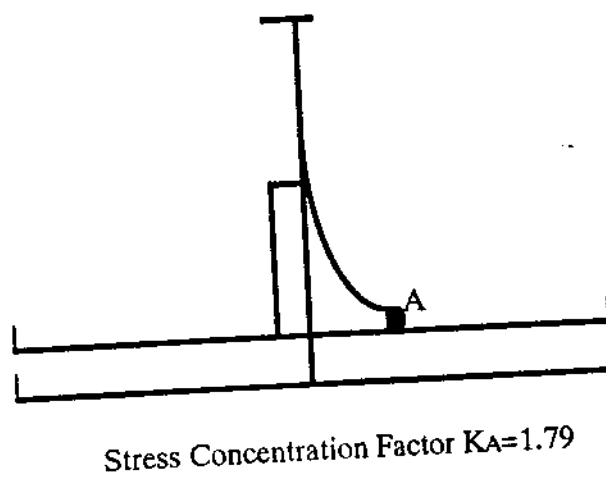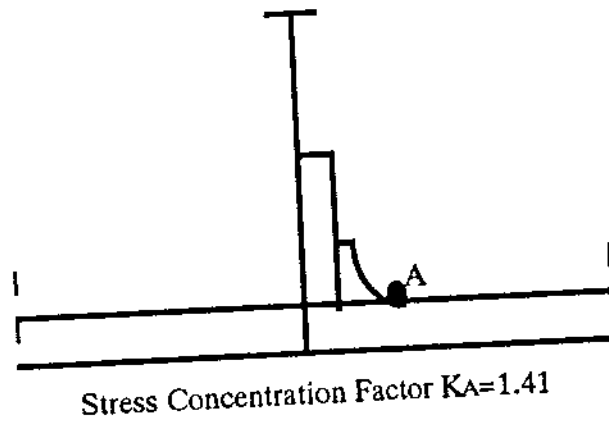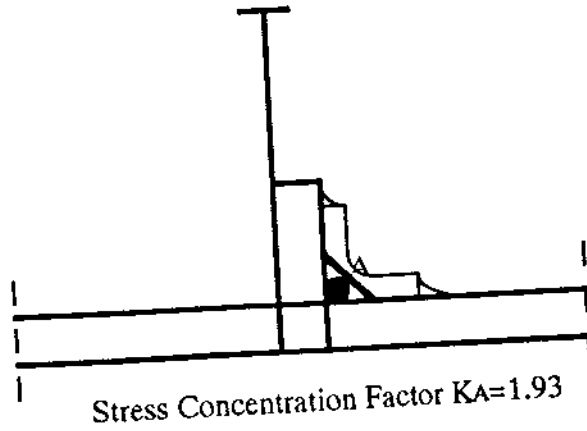
Fig 4.20B Stress Concentration Factors for Stiffener and Bracket-toes
for Transverse Bulkhead Connection

214

Chapter 5

Fatigue Damage Evaluation

5.1 Introduction

Fatigue may be defined as a process of cycle by cycle accumulation of damage in a structure subject to fluctuating stress and strain.

A significant feature of this process is that the load is less and often significantly less than the load necessary to cause immediate failures such as buckling or yielding of the structure. Failure occur after a certain number of load cycles of constant or varying magnitude. Cracks develop in a CSD to the extent that the structure can no longer support the load.

The fatigue analyses methodology was presented in detail in the previous reports (Ref 1.2.3). This chapter summarizes the theoretical model and addresses the analyses results for various CSD and some specific considerations.

5.2 Fatigue Damage Evaluation Model

In this study the S-N curve approach combined with the use of Miner's summation rule is used to calculate fatigue damage. Weibull approximation for the randomness in loading are applied in probabilistic fatigue analysis.

5.2.1 S-N Classification

The accuracy of the estimated fatigue life of a structural detail depends strongly on the load and capacity. The capacity to resist metal fatigue can be expressed by the S-N curve used for the hotspot location that is of interest. The S-N curve recommended by the Department of Energy (DnE) is used to describe the fatigue strength at the hotspots of the CSD. Fig 5.1 shows these S-N curves and a summary of the curve parameters. The S-N curve classification for different hotspots of CSD is described in Ref.1 and Ref.2. It should be pointed out that the S-N curve for deterministic analysis is the mean curve while the S-N curve for probabilistic analysis is the curve with median value = 1.0 and standard deviation = 0.3.

U.K. Department of Energy Design S-N Curves
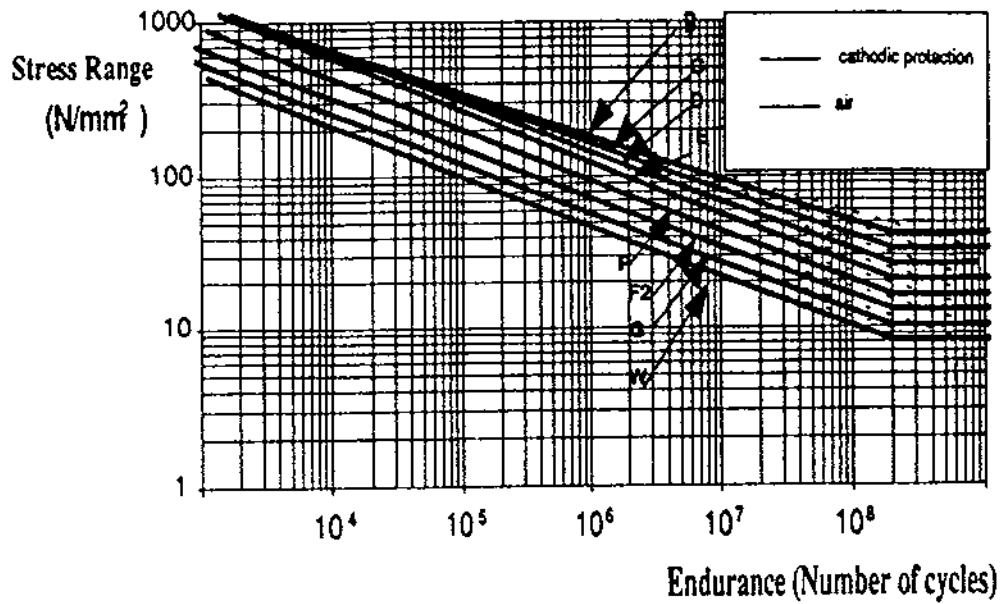
Figure 3.7: S-N curves

Table 3.4: The data of S-N relations

Class	m	C_{50}	log s
B	4	$2.343*10^{15}$	0.1822
C	3.5	$1.082*10^{14}$	0.2041
D	3	$3.988*10^{12}$	0.2095
E	3	$3.289*10^{12}$	0.2509
F	3	$1.726*10^{12}$	0.2183
F2	3	$1.231*10^{12}$	0.2279
G	3	$0.566*10^{12}$	0.1793
W	3	$0.368*10^{12}$	0.1846

Fig 5.1 UK. DeN S-N Curves

216

5.2.2 Fatigue Damage Assessment

It is assumed that the curve characterizing fatigue behavior under constant cyclic loading is of the form

$$NS^m = K$$

where

N = Number of cycles to failure
S = Stress range
m = Empirical constant
K = Empirical constant

When the Miner's rule is applied, Fatigue damage is given by

$$D = N_T D E(S^m) / K$$

where

N_T = Total number of cycles in time T
T = Time
D = Damage
$E(S^m)$ = Expected, mean, or average value of S^m
S = Stress range (random variable)

To account for the uncertainties in the stress calculation the following relation between the actual stress range Sa, and the estimated stress range S is introduced

$$Sa = BS$$

where

B the bias that quantifies the modeling error. (random variable)

If we define the average frequency of stress cycles as

$$fo = N_T/T$$

Then the fatigue damage can be rewritten as

$$D = T\, B^m \Omega / K$$

where

$$\Omega = foE(S^m) = \text{stress parameter}$$

5.2.3 Weibull Model

The Weibull distribution is currently used to calculate Ω and thus the fatigue damage. It is assumed that the long-term distribution of the stress range can be fitted by the Weibull distribution. The three important Weibull parameters in this distribution are S_m, ξ and N_T. Then the stress parameter can be calculated as

$$\Omega = \lambda(m)fo S_m^m [\ln N_T]^{-m/\xi} \Gamma(\frac{M}{\xi} + 1)$$

where

S_m = Extreme stress range during the life time
ξ = Stress range parameter (Weibull shape parameter)
N_T = Total number of stress ranges in design life
λ = 1, unless Rayleigh assumption was made in analysis

5.2.4 Deterministic Analysis :

Based on the stress transfer function, Wave data for the TAP trade and selected S-N curve, fatigue life is predicted for the locations of structural details of interest using the Miner's cumulative damage hypothesis. Evaluation of fatigue life was carried out on the following criteria:

Estimated Life:

$$Lt = (\frac{0.5}{Lf} + \frac{0.5}{Lb})^{-1} > 20 \text{ years}$$

where,

Lt : total fatigue life
Lf: fatigue life for full load condition
Lb: fatigue life for ballast condition

5.2.5 Probabilistic Analysis :

It is assumed that the lognormal format for the probability distributions of all factors of the fatigue damage expressions. This format has been demonstrated to be valid for the variables involved in the fatigue damage analysis, specially for the variables Δ and K. Miner's rule, which states the failure occurs when the fatigue damage $D > 1$ is modified to

$$D > \Delta$$

218

where Δ is a random variable denoting damage at failure. This quantifies the modeling errors associated with Miner's rule.

To account for the uncertainties in fatigue strength, the S-N curve parameter K is defined as a random variable.

The time to failure T is then given as

$$T = \frac{\Delta K}{B^m \Omega}$$

Since Δ, K, B are random variables, T is also a random variable. The probability of fatigue failure is defined as

$$Pf = P\,(T < Ts\,)$$

where
  Ts = Service life of the structure.

The use of the lognormal format has the advantage that a simple closed form expression for Pf can be found.

$$Pf = \Phi(-\beta)$$

where

Φ = standard normal distribution function and β = safety index

$$\beta = \frac{\ln(T/\tilde{T})}{\sigma_{\ln T}}$$

where $\tilde{T}$ is the median value of T and is equal to

$$\tilde{T} = \frac{\Delta K}{B^m \Omega}$$

The standard deviation of ln T is given by

$$\sigma_{\ln T} = (\ln(1 + C_A^2)(1 + C_K^2)(1 + C_B^2)^{m^2})^{1/2}$$

where the C's denote the coefficients of variation, COV, of each variable.

43

Bias for the Probabilistic Model

For a reliability analysis it is necessary to specify the median and the coefficient of variation of K,B and Δ, which are assumed to be lognormally distributed. The median value for K is obtained from least square analysis of the S-N data. The COV of K, C_k is obtained by approximating an equal probability curve with a straight line.

The variables B and Δ are used to quantify the modeling bias associated with assumptions made in the stress analysis and the description of fatigue strength. Several sources can contribute to the bias B. That is

B_M = Fabrication and assembly operations
B_S = Sea state description
B_F = Wave load prediction
B_N = Nominal member loads
B_H = Estimation of hotspot stress concentration factors.

Table 5.2 summarizes frequently used values for the medians and COV's of the B's .

Using these 5 bias factors, the following representation of B is obtained

$$B = B_M B_S B_F B_N B_H$$

Assuming that each random variable is lognormally distributed the median and the COV of B are, respectively

$$B = B_M B_S B_F B_N B_H$$

$$C_B = \sqrt{(1 + C_M^2)(1 + C_S^2)(1 + C_F^2)(1 + C_N^2)(1 + C_H^2) - 1}$$

For the random variable Δ, describing the model error associated with Miner's rule, the following values for Δ and C_Δ are widely used. $\Delta = 1.0$ and $C_\Delta = 0.3$.

Uncertainties in Proposed Calculation

Uncertainties are involved in the estimation of the long-term stress distribution. These uncertainties account for the total modeling error involved in the fatigue damage evaluation procedure. It's the reasonable assumption that the uncertainties follow the log-

44

normal distribution so that the uncertainty information can be represented through the two parameters mean value and coefficient of variation.

A lot of different contributors to the modeling error are involved in the fatigue damage evaluation. A good comprehensive summary of the uncertainties in the cumulative fatigue damage is given in (Ref. 7).

The combination of the different contributing factors for the modeling errors defines the total modeling error or bias. The total coefficient of variation of the modeling error or bias is obtained through a combination of the individual coefficients of variation.

For the evaluation of the fatigue damage for the CSD in this Chapter, only the total modeling bias (its mean and coefficient of variation) are varied. These values essential represent the systematic error and the confidence in the estimation of the long-term stress range distribution.

The selection of bias values and the coefficients of variation for these values are discussed extensively in (Ref. 7). Based on the previous study, the following ranges for the bias and the coefficient of variation of the bias have been selected for the proposed CSD.

	Bias	Median Value	CovBias
1	Fabrication and Assembly	1.20	0.1
2	Seastate Characteristics	1.10	0.3
3	Wave Load Prediction	0.80	0.2
4	Determination of Member Load	0.90	0.4
5	Estimation of SCF	1.00	0.1
	Median Bias	Cov Bias	
	1.07	0.3	

	Median	Cov
S-N Curve	1.0	0.3

5.3 Fatigue Analyses for General Sideshell CSD

From the SMP databases and previous experience, it appears that the highest crack frequency is experienced in tanker sideshell longitudinals. Thus the fatigue analyses for the general sideshell CSD with various configurations have been conducted to evaluate the fatigue damage. The proposed general sideshell CSD is located at longitudinal L34 with Frame 52 which is the ballast water-line which corresponds to the region with highest dynamic loads. (see Fig 5.2)

45

221
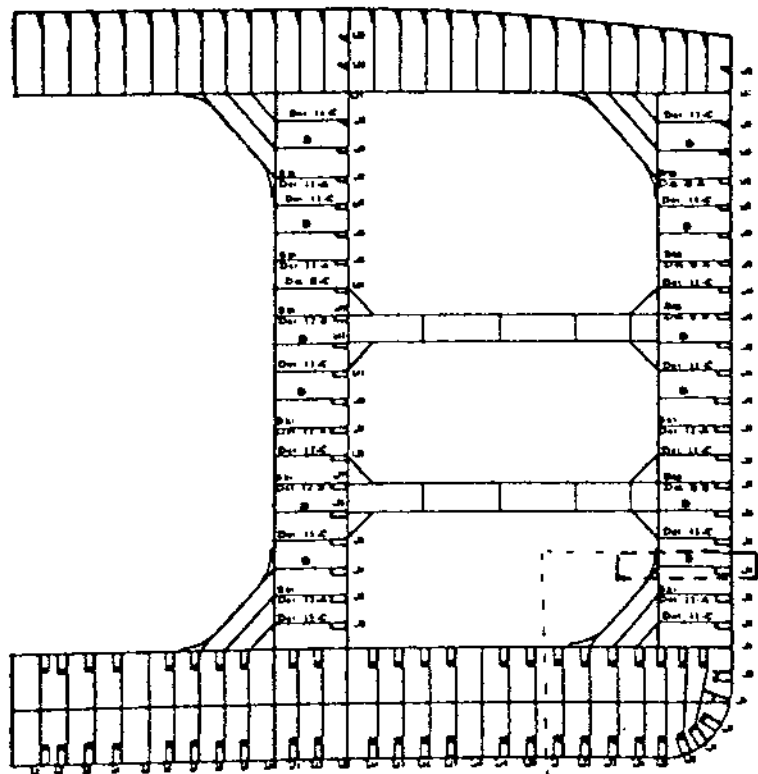
Fig 5.2 CSD Location in Web Frame Section

5.3.1 Fatigue of Stiffeners and Bracket-toes for the General Sideshell CSD

The stiffener and bracket-toes for the general sideshell CSD are one of the most severe fatigue damage areas. Several different configurations for stiffeners and bracket-toes are conducted in this project. The analysis procedure for the long-term loading and fatigue analysis is based on fatigue analysis procedure developed by SMP project.(Ref 1. and 2). The approach used was to calculate the long-term Weibull scale parameter by SMP software while the shape parameter is determined by ABS empirical formula as follows: (Ref. 8)

$$\varepsilon = 1.40 - 0.036\alpha L^{1/2} \quad \text{for } 190 < L < 305m$$
$$= 1.40 - 0.036\alpha L^{1/2} \quad \text{for } L > 305$$

where:

α =1.00   for deck structures

α =0.93   for bottom structures

α =0.86   for sideshell and longitudinal bulkhead structures

Thus the long-term loading is determined by two Weibull parameter instead of the Weibull scale parameter and zero crossing rate in SMP procedure.(Ref 1. and 2) Fig 5.3 is the typical analysis results.

Fig 5.2A Unit Load Load FEA to Determine Stress Vectors for Stiffeners and Bracket-toes
(Unit Axial Force)

Weibull parameter
Scale = 3.43 | Shape = 0.832

A

Probability of Failure During 20 Years = 3.88%

Weibull Parameter
Scale = 5.13 | Shape = 0.93

A

Probability of Failure During 20 Years = 18.4%
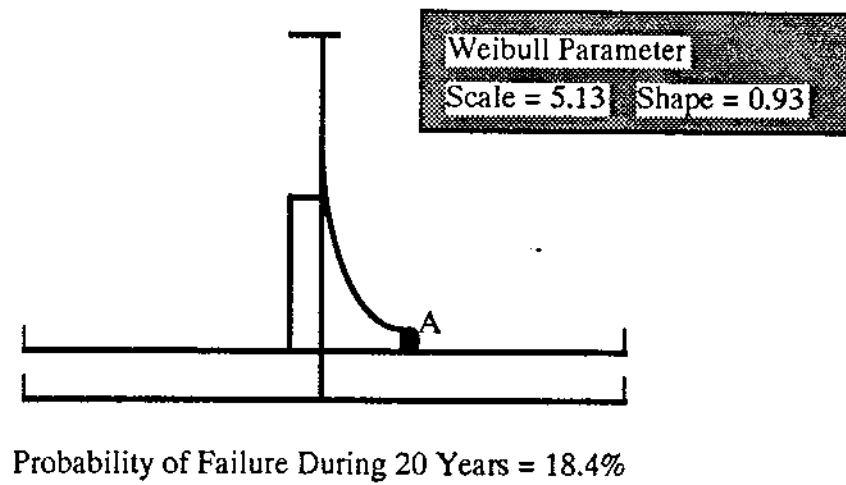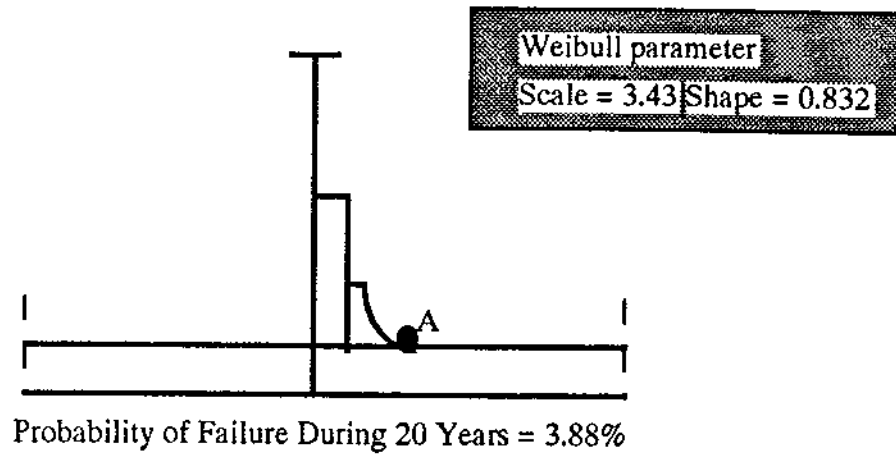
Fig 5.3 Fatigue Analysis for General Sideshell CSD Stiffener and Bracket-toe

226

Fig 5.2B Unit Load FEA to Determine Stress Vectors for Stiffeners and Bracket-toes
(Unit Pressure)

Weibull Parameter B
Scale=4.531   Shape=0.943

Weibull Parameter A
Scale=4.531   Shape=0.943
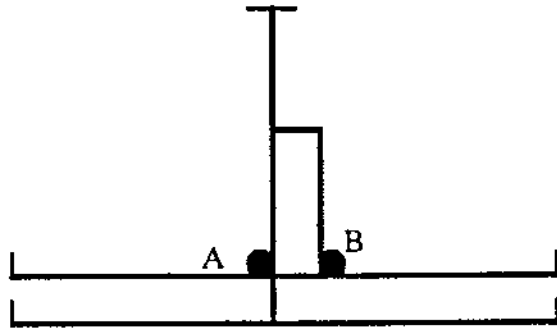
Probability of Failure During 20 years = 8.5% Fatigue Life =119 Years

Probability of Failure During 20 years =7.6% Fatigue Life = 179 Years

Weibull Parameter
Scale =3.274 Shape=0.853
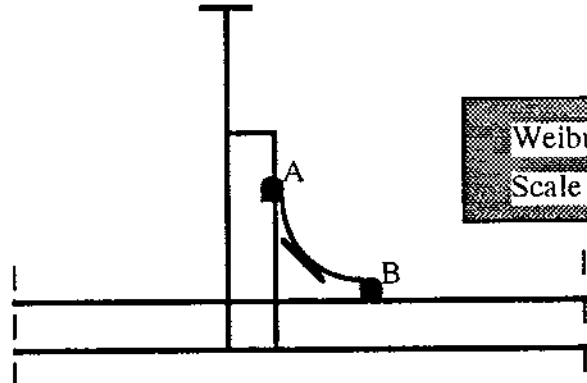
Probability of Failure During 20 Years =3.7% Fatigue Life = 254 Years

Weibull Parameter B
Scale = 5.23   Shape=0.866

Weibull Parameter A
Scale = 4.64   Shape=0.866
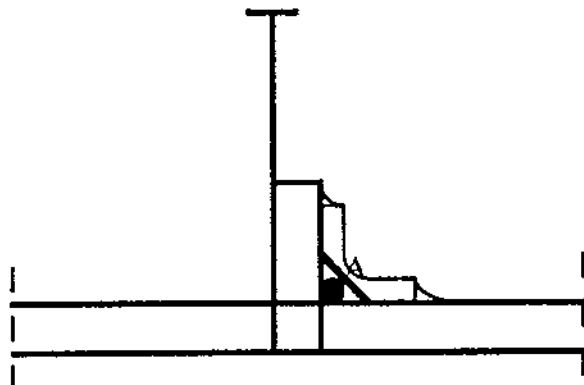
Probability of Failure During 20 Years =9.73% Fatigue Life = 163 Years

Probability of Failure During 20 Years = 15.47% Fatigue Life = 98 Years

49

225

5.3.2 Load Effects on Fatigue Damage for General Sideshell CSD

High dynamic loading and high local stress concentrations contribute to the high damage frequencies of general sideshell CSD. Fatigue is basically due to the cyclic axial forces due to the hull girder wave bending and local dynamic pressures. For general sideshell CSD, the fluctuating stress is mainly caused by local bending of the longitudinal subject to fluctuating hydrostatic pressure. The fluctuating stress for deck is mainly axial stresses caused by hull girder wave bending moment. It is informative to investigate these two load effects for the general sideshell CSD fatigue. The following analyses were conducted to determine the load effects.

Case 1 General Sideshell CSD Stiffener

The load effects for general sideshell CSD stiffener was carried out in two steps. The CSD is shown in Fig 4.2.

1) Fatigue analysis was carried out based on SMP fatigue analysis procedure with the stress vector due to unit axial force only. That is to say that the long-term Weibull scale parameter is determined with the stress vectors f1 = 1.037 and f2=0.

2) Fatigue analysis was carried out based on SMP fatigue analysis procedure with the stress vector due to unit local pressure only. That is to say that the long-term Weibull scale parameter is determined with the stress vectors f1 = 0 and f2=1020.

Table 5.3 and Table 5.4 show the Weibull Parameters and corresponding fatigue damage. It has been found that fatigue damage due to local pressure is about as twice as fatigue damage due to the axial force.

Unit Axial	Stress Vector	Weibull Scale	Weibull Shape	Damage
1	1.037	2.748	0.942	0.107

Table 5.3 Fatigue Damage due to Unit Axial Force for Stiffener

Unit Pressure	Stress Vector	Weibull Scale	Weibull Shape	Damage
1	1030	3.586	0.942	0.23

Table 5.4 Fatigue Damage due to Unit Pressure for Stiffener

It should be pointed out that the sum of the fatigue damage due to these two separated cases are not the same as the previous analysis results. The reason is obviously due to the long-term loading combination of these two stresses.

51

227

Case 2 General Sideshell CSD Bracket-toe

The same procedure is applied to the general sideshell CSD bracket-toe on Fig 4.4. Table 5.5 and 5.6 are the analysis results.

Unit Axial	Stress Vector	Weibull Scale	Weibull Shape	Damage
1	1.07	2.375	0.942	0.087

Table 5.5 Fatigue Damage due to Unit Axial Force Bracket-toe

Unit Pressure	Stress Vector	Weibull Scale	Weibull Shape	Damage
1	1020	3.756	0.942	0.157

Table 5.6 Fatigue Damage due to Unit Pressure for Bracket-toe

Based on these two case studies, the following conclusions can be derived.

1) For general sideshell longitudinal CSD around the ballast waterline, fatigue damage due to local pressure is about 67% while the fatigue damage due to axial loads is about 33%.

2) It's expected that fatigue damage for deck longitudinal CSD due to the axial loads will be the major part of fatigue damage.

3) The major part of the cyclic stress for general sideshell CSD is caused by local bending of the longitudinal subject to fluctuating hydrostatic pressure. The fluctuation in pressure is caused by roll and heave motion of the tanker, waves and combination of these effects. Combined roll and setting create dynamic stresses in.general sideshell longitudinal in the region between full loaded and ballast waterlines considerably greater than that in bottom longitudinal. (see Fig 5.6)
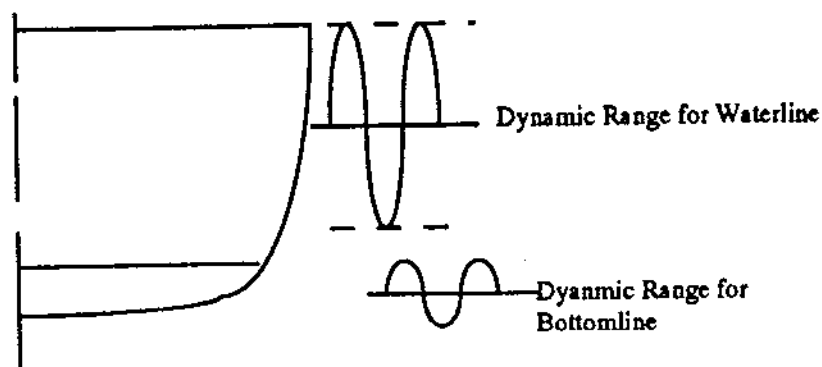
Fig 5.6 Dynamic Pressure Range for Waterline and Bottom line

5.3.3 Cut-out in Transverse Web Frame

Due to the experience in long-term loading analysis in SMP project, there is uncertainty in determination of the long-term loading for the hotspots on cutout while the fatigue analysis for stiffeners and bracket-toes are quite reasonable. The modified long-term loading analysis procedure for cutout in transverse web frame is developed based on the SMP long-term loading procedure.

First, Weibull shape parameter was determined by the ABS empirical formula as follows (Ref. 8)

$$\varepsilon = 1.40 - 0.036\alpha L^{1/2} \quad \text{for } 190 < L < 305m$$
$$= 1.40 - 0.036\alpha L^{1/2} \quad \text{for } L > 305$$

where:

α	=1.00	for deck structures
α	=0.93	for bottom structures
α	=0.86	for sideshell and longitudinal bulkhead structures

Two unit load cases for global FEA were conducted to determine the boundary displacements for the proposed general sideshell CSD. The local FEA for unit loads were conducted based on the displacements derived from the two unit load cases global FEA. The transfer functions for the CSD location were applied to determine the Weibull Scale parameter.

Based on the Weibull scale parameter and shape parameter and fatigue S-N curves, the fatigue analysis for cutout in transverse web frame was conducted.

Fig 5.5 shows the analysis results. The stress contours for the two unit load case global FEA and corresponding local FEA stress vectors are in Ref .3
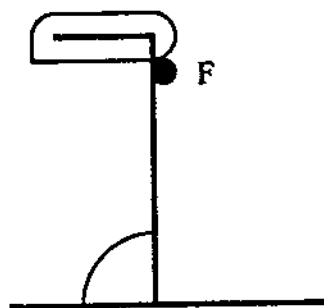
Extreme Stress Range P	202.55
Extreme Stress Range T	78.69
Weibull Shape =	0.942

Cutout Design 9

Probability of Failure During 20 Years = 0.84%

53

229

Extreme Stress Range P 164.74
Extreme Stress Range T 78.69
Weibull Shape = 0.942
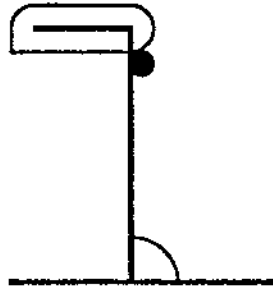
Cutout Design 10
Probability of Failure During 20 Years = 0.037%

Extreme Stress Range P 176.67
Extreme Stress Range T 78.69
Weibull Shape = 0.942
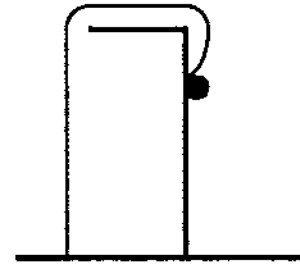
Cutout Design 6
Probability of Failure During 20 Years = 0.1%

Extreme Stress Range P 153.76
Extreme Stress Range T 78.69
Weibull Shape = 0.942
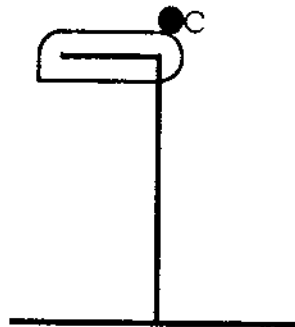
Cutout Design 8
Probability of Failure During 20 Years = 0.0

Unit : Stress Range N/mm**2

Fig 5.6 Fatigue Analysis for Cutout in Transverse Web Frame.

230

5.4 General Nonsideshell CSD

Two nonsideshell CSD were studied to evaluate their fatigue lives. One is the general sideshell transverse bulkhead and the other is the double-bottom connections.

5.4.1 Longitudinal Transverse Bulkhead Connection

Based on SMP databases, the second most fatigue cracks of side shell longitudinal has been found at their connection to transverse bulkhead where relative transverse deflection between the bulkhead and adjacent web frames generates additional bending stresses.

The long-term loading procedure is different from the procedure for general sideshell CSD. Several modifications have been made based on the existing SMP procedure. There are some uncertainties in the proposed procedure due to the simplified long-term loading strategy. The modified long-term loading procedure is as follows:

1) The global FEA was conducted based on the nominal loading for the stillwater ballast tanker . For this case tanks 5P, 5S, 3P and 3S are filled with saltwater ballast. (See Fig 3.1). Two separated nominal loading cases were conducted. 1) One is the nominal pressure. 2) The other is the nominal longitudinal bending moments.

2) Local FEA was conducted to determine the hotspot stress based on the applied displacement boundary conditions derived from the above global FEA. Two separated load cases were conducted in local level.

3) Calculate the ratio for the long-term extreme wave bending moment and nominal wave bending moment, the ratio for the long-term extreme pressure and the nominal pressure for specific location.

4) Multiple the hotspot stress derived from Local FEA multiplied by the corresponding ratio to determine the long-term stress due to pressure and longitudinal bending.

5) The extreme stress range is the twice of the results in Step 4.

The fatigue evaluation criteria is as follows :

Based on the extreme stress range and selected S-N curve, fatigue life is predicted for the locations of structural details of interest using the Miner's cumulative damage hypothesis. Weibull shape parameter is determined by ABS empirical formula. Evaluation of fatigue life was carried out on the following criteria:

231

$$\varepsilon = 1.40 - 0.036\alpha L^{1/2} \quad \text{for } 190 < L < 305m$$
$$= 1.40 - 0.036\alpha L^{1/2} \quad \quad \text{for } L > 305$$

where:

α =1.00   for deck structures

α =0.93   for bottom structures

α =0.86   for sideshell and longitudinal bulkhead structures

Estimated Life:

$$Lt = (\frac{0.5}{Lf} + \frac{0.5}{Lb})^{-1} > 20 \text{ years}$$

where,

Lt : total fatigue life
Lf: fatigue life for local pressure
Lb: fatigue life for longitudinal bending.

The two load case global and local finite element analysis results were shown in Ref. 3 Following is the stress range and calculated fatigue life.
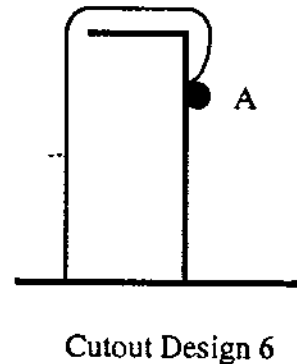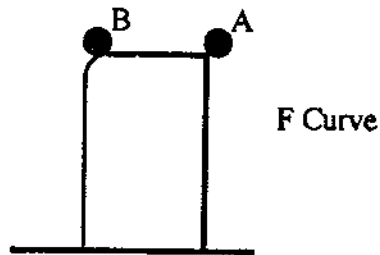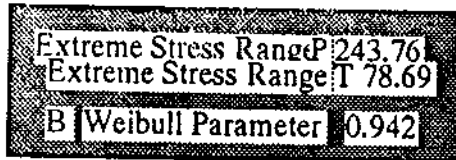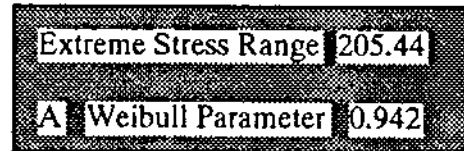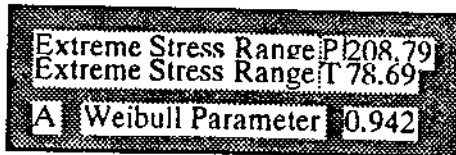
Extreme Stress Range	P	208.79
Extreme Stress Range	T	78.69
A	Weibull Parameter	0.942

Extreme Stress Range	P	243.76
Extreme Stress Range	T	78.69
B	Weibull Parameter	0.942

| Extreme Stress Range | 205.44 |
| A | Weibull Parameter | 0.942 |

F Curve

Cut-out Design 1

A: Probability of Failure During 20 Years = 0.7%
B: Probability of Failure During 20 Years = 16.43%

Cutout Design 6

Probability of Failure During 20 Years = 0.45%

Unit : N/mm**2

Fig 5.5 Fatigue Analysis for Cut-out in Transverse Bulkhead

Extreme Stress Range 276.76
Weibull Shape 0.972 B

Extreme Stress Range 234.34
Weibull Shape 0.972 A
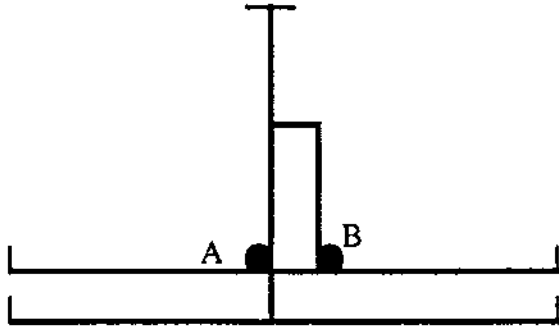
Probability of Failure During 20 years = 34.76%
Probability of Failure During 20 years =19.78%

Extreme Stress Range 156.45
Weibull Shape 0.972 A

Probability of Failure During 20 Years =0.0%

233
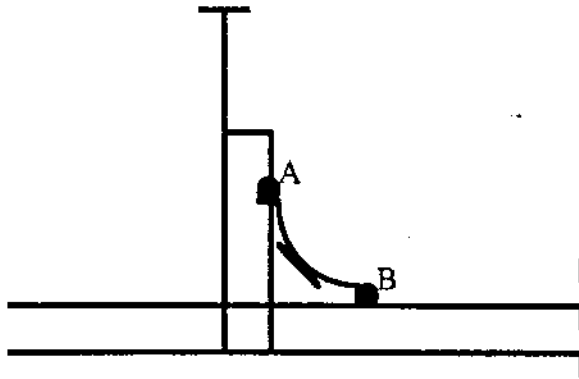
Double-Bottom Connection
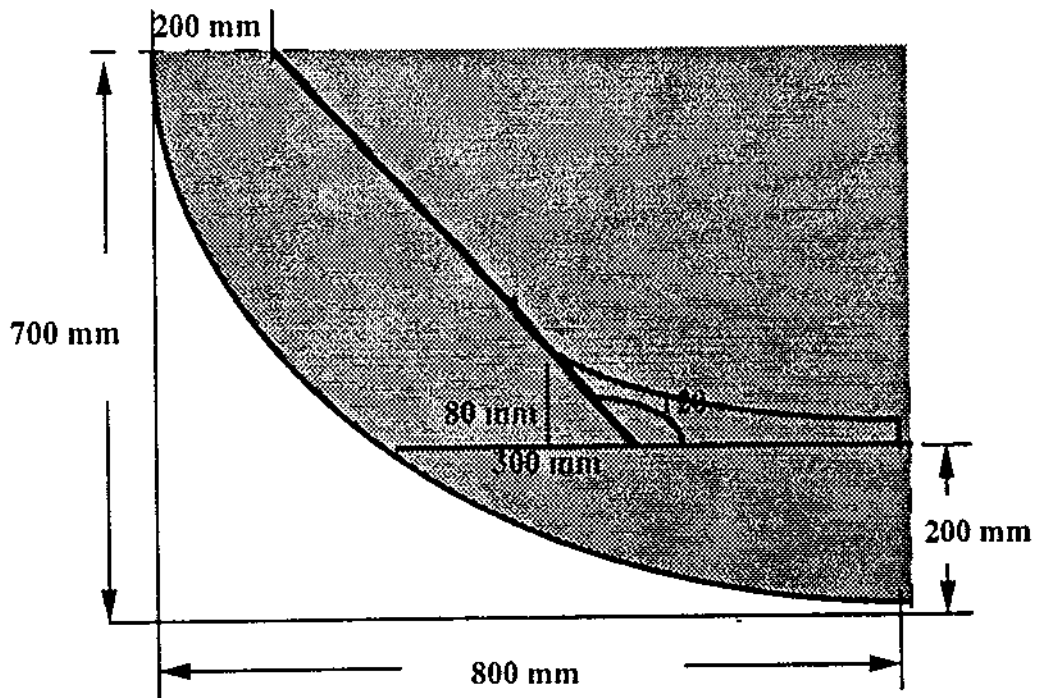
Fig 5.8 Proposed Double-Bottom Geometry and Dimensions

234
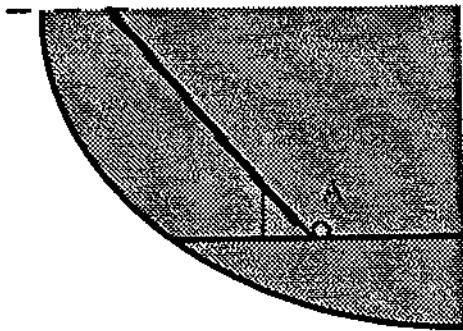
Extreme Stress Range	269.5
Weibull Parameter	0.942

Probability of Failure = 39.8%
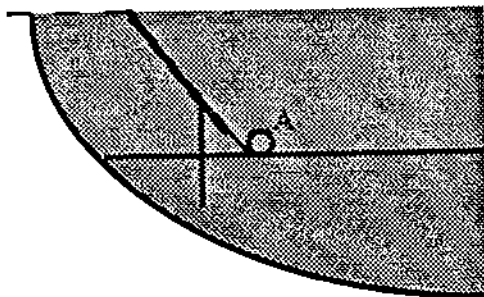
Extreme Stress Range	302.4
Weibull Parameter	0.942

Probability of Failure = 43.68%
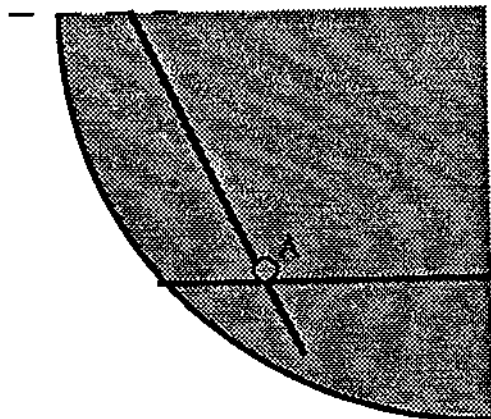
Extreme Stress Range	225.47
Weibull Parameter	0.942

Probability of Failure = 21.34%

Unit : N/mm**2

Fig 5.9 Fatigue Analysis for Double-Bottom Connection

235

5.4 Fatigue Design Procedure for CSD in Tankers

This section discusses the general fatigue design procedure for CSD in tankers. In general, fatigue design for CSD has four principal lines of definse. (Ref . 6)

1 Minimize Stress-strain Risers (stress concentration) and cyclic straining-stressing through good engineering of the frame system and its details.

2 Minimize Flaws (misalignments, poor materials, porosity-voids, etc.) through good, practical material and fabrication specifications and practices.

3 Minimize Degradation at the Local Element through selection of good materials and fabrication practice, and good engineering designs (e.g. crack stoppers, damage localizes and repairable elements)

4 Minimize Degradation at Frame System Level so that when (not if) local fatigue degradation occurs, there are no significant effects on the framing system's ability to perform satisfactorily

One of the simplest forms for fatigue design for CSD is allowable stress and stress range approach. The S-N approach can be expressed as an allowable stress range, S_{rf}, for a CSD:

$$Srf = [\frac{K}{NcY}]^{1/m} (\ln Nc)^{1/\varepsilon}$$

where:

K - life intercept of design S-N curve,
m - slope of design S-N curve,
ε - Weibull shape parameter for long-term stress distribution
Nc- Total number of stress cycles during the design service life.

$Y - \Gamma(1+\frac{m}{\varepsilon})$, and

Γ - Gamma Function

The Weibull shape parameter, ε can be determined as

$$\varepsilon = 1.40 - 0.036\alpha L^{1/2} \quad \text{for } 190 < L < 305m$$
$$= 1.40 - 0.036\alpha L^{1/2} \quad \text{for } L > 305$$

where:

α = 1.00 for deck structures

α = 0.93 for bottom structures

α = 0.86 for sideshell and longitudinal bulkhead structures

Nc is based on the design life of the CSD and the average frequency of cyclic loading during the design life. The design life may incorporate a factor of safety (design life = factor of safety x service life)

CSD Design Procedure for a Fatigue Design Check

Based on above model, CSD design procedure for a fatigue design check proceeds through six steps:

Step 1 - Define an appropriate value of the Weibull stress range shapes parameter.

Step 2 - Define an appropriate stress ratio. ($R = S_{min}/S_{max}$)

Step 3 - Define an appropriate S-N curve slope and use S-N curve to establish the design stress range $S_{fd} = S_R$ for desired service life T. (normally 20 years for tanker)

Step 4 - The peak stress value for the hotspot is computed as $S_{PD} = S_{fd}/(1-R)$

Step 5 - The fatigue strength can be stated in terms of a nominal stress by using an appropriate stress concentration factor (SCF).

Step 6 - The CSD is taken as satisfactory if $S_m < S_{PD}$, where S_m is the hotspot stress corresponding to the service life.

5.6 Fatigue Analysis Based on Calibrated S-N Curves

The procedure for the evaluation of fatigue damage for engineering applications is basically based on the use of S-N curves in combination with the Palmgren-Miner summation rule.

The use of S-N curves for fatigue life evaluations requires that the stresses used in the analysis are compatible with the stresses used for the derivation of the S-N curves. In the case of the S-N curves derived from tests of tubular joints the curves are based on the measured hotspot stress. This requires that the hotspot stress has to be determined for the fatigue analysis of a tubular joint.

227

S-N data for most specimens is represented based on the nominal stress. In order to use these curves for the fatigue life evaluation of complex details the nominal stress has to be determined.

If the nominal stress is used in fatigue life evaluation, the influence of the local geometry on the hotspot stress has to be accounted for through the choice of the S-N curve. For complex CSD the nominal stress can not be easily evaluated whereas the hotspot stress can be obtained from finite element analysis in a straightforward manner. It is therefore desirable to develop calibrated S-N curves that are suitable for the use of hotspot stress obtained from finite element analyses.

The above fatigue analysis is basically based on hotspot stress approach in SMP project. The S-N curves are selected one level higher than the curves in nominal stress. This section discussed the fatigue evaluation for CSD based on the new calibrated S-N curves developed by **Fatigue Classification of Critical Structural Details in Tankers** conducted by Department of Naval Architecture & Offshore Engineering, University of California at Berkeley.

Calibrated S-N Curves

The calibration model is derived based on the assumption that the S-N curve resulting from a series of S-N tests are represented in terms of the nominal stress σ_{nom}. The nominal stress is defined as

$$\sigma_{nom} = F/A \quad \text{Uniaxial tension loading}$$
$$\sigma_{nom} = M/W \quad \text{bending moment}$$

where:

F	axial force
A	area of cross-section
M	bending moment
W	section modules

The general form of this type of S-N curve is thus given by

$$N = C(\Delta\sigma_{nom})^{-m}$$

where:

$\Delta\sigma_{nom}$ stress range based on nominal stress
m   negative inverse slope of S-N curve
logC   intercept with logN axis

228

The parameters C and m are based on the curve fitting procedure that has been used to define the S-N curve. m represents the negative, inverse slope of the S-N curve in a log-log scale Most S-N curves for welded geometry's therefore have a slope parameter m=3.0

In order to calibrate existing S-N curves the parameter m is held constant. Fig 5.12 shows a schematic view of the stress distribution in a test specimen. The nominal stress σ_{nom} is based on F/A or M/W. Due to the presence of the welded attachment this stress is increased with a maximum value of $K_t\sigma_{nom}$ at the beginning of the attachment. Here Kt represents the stress concentration factor and defined as:

$$Kt = \frac{\sigma_{max}}{\sigma_{nom}}$$

In order to use the hotspot stress for the calculation of the fatigue damage the S-N curve has to be modified. The number of cycles to failure at a given stress range for a particular test specimen is based on constant amplitude tests. The modified S-N curve there fore has to be the same number of cycles to failure for a given hotspot stress. Fig 5.12 shows the relation between the modified and original S-N curve. The two curves have the same slope but the parameter C has been replaced by C. The following equation has been used to derive C:

$$N==C(\Delta\sigma_{nom})^{-m}=C(Kt\Delta\sigma_{nom})^{-m}$$

The curve parameter C of the modified S-N curve can therefore be expressed as

$$C=CKt^m$$

The modified S-N curve depends on the method for obtaining the hot spot stress. The curve has to be used in combination with hot spot stresses that are obtained in the same was as the hot spot stress used for the determination of C.

Based on the previous procedure, the calibrated S-N was developed in **Fatigue Classification of Critical Structural Details in Tankers** Fig 5.10 is the calibrated results which includes the original and calibrated S-N curves (Ref. 7). In addition, the S-N curve database was developed in that project which is used by Microsoft Access.
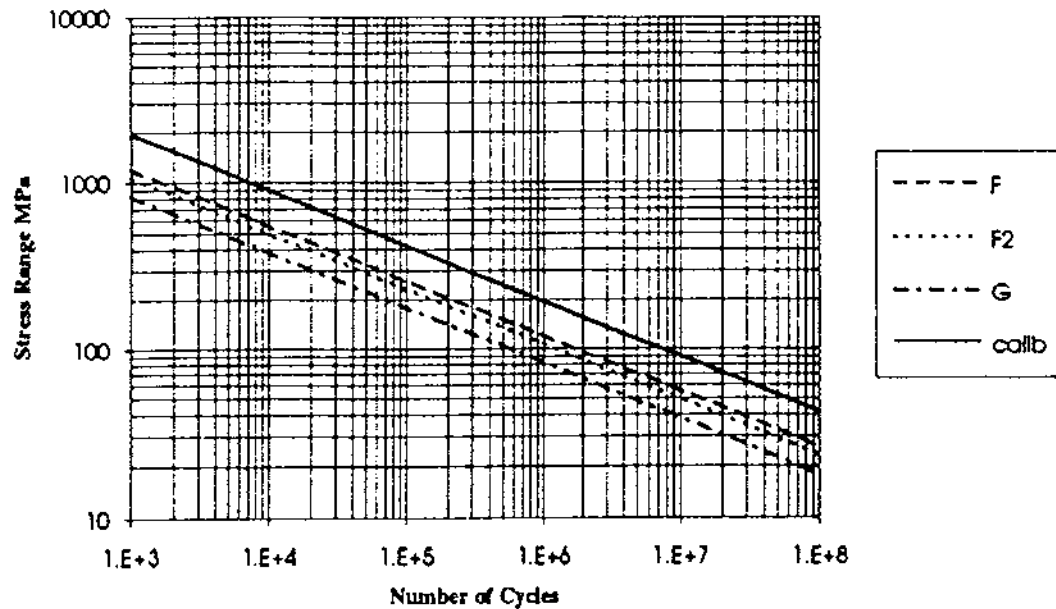
Fig 5.10 Original and Calibrated S-N Curves

The calibrated S-N curves obtained through the Joint Industry Project **Fatigue Classification of Critical Structural Details in Tankers** has been used in fatigue analysis for proposed CSD in double-hull tankers by using SMP fatigue life evaluation software.

The proposed CSD was illustrated in Fig 5.2. The same log-term loading and calibrated S-N curves were applied in this case. It has been found that the fatigue probability due to the calibrated S-N curves is smaller that derived from the original S-N curves. The results indicated the uncertainties in S-N curves selection and hotspot stress determination played important role in fatigue analysis. Due to the current experience, it's still hard to determine which is best among these two selections.

f1	f2	Scale	shape	Original	calibrate	Original	calibrate
1.037	1030	4.238	0.942	F curve	New	12.7%	2.37%

Table 5.5 Fatigue Comparison between Original and Calibrated Curves

5.7 Discussion and Conclusion

This chapter addresses the general fatigue analysis for various CSD in the second proposed double-bottom tanker. The fatigue analysis was based on an updated fatigue analysis procedure. We found that the fatigue assessment problem is one having very high levels of complexity. This is because to do the assessment correctly, one must address numerous issues such as the establishment of the long-term loading, the finite element modeling for the CSD, the selection of appropriate S-N curves and corresponding stress concentration factors. This information was documented in the project reports **Fatigue Analysis of Proposed CSD in a Double-Hull Tankers** and **Fatigue Analysis of Proposed CSD in a Double-Bottom Tanker.**

The fatigue assessments addressed here were those resulting from hull-girder bending and local pressures. The relative importance of the mechanism depends upon the location of the CSD. It's clear that about 67% of the fatigue damage for general sideshell CSD is due to local pressure while 33% of the fatigue damage is due to hull-girder bending. For deck CSD, fatigue damage is mainly due to hull girder bending while the bottom CSD is mainly due to local pressure.

For general sideshell CSD fatigue evaluation, the cutout in transverse web frame is not the critical area for general sideshell CSD due to the new design such as two-side lug, tight connection between longitudinal and web frame and smooth shape for the cutout. Most fatigue problems occur at the sideshell longitudinal stiffener or bracket connection or the bracket-toe connection. The basic reason is not only due to the high stress concentration factors but also due to the high level S-N curves. The new design of the sideshell CSD without stiffener can dramatically improve the fatigue performance.

For general nonsideshell CSD, it can be concluded that the critical area is the side longitudinal in sideshell transverse bulkhead. Compared with the general sideshell at the similar location, fatigue life is relatively shorter. One of the reasons is caused by the difference about the transverse flexibility for transverse bulkhead and transverse web frame. Another reason is the uncertainties in the long-term loading analysis. Fatigue damage is severe in double-bottom connections. Due to the limited information for the bottom connection in double-hull, only several cases about the connection in double-bottom tankers have been performed. The different configurations have large difference in stress concentration factors and fatigue life.

241

The experience obtained from this project in CSD fatigue design alternatives will be addressed in detail in next chapter.

242

Chapter 6

CSD Fatigue Design Alternatives

6.1 Introduction

From previous experience, we know that fatigue damage for CSD in tankers are mainly due to the result of excessively high nominal stresses in the CSD that are derived from the use of higher strength steels, improper configured details and misaligments.This chapter summarizes the current state of art for CSD fatigue design based on the study in this project. It focuses on the general sideshell CSd fatigue while the sideshell transverse bulkhead is also discussed here. The objective of this chapter is to simplify the complex fatigue design based on the previous studies and the study in this project.

6.2 General Sideshell Stiffener and Bracket-toe

From the previous SMP databases, fatigue damage is most severe for sideshell longitudinal transverse web frame CSD. Recent experience in CSD has proved the that the fatigue damage is most severe in sideshell CSD stiffener and bracket-toe.

The stiffener or bracket-toe is used in ship structural design in longitudinal as well as transverse members and has frequently shown severe fatigue damages. For brackets on continuous plates or flanges, different shape exist: without or with soft transition and without or with additional buckling stiffener (types A-D according to Fig.6.1) The systematic variation has been performed with the following geometric parameters and validity ranges, see Fig 6.1

$$\eta = H/(30*T) \qquad (0.33 - 3.3)$$

$$\gamma = G/H \qquad (0.40 - 2.5)$$

$$\rho = R/(H*T\kappa/T) \qquad (0.60 - 1.5 \text{ for } \eta = 0.33)$$
$$(0.40 - 1.0 \text{ for } \eta = 1.00)$$
$$(0.25 - 0.6 \text{ for } \eta = 3.3)$$

$$v1 = T_G/T \qquad (1.5 - 2.5)$$

$$v2 = T_K/T \qquad (0.5 - 1.5)$$

$$\varphi = \varphi_0 * \pi/180° \qquad (\pi/9 - \pi/4)$$

Load Case 1 **Load Case 2** **Load Case 3**
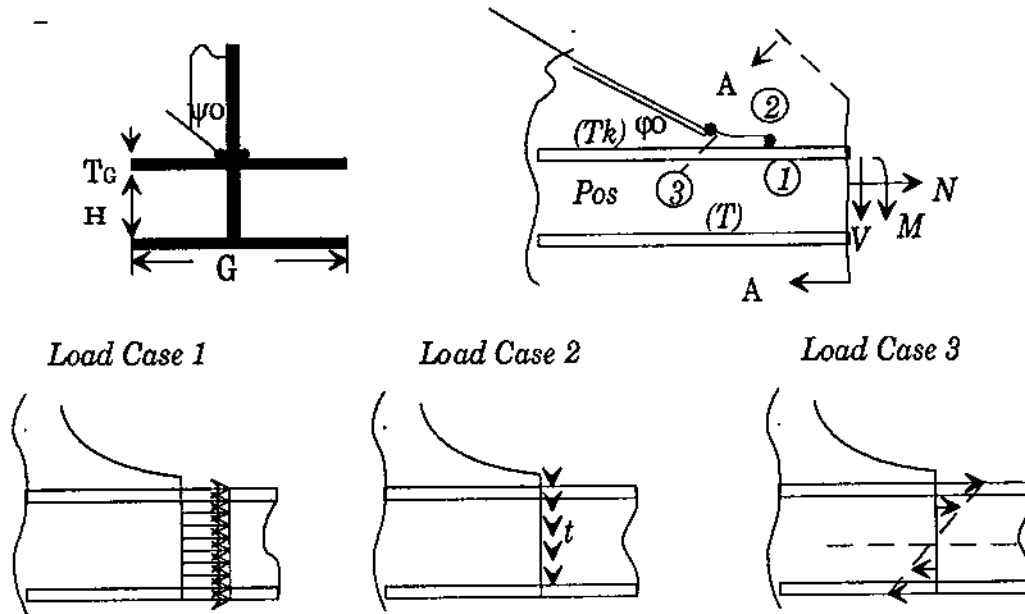
Types of Bracket

A : Straight End (R=0), without Stiffener

B : Straight End, with Stiffener

C: Soft Transition, without Stiffener

D: Soft Transition, with Stiffener

Fig 6.1 Stiffener or Bracket-toe Investigated

The different validity ranges of the parameter ρ consider the relatively large end radii in thick-walled structure (bracket on T-bar) compared to thin-walled structures (bracket on web frames in tankers). Further scantlings such as flank angle φ_0, depth of bracket toe, height and thickness of buckling stiffener as well as throat thickness of weld have been set to usual values.

Two or three typical values of each geometric parameter were selected, for which the variation were performed with all possible combinations. In this way also extreme combinations of the geometric parameters are taken into account.

Three unit load case (LC) as shown in Fig 6.1 are considered, corresponding to common forces and moments. The shear load case is defined such that only a unit shear stress acts in the web below the bracket toe. Equilibrium conditions were applied to the proposed CSDs.

As shown in Fig. 6.1, three critical positions are considered, which are located at the weld toes at the end of the bracket and buckling stiffeners as well as the rounded plate edge of the soft transition. According to the above considerations concerning the determination of the hotspot stresses, the structure was modelled using shell plate elements. The finite element model was clamped at the end of the bracket, i.e. far away from the notch area investigated.

Fig. 6.2 shows the calculated hot-spot SCF, K_{SN}, for the pos. 1 and 3 of bracket type D under normal load. The results are valid for selected geometric parameters as given in Fig. 6.1. The resulsts show the large influence of the parameter H/T and particularly of the thickness ratios T_G/T and T_K/T.

It becomes apparent that a relatively thick bracket plate may cause a high hotspot stress at the bracket-toe (Pos. 1) while the hotspot stress at the end of the buckling stiffener (Pos. 3) is much reduced. This effect may be well known to experienced structural engineers, but now it can be quantified. For instance, the plate thickness of the bracket can be determined such that equivalent hot-spot stress are obtained at both positions, with the objective of a structural optimization. By the way, the angle φ_0 of the sniped end of the buckling stiffener has a negligible effect on the hot-spot stress.

6.2.1 Approximate Formula for Bracket-toe SCFs

Apart from a direct interpolation between the numerical results, the development of approximation formulae is of great interest for practical application. An empirial formula has been developed, which better considers the dependence between the different geometric parameters. This formula is based on the Almar-Naess 's fatigue handbook (Ref. 7).

$$K_S = X_1(\eta^{X2+X14 \, * \, \eta+X15 \, * \, \gamma+X16 \, * \, \rho+X17 \, * \, v1+X18 \, * \, v2} + X_3)\gamma^{X4} \, * \rho^{X6} \, * v_1^{X8} \, * v_2^{X10} \, * \psi^{X12} + X_{20}$$

Table 6.1 Regression Coefficients for the Calculation of hot-spot SCFs of Bracket Toes

Type	Pos.	LC	X1	X2	X3	X4	X6	X8	X10	X12	X14	X15	X16	X17	X18	X20
A	1	1	-1.64	-0.14	-1.93	0.184	0.0	-0.6	0.47	0.0	0.0	0.03	0.0	0.0	-0.12	0.97
		2	1.23	0.04	-2.05	0.184	0.0	-1.05	0.61	0.0	0.0	0.03	0.0	0.06	-0.31	0.07
		3	-1.96	-0.17	-2.04	0.24	0.0	-0.56	0.50	0.0	0.0	0.05	0.0	0.0	-0.13	0.94
B	1	1	-1.80	-0.10	-1.95	0.17	0.0	-0.51	0.34	0.0	-0.05	0.0	0.0	0.0	-0.10	0.81
		2	-1.26	0.0	-2.07	0.23	0.0	-1.24	0.54	0.0	-0.05	0.05	0.0	0.0	-0.27	0.25
		3	-2.58	-0.19	-1.84	0.26	0.0	-0.54	0.40	0.0	0.0	0.04	0.0	0.0	-0.07	0.95
C	1	1	-1.2	0.0	-1.82	0.155	-0.17	-0.61	0.56	0.0	0.03	0.02	0.0	0.02	-0.11	0.92
		2	-1.08	0.192	-1.29	0.36	-0.55	-0.8	0.40	0.0	-0.05	0.0	0.0	-0.25	-0.05	0.24
		3	1.30	0.05	-1.83	0.21	-0.23	-0.61	0.56	0.0	0.0	0.04	0.0	0.03	-0.3	0.90
D	1	1	1.19	0.0	-1.82	0.155	-0.17	-0.61	0.56	0.0	0.03	0.02	0.0	0.02	-0.11	0.93
		2	-1.08	0.19	-1.29	0.36	-0.55	-0.8	0.40	0.0	-0.05	0.0	0.0	0.02	-0.05	-0.05
		3	-1.26	0.13	-1.88	0.20	-0.25	-0.58	0.49	0.0	0.0	0.0	0.0	0.03	-0.11	0.89
C	3	1	-1.51	-0.28	-2.63	0.16	0.0	0.21	-0.70	-0.01	-0.31	0.0	0.0	0.0	0.0	-1.02
		2	-2.85	-0.07	-2.76	0.05	0.0	0.03	-0.61	0.01	-0.04	-0.03	0.0	0.0	-0.10	-1.66
		3	-2.31	-0.28	-2.67	0.26	0.0	0.28	-0.70	-0.005	-0.10	0.0	0.0	0.0	-0.05	-1.22
D	3	1	-1.58	-0.26	-1.98	0.177	-0.26	0.22	-0.67	-0.01	0.06	0.02	0.113	0.0	-0.67	-0.61
		2	1.251	0.0	0.70	-0.05	-0.25	-0.11	-0.88	0.01	-0.17	0.031	-0.28	-0.06	0.35	0.41
		3	-1.88	-0.23	-2.39	0.25	-0.26	0.26	-0.66	0.0	0.09	0.04	0.12	0.0	-0.10	-1.0

From the results of systematic calculations, the regression coefficients Xi given in Table 6.2 have been detemined for the calculation of hot-spot SCFs at pos. 1 and 3. For combined loading the hotspot SCFs, KsN, Ksv and KsM have to calculated separately for the different unit load cases. The hotspot stress is calculated with the actual nominal stresses, σ_N, τ and σ_M as follows:

$$\sigma_s = K_{SN} * \sigma_N + K_{SV} * \tau + K_{SM} * \sigma_M$$

A typical bracket subject to combined loads is considered in order to comapre the four bracket types with each other. Table 2.2 shows the chosen geometric parameters, nominal stresses as well as the resulting hot-spot SCFs and combined stress according to the empirial formula at pos. 1. The effect of a soft transition can clearly be seen at the reduced combined hot-spot stresses for types C and D. The individual hot-spot SCFs show that the stress reduction due to a soft transition is particularly pronounced under shear load, but also under bending load. This means that the advantage of soft transitions may be under estimated if only a normal load is considered. Under combined loads, the benefical effect of a soft transition is much greater.

Table 6.2 Hot-spot SCFs and Combined Stress Derived From Empirial Formula

Type of Bracket	A	B	C	D
Geometric Parameters				
$\eta = H/(30 * T)$	1.0	1.0	1.0	1.0
$\gamma = G/H$	1.0	1.0	1.0	1.0
$\rho = R/(H * T_K/T)$	-	-	0.65	0.65
$\nu_1 = T_G/T$	2.0	2.0	2.0	2.0
$\nu_2 = T_K/T$	1.5	1.5	1.5	1.5
$\varphi = \varphi_0 * \pi/180°$	-	$\pi/4$	-	$\pi/4$
Nominal Stress				
σ_N (N/mm²)	100	100	100	100
τ (N/mm²)	50	50	50	50
σ_M (N/mm²)	50	50	50	50
Hot-Spot SCFs at Pos. 1				
K_{SN}	2.175	2.186	1.786	1.795
K_{SV}	0.864	0.954	0.204	0.217
K_{SM}	2.635	2.702	1.861	1.866
Hotspot Stresses				
σ_s (N/mm²)	392.4	401.6	281.8	283.6

6.2.2 Fatigue Design for Stiffener or Bracket-toe

In the previous sections, we discussed about the SCF for bracket-toe or stiffener. Usually, High SCF will have severe fatigue damage. Thus several stress relaxation methods are presented to reduce the SCF.

1) Installation of backing bracket or stiffener
2) Using soft bracket-toe

It should be pointed out the fatigue is not only due to high SCF only although high SCF plays the important role in fatigue design. Another factor is the S-N curve selection which is associated with welding or construction. This requires high-quality construction and maintenance.

Recent experience has shown that fatigue on side longitudinal stiffener or bracket connection is still the most severe fatigue damage areas. (Ref. 6) Some Japanese shipyards have proposed new CSD design without stiffener. This may be the best alternative for the stiffener or bracket-toe design.

248

6.2 Cutout in Transverse Web Frame

Since the relative new CSD design is the CSD without stiffener or bracket. Cut-out , another critical area about fatigue damage in CSD becomes much more important in CSD fatigue design.

10 cutouts in transverse web frame were analysised in this project, Based on the analysis results, the design alternatives for cutout were discussed here.

Generally speaking, cutout with two side lug can satisfy the general fatigue requirement.

From the case studies in this project, following is relatively better design for cutout based on stress concentration factors.
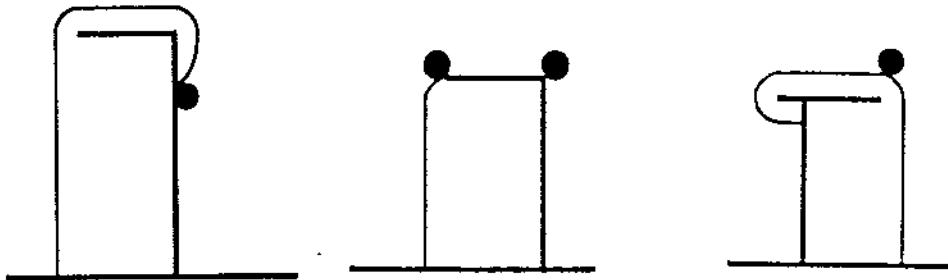
Fig 6.2 Realtively Better Cutout Design

It's hard to derive a reasonable formula for the SCF of cutout. But we can derive the general relationship about the stress and cutout size.
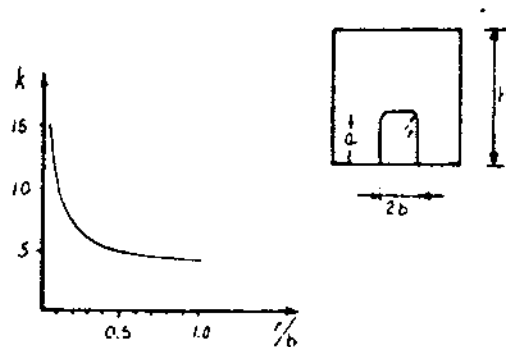
Fig 6.3 General Relationship Between Stress and Cutout Size.

It should be pointed out that a low SCF doesn't mean short fatigue life since the fatigue is due to the stress range and S-N curve selection. For example, Fig 6.4 shows one typical cutout design, Hotspot with stress concentration factor 2.12, the S-N curve is C curve while the hotspot with stress concentration factor 1.47, the S-N curve is F curve. The fatigue analysis results on Fig 6.5 shows the difference between SCF and fatigue damage.

SCF=1.33

SCF=2.31

Cutout Design 6

Cutout Design 10
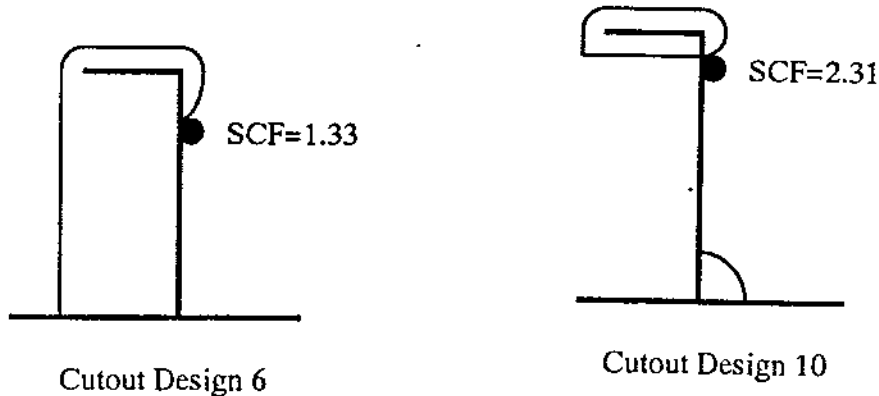
Fig 6.4 Typical Cutout Stress Concentration Factor (SCF)

Extreme Stress Range P	176.67
Extreme Stress Range T	78.69
Weibull Shape = 0.942	

Extreme Stress Range P	164.74
Extreme Stress Range T	78.69
Weibull Shape = 0.942	

Unit : Stress Range N/mm**2
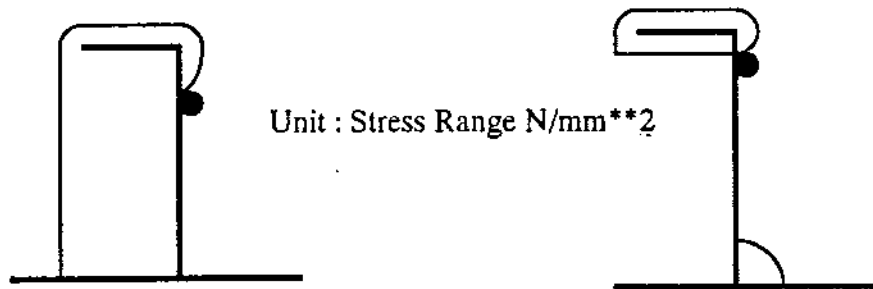
Probability of Failure During 20 Years = 0.1%

Probability of Failure During 20 Years = 0.037%

Fig 6.5 Fatigue Life for Cutout

Relatively speaking, fatigue for cutout in sideshell CSD is not as severe as stiffener or bracket. For general relatievly new design, especially the two side lug design, the fatigue performance can be satisfied.

250

6.3 General Nonsideshell CSD

Two nonsideshell CSD have been conducted in this project. Following is the summary from the analysis for CSD fatigue design.

6.3.1 Sideshell Longitudinal Transverse Bulkhead

The basic fatigue design consideration in sideshell longitudinal TBHD is nearly the same as that in general sideshell CSD. The approximate formula can be applied in the bracket-toe or stiffener connection in sideshell longitudinal TBHD. The SCF table for cutout in transverse bulkhead is presented in Chapter 4.

It should be pointed out that the fatigue damage in transverse bulkhead is not smaller than that in general sideshell CSD although the SMP database shows that most fatigue cracks are general sideshell CSD. From another point of view, fatigue damage in transverse bulkhead is severe.

6.3.2 Double-Bottom Connection

It has been found that the fatigue damage is severe on double-bottom connection although there are some uncertainties in the long-term loading procedure. Due to the limited information, we have no chance to perform the analysis for the bottom connection in double-hull tankers. Based on the experence in the study of the bottom connection in double-bottom in this project, several recommendation was presented here.

It's recongized that the double-bottom connection's SCF is usually high.

It highly recommended that the soft connection should be applied here which can reduce the stress concentration factors greatly.

Adding bracket with soft-toe is one of the effect way to reduce the stress concentration factors and fatigue damage.

Up to now, it's hard to conclude more results for the new design due to the limited analytical experience and database. Further studies about the different bottom connections should be conducted to improve design of the double-hull bottom connection.

Chapter 7

Summary and Conclusions

7.1 Summary

A detailed fatigue analysis was performed for a 190,000 DWT double-bottom tanker. The fatigue analysis for the double-bottom tanker focused on several specific CSD with different configurations at the same locations to evaluate fatigue performance with different design alternatives. Both probabilistic and deterministic fatigue analyses were conducted to determine the probability of failure during the tanker's service life and fatigue life of the specific CSD in the proposed double-bottom tanker. The stress concentration factors (SCF) table for various cutout, bracket and stiffener or double-bottom connection has been developed. The relatively new simple formula for the SCF calculation for bracket-toe or stiffener is presented for preliminary CSD design. The load effects on fatigue damage has been investigated for local pressure and axial loads.

7.2 Conclusions

Several conclusions have been made from the analysis.

1) Fatigue damage on side longitudinal around the load water line is severe.

2) Fatigue damage on side longitudinal with the transverse bulkhead is severe.

3) The most critical area for fatigue damage for general sideshell CSD is the longitudinal stiffener or bracket connection.

4) A new design based on an apple-shaped slot opening at the connections between longitudinal and web frame without stiffeners may be the most effective way to reduce the fatigue damage on side longitudinal stiffeners or bracket connections.

5) Fatigue damage for the new design about cut out especially the two side lug cutout appears to be acceptable.

252

6) A relatively simple formula for the SCF calculation for bracket-toe or stiffener is proposed for preliminary optimized fatigue design.

7) A SCF table for various cutout, bracket and stiffener or double-bottom connection has been developed.

8) Fatigue damage due to local pressure for general sideshell CSD is about as twice that due to axial loads.

There are uncertainties in fatigue analyses especially the long-term loading for the nonsideshell CSD. An uncertainty analysis has been performed in the analysis of the 150,000 DWT double-hull tanker (Ref. 3). It has been shown that fatigue analysis results are very sensitive to the loading uncertainties. Further studies of the fatigue long-term loading uncertainties are recommended.

253

Reference

1 Structural Maintenance for New and Existing Ships, Research Report SMP 1-1 through SMP 5-2. Dept. of Naval Architecture & Offshore Engineering, University of California at Berkeley, Berkeley, CA 94720. October, 1992

2 Tao Xu and Robert, G Bea "CSD Library and Finite Element Stress Contours" Research Report, SMPII 1-3. Dept. of Naval Architecture & Offshore Engineering, University of California at Berkeley, Berkeley, CA 94720. October, 1993

3 Tao Xu and Robert, G Bea "Fatigue Analysis of a 150,000 DWT Double-Hull Tanker" Research Report, SMPII 1-1. Dept. of Naval Architecture & Offshore Engineering, University of California at Berkeley, Berkeley, CA 94720. October, 1993

4 Guide for the Fatigue Strength Assessment of Tankers, American Bureau of Shipping, New York, NY, 1992

5 Rolf Schulte-Strathaus and Robert, G Bea "Development of Calibrated S-N Curves and System for the Selection of S-N Curves". Research Report, FACTS 1-1. Dept. of Naval Architecture & Offshore Engineering, University of California at Berkeley, Berkeley, CA 94720. September, 1993

6 A. Almar-Naess "Fatigue Handbook". Tapair, Trondheim, 1985

7 Huges, O.F. "Ship Structural Design, A Rationally Based Computer-Aided Optimization Approach". SNAME, Jersey City, NJ, 1988

8 U.K. Department of Energy, London. Offshore Installation : Guidance on Design, Construction and Certification, Section 21 : Steel Fourth Edition, January 1990

Study of Fatigue of Proposed Critical Structural Details in Double Hull Tankers

Critical Structural Detail Library and Finite Element Stress Contours

Tao Xu
and
Professor Robert G. Bea

Department of Naval Architecture and Offshore Engineering
University of California, Berkeley

Table of Contents

257, 258*

Chapter 1

Introduction

The one year Joint Industry Research Project " **Study of Fatigue of Proposed Critical Structural Details (CSD) in Double-Hull Tankers** " was initiated in October 1992 by the Department of Naval Architecture & Offshore Engineering of the University of California at Berkeley as an extension of two year International Joint Industry Research Project " **Structural Maintenance for New and Existing Ships** ". The objective of this project is :

To conduct analyitcal studies of proposed CSD for new double-hull tanker to assure that they have desirable durability and robustness characteristics.

In this study, we performed analyses for two tankers that are proposed for the next generation of VLCC's and ULCC's. The first study on a 150,000 DWT double-hull tanker which focused on the complete fatigue analysis for the whole structure was documented in Ref.3. The second study on a 190,000 DWT double-bottom tanker which focused on fatigue design alternatives for specific CSD was documented in Ref.2. This report summarizes the general CSD library and finite element stress contours which were performed in this project.

3

259

Chapter 2

CSD Library

2.1 Introduction

A typical generic sideshell longitudinal structural detail module library has been developed in SMP project. The library of fine-mesh FE models acted as a set of "basic components" for a complete sideshell CSD. The user selected, dimensioned and positioned the desired components through the graphic interface, and once the necessary choices have been confirmed, the appropriate complete CSD fine-mesh model will be assembled automatically. Fig 2.1 is the typical sideshell CSD and Fig 2.2 is the CSD library structure in SMP project.

Fig 2.1 General Sideshell Longitudinal CSD

260

CSD Library

```
                    CSD Library
                        |
        ┌───────────────┴───────────────┐
  Finite Element Directory          S-N Curve Directory
        |                               |
   ┌────┴────┐                     ┌─────┴─────┐
Sideshell  Nonsideshell        Sideshell   Nonsideshell
```
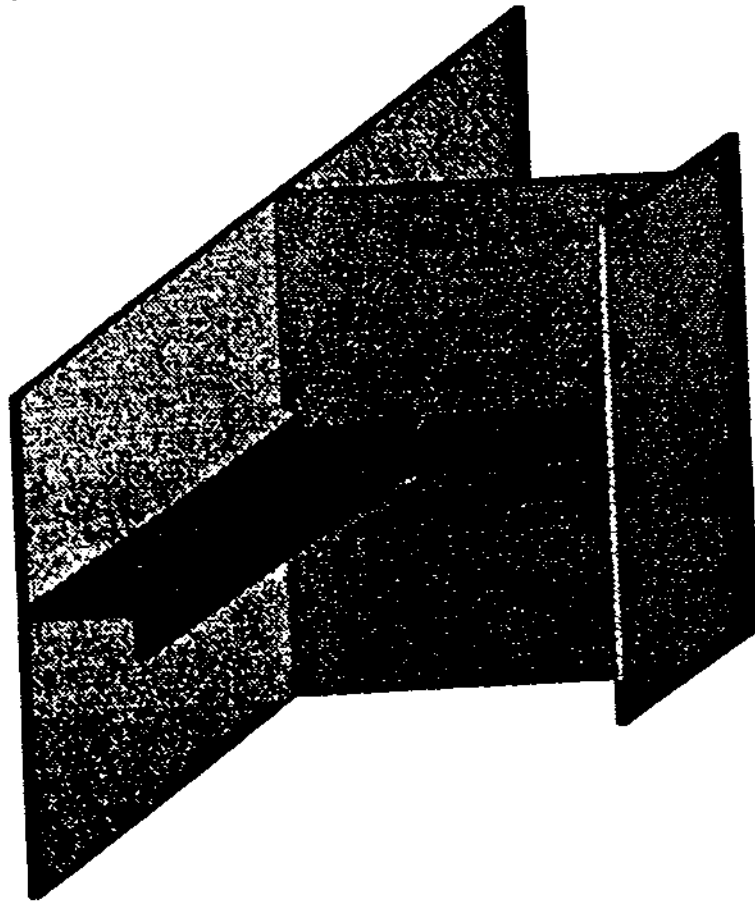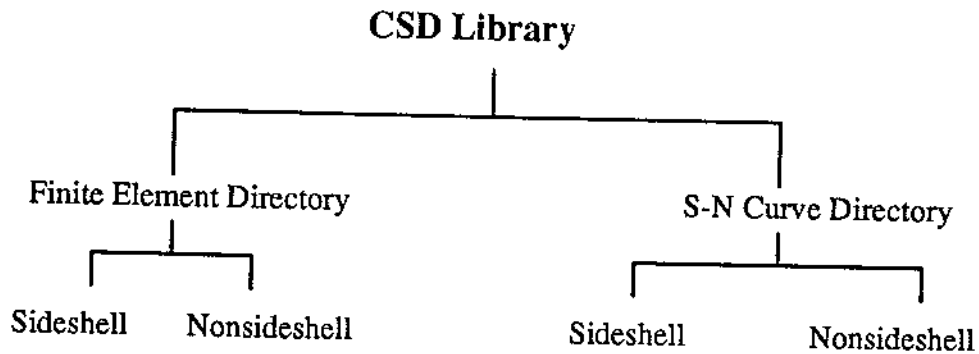
Fig 2.2 SMP CSD Library Structure

Based on the previous SMP project, the update CSD library was developed in this project, the CSD library includes Finite Element Directory and S-N Curve Directory. The finite element directory focused on the generic sideshell CSD with different configurations about cutout , stiffener and bracket with same dimensions. The S-N curve diectory is developed by SMP project based on hotspot stress.

2.2 CSD Finite Element Directory

The CSD Finite element library developed in this project is a little different from the previous SMP project due to the objective of this project. Fig 2.3 is the general structure for the FE library.

CSD Finite Element Directory

```
              CSD Finite Element Directory
                        |
        ┌───────────────┴───────────────┐
  General Sideshell Detail         Nonsideshell Detail
        |                               |
   ┌────┴────┐                     ┌─────┴─────┐
FEA Loading  Fatigue Loading    FEA Loading  Fatigue Loading
```
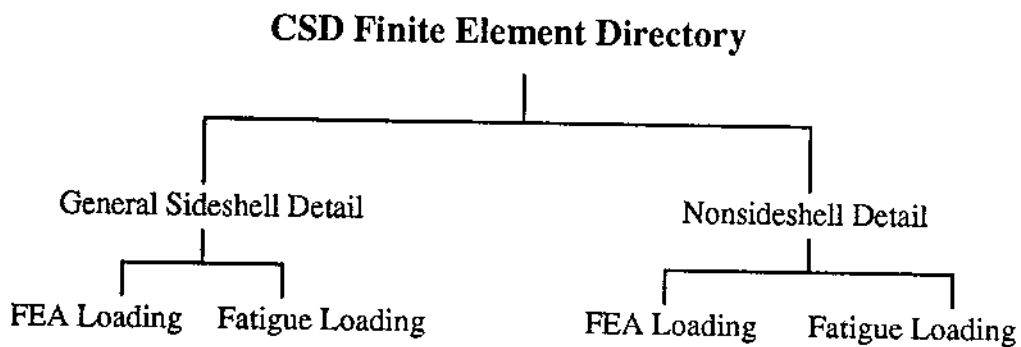
Fig 2.3 Finite Element Directory Structure

One of the tasks in this project is to evaluate the different CSD design alternatives. The CSD finite element models were generate to conduct this task. The FE model is the same dimensions with different configurations. Fig 2.4 shows the dimensions for the general sideshell CSD. Fig 2.5 is the typical FE model.

261

10"

30"

105" x 0.46"

6"

20"

25"

404" x 0.46"

105" x 0.46"
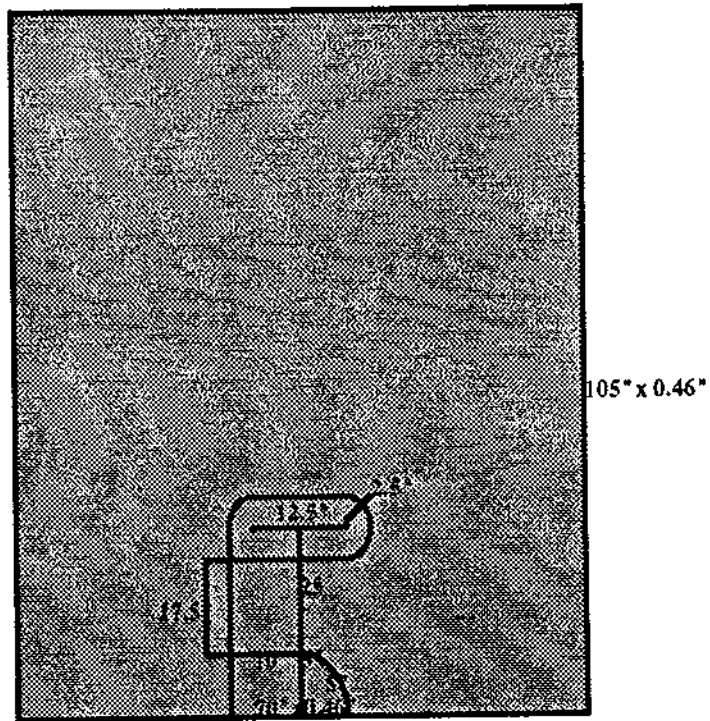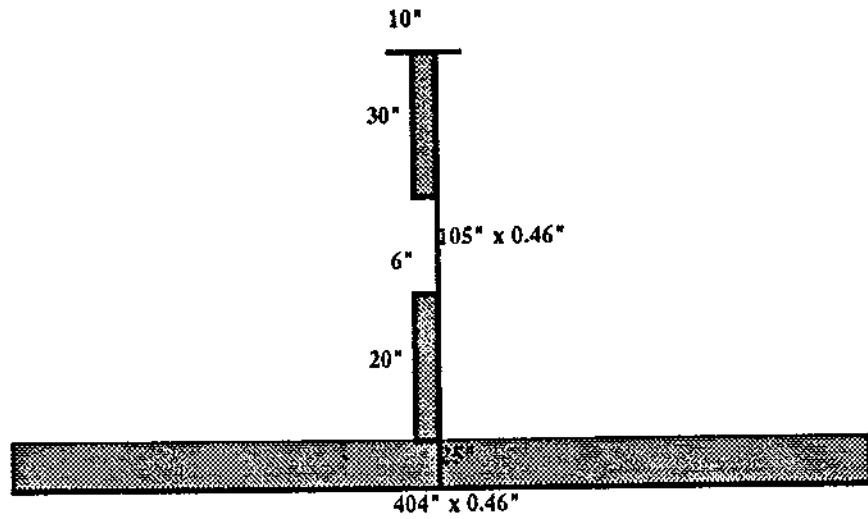
Fig 2.4 Dimesnions of the CSD in Finite Element Directory

In the subdirectory of the general sideshell, several different configurations about cutout , stiffener and bracket. Fig 2.6 and Fig 2.7 show the cutouts, stiffener and brackets in this directory. In the subdirectory of the nonsideshell details, several design alternatives for the double-bottom connections were included here. Fig 2.8 is the configurations for these deatils.

6

262
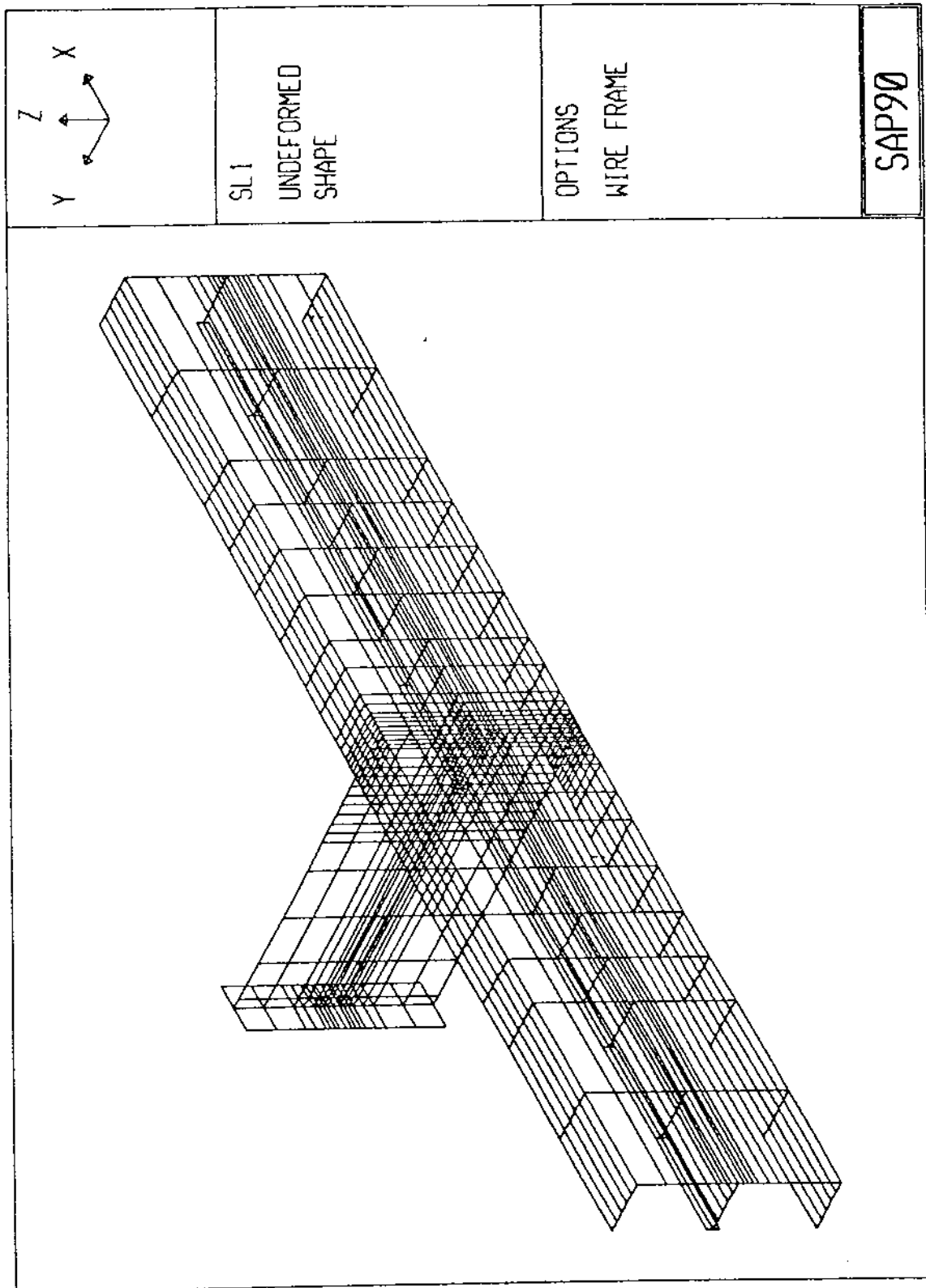
Fig 2.5 Typical FE Model for CSD

263
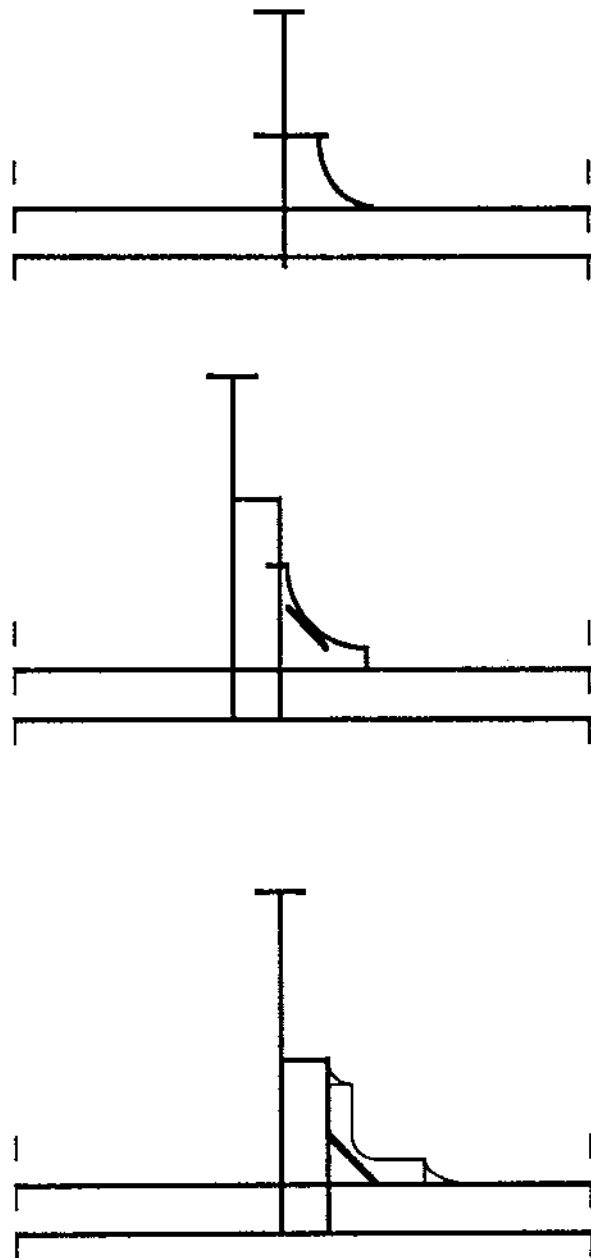
Fig 2.6 Design Alternatives for Stiffener, Bracket

264
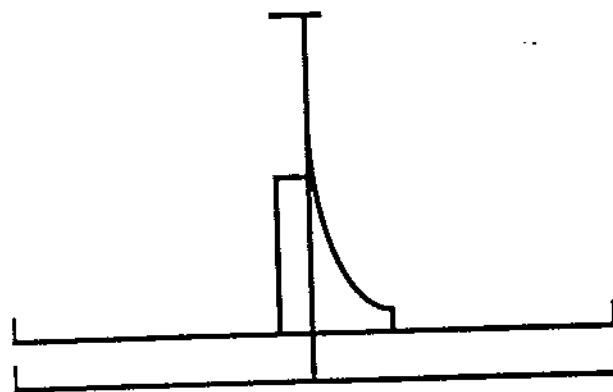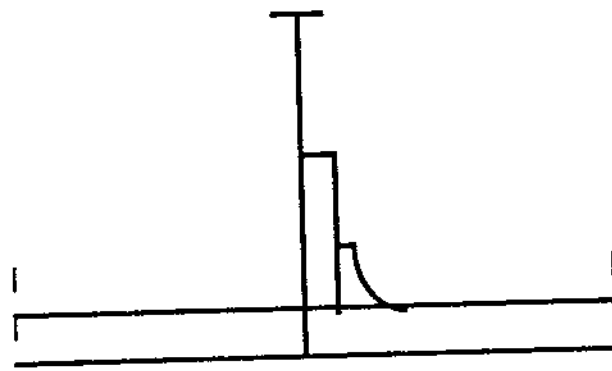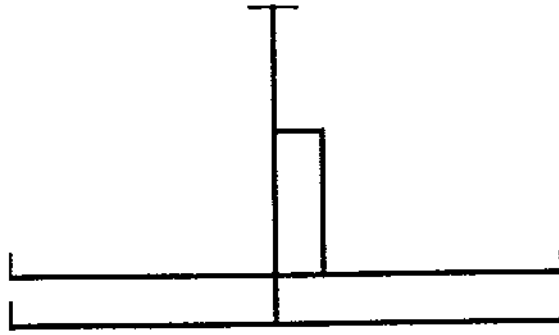
Fig 2.6 Design Alternatives for Stiffener and Bracket (Continued)

9
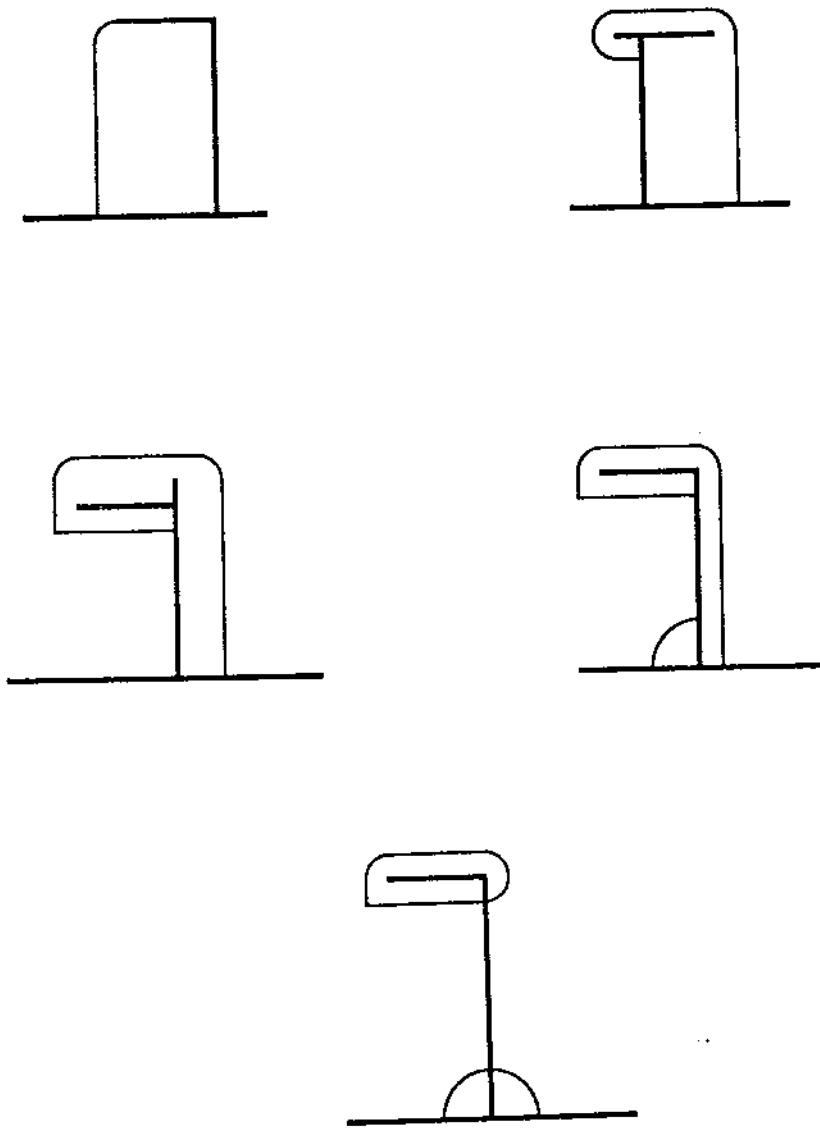
Fig 2.7 Design Alternatives for Cutouts

266
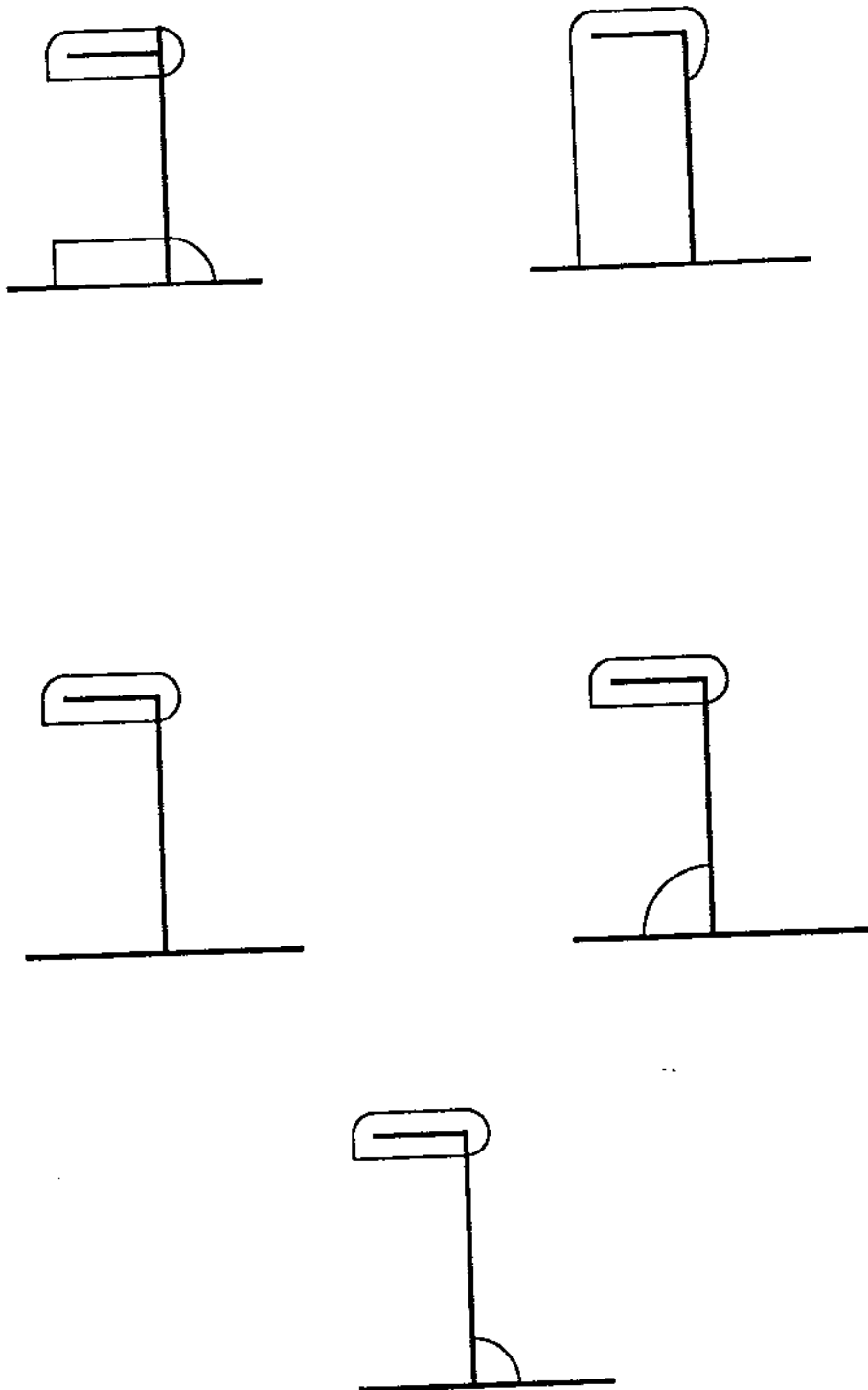
Fig 2.7 Design Alternatives for Cutout (Continued)
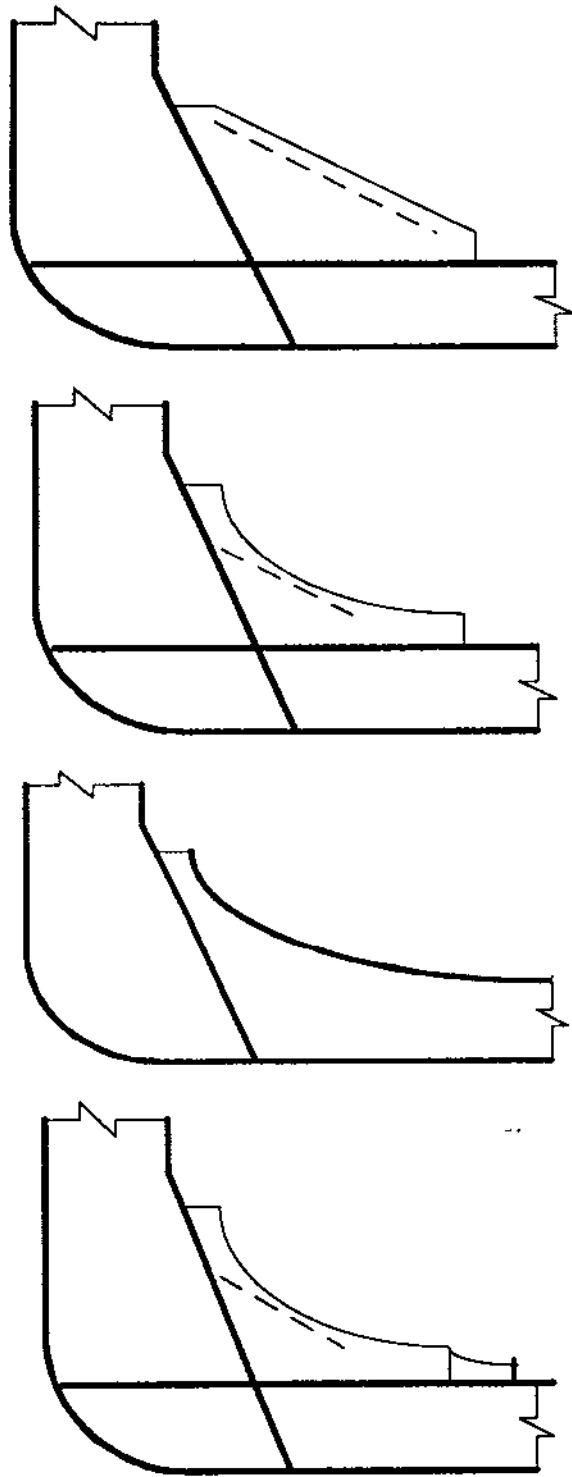
11

267

Fig 2.8 Design Alternatives for Double-Bottom Connections

268
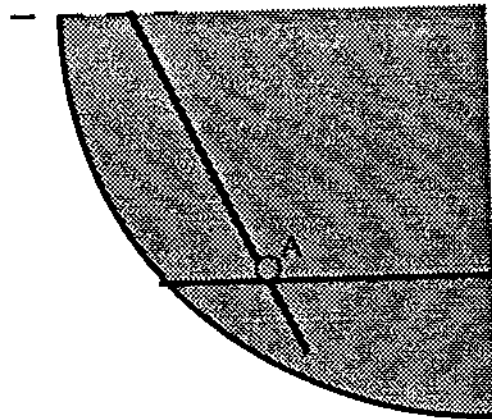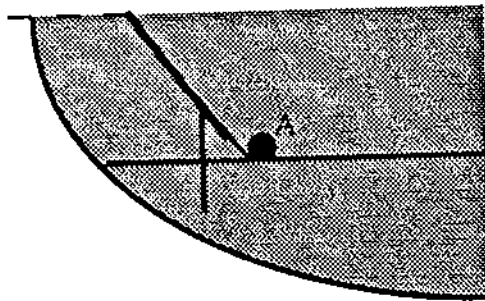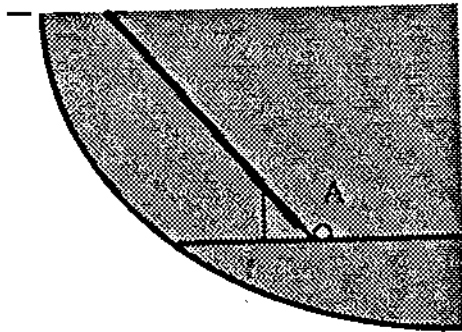
Fig 2.8 Design Alternatives for Double-Bottom Connections (Continued)

2.3 CSD S-N Curve Directory

The fatigue S-N curves for hotspot stress for CSD in tanker is developed based on the study of SMP project, the current project and **"Fatigue Classification of Critical Structural Details in Tankers"**. The detailed fatigue classification for general sideshell CSd and bottom connection is documented in Section 4

The fatigue S-N curve database or library was created by Microsoft Access in **"Fatigue Classification of Critical Structural Details in Tankers"** project. The detail was documented in Ref. 5.

270

Chapter 3

Finite Element Analysis Stress Plots

3.1 Introduction

During this project, a global-local finite element analysis was performed to detrmine the stress concentration factors and fatigue stress ranges by SAP90. The genearl results were documented in Ref.1 and 2. The stress plots were presented here.

The stress plots were presented here in three sections. Section 1 is the global analysis for the 190,000DWT double-bottom tanker. Section 2 is the local finite element analysis for general sideshell CSD. Section 3 is the local finite element analysis for nonsideshell CSD.

For graphical display of stress output, SAP90 has an option which allows the user to display stresses parallel to a global reference axis. This option has been utilized for all of the stress plots in this chapter.

Fot the output plots, the data has been arranged as follows:

For Section 1

1) Global Finite Element Model - 3D display
2) Global Finite Element Model - 2D display on Web Frame of the fore
3) Global Finite Element Model - 2D display on Web Frame of the aft
4) Global Finite Element Deformation
5) Global Finite Element Stress Plot - 3D display on Max Stress
6) Global Finite Element Stress Plot - 3D display on Shear Stress
7) Global Finite Element Stress Plot - 2D display on Max Stress of the fore Web Frame
8) Global Finite Element Stress Plot - 2D display on Shear Stress of the fore Web Frame
9) Global Finite Element Stress Plot - 2D display on Max Stress of the aft Web Frame

271

10) Global Finite Element Stress Plot - 2D display on Shear Stress of the aft Web Frame

For Section 2

1) Finite Element Model - 3D display
2) Finite Element Model - 2D dispaly on Transverse
3) Finite element Model - 2D display on Longitudinal
4) Finite Element Deformed Shape - 3D display
5) Finite Element Stress Plot - 3D display Max Stress
6) Finite Element Stress Plot - 3D display Shear Stress
7) Finite Element Stress Plot - 2D display Max Stress on Transverse
8) Finite Element Stress Plot - 2D display Shear Stress on Transverse
9) Finite Element Stress Plot - 2D display Max Stress on Longitudinal
10) Finite Element Stress Plot - 2D display Shear Stress on Longitudinal

For Section 3

1) Finite Element Model - 2D display
2) Finite Element Deformed Shape - 2D display
3) Finite Element Stress Plot - 2D display Max Stress
4) Finite Element Stress Plot - 2D display Shear Stress

3.2 Stress Plots

The global-local finite element analysis was conducted in this project. Detail about loading, boundary conditions and so on are presented in Ref. 2. The stress plots are presented later.

272

Section 1 Global Finite Element Analysis

273

arco1
UNDEFORMED
SHAPE

OPTIONS
WIRE FRAME

Z
Y X
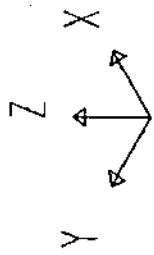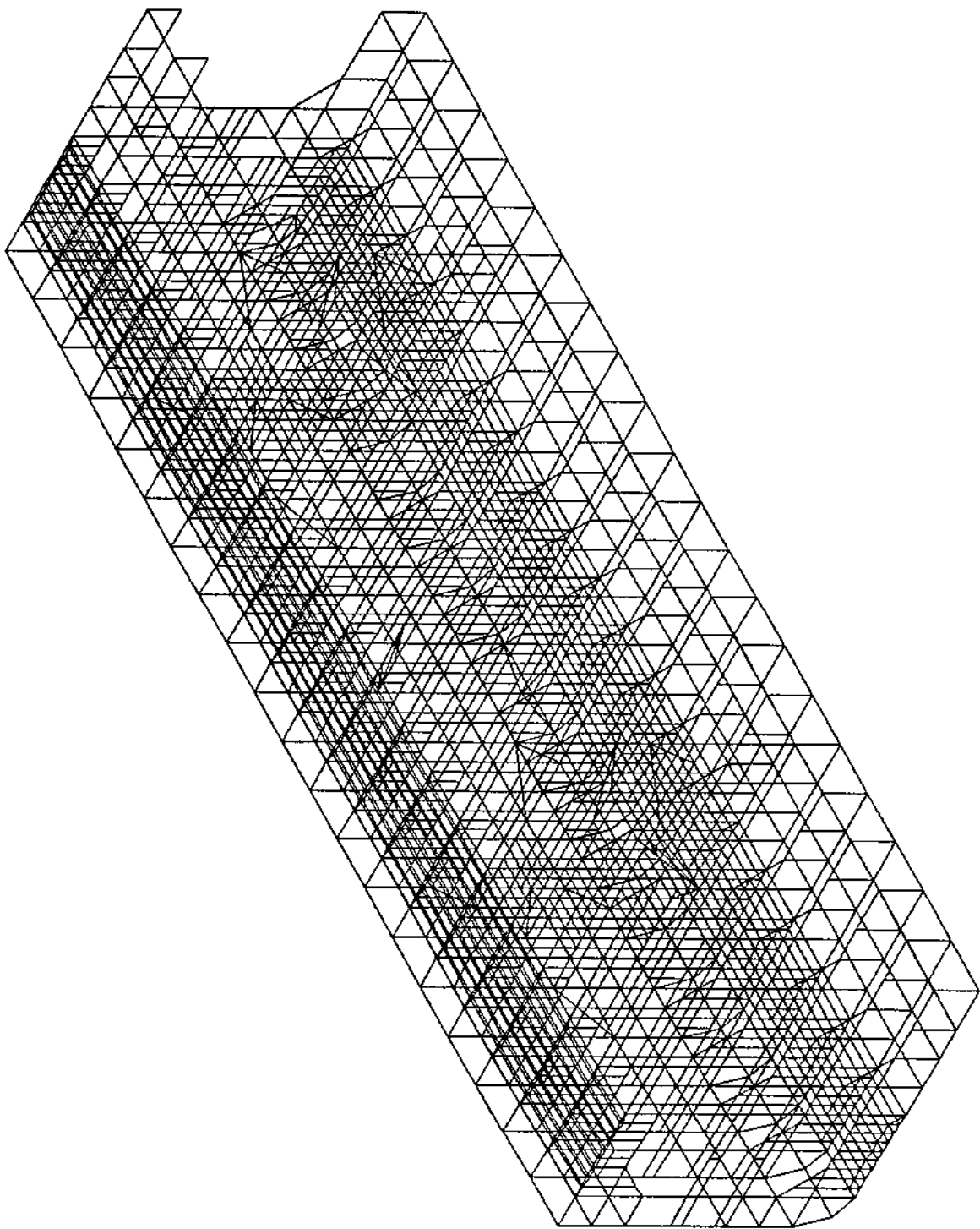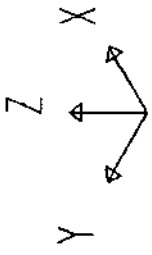
SAP90

arco1
DEFORMED
SHAPE
LOAD   1

MINIMA
X-0.4556E+01
Y-0.4204E+00
Z-0.1667E+01
MAXIMA
X 0.7167E+00
Y 0.3356E+00
Z 0.1668E+01

SAP90

Y

Z

X
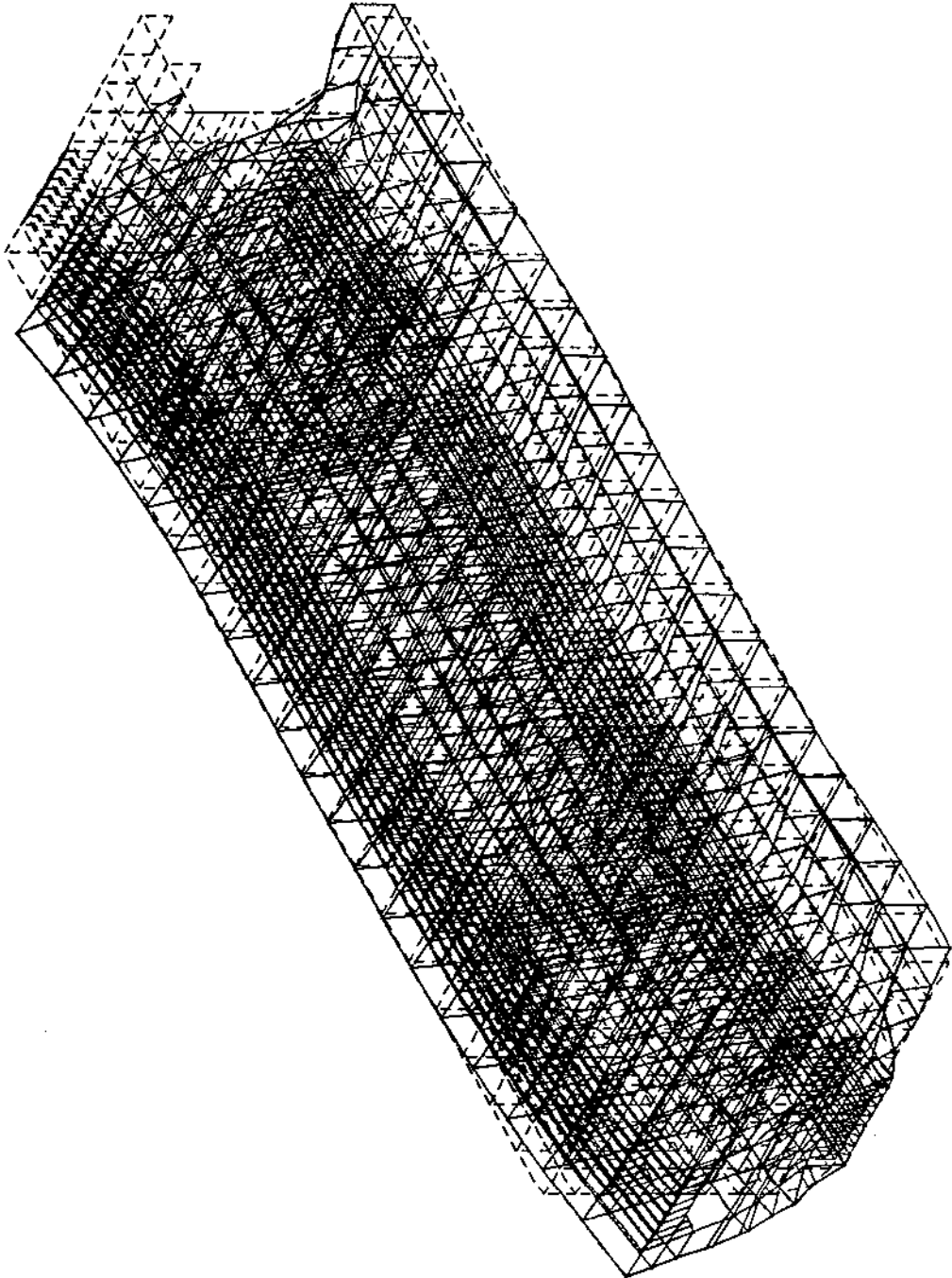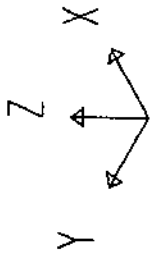
arco1
SHELL
OUTPUT   S12T
LOAD   1

$\times\ 10^{-1}$

104
52
0
-52
-104
-156
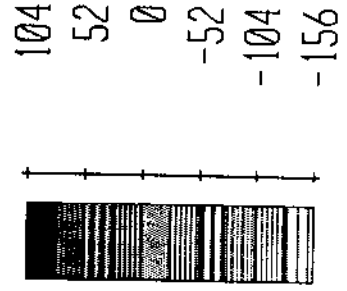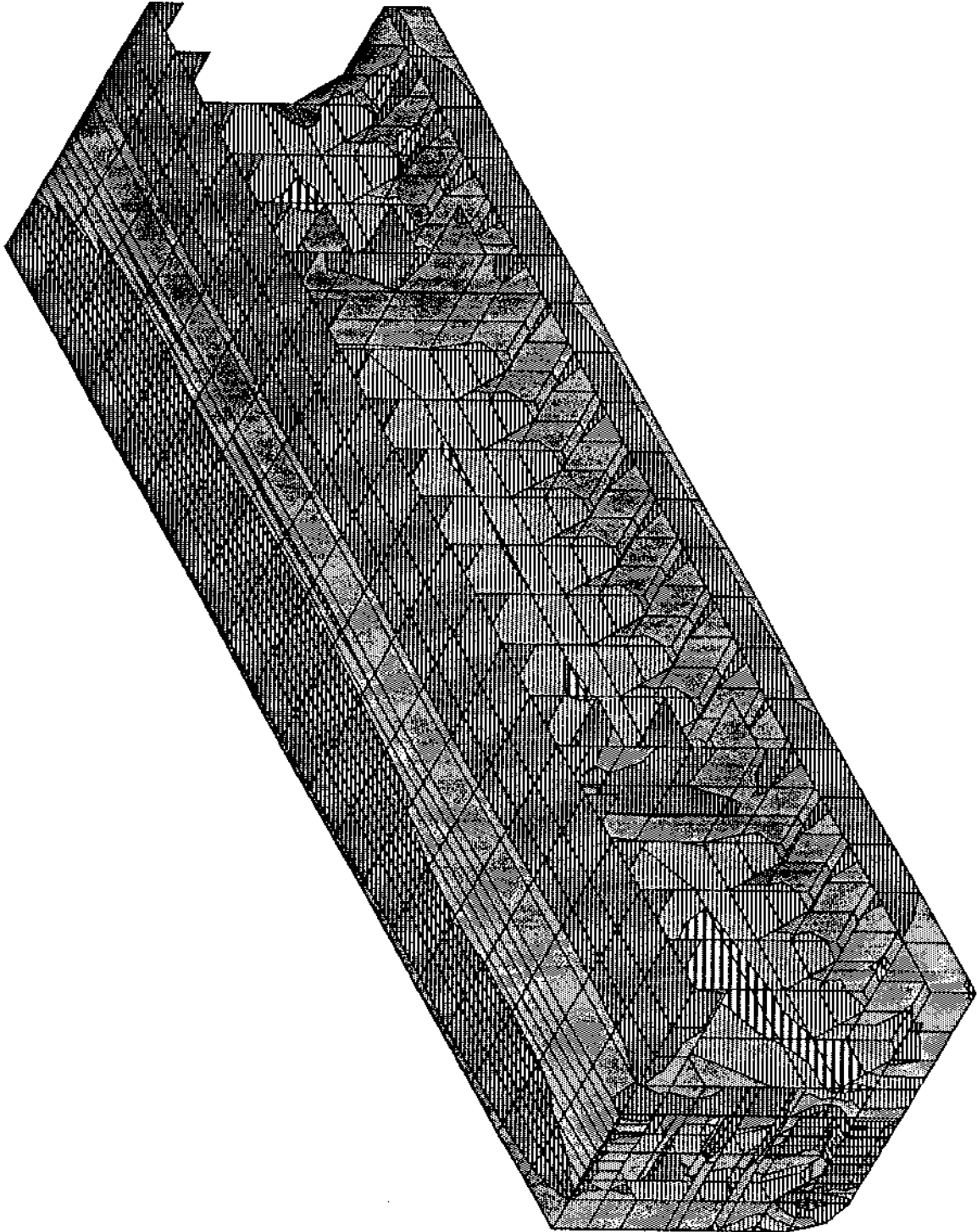
SAP90

MIN IS -0.149E+02 <JOINT 4035>   MAX IS   0.897E+01 <JOINT   2491>

Z

X

Y

arco1
SHELL
OUTPUT SMXT
LOAD   t

X 10⁻¹

640
480
320
160
0
-160
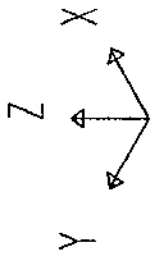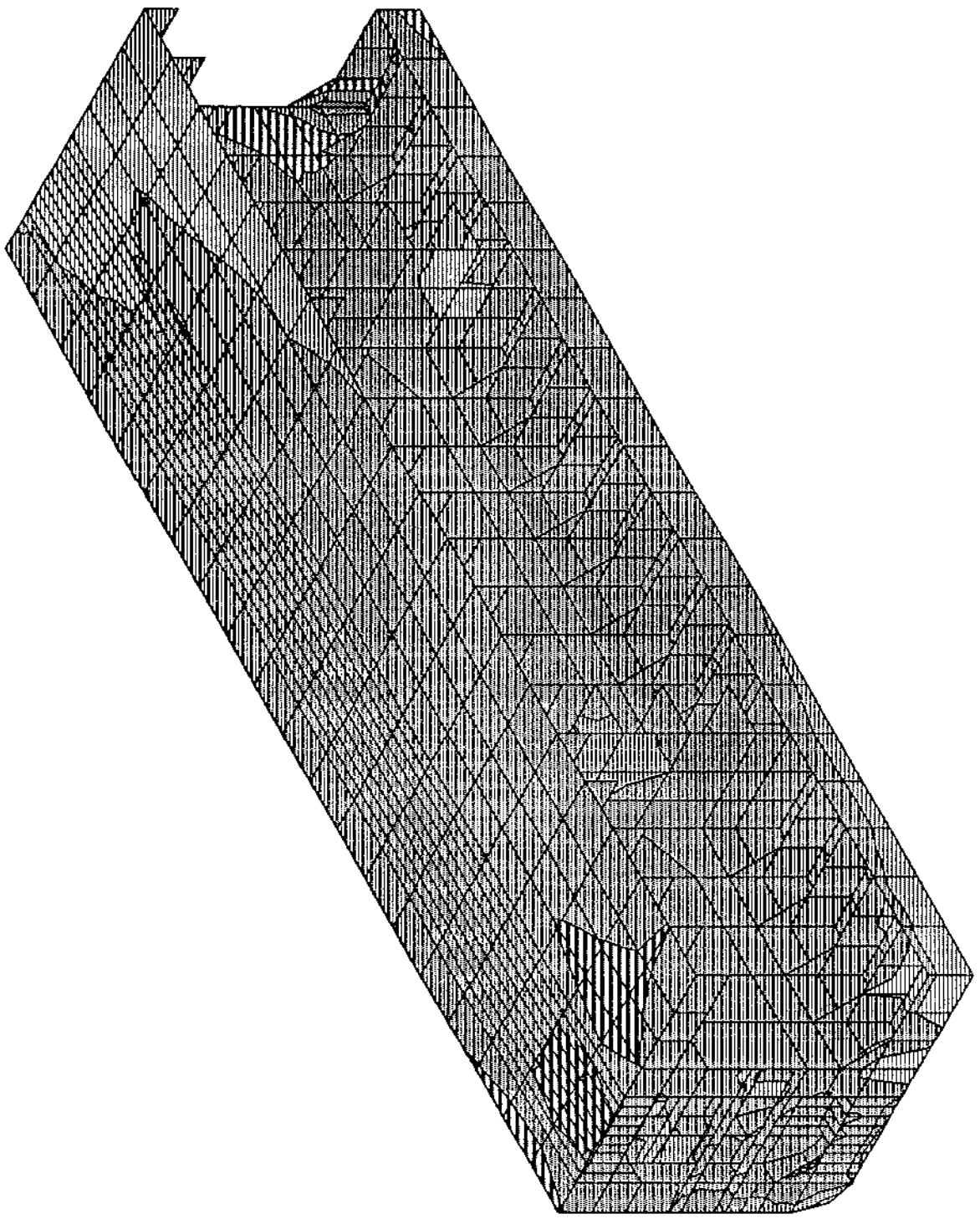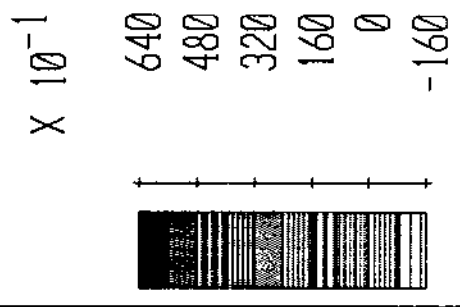
SAP90

MIN IS -0.149E+02 <JOINT   35>   MAX IS   0.546E+02 <JOINT   4035>

264

Z

Y

arco1
UNDEFORMED
SHAPE

OPTIONS
WIRE FRAME

SAP90

Z

Y
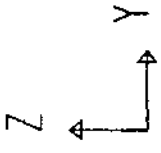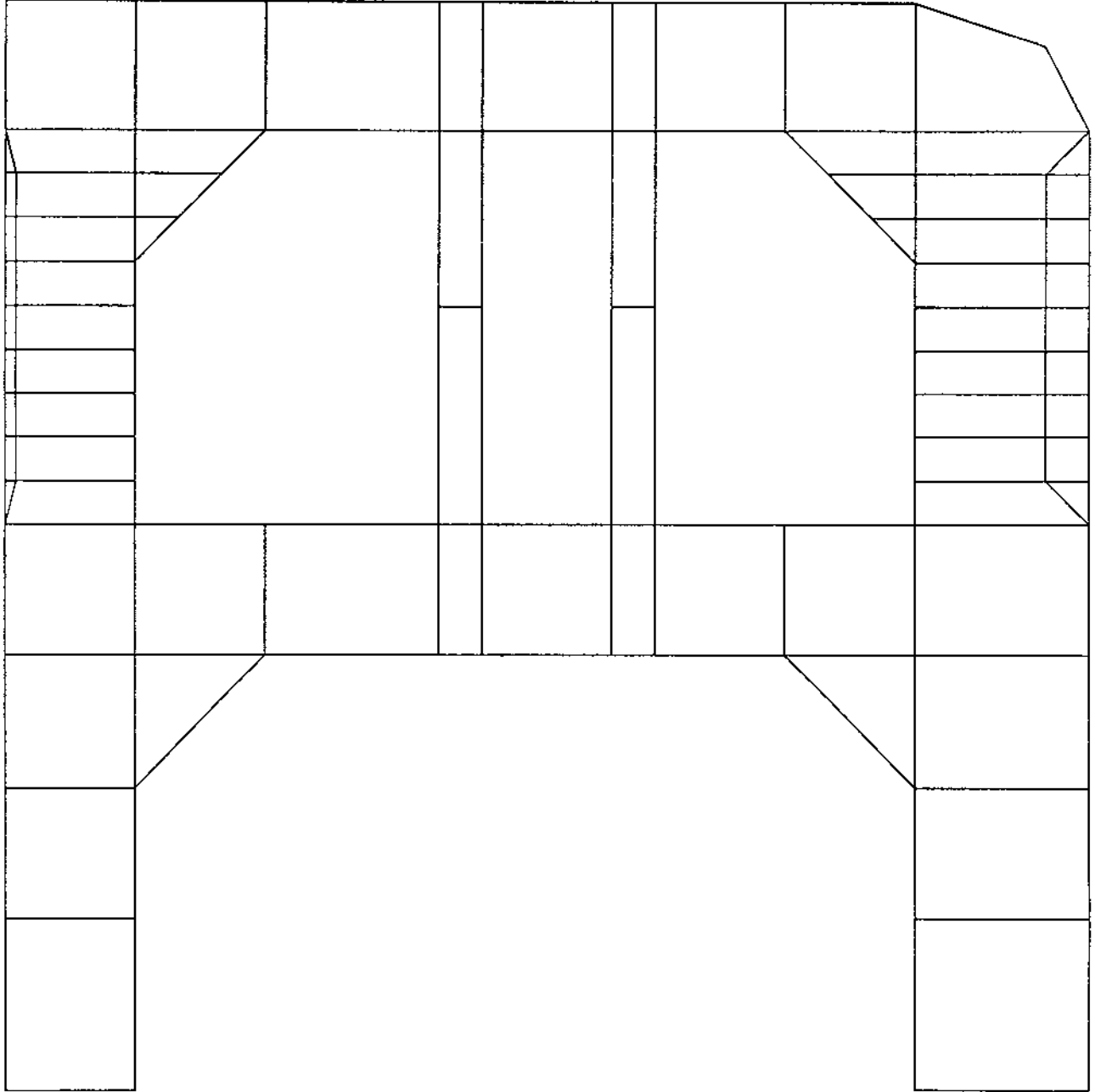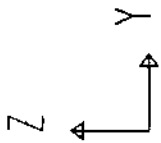
arcol
SHELL
OUTPUT S12T
LOAD   1

X 10⁻¹
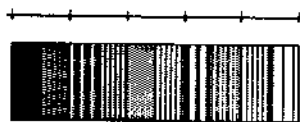
280
210
140
70
0
-70
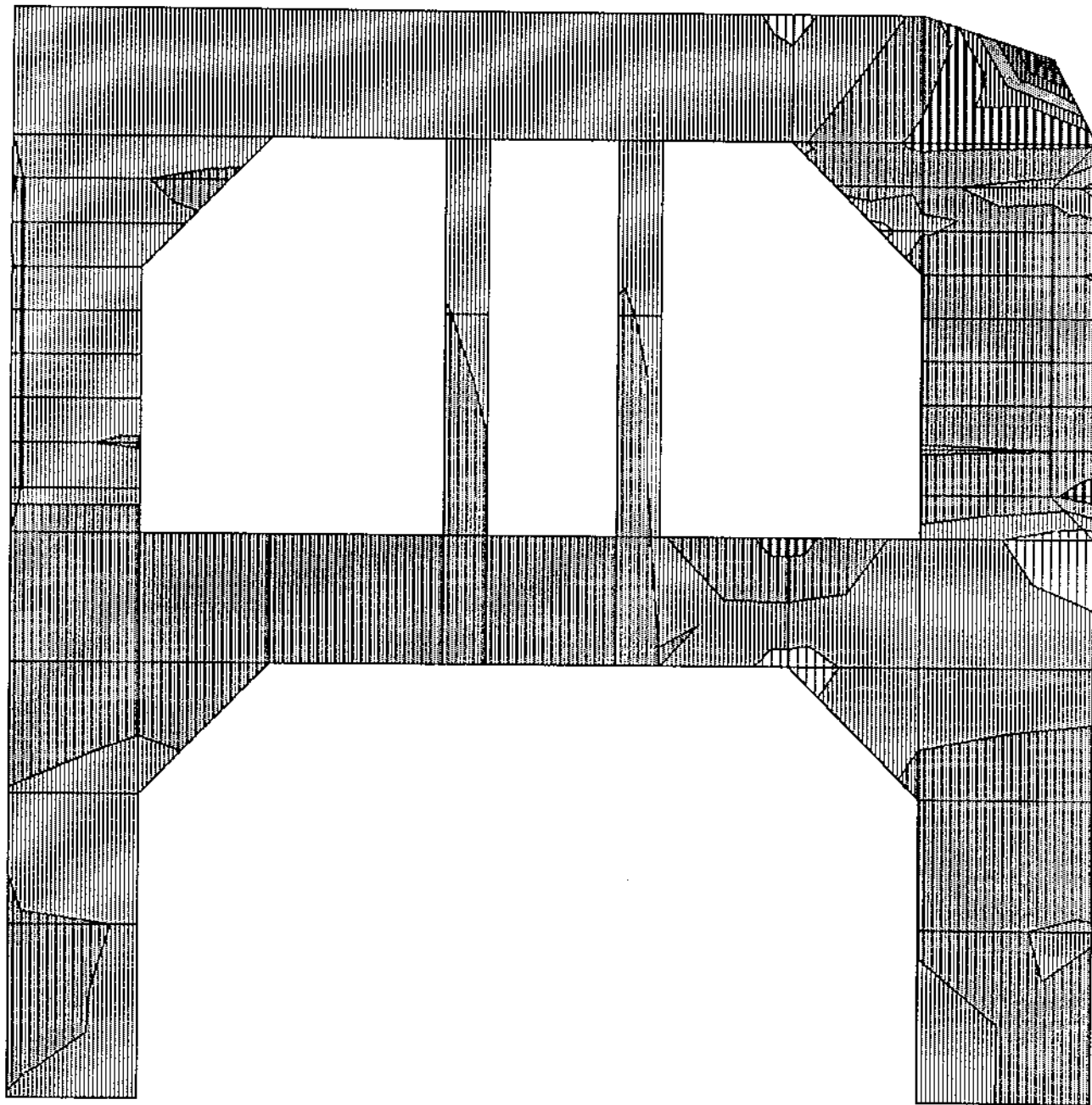
MIN IS -0.566E+01 <JOINT   29>   MAX IS   0.247E+02 <JOINT   35>

SAP90

279

Z
Y

arco1
SHELL
OUTPUT SMXT
LOAD 1

$X \ 10^{-1}$

240
120
0
-120
-240
-360
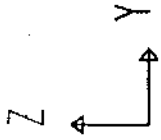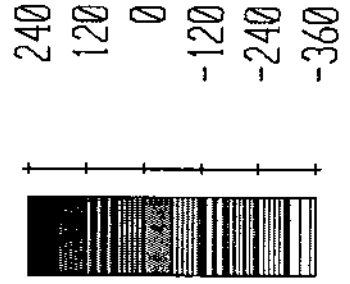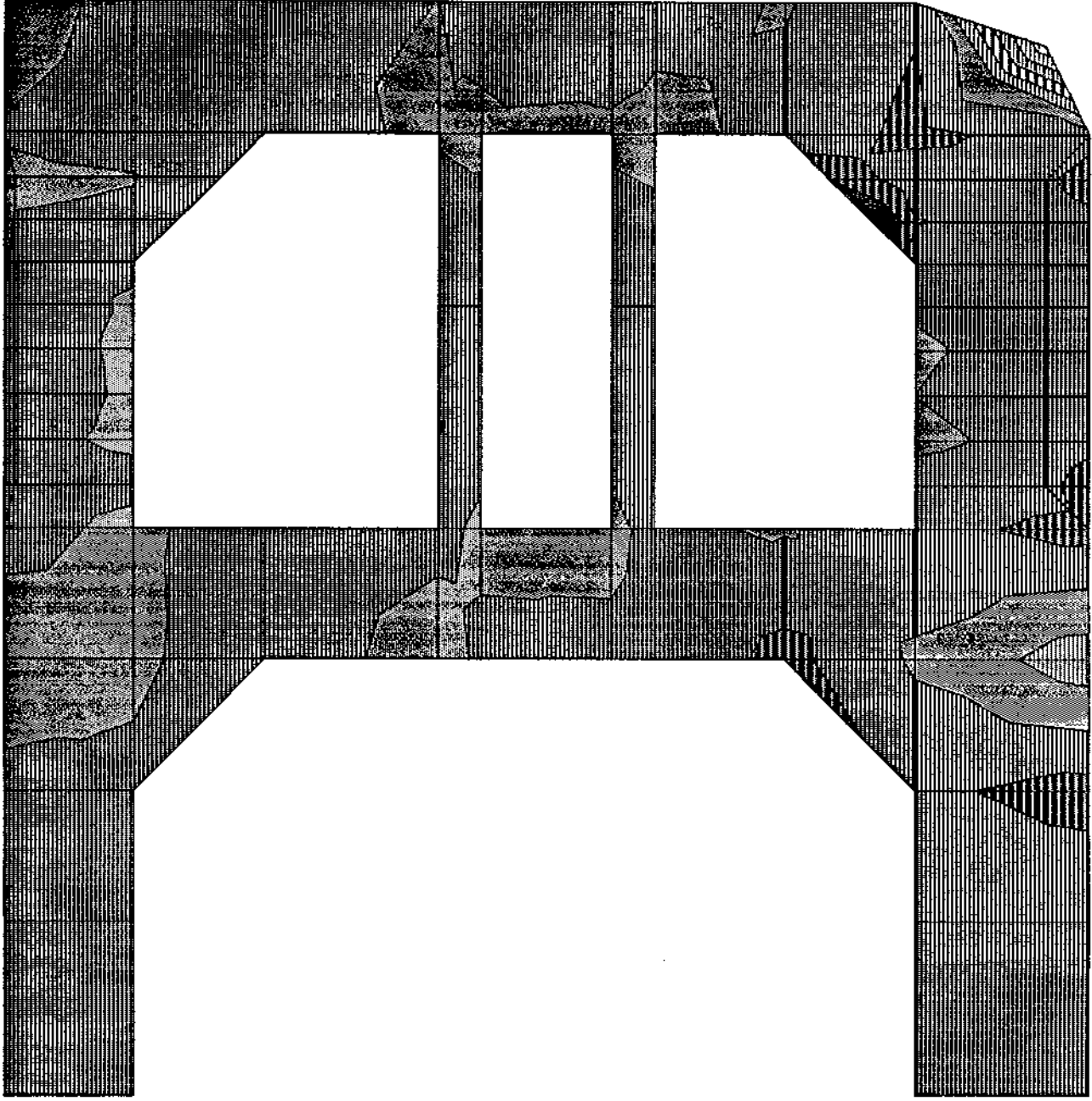
SAP90

MIN IS -0.349E+02 <JOINT 35>   MAX IS 0.235E+02 <JOINT 91>
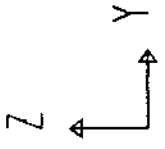
280

Section 2 General Sideshell CSD Analysis

Z

Y

arco1
UNDEFORMED
SHAPE

OPTIONS
WIRE FRAME

SAP90

282

Z

Y

arco1
SHELL
OUTPUT S12T
LOAD   1

X 10⁻¹

105
35
-35
-105
-175
-245
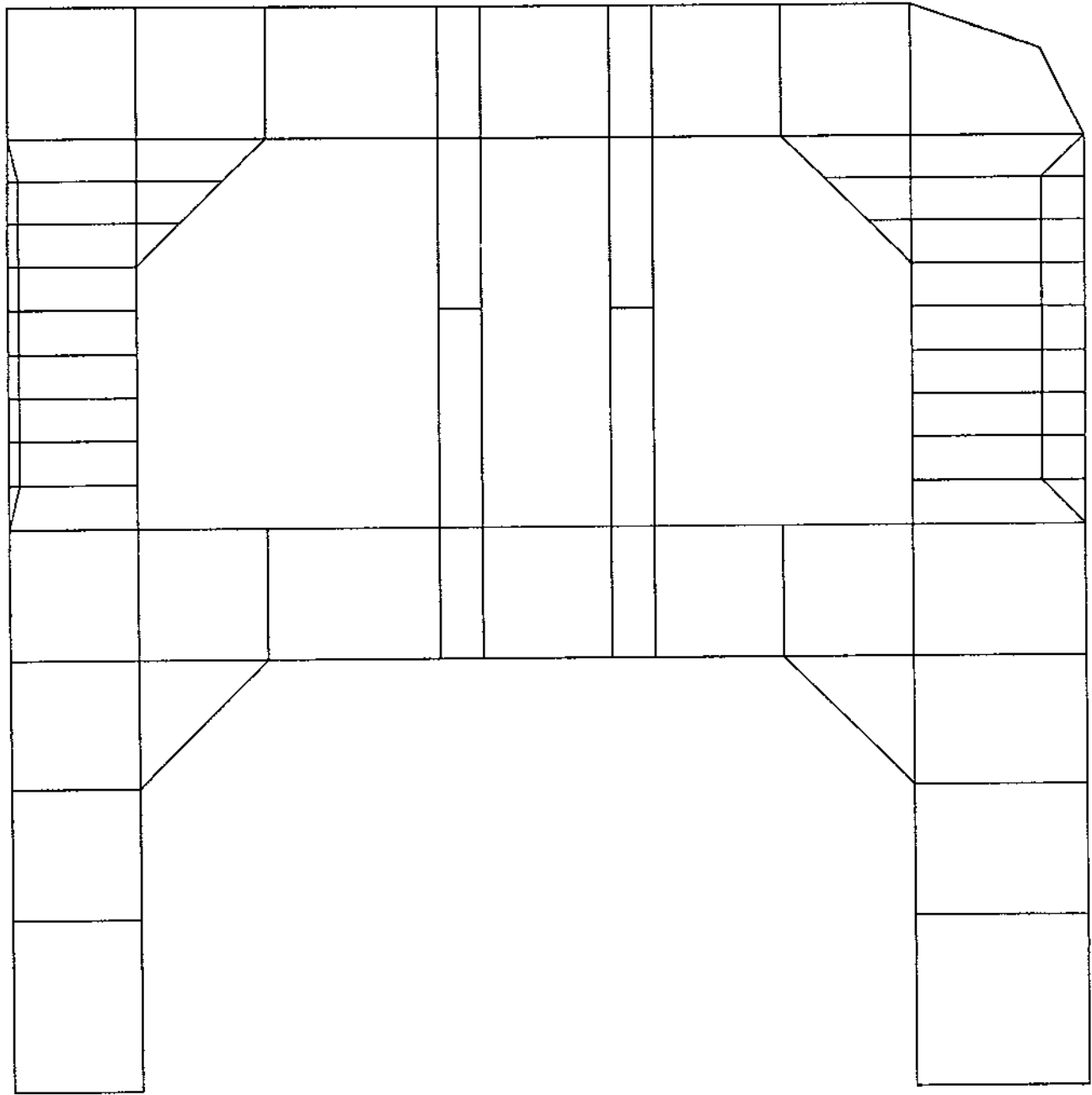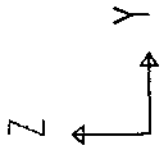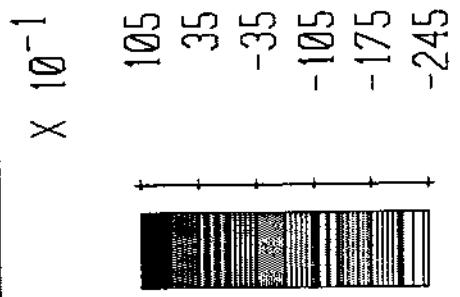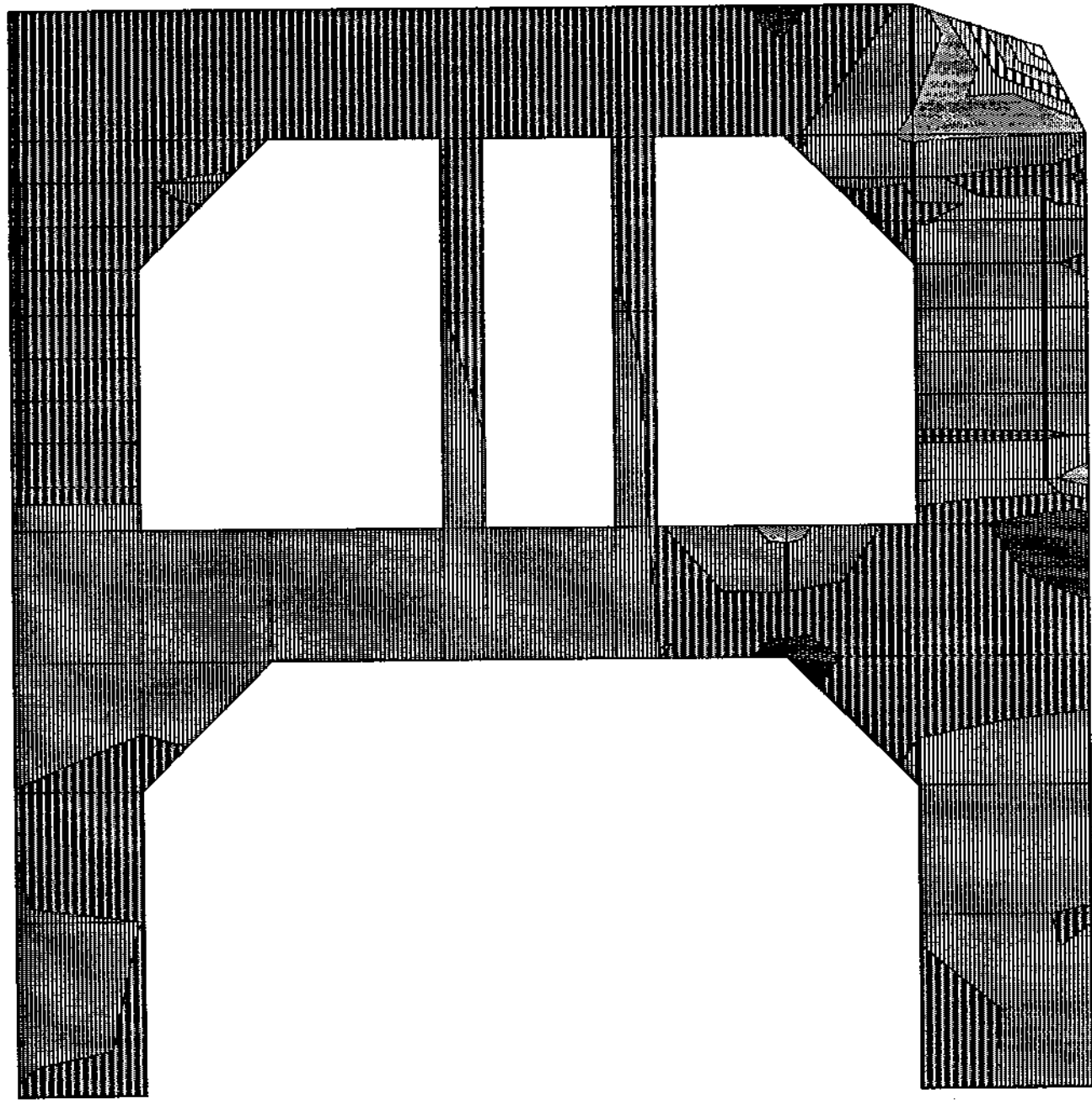
SAP90

MIN IS -0.245E+02 <JOINT 4035>   MAX IS   0.590E+01 <JOINT 4029>

283

Section 2 General Sideshell CSD Analysis

10"

30"

105" x 0.46"

6"

20"

2.5"

404" x 0.46"

105" x 0.46"

2.5"

12.5"

25"

12.5"

5.0"

70" x 0.46"

286

detail1
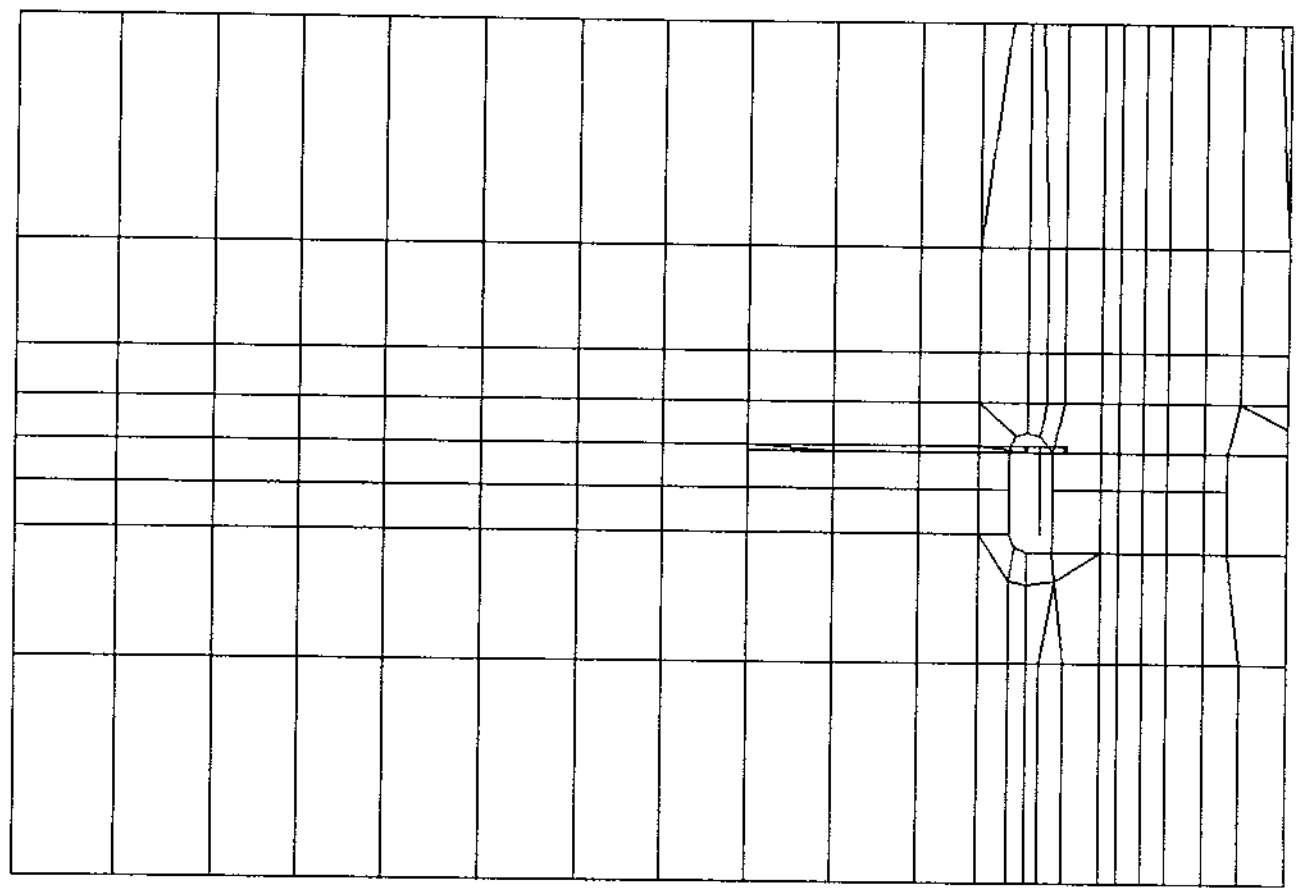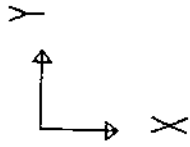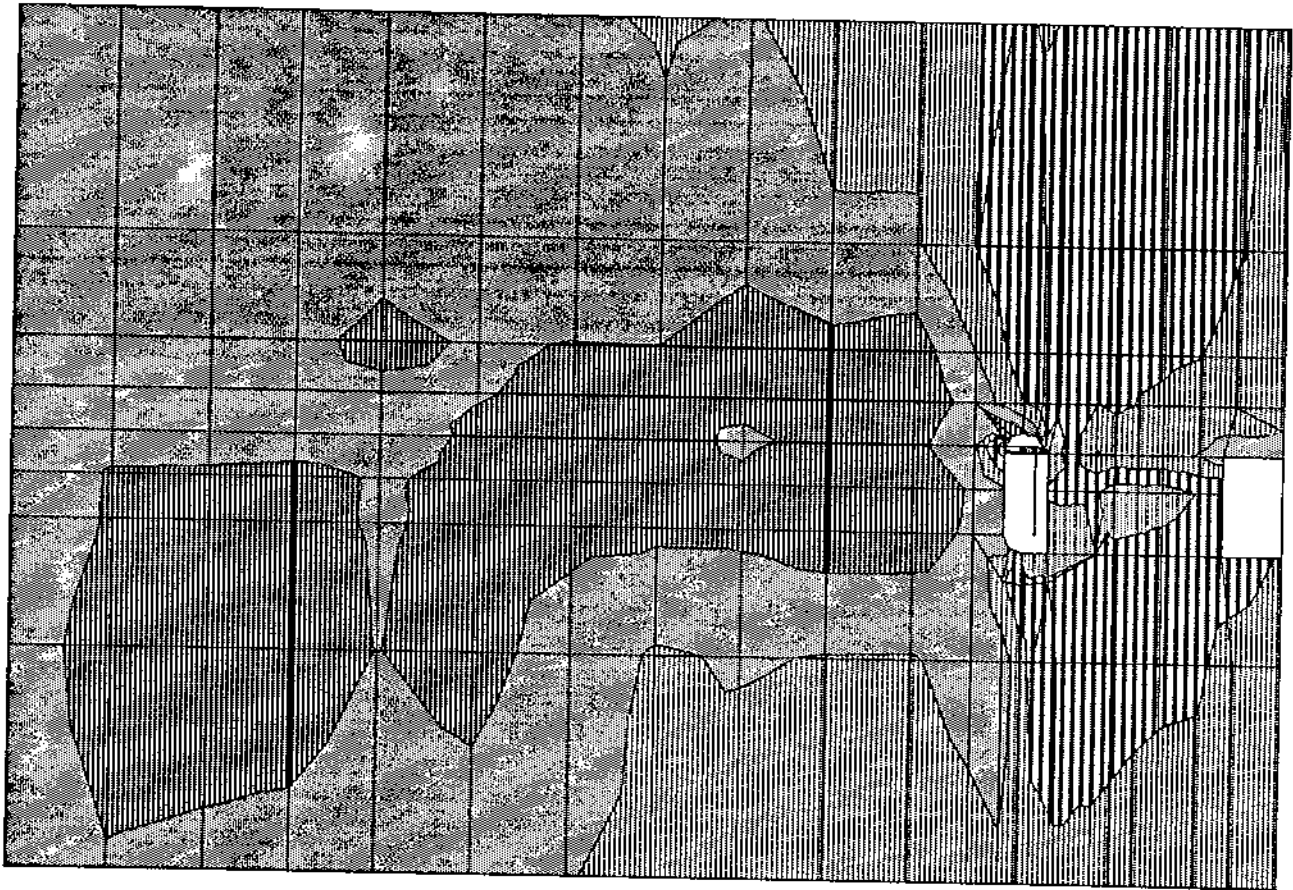
UNDEFORMED
SHAPE

OPTIONS

WIRE FRAME

SAP90

detail1

DEFORMED
SHAPE

LOAD   1

MINIMA
X-0.4483E-01
Y-0.2375E+01
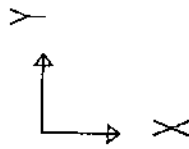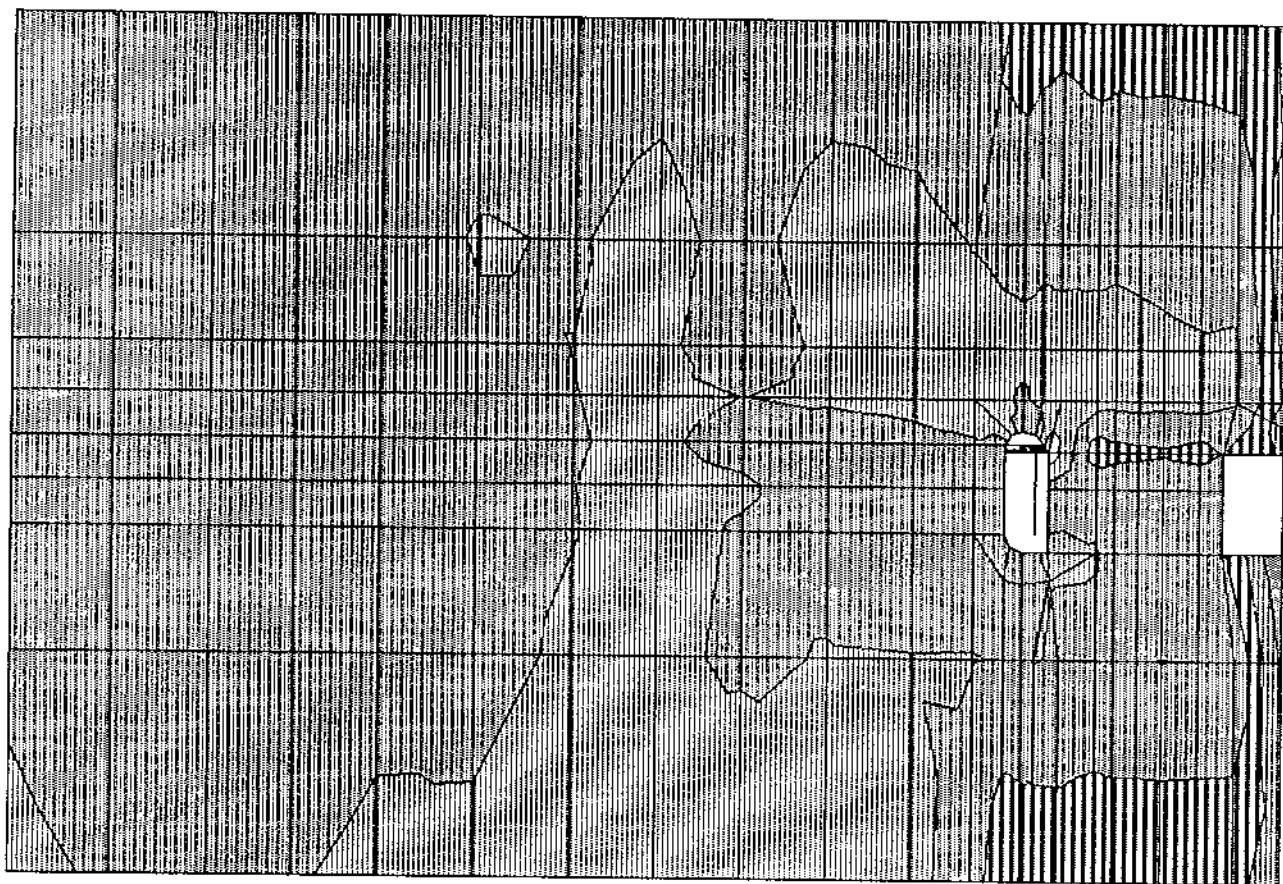Z-0.1548E+00
MAXIMA
X 0.6452E-01
Y-0.2329E+01
Z-0.3119E-01

SAP90

detail1

SHELL
OUTPUT   S11T
LOAD   1

21000
14000
7000
0
-7000
-14000

SAP90

MIN IS   -0.136E+05 <JOINT   1172>   MAX IS   0.176E+05 <JOINT   2441>

detail1

SHELL

OUTPUT   S22T

LOAD   1

21000
14000
7000
0
-7000
-14000

MIN IS -0.139E+05 <JOINT 1172>   MAX IS   0.164E+05 <JOINT 2412>

SAP90

arco1
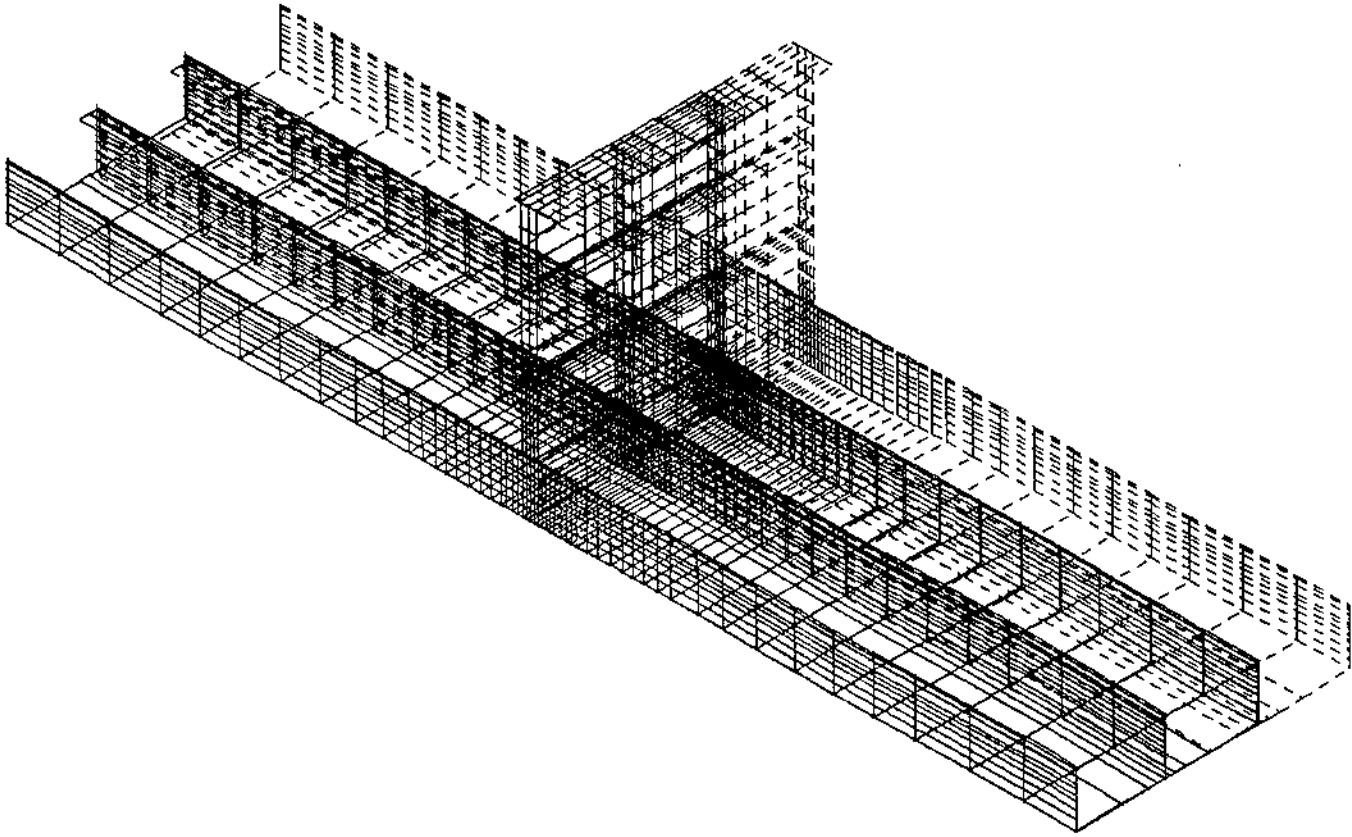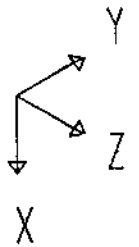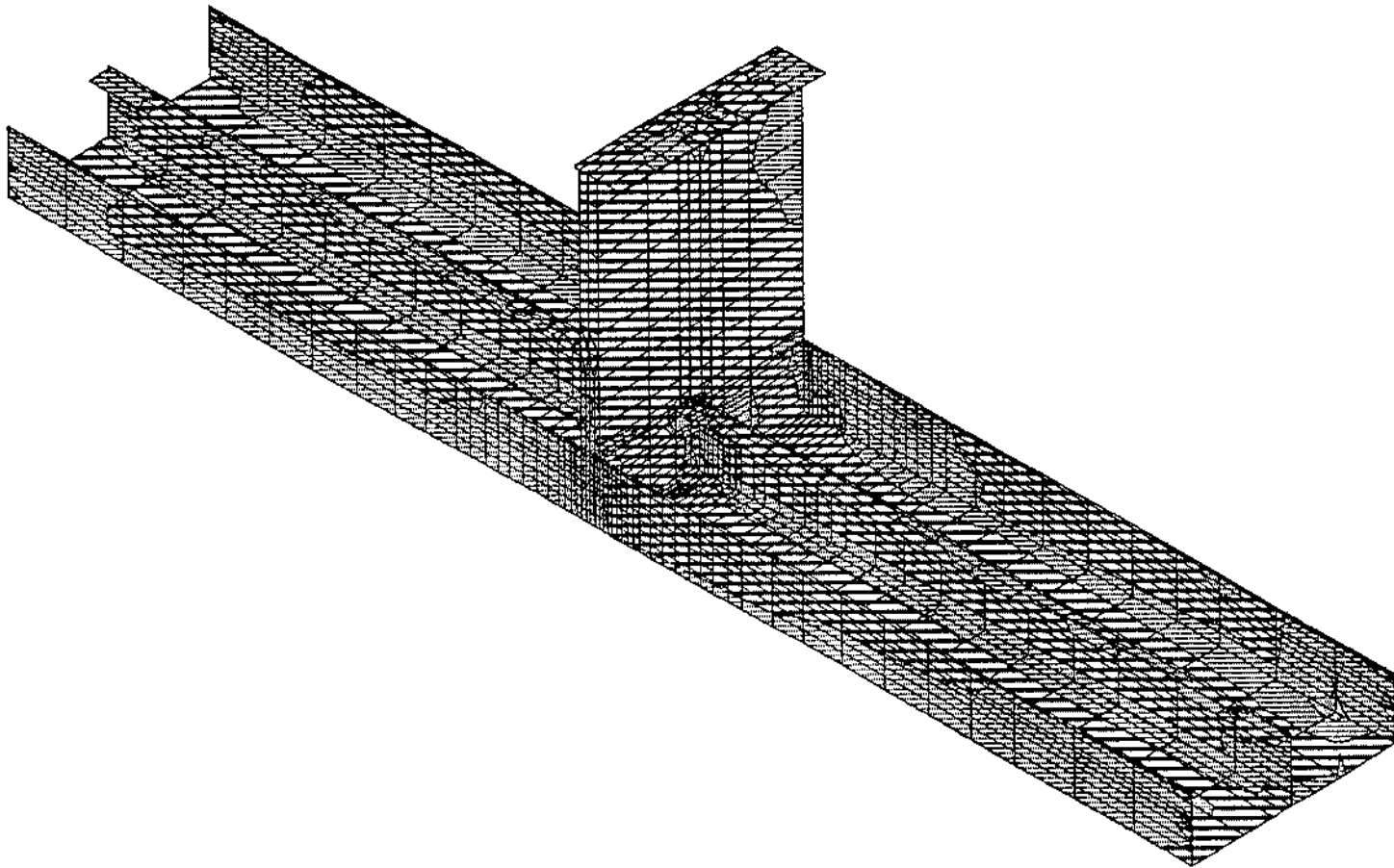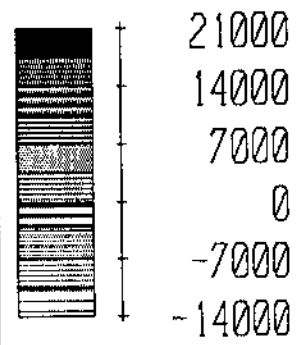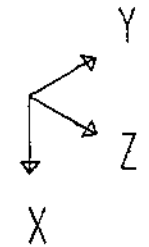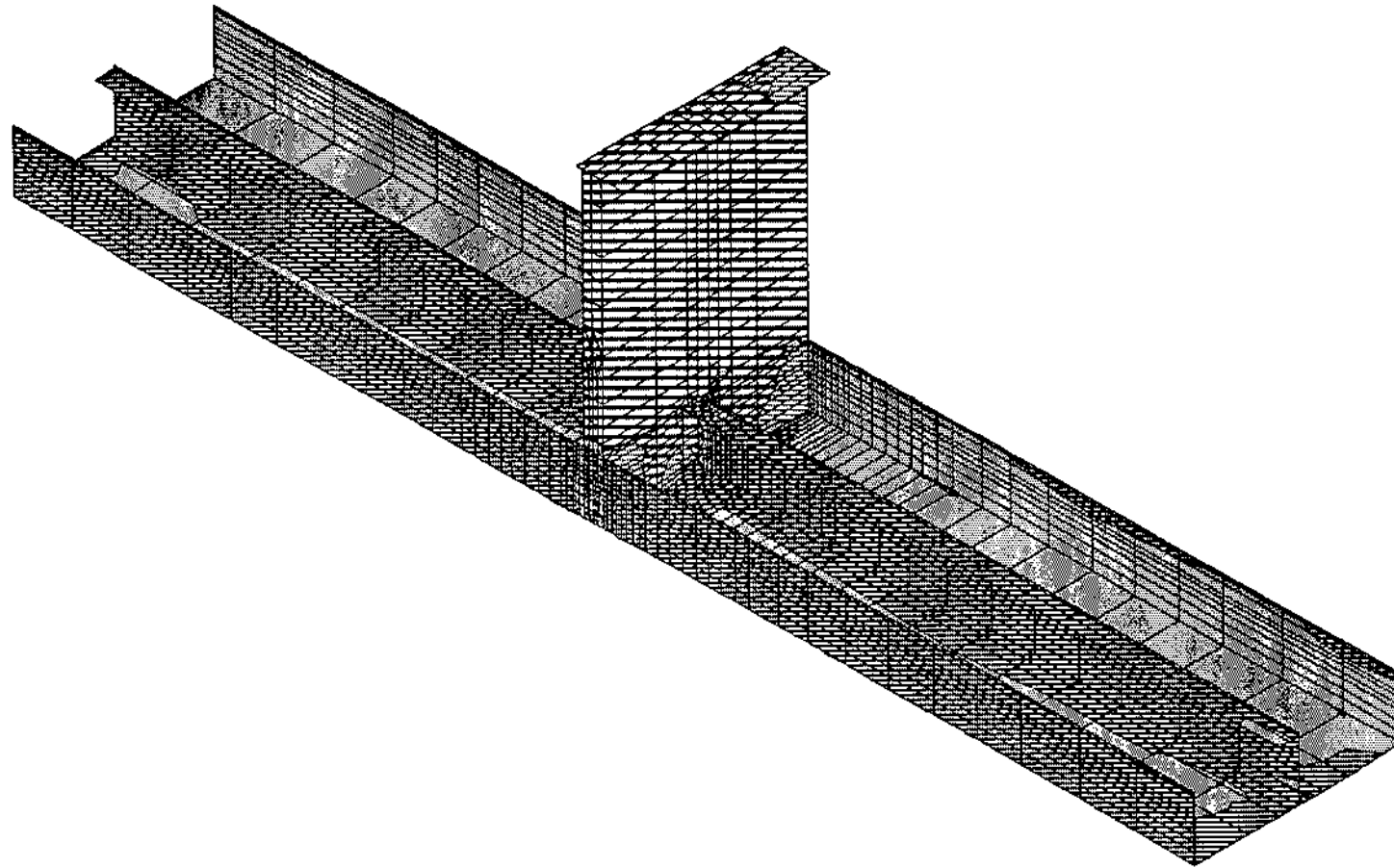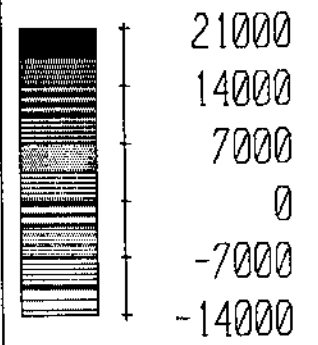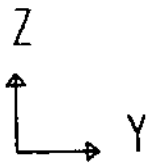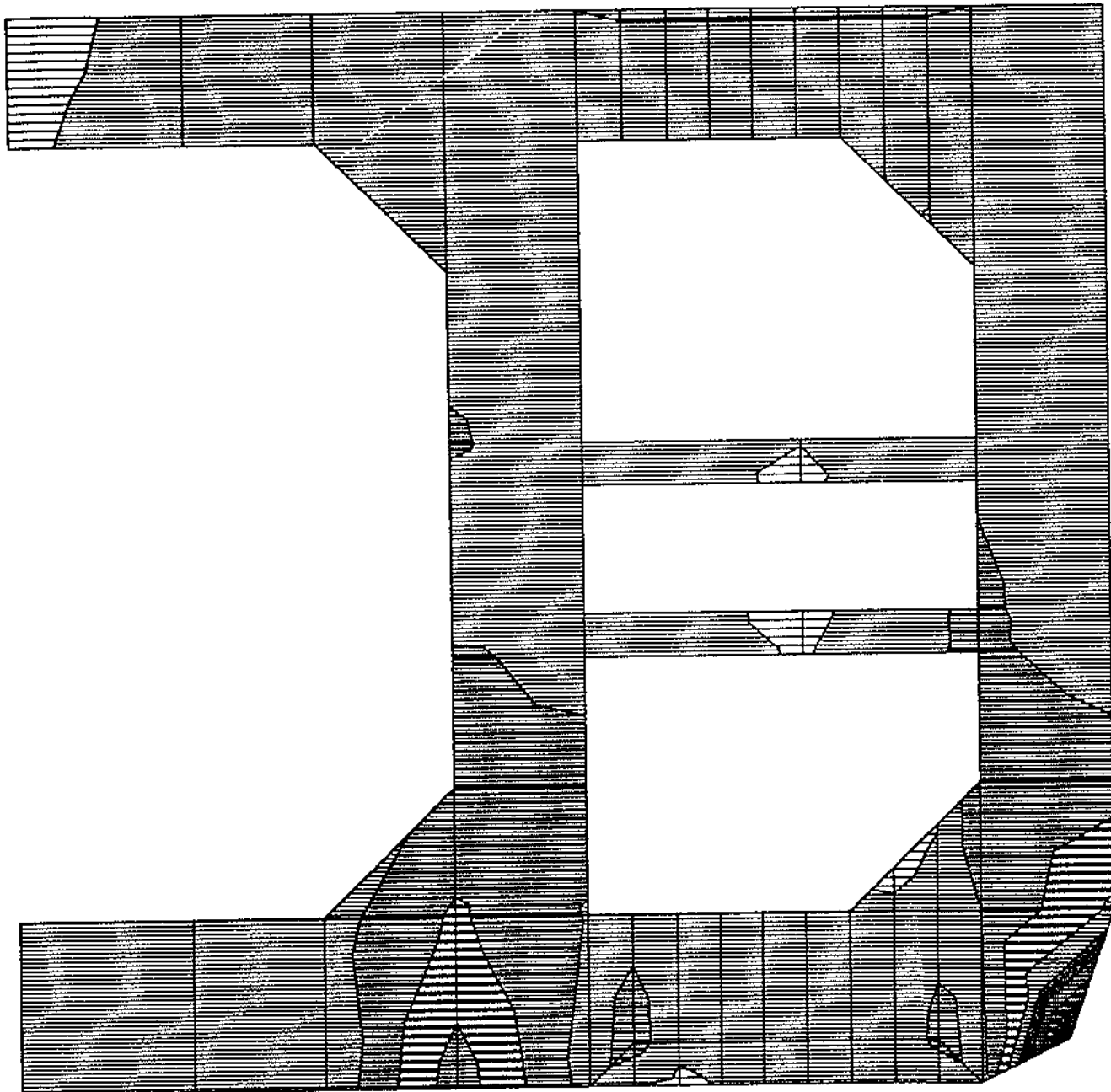
SHELL

OUTPUT   SMXT

LOAD   1

99
77
55
33
11
-11
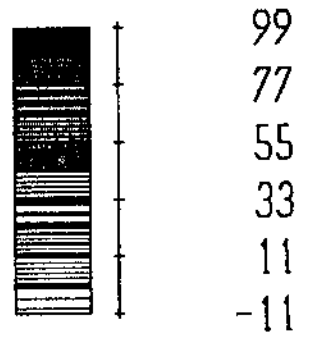
MIN IS -0.818E+01 <JOINT 4091>   MAX IS   0.957E+02 <JOINT   4035>

SAP90
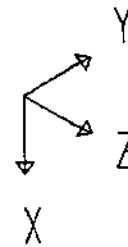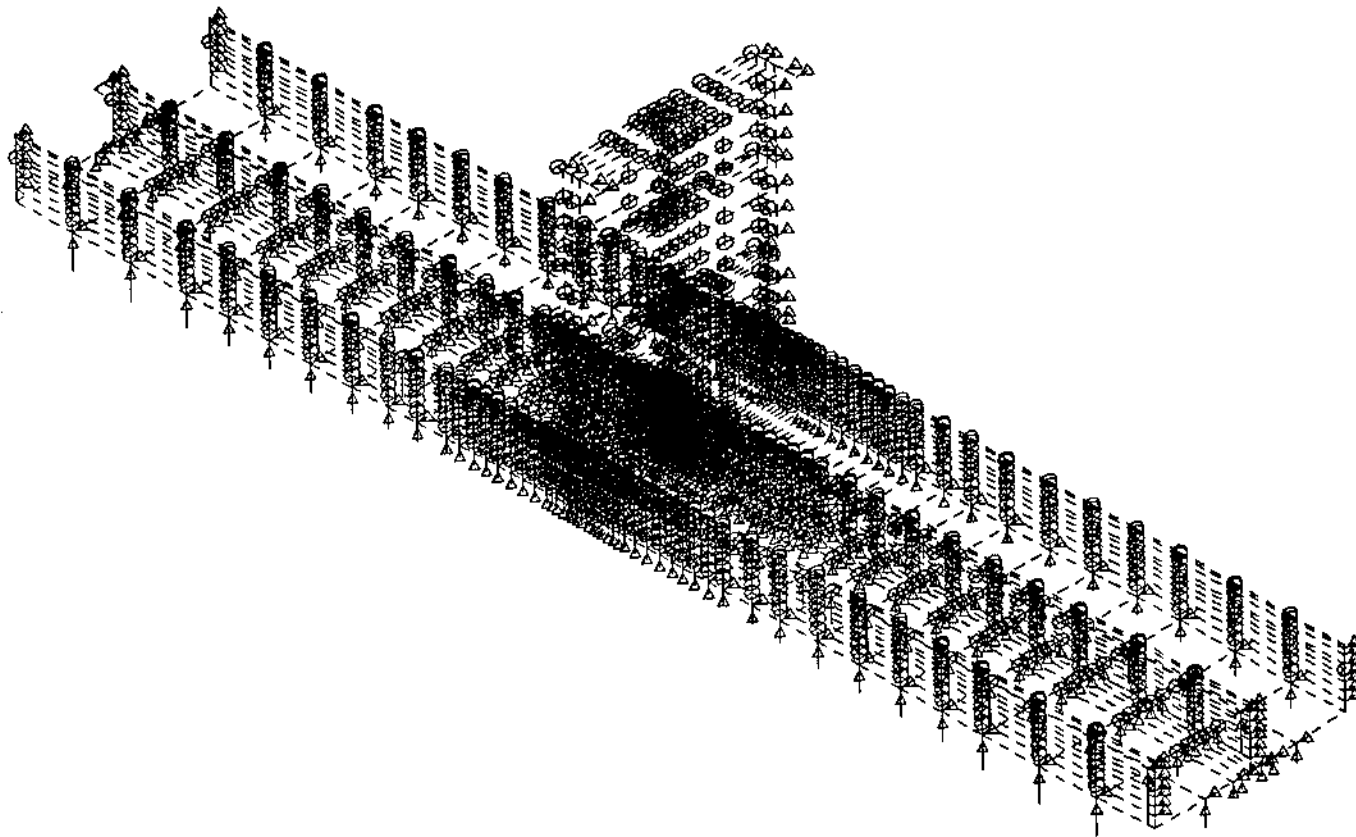
detail1

JOINT
LOADS

LOAD   1
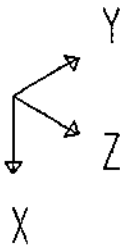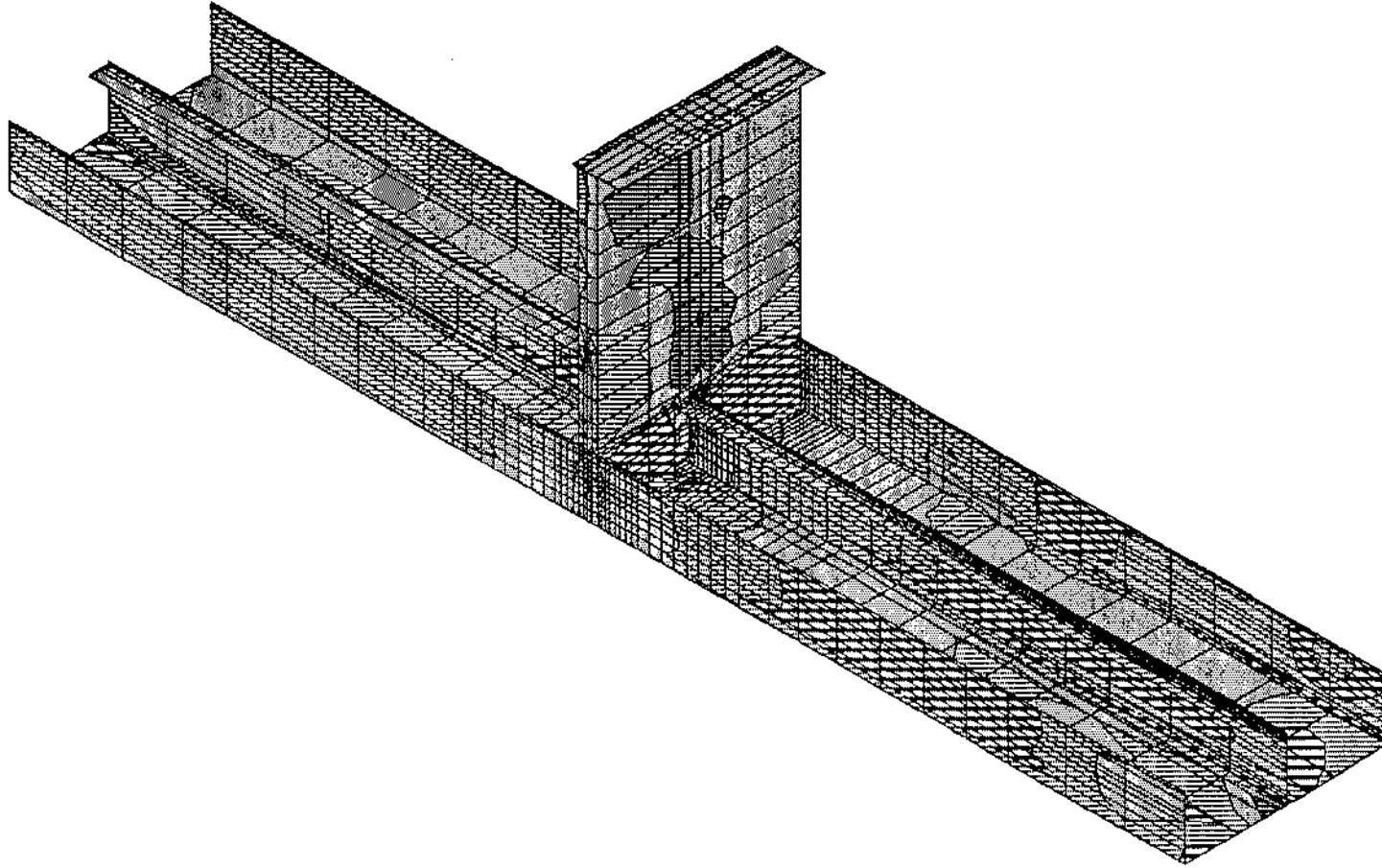
MINIMA
P-0.1563E+04
MAXIMA
P-0.2288E-01

SAP90

detail1
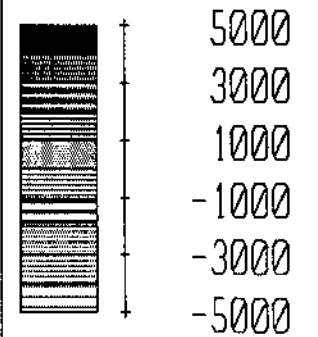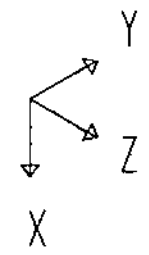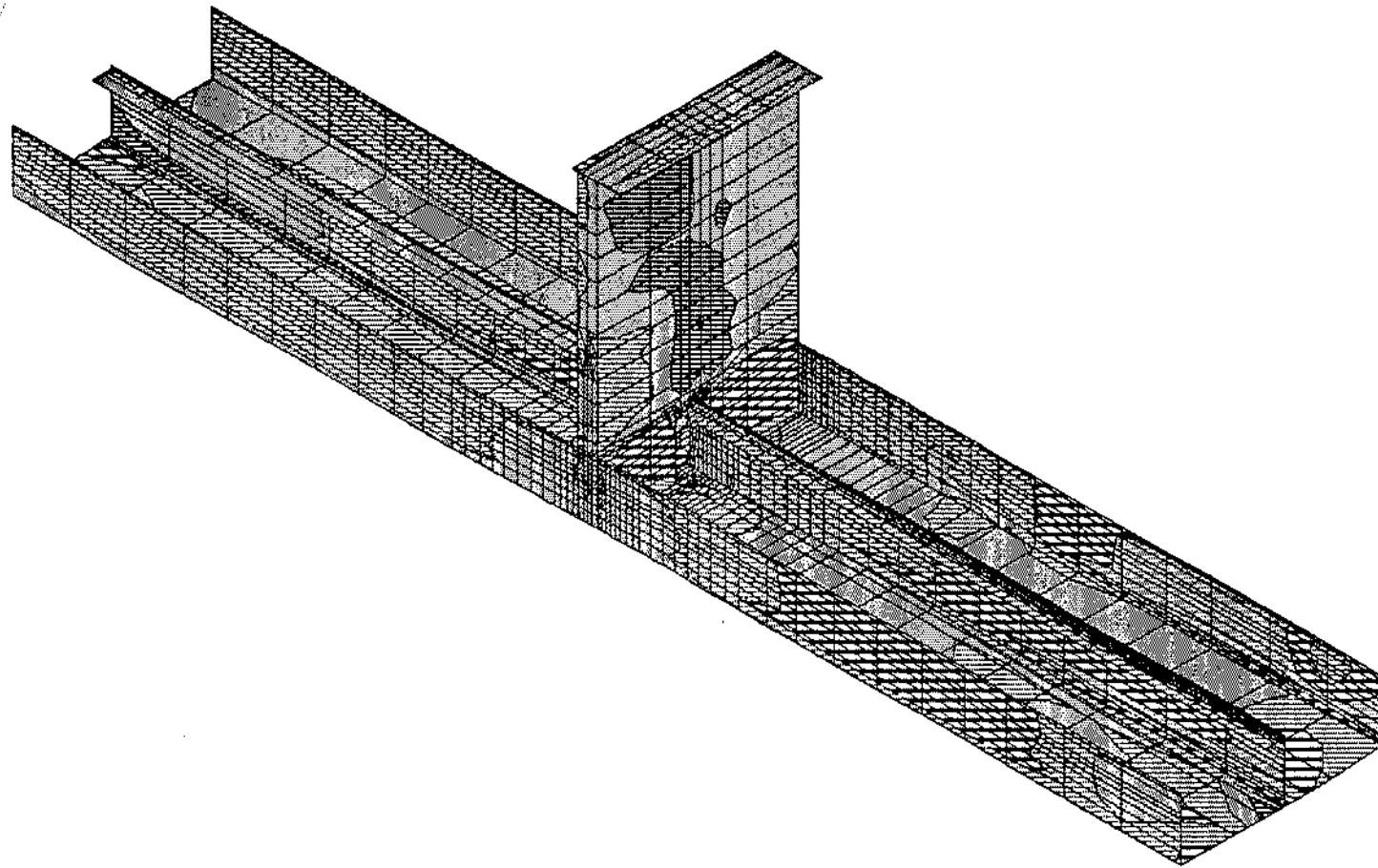
SHELL
OUTPUT   S12T
LOAD   1

5000
3000
1000
-1000
-3000
-5000

MIN IS   -0.494E+04 ⟨JOINT   2388⟩   MAX IS   0.460E+04 ⟨JOINT   2324⟩

SAP90

detail1

SHELL
OUTPUT   S12T

LOAD   1

5000
3000
1000
-1000
-3000
-5000

SAP90

MIN IS -0.494E+04 <JOINT 2388>   MAX IS   0.460E+04 <JOINT 2324>

detail l

SHELL

OUTPUT SMXT

LOAD 1

20800
15600
10400
5200
0
-5200

MIN IS -0.486E+04 <JOINT 1172>   MAX IS 0.187E+05 <JOINT 1171>

SAP90

Z

X
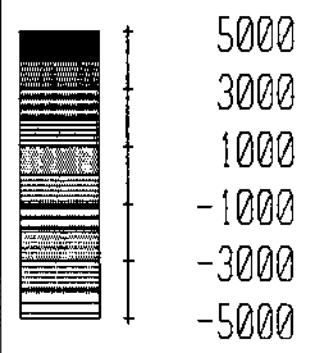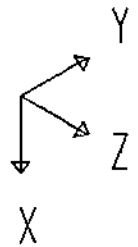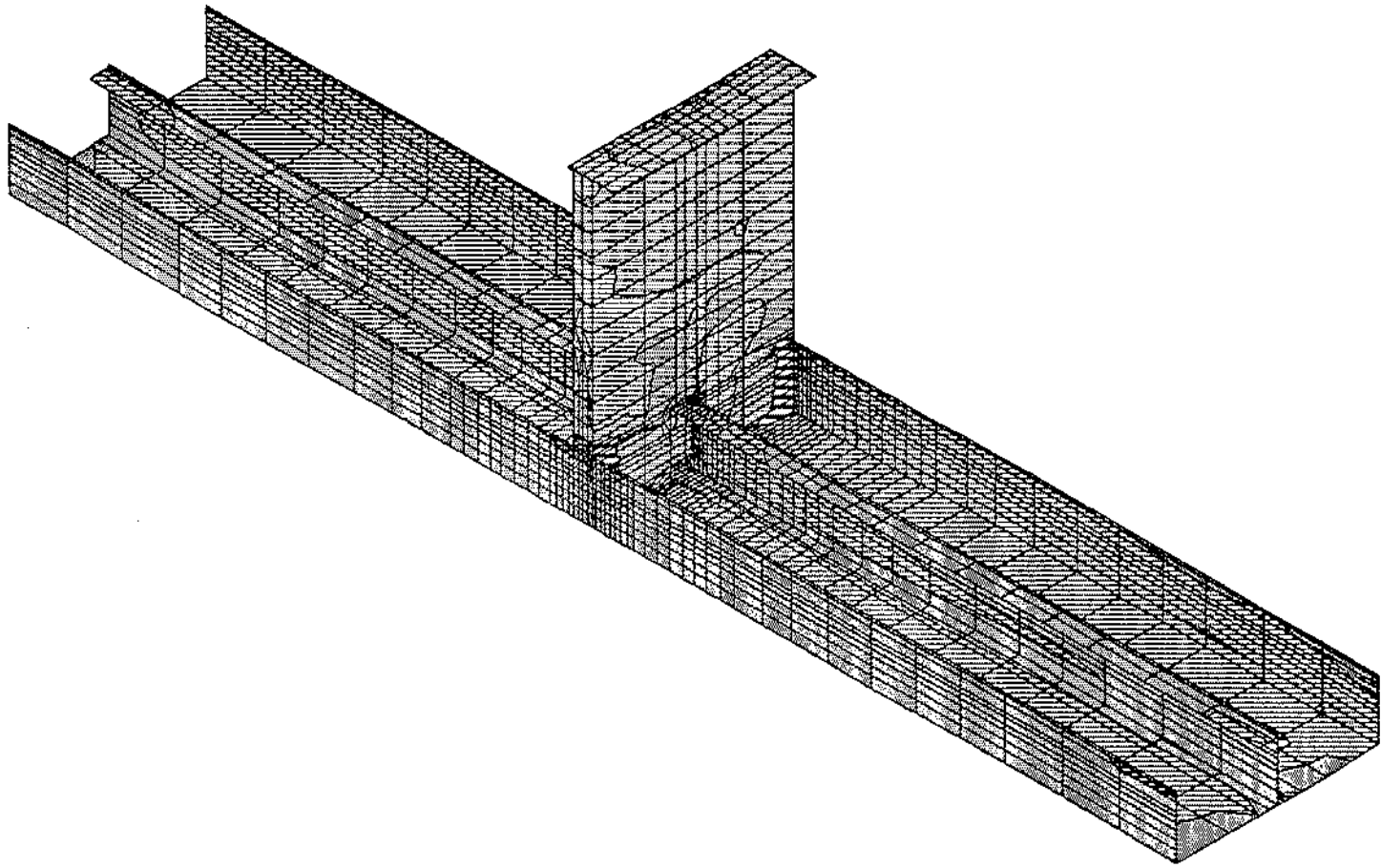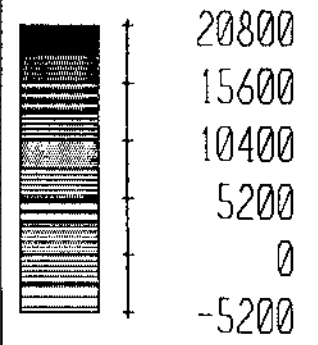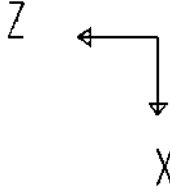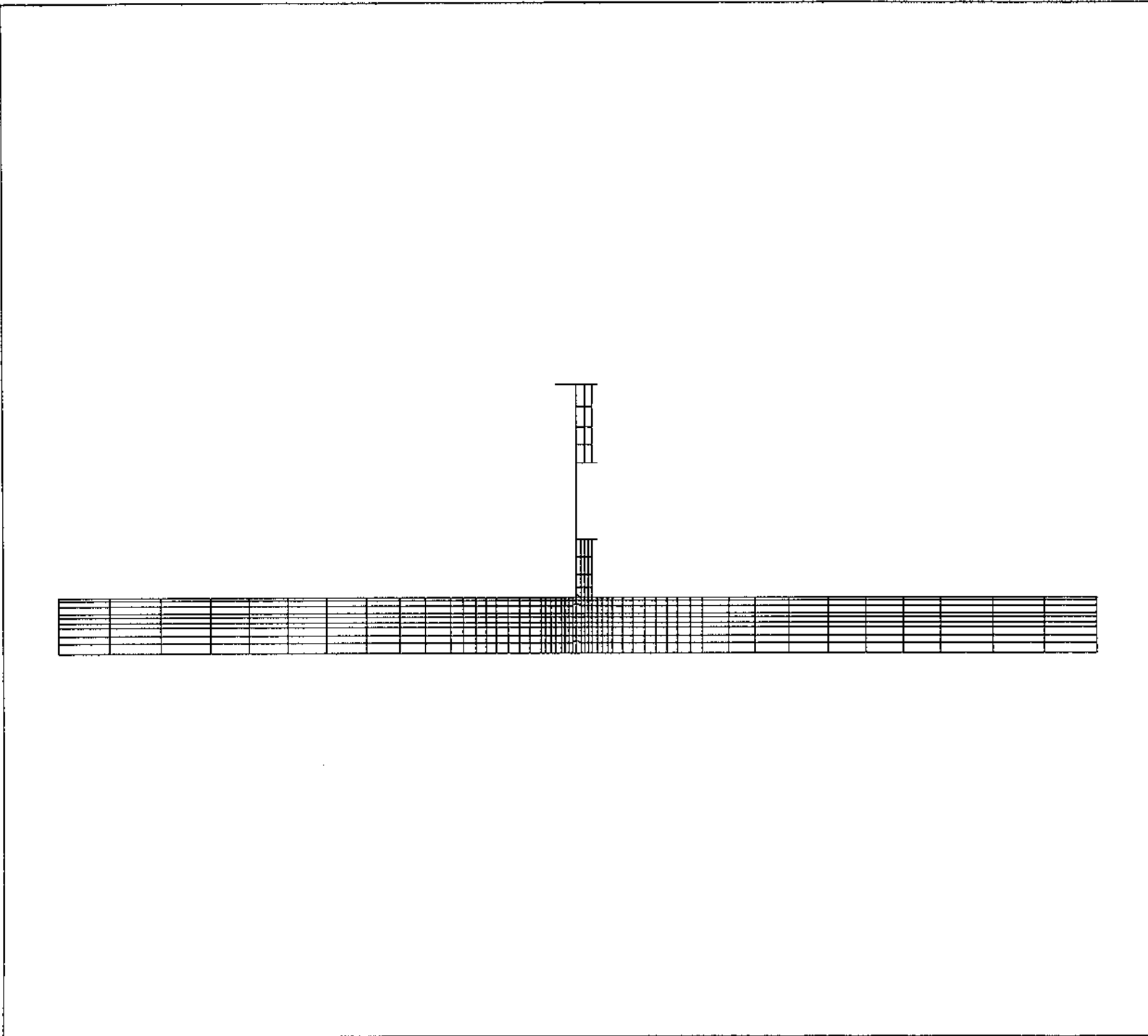
detail1

UNDEFORMED
SHAPE

OPTIONS

WIRE FRAME

SAP90

245

Z ←

X
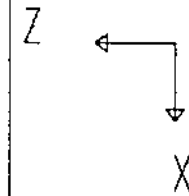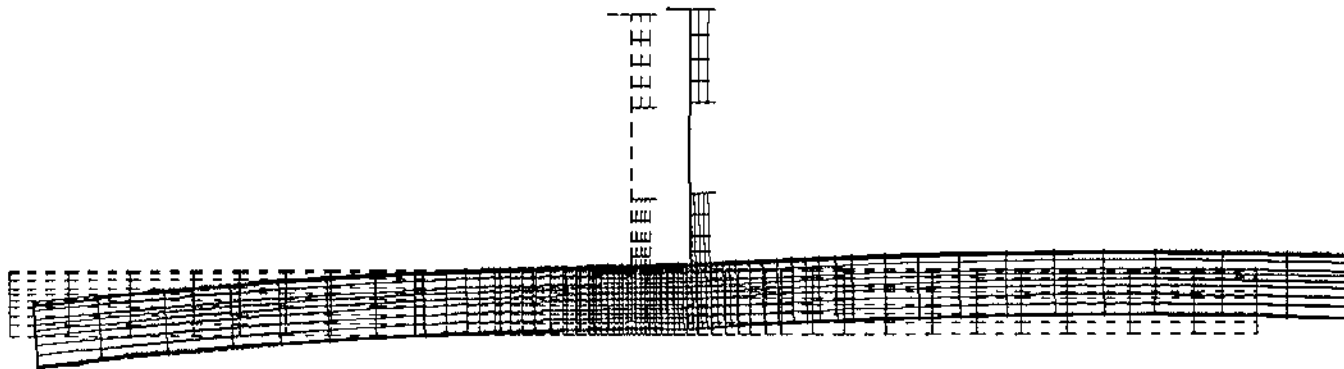
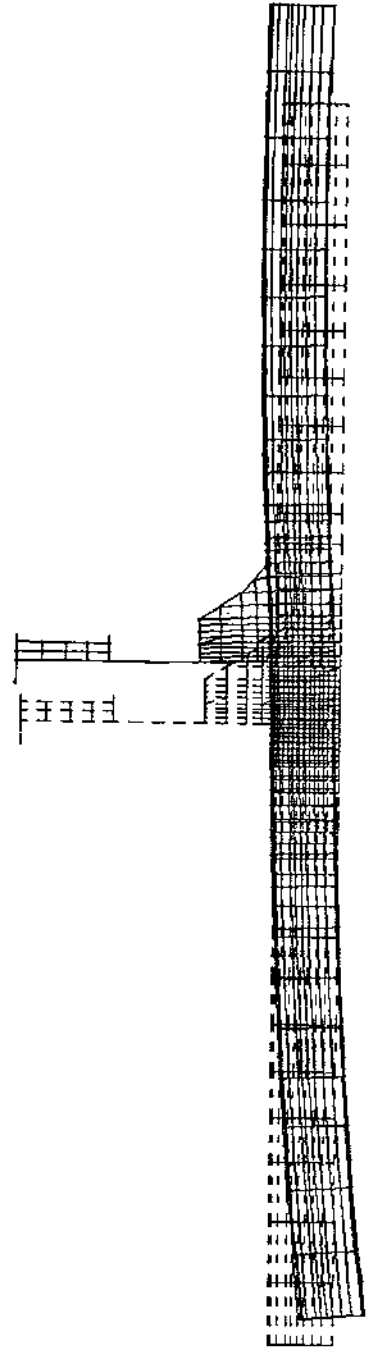detail 1
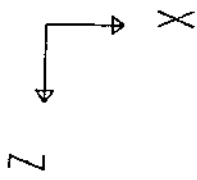
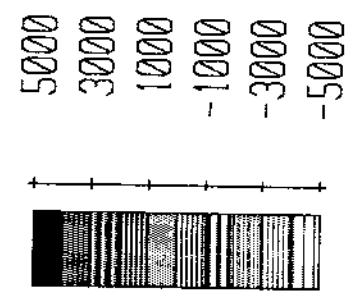DEFORMED
SHAPE

LOAD   1

MINIMA
X-0.3174E-01
Y-0.2363E+01
Z-0.1464E+00
MAXIMA
X 0.4849E-01
Y-0.2333E+01
Z-0.3977E-01

SAP90

Z

X

detail1
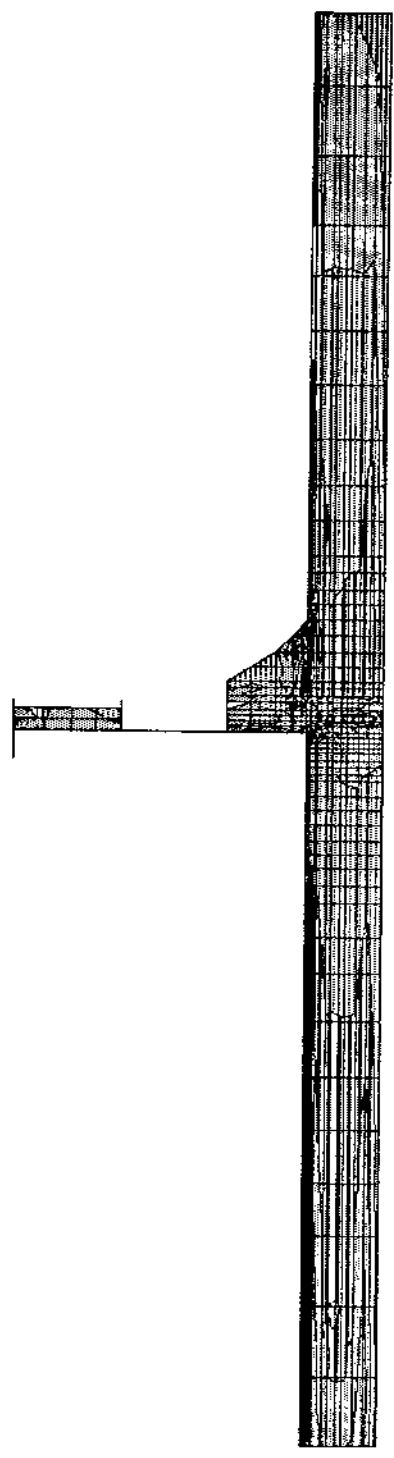
SHELL
OUTPUT   S11T

LOAD   1

21000
14000
7000
0
-7000
-14000
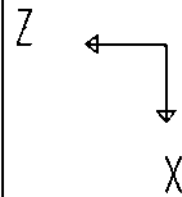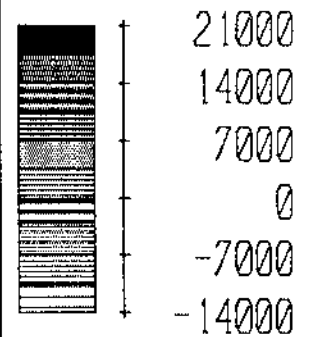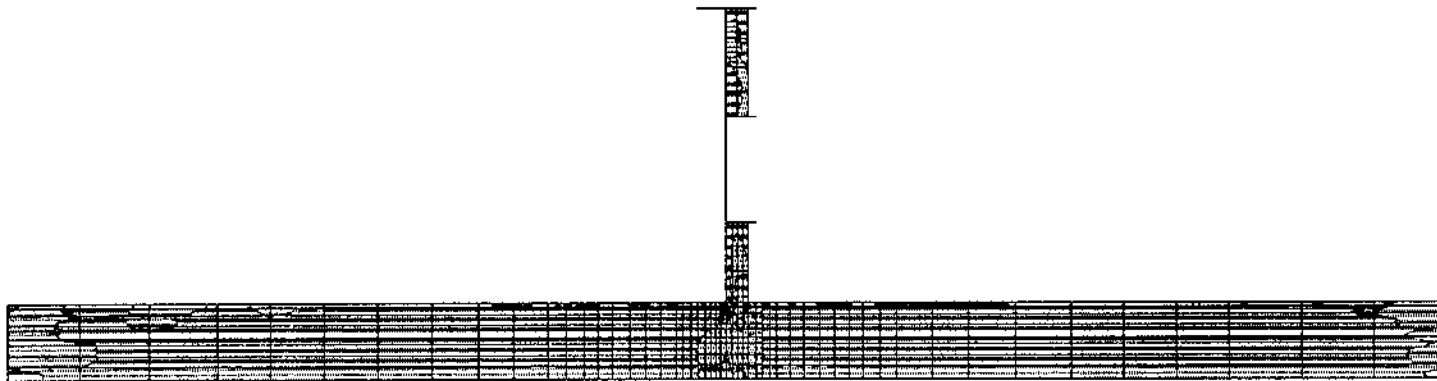
MIN IS   -0.136E+05 <JOINT   1172>   MAX IS   0.161E+05 <JOINT   894>

SAP90

Z

X

detail1

SHELL
OUTPUT   S22T

LOAD   1

14000
8400
2800
-2800
-8400
-14000
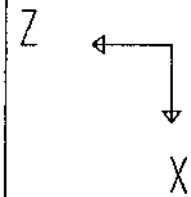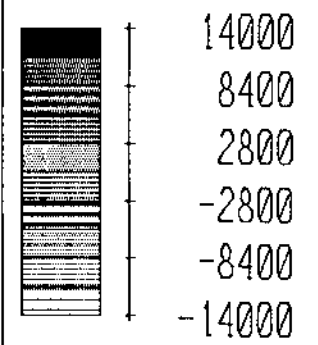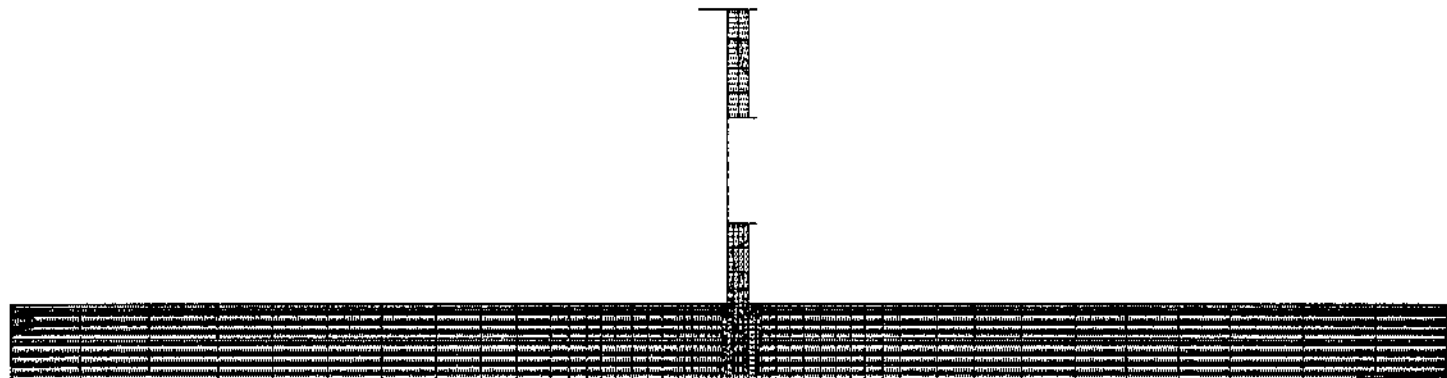
MIN IS   -0.139E+05 <JOINT   1172>   MAX IS   0.138E+05 <JOINT   1171>

SAP90
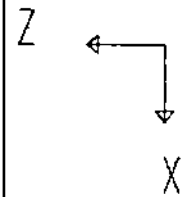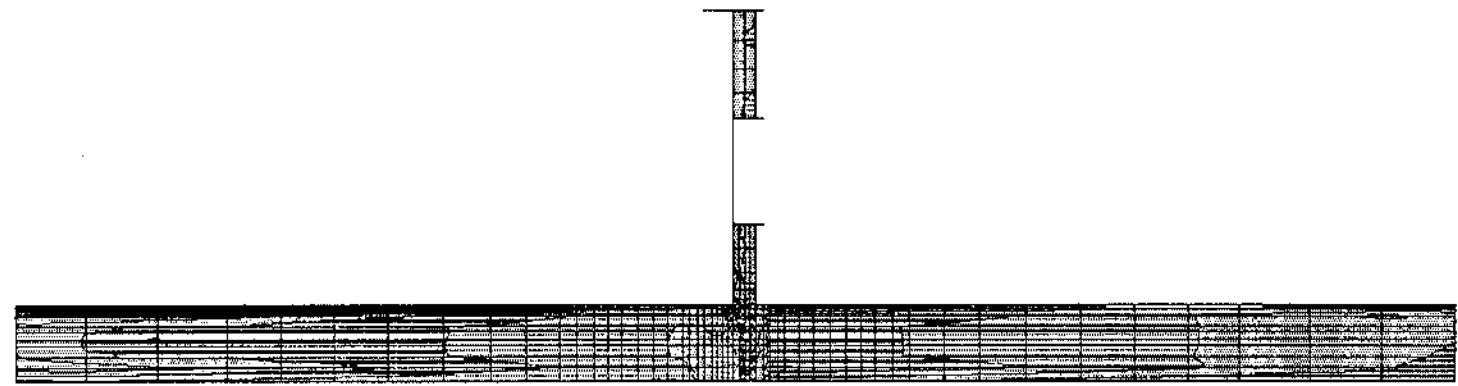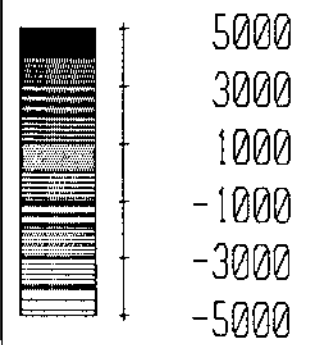
detail1

SHELL

OUTPUT   S12T

LOAD   1

5000
3000
1000
-1000
-3000
-5000

MIN IS   -0.494E+04 <JOINT 2388>   MAX IS   0.372E+04 <JOINT 2350>

SAP90

Z

X

detail1

SHELL

OUTPUT   SMXT

LOAD   1

20800
15600
10400
5200
0
-5200

300
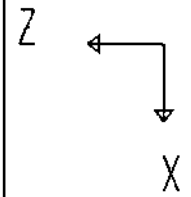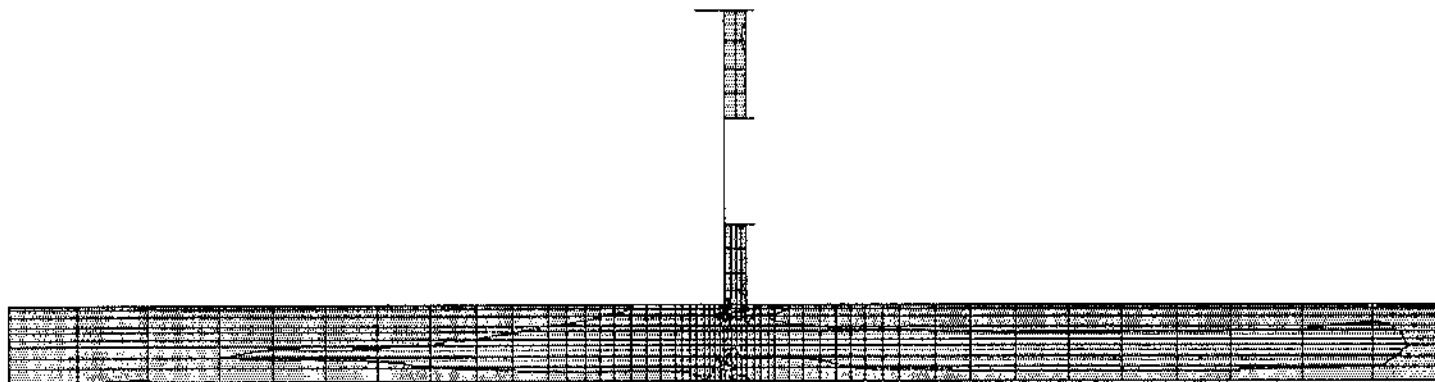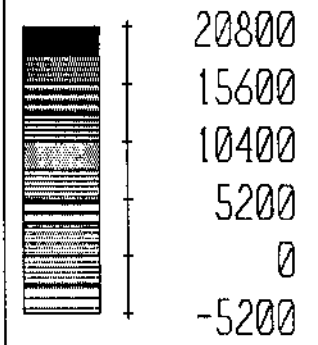
MIN IS   -0.486E+04 <JOINT   1172>   MAX IS   0.187E+05 <JOINT   1171>

SAP90

detail1

UNDEFORMED
SHAPE
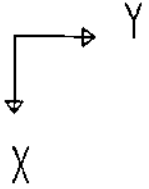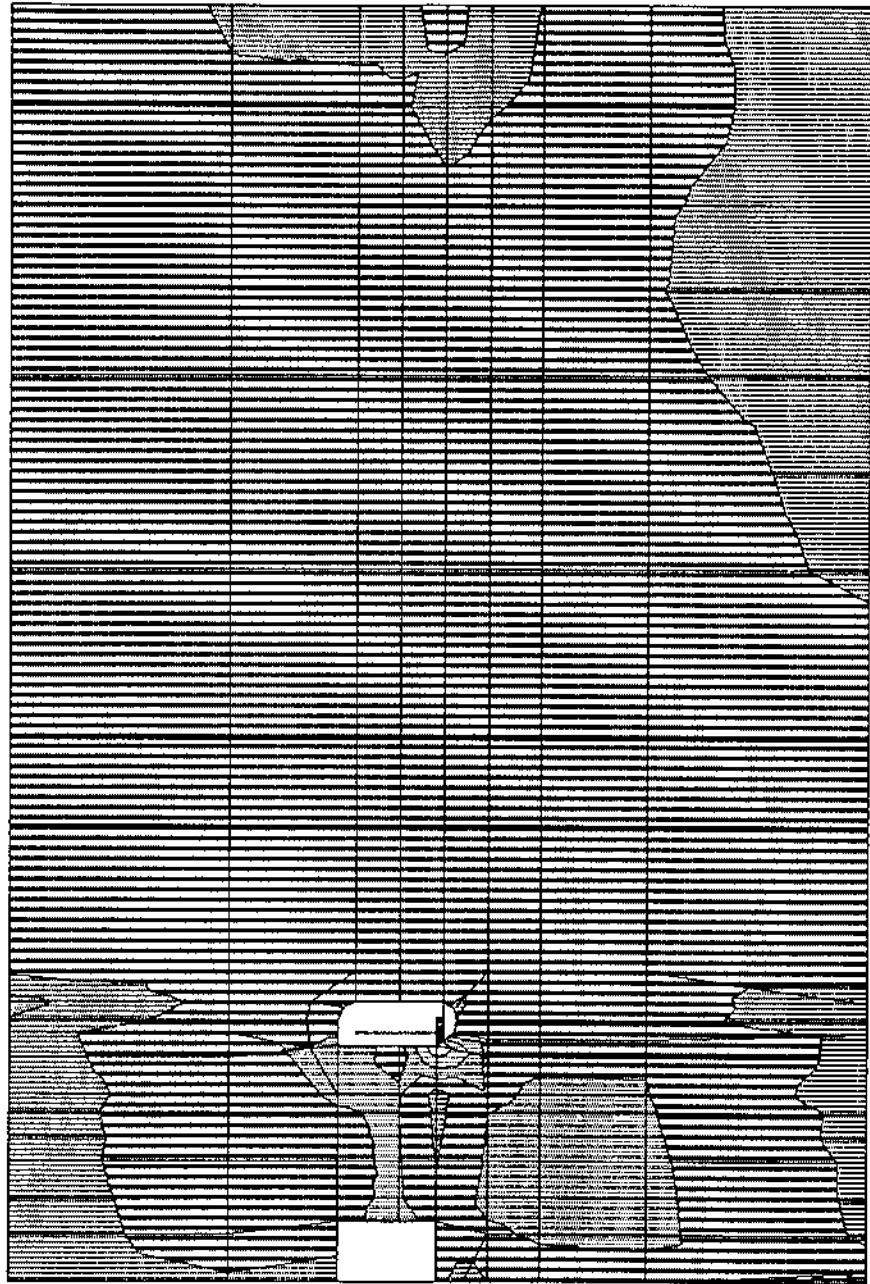
OPTIONS

WIRE FRAME

SAP90

detail1

SHELL
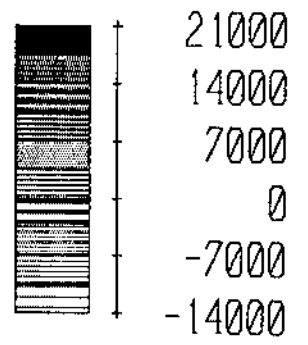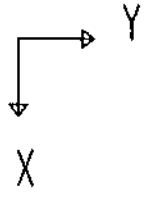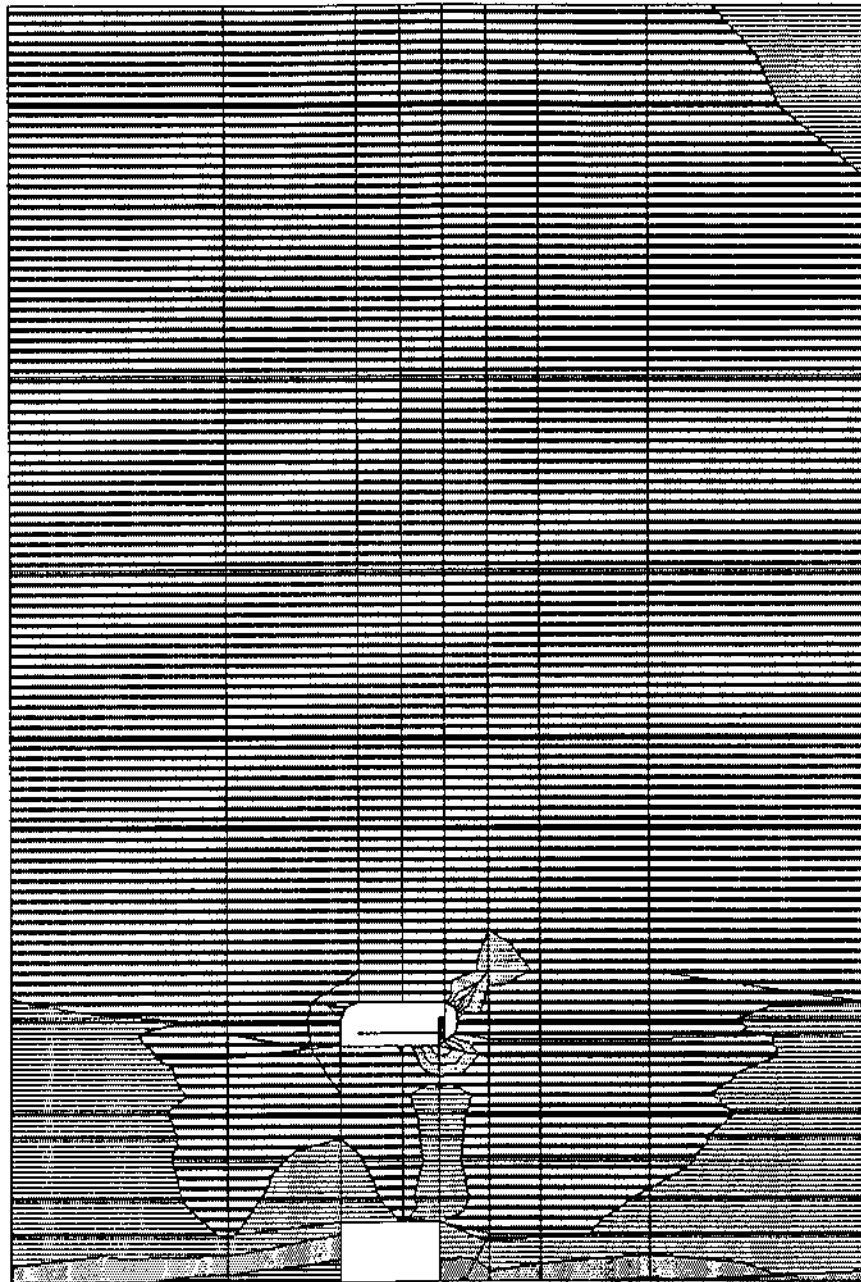
OUTPUT S11T

LOAD 1

21000
14000
7000
0
-7000
-14000

MIN IS -0.136E+05 <JOINT 1172>   MAX IS 0.176E+05 <JOINT 2441>

SAP90

Y

X

detail1

SHELL
OUTPUT   S22T

LOAD   1

21000
14000
7000
0
-7000
-14000

MIN IS -0.139E+05 <JOINT   1172>   MAX IS   0.164E+05 <JOINT   2412>

SAP90

detail1

SHELL
OUTPUT S12T

LOAD   1

5000
3000
1000
-1000
-3000
-5000

SAP90

MIN IS -0.494E+04 <JOINT 2388>   MAX IS   0.460E+04 <JOINT 2324>

detail1

SHELL
OUTPUT   SMXT

LOAD   1

20800
15600
10400
5200
0
-5200

MIN IS   -0.486E+04 ⟨JOINT   1172⟩   MAX IS   0.187E+05 ⟨JOINT   1171⟩

SAP90

10"

30"

105" x 0.46"

6'

20"

25"

404" x0.46"

12.5"   2.5"

3"

25"

105" x 0.46"

70" x 0.46"

306
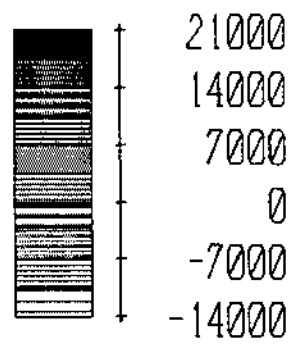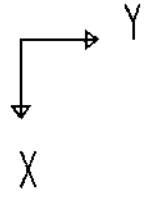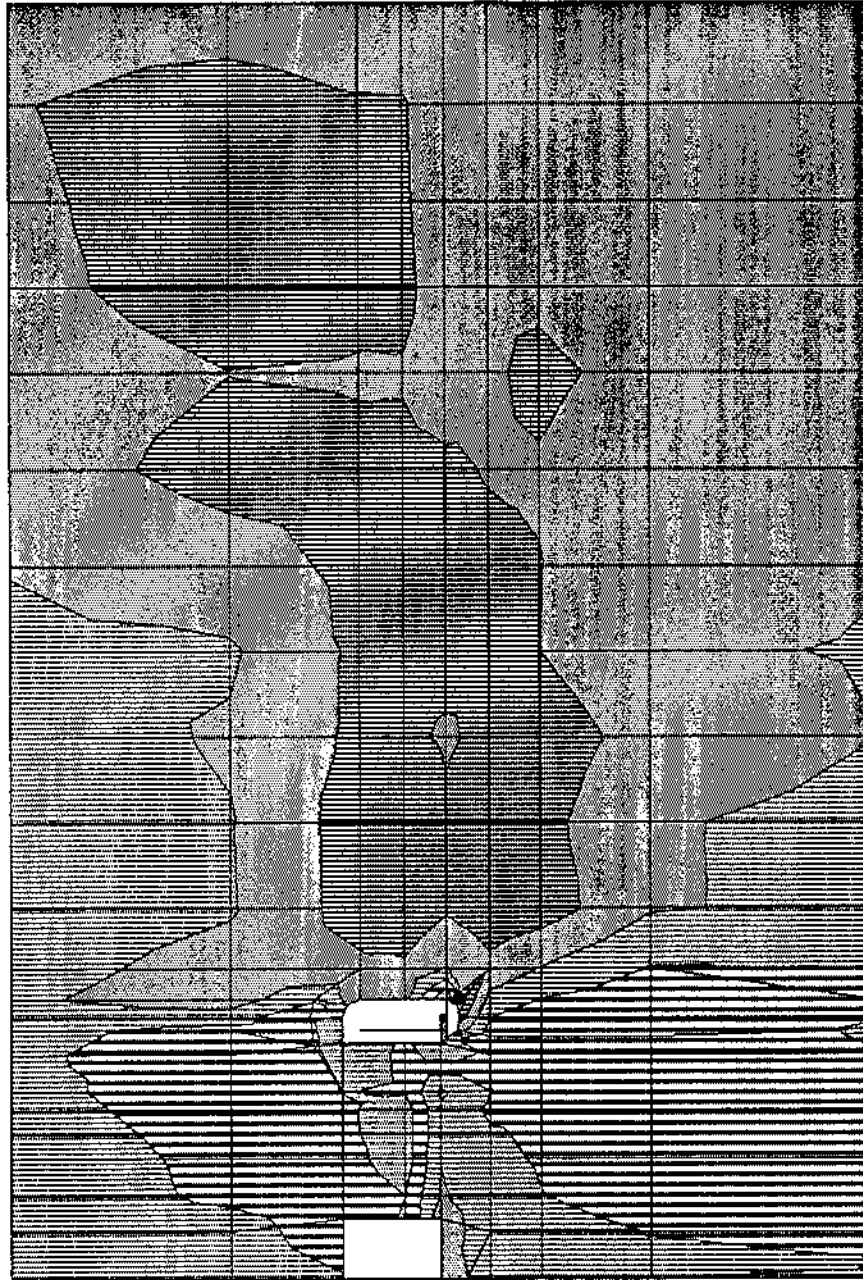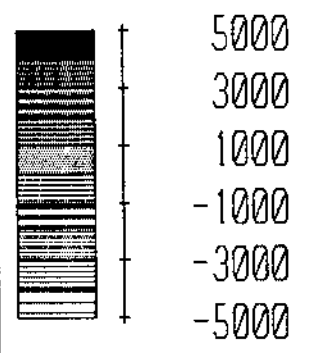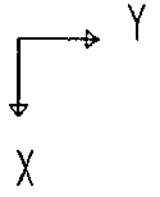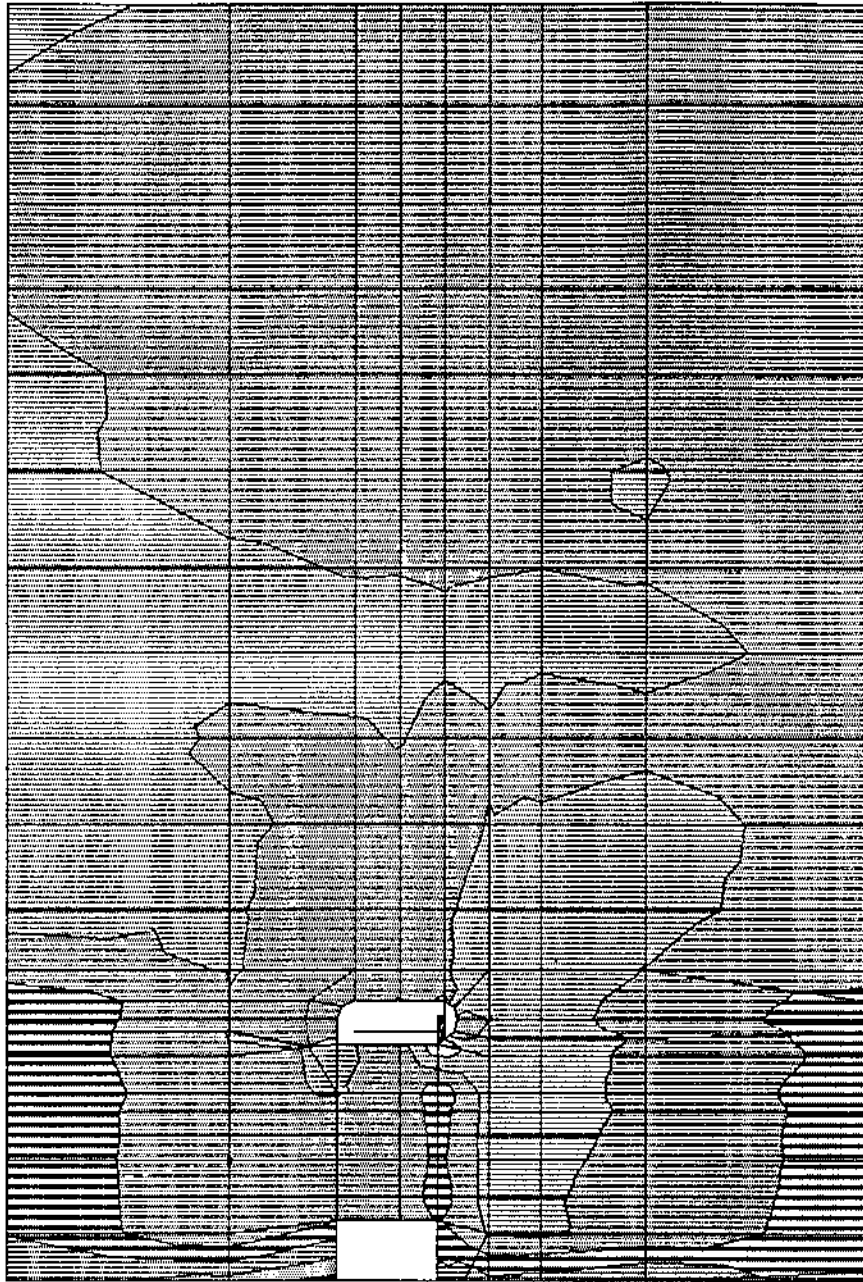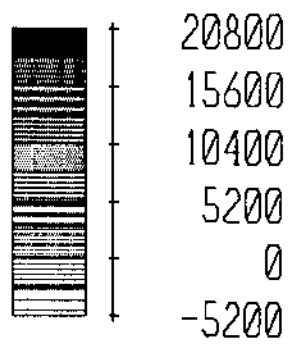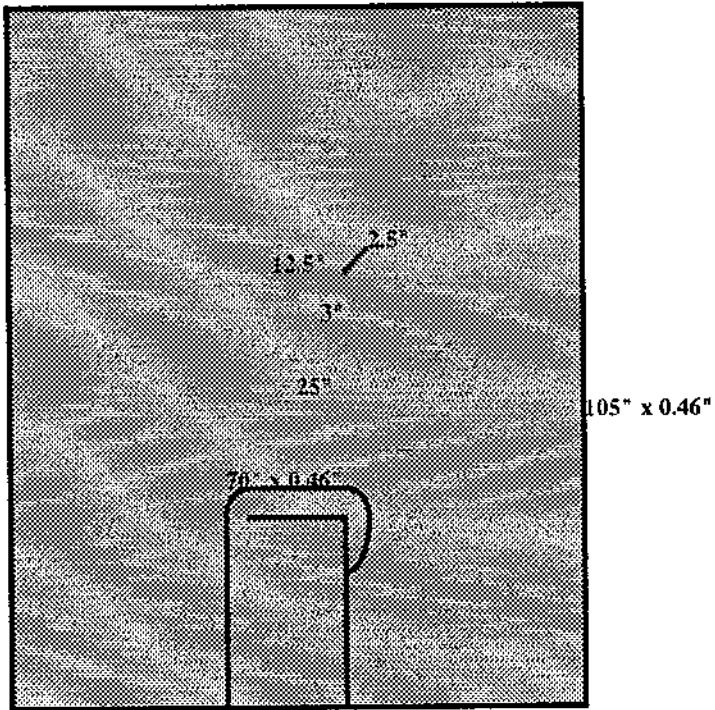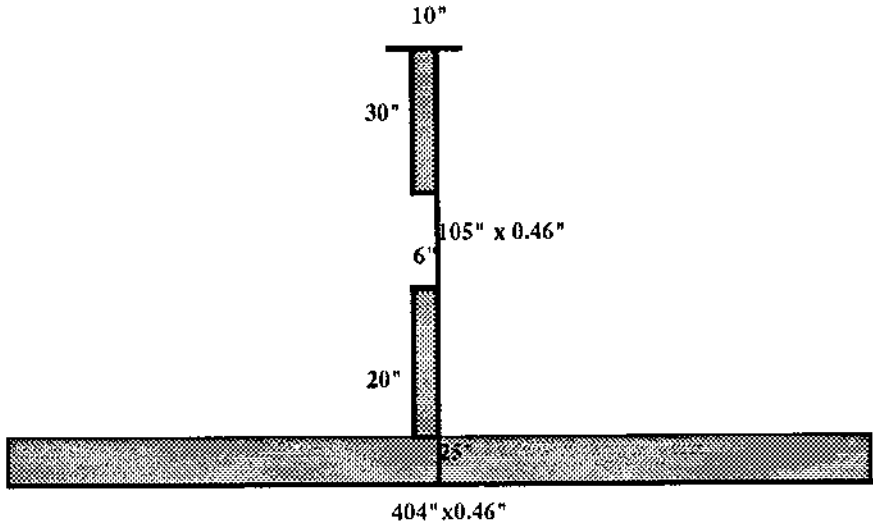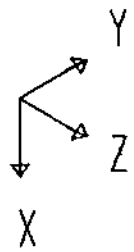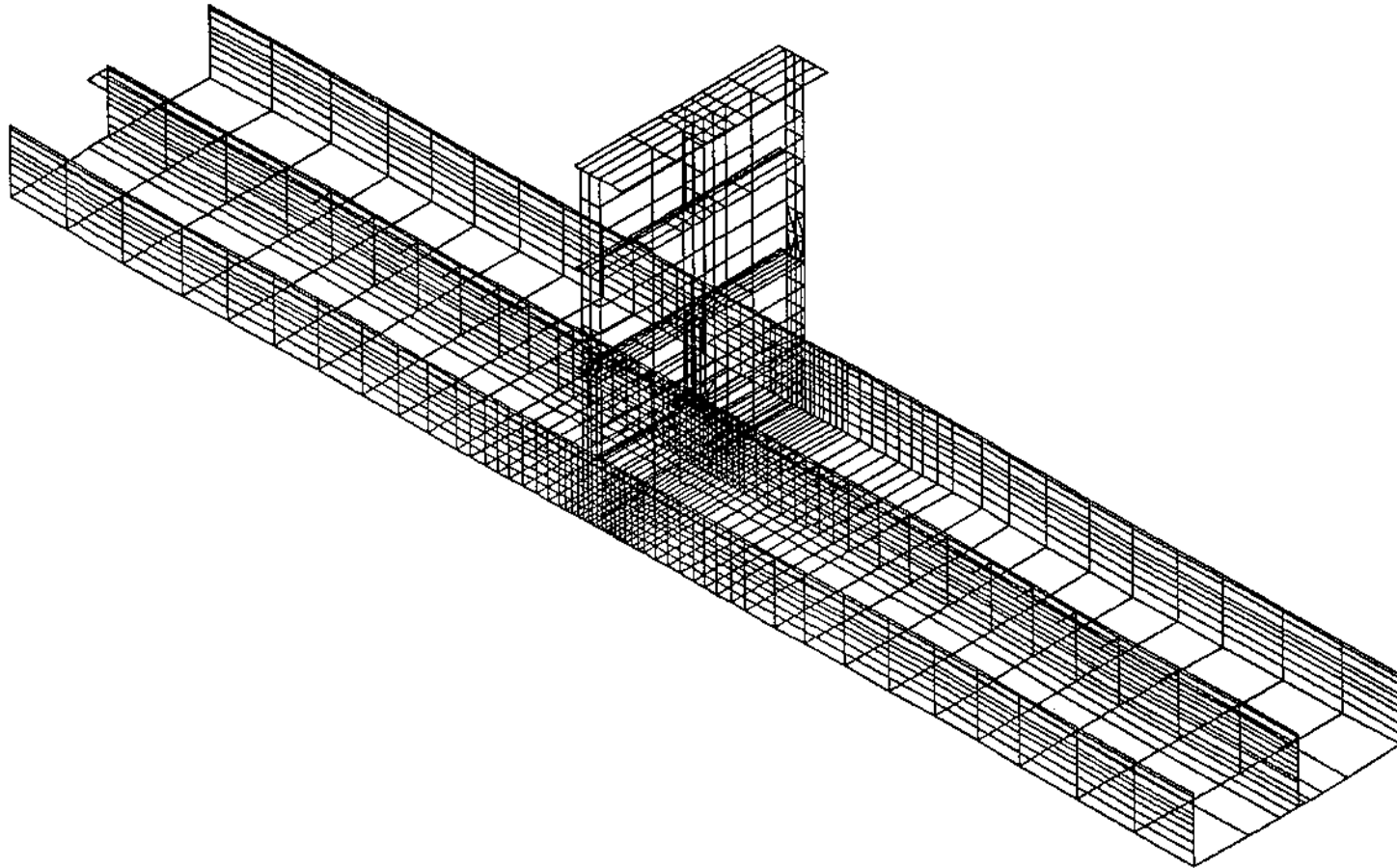
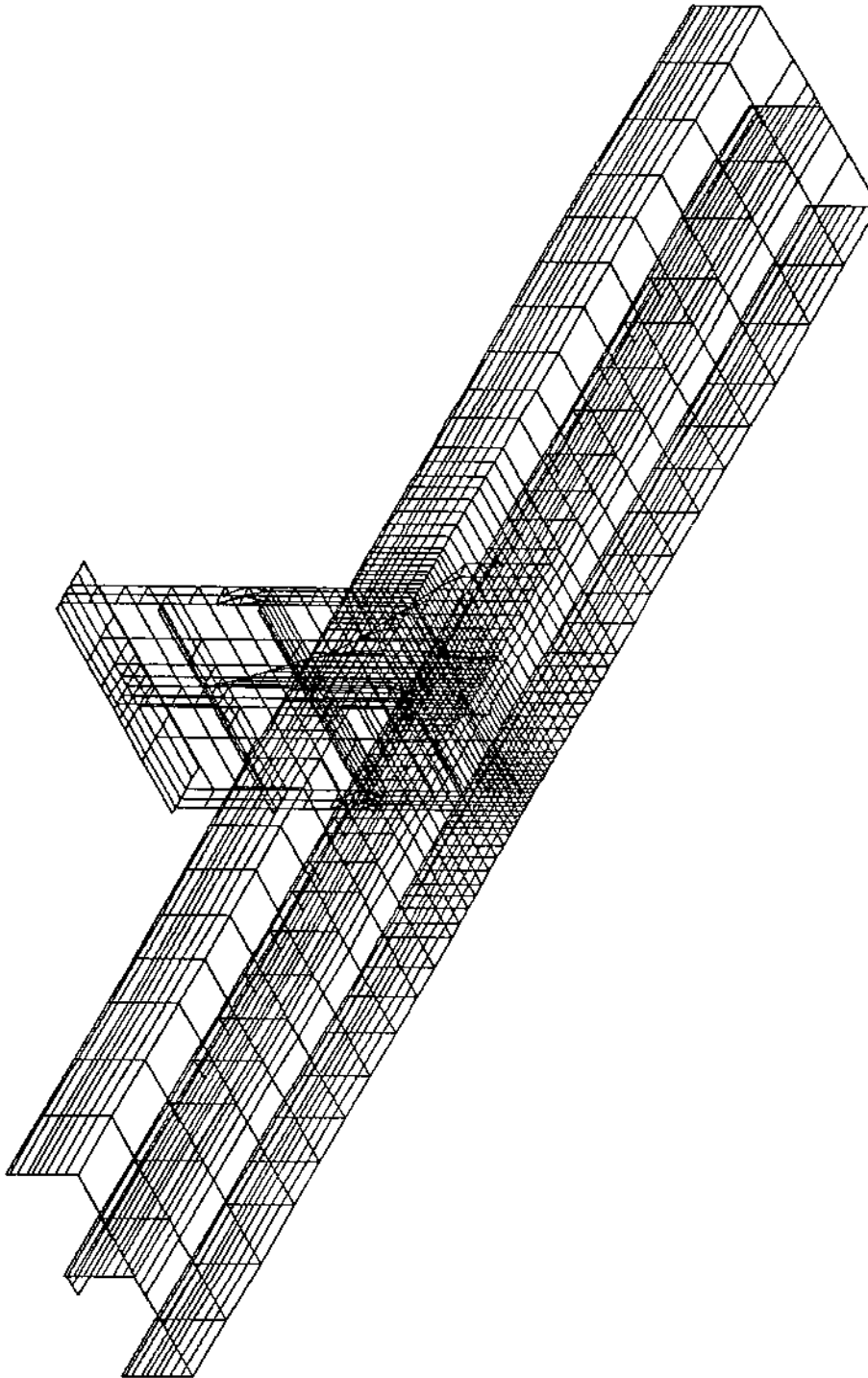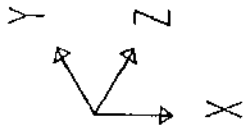detail2
UNDEFORMED
SHAPE

OPTIONS
WIRE FRAME
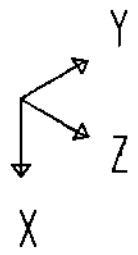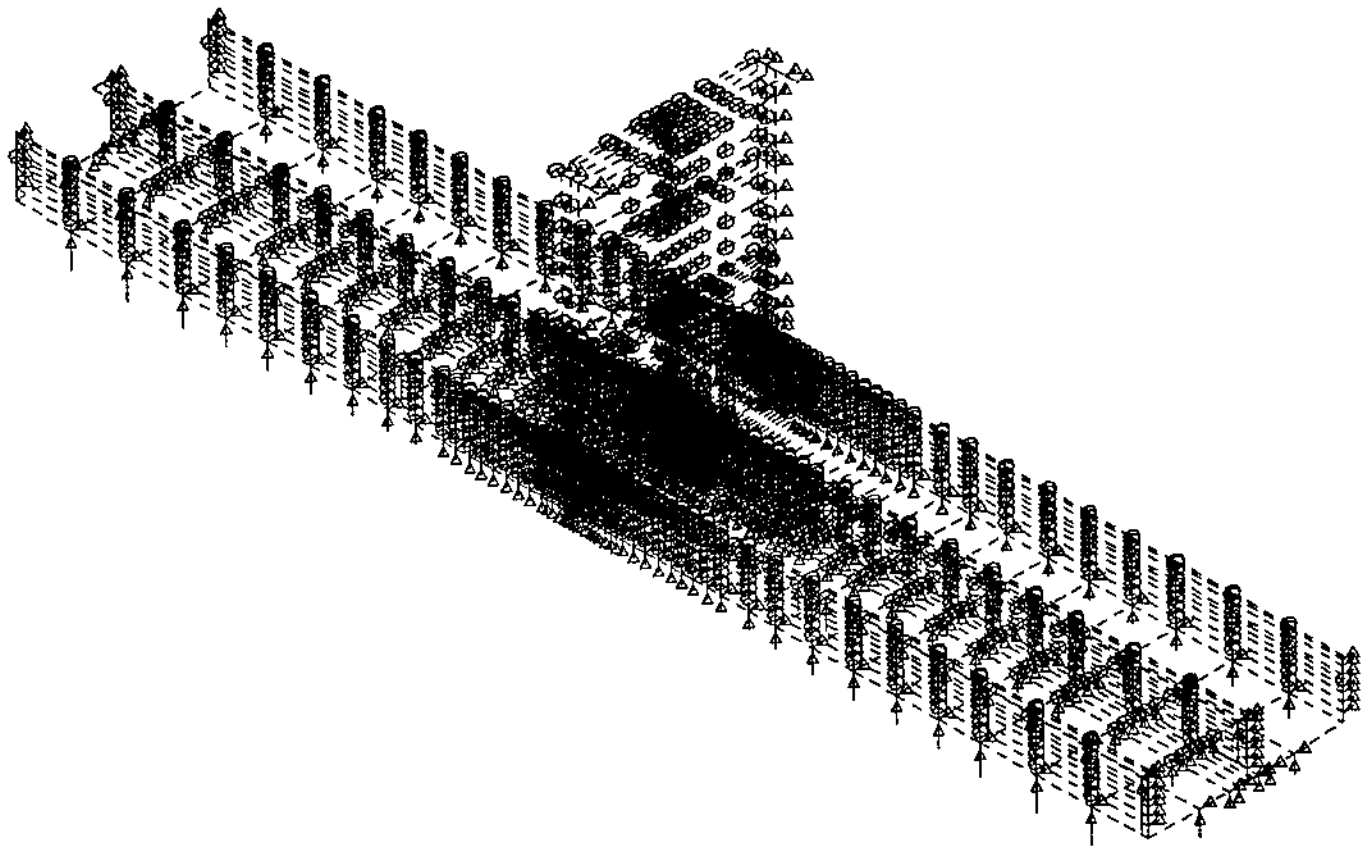
SAP90

detail2

JOINT
LOADS

LOAD   1

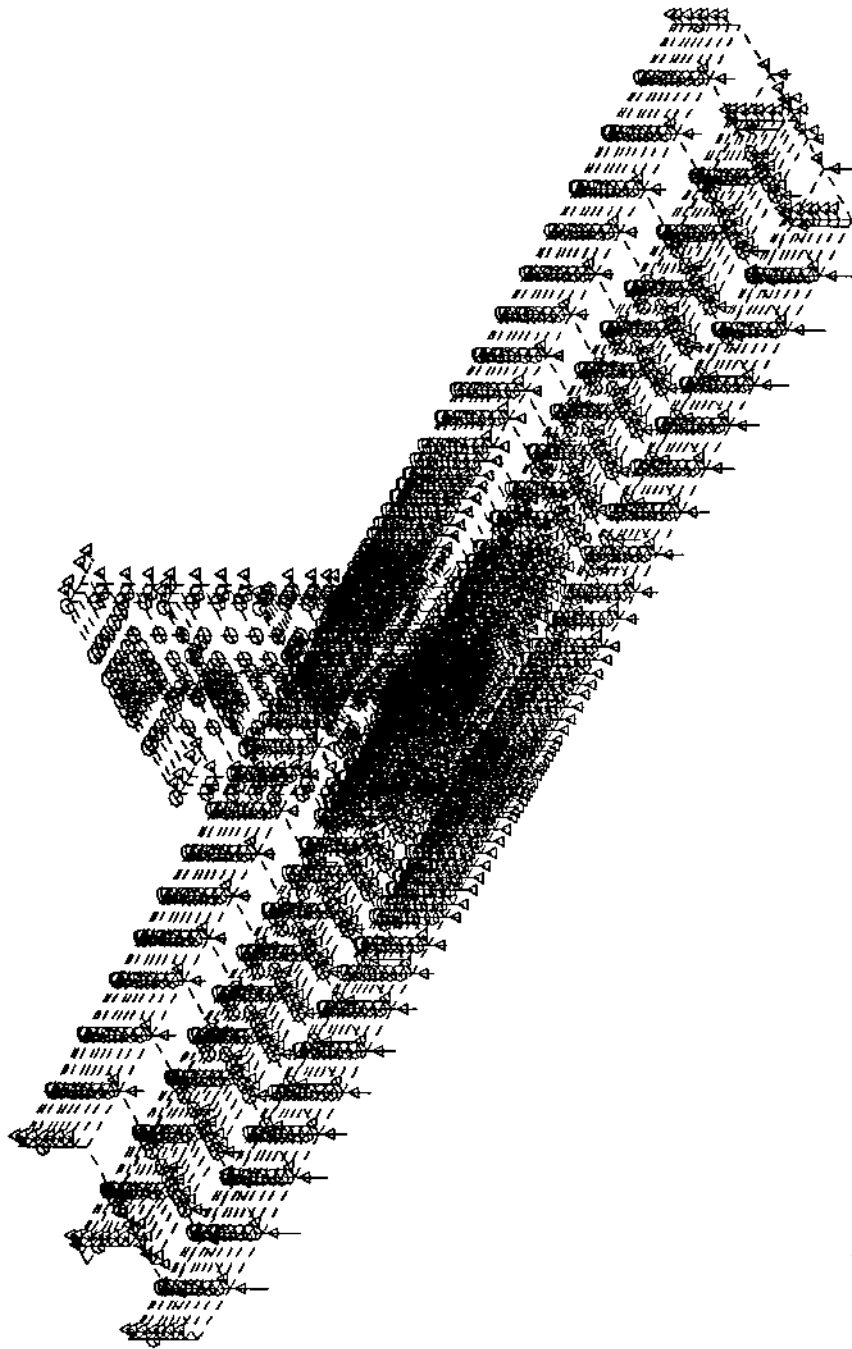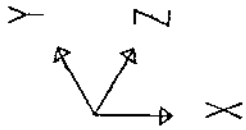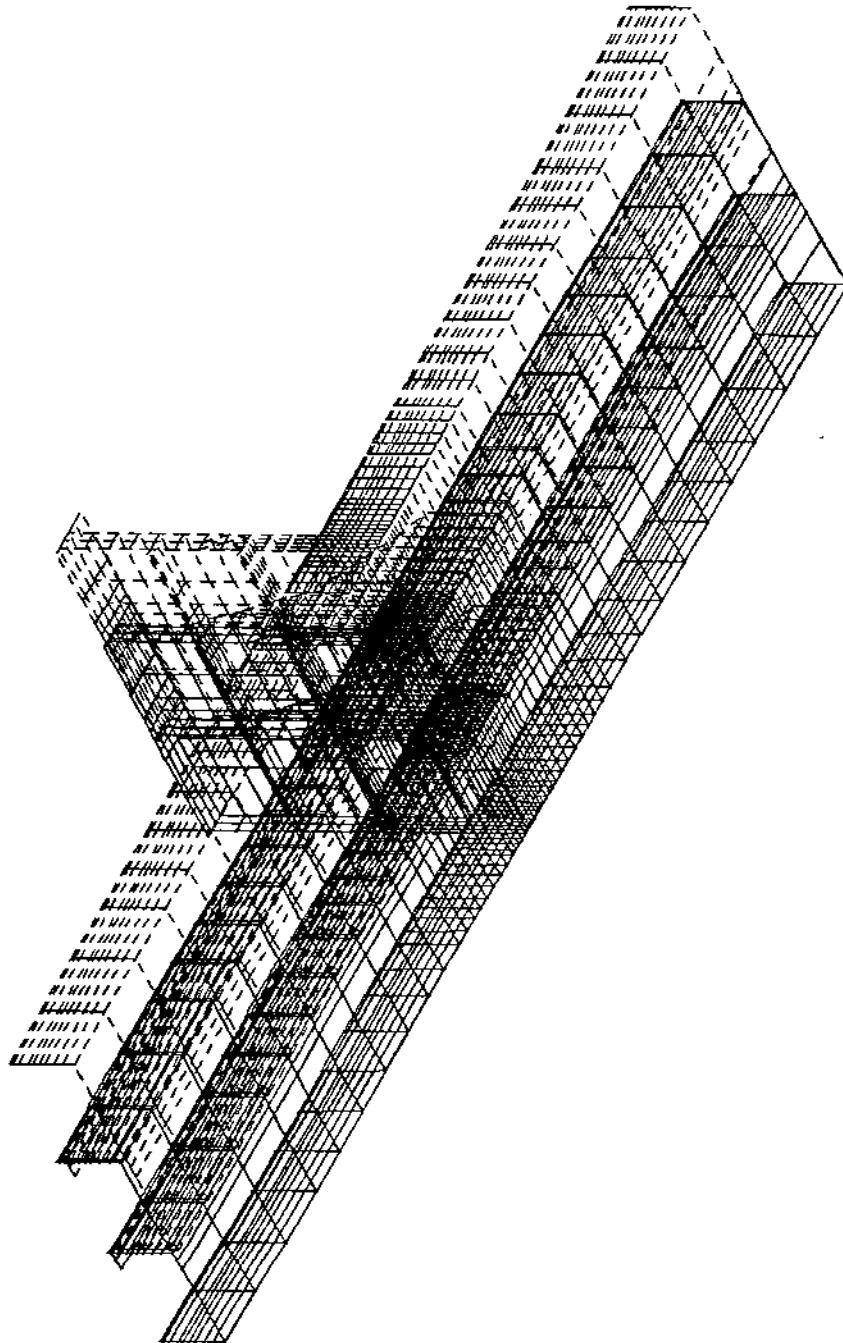MINIMA
P-0.1563E+04
MAXIMA
P-0.2288E-01
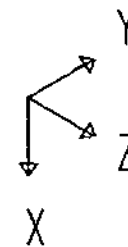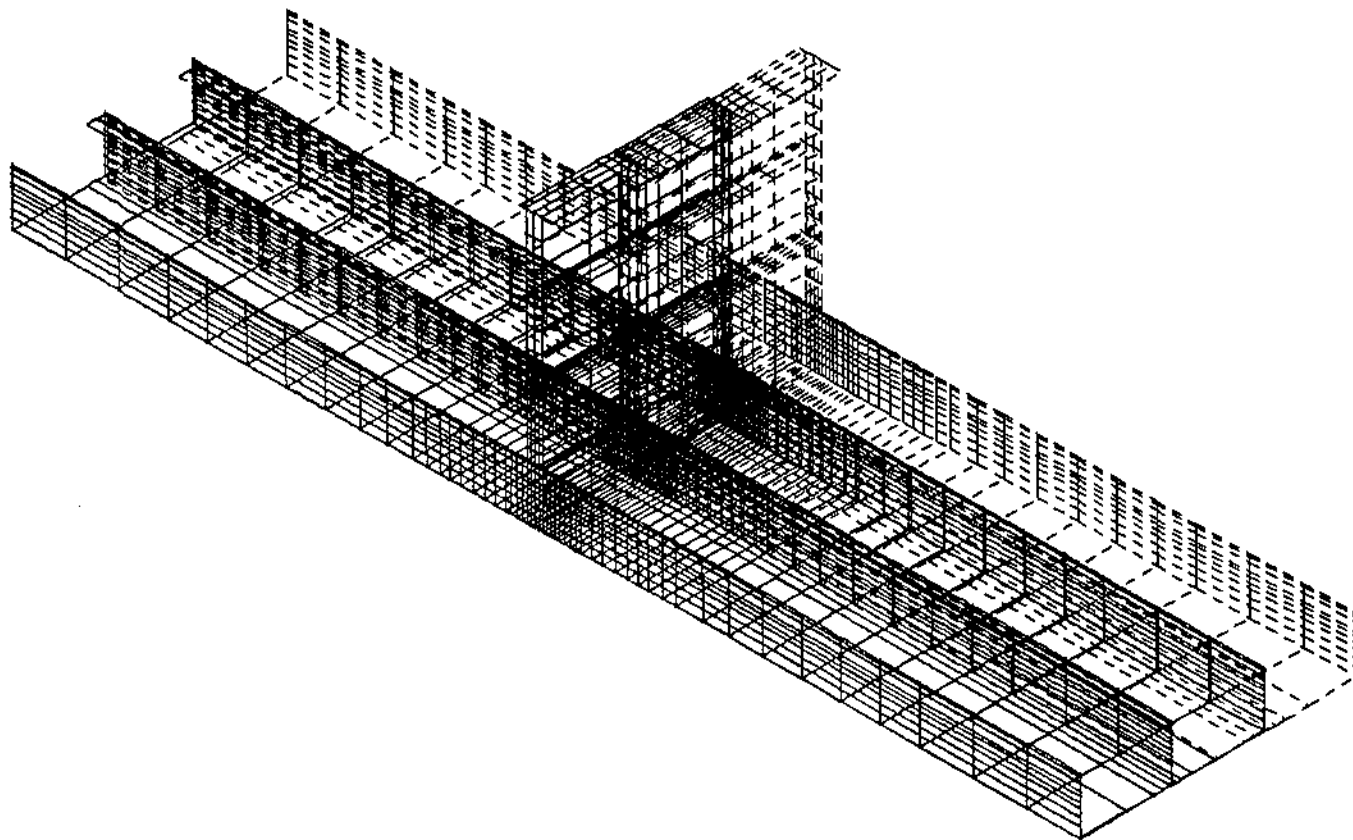
SAP90

detail2

DEFORMED
SHAPE

LOAD   1

MINIMA
X-0.4494E-01
Y-0.2375E+01
Z-0.1548E+00
MAXIMA
X 0.6452E-01
Y-0.2329E+01
Z-0.3119E-01
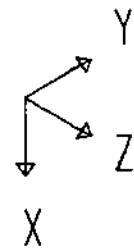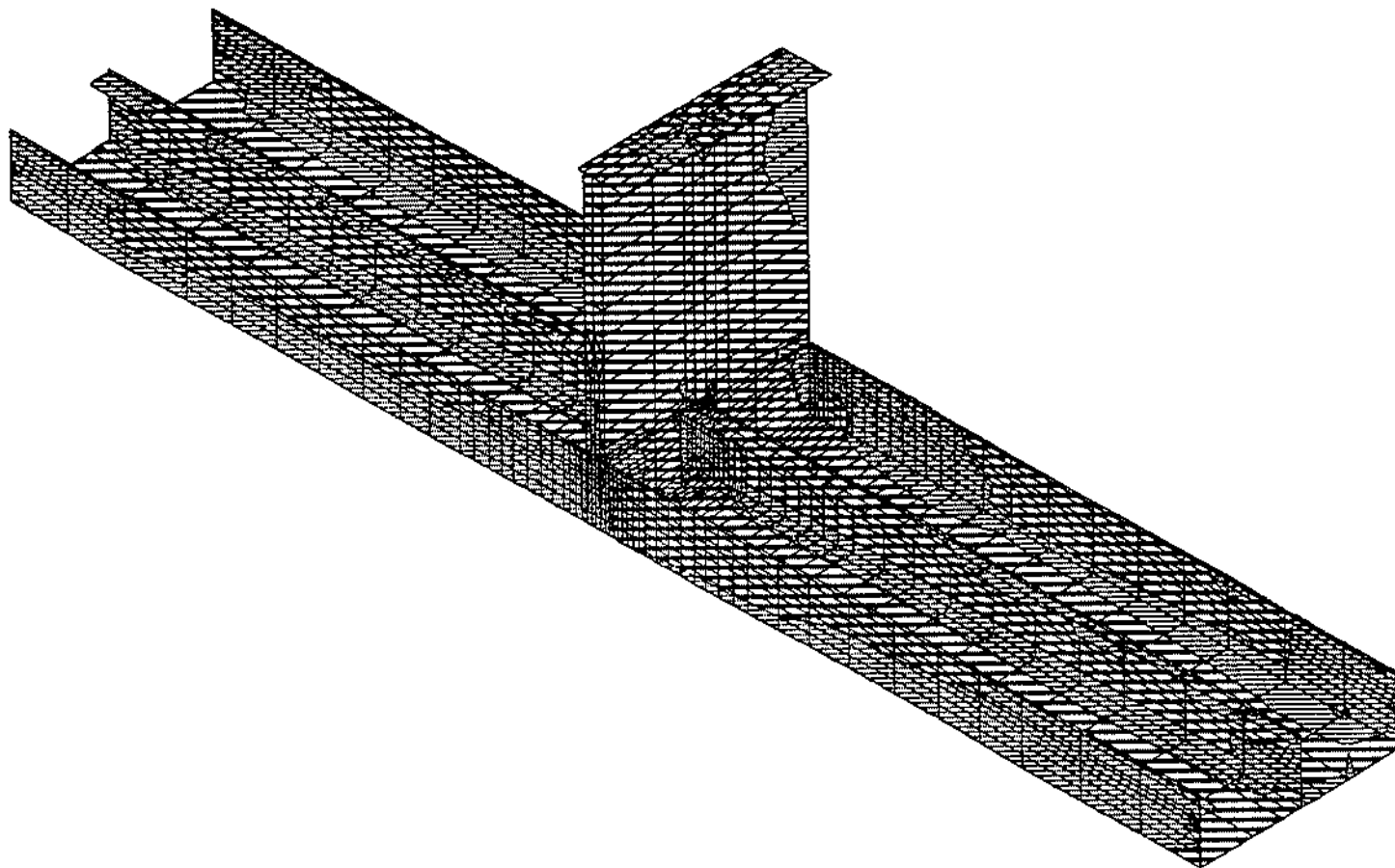
SAP90

detail2

SHELL

OUTPUT   S11T

LOAD   1

24000
16000
8000
0
-8000
-16000

SAP90

MIN IS -0.155E+05 ‹JOINT 1172›   MAX IS   0.176E+05 ‹JOINT 2441›

310

Y

Z

X

detail2

SHELL

OUTPUT   S22T

LOAD   1

22500
13500
4500
-4500
-13500
-22500
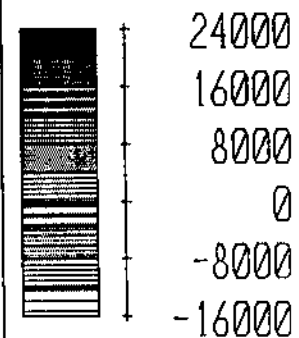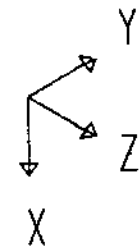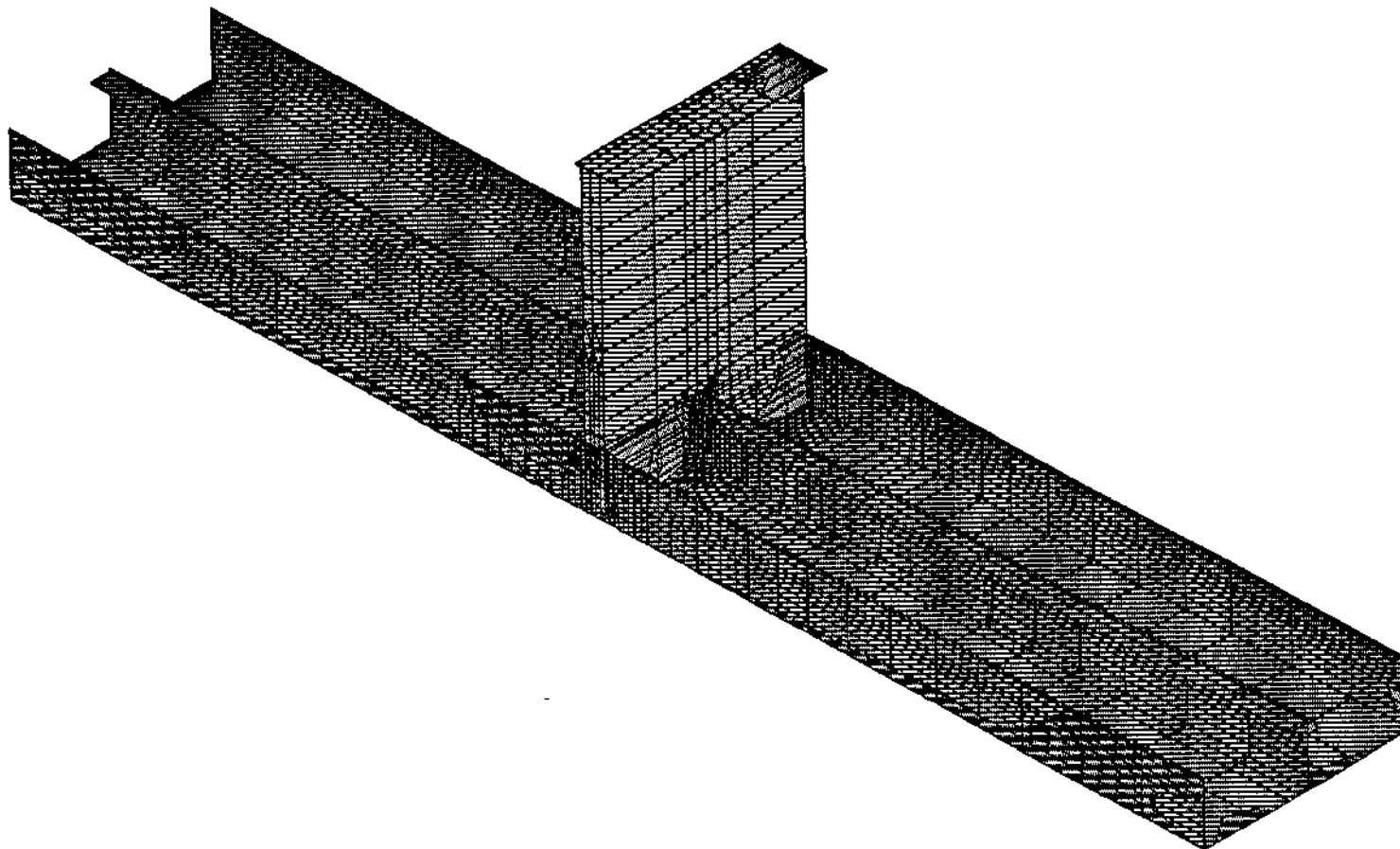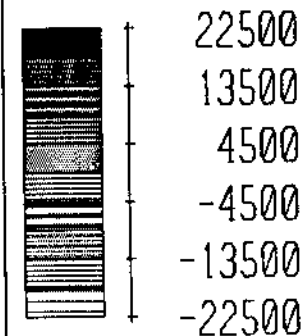
SAP90

MIN IS -0.210E+05 <JOINT 1180>   MAX IS   0.164E+05 <JOINT 2412>
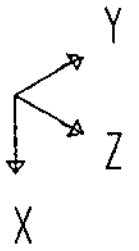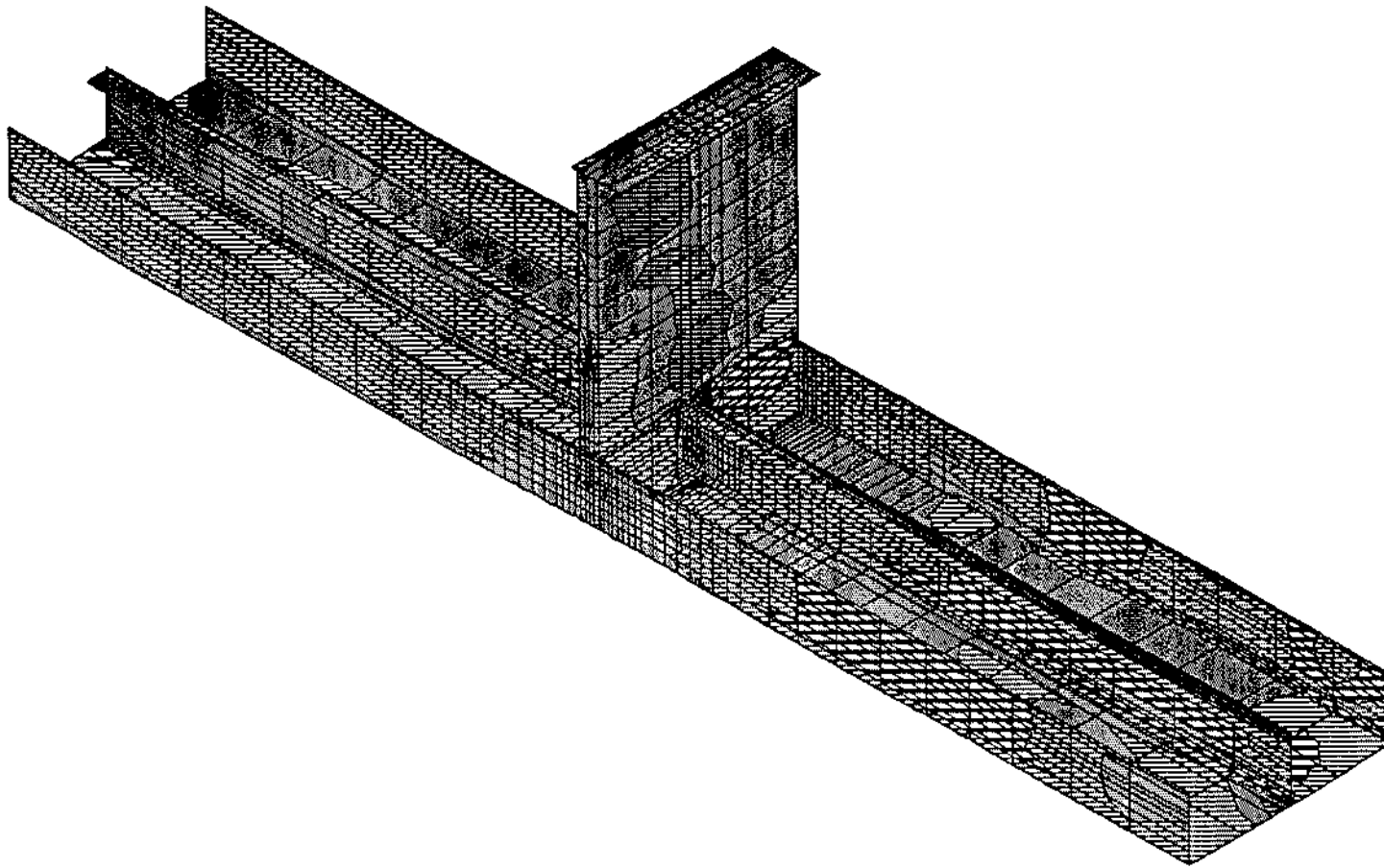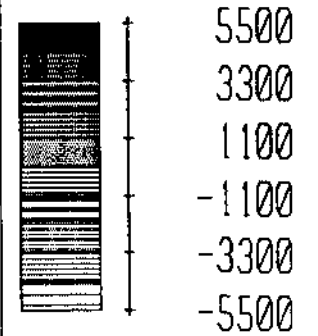
detail2

SHELL

OUTPUT S12T

LOAD   1

	5500
	3300
	1100
	-1100
	-3300
	-5500

SAP90

MIN IS -0.501E+04 <JOINT 2388>   MAX IS   0.482E+04 <JOINT 1180>

detail2

SHELL

OUTPUT SMXT

LOAD 1

19600
14000
8400
2800
-2800
-8400

MIN IS -0.693E+04 <JOINT 1172>   MAX IS 0.184E+05 <JOINT 1171>

SAP90

detail2

UNDEFORMED
SHAPE

OPTIONS

WIRE FRAME

SAP90

detail2

SHELL

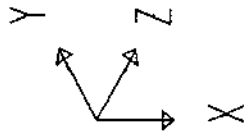OUTPUT   S12T

LOAD   1

5500
3300
1100
-1100
-3300
-5500

SAP90

MIN IS   -0.501E+04 <JOINT   2388>   MAX IS   0.482E+04 <JOINT   1180>

detail2

SHELL

OUTPUT   SMXT

LOAD   1

19600
14000
8400
2800
-2800
-8400

MIN IS -0.693E+04 <JOINT 1172>   MAX IS   0.184E+05 <JOINT 1171>

SAP90

Z

X
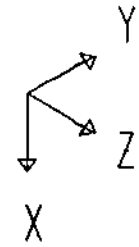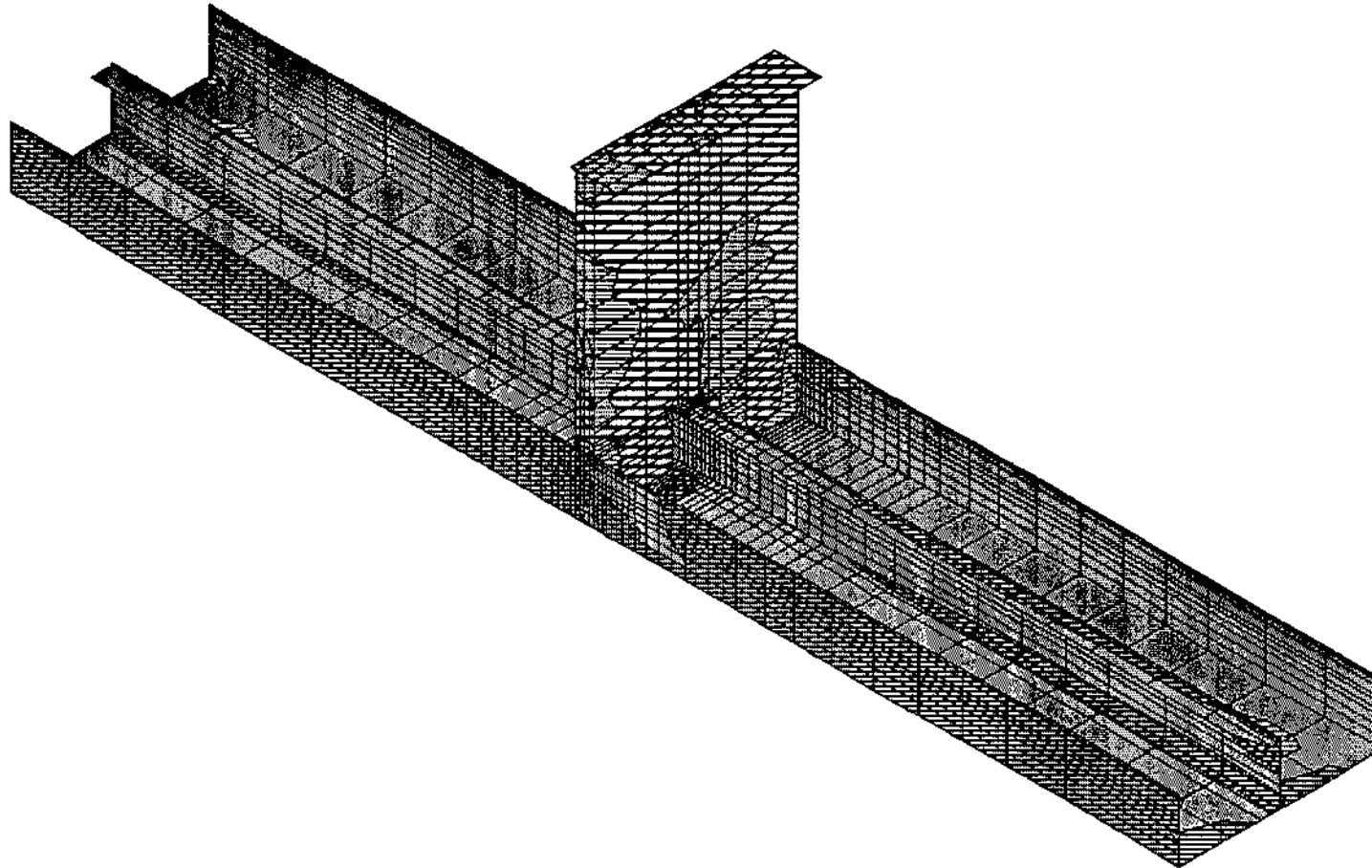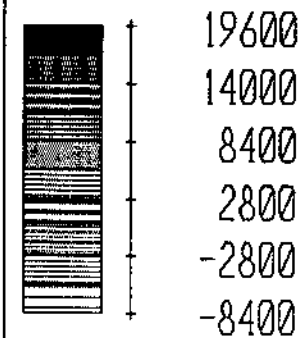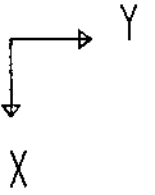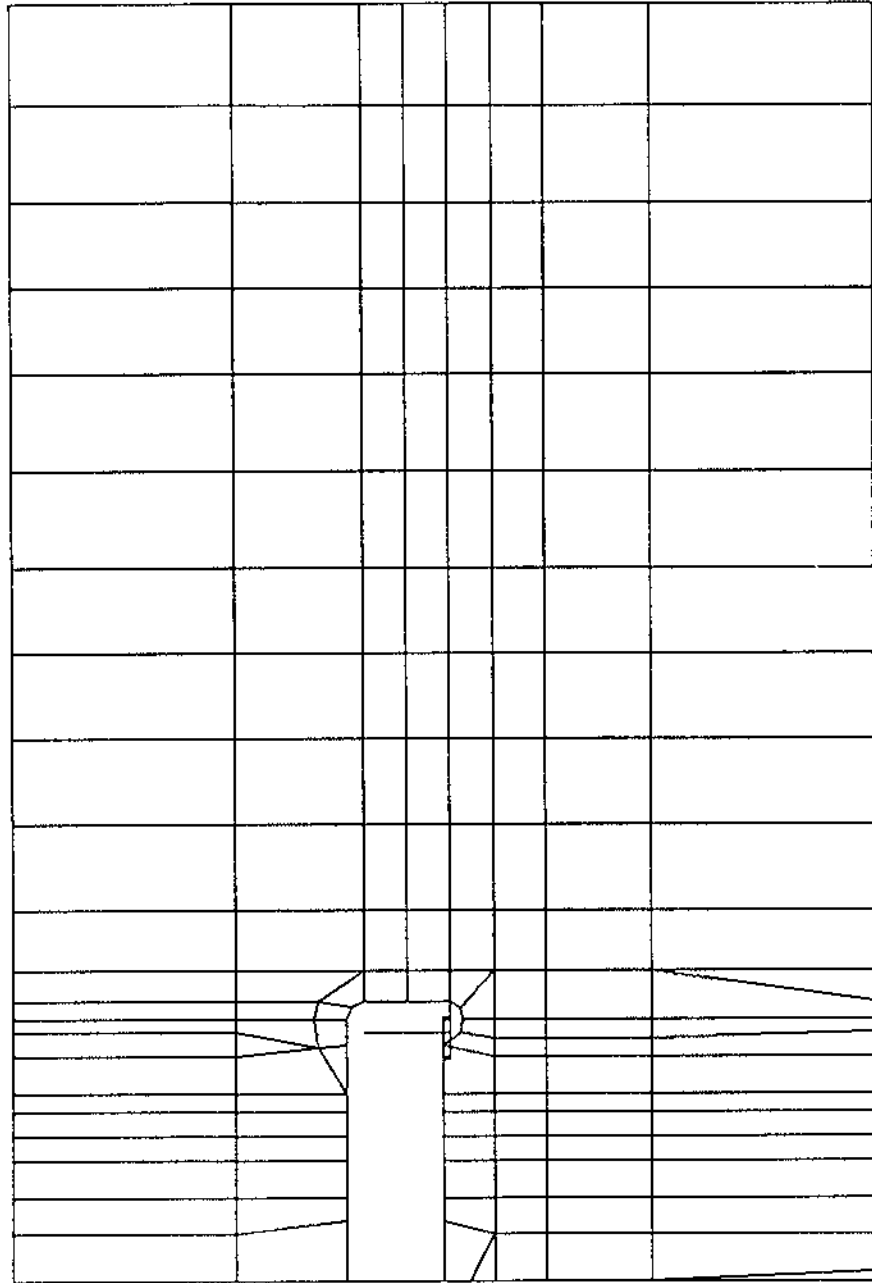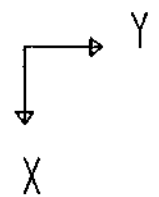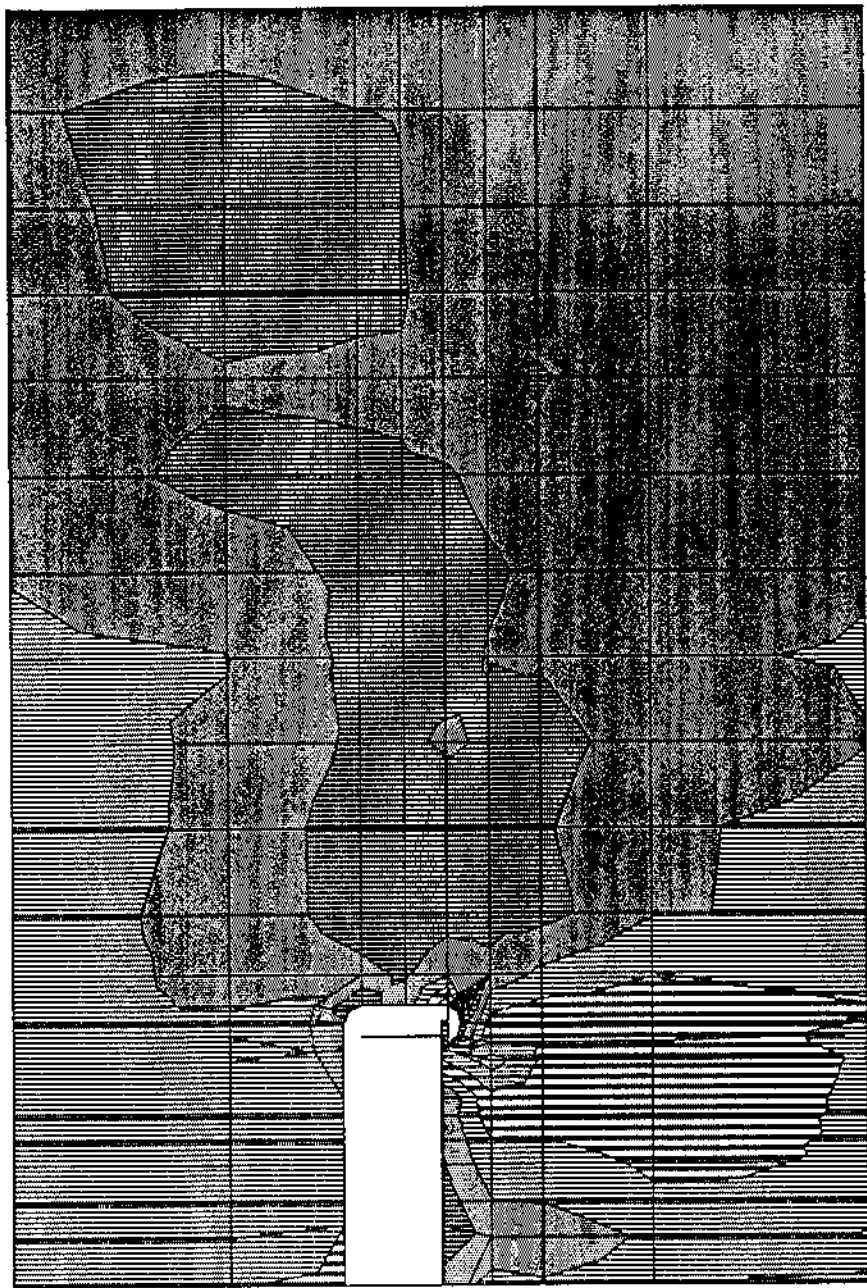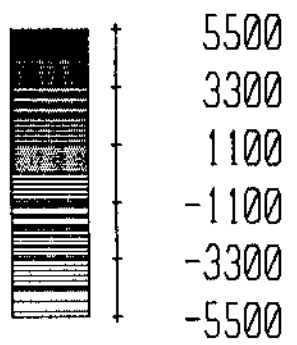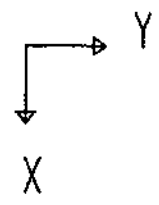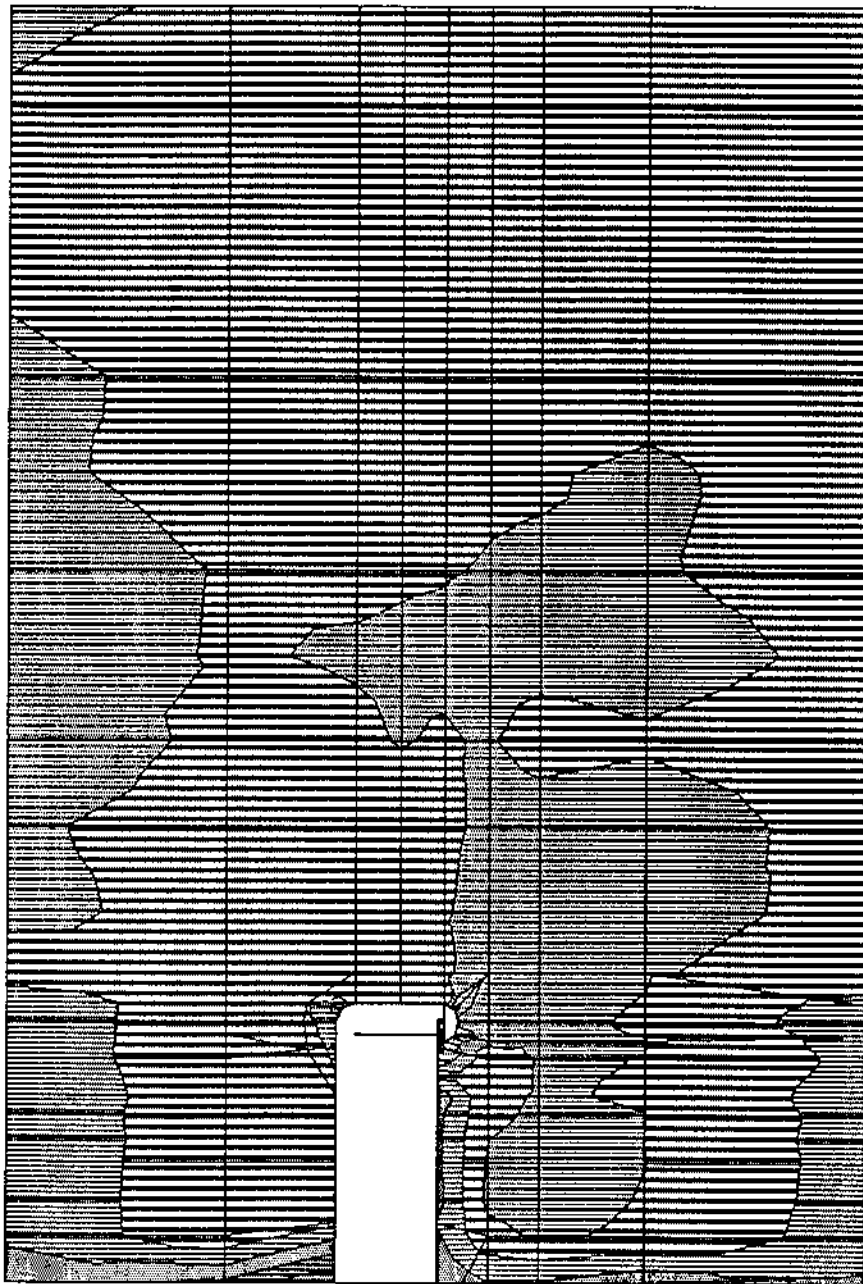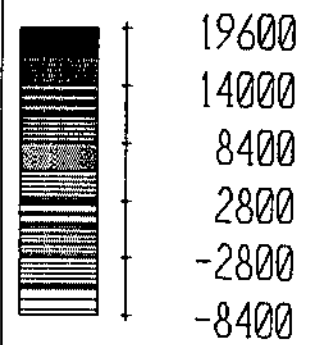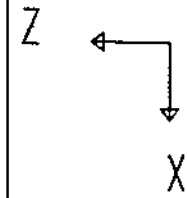
detail2
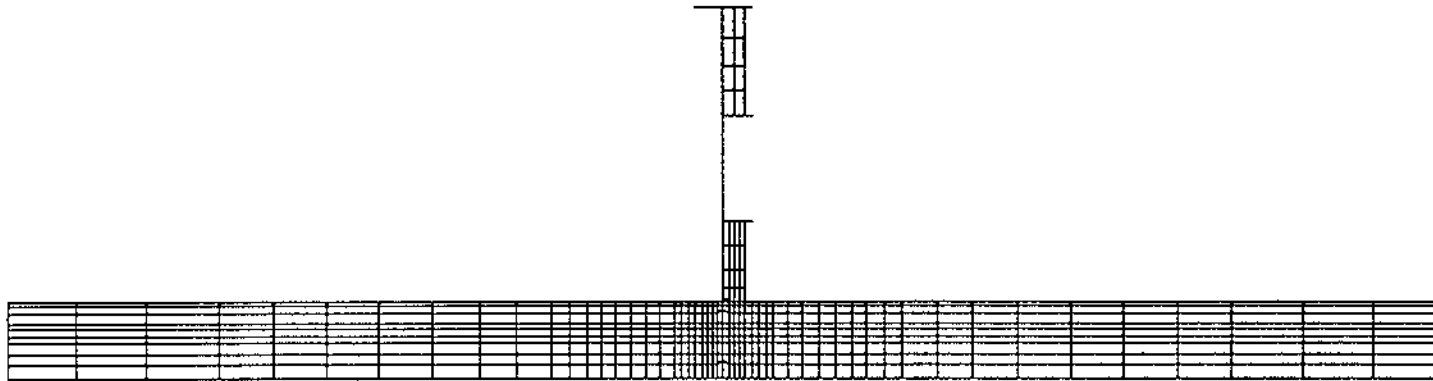
UNDEFORMED
SHAPE

OPTIONS
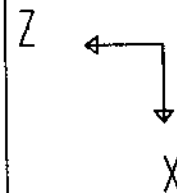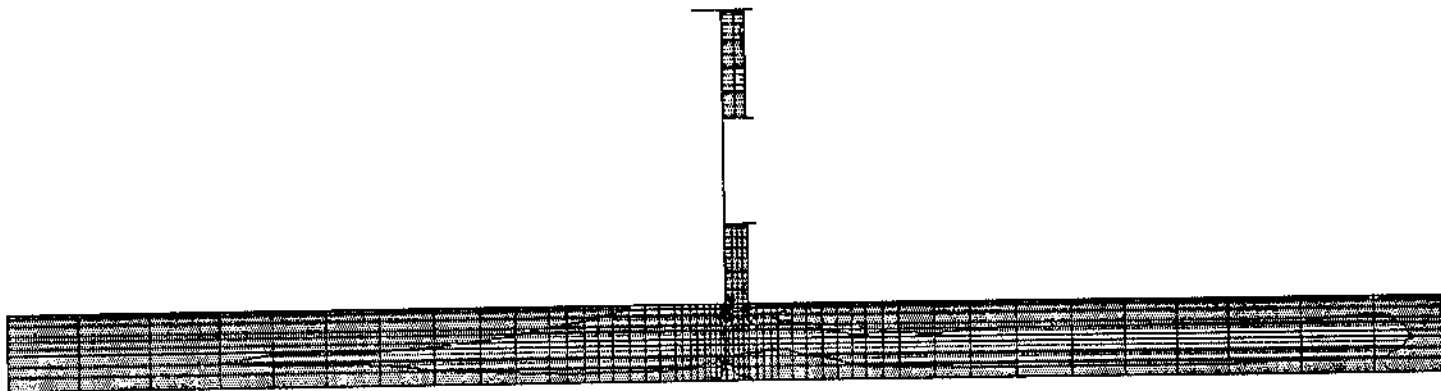
WIRE FRAME

SAP90

detail4

SHELL

OUTPUT SMXT
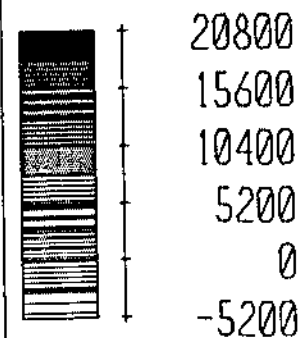
LOAD   1

20800
15600
10400
5200
0
-5200

MIN IS -0.489E+04 <JOINT 1172>   MAX IS   0.185E+05 <JOINT   1171>

SAP90

10"

30"

105" x 0.46"

6"

20"

404" x 0.46"

105" x 0.46"

2.5"   2.5"
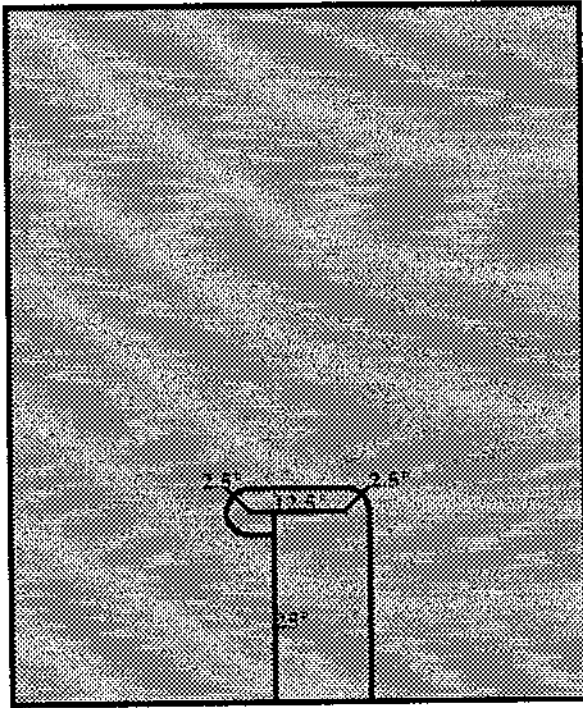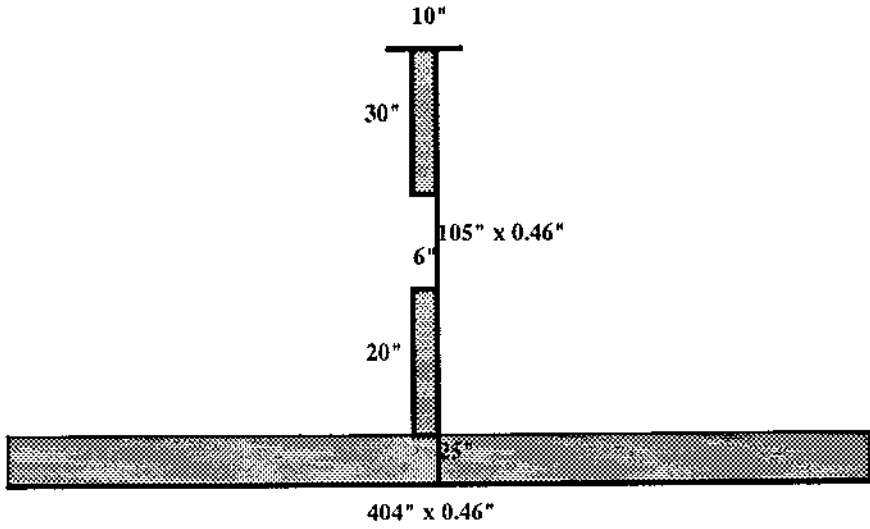
70" x 0.46"
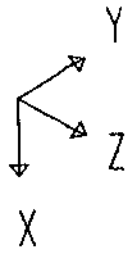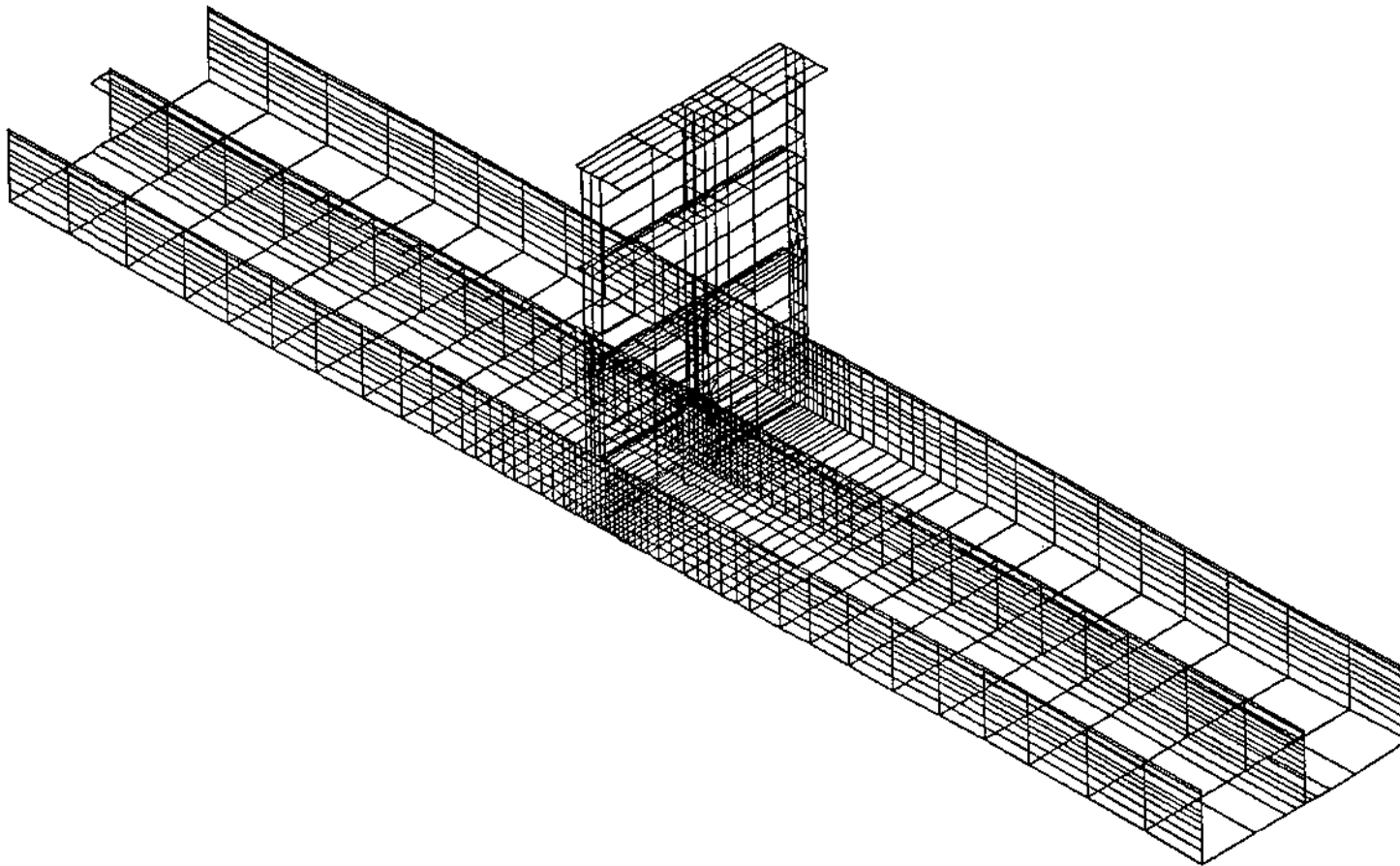
detail5

UNDEFORMED
SHAPE

OPTIONS

WIRE FRAME
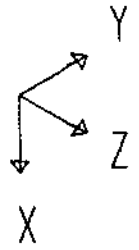
SAP90

detail5

DEFORMED
SHAPE

LOAD   1

MINIMA
X-0.4495E-01
Y-0.2375E+01
Z-0.1548E+00
MAXIMA
X 0.6452E-01
Y-0.2329E+01
Z-0.3119E-01
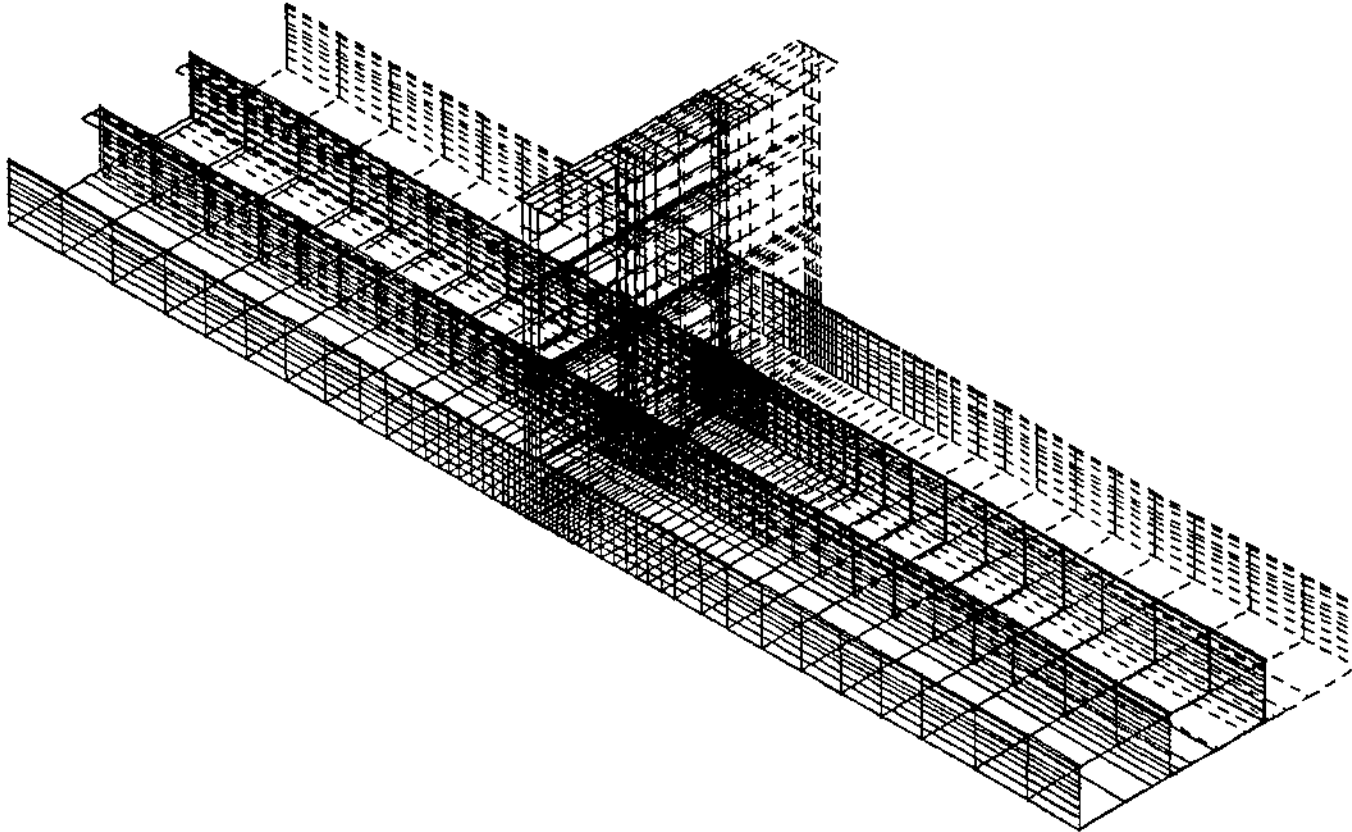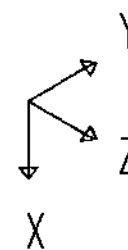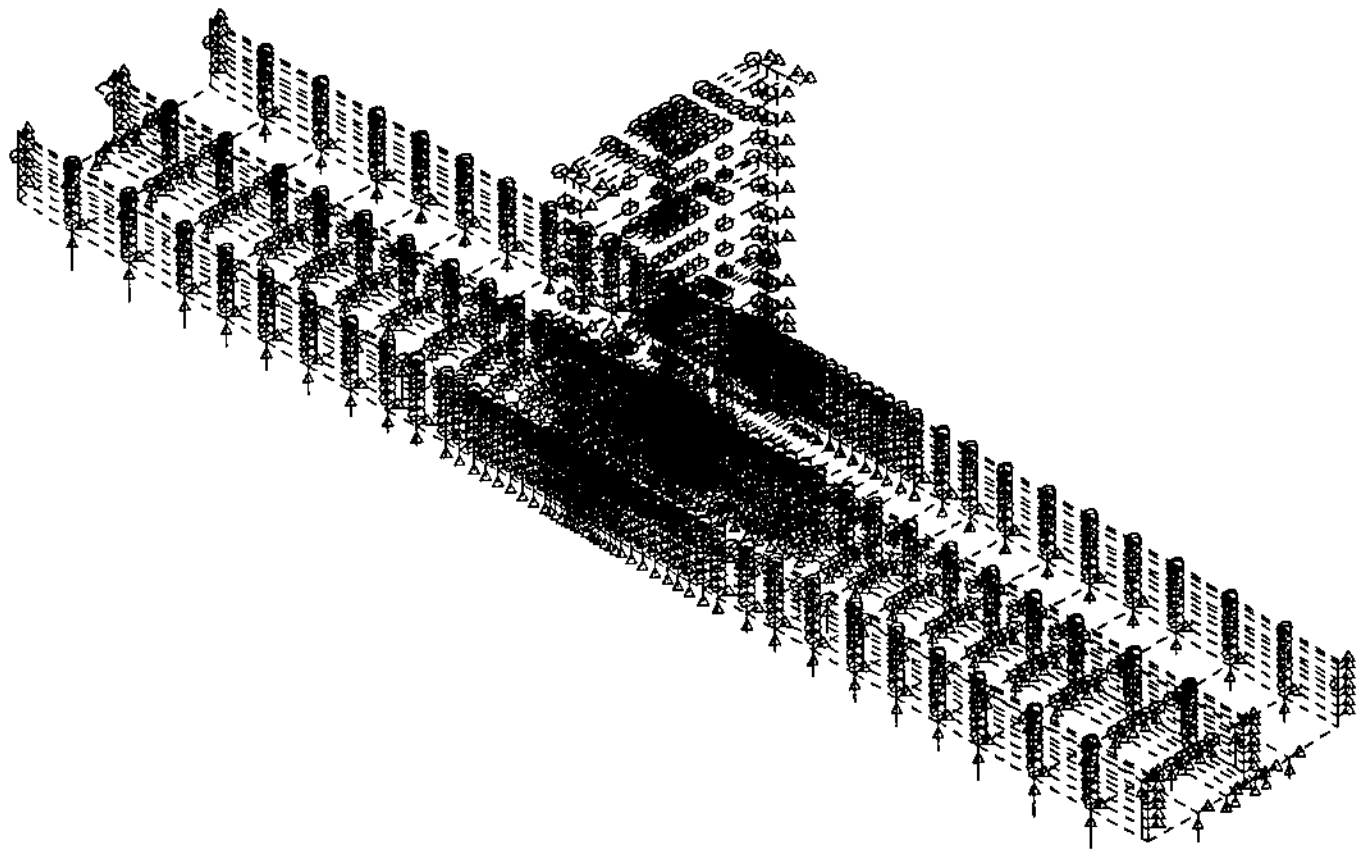
SAP90

detail5

JOINT
LOADS

LOAD   1

MINIMA
P-0.1563E+04
MAXIMA
P-0.2288E-01

SAP90

Y
Z
X

detail5

SHELL
OUTPUT   S11T

LOAD   1

20000
12000
4000
-4000
-12000
-20000
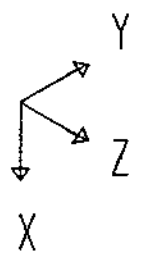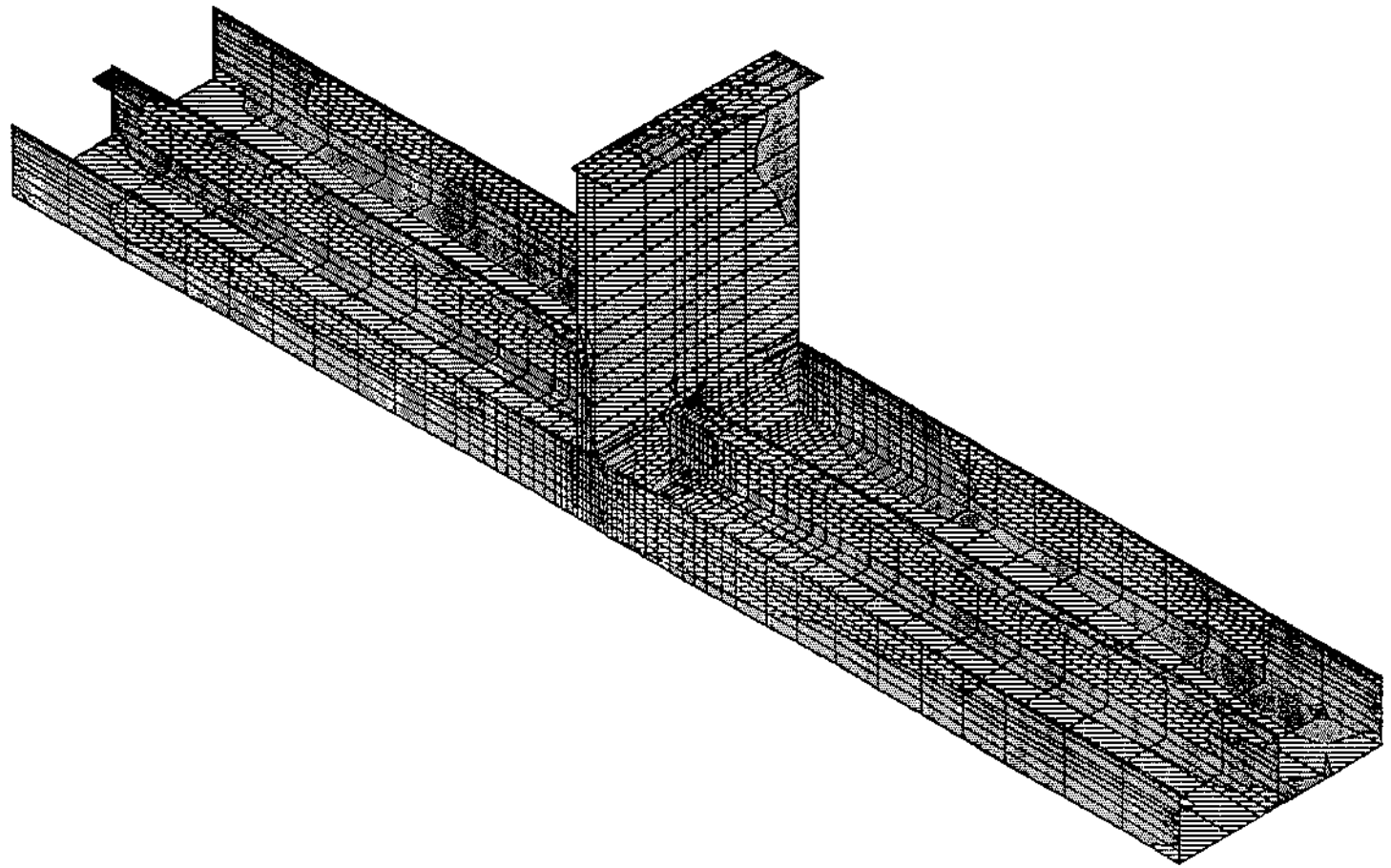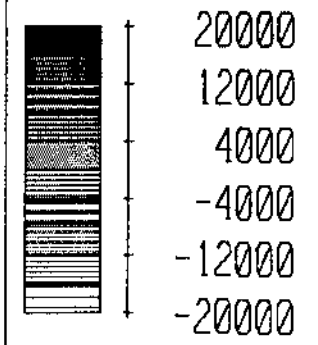
MIN IS -0.171E+05 <JOINT 1172>   MAX IS   0.176E+05 <JOINT 2441>

SAP90

Y

Z

X
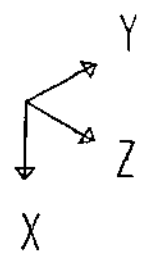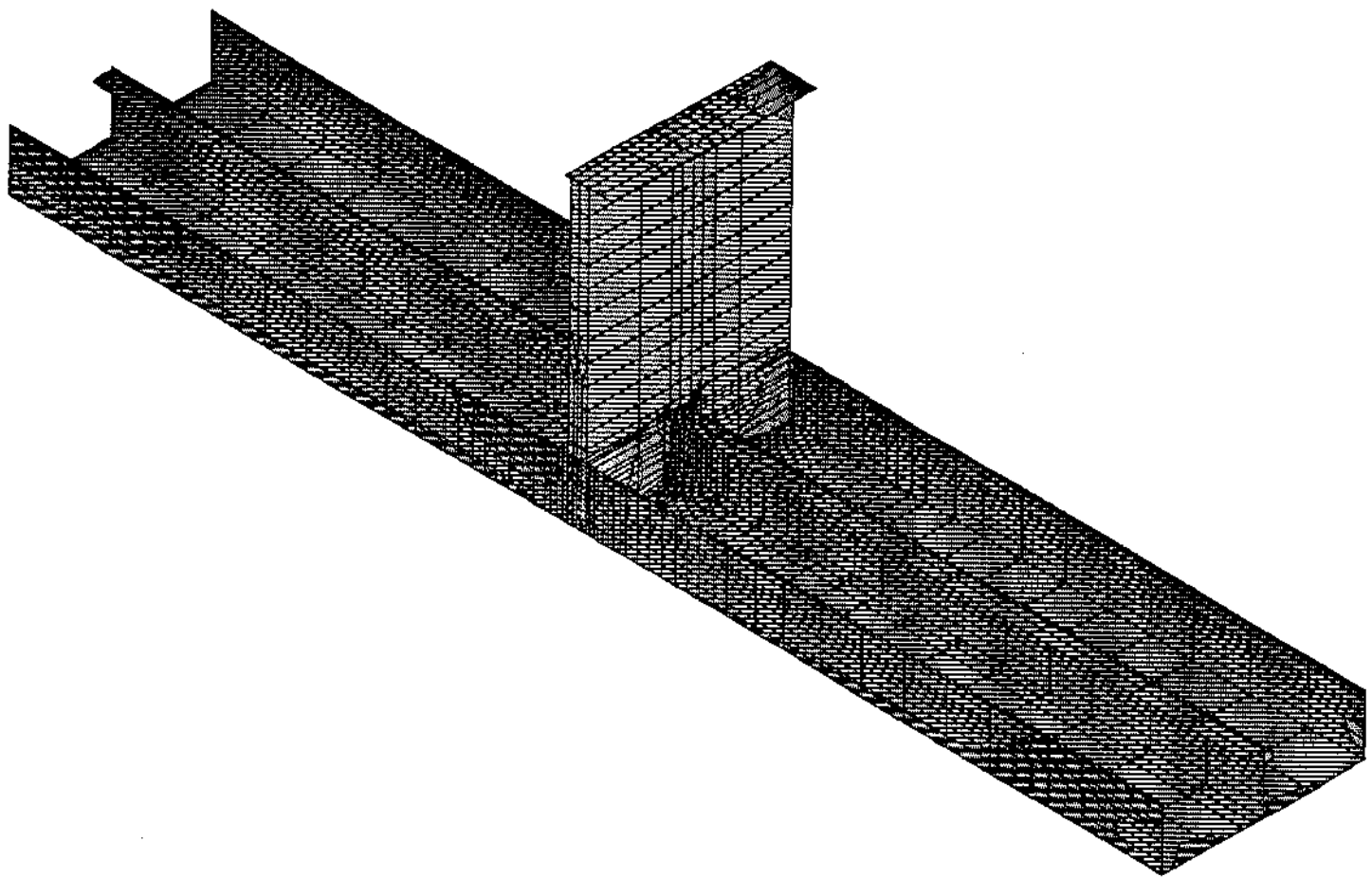
detail5

SHELL

OUTPUT S22T

LOAD   1

22500
13500
4500
-4500
-13500
-22500
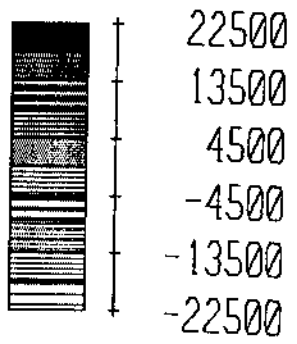
MIN IS -0.207E+05 <JOINT 1180>   MAX IS   0.164E+05 <JOINT 2412>

SAP90

MIN IS -0.501E+04 ⟨JOINT 2388⟩   MAX IS   0.461E+04 ⟨JOINT 2324⟩

detail5
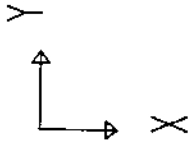
SHELL

OUTPUT SMXT

LOAD 1

18200
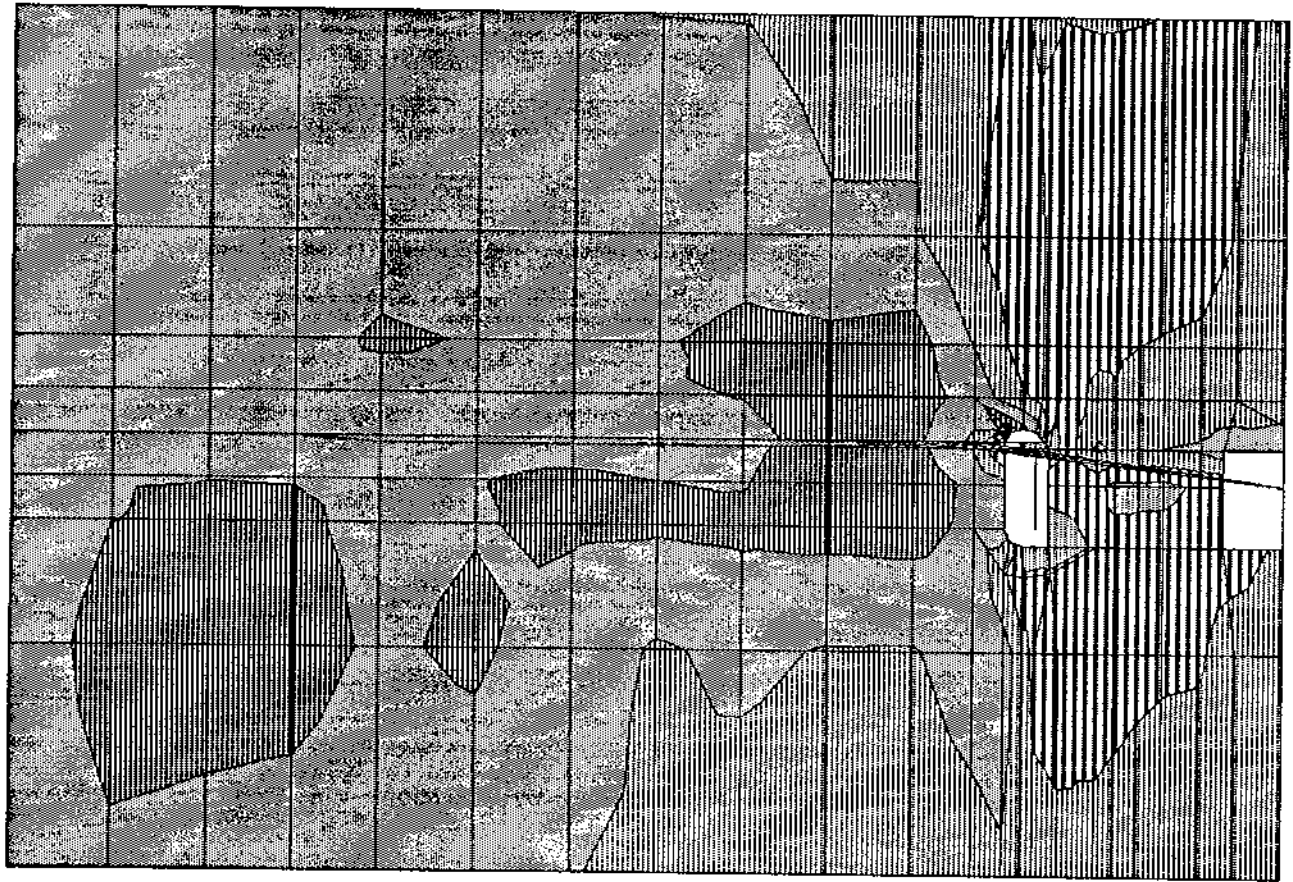13000
7800
2600
-2600
-7800

SAP90

Y

X

detail5

UNDEFORMED
SHAPE

OPTIONS
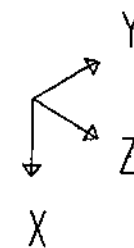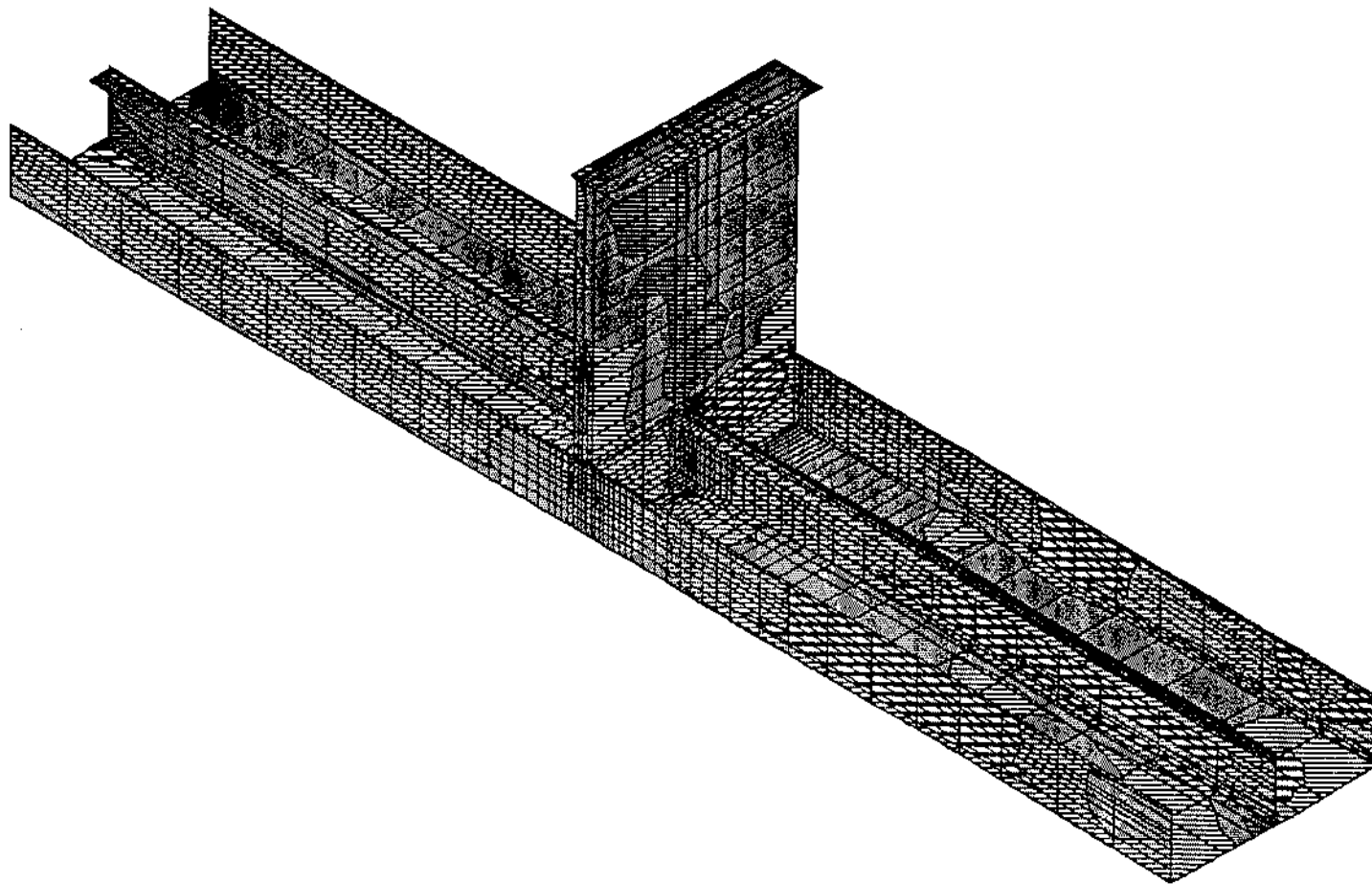
WIRE FRAME

SAP90

detail5

SHELL

OUTPUT   S12T

LOAD   1

5500
3300
1100
-1100
-3300
-5500
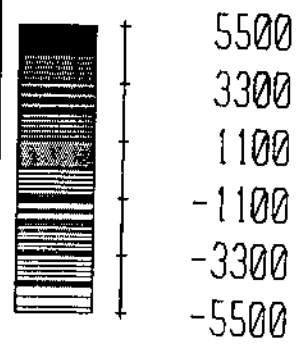
MIN IS -0.501E+04 <JOINT 2388>   MAX IS   0.461E+04 <JOINT 2324>

SAP90
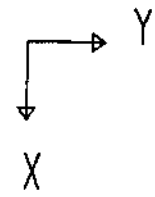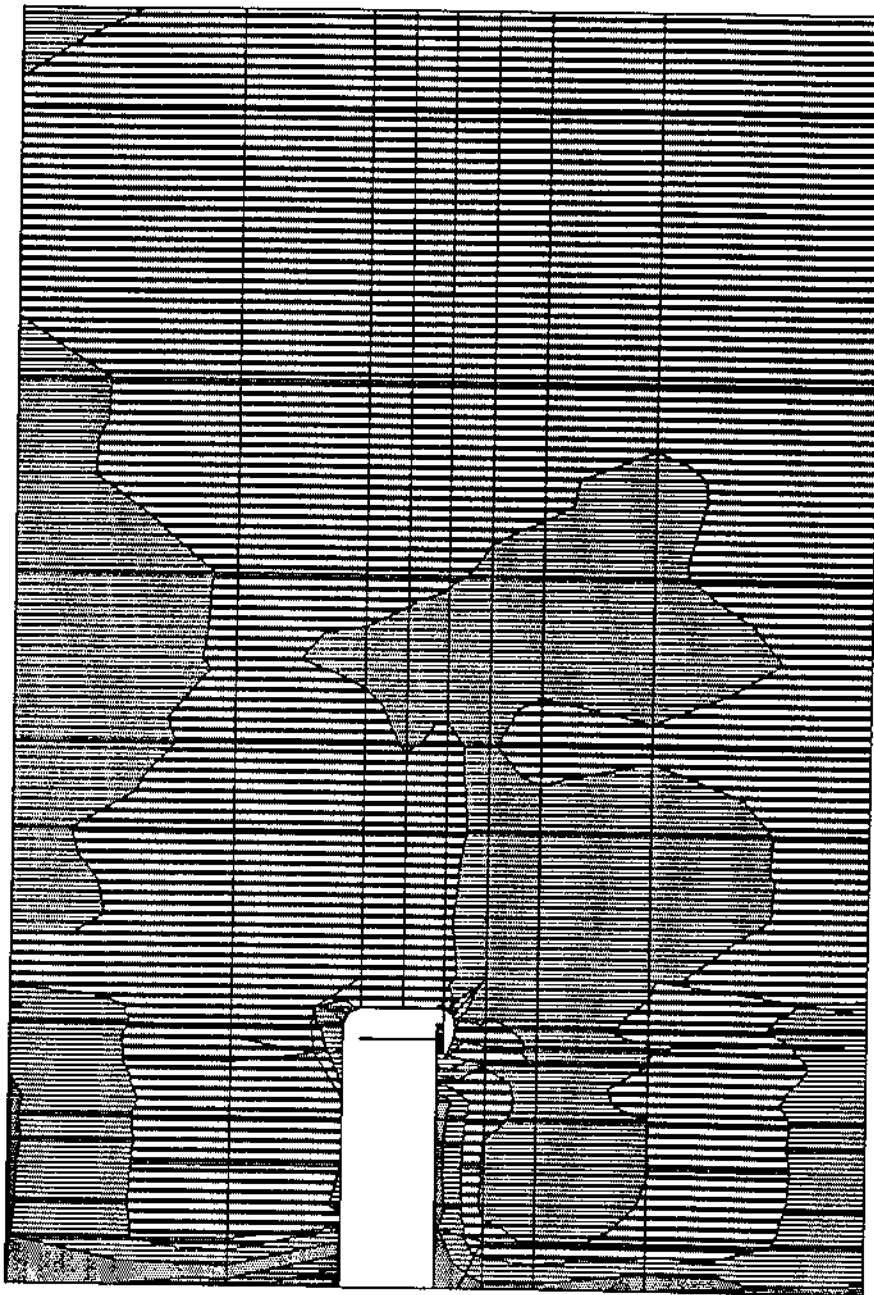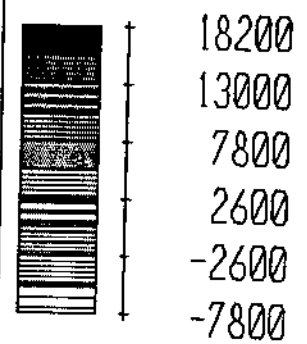
detail5

SHELL

OUTPUT SMXT

LOAD   1

18200
13000
7800
2600
-2600
-7800

MIN IS -0.706E+04 <JOINT   1172>   MAX IS   0.180E+05 <JOINT   2441>   SAP90
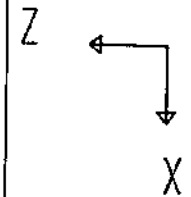
Z

X

detail5

UNDEFORMED
SHAPE

OPTIONS

WIRE FRAME

SAP90

Z ←
   ↓
      X

detail5

SHELL

OUTPUT S12T

LOAD   1

5500
3300
1100
-1100
-3300
-5500
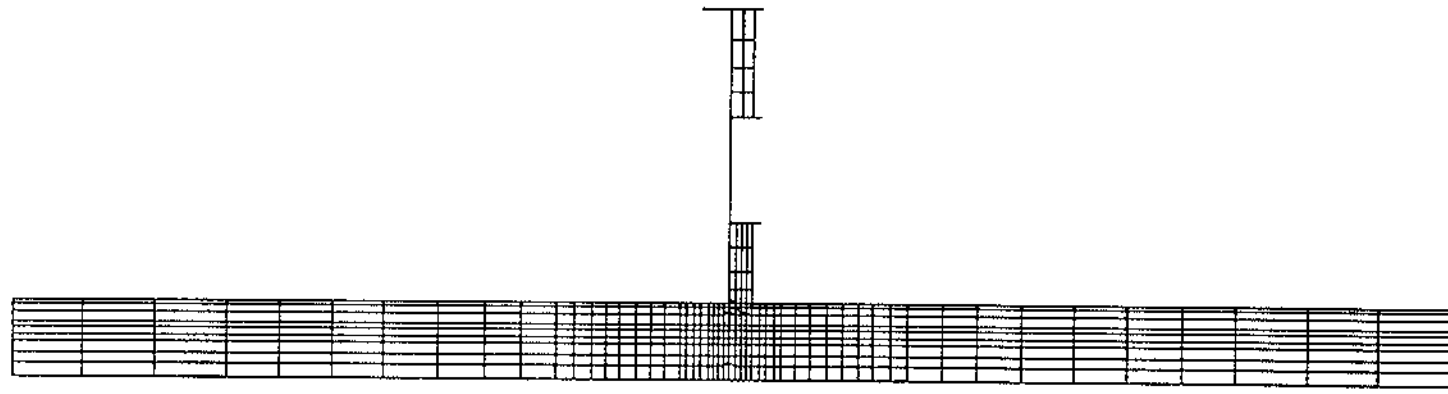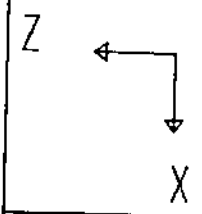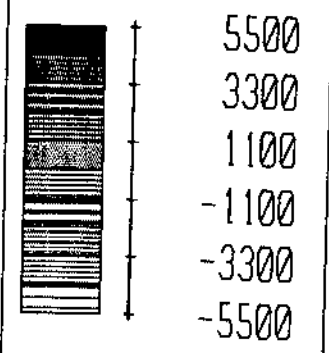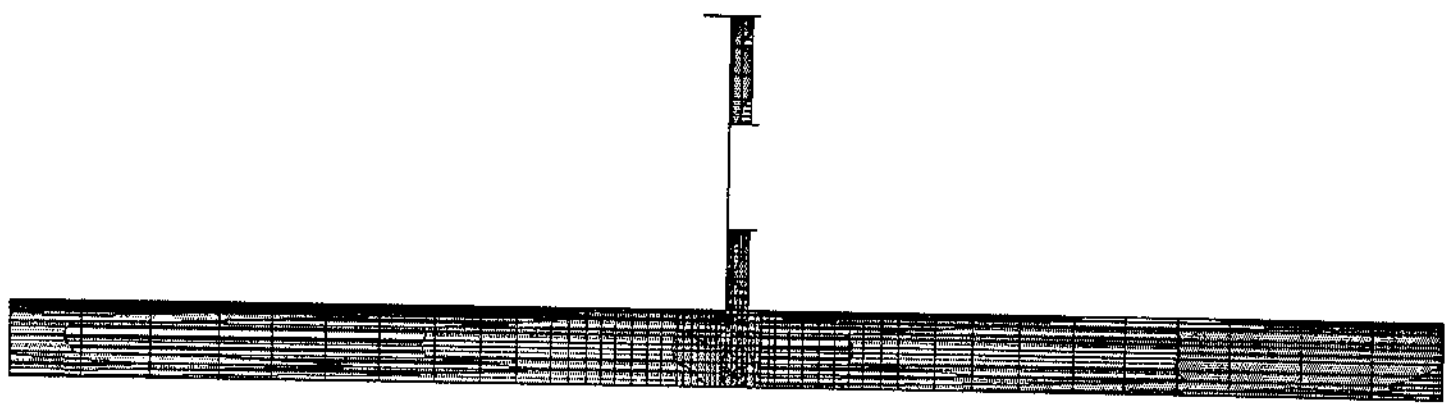
MIN IS -0.518E+04 <JOINT 1192>   MAX IS   0.457E+04 <JOINT 1180>

SAP90

Z

X

detail5

SHELL

OUTPUT   SMXT

LOAD   1

17500
12500
7500
2500
-2500
-7500
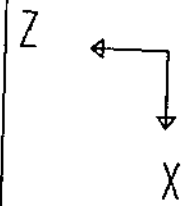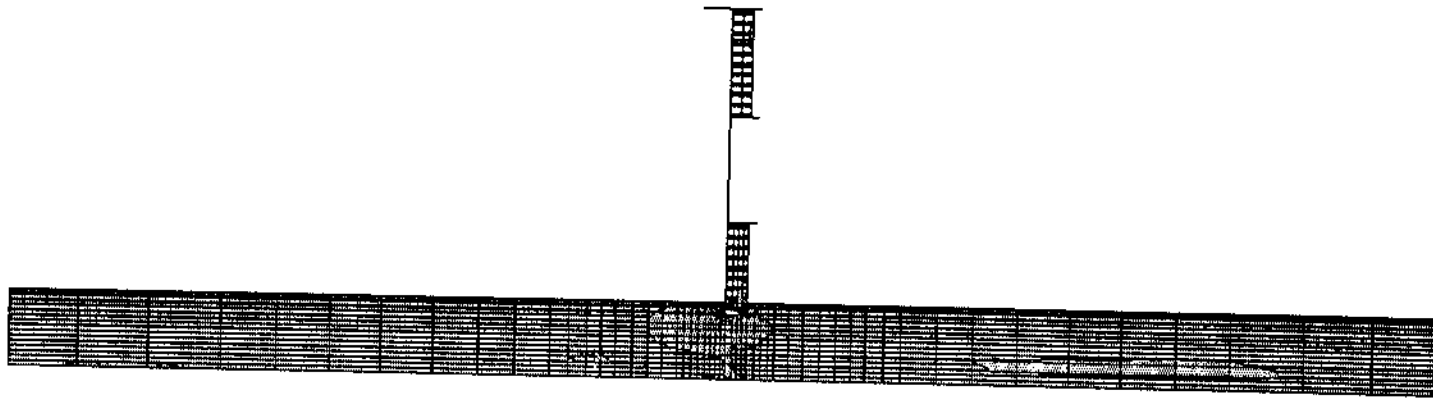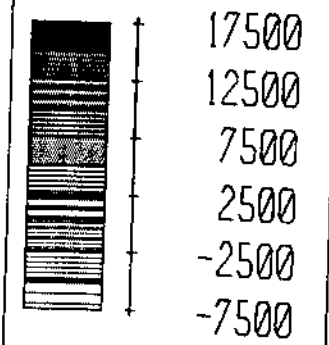
MIN IS -0.706E+04 <JOINT 1172>   MAX IS   0.174E+05 <JOINT 1171>   SAP90

10"

30"

105" x 0.46"

6'
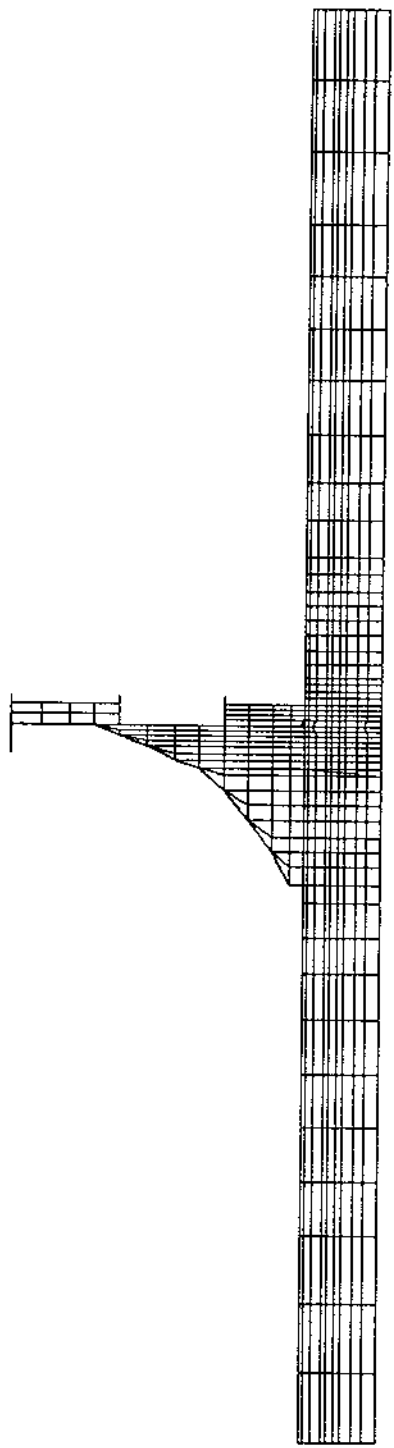
20"

2.5"

404" x 0.46"

105" x 0.46"

2.5"

12.5"

2.5"

70" x 0.46"

362

Y

Z

X
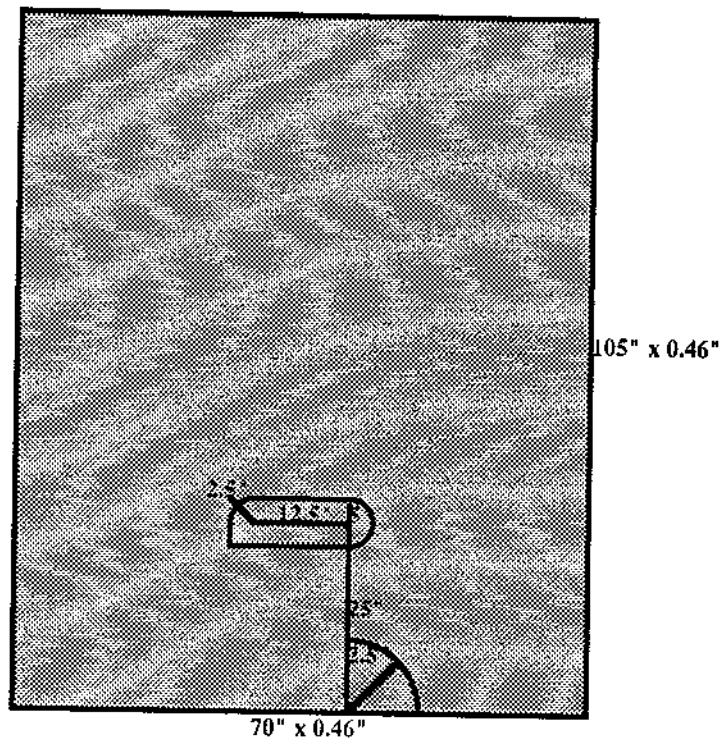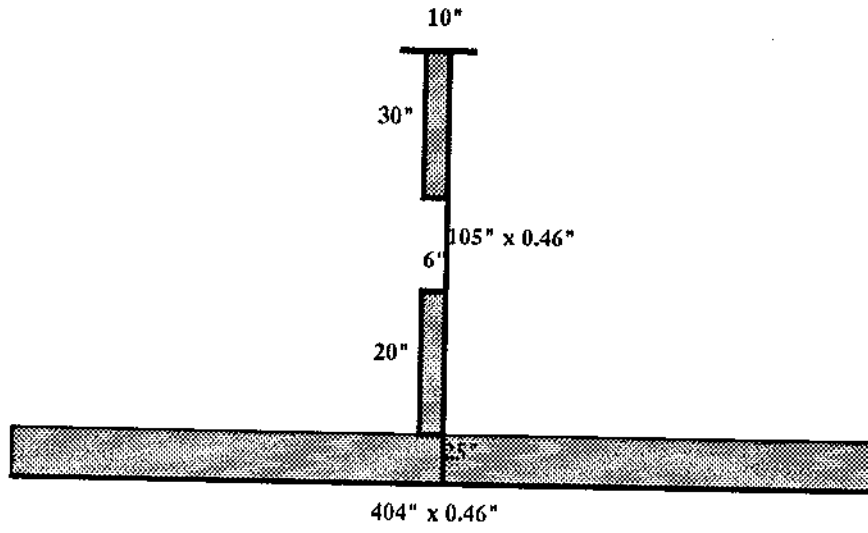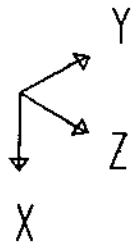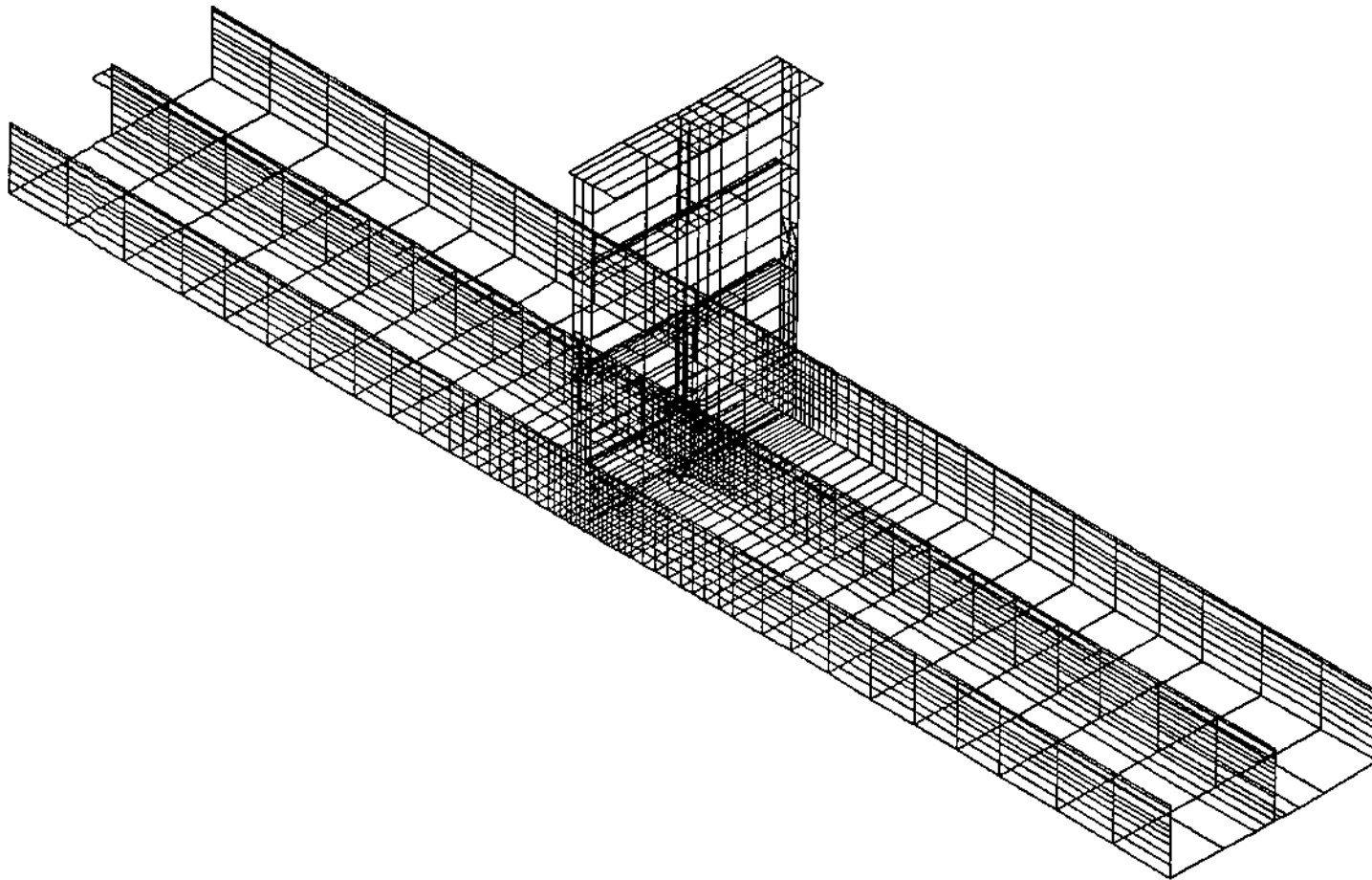
detail6

UNDEFORMED
SHAPE

OPTIONS

WIRE FRAME
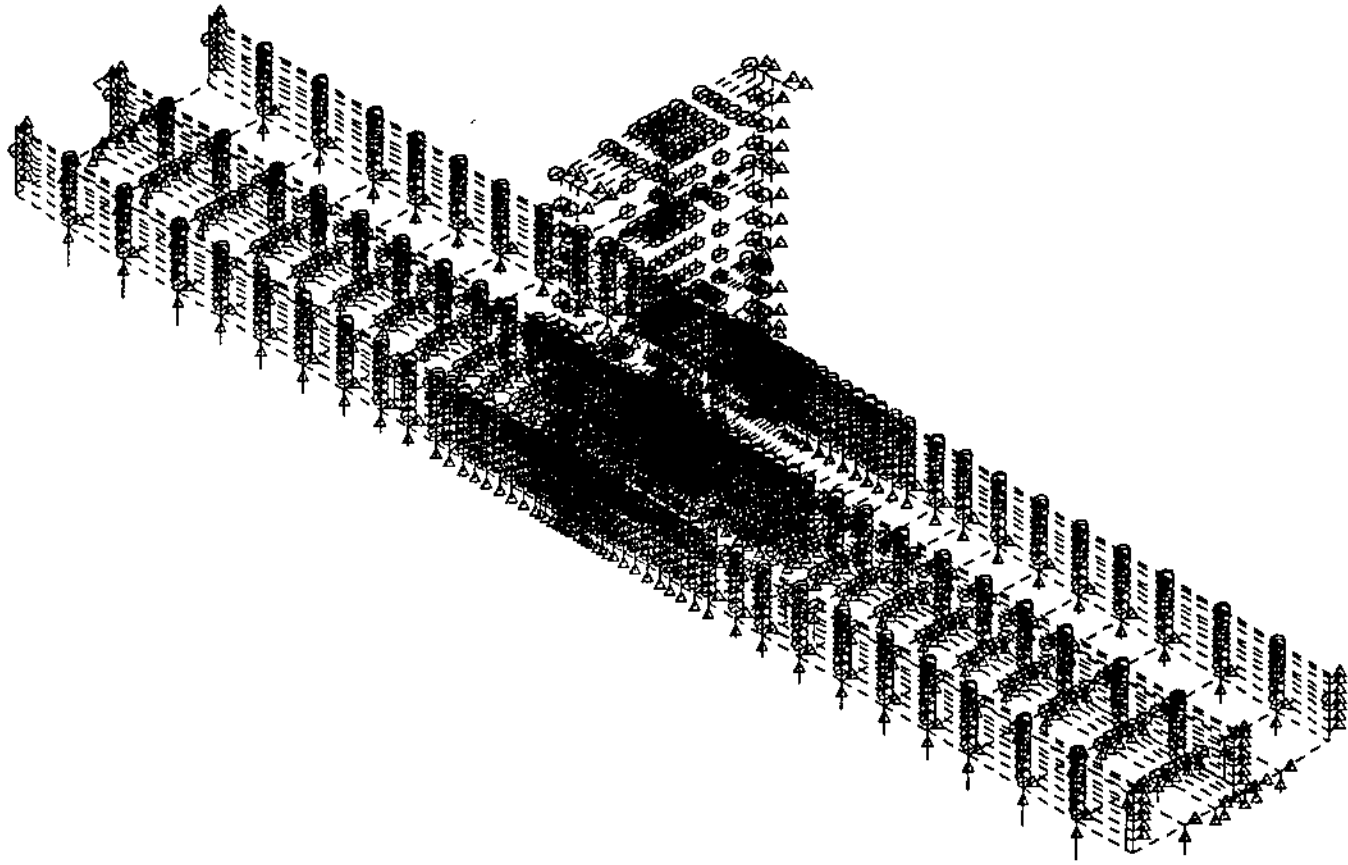
SAP90

detail6

JOINT
LOADS

LOAD   1

MINIMA
P-0.1563E+04
MAXIMA
P-0.2288E-01
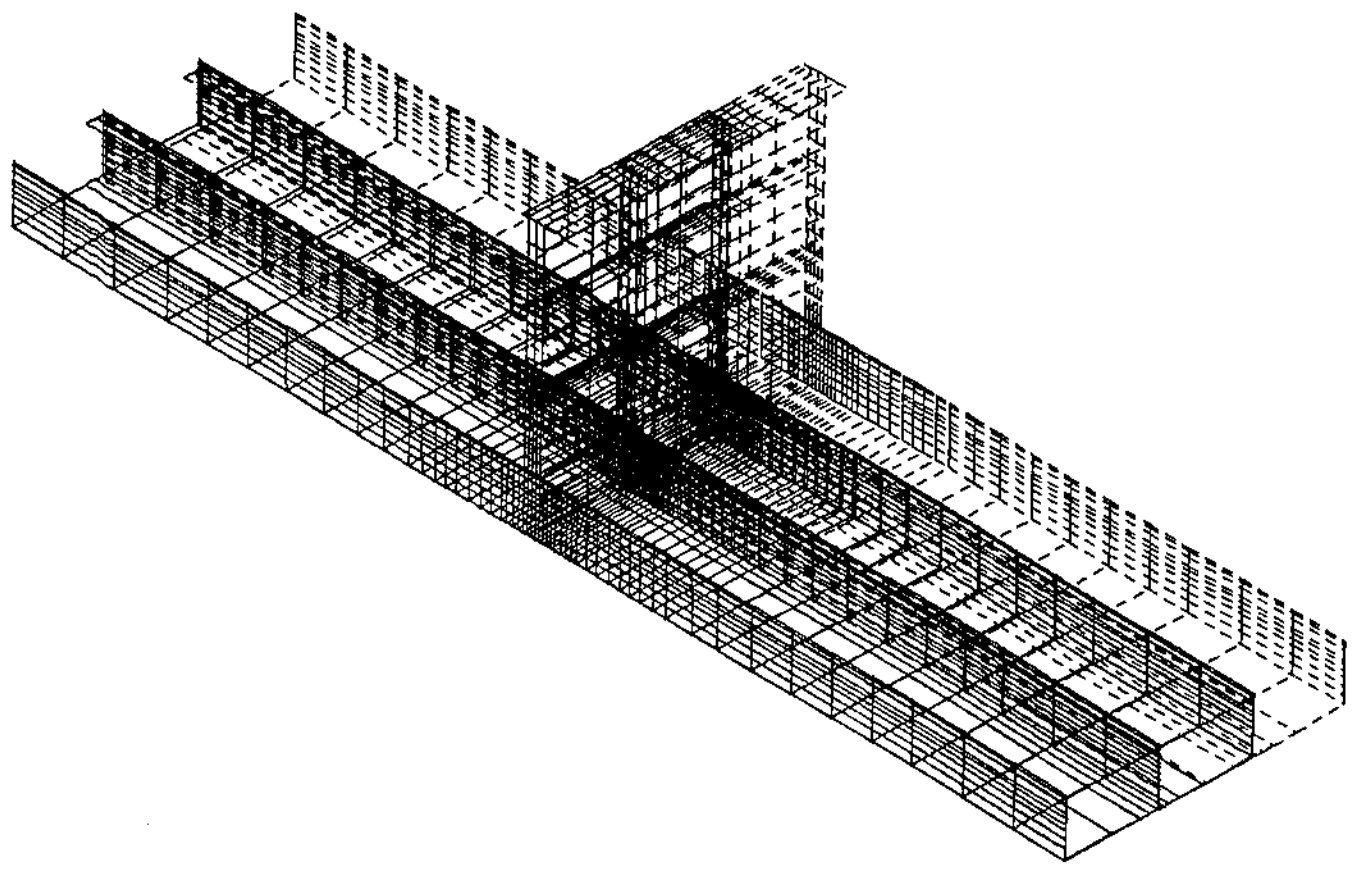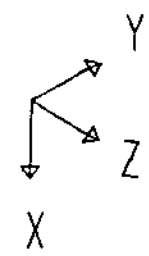
SAP90

detail6

DEFORMED
SHAPE

LOAD   1

MINIMA
X-0.4480E-01
Y-0.2375E+01
Z-0.1548E+00
MAXIMA
X 0.6452E-01
Y-0.2329E+01
Z-0.3119E-01

SAP90

detail6

SHELL

OUTPUT S11T

LOAD 1

21000
14000
7000
0
-7000
-14000

MIN IS -0.136E+05 <JOINT 1172>   MAX IS 0.176E+05 <JOINT 2441>
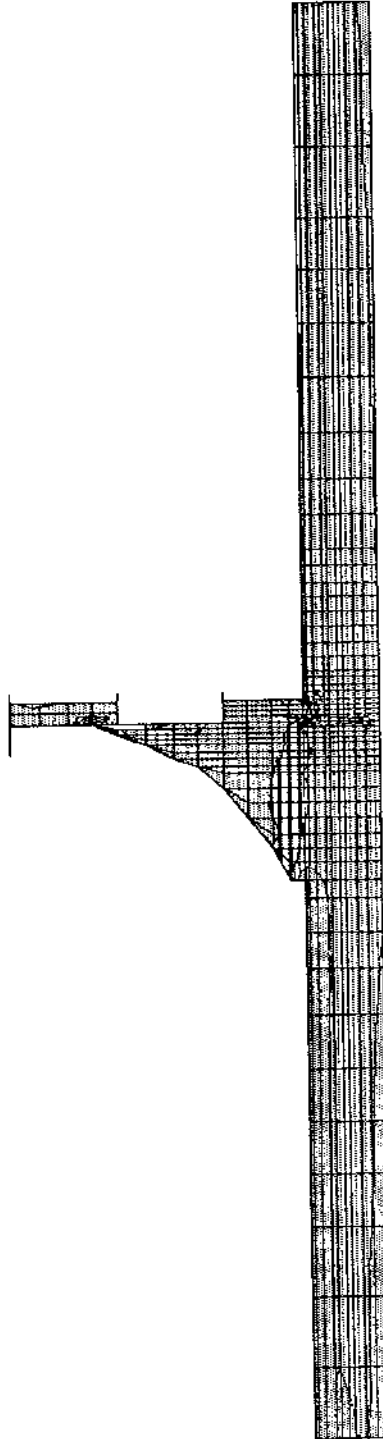
SAP90

detail6

SHELL
OUTPUT   S22T

LOAD   1

21000
14000
7000
0
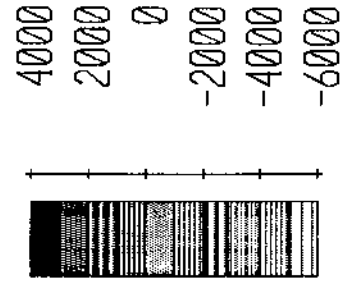-7000
-14000

SAP90

MIN IS -0.138E+05 <JOINT 1172>   MAX IS   0.164E+05 <JOINT 2412>

detail6

SHELL
OUTPUT   S12T

LOAD   1

5000
3000
1000
-1000
-3000
-5000

SAP90

MIN IS -0.493E+04 <JOINT 2388>   MAX IS   0.460E+04 <JOINT 2324>

detail6

SHELL

OUTPUT   SMXT

LOAD   1

20800
15600
10400
5200
0
-5200

MIN IS -0.489E+04 <JOINT   1172>   MAX IS   0.185E+05 <JOINT   1171>

SAP90

detail6

UNDEFORMED
SHAPE

OPTIONS

WIRE FRAME

SAP90

MIN IS -0.493E+04 ⟨JOINT 2388⟩   MAX IS   0.460E+04 ⟨JOINT 2324⟩

Y

X

detail6

SHELL
OUTPUT   SMXT
LOAD   1

20800
15600
10400
5200
0
-5200

SAP90

MIN IS   -0.489E+04 <JOINT   1172>   MAX IS   0.185E+05 <JOINT   1171>

Z

X

detail6

UNDEFORMED
SHAPE

OPTIONS

WIRE FRAME

SAP90

Z ←
X

detail6

SHELL
OUTPUT   SMXT
LOAD   1

20800
15600
10400
5200
0
-5200
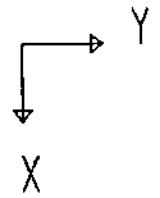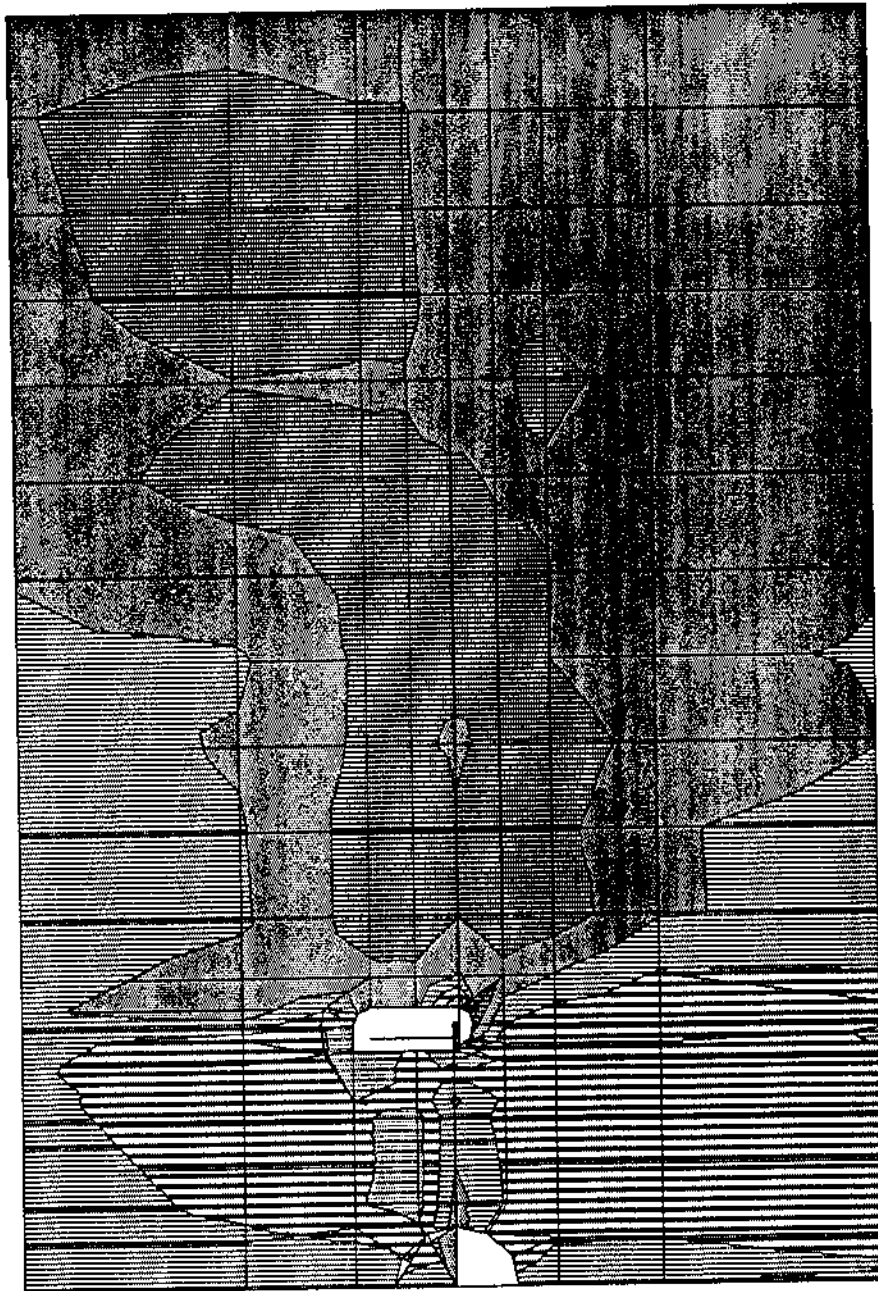
SAP90

MIN IS -0.489E+04 <JOINT 1172>   MAX IS   0.185E+05 <JOINT   1171>

detail7

SHELL

OUTPUT S11T

LOAD   1

21000
14000
7000
0
-7000
-14000

380

MIN IS -0.135E+05 〈JOINT 1172〉   MAX IS   0.176E+05 〈JOINT 2441〉

SAP90

detail7

SHELL

OUTPUT   S22T

LOAD   1

21000
14000
7000
0
-7000
-14000

MIN IS   -0.138E+05 <JOINT   1172>   MAX IS   0.164E+05 <JOINT   2412>

SAP90

Y

Z

X

detail7

SHELL

OUTPUT S12T

LOAD   1

5000
3000
1000
-1000
-3000
-5000

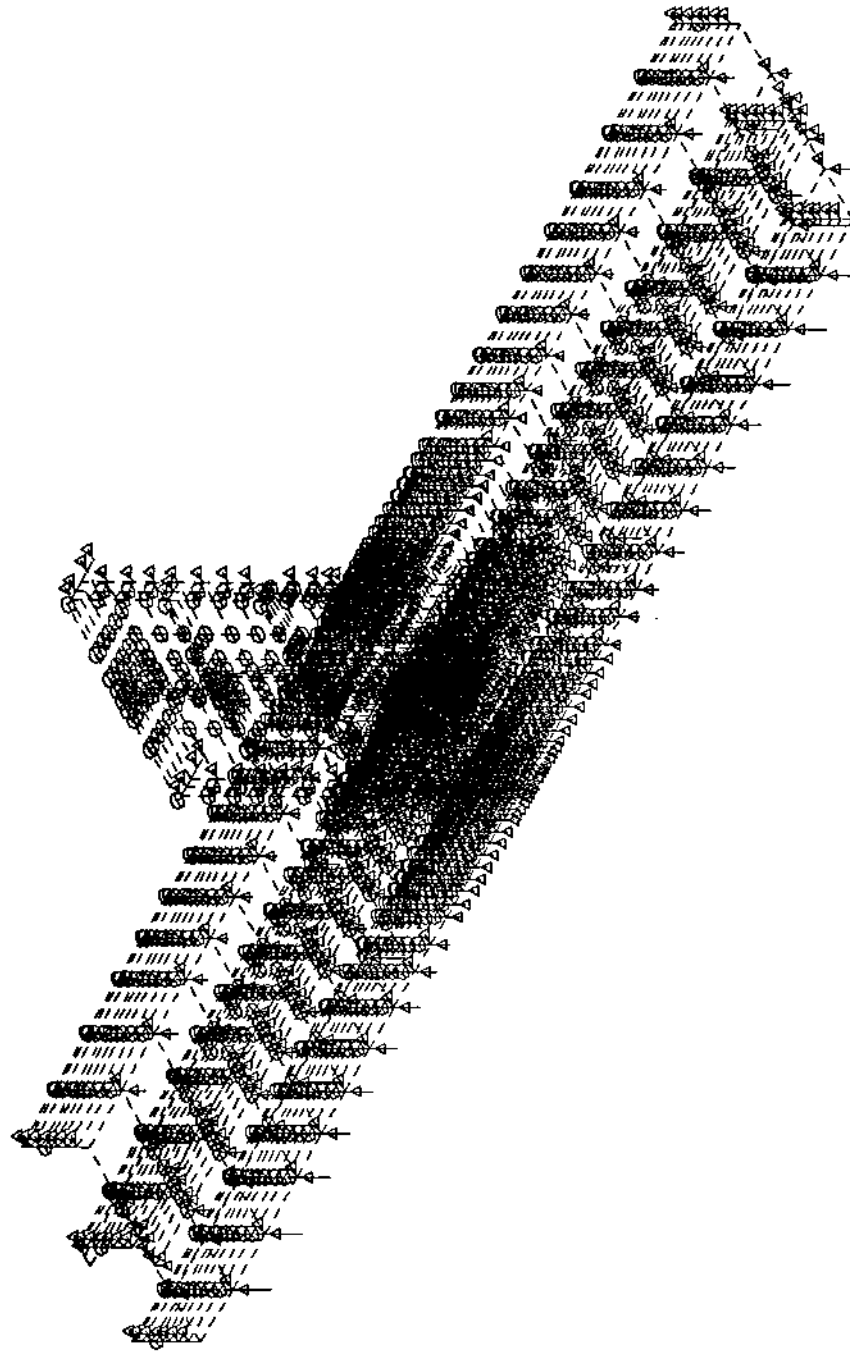MIN IS -0.494E+04 <JOINT 2388>   MAX IS   0.460E+04 <JOINT 2324>

SAP90

detail7

JOINT
LOADS

LOAD   1

MINIMA
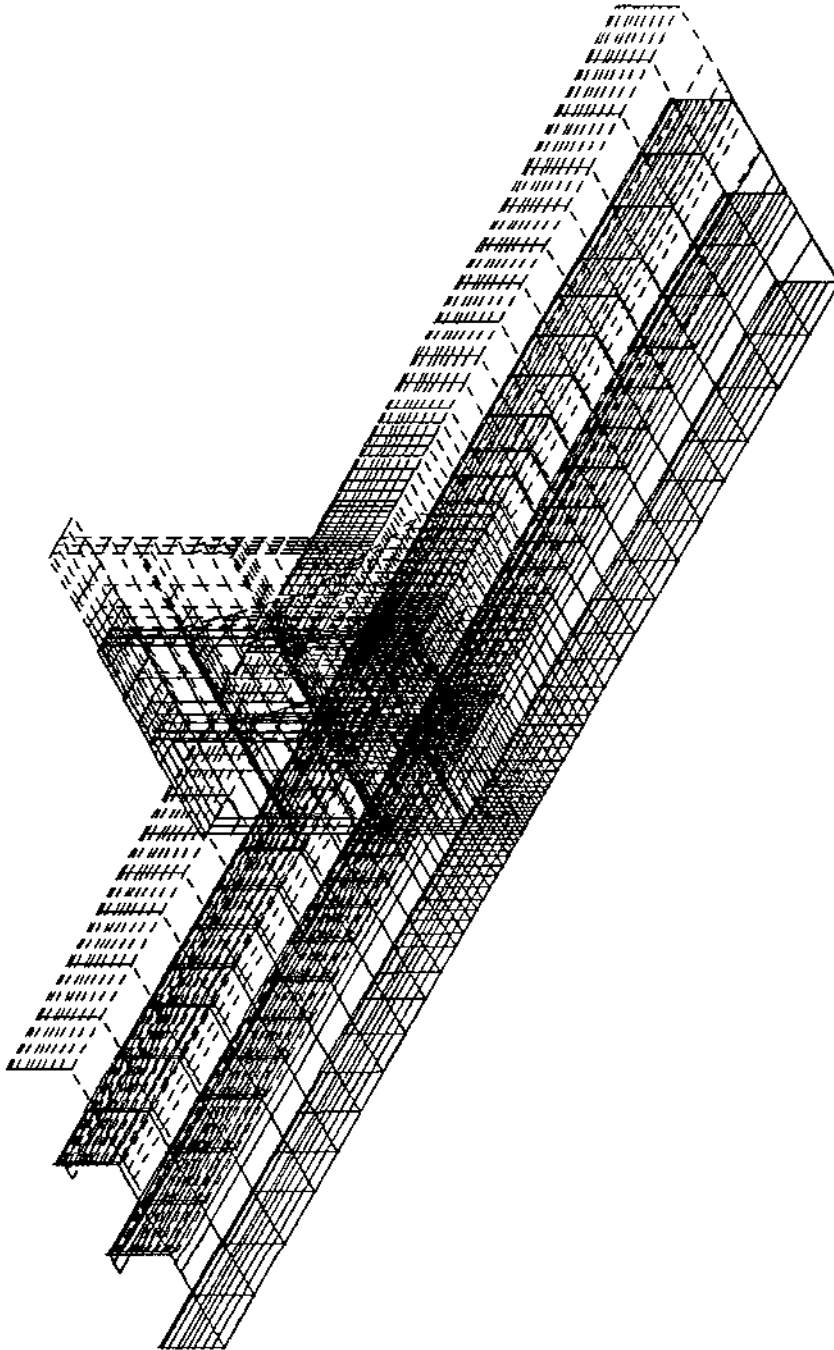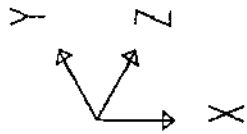P-0.1563E+04
MAXIMA
P-0.2288E-01

SAP90

Y
Z
X
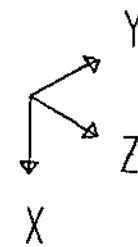
detail7

DEFORMED
SHAPE

LOAD   1

MINIMA
X-0.4482E-01
Y-0.2375E+01
Z-0.1548E+00
MAXIMA
X 0.6452E-01
Y-0.2329E+01
Z-0.3119E-01
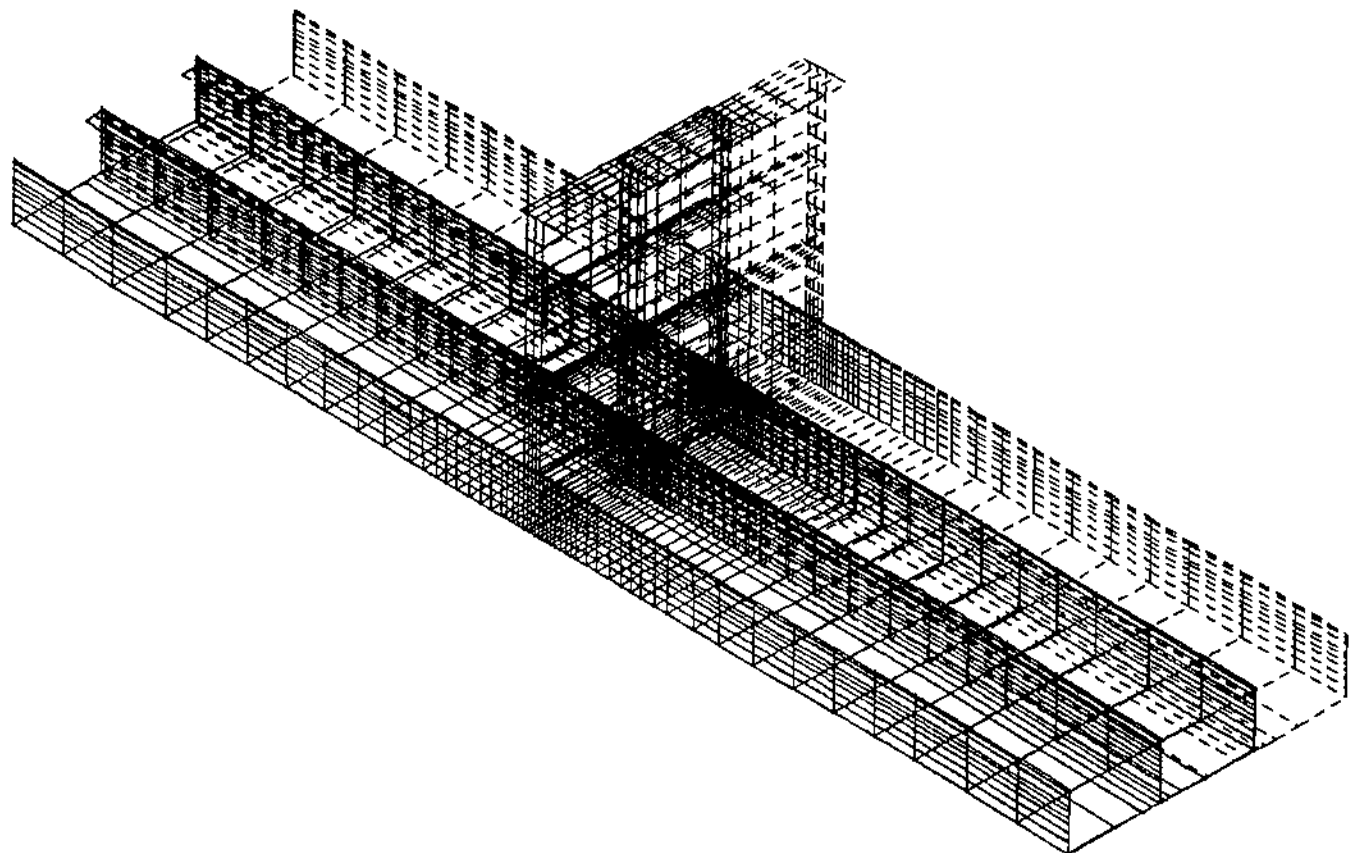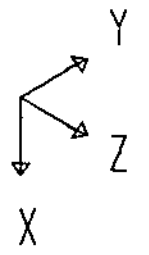
SAP90

Y
Z
X

detail7

UNDEFORMED
SHAPE

OPTIONS
WIRE FRAME

SAP90

10"

30"

105" x 0.46"

6"

20"

25"

404" x 0.46"

105" x 0.46"

2.5"

25"

70" x 0.46"

326

Z

X

detail6

SHELL
OUTPUT S12T

LOAD   1

5000
3000
1000
-1000
-3000
-5000
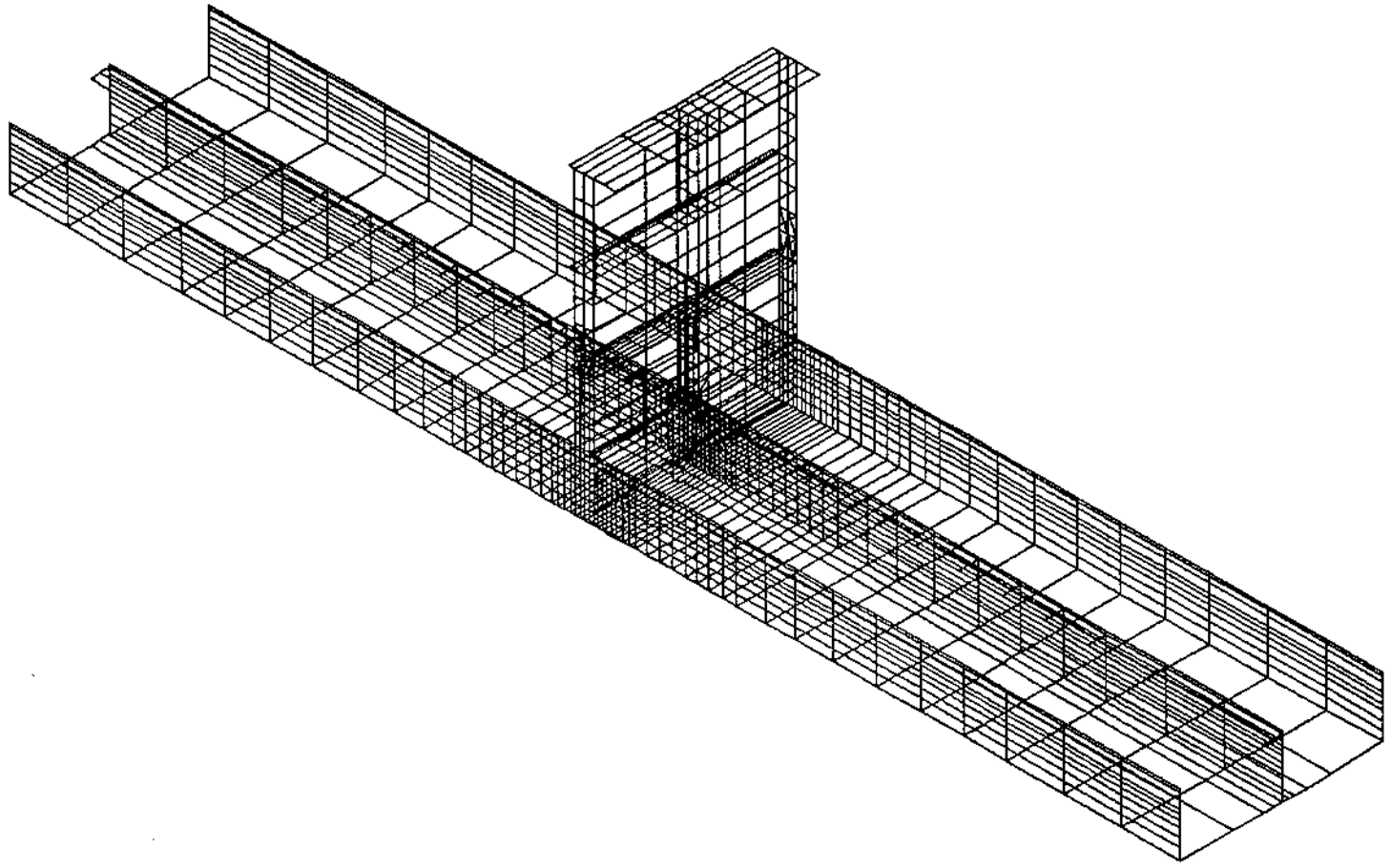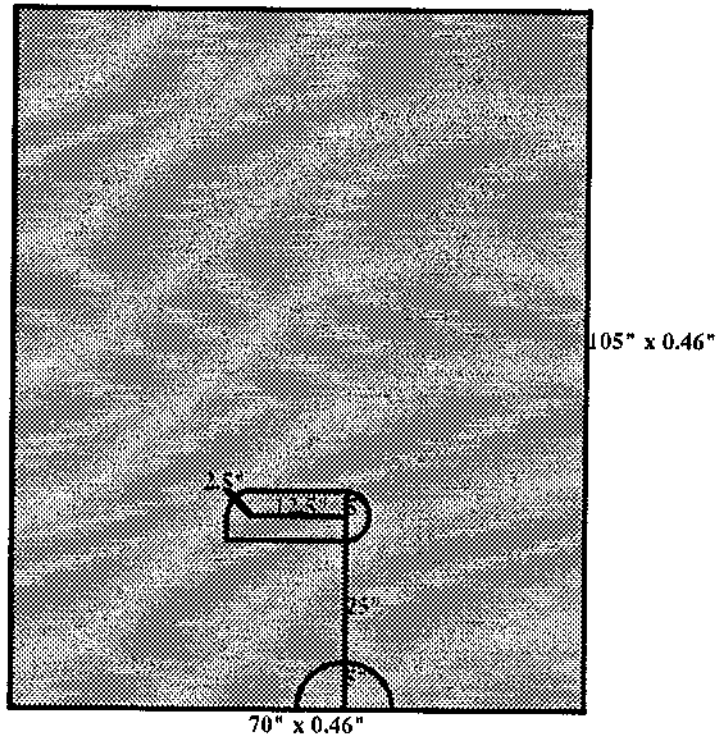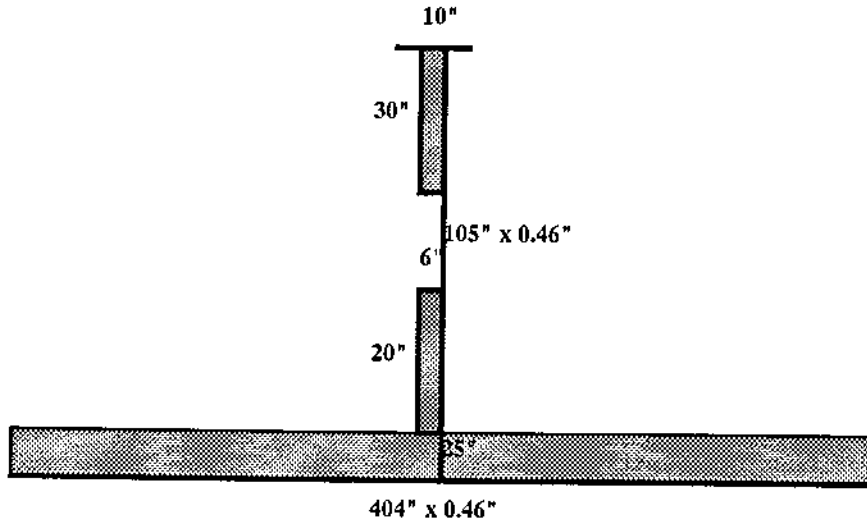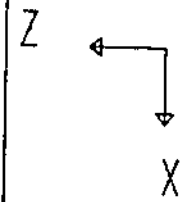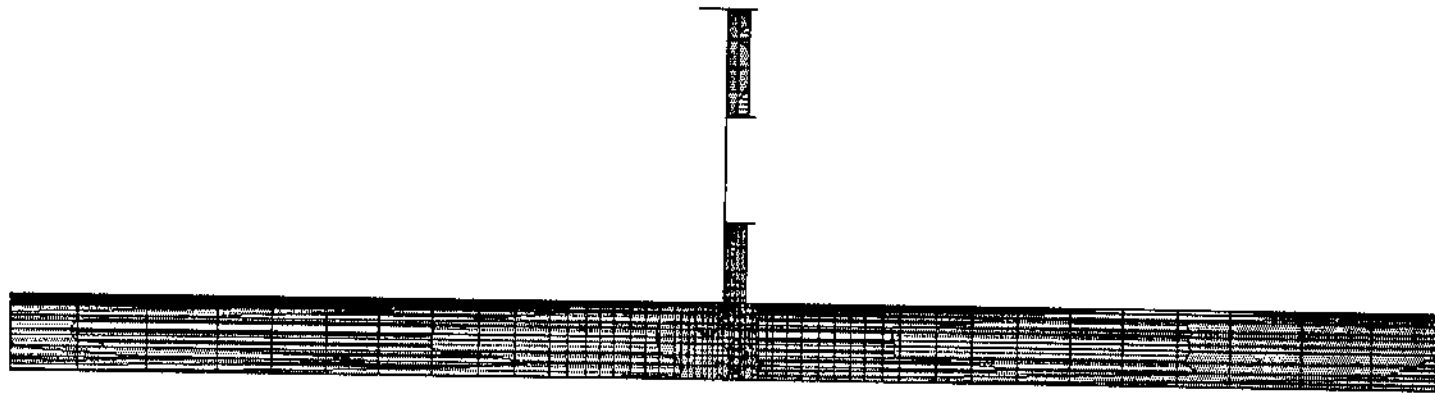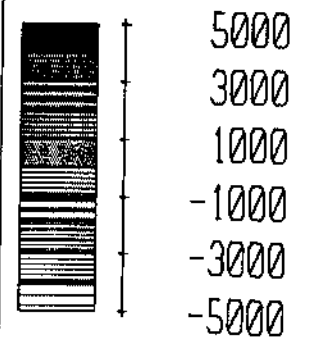
MIN IS -0.493E+04 <JOINT 2388>   MAX IS   0.371E+04 <JOINT 2350>

SAP90

SAP90

Y

Z

X

detail7

SHELL
OUTPUT SMXT
LOAD   1

20800
15600
10400
5200
0
-5200

MIN IS -0.481E+04 <JOINT 1172>   MAX IS   0.186E+05 <JOINT 1171>

383

detail7
UNDEFORMED
SHAPE

OPTIONS
WIRE FRAME

SAP90

Y
X

384

detai17

SHELL
OUTPUT S12T

LOAD   1

5000
3000
1000
-1000
-3000
-5000

SAP90

Y
X

MIN IS -0.494E+04 <JOINT 2388>   MAX IS   0.460E+04 <JOINT 2324>

385

detail7

SHELL

OUTPUT SMXT

LOAD   1

Y
X
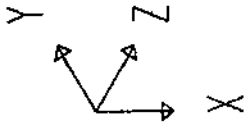
20800
15600
10400
5200
0
-5200

SAP90

MIN IS -0.481E+04 <JOINT 1172>   MAX IS   0.186E+05 <JOINT 1171>
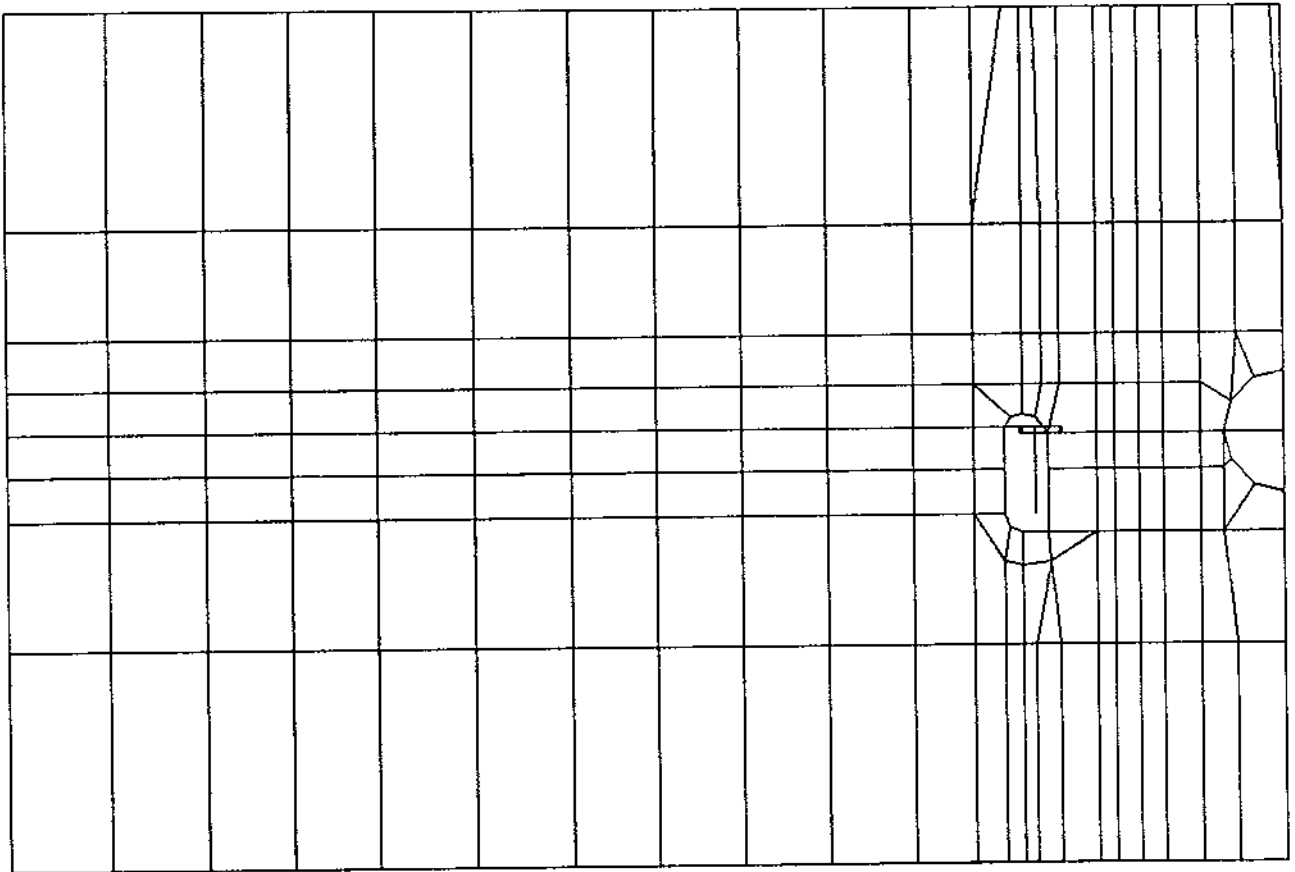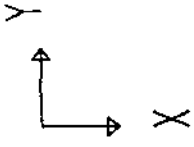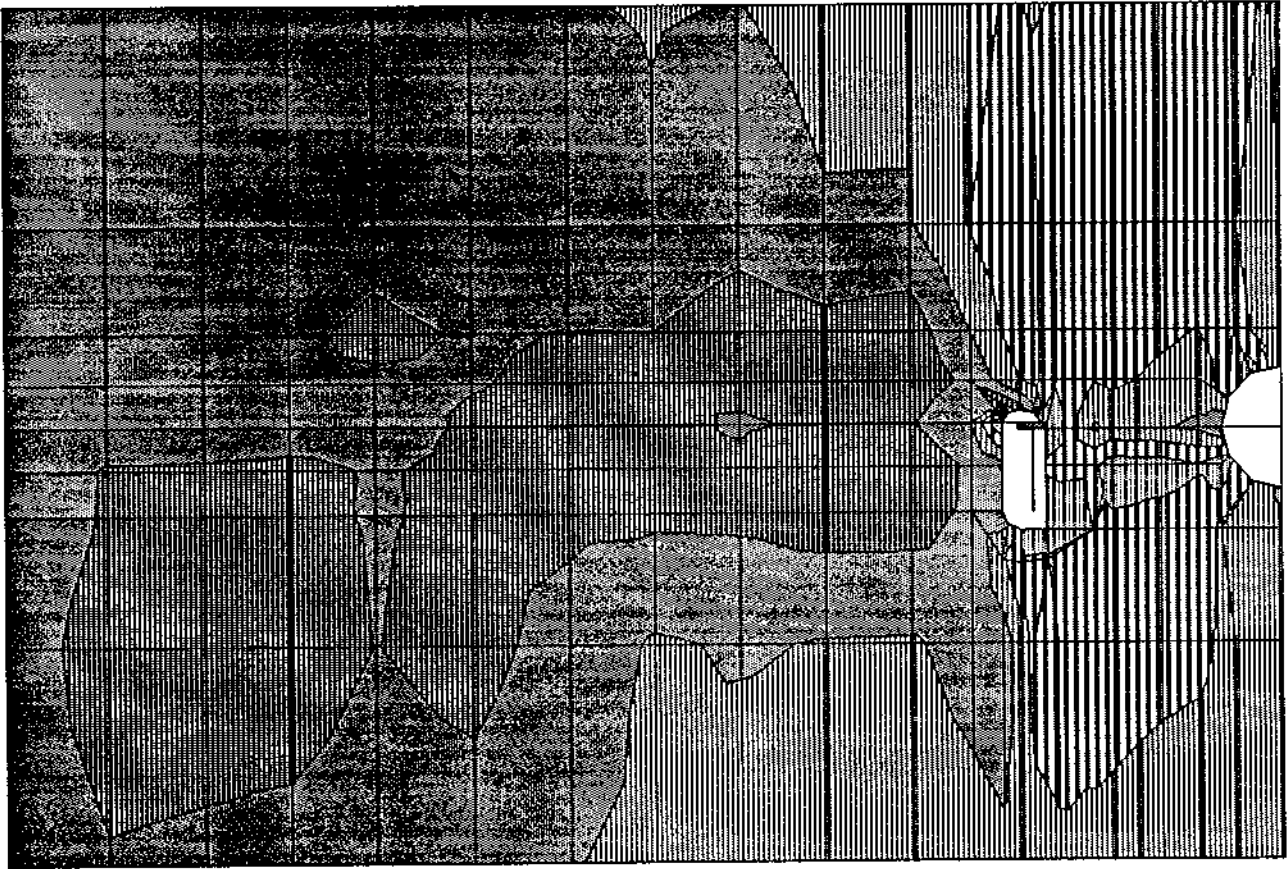
Z
X

detail7
UNDEFORMED
SHAPE

OPTIONS
WIRE FRAME

SAP90

387

Z

X

detail7

SHELL
OUTPUT   S12T

LOAD   1

5000
3000
1000
-1000
-3000
-5000

SAP90

MIN IS -0.494E+04 <JOINT 2388>   MAX IS   0.372E+04 <JOINT 2350>

388

Z

X ← → X

Z

detail7

SHELL
OUTPUT SMXT

LOAD   1

20800
15600
10400
5200
0
-5200

MIN IS -0.481E+04 <JOINT 1172>   MAX IS   0.186E+05 <JOINT 1171>

SAP90

389

10"

30"

105" x 0.46"

6"

20"

35"
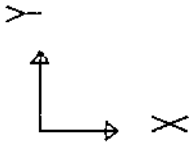
404" x 0.46"

105" x 0.46"

2.5"

11.5"

28"

15"

5"

70" x 0.46"

390

Y

Z

X

detail8
UNDEFORMED
SHAPE

OPTIONS
WIRE FRAME

SAP90

391

Y

Z

X
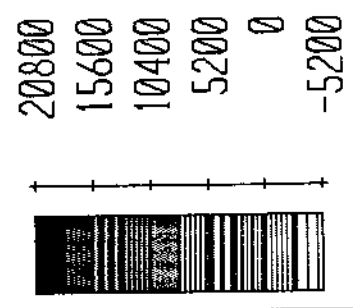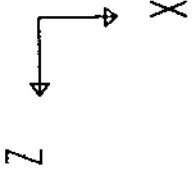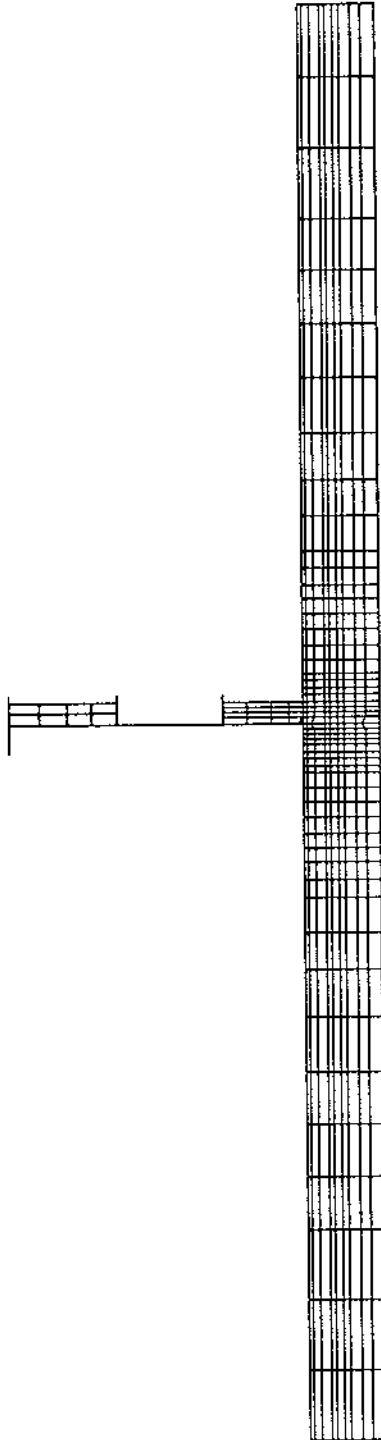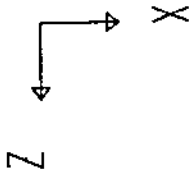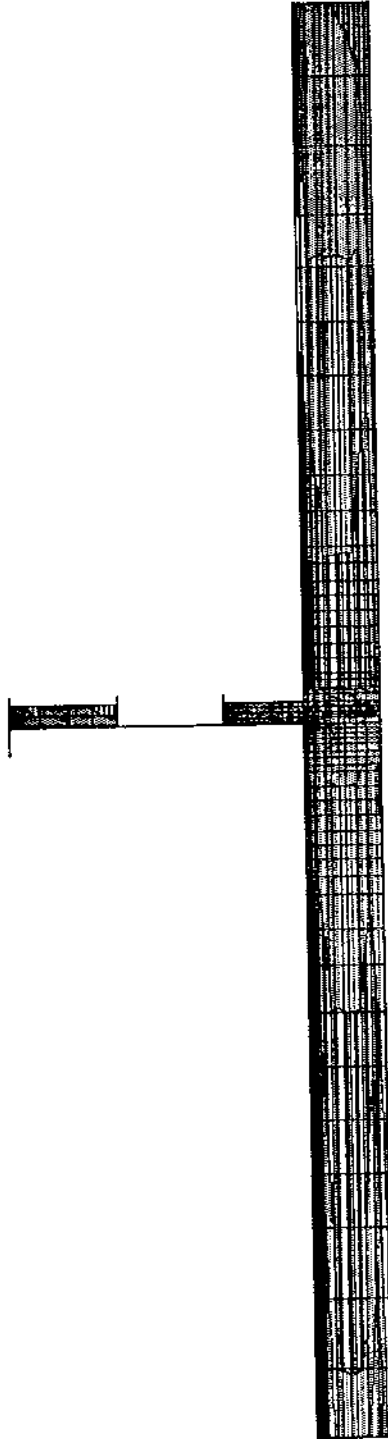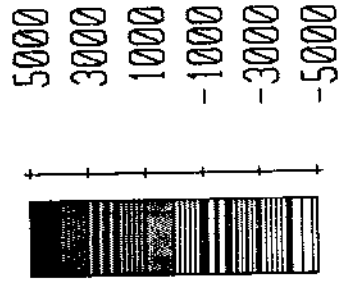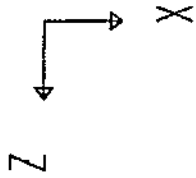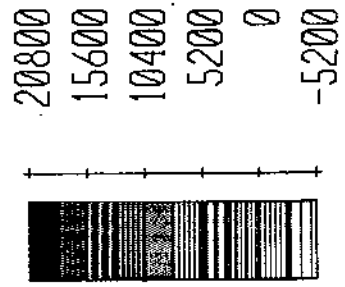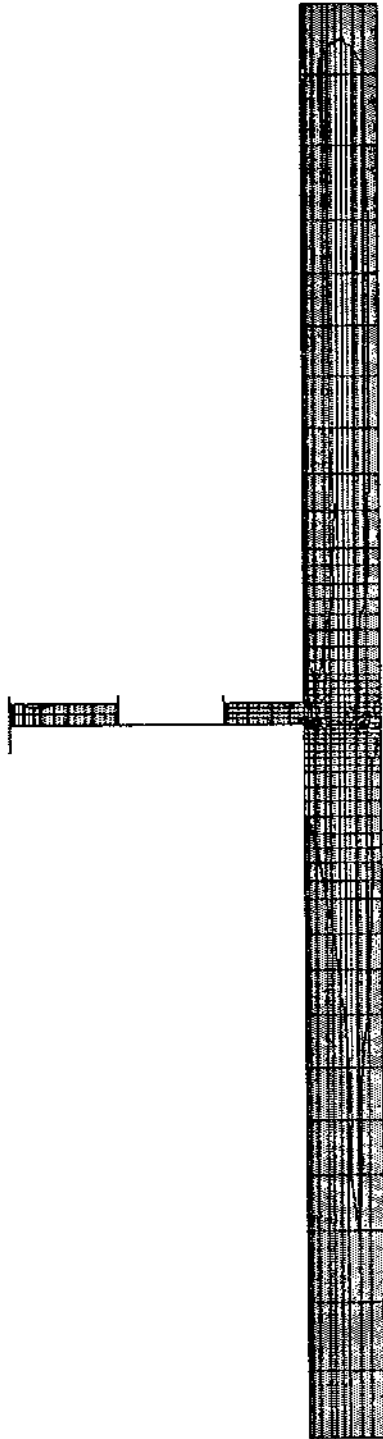
detail8

JOINT
LOADS
LOAD   1

MINIMA
P-0.1563E+04
MAXIMA
P-0.2288E-01
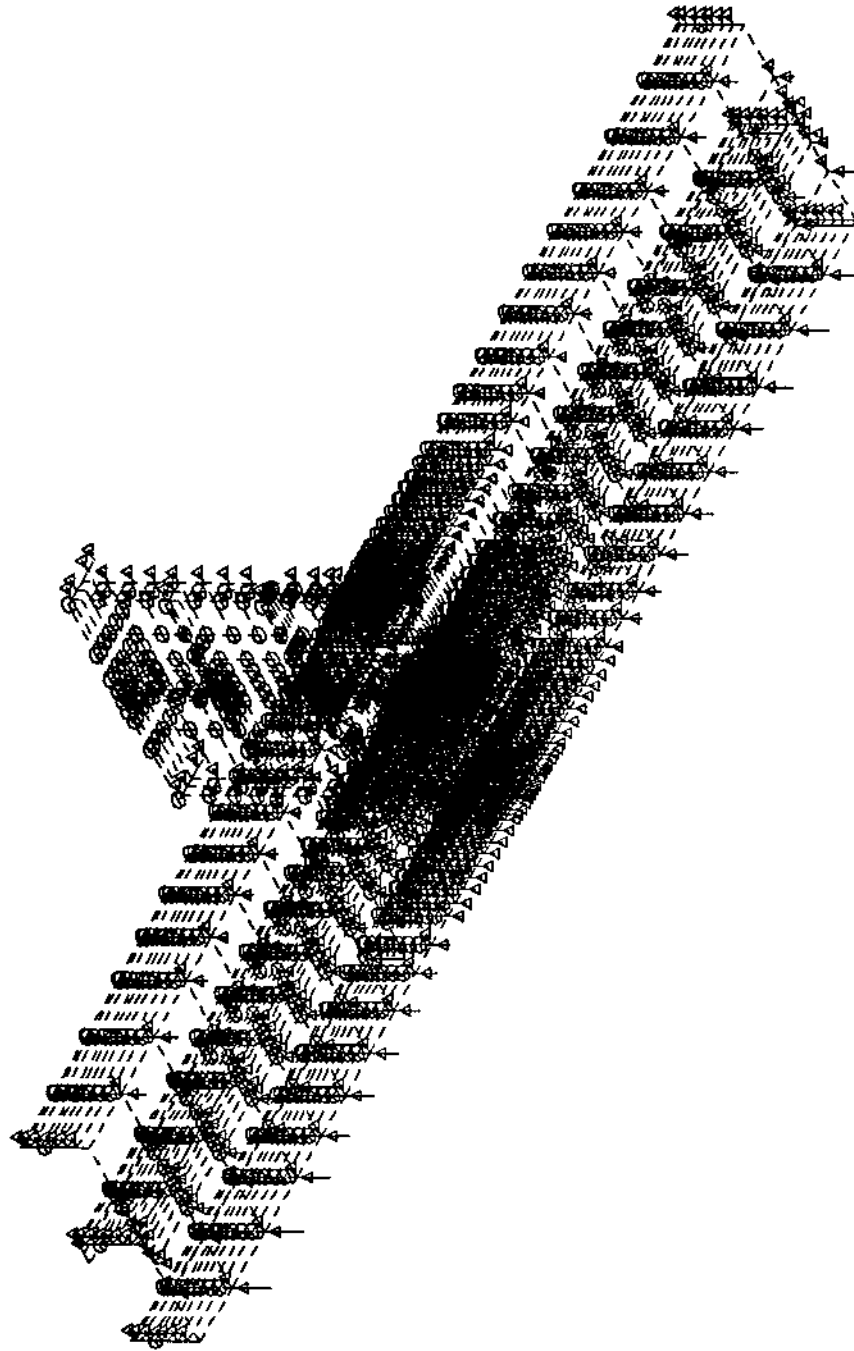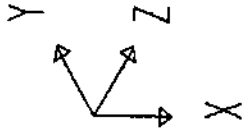
SAP90

detail8
DEFORMED
SHAPE
LOAD   1

MINIMA
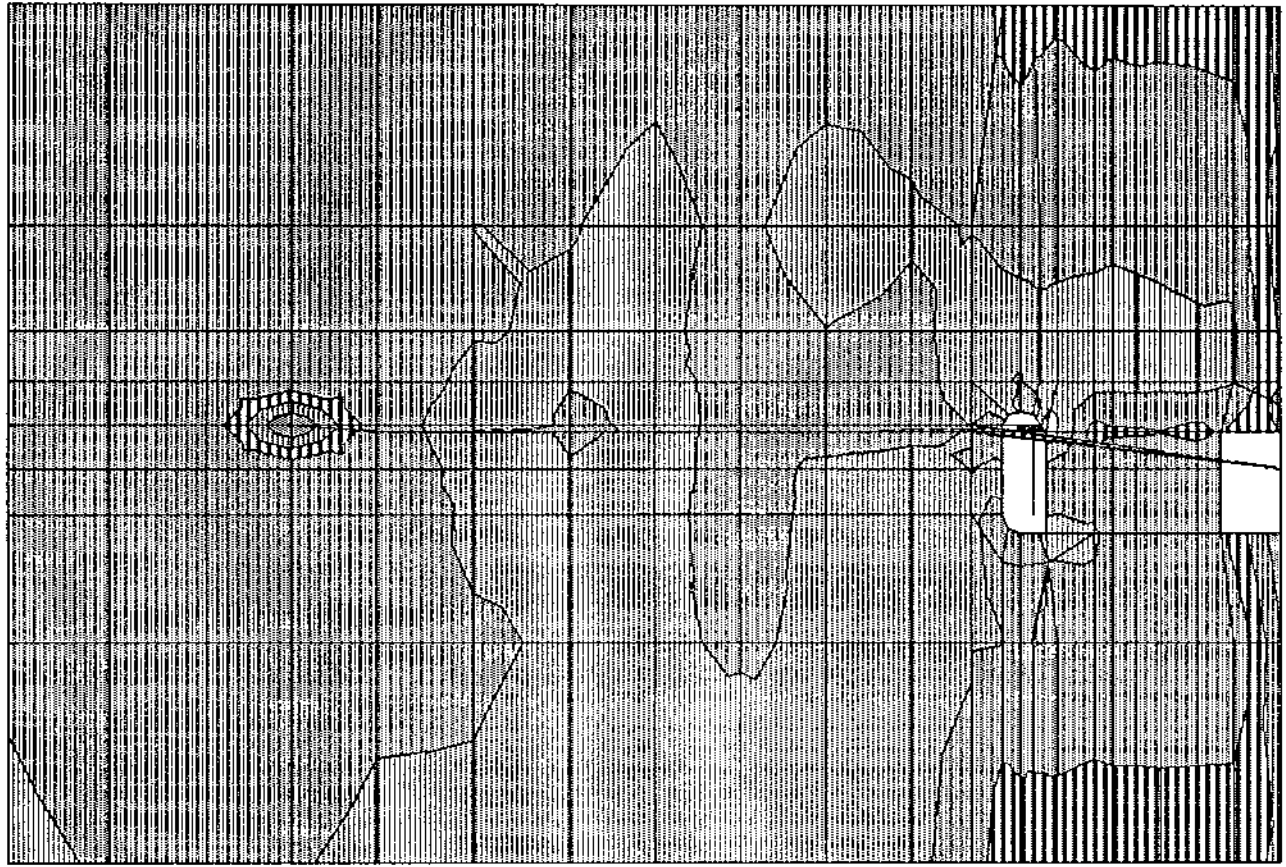X-0.4483E-01
Y-0.2375E+01
Z-0.1548E+00
MAXIMA
X 0.6452E-01
Y-0.2329E+01
Z-0.3119E-01

SAP90

393

detail8
SHELL
OUTPUT S11T
LOAD   1

21000
14000
7000
0
-7000
-14000

Y
Z
X
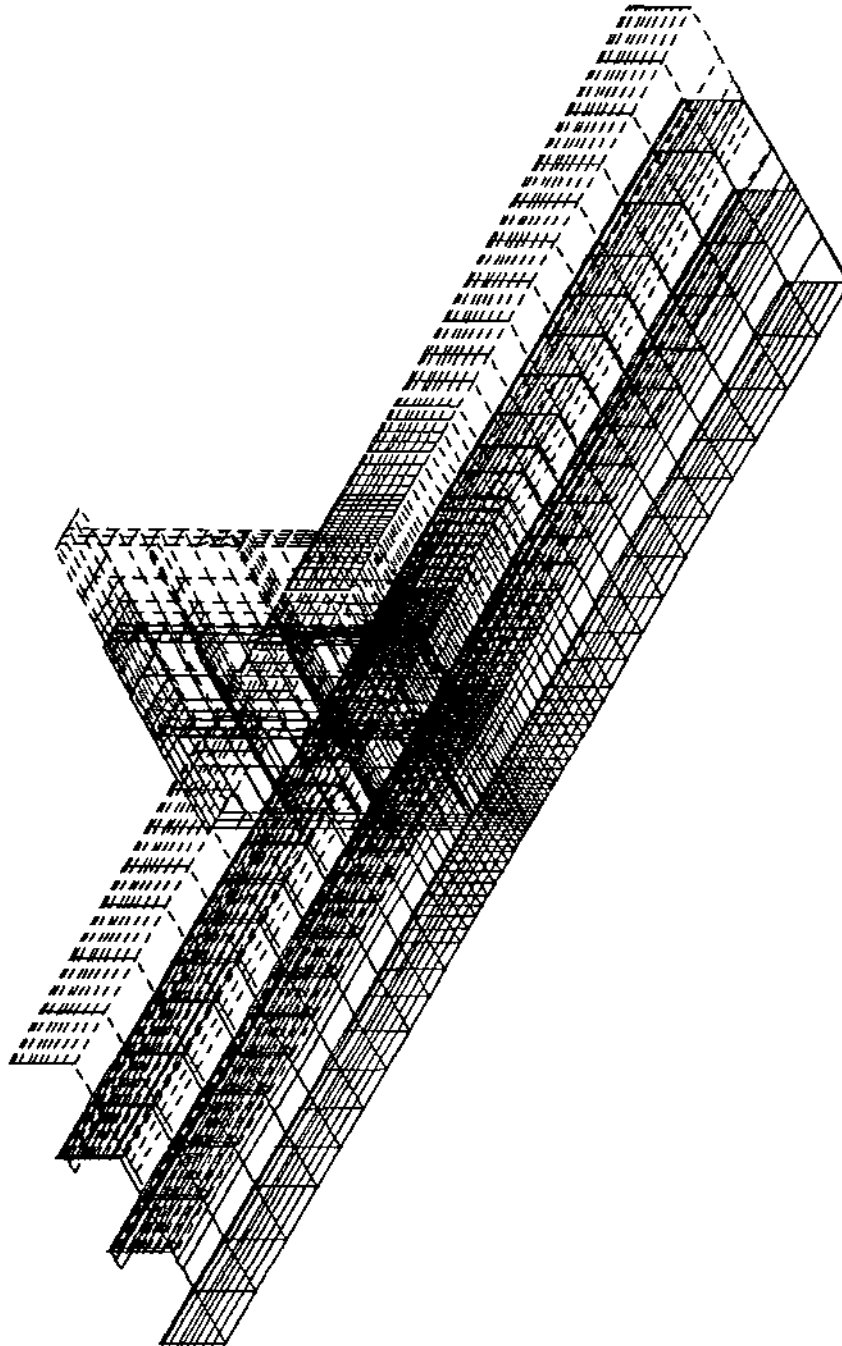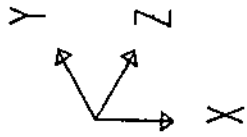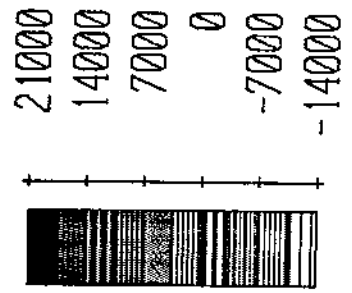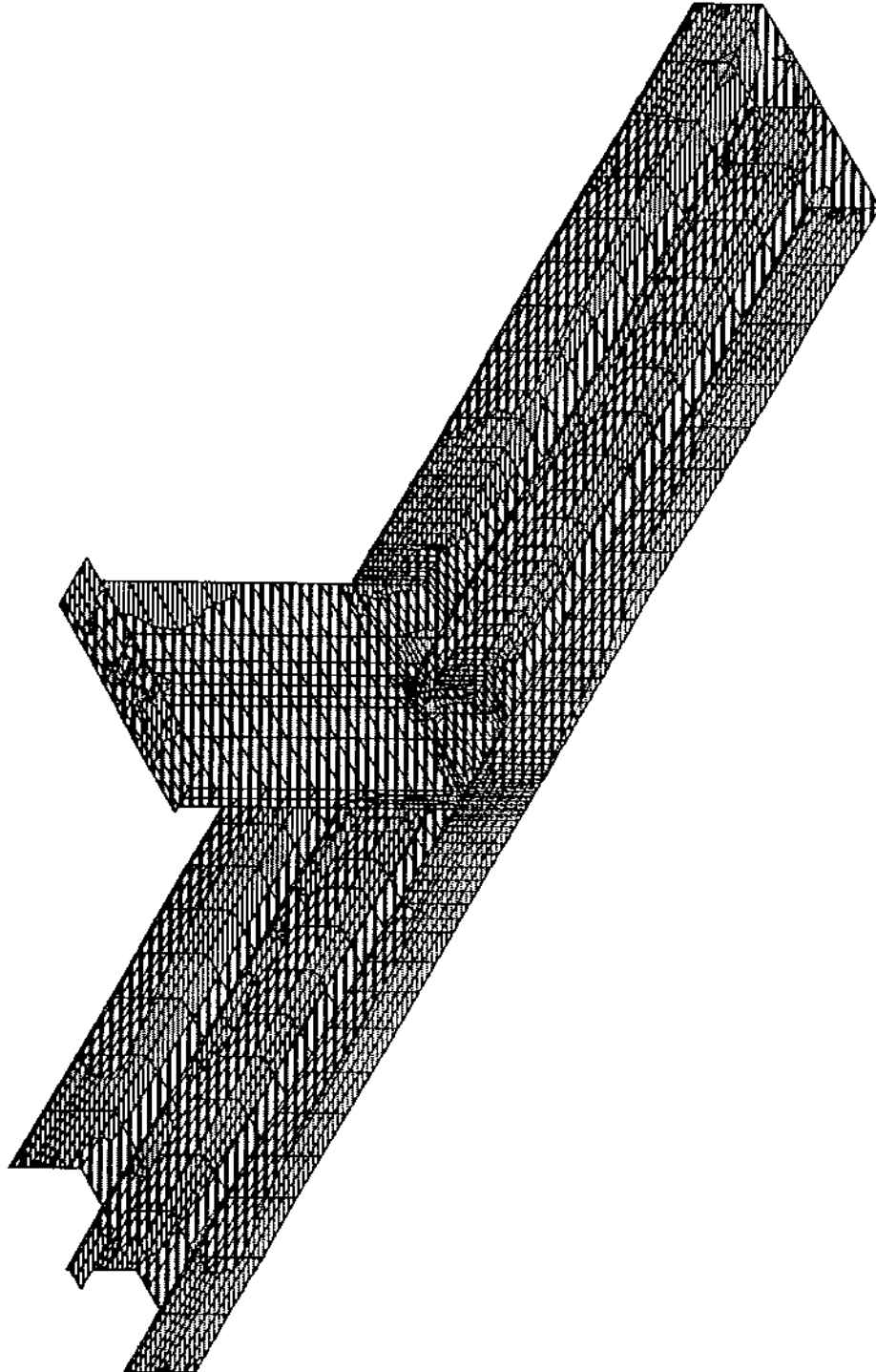
MIN IS -0.135E+05 <JOINT 1172>   MAX IS   0.176E+05 <JOINT 2441>

SAP90

394

Y
Z
X

detail8
SHELL
OUTPUT S22T
LOAD   1

21000
14000
7000
0
-7000
-14000

SAP90

MIN IS -0.139E+05 <JOINT 1172>   MAX IS 0.164E+05 <JOINT 2412>

395

Y Z X

detail8
SHELL
OUTPUT S22T
LOAD   1

21000
14000
7000
0
-7000
-14000

SAP90

MIN IS -0.139E+05 <JOINT 1172>   MAX IS   0.164E+05 <JOINT 2412>

396

Y

Z

X

detail8

SHELL
OUTPUT S12T

LOAD   1

5000
3000
1000
-1000
-3000
-5000

SAP90

MIN IS -0.494E+04 <JOINT 2388>   MAX IS   0.460E+04 <JOINT 2324>

Y
Z
X

detail8
SHELL
OUTPUT SMXT
LOAD   1

19200
14400
9600
4800
0
-4800

SAP90

MIN IS -0.480E+04 <JOINT 1172>   MAX IS   0.186E+05 <JOINT 1171>

398

Y

X

detail8
UNDEFORMED
SHAPE

OPTIONS
WIRE FRAME

SAP90

399

Y
X

detail8
SHELL
OUTPUT S12T
LOAD   1

5000
3000
1000
-1000
-3000
-5000

SAP90

MIN IS -0.494E+04 <JOINT 2388>   MAX IS 0.460E+04 <JOINT 2324>

402

detail8

SHELL
OUTPUT SMXT
LOAD   1

Y
X

19200
14400
9600
4800
0
-4800

SAP90

MIN IS -0.480E+04 <JOINT 1172>   MAX IS   0.186E+05 <JOINT 1171>

Z

X

detail8
UNDEFORMED
SHAPE

OPTIONS
WIRE FRAME

SAP90

Z

X

detail8

SHELL
OUTPUT S12T
LOAD   1

5000
3000
1000
-1000
-3000
-5000

SAP90

MIN IS -0.494E+04 <JOINT 2388>   MAX IS   0.372E+04 <JOINT 2350>

403

Z

X

detail8

SHELL
OUTPUT   SMXT

LOAD   1

19200
14400
9600
4800
0
-4800

MIN IS -0.480E+04 <JOINT 1172>   MAX IS   0.186E+05 <JOINT 1171>

SAP90

10"

30"

6" 105" x 0.46"

20"

2.5"

404" x 0.46"

105" x 0.46"

2.5" 2.5"

1 x 5"

.5"

.5"

70 ' x 0.46"

405

Y

Z

X

detail9

UNDEFORMED
SHAPE

OPTIONS

WIRE FRAME

SAP90

detail9

JOINT
LOADS

LOAD   1

MINIMA
P-0.1563E+04
MAXIMA
P-0.2288E-01
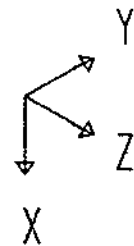
SAP90

detail9

DEFORMED
SHAPE

LOAD   1

MINIMA
X-0.4480E-01
Y-0.2375E+01
Z-0.1548E+00
MAXIMA
X 0.6452E-01
Y-0.2329E+01
Z-0.3119E-01

SAP90

detail9

SHELL

OUTPUT   S11T

LOAD   1

21000
14000
7000
0
-7000
-14000

SAP90

MIN IS -0.131E+05 <JOINT 1172>   MAX IS   0.176E+05 <JOINT 2441>

detail9

SHELL
OUTPUT S22T

LOAD   1

21000
14000
7000
0
-7000
-14000

SAP90

MIN IS -0.129E+05 〈JOINT 1172〉   MAX IS   0.164E+05 〈JOINT 2412〉

detail9

SHELL

OUTPUT S12T

LOAD 1

5000
3000
1000
-1000
-3000
-5000

MIN IS -0.493E+04 〈JOINT 2388〉　　　MAX IS　0.460E+04 〈JOINT 2324〉

SAP90

detail9

SHELL
OUTPUT   SMXT
LOAD   1

19200
14400
9600
4800
0
-4800

MIN IS -0.479E+04 <JOINT 1172>   MAX IS   0.180E+05 <JOINT 2441>

SAP90

Y

X

detail9

UNDEFORMED
SHAPE

OPTIONS

WIRE FRAME

SAP90

detail9

SHELL

OUTPUT S12T

LOAD   1

5000
3000
1000
−1000
−3000
−5000

MIN IS −0.493E+04 <JOINT 2388>   MAX IS   0.460E+04 <JOINT 2324>

SAP90

Y

X

detail9

SHELL

OUTPUT   SMXT

LOAD   1

SAP90

19200
14400
9600
4800
0
-4800

MIN IS -0.479E+04 <JOINT 1172>   MAX IS   0.180E+05 <JOINT 2441>

Z ←
X

detail9

UNDEFORMED
SHAPE

OPTIONS

WIRE FRAME

SAP90

Z

X

detail9

SHELL
OUTPUT S12T
LOAD   1

5000
3000
1000
-1000
-3000
-5000
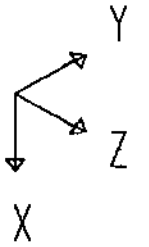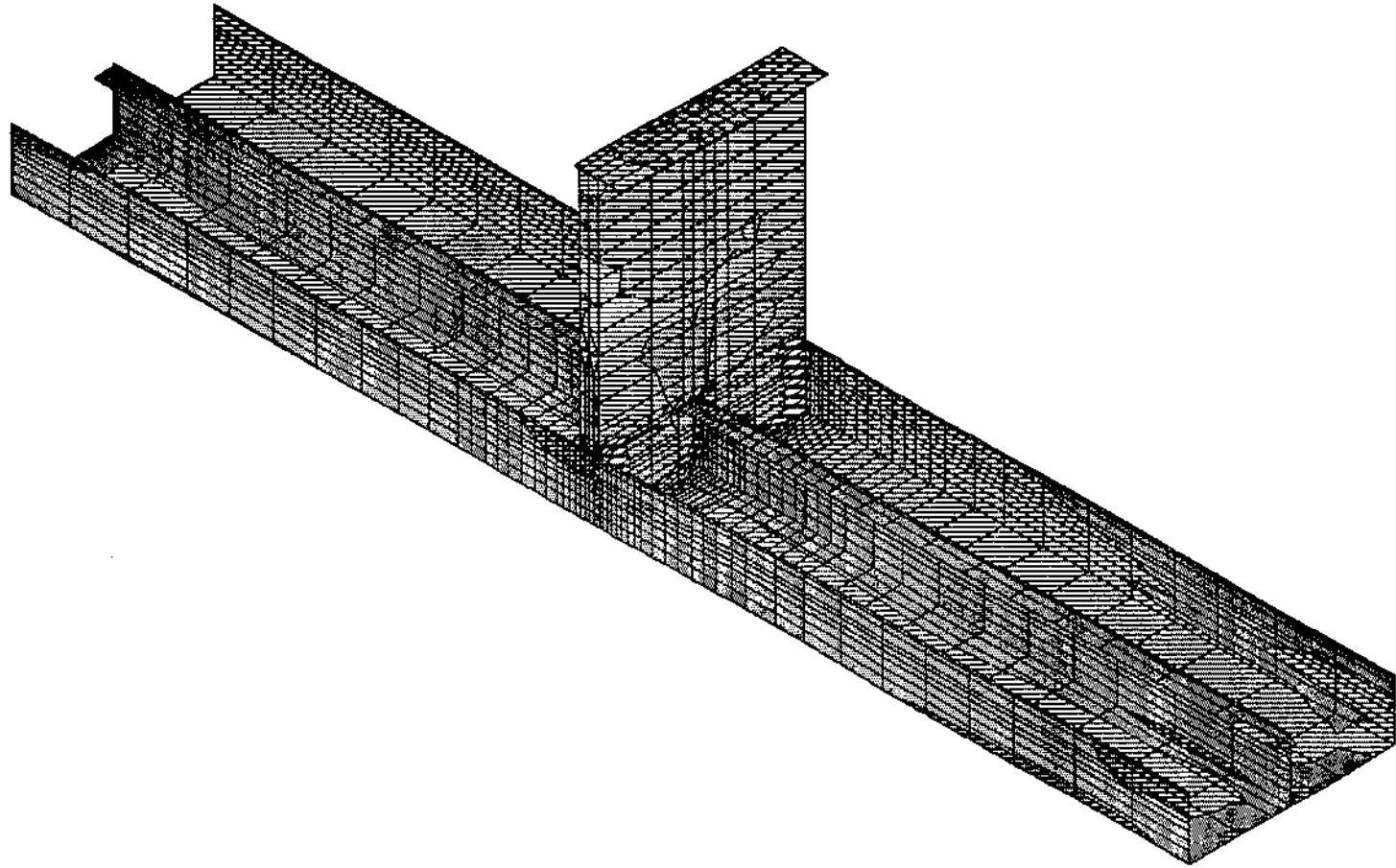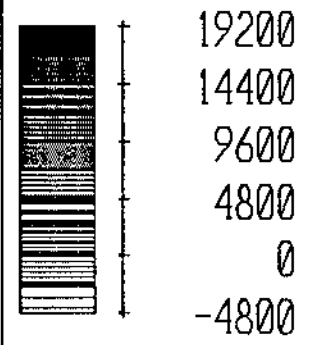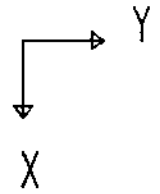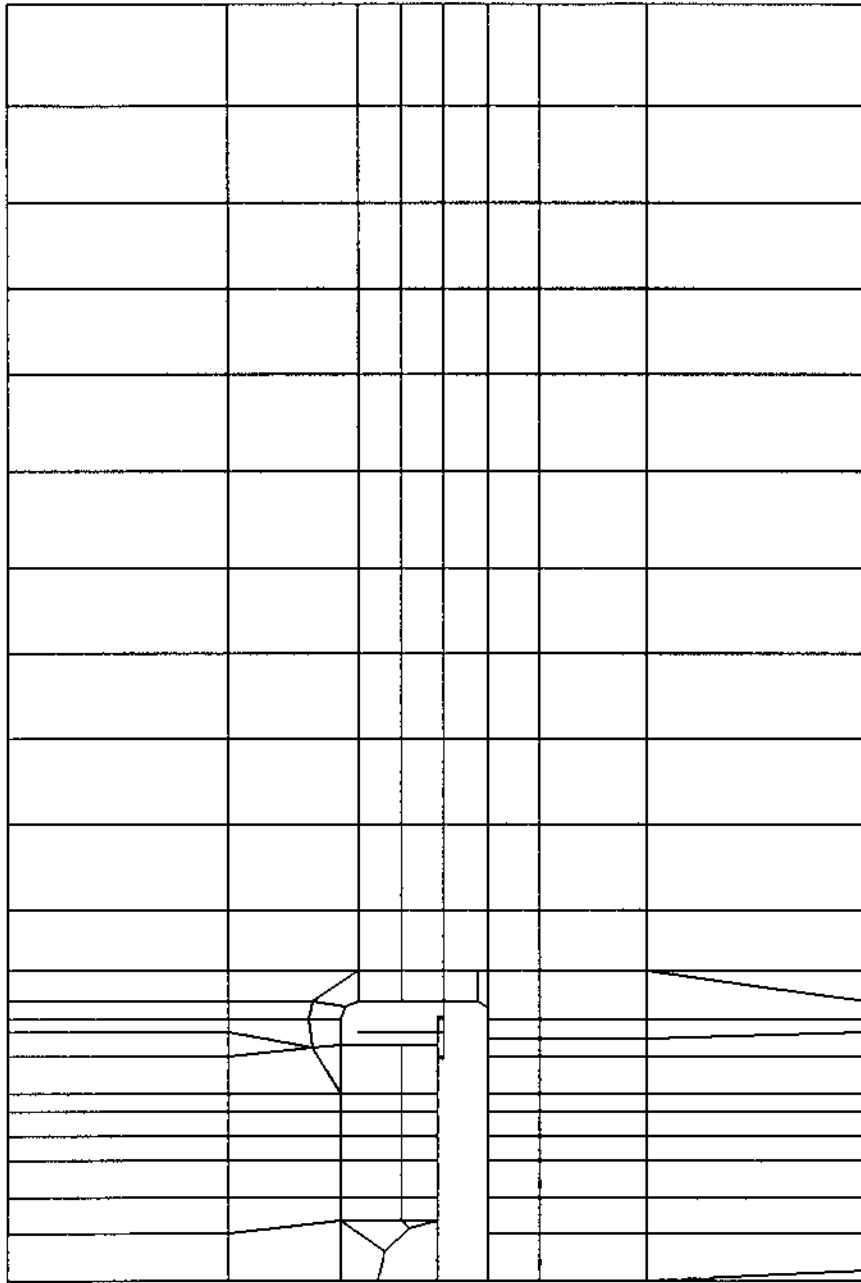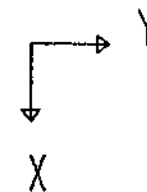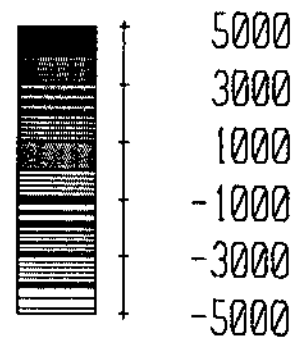
MIN IS -0.493E+04 <JOINT 2388>   MAX IS   0.366E+04 <JOINT 2350>

SAP90

Z

X

detail9

SHELL

OUTPUT   SMXT

LOAD   1

19200
14400
9600
4800
0
-4800
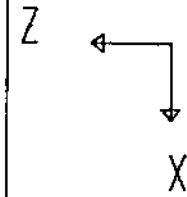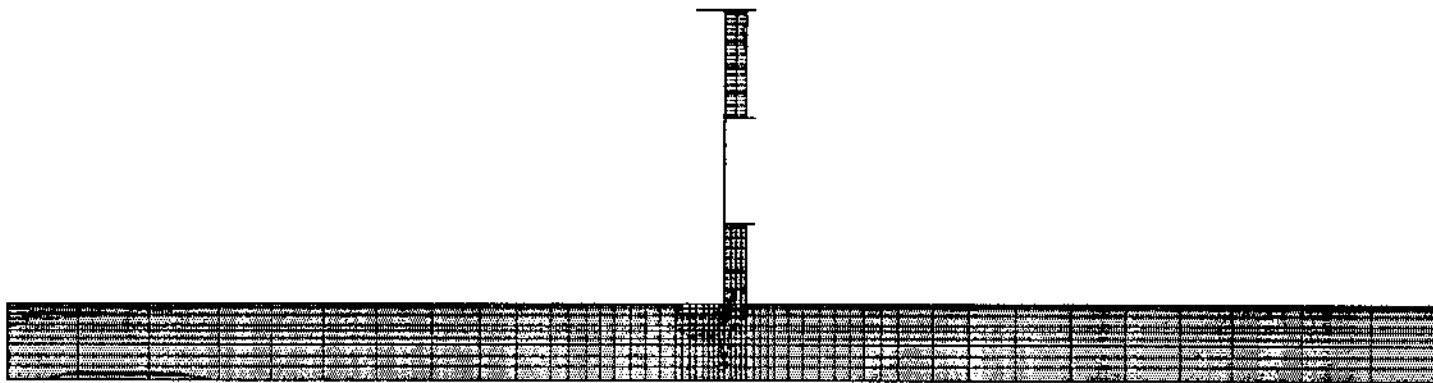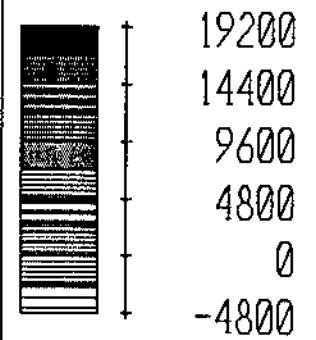
MIN IS   -0.479E+04 <JOINT   1172>   MAX IS   0.169E+05 <JOINT   894>

SAP90

10"

30"

6" 105" x 0.46"

20"

0.5"

404" x 0.46"

105" x 0.46"

3.5" 3.5"

12.5"

25"

70 ' x 0.46"

419

Y
Z
X

detail 10

UNDEFORMED
SHAPE

OPTIONS

WIRE FRAME

SAP90

Y

Z

X
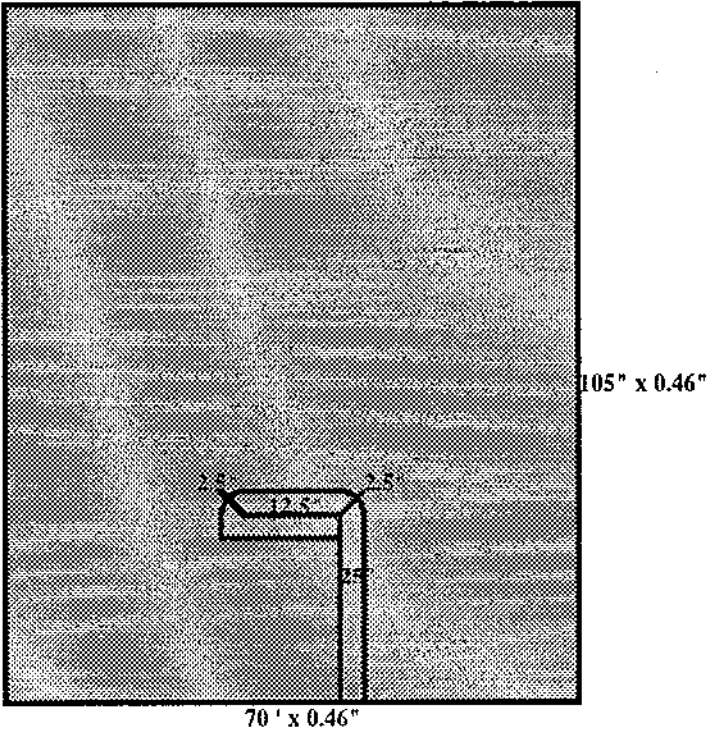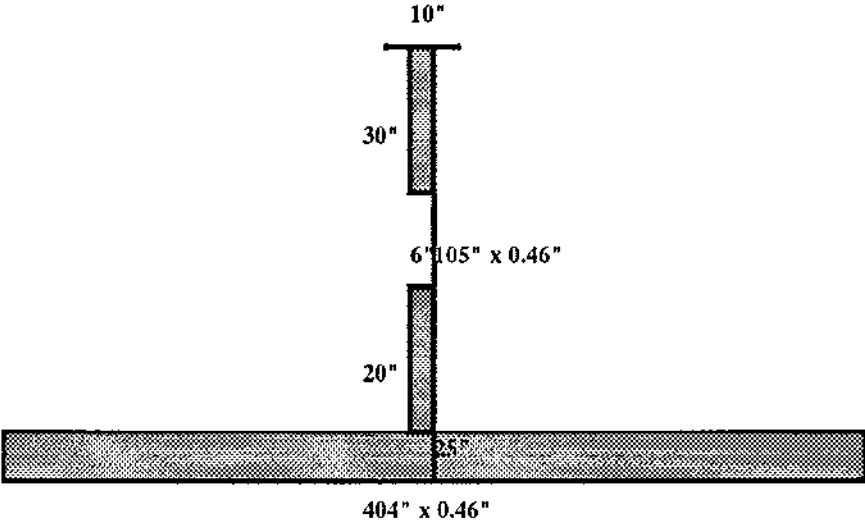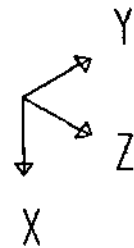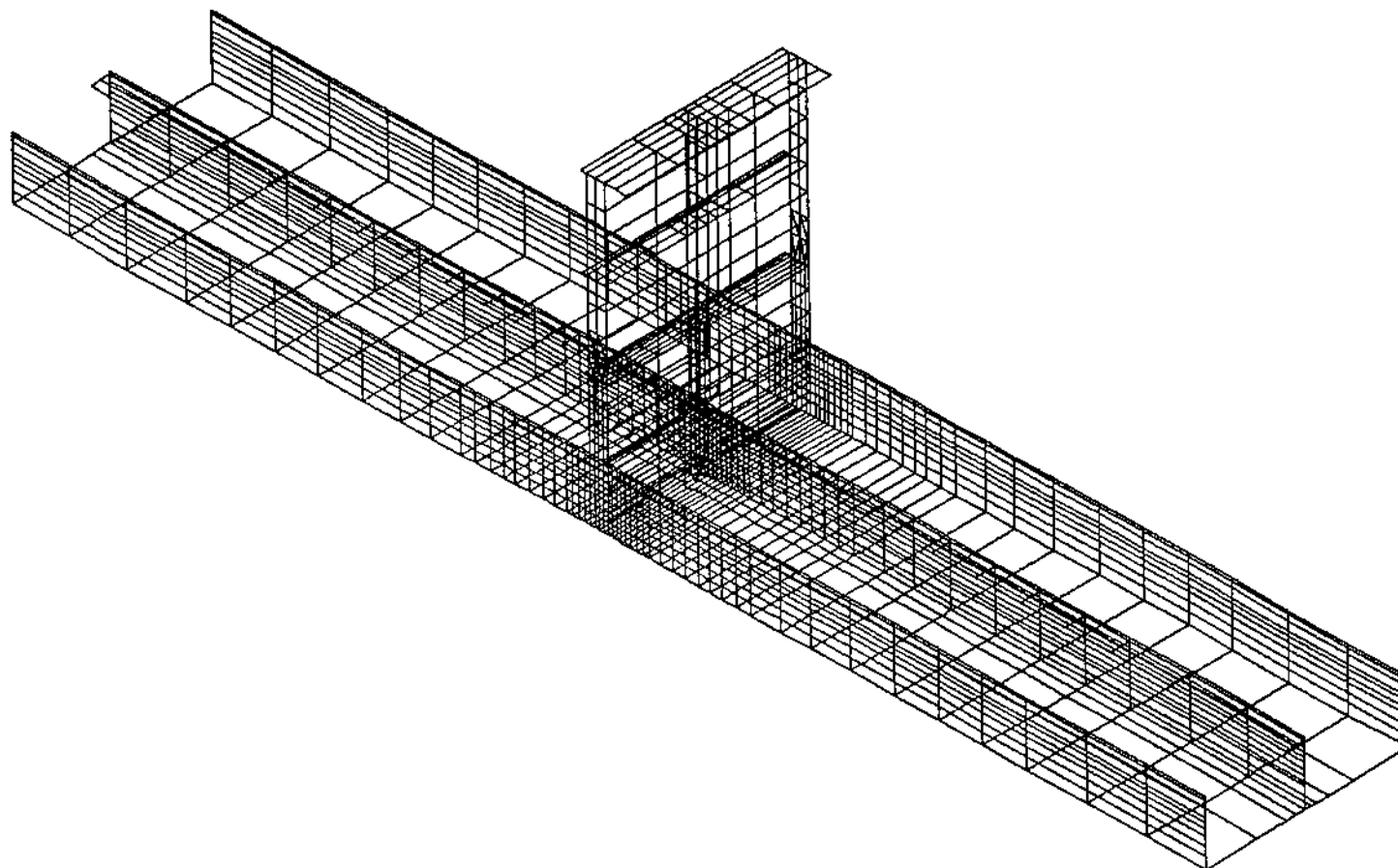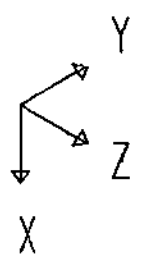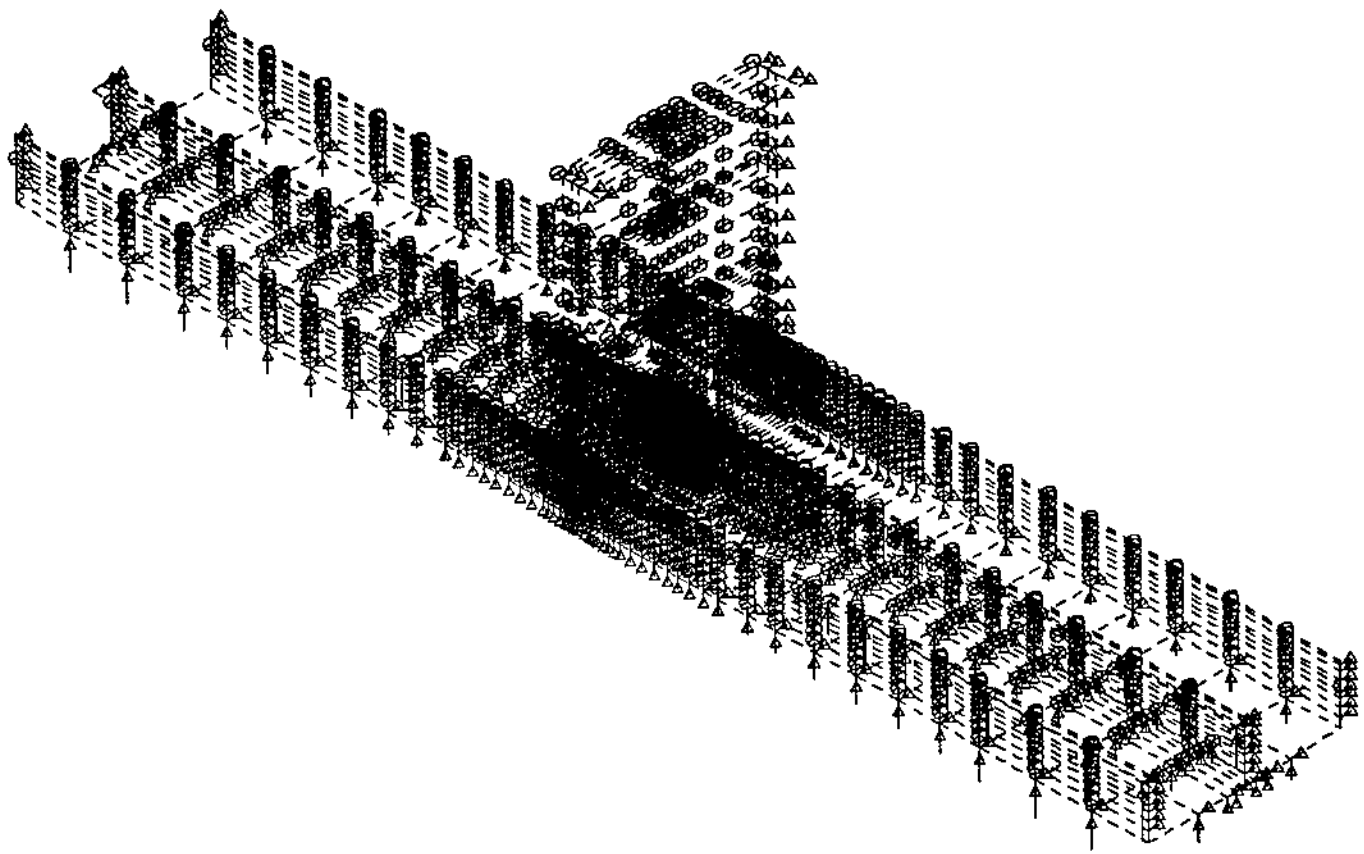
detail 10

JOINT
LOADS

LOAD   1
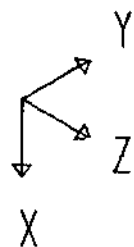
MINIMA
P-0.1563E+04
MAXIMA
P-0.2288E-01

SAP90

422

Y

Z

X

detail 10

SHELL

OUTPUT   S11T

LOAD   1

21000
14000
7000
0
-7000
-14000

SAP90

MIN IS   -0.131E+05 <JOINT   1172>   MAX IS   0.176E+05 <JOINT   2441>

Y

Z

X

detail10

SHELL
OUTPUT   S22T
LOAD   1

21000
14000
7000
0
-7000
-14000
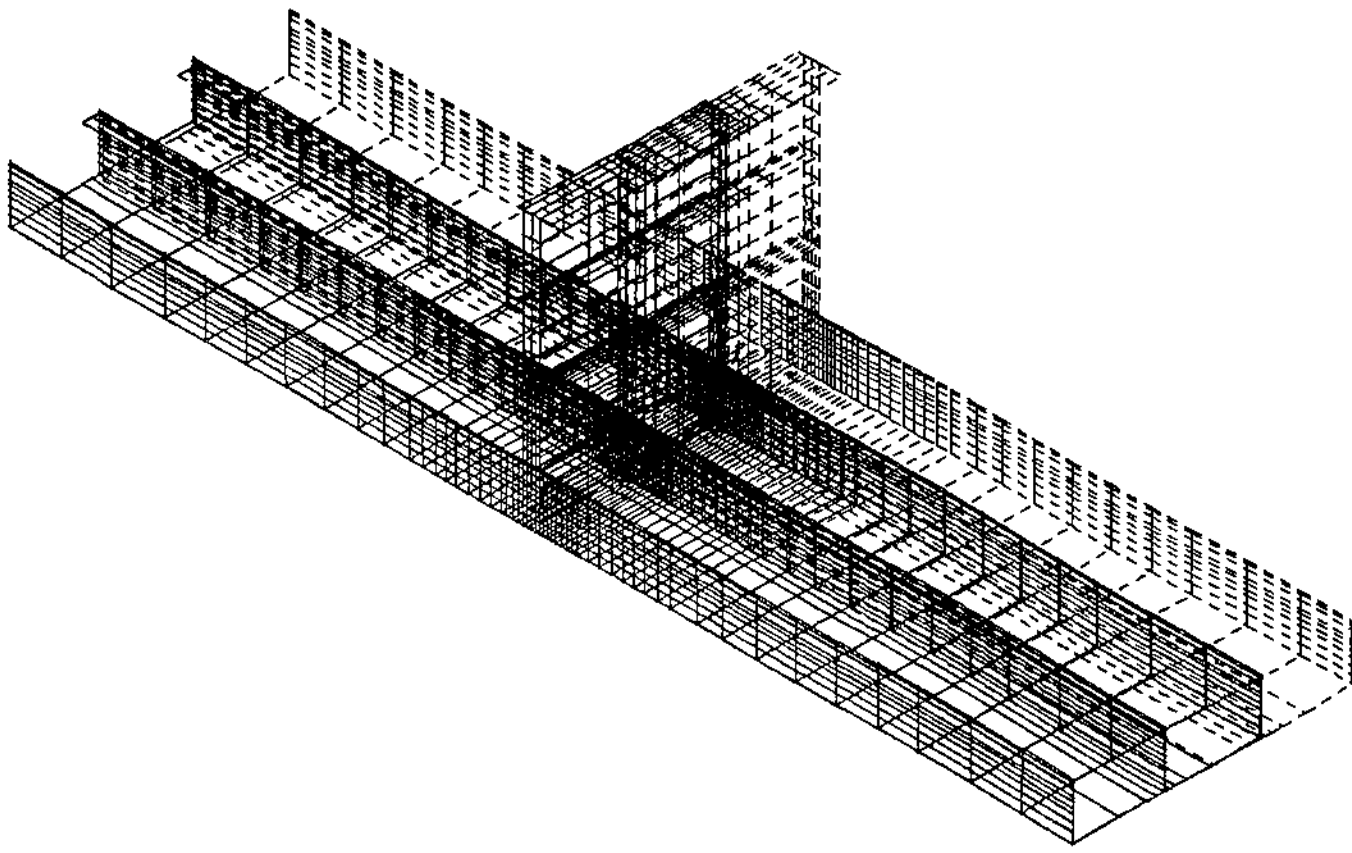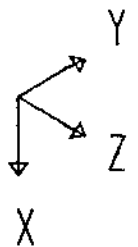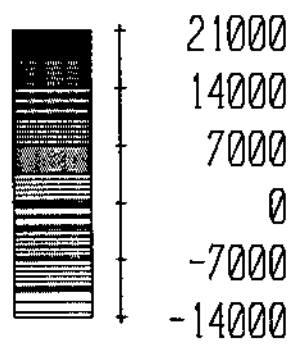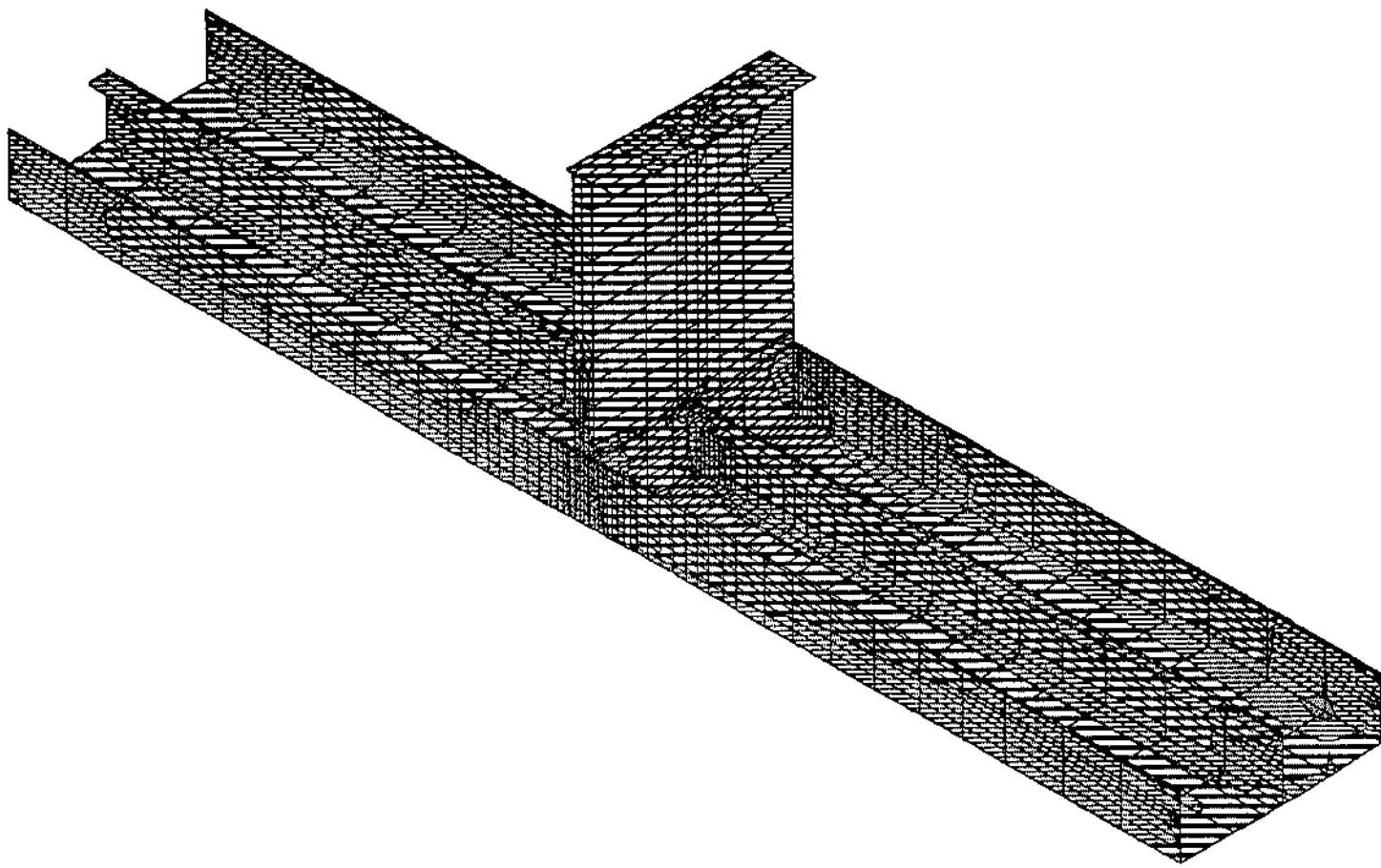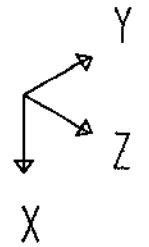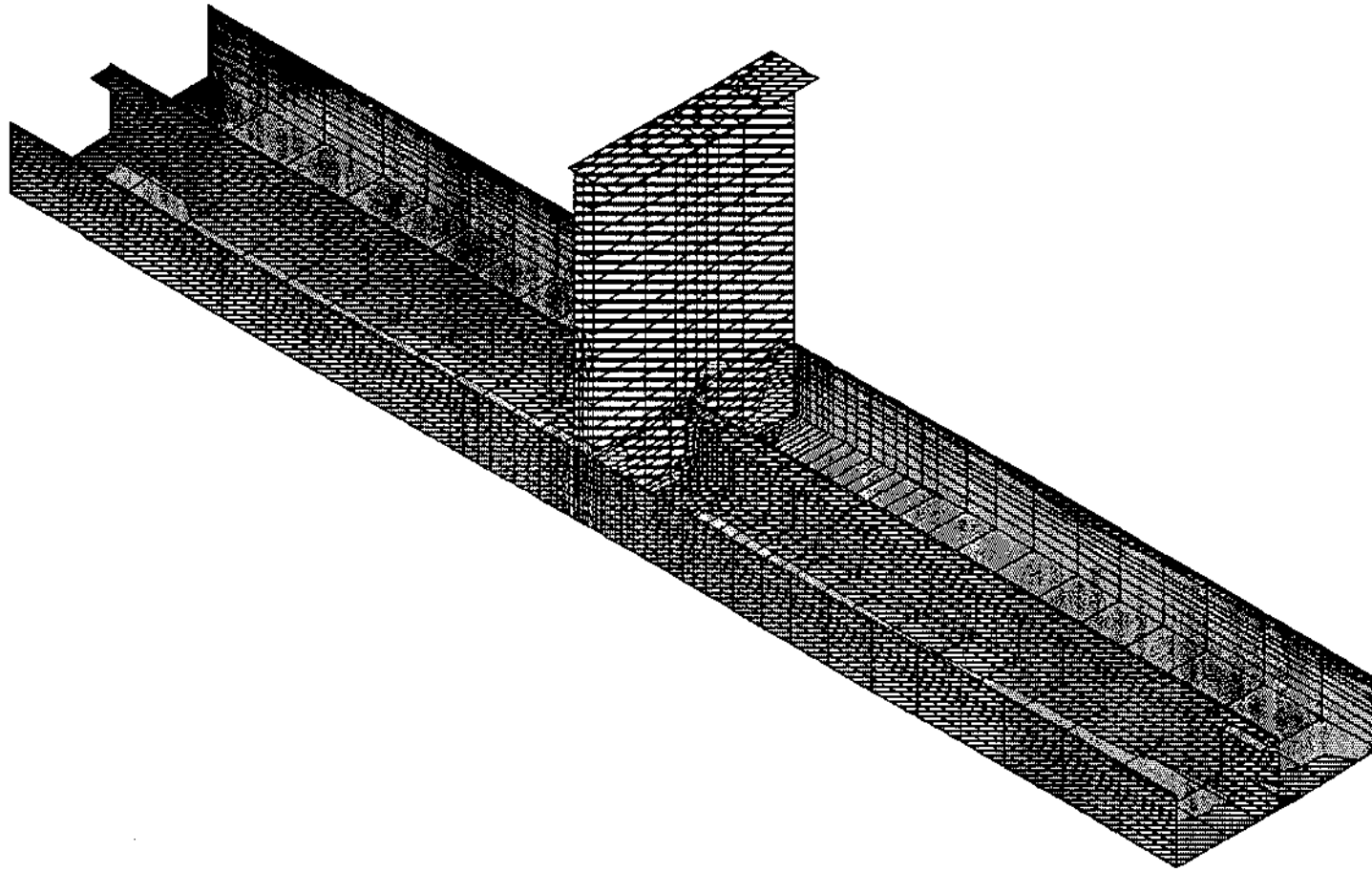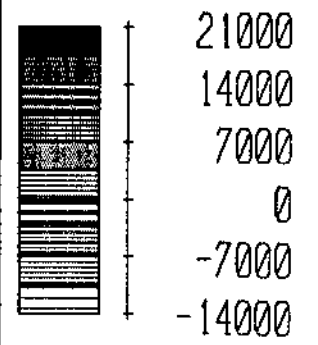
MIN IS   -0.126E+05 <JOINT   1172>   MAX IS   0.164E+05 <JOINT   2412>

SAP90

detail 10

SHELL
OUTPUT   S12T

LOAD   1

5000
3000
1000
-1000
-3000
-5000

MIN IS   -0.491E+04 <JOINT   2388>   MAX IS   0.460E+04 <JOINT   2324>

SAP90

detail 10

SHELL

OUTPUT   SMXT

LOAD   1

20800
15600
10400
5200
0
−5200

MIN IS −0.503E+04 <JOINT 1172>   MAX IS   0.180E+05 <JOINT 2441>

SAP90

detail 10

SHELL

OUTPUT S12T

LOAD 1

5000
3000
1000
-1000
-3000
-5000

SAP90

MIN IS -0.491E+04 <JOINT 2388>   MAX IS   0.460E+04 <JOINT 2324>

427

Y

X

detail 10

UNDEFORMED
SHAPE

OPTIONS

WIRE FRAME

SAP90

detail 10

SHELL
OUTPUT SMXT
LOAD   1

20800
15600
10400
5200
0
-5200

SAP90
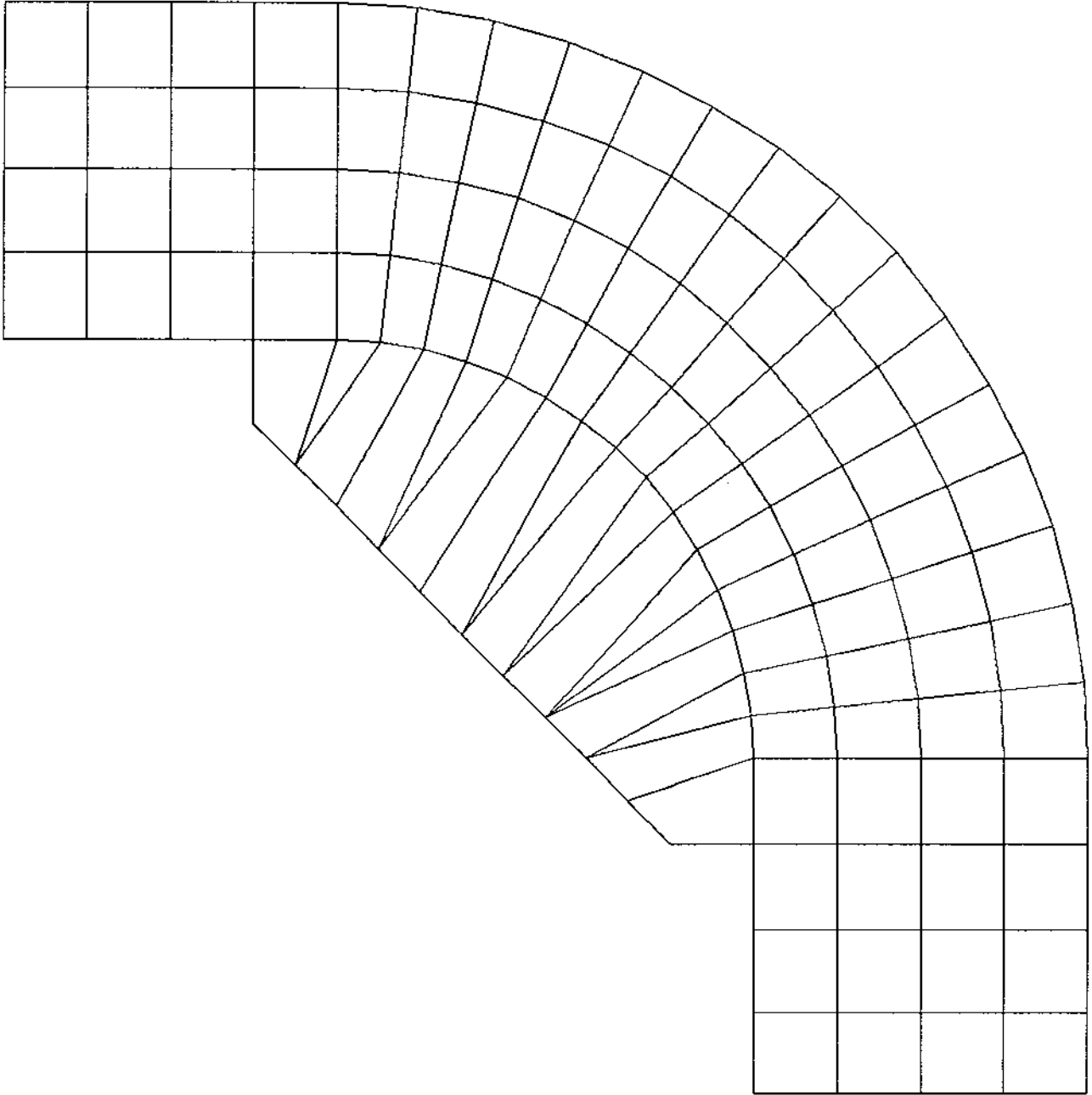
MIN IS -0.503E+04 <JOINT 1172>   MAX IS   0.180E+05 <JOINT 2441>

Z

X

detail 10

UNDEFORMED
SHAPE

OPTIONS

WIRE FRAME

SAP90

430

Z

X

detail 10

SHELL

OUTPUT SMXT

LOAD   1

16800
12000
7200
2400
-2400
-7200
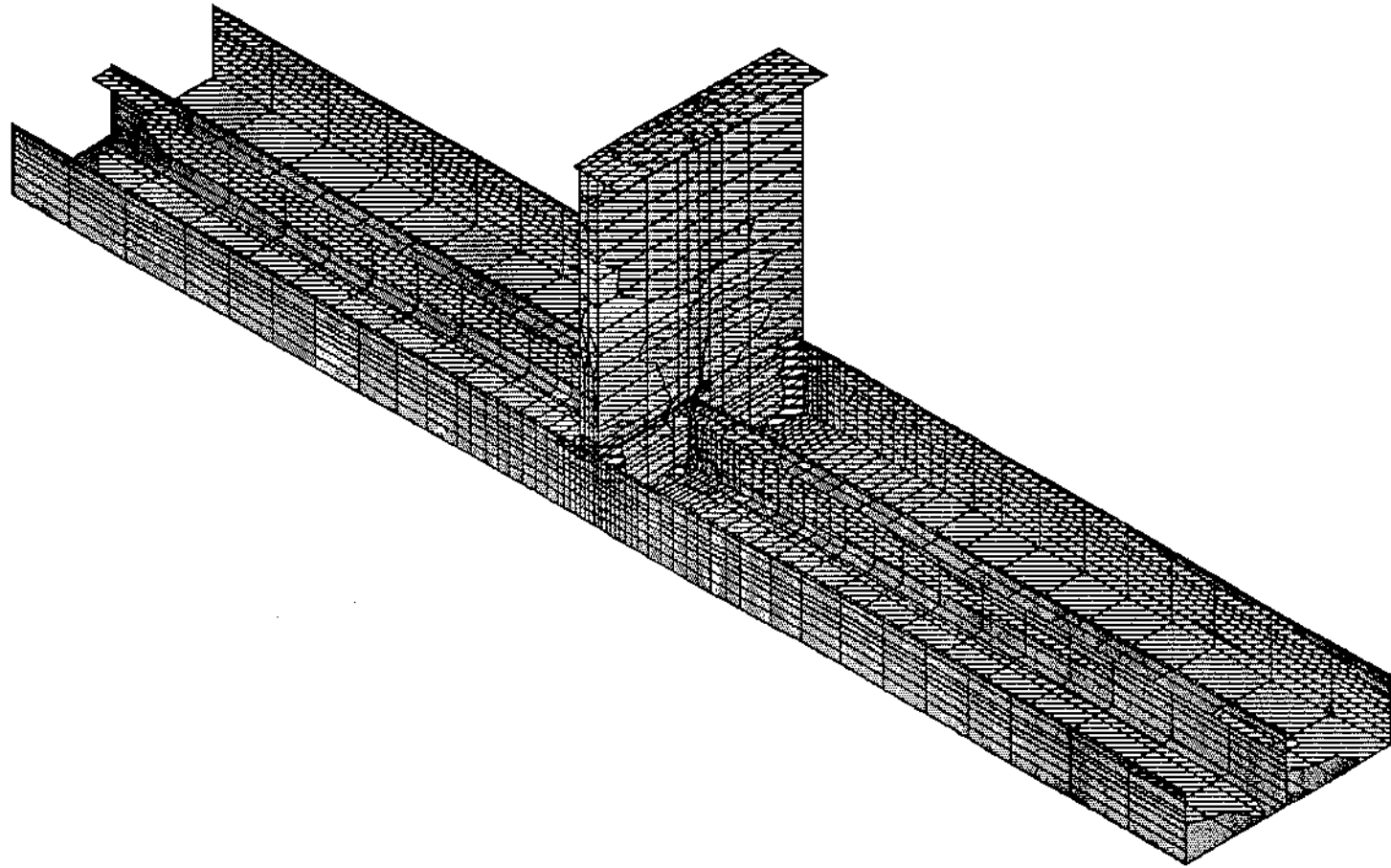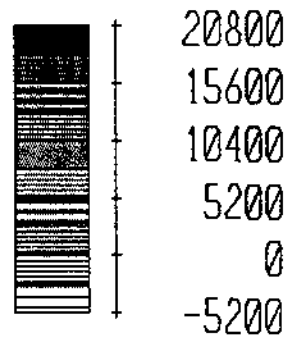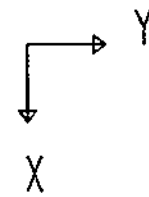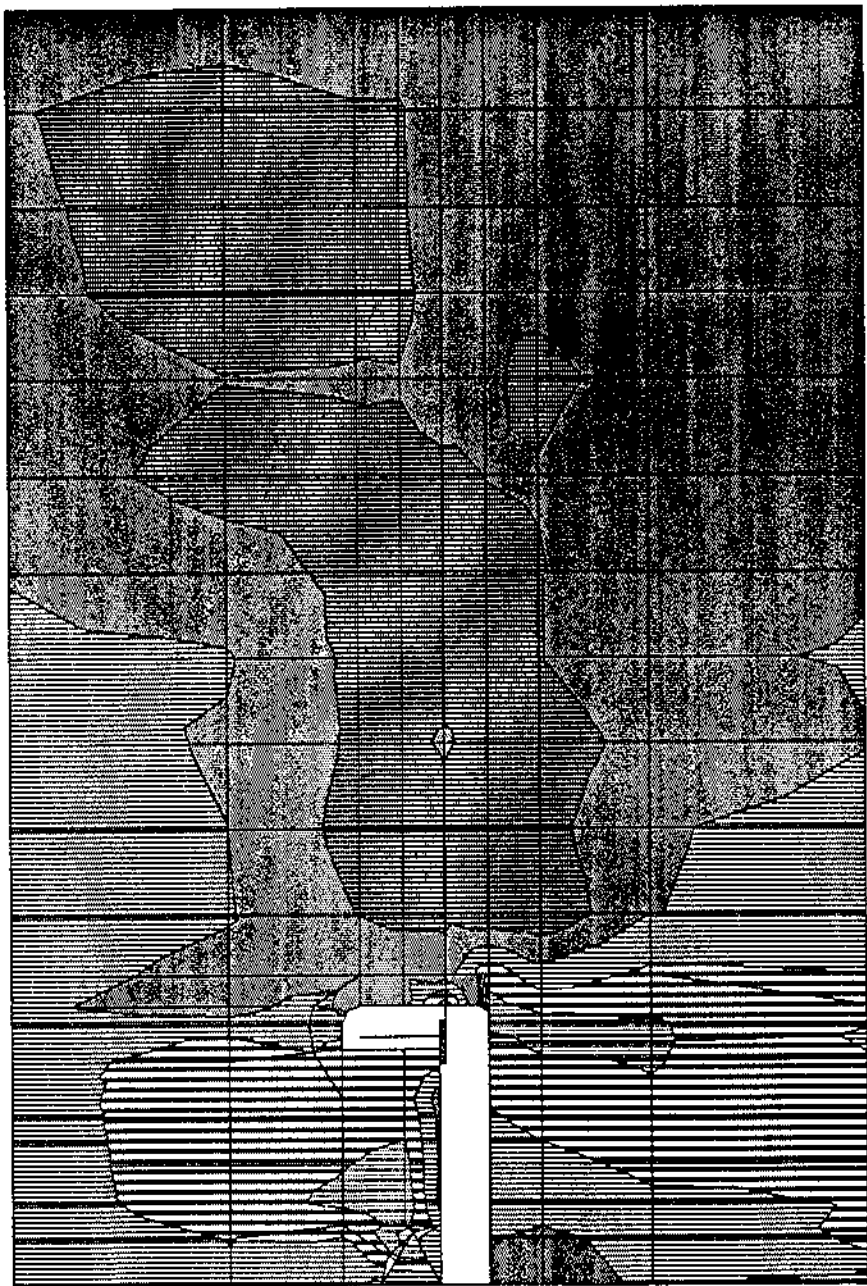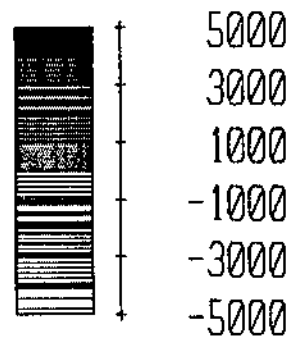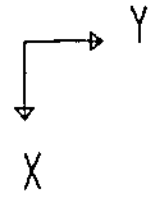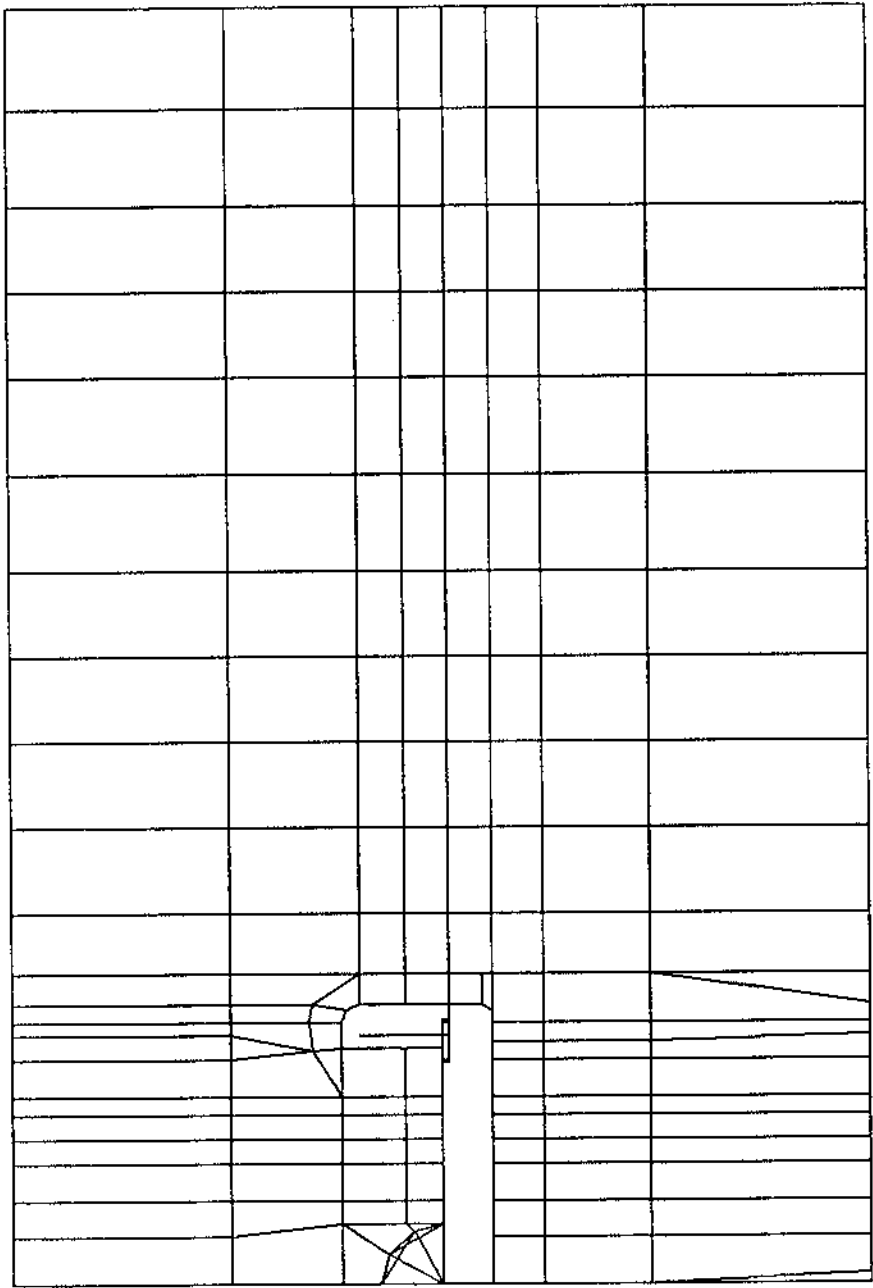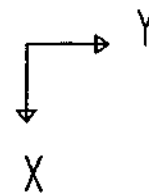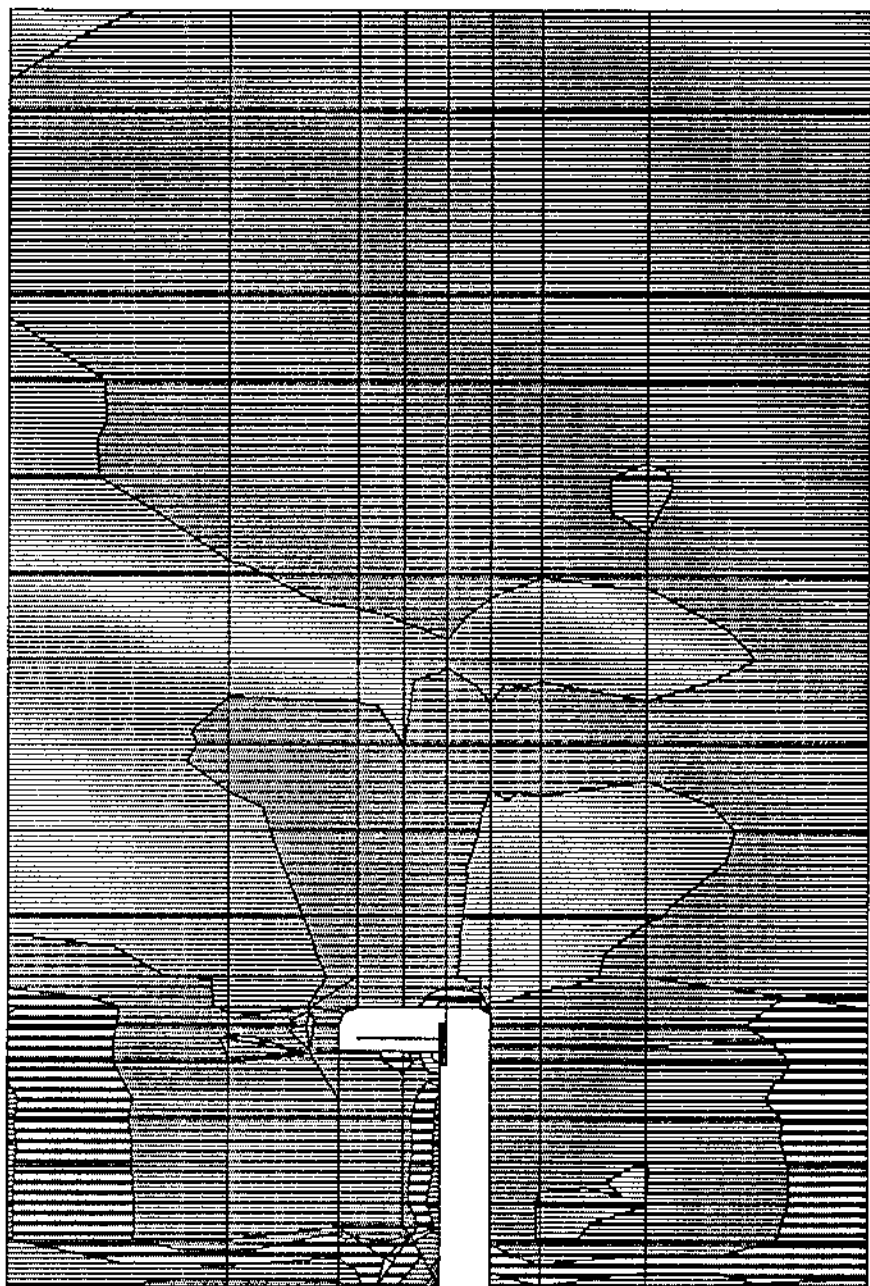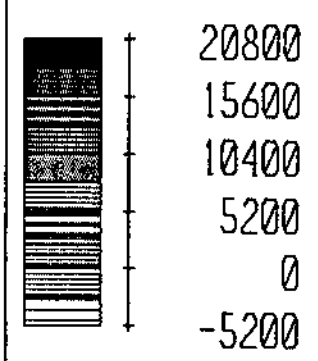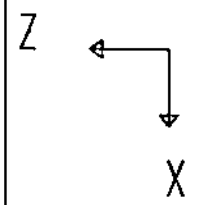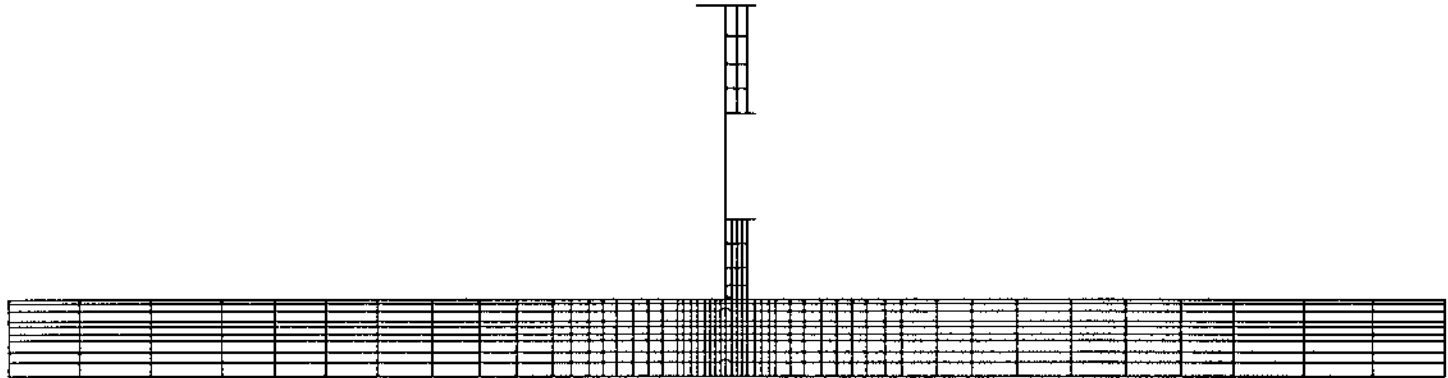
MIN IS -0.503E+04 <JOINT 1172>   MAX IS   0.168E+05 <JOINT   894>

SAP90
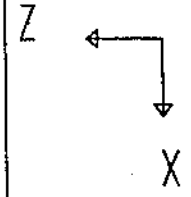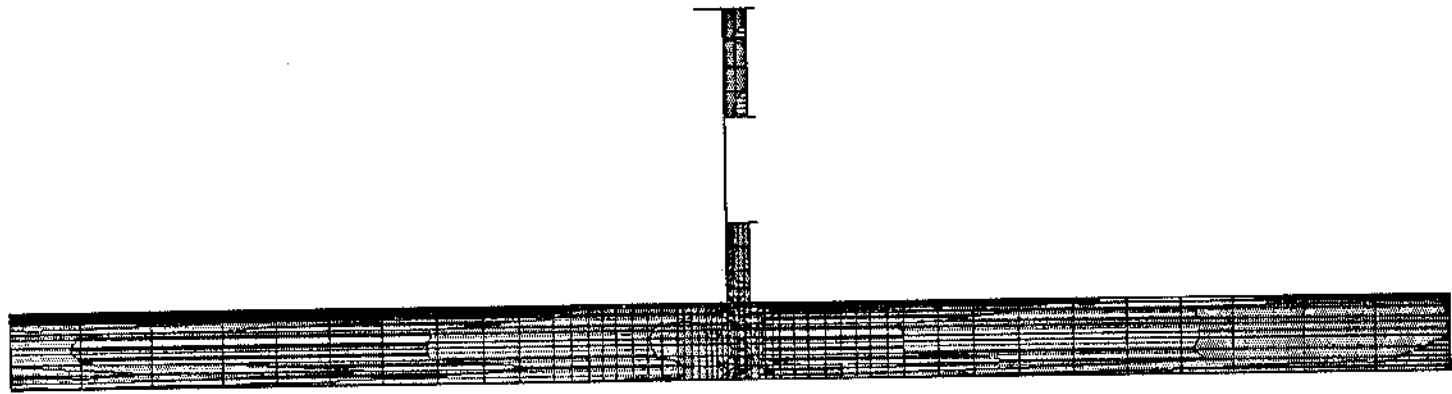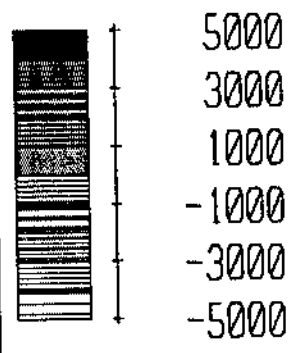
431

Z ← X

detail 10

SHELL
OUTPUT   S12T

LOAD   1

5000
3000
1000
-1000
-3000
-5000

SAP90

MIN IS   -0.491E+04 〈JOINT   2388〉   MAX IS   0.364E+04 〈JOINT   2350〉

10"

30"

105" x 0.46"

6"

20"

1" 10"

15"

25"

404" x 0.46"



105" x 0.46"

12.5"

17.5"

stiffen1

UNDEFORMED
SHAPE

OPTIONS

WIRE FRAME

SAP90

Z   Y

X
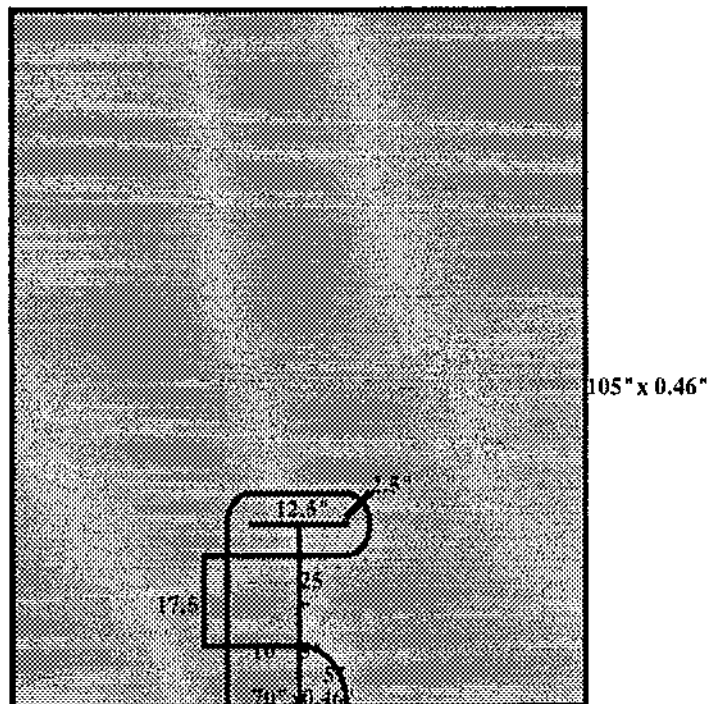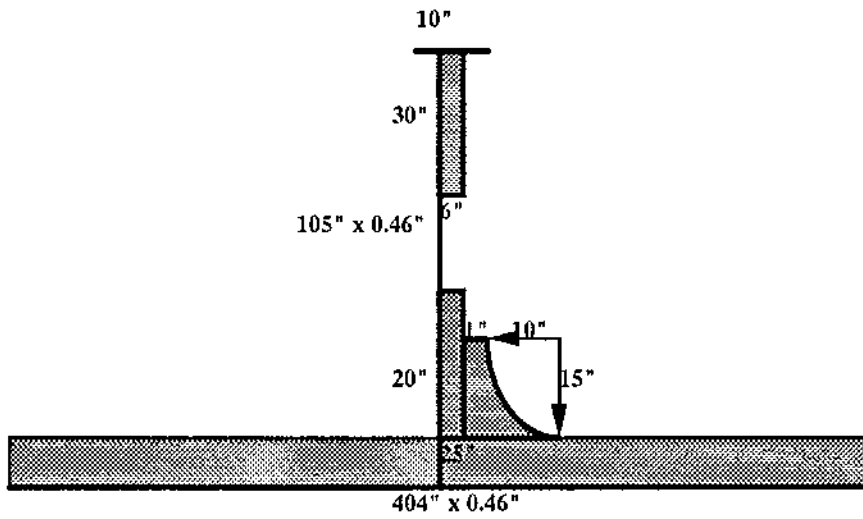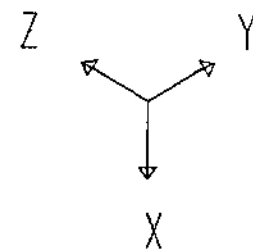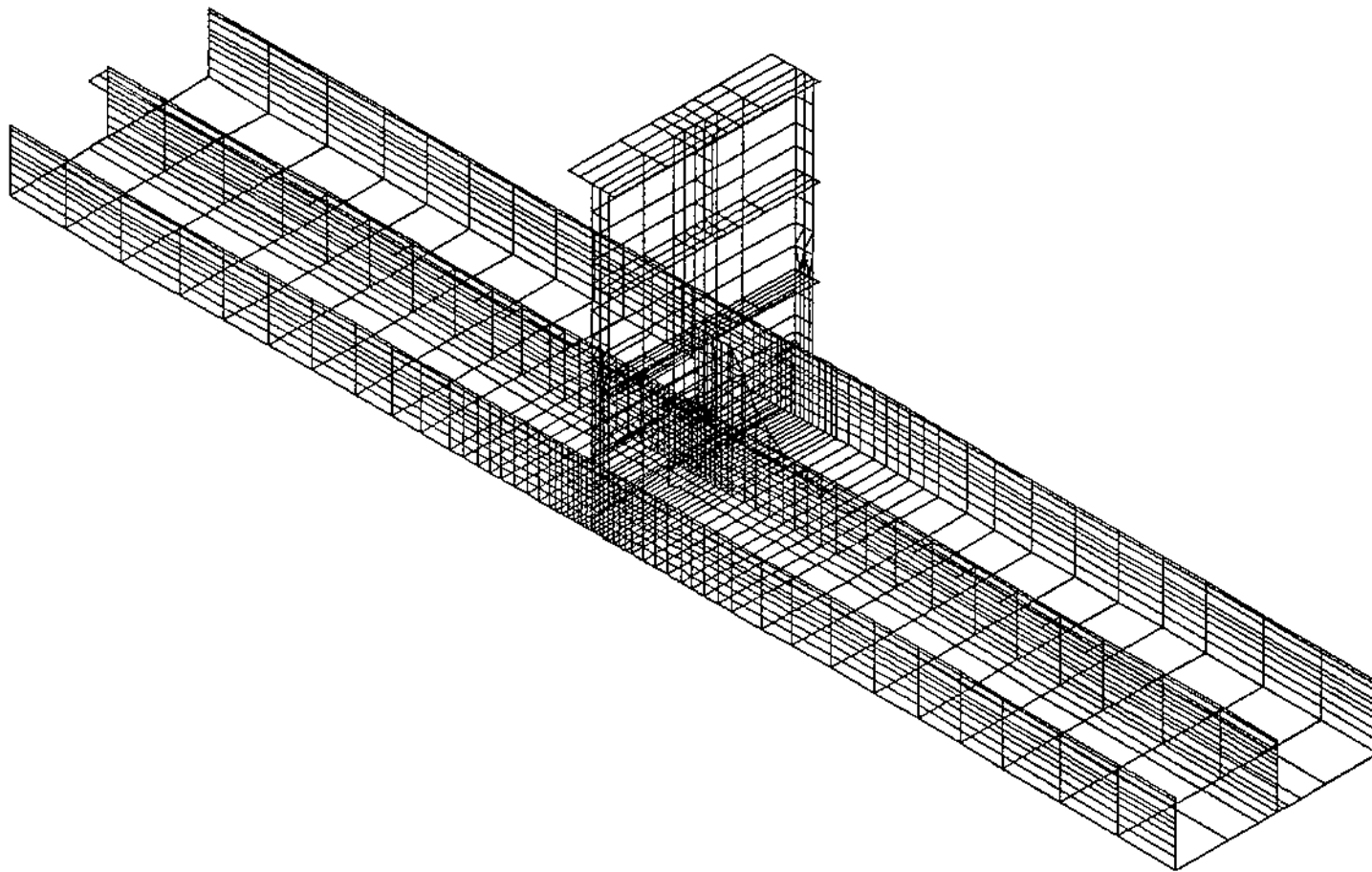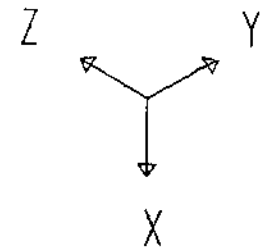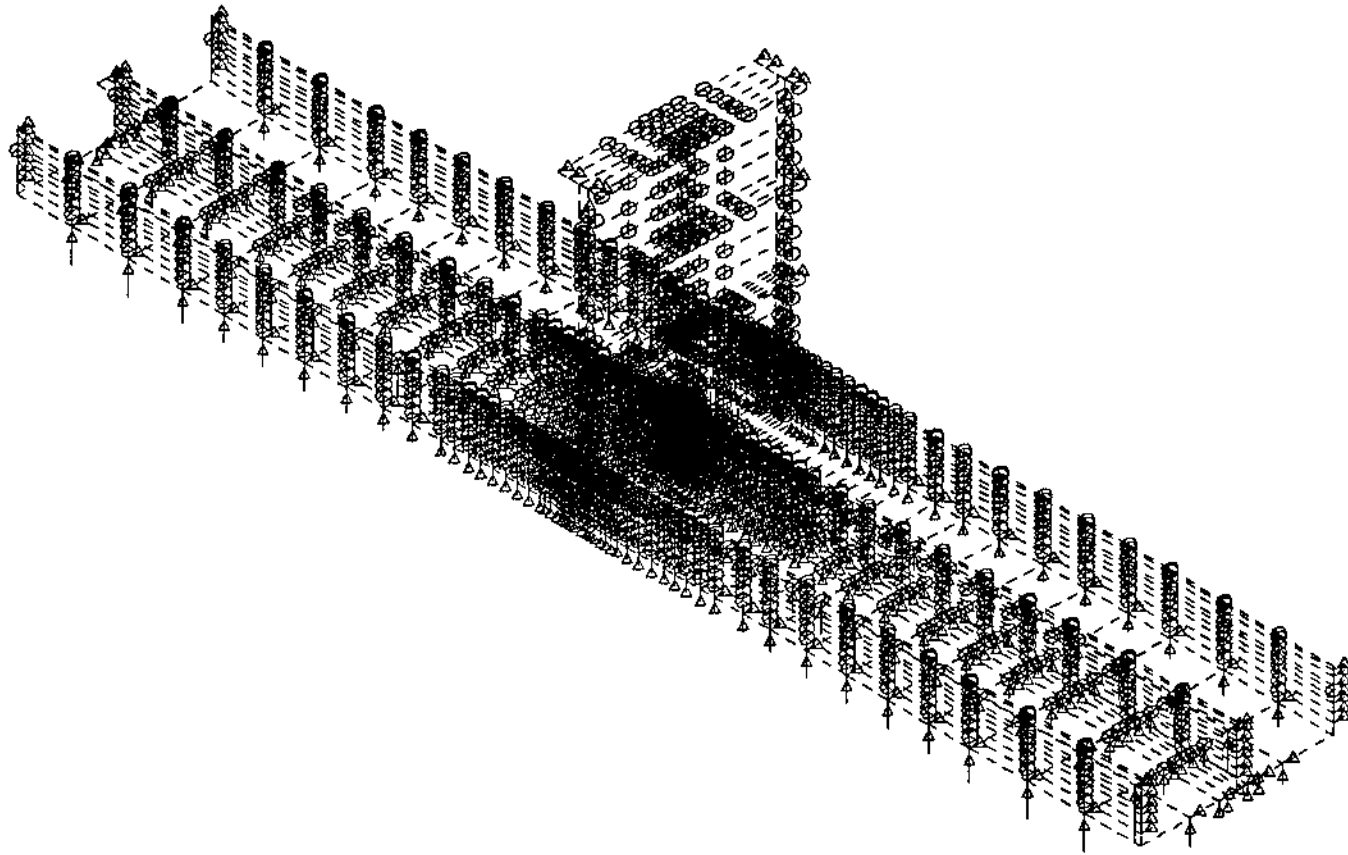
stiffen1

JOINT
LOADS

LOAD   1

MINIMA
P-0.1563E+04
MAXIMA
P-0.2288E-01

SAP90

435

stirren1
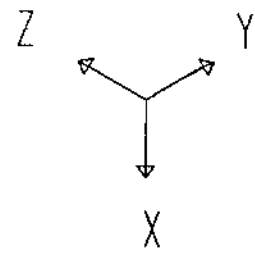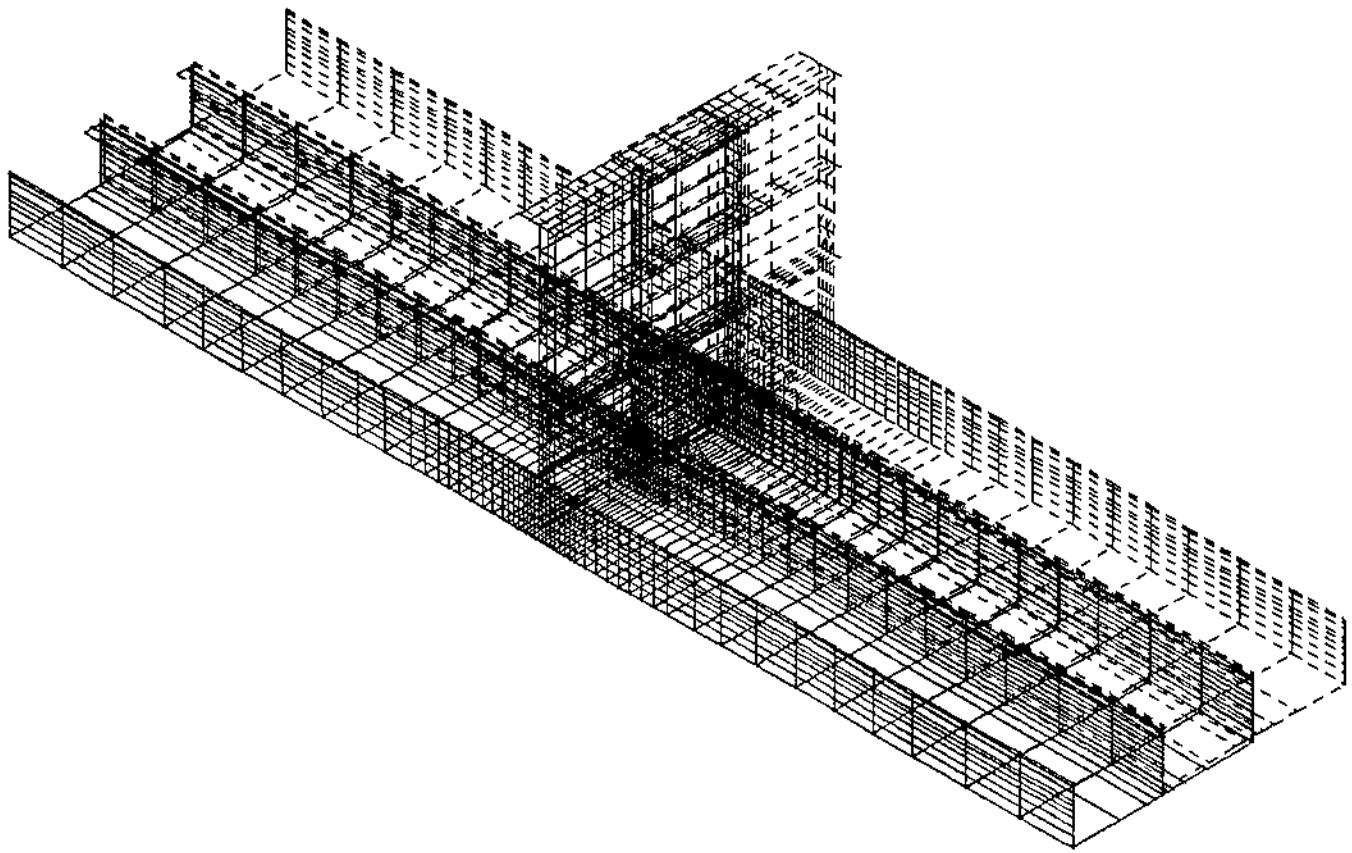
DEFORMED
SHAPE

LOAD   1

MINIMA
X-0.4484E-01
Y-0.2375E+01
Z-0.1548E+00
MAXIMA
X 0.6452E-01
Y-0.2329E+01
Z-0.3119E-01
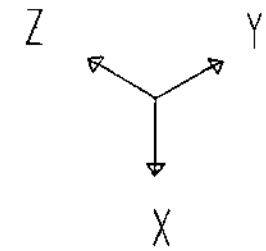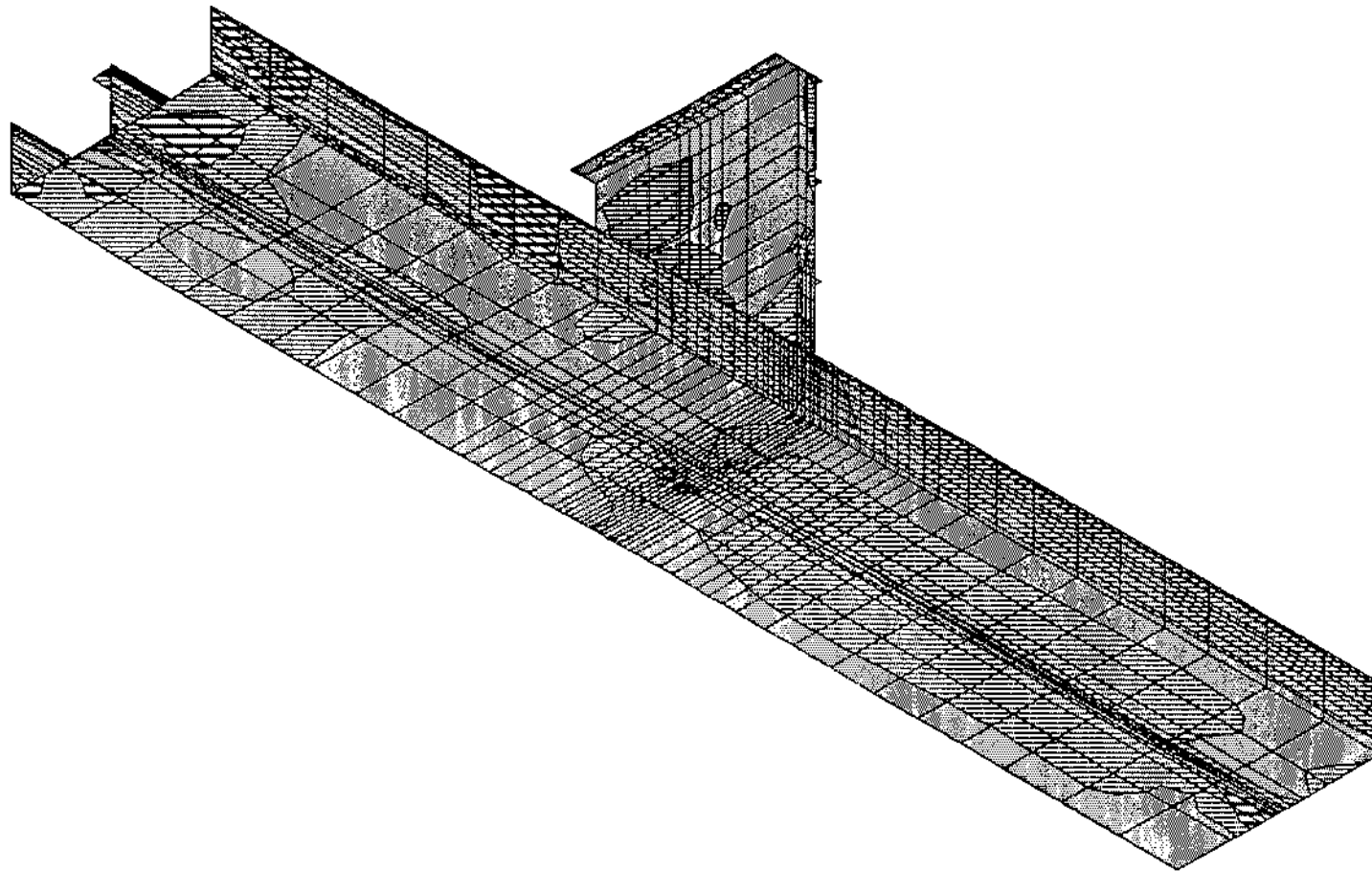
SAP90

Z   Y

X

stirrenl

SHELL
OUTPUT   S12T
LOAD   1

5000
3000
1000
-1000
-3000
-5000

SAP90

MIN IS -0.495E+04 <JOINT 2388>   MAX IS   0.460E+04 <JOINT 2324>

Z

Y

X

stiffen1
SHELL
OUTPUT SMXT
LOAD   1

22400
16800
11200
5600
0
-5600

SAP90

MIN IS -0.489E+04 <JOINT 1172>   MAX IS   0.190E+05 <JOINT 1171>

438

Y
X
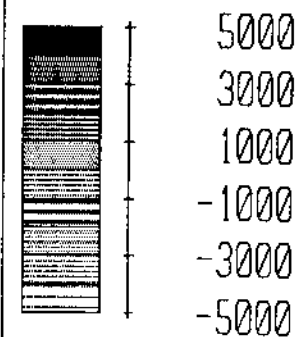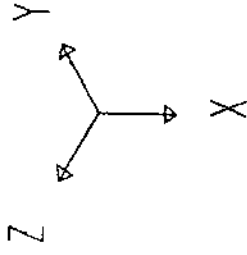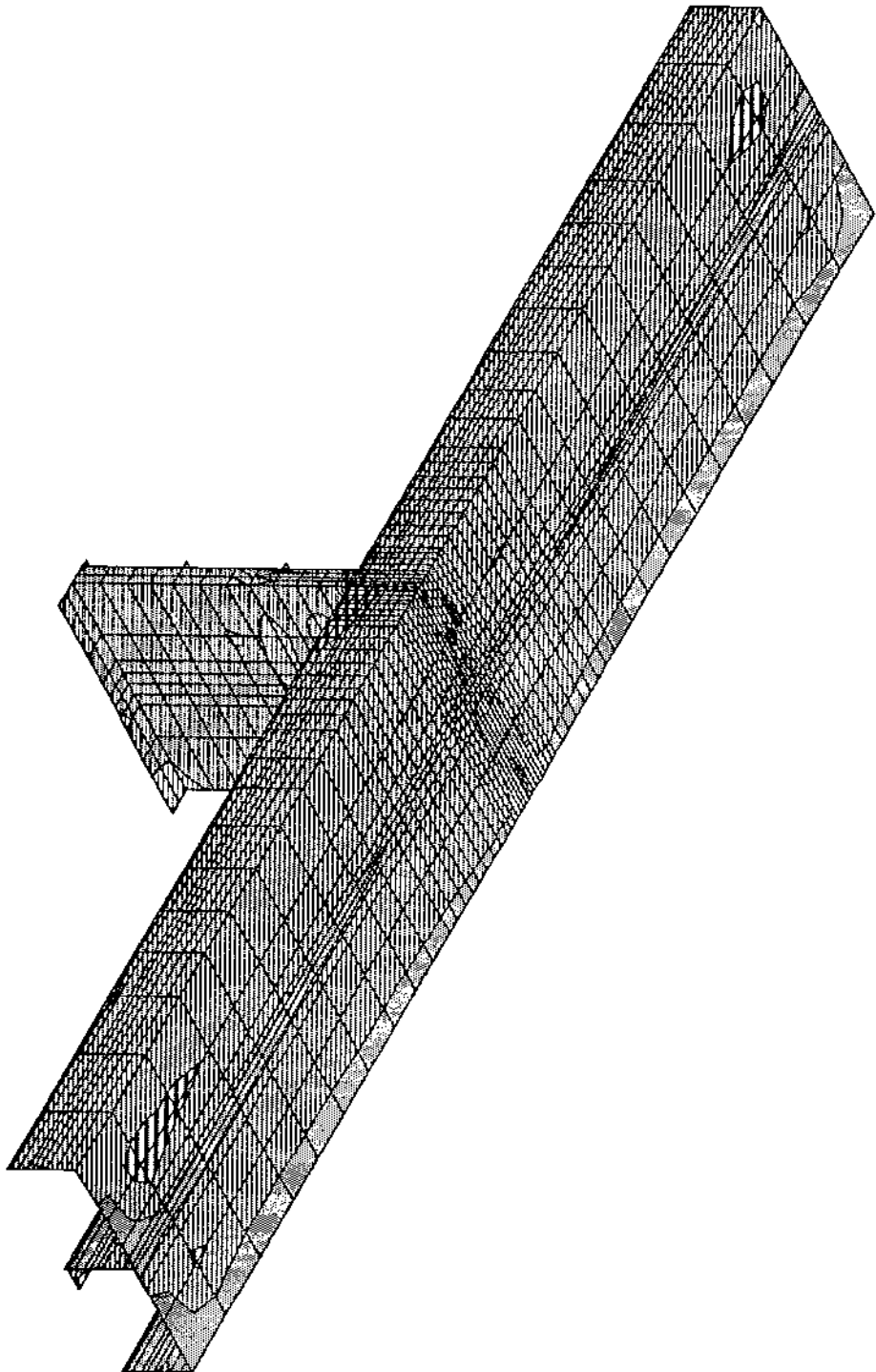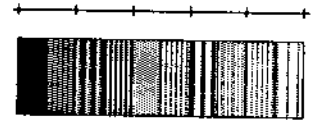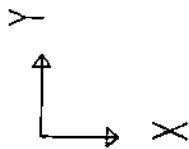
stiffen1
UNDEFORMED
SHAPE

OPTIONS
WIRE FRAME

SAP90

stiffen1

SHELL
OUTPUT S12T
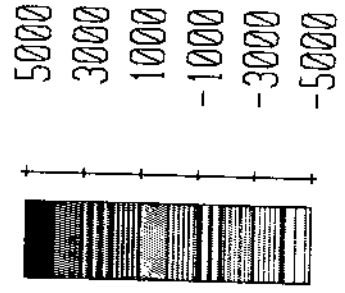
LOAD   1

Y
X

5000
3000
1000
-1000
-3000
-5000

SAP90

MIN IS -0.495E+04 <JOINT 2388>   MAX IS 0.460E+04 <JOINT 2324>

440

Y
↑
└→ X

stiffen1

SHELL
OUTPUT SMXT
LOAD   1

22400
16800
11200
5600
0
-5600

MIN IS -0.489E+04 <JOINT 1172>   MAX IS   0.190E+05 <JOINT 1171>

SAP90

441

Z

X
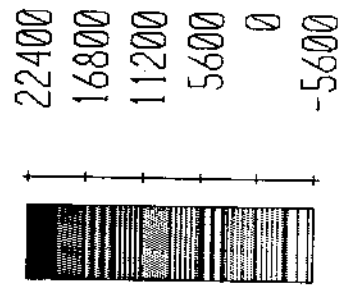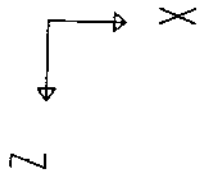
stiffen1
UNDEFORMED
SHAPE

OPTIONS
WIRE FRAME
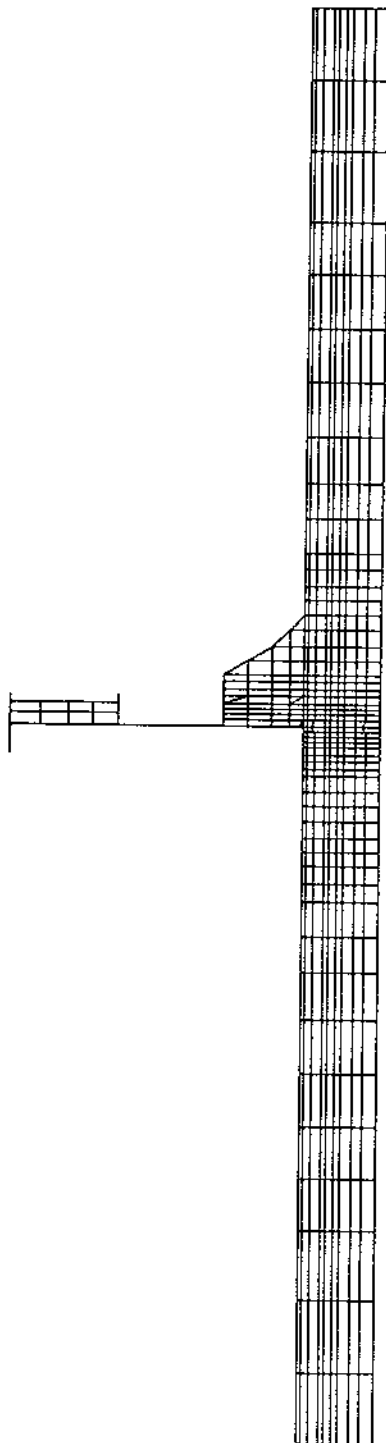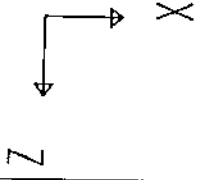
SAP90

stiffen1
DEFORMED
SHAPE
LOAD   1

Z
X

MINIMA
X -0.3179E-01
Y -0.2363E+01
Z -0.1464E+00
MAXIMA
X 0.4849E-01
Y -0.2333E+01
Z -0.3977E-01

SAP90

443

Z

X

stiffen1

SHELL
OUTPUT S12T
LOAD   1

5000
3000
1000
-1000
-3000
-5000

SAP90

MIN IS -0.495E+04 <JOINT 2388>   MAX IS   0.373E+04 <JOINT 2350>
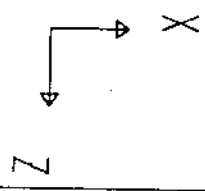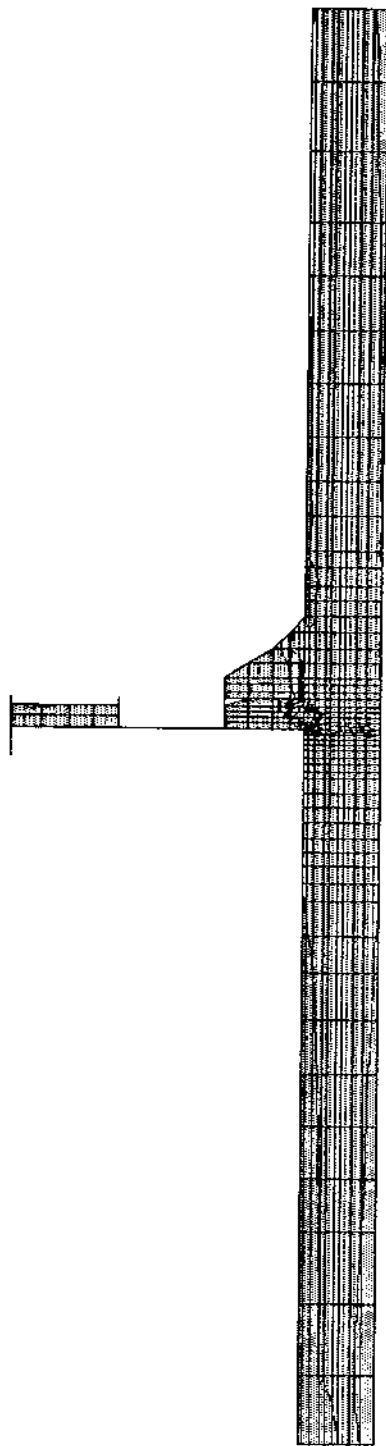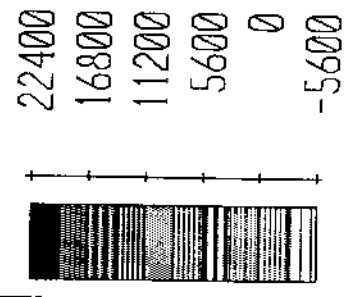
444

Z
X
stiffen1
SHELL
OUTPUT SMXT
LOAD   1

22400
16800
11200
5600
0
-5600

MIN IS -0.489E+04 <JOINT 1172>   MAX IS   0.190E+05 <JOINT 1171>

SAP90

445

10"

30"

105"x0.46" 6"

20"

6'

30"

20"

1"

2.5

404" x 0.46"

105" x 0.46"

2.5"

12.5

25

17.5

10

70"

5

70" x 0.46"

446
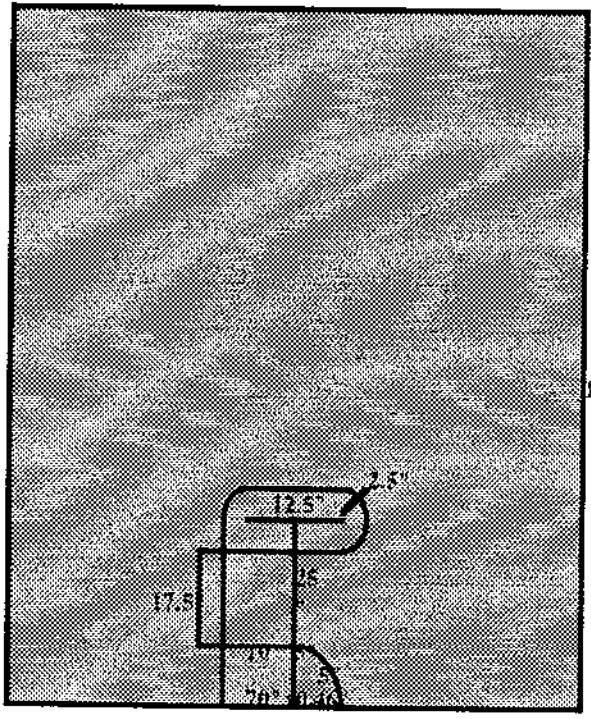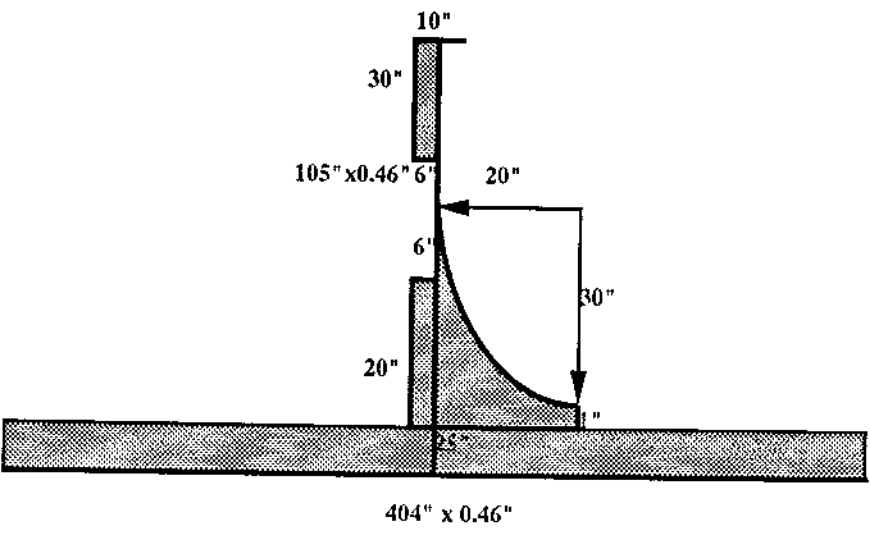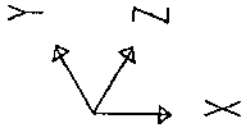
stiffen2
UNDEFORMED
SHAPE

OPTIONS
WIRE FRAME

SAP90

stiffen2

JOINT
LOADS
LOAD   1

MINIMA
P-0.1563E+04
MAXIMA
P-0.2288E-01

SAP90

Y
Z
X

stiffen2
DEFORMED
SHAPE
LOAD   1

MINIMA
X-0.4489E-01
Y-0.2375E+01
Z-0.1548E+00
MAXIMA
X 0.6452E-01
Y-0.2329E+01
Z-0.3119E-01

SAP90

449

Y
Z
X

stiffen2

SHELL
OUTPUT S12T

LOAD 1

5500
3300
1100
-1100
-3300
-5500

SAP90

MIN IS -0.511E+04 <JOINT 2388>   MAX IS 0.460E+04 <JOINT 2324>

450

Y
Z
X

stiffen2
SHELL
OUTPUT SMXT
LOAD   1

22400
16800
11200
5600
0
-5600

SAP90

MIN IS -0.463E+04 <JOINT 1172>   MAX IS   0.212E+05 <JOINT 894>

457

Y
X

stiffen2
UNDEFORMED
SHAPE

OPTIONS
WIRE FRAME

SAP90

452

stiffen2
SHELL
OUTPUT S12T
LOAD   1

5500
3300
1100
-1100
-3300
-5500
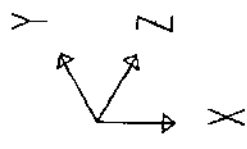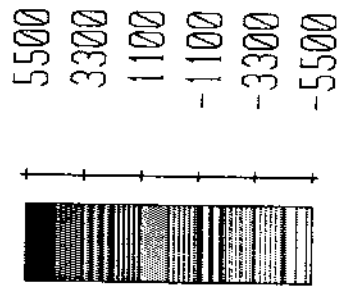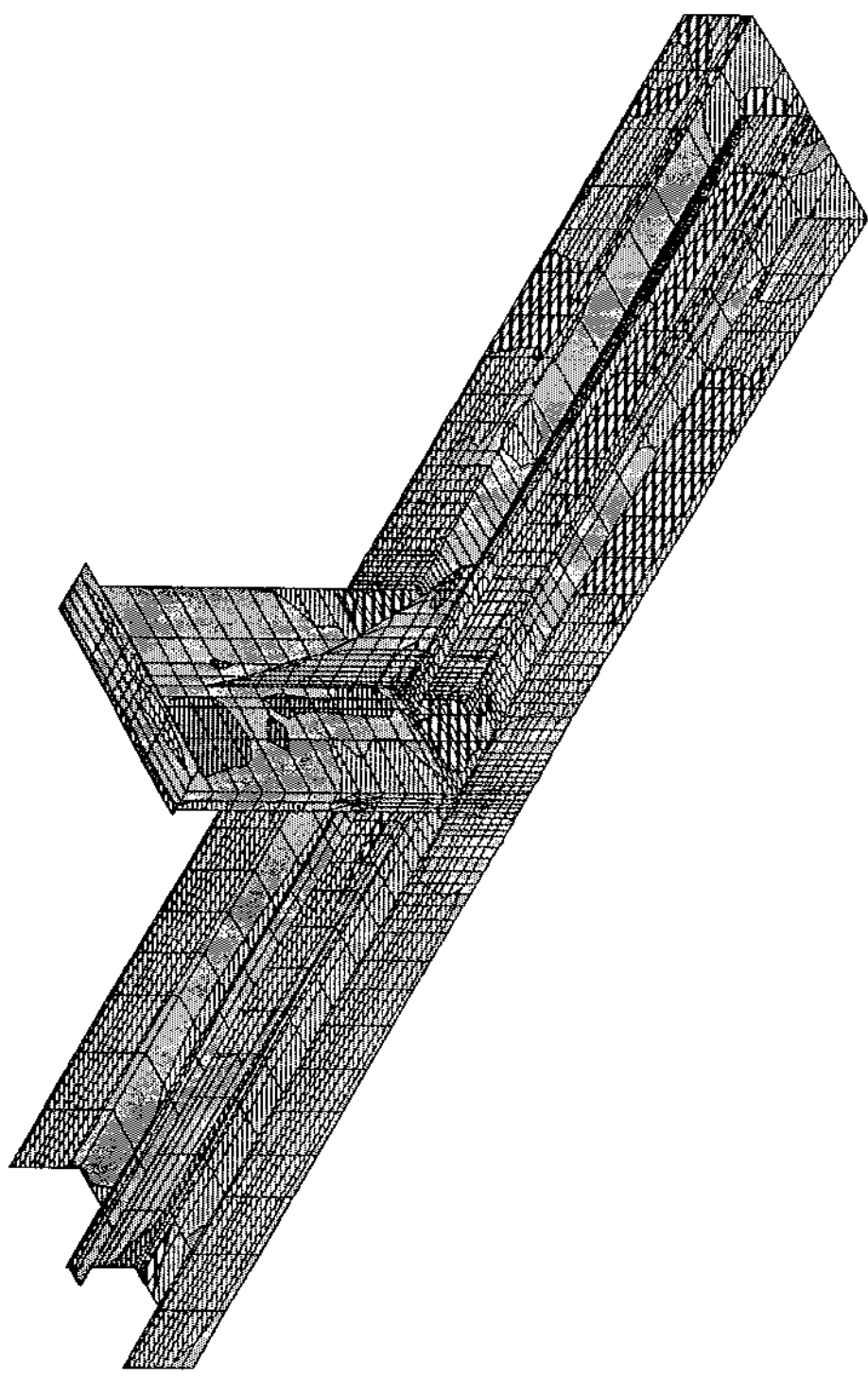
SAP90

MIN IS -0.511E+04 <JOINT 2388>   MAX IS 0.460E+04 <JOINT 2324>

stiffen2

SHELL
OUTPUT SMXT
LOAD   1

22400
16800
11200
5600
0
-5600

SAP90

MIN IS -0.463E+04 <JOINT 1172>   MAX IS   0.212E+05 <JOINT 894>

454

Z

X

stiffen2
UNDEFORMED
SHAPE

OPTIONS
WIRE FRAME

SAP90

455

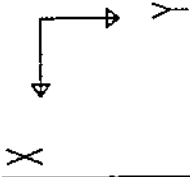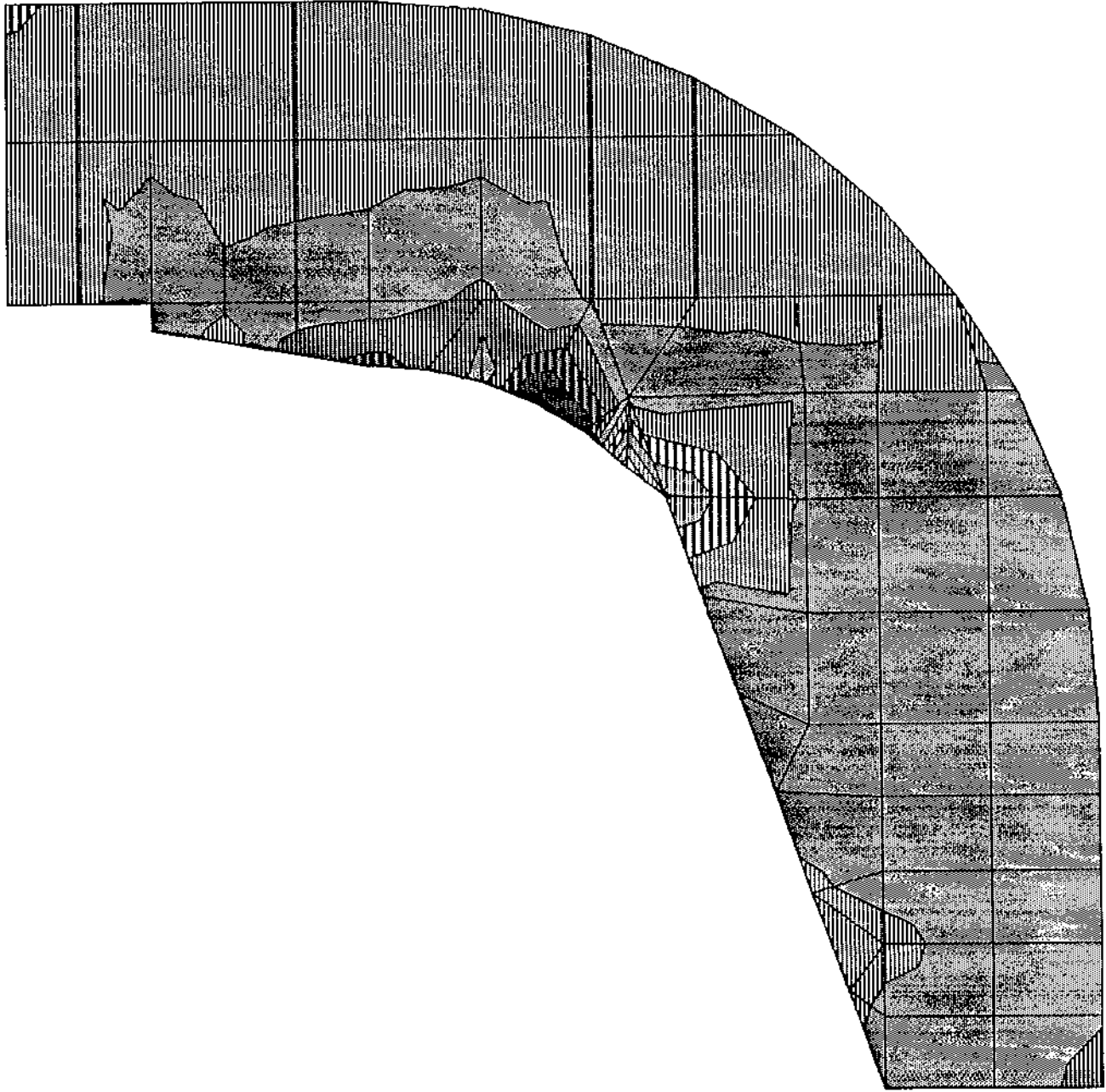stiffen2

SHELL
OUTPUT SMXT

LOAD   1

X

Z

22400
16800
11200
5600
0
-5600

SAP90

MIN IS -0.463E+04 <JOINT 1172>   MAX IS   0.212E+05 <JOINT 894>

Z

X

stiffen2
SHELL
OUTPUT S12T
LOAD 1

4000
2000
0
-2000
-4000
-6000
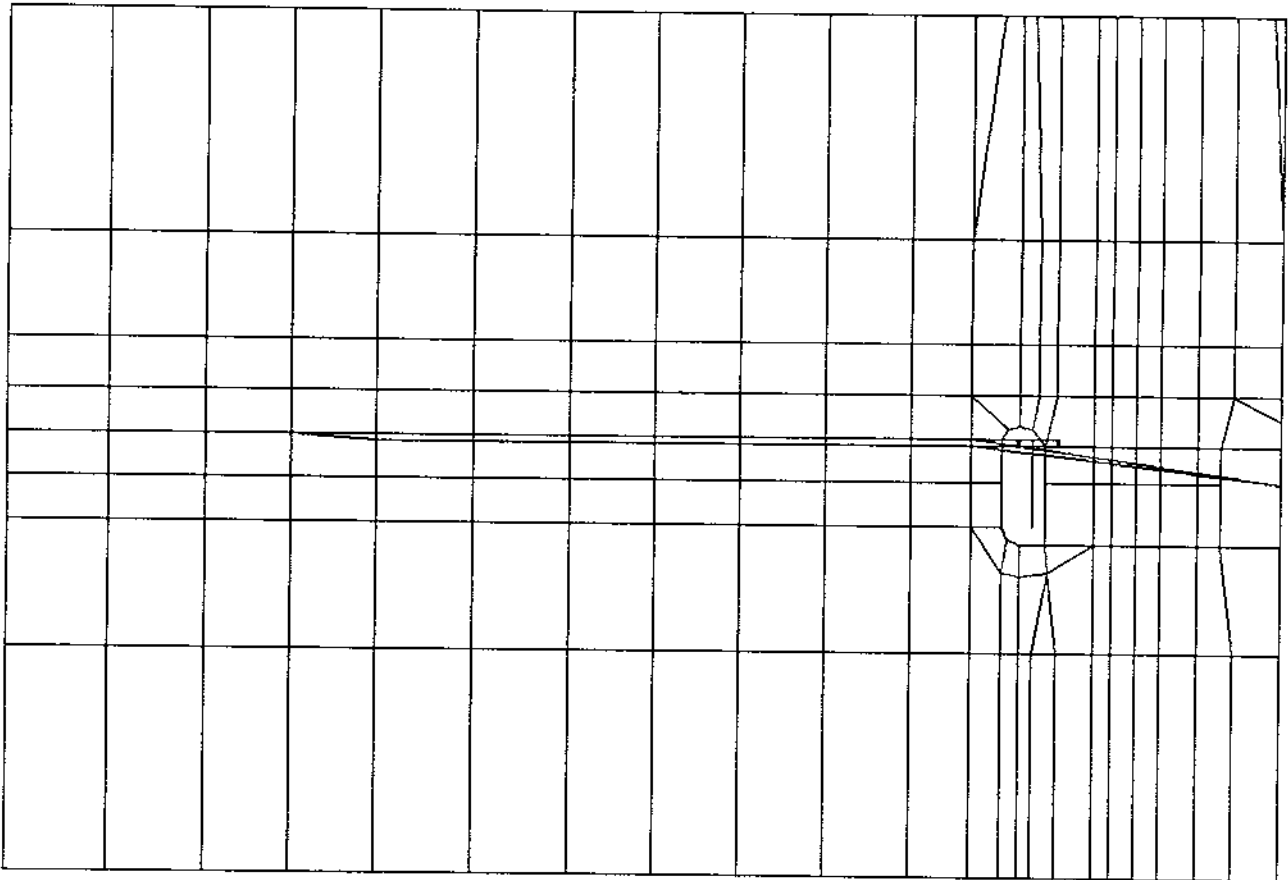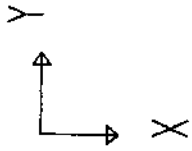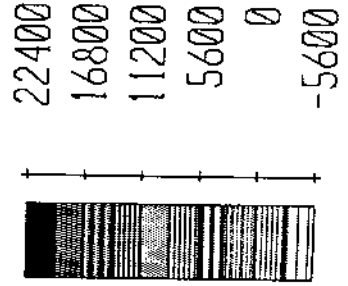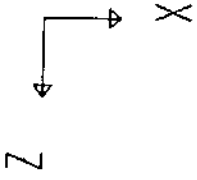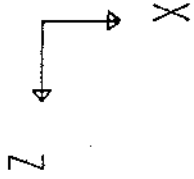
SAP90

MIN IS -0.511E+04 <JOINT 2388>   MAX IS 0.381E+04 <JOINT 2350>

457

10"

30"

105" x0.46" 6"   20"

6"

30"

20"

1"   1"

.5"

404" x 0.46"

105" x 0.46"

12.5"   1.5"

17.5"

1"

20"   1"

70" x 0.46"

458

Y
Z
X
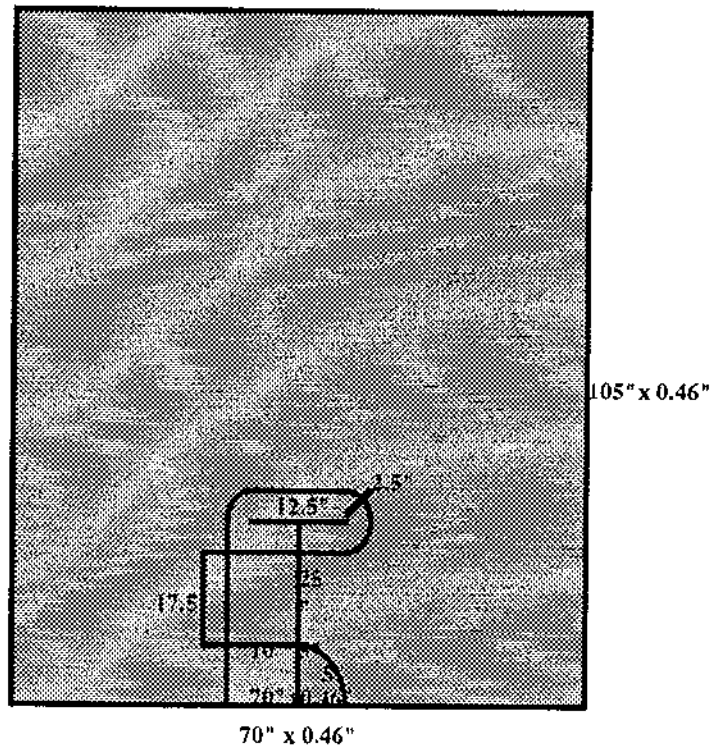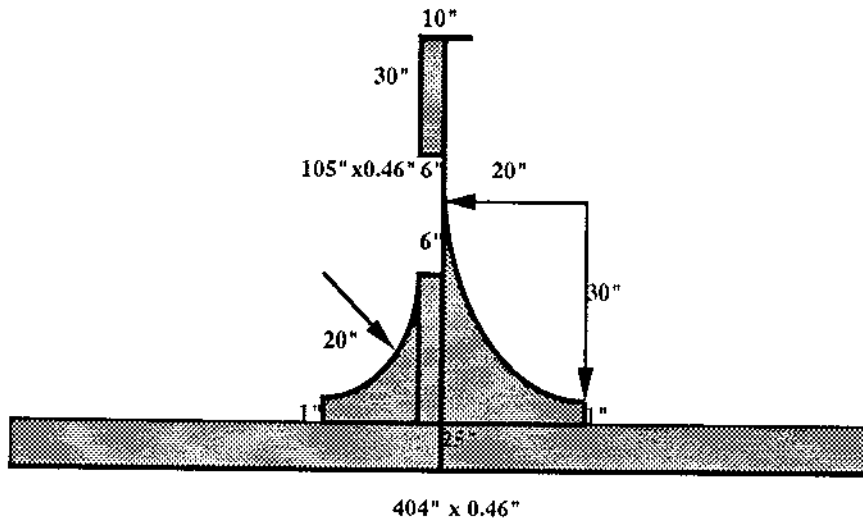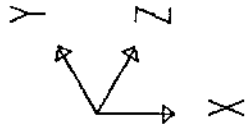
stiffen3
UNDEFORMED
SHAPE

OPTIONS
WIRE FRAME
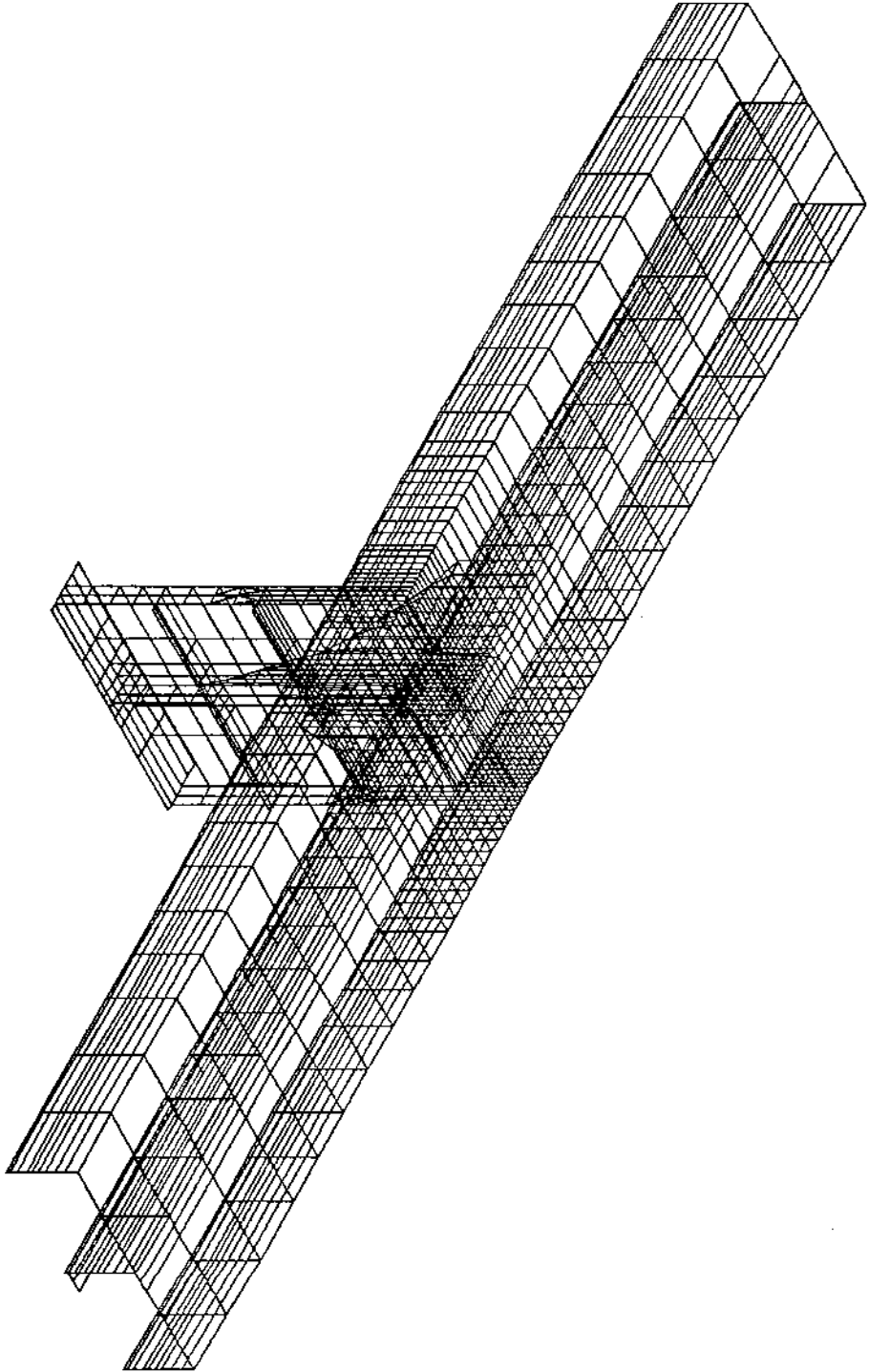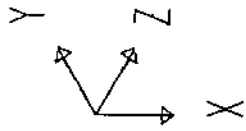
SAP90

stiffen3

JOINT
LOADS
LOAD   1

Y
Z
X

MINIMA
P-0.1563E+04
MAXIMA
P-0.2288E-01
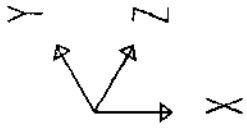
SAP90

stiffen3

DEFORMED

SHAPE

LOAD   1

MINIMA
X-0.4499E-01
Y-0.2375E+01
Z-0.1548E+00
MAXIMA
X 0.6452E-01
Y-0.2329E+01
Z-0.3119E-01

SAP90

461

Y
Z
X

stiffen3
SHELL
OUTPUT S12T
LOAD   1

5500
3300
1100
-1100
-3300
-5500

SAP90

MIN IS -0.515E+04 <JOINT 2388>   MAX IS   0.460E+04 <JOINT 2324>

462

MIN IS -0.524E+04 <JOINT 1172>   MAX IS   0.203E+05 <JOINT 1171>

stiffen3
UNDEFORMED
SHAPE

OPTIONS
WIRE FRAME

Y
X

SAP90

stiffen3
SHELL
OUTPUT S12T
LOAD   1

Y
X

5500
3300
1100
-1100
-3300
-5500

SAP90

MIN IS -0.515E+04 <JOINT 2388>   MAX IS   0.460E+04 <JOINT 2324>

465

Y
X

stiffen3
SHELL
OUTPUT SMXT
LOAD 1
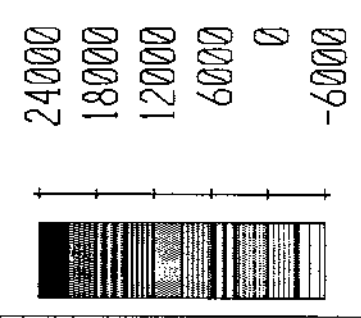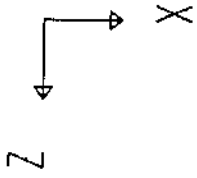
24000
18000
12000
6000
0
-6000

SAP90

MIN IS -0.524E+04 <JOINT 1172>   MAX IS 0.203E+05 <JOINT 1171>

466

Z

X

stiffen3
UNDEFORMED
SHAPE

OPTIONS
WIRE FRAME

SAP90

467

Z

Z ——→ X

stiffen3

SHELL
OUTPUT S12T
LOAD   1

4000
2000
0
-2000
-4000
-6000
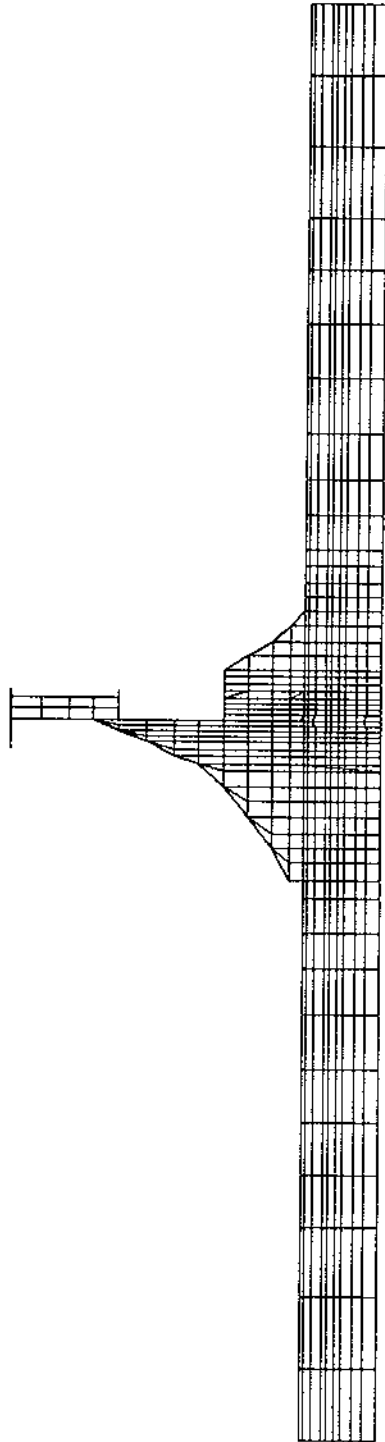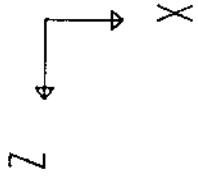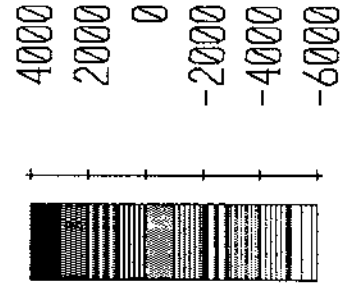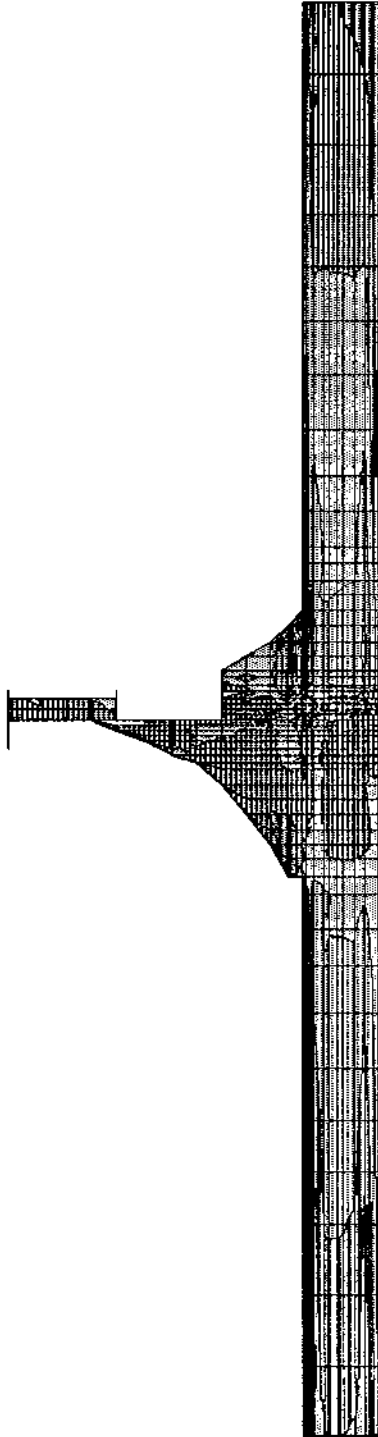
SAP90

MIN IS -0.515E+04 <JOINT 2388>   MAX IS   0.383E+04 <JOINT 2350>

468

Section 3 General Nonsideshell CSD Analysis
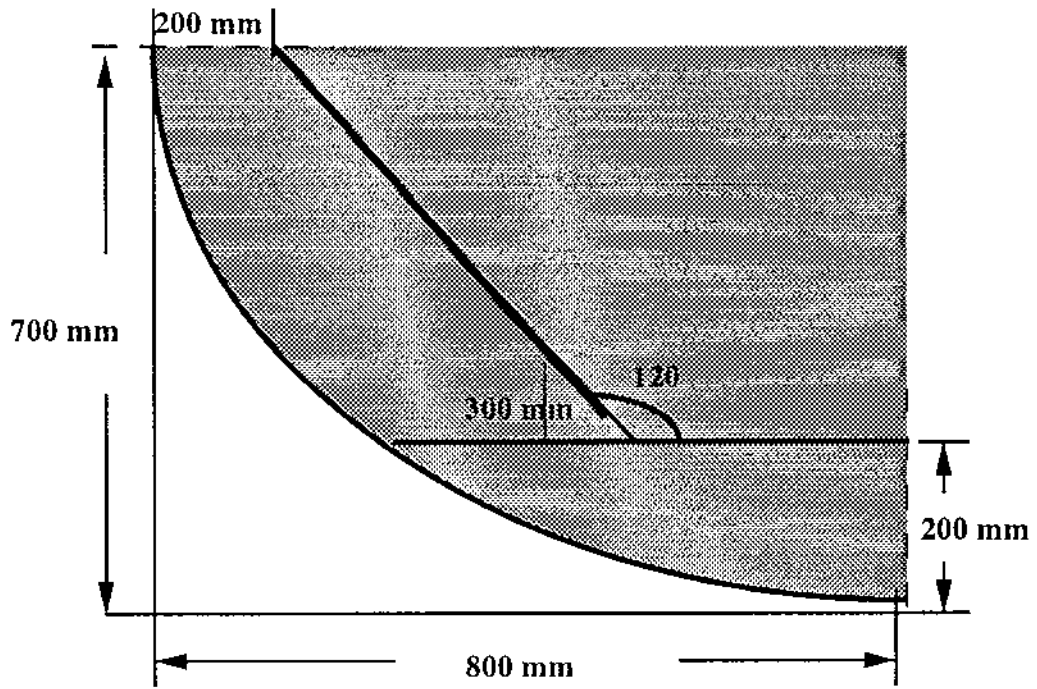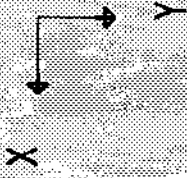
Double-Bottom Connection

WEBFRAME
UNDEFORMED
SHAPE

OPTIONS
WIRE FRAME

SAP90

471
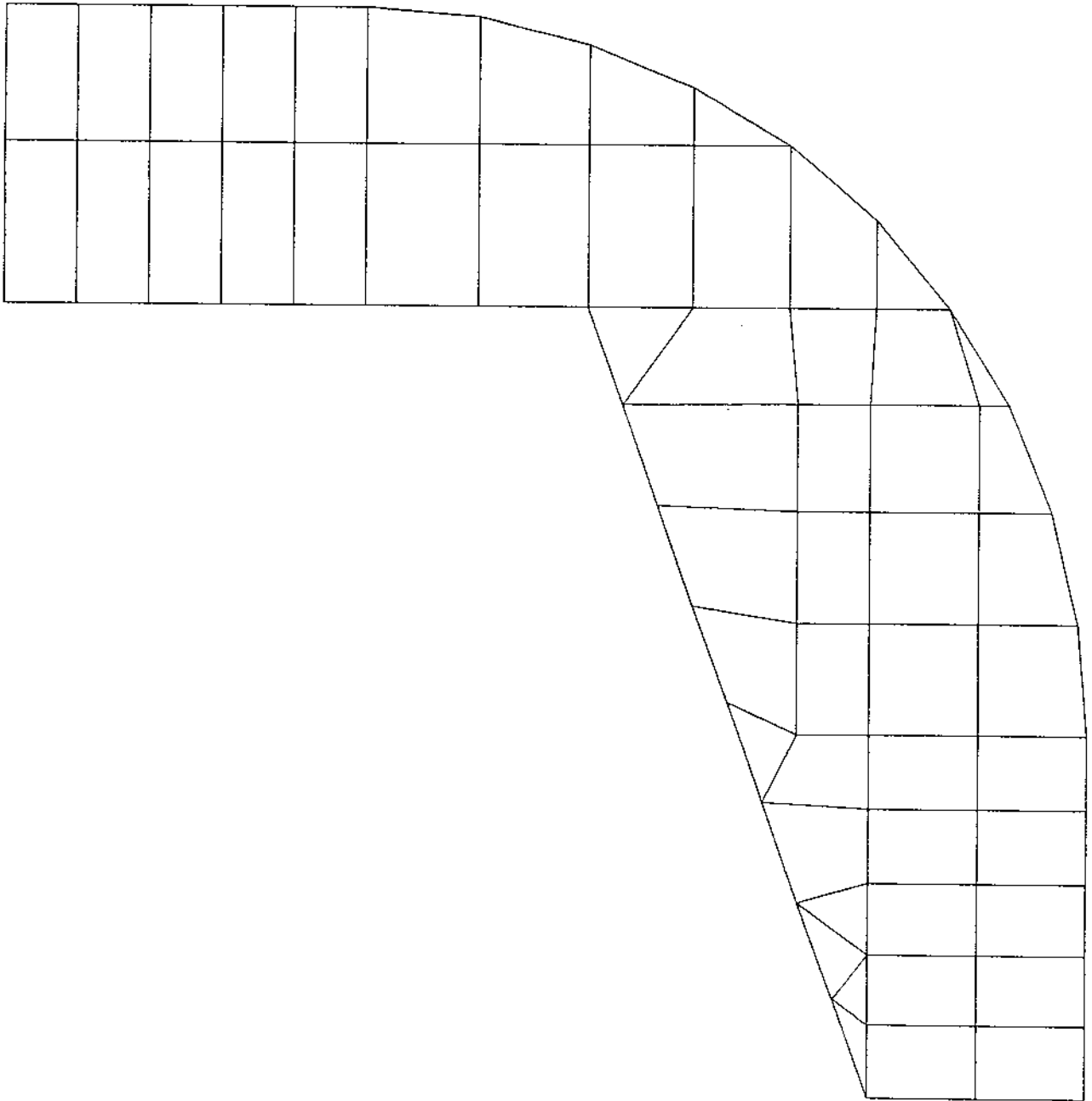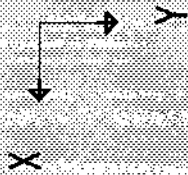
WEBFRAME

DEFORMED
SHAPE
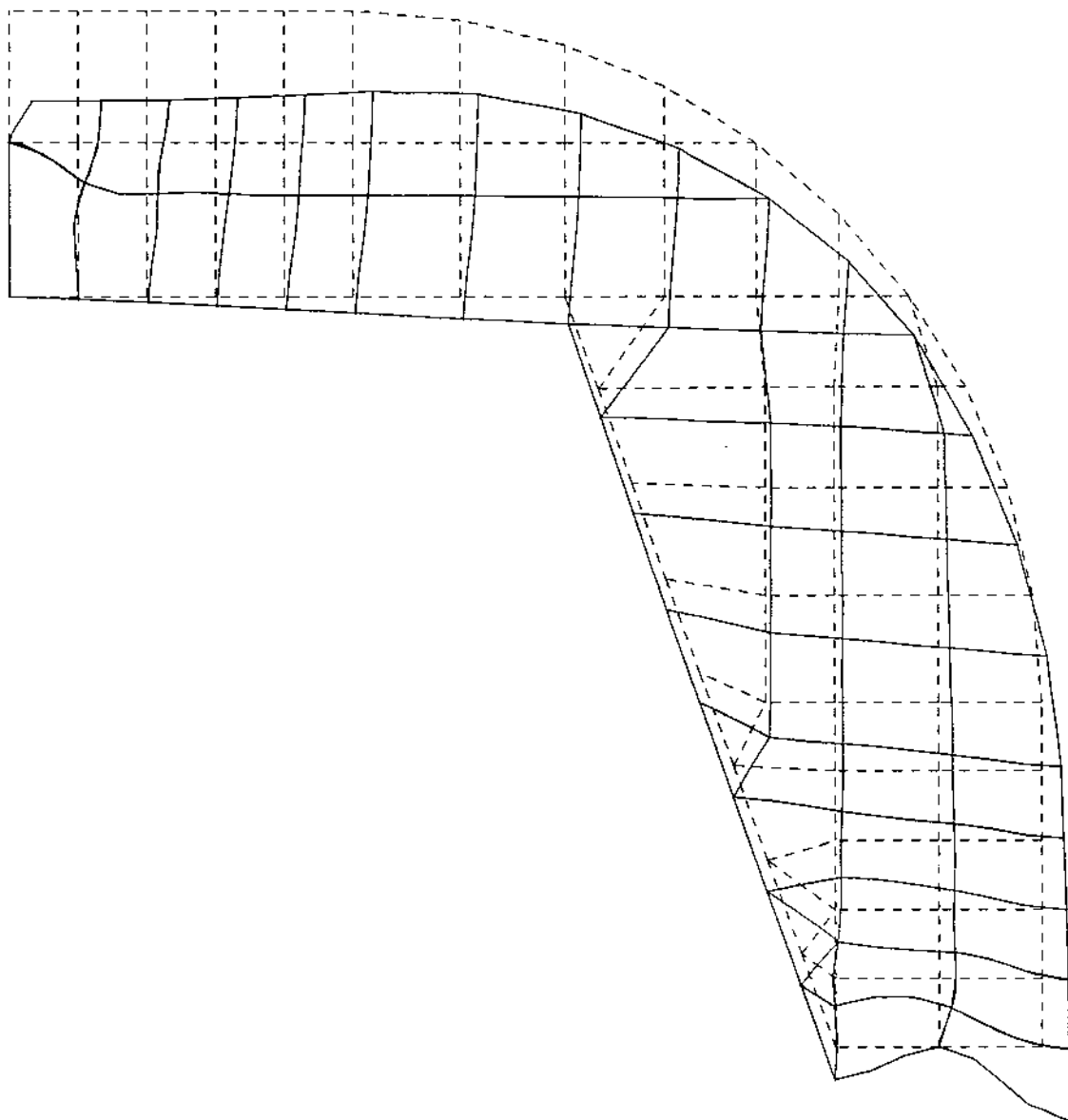
LOAD   1

MINIMA
X 0.0000E+00
Y-0.4144E-05
Z 0.0000E+00
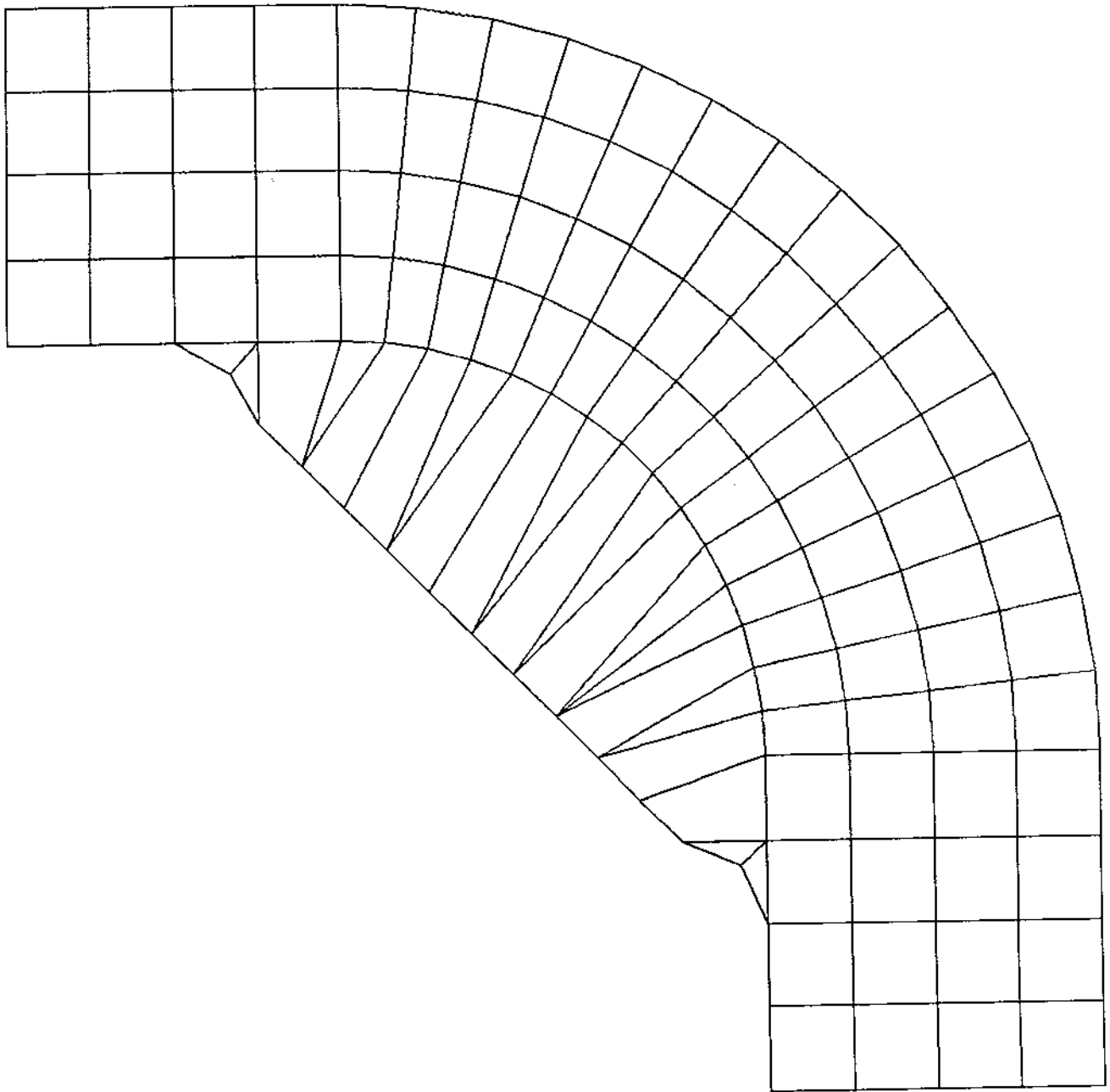MAXIMA
X 0.3349E-03
Y 0.1028E-03
Z 0.0000E+00

SAP90

X

Y

X

webframe
SHELL
OUTPUT S11T
LOAD   1

X 10⁻⁵

168
112
56
0
-56
-112
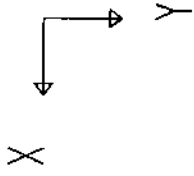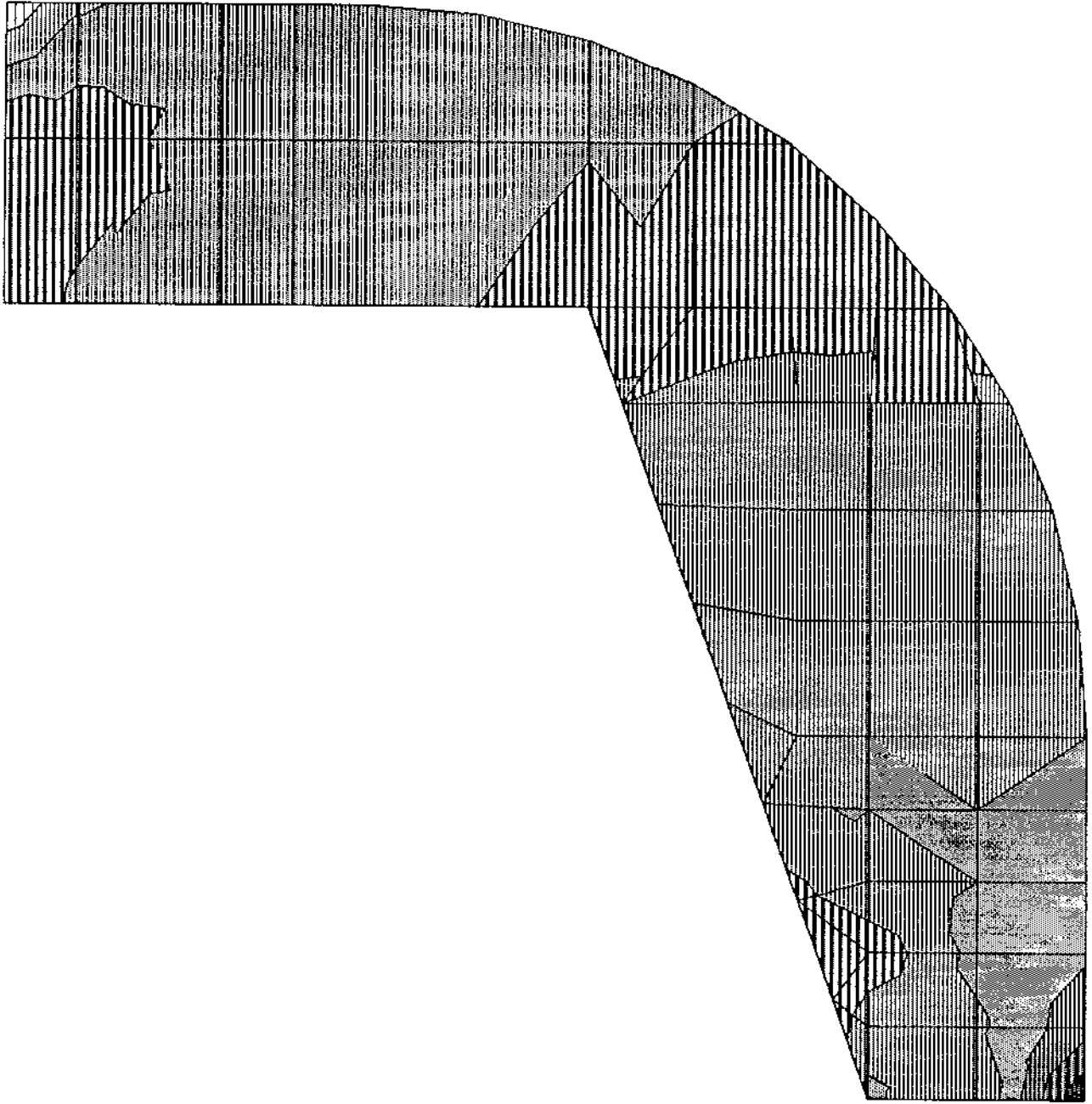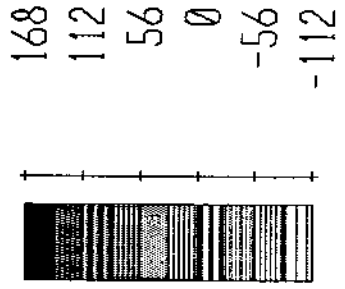
MIN IS -0.107E-02 <JOINT   17>   MAX IS   0.139E-02 <JOINT   22>

SAP90

473

X

Y↓ X→
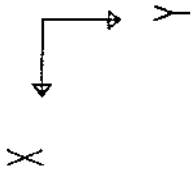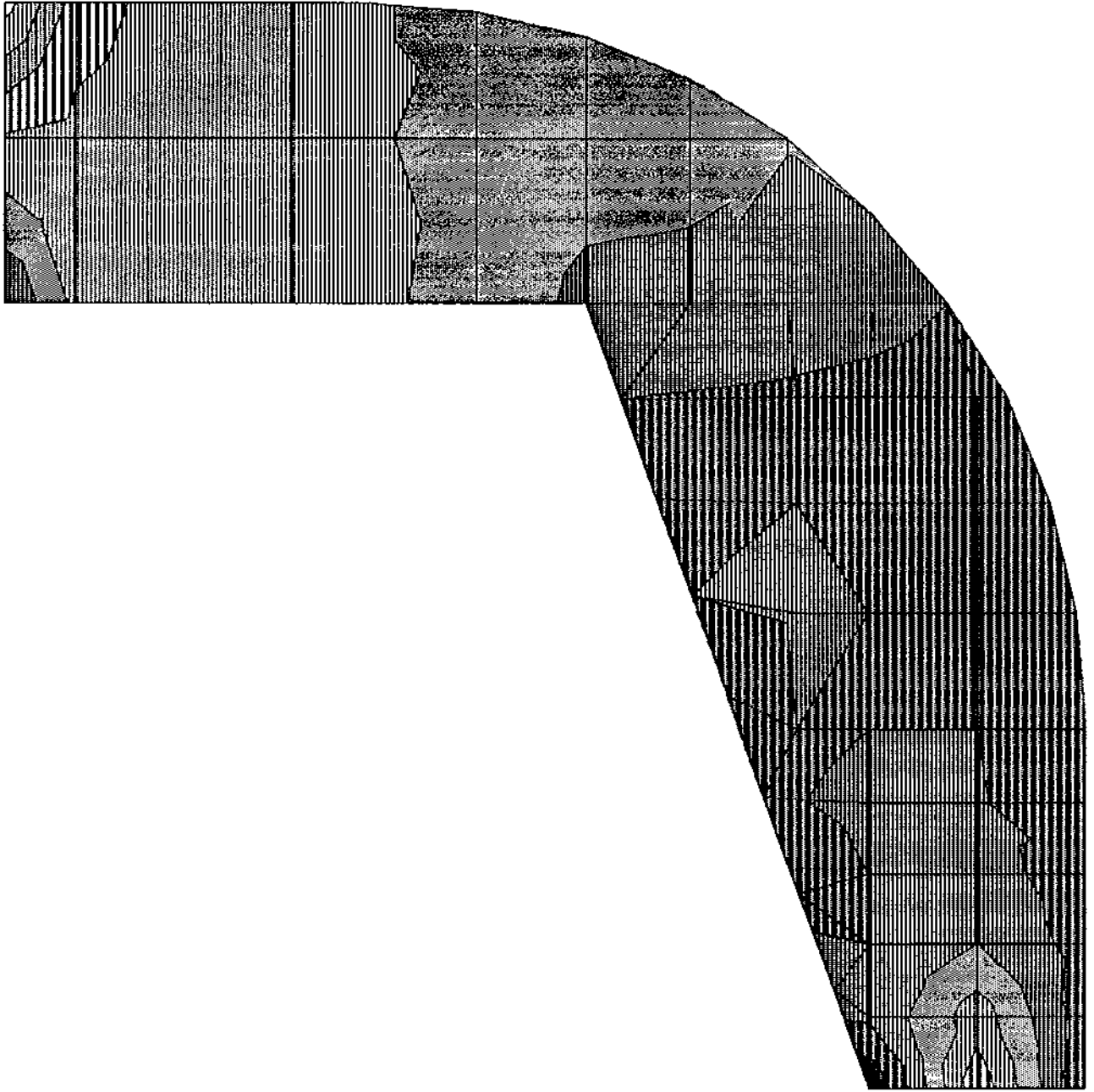
webframe

SHELL
OUTPUT S22T
LOAD   1

X 10⁻⁵

165
55
-55
-165
-275
-385
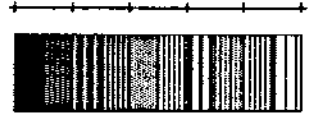
SAP90

MIN IS -0.353E-02 <JOINT   17>   MAX IS   0.105E-02 <JOINT   162>

47a

X
Y
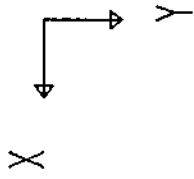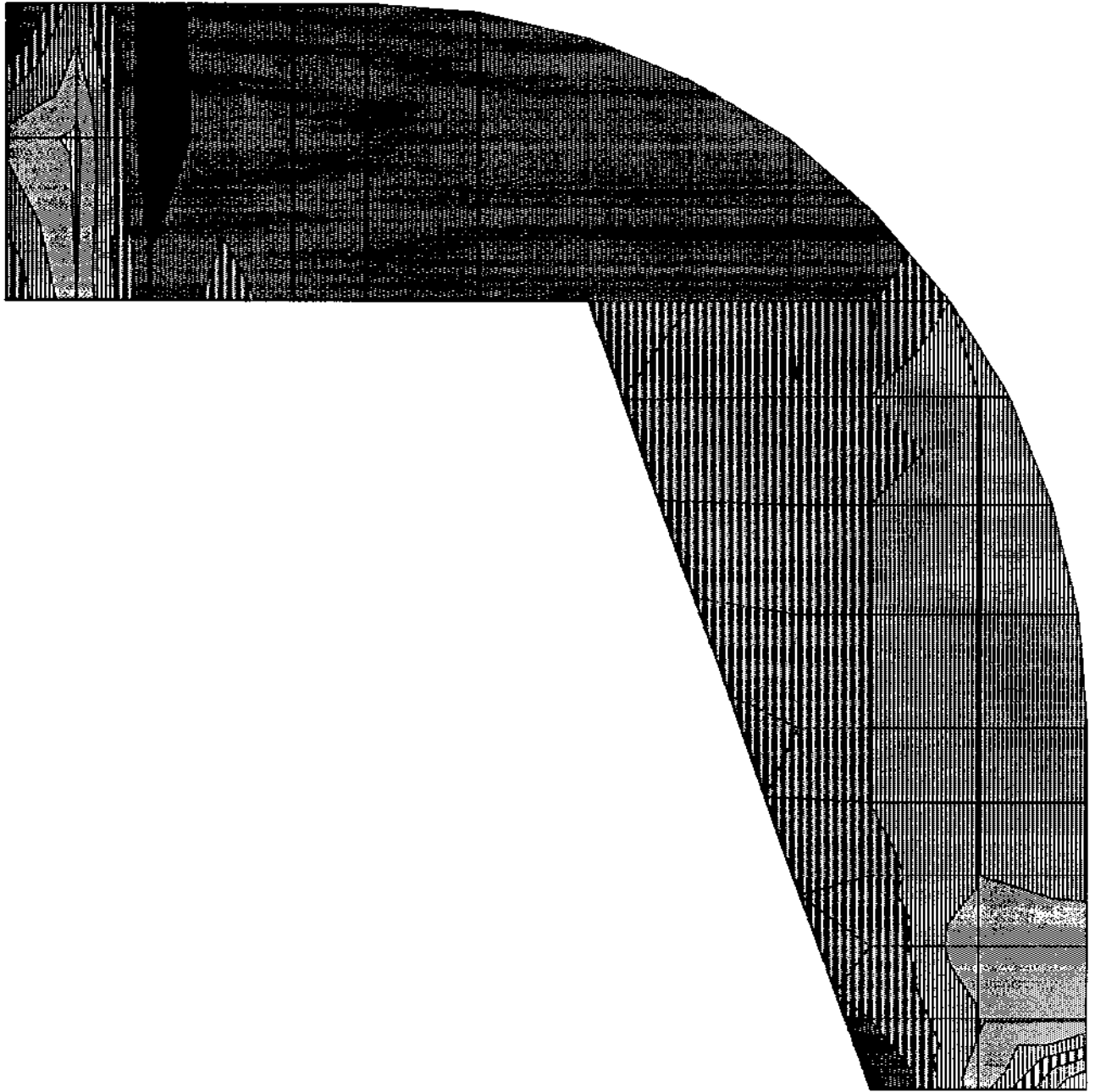
webframe
SHELL
OUTPUT S12T
LOAD   1

$X \ 10^{-5}$

34
0
-34
-68
-102
-136
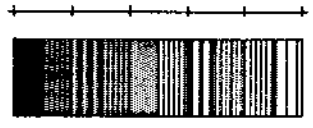
MIN IS -0.126E-02 <JOINT   22>   MAX IS   0.331E-03 <JOINT   17>

SAP90

475

X

↓ Y
X

webframe
SHELL
OUTPUT SMXT
LOAD   1
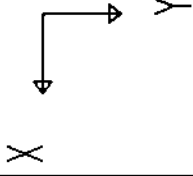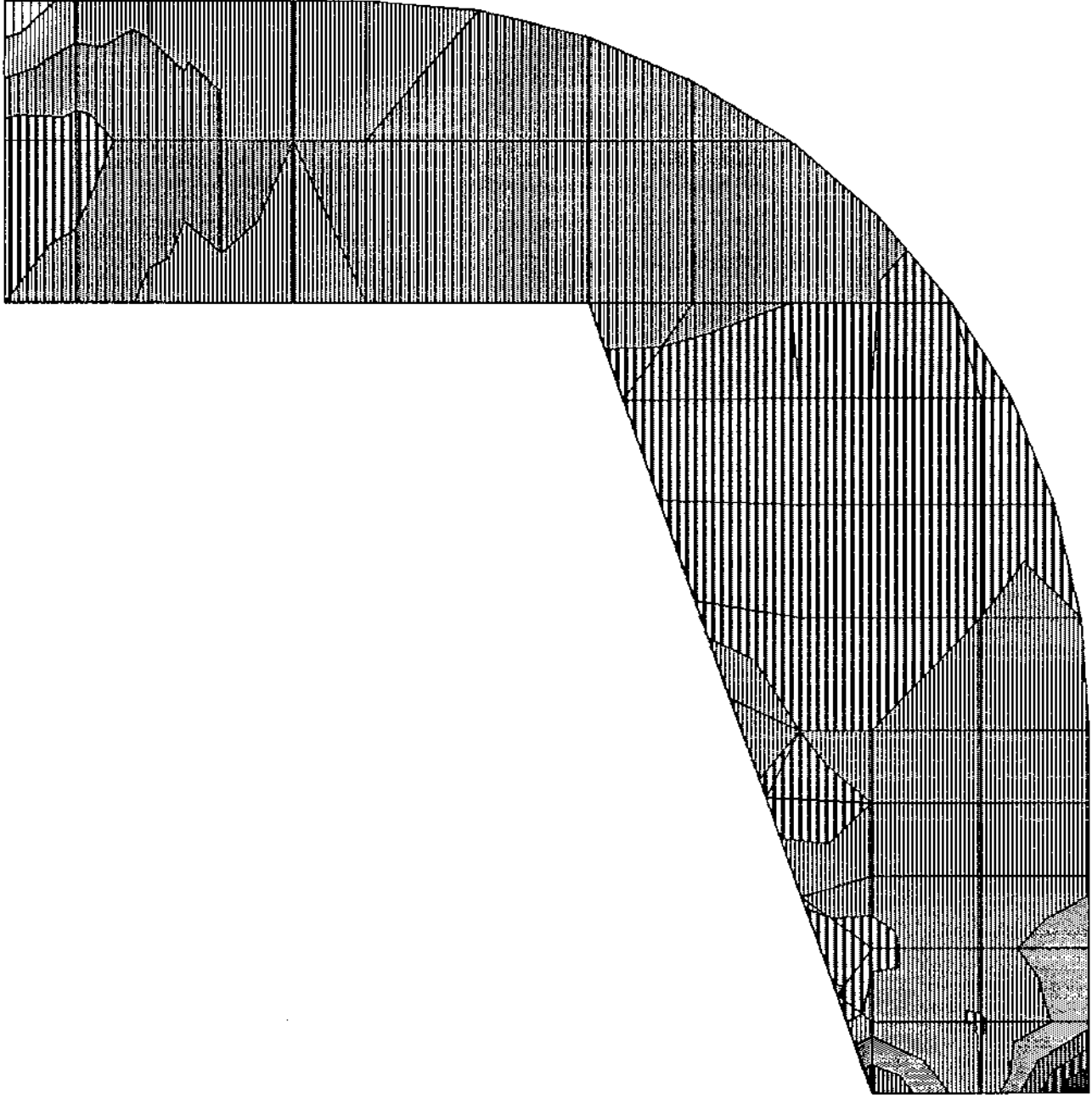
X 10^{-5}
245
175
105
35
-35
-105
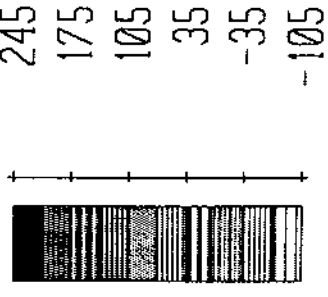
SAP90

MIN IS -0.102E-02 <JOINT   17>   MAX IS   0.226E-02 <JOINT   22>

Double-Bottom Connection

200

50

400

700 mm

450

50

200

800 mm

webframe
UNDEFORMED
SHAPE

OPTIONS
WIRE FRAME

Y
X
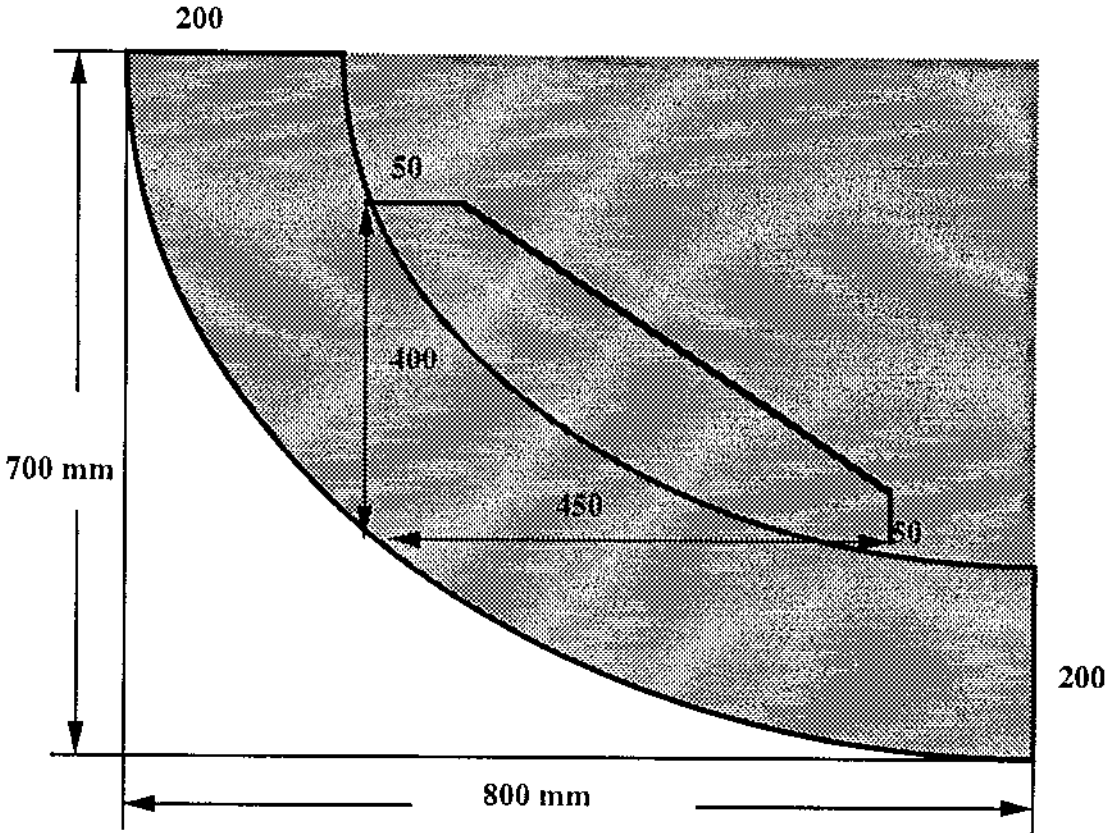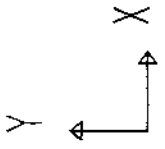
SAP90

webframe
DEFORMED
SHAPE
LOAD   1
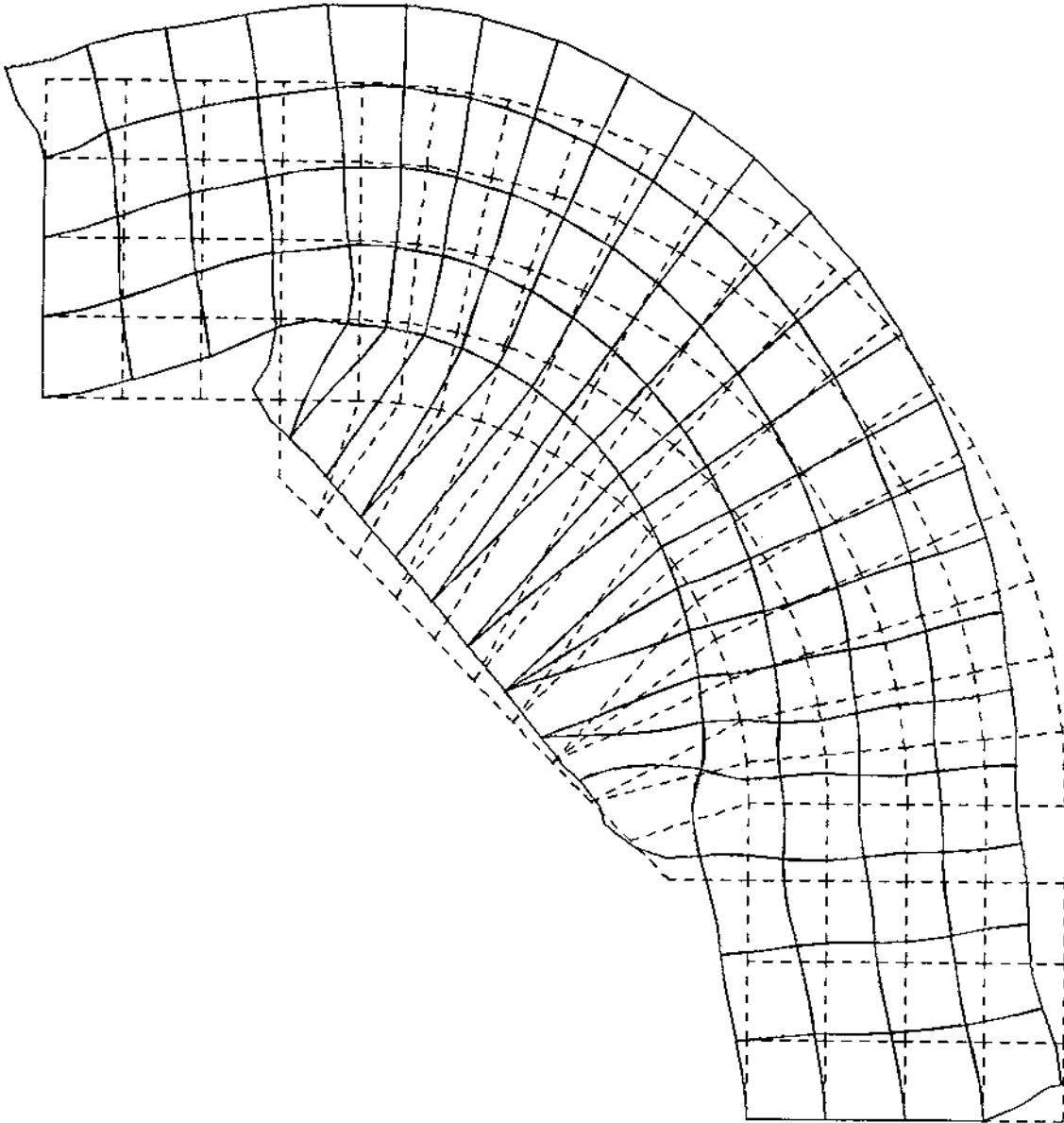
MINIMA
X -0.9787E-07
Y -0.8306E-06
Z 0.0000E+00
MAXIMA
X 0.6992E-05
Y 0.5163E-05
Z 0.0000E+00

SAP90

Y
X

479
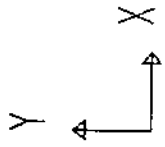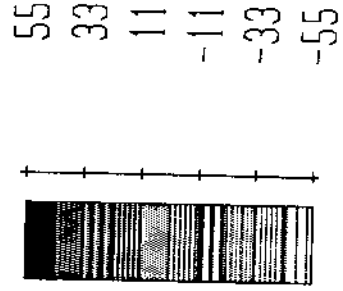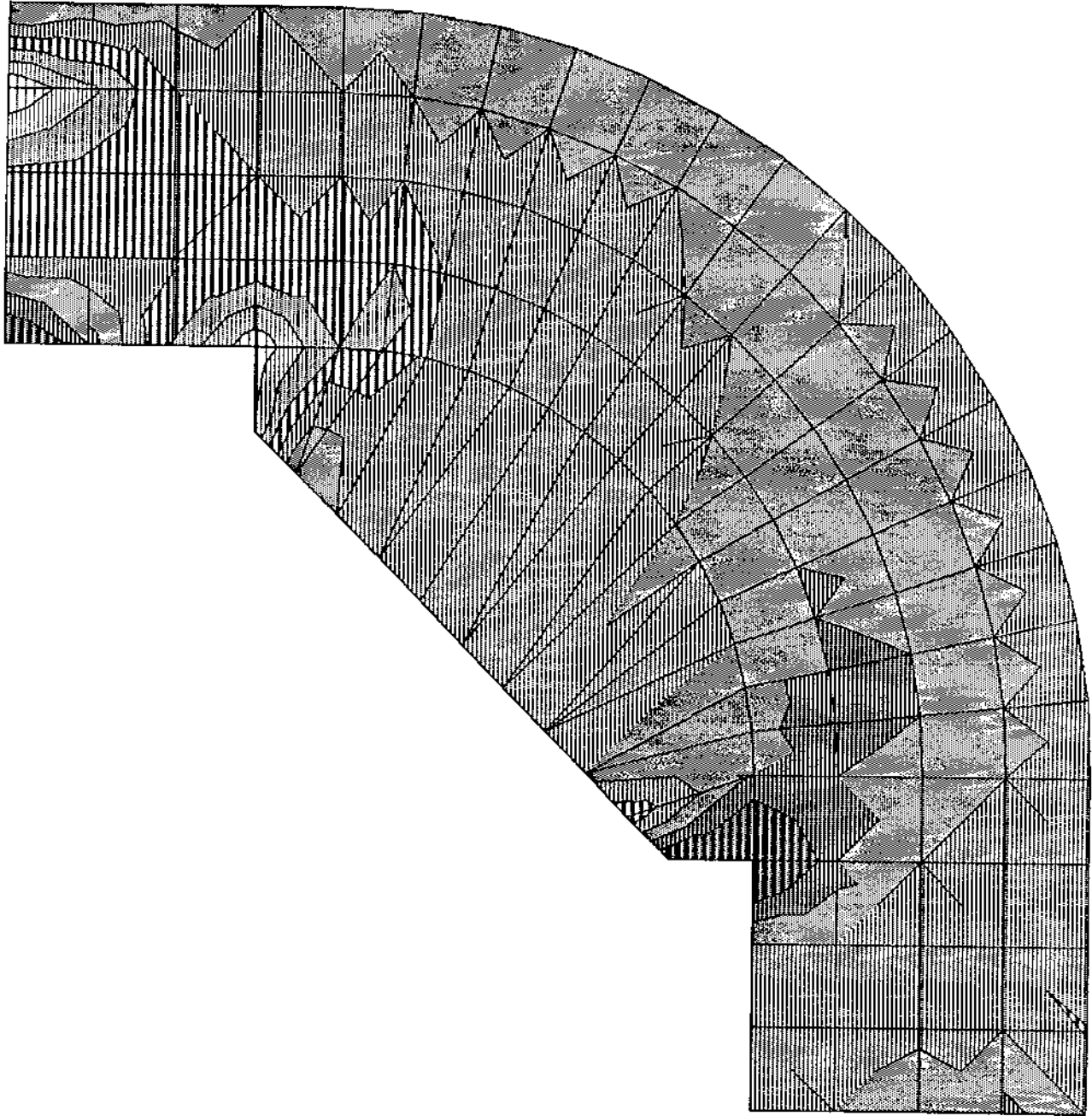
MIN IS -0.549E-03 <JOINT 117>   MAX IS 0.427E-03 <JOINT 98>

Y
X

webframe
SHELL
OUTPUT S11T
LOAD 1

X 10⁻⁵
55
33
11
-11
-33
-55
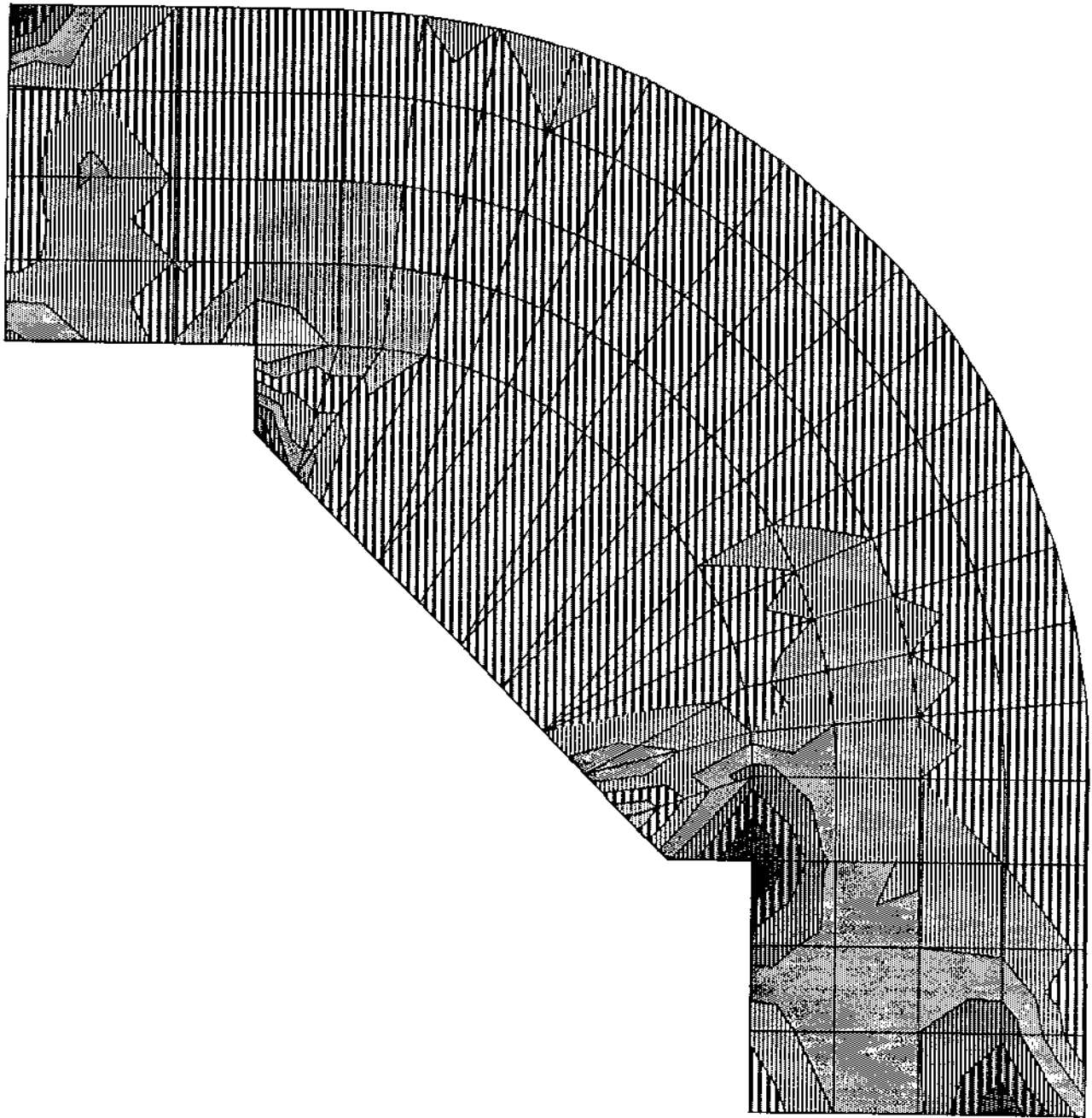
SAP90

MIN IS -0.263E-03 <JOINT 102>   MAX IS 0.775E-03 <JOINT 98>
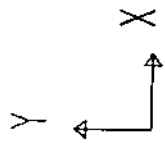
Y
└→ X

webframe
SHELL
OUTPUT SMXT
LOAD   1

X 10⁻⁵

84
60
36
12
-12
-36

SAP90

Y
L→ X
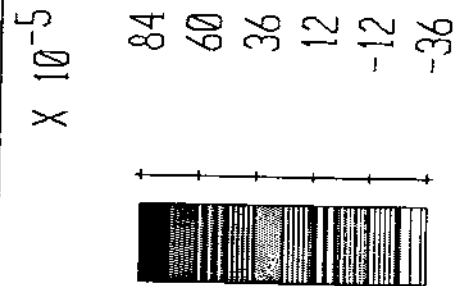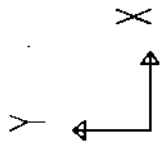
webframe
SHELL
OUTPUT S22T
LOAD 1

X 10⁻⁵
85
51
17
-17
-51
-85
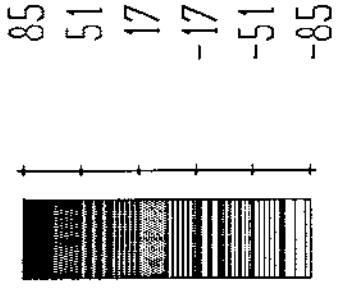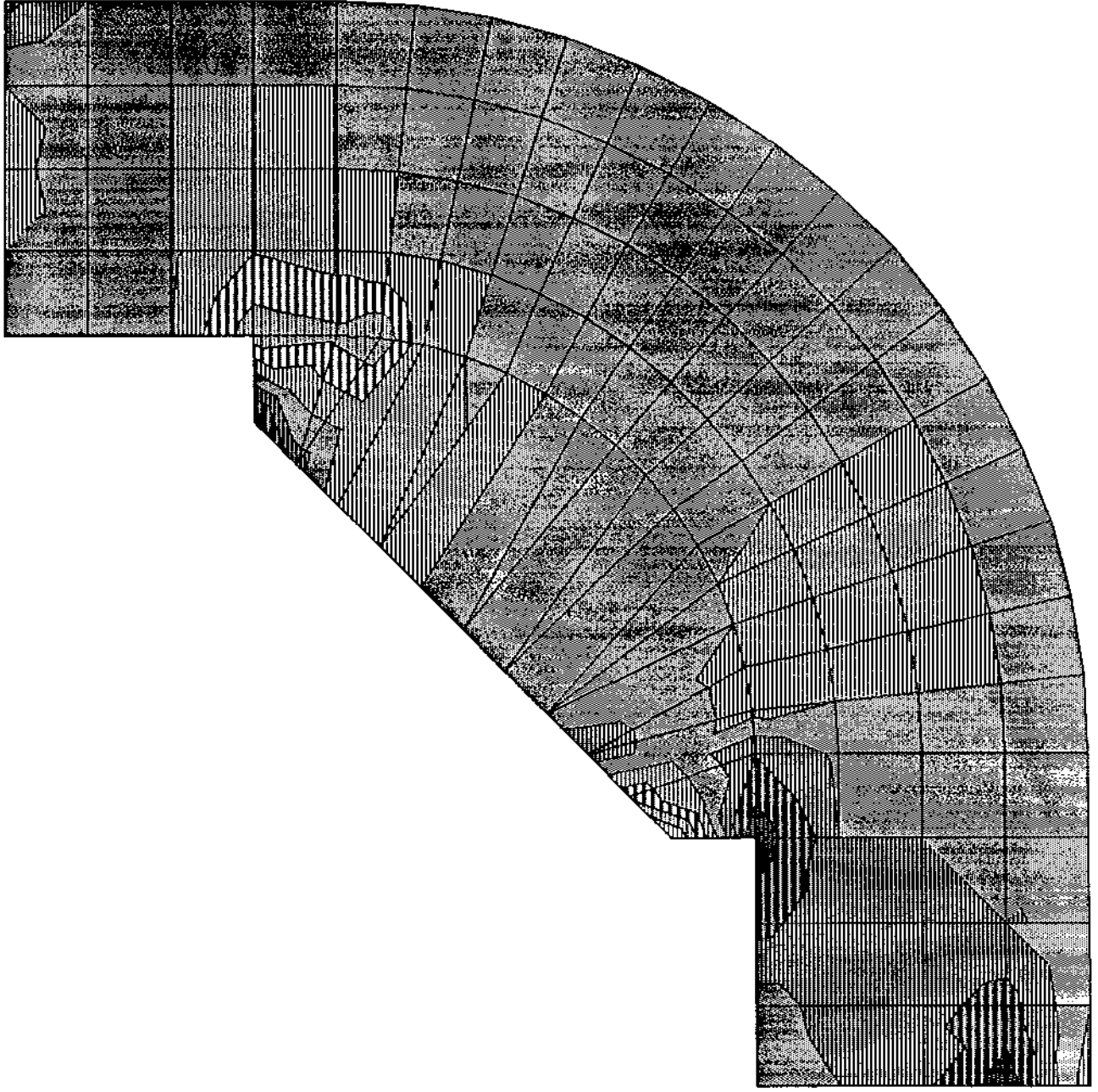
SAP90

MIN IS -0.751E-03 <JOINT 132>   MAX IS 0.631E-03 <JOINT 122>

482

Y

X

webframe

SHELL
OUTPUT S12T
LOAD   1

$X \times 10^{-5}$
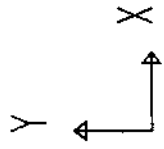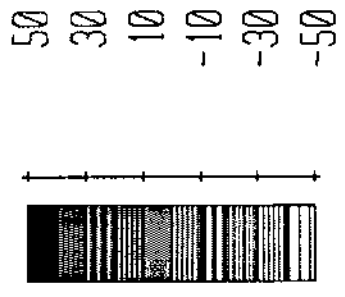
50
30
10
-10
-30
-50
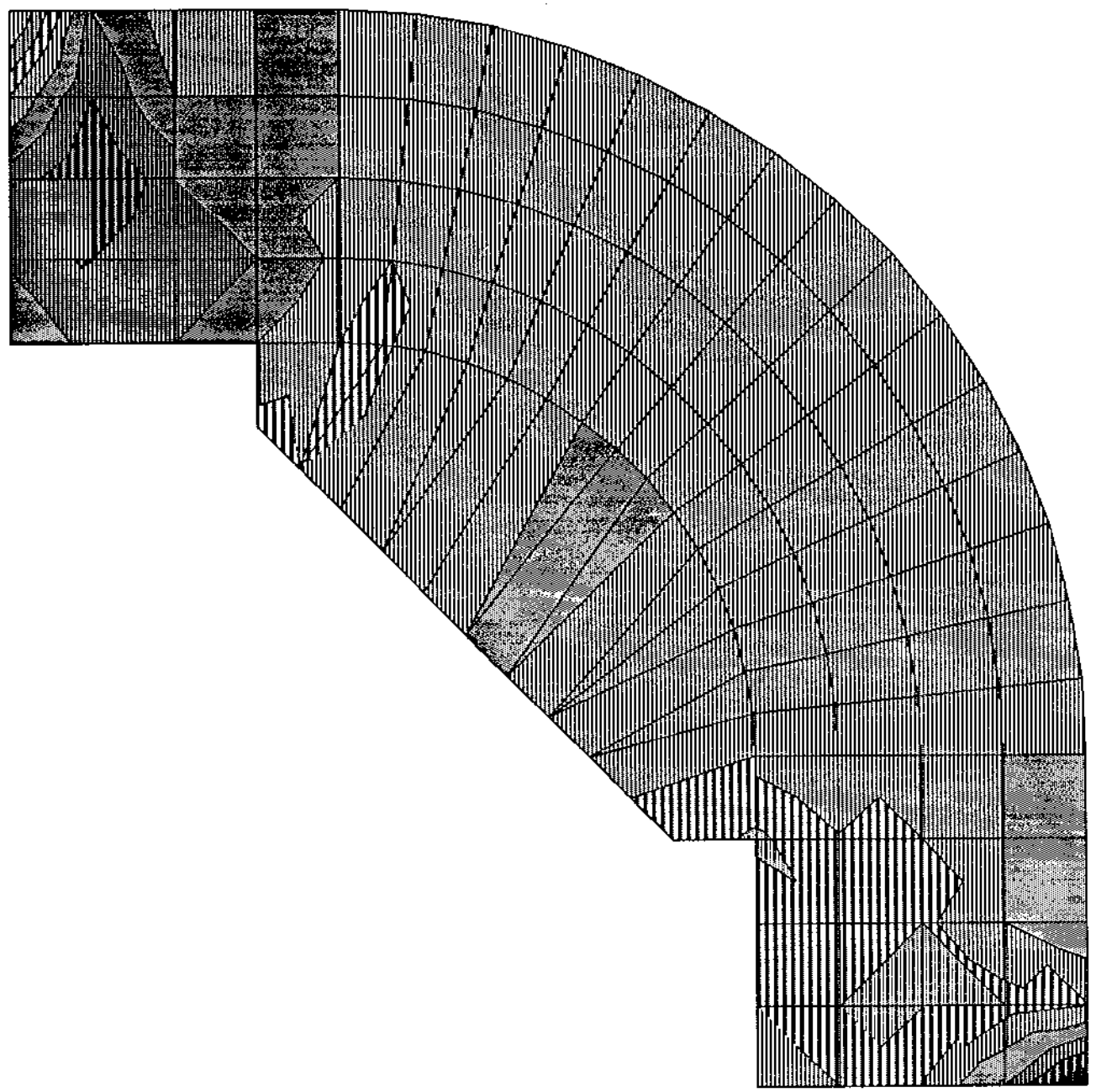
MIN IS -0.464E-03 <JOINT   121>   MAX IS   0.418E-03 <JOINT   85>

SAP90

483

Double-Bottom Connection

484

X

Y
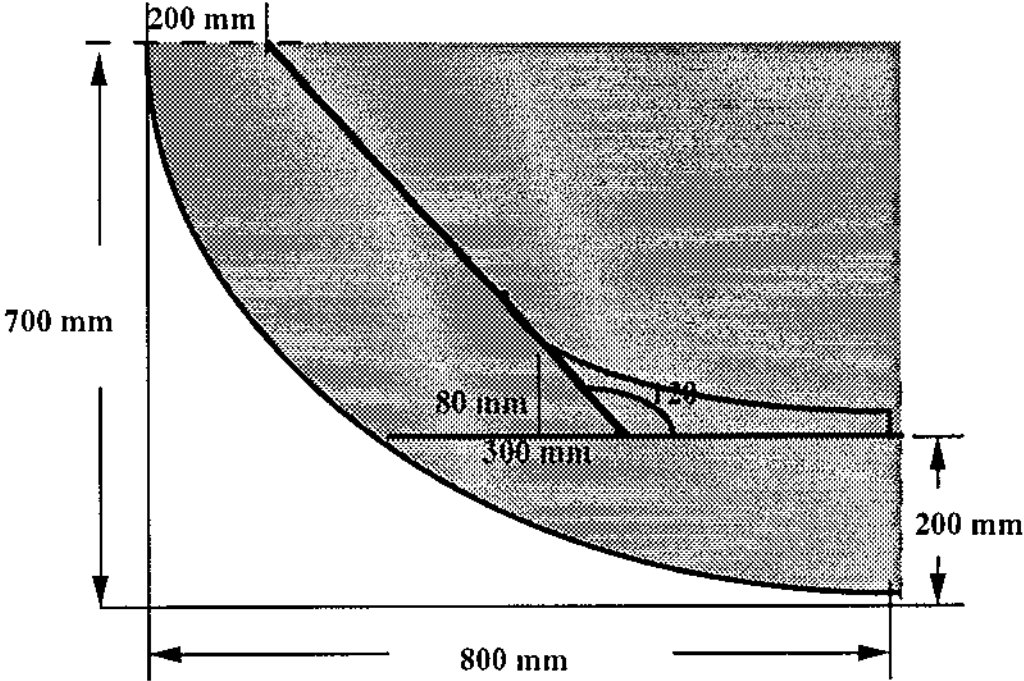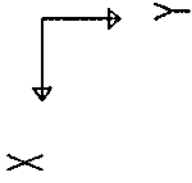
webfram2
UNDEFORMED
SHAPE

OPTIONS
WIRE FRAME

SAP90

X

Y
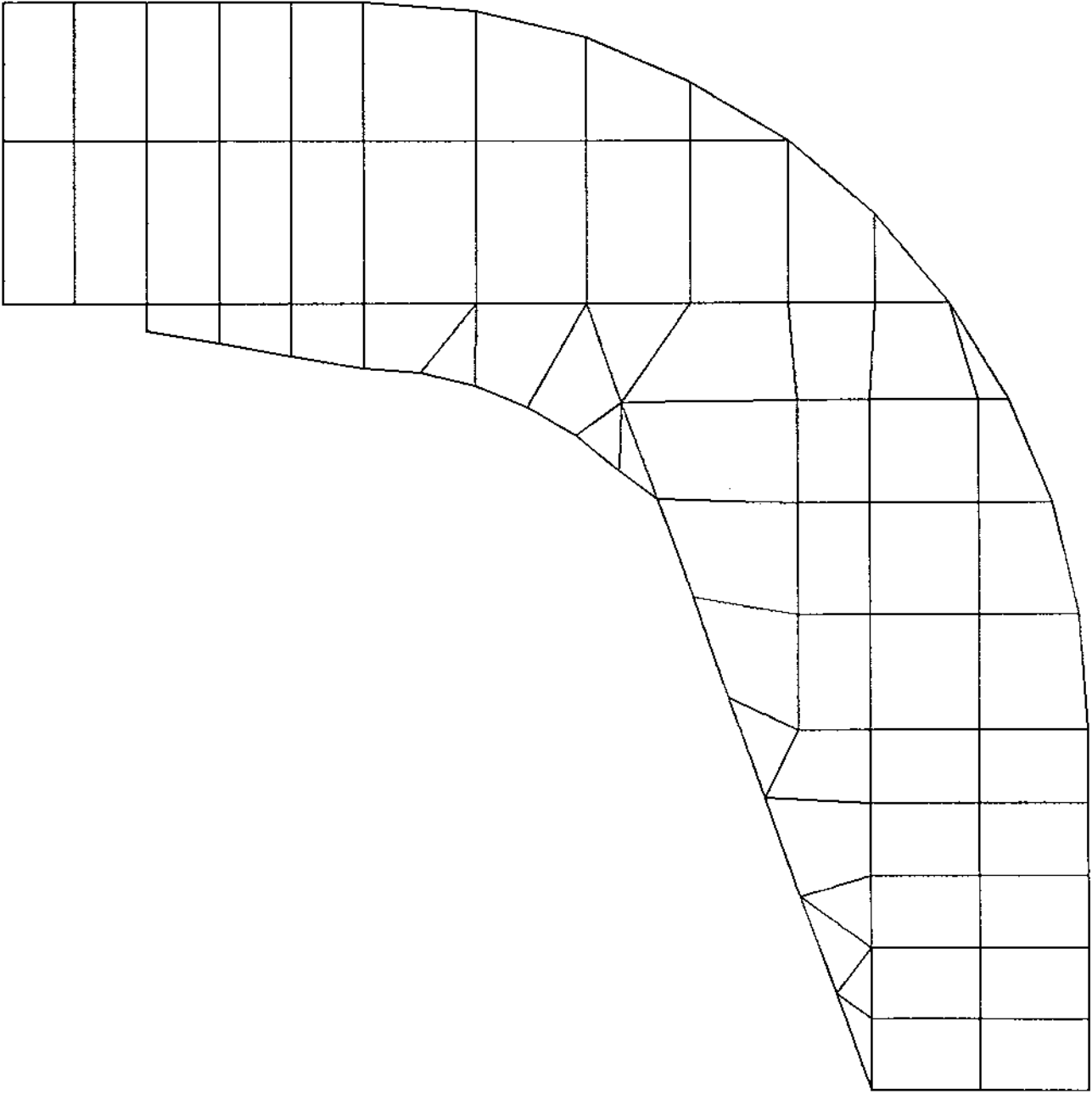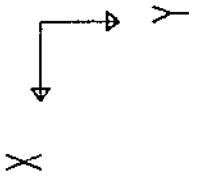
webfram2

DEFORMED
SHAPE

LOAD   1

MINIMA
X 0.0000E+00
Y-0.4204E-05
Z 0.0000E+00
MAXIMA
X 0.4691E-03
Y 0.2358E-03
Z 0.0000E+00
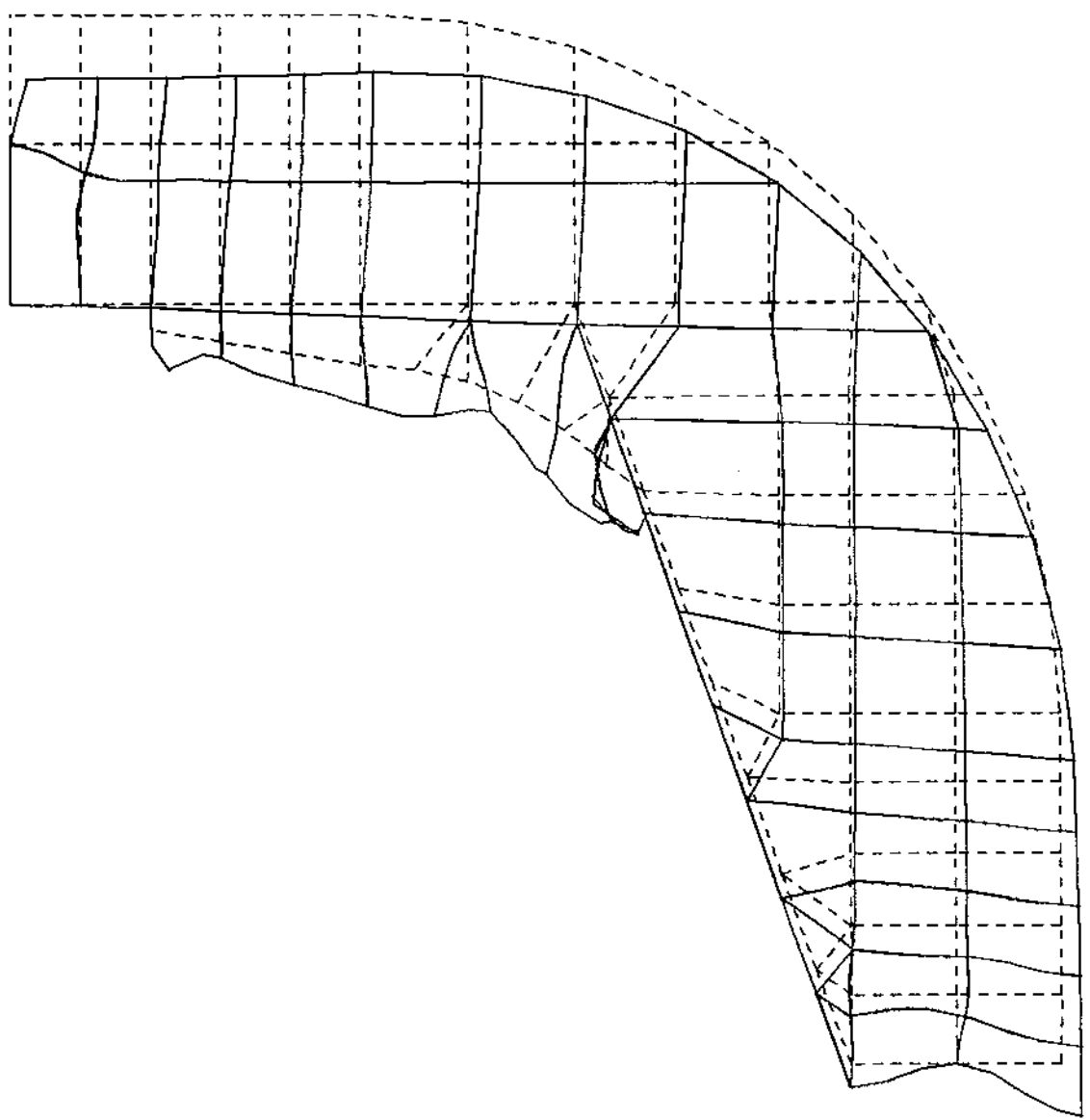
SAP90

X

Y

webfram2
SHELL
OUTPUT S11T
LOAD   1

X 10⁻⁵

425
255
85
-85
-255
-425

MIN IS -0.415E-02 ⟨JOINT 192⟩   MAX IS   0.377E-02 ⟨JOINT   190⟩

SAP90

487

X

X ——→ Y
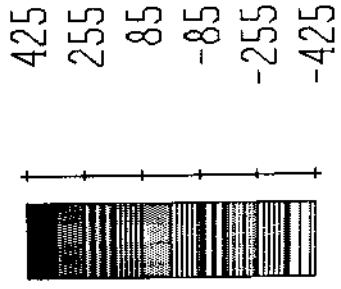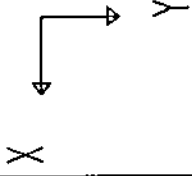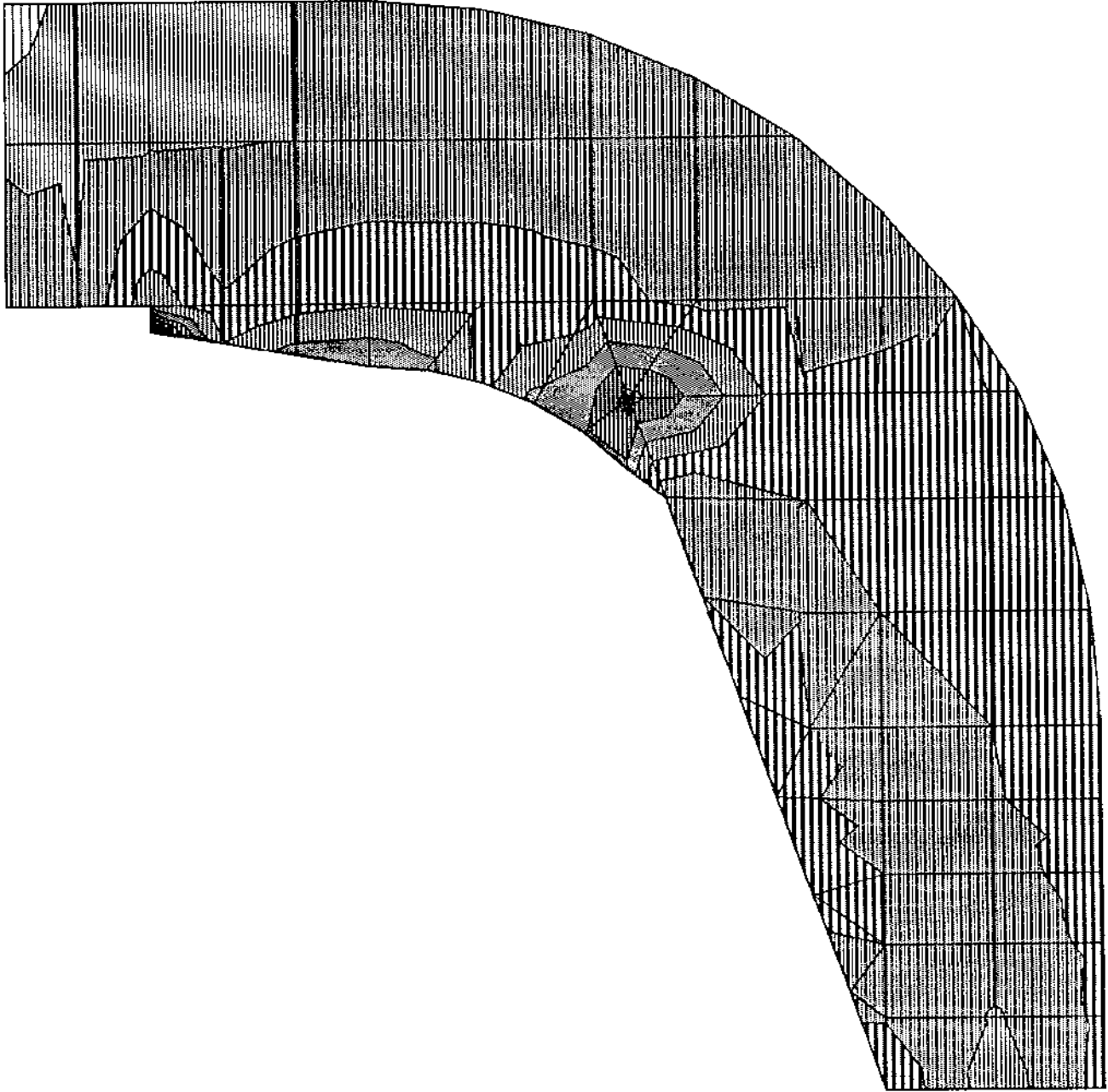
webfram2

SHELL
OUTPUT S22T
LOAD   1

X 10⁻⁴

91
65
39
13
-13
-39
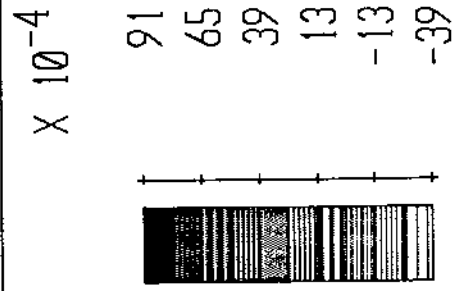
SAP90

MIN IS -0.357E-02 <JOINT   17>   MAX IS   0.885E-02 <JOINT   184>

X

Y

webfram2
SHELL
OUTPUT S12T
LOAD   1

X 10⁻⁵

100
0
-100
-200
-300
-400
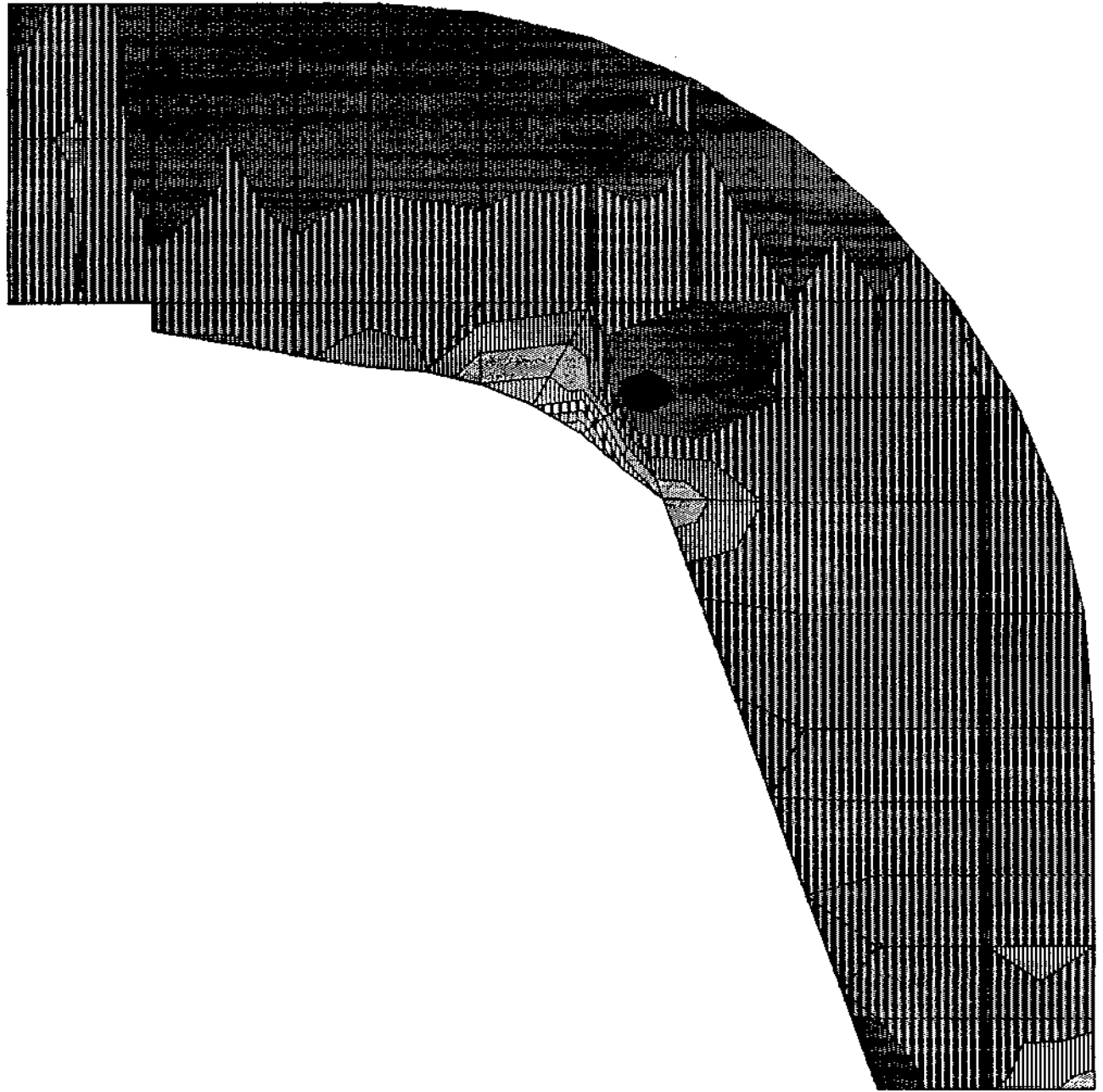
MIN IS -0.365E-02 <JOINT   191>   MAX IS   0.731E-03 <JOINT   43>

SAP90

489

X

Y
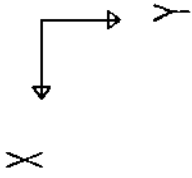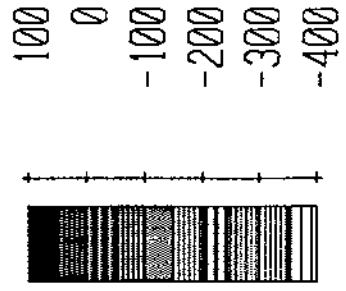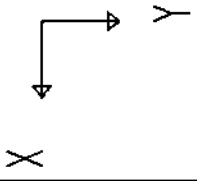
webfram2
SHELL
OUTPUT SMXT
LOAD   1

X 10⁻⁴
99
77
55
33
11
-11
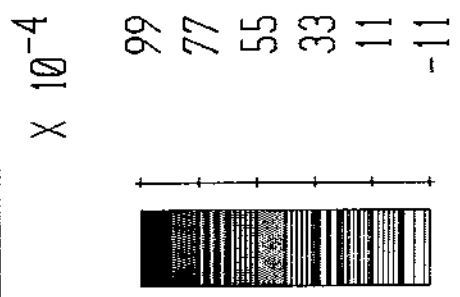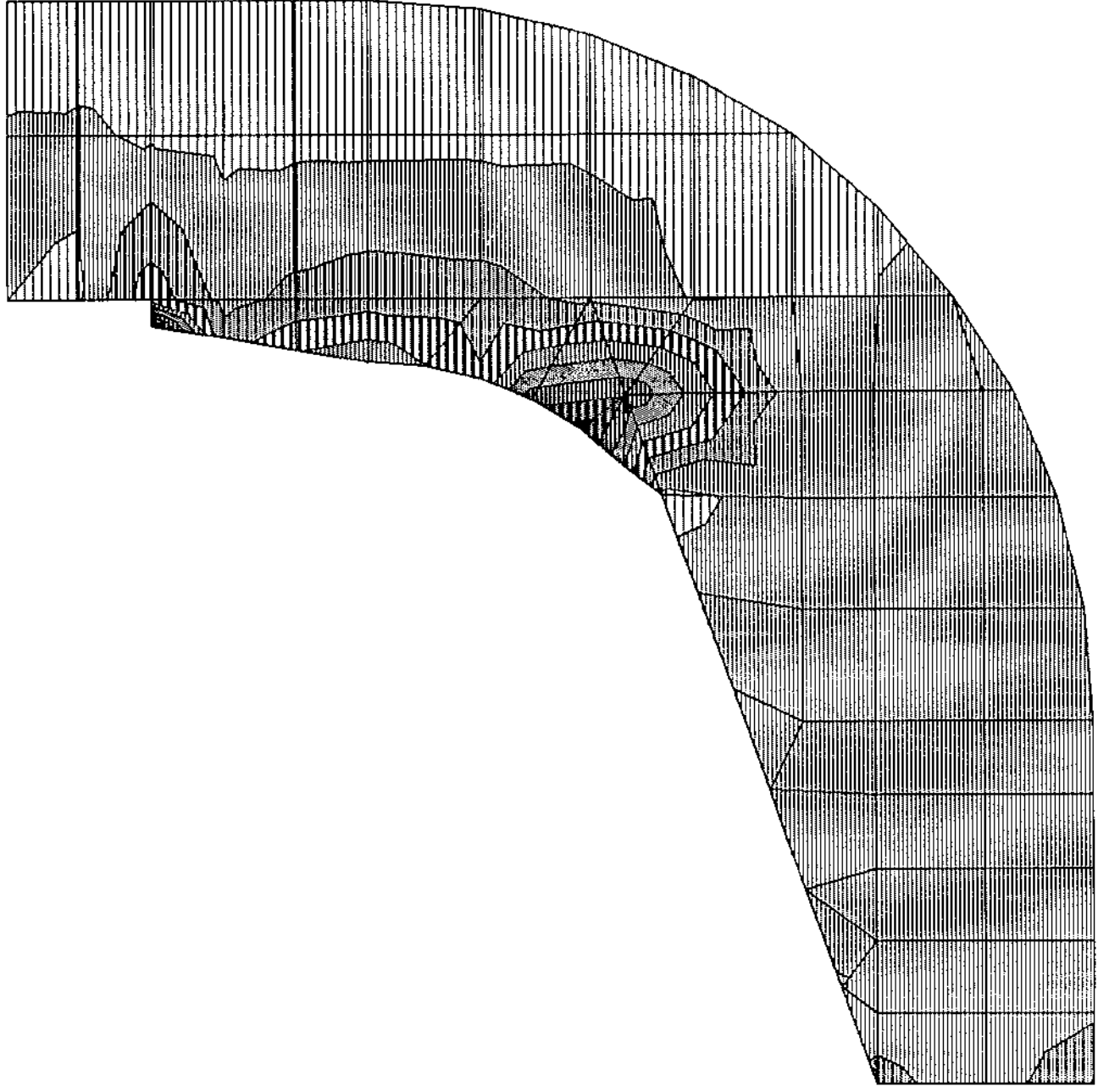
SAP90

MIN IS -0.104E-02 <JOINT   17>   MAX IS   0.887E-02 <JOINT   184>

490

Double-Bottom Connection

200

700 mm

50

400

450

50

200

800 mm

Y
X
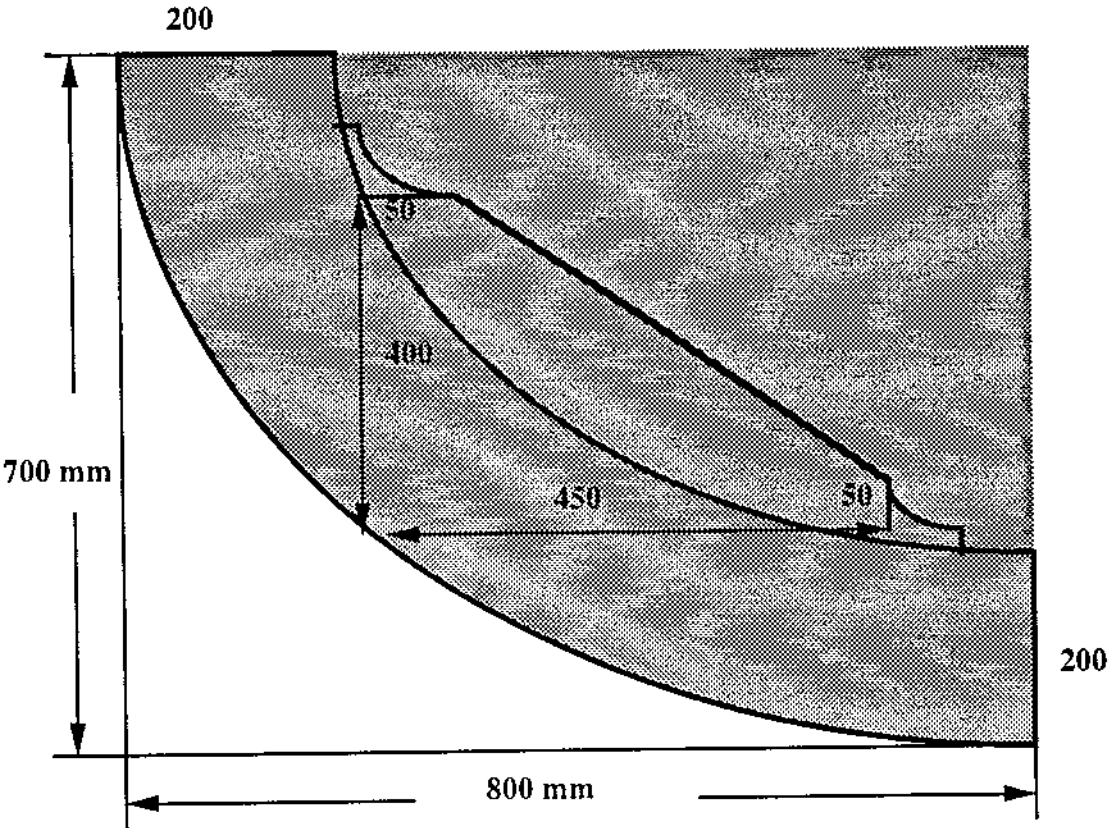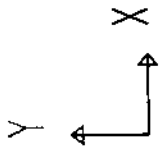
webframe1
UNDEFORMED
SHAPE

OPTIONS
WIRE FRAME

SAP90

Y
X
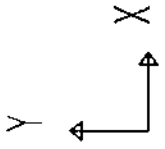
webframe1
SHELL
OUTPUT S11T
LOAD   1

X 10⁻⁵

60
36
12
-12
-36
-60
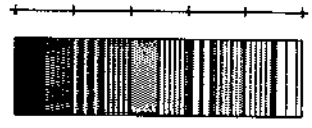
SAP90
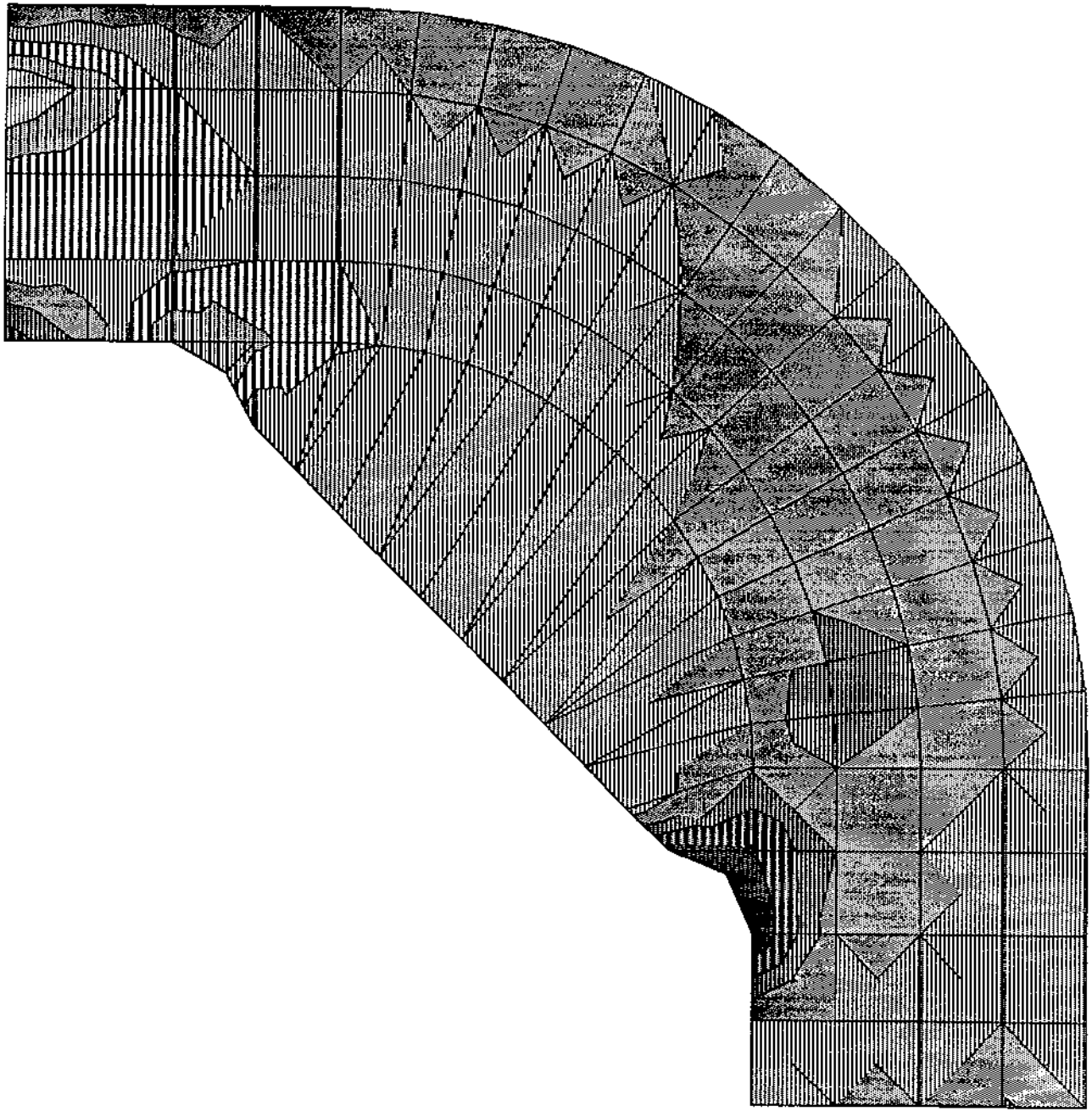
MIN IS -0.514E-03 <JOINT 117>   MAX IS   0.487E-03 <JOINT   135>

493
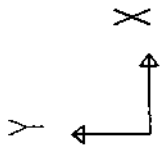
webframe1
DEFORMED
SHAPE
LOAD   1

MINIMA
X 0.0000E+00
Y-0.7019E-06
Z 0.0000E+00
MAXIMA
X 0.5809E-05
Y 0.3845E-05
Z 0.0000E+00

SAP90

Y

X
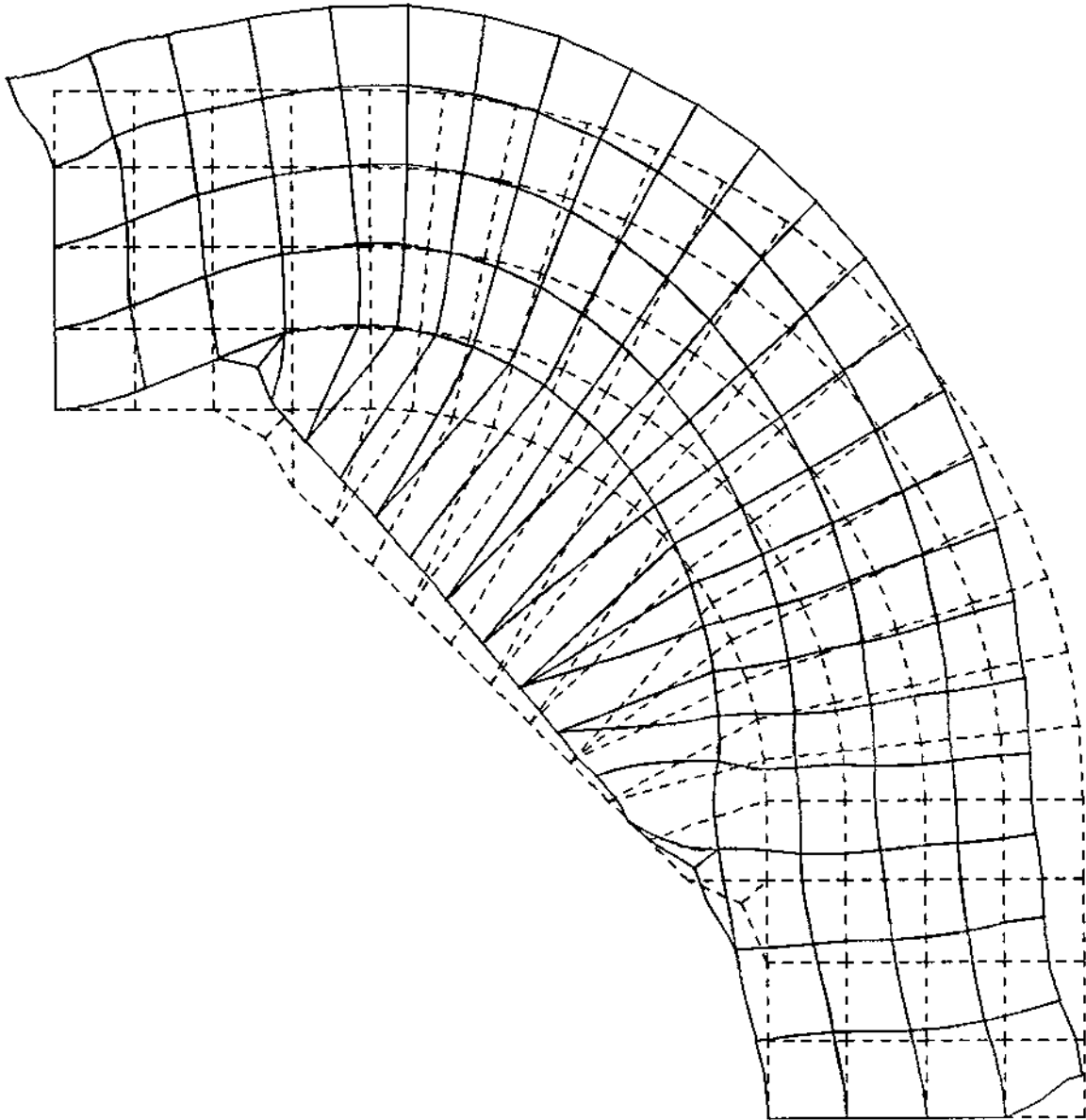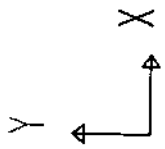
webframe1

SHELL
OUTPUT   S22T
LOAD   1

X 10⁻⁵

102
68
34
0
-34
-68
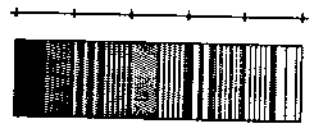
SAP90
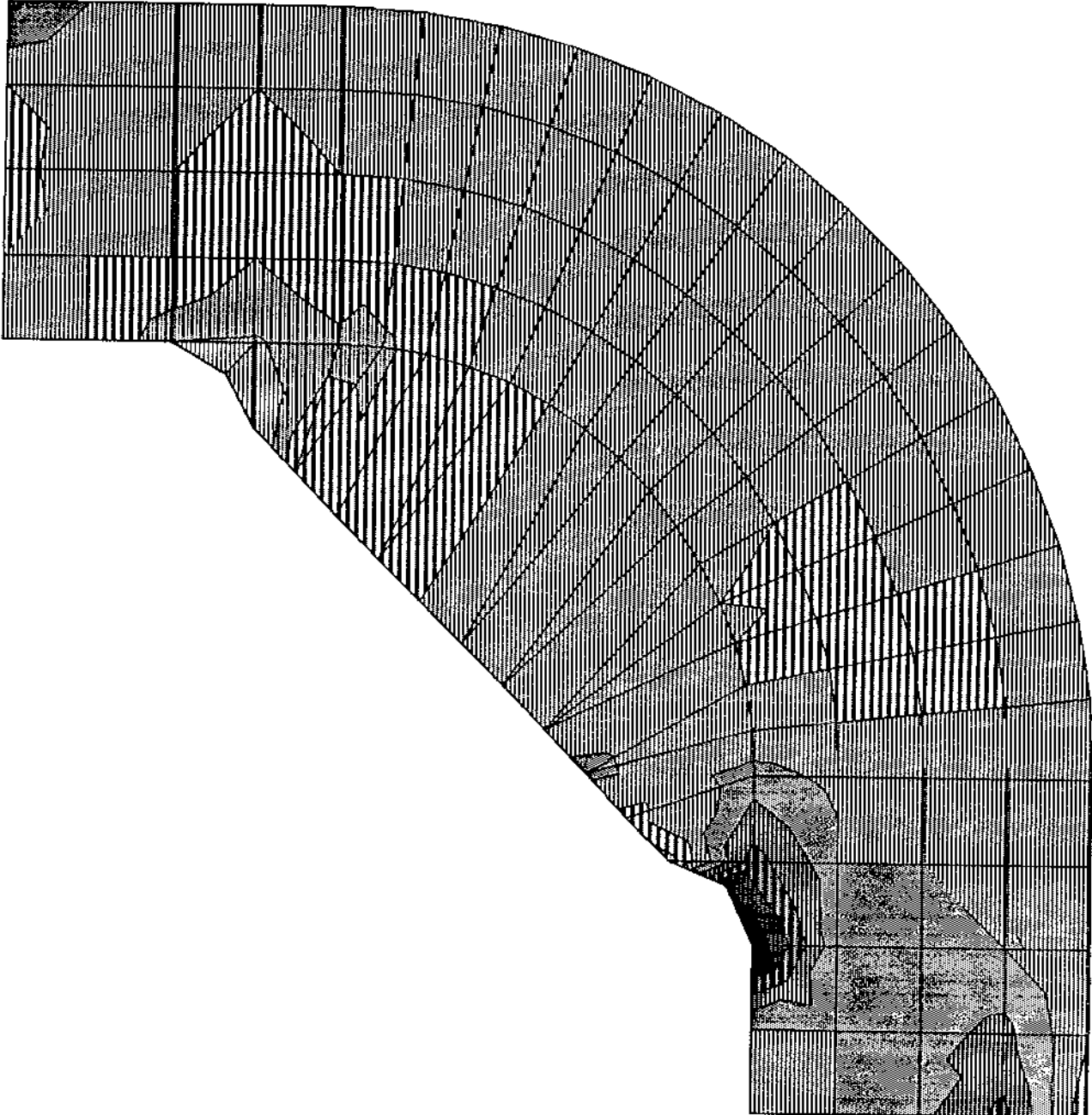
MIN IS -0.571E-03 <JOINT   122>   MAX IS   0.101E-02 <JOINT   99>

495

Y
X
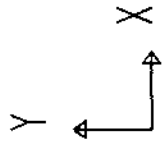
webframe1
SHELL
OUTPUT   S12T
LOAD   1

X 10^{-5}

50
30
10
-10
-30
-50
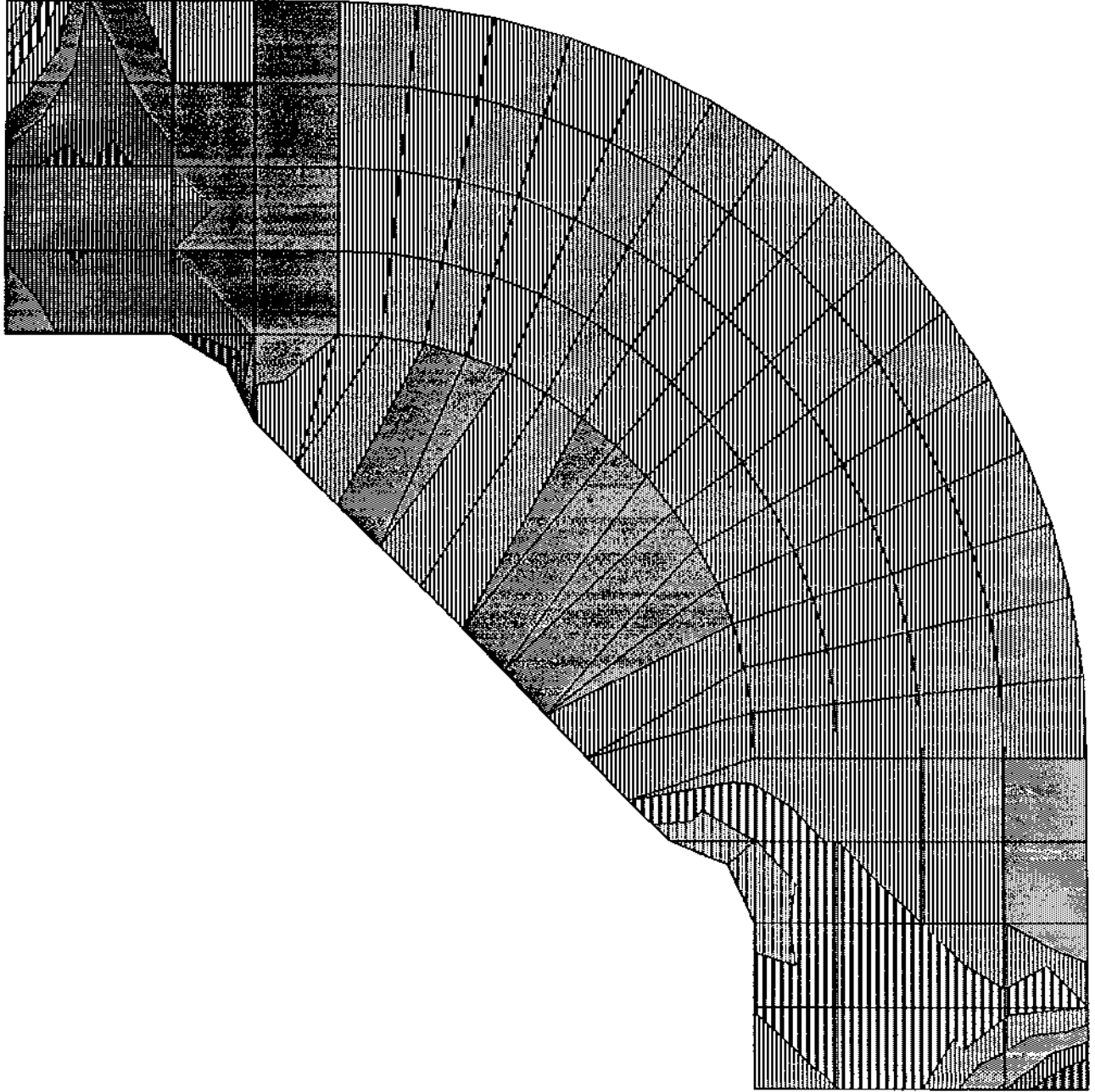
SAP90

MIN IS -0.434E-03 <JOINT   121>   MAX IS   0.387E-03 <JOINT   85>

496
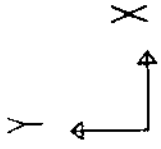
webframe1
SHELL
OUTPUT SMXT
LOAD   1

X 10⁻⁵

117
91
65
39
13
-13

Y
X
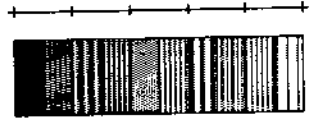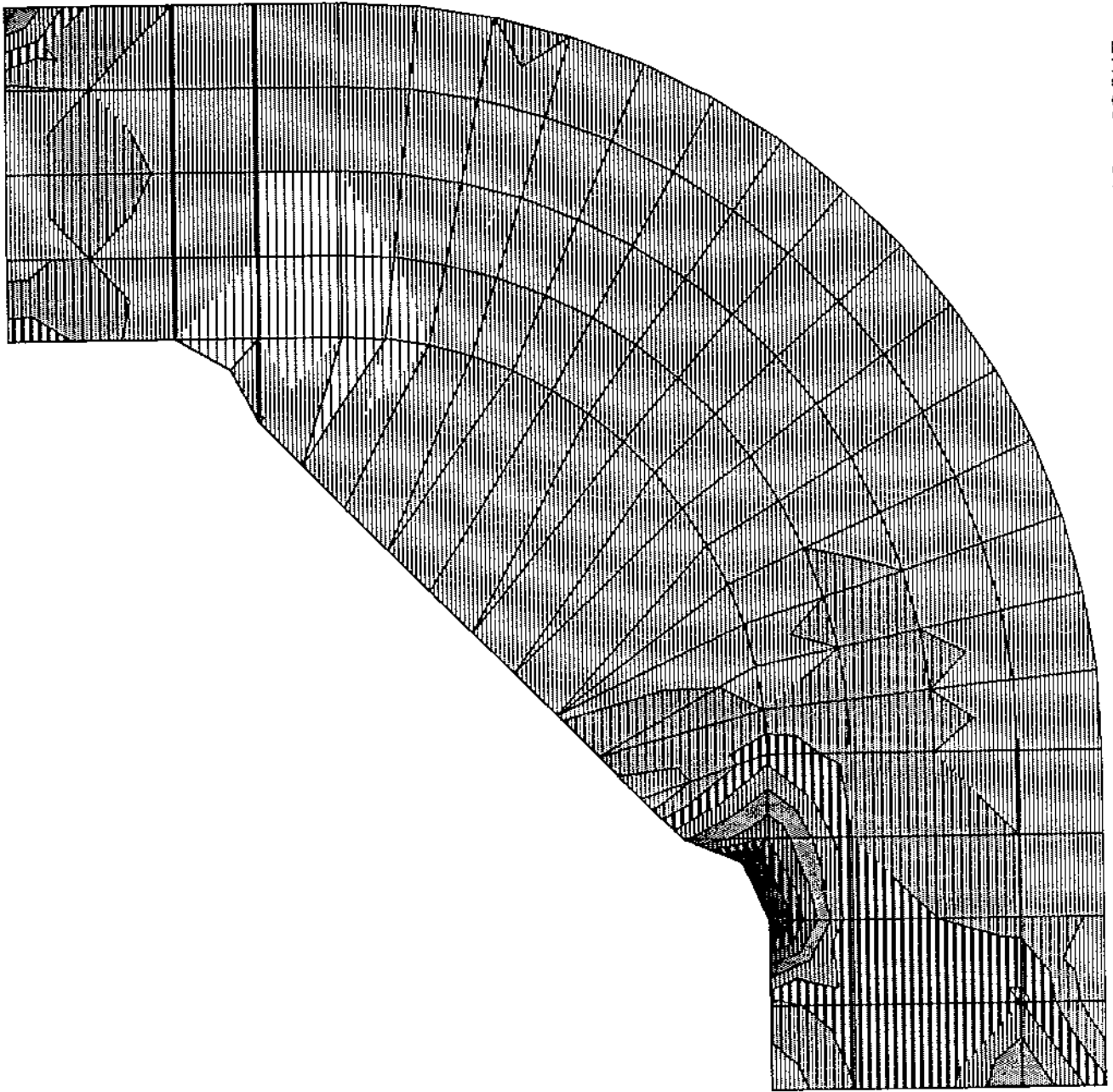
MIN IS -0.590E-04 <JOINT   102>   MAX IS   0.112E-02 <JOINT   135>

SAP90

Section 4 Fatigue Classification for CSD in Tankers
Based on Hotspot Stress
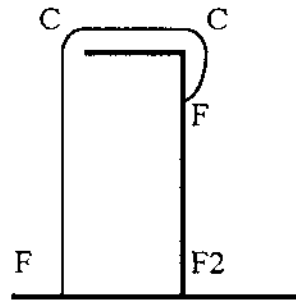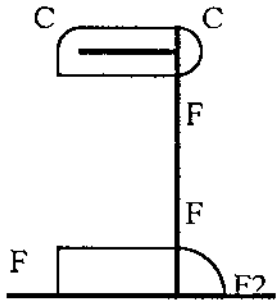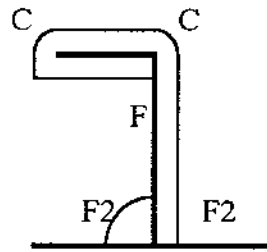
U.K. Department of Energy Design S-N Curves
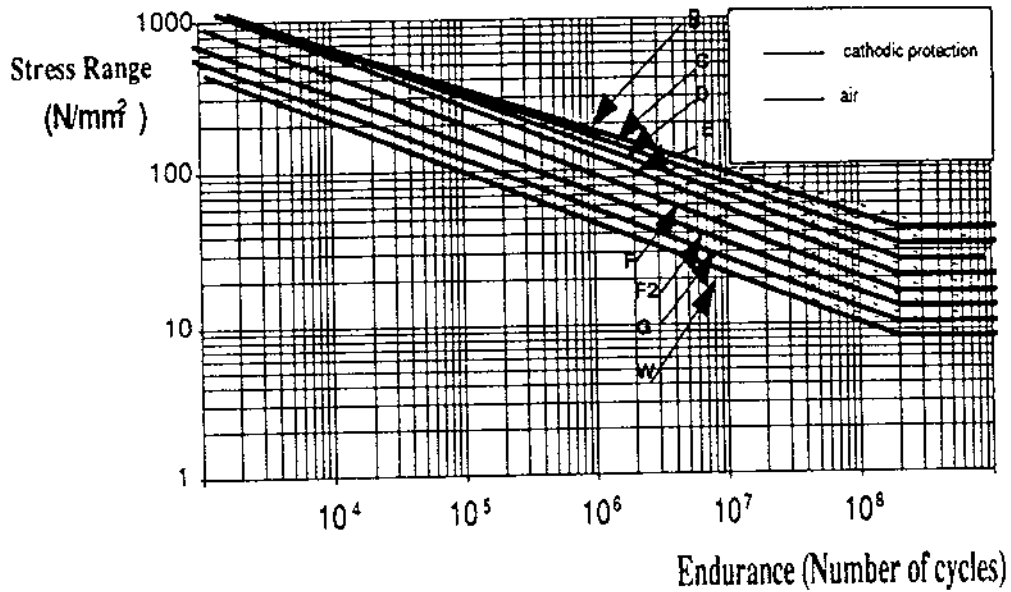
Figure 3.7: S-N curves

Table 3.4: The data of S-N relations

Class	m	C_{50}	log s
B	4	$2.343*10^{15}$	0.1822
C	3.5	$1.082*10^{14}$	0.2041
D	3	$3.988*10^{12}$	0.2095
E	3	$3.289*10^{12}$	0.2509
F	3	$1.726*10^{12}$	0.2183
F2	3	$1.231*10^{12}$	0.2279
G	3	$0.566*10^{12}$	0.1793
W	3	$0.368*10^{12}$	0.1846

C   F

F   F2

C   C

F

F2   F

C   C

F

F2   F2

C   C

F

F2   F2

C   C

F

F

F   F2

C   C

F

F   F2

C C

F

F or F2

C C

F

F or F2 F or F2

C C

F or F2 F or F2

C C

F or F2 F or F2

F2   F or F2

F2   F

F   C
F2   F2

502

F2   F or F2

F

F or F2   F2   F2

F

F2   C

F

503

F2

F2

F2

F2

F2

F2

F2

F

504

F2

F2

F2 or G

505
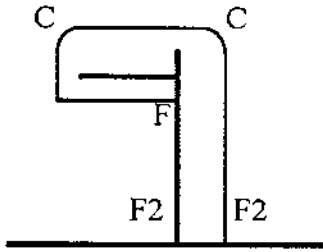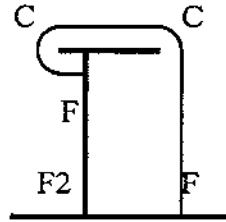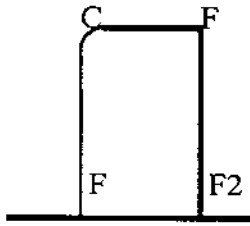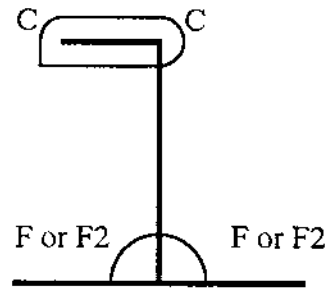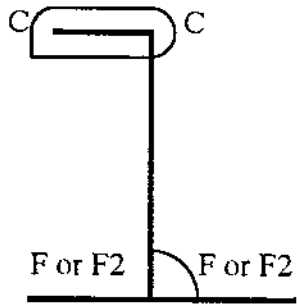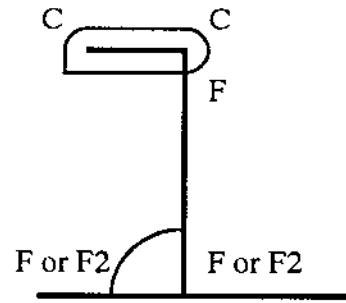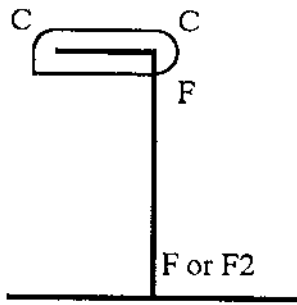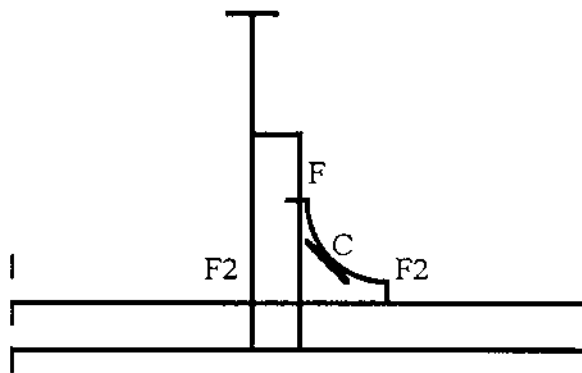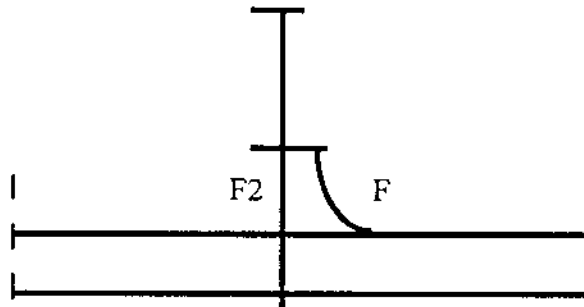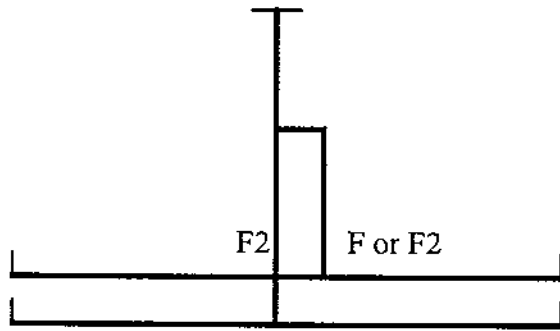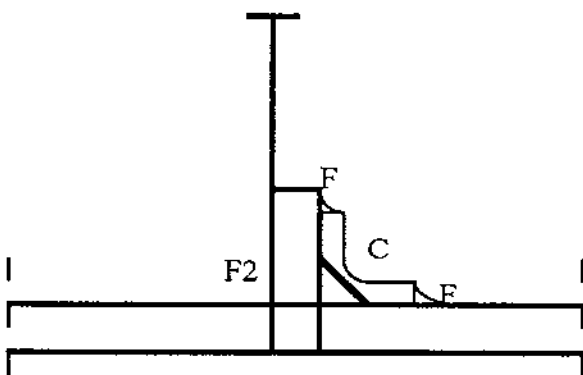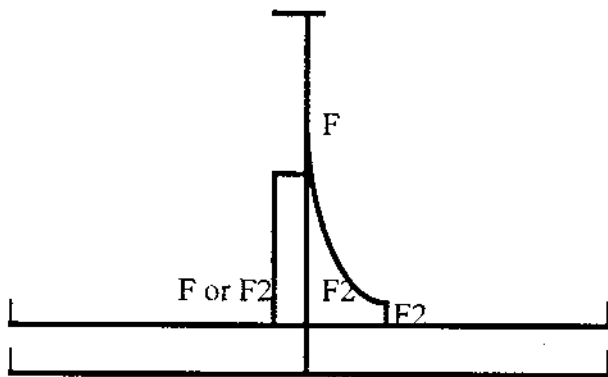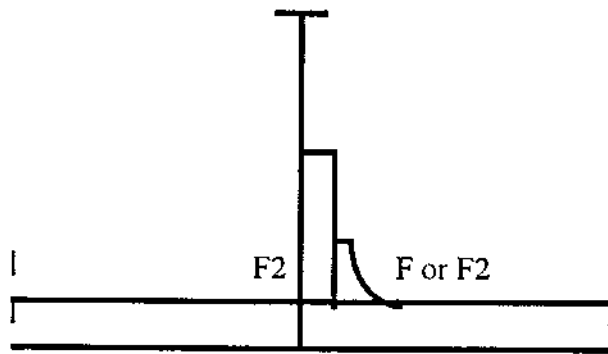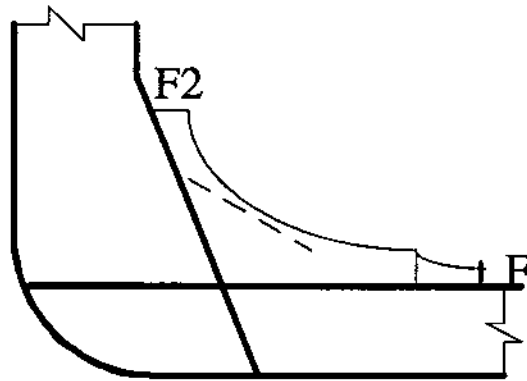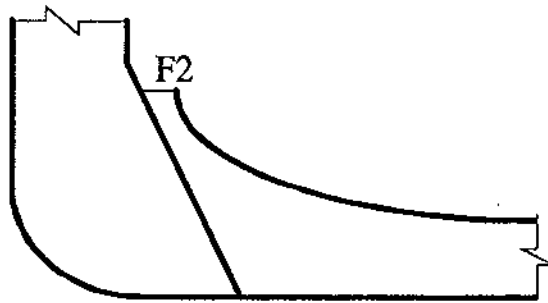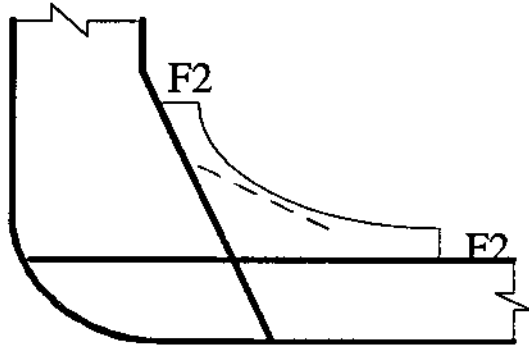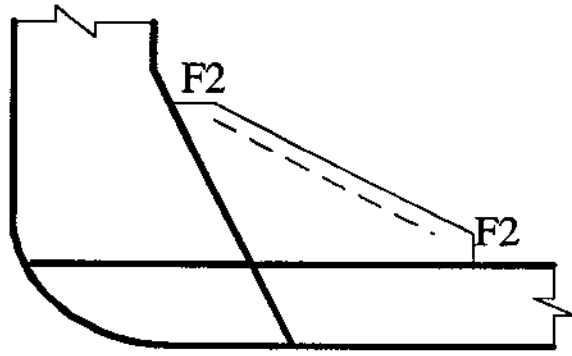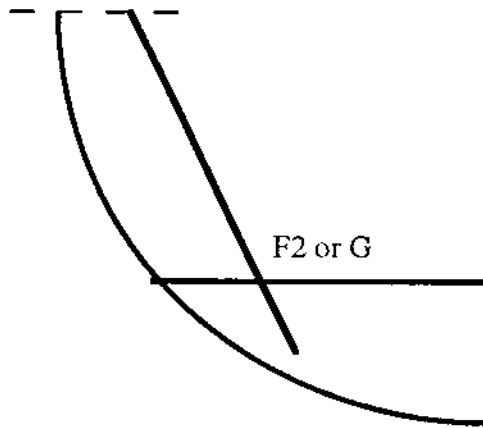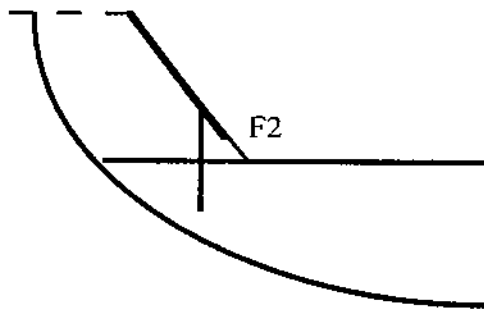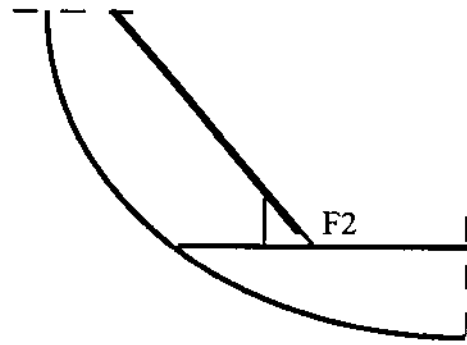
Chapter 4

Summary

This report documents CSD library developed and some finite element stress contours performed in this project. The CSD library is a little different from previous SMP project (Ref. 1). The stress contours which were major part of the tedious and hard work in this project will be very useful for the coming new project "Fitness for Purpose Evaluation for Cracked CSD in Tankers". More detailed conclusions including stress concentration factors and CSD fatigue design can be found in Ref. 2.

Reference

1 Structural Maintenance for New and Existing Ships, Research Report SMP 1-1 through SMP 5-2. Dept. of Naval Architecture & Offshore Engineering, University of California at Berkeley, Berkeley, CA 94720. October, 1992

2 Tao Xu and Robert, G Bea "Fatigue Analysis of a 190,000 DWT Double-Bottom Tanker" Research Report, SMPII 1-2. Dept. of Naval Architecture & Offshore Engineering, University of California at Berkeley, Berkeley, CA 94720. October, 1993

3 Tao Xu and Robert, G Bea "Fatigue Analysis of a 150,000 DWT Double-Hull Tanker" Research Report, SMPII 1-1. Dept. of Naval Architecture & Offshore Engineering, University of California at Berkeley, Berkeley, CA 94720. October, 1993

4 SAP-90 User's Manual Computer and Structure Inc. 1991

5 Rolf Schulte-Strathaus and Robert, G Bea "Development of calibrated S-N Curves and System for the Selection of S-N Curves". Research Report, FACTS 1-1. Dept. of Naval Architecture & Offshore Engineering, University of California at Berkeley, Berkeley, CA 94720. September, 1993

COMMITTEE ON MARINE STRUCTURES

Commission on Engineering and Technical Systems

National Academy of Sciences - National Research Council

The **COMMITTEE ON MARINE STRUCTURES** has technical cognizance over the interagency Ship Structure Committee's research program.

Dr. John Landes, *Chairman*, University of Tennessee, Knoxville, TN

Mr. Howard M. Bunch, University of Michigan, Ann Arbor, MI

Dr. Dale G. Karr, University of Michigan, Ann Arbor, MI

Mr. Andrew Kendrick, NKF Services, Montreal, Quebec

Dr. John Niedzwecki, Texas A & M University, College Station, TX

Dr. Alan Pense, NAE, Lehigh University, Bethlehem, PA

Dr. Barbara A. Shaw, Pennsylvania State University, University Park, PA

Dr. Robert Sielski, National Research Council, Washington, DC

CDR Stephen E. Sharpe, Ship Structure Committee, Washington, DC

DESIGN WORK GROUP

Dr. John Niedzwecki, *Chairman*, Texas A&M University, College Station, TX

Dr. Bilal Ayyub, University of Maryland, College Park, MD

Mr. Ovide J. Davis, Pascagoula, MS

Mr. Andy Davidson, NASSCO, San Diego, CA

Dr. Maria Celia Ximenes, Chevron Shipping Co., San Francisco, CA

Mr. Jeffrey Geiger, Bath Iron Works, Bath, ME

Mr. Hugh Rynn, Sea-Land Services, Elizabeth, NJ

MATERIALS WORK GROUP

Dr. Barbara A. Shaw, *Chairman*, Pennsylvania State University, University Park, PA

Dr. David P. Edmonds, Edison Welding Institute, Columbus, OH

Dr. John F. McIntyre, Advanced Polymer Sciences, Avon, OH

Dr. Harold S. Reemsnyder, Bethlehem Steel Corp., Bethlehem, PA

Dr. Bruce R. Somers, Lehigh University, Bethlehem, PA

C.2

C3

RECENT SHIP STRUCTURE COMMITTEE PUBLICATIONS

Ship Structure Committee Publications - A Special Bibliography This bibliography of SSC reports may be downloaded from the internet at: "http://www.dot.gov/dotinfo/uscg/hq/nmc/nmc/ssc1/index.htm".

SSC-394   Strength Assessment of Pitted Plate Panels J. Daidola, J. Parente, I. Orisamolu, K-t. Ma 1997

SSC-393   Evaluation of Ductile Fracture Models R. Dexter, M. Gentilcore 1997

SSC-392   Probability Based Ship Design: Implementation of Design Guidelines A. Mansour, P. Wirsching, G. White, B. Ayyub 1996

SSC-391   Evaluation of Marine Structures Education in North America R. Yagle 1996

SSC-390   Corrosion Control of Inter-hull Structures M. Kikuta, M. Shimko, D Ciscom 1996

SSC-389   Inspection of Marine Structures L. Demsetz, R. Cario, R. Schulte-Strathaus, B. Bea 1996

SSC-388   Ship Structural Integrity Information System-Phase II M. Dry, R. Schulte-Strathaus, B. Bea 1996

SSC-387   Guideline for Evaluation of Finite Elements and Results R. I. Basu, K. J. Kirkhope, J. Srinivasan 1996

SSC-386   Ship's Maintenance Project R. Bea, E. Cramer, R. Schulte-Strauthaus, R. Mayoss, K. Gallion, K. Ma, R. Holzman, L. Demsetz 1995

SSC-385   Hydrodynamic Impact on Displacement Ship Hulls - An Assessment of the State of the Art J. Daidola, V. Mishkevich 1995

SSC-384   Post-Yield Strength of Icebreaking Ship Structural Members C. DesRochers, J. Crocker, R. Kumar, D. Brennan, B. Dick, S. Lantos 1995

SSC-383   Optimum Weld-Metal Strength for High Strength Steel Structures R. Dexter and M. Ferrell 1995

SSC-382   Reexamination of Design Criteria for Stiffened Plate Panels by D. Ghose and N. Nappi 1995

SSC-381   Residual Strength of Damaged Marine Structures by C. Wiernicki, D.

PROJECT TECHNICAL COMMITTEE MEMBERS

The following persons were members of the committee that represented the Ship Structure Committee to the Contractor as resident subject matter experts. As such they performed technical review of the initial proposals to select the contractor, advised the contractor in cognizant matters pertaining to the contract of which the agencies were aware, performed technical review of the work in progress and edited the final report.

Chairman

Paul Cojeen   U. S. Coast Guard

Members

LT Robert Holzman   U. S. Coast Guard

Fred Seibold   Maritime Administration

Dr. Walter MacLean   U. S. Merchant Marine Academy

Chao Lin   Maritime Administration

Dr. Y-k Chen   American Bureau of Shipping

William Siekierka   Naval Sea Systems Command,
                               Contracting Officer's
                               Technical Representative

Dr. Robert Sielski   National Academy of Science,
                               Marine Board Liaison

CDR Steve Sharpe   U.S. Coast Guard, Executive Director
                               Ship Structure Committee

509
510x , 511x , 512x all